A mechanistic insight into the synthesis of enantiopure -amino acids using the enamido Ireland Claisen rearrangement

Harker, Wesley

Award date:
2011

Awarding institution:
University of Bath

A Mechanistic Insight into the Synthesis of Enantiopure β-Amino Acids using the Enamido Ireland Claisen Rearrangement

Wesley R. R. Harker

A Thesis Submitted for the Degree of Doctor of Philosophy

University of Bath

Department of Chemistry

March 2011

…… ……

Wesley R. R. Harker Date

'Just make and rearrange 9 arylacetates and we'll get a quick communication in a fortnight'

ABSTRACT

The Ireland-Claisen rearrangement is a powerful synthetic technique allowing predictable diastereocontrol and chirality transfer within the synthesis of γ,δ-unsaturated carboxylic acids. The Carbery group has recently disclosed a novel enamido-Ireland-Claisen rearrangement (EICR) allowing access to $\beta^{2,3}$-amino acid precursors, where a strong dependency between diastereoselectivity and the substrate acyl moiety was noted. Development of this seminal work in terms of mechanistic rationale and synthetic utility subsequently ensued.

Initial focus, covered in Chapter 2, began with a thorough optimisation of rearrangement conditions and resulted in a desire to probe the electronic dependency of the diastereoselective phenylacetate EICR. With this in mind, rearrangement of a range of electronically differentiated arylacetates demonstrated that diastereoselectivity is profoundly susceptible to electronic perturbation as shown by a non-linear Hammett type plot involving that of *para*-substituents.

In order to evaluate the origins of this free energy relationship, Chapter 3 covers the *in-situ* ^{1}H- and ^{13}C-NMR mechanistic studies undertaken, involving model silyl ketene acetal (SKA) formation and EICR monitoring. These studies demonstrated that poor *E/Z*-SKA generation and rearrangement through a chair transition state may be operative in the case of electron rich aryl substitution; however selective formation of the *E*-SKA and subsequent rearrangement *via* competing chair and boat transition states may be operative for electron poor aryl substitution. A useful synthetic transformation brought about by these mechanistic studies was seen to be the isolation of phenylacetate derived SKAs in excellent yield and far superior *E*-geometric control to that currently published.

Finally, Chapter 4 involves investigations into improving the diastereoselectivity of the non-α-arylacetates and results in the rearrangement of alkyl- and arylacetate-*N*-allylsulfonamides in high diastereoselectivity and utilisation of an optically enriched substrate demonstrated good chirality transfer (>88% e.e.). Utilisation of these products has been shown within the synthesis of β-proline analogues.

CONTENTS

ACKNOWLEDGEMENTS

Throughout my PhD studies there has been a large support network, both within the Carbery group and external to it, which has allowed me to get to the stage that I am at today.

First and foremost I thank Dr. David R. Carbery for his constant and unwavering resilience in coping with my paranoid tendencies and always being there for the problem solving discussions and counsel. The mechanistic direction my research pursued has been challenging and the ability to face demanding topics has demonstrated that adaptation is the key to personal growth and success. Cheers Dave!

Thanks go out to Dr. Emma L. Carswell for her support and willingness to sign ridiculously awkward order forms involving $^{2}H/^{13}C$-labelled materials and also for all the '5 minute phone calls' and advice.

Special thanks go out to Dr. John P. Lowe for showing me the power of NMR and also to Dr. Samantha Rutherford and Mr. Ross Lennen from M.S.D, as without their friendly and knowledgeable guidance the mechanistic studies would not have been achievable. Further analytical thanks go to Dr. Anneke T. Lubben for all the manual injections into the mass spectrometer and also to Dr. Mary F. Mahon for XRD analysis.

In addition I also thank Prof. Ian H. Williams and Dr. Ian R. Greig for discussions surrounding *in-silico* modelling and physical organic chemistry.

Penultimately I thank Dr. Morwenna S. M. Pearson-Long, Dr. Barrie J. Marsh, Dr. James P. Tellam, Dr. Andrew C. Silvanus, Mr Stephen J. Heffernan and Mr. Matthew R. Crittall. In addition I am eternally grateful to Mr. Nathan W. G. Fairhurst for acting as an un-official I.T-guru. Team work really works!

I finally thank Trixie Stirling, Rexie Shaw & Misty Mirtle.

Cheers!

ABBREVIATIONS

ACPC ..... *trans*-2-aminocyclopentanecarboxylic acid

APC ..... *trans*-3-aminopyrrolidine-4-carboxylic acid

ADHD ..... Attention Deficit Hyperactivity Disorder

Adda ..... (2*S*,3*S*,8*S*,9*S*)-3-Amino-9-methoxy-2,8-dimethyl-10-phenyl-deca-4,6-dienoic acid

Amha……..3-Amino-2-methylhex-enoic acid

app ..... Apparent

Bn ..... Benzyl

Boc ..... ^{t}Butoxycarbonyl

bs ..... Broad singlet

CAN ..... Ceric(IV)ammonium nitrate

Cat ..... Catalytic

Cbz ..... Carbobenzyloxy

Conform ..... Conformation

Cp ..... Cycopentadienyl

DCC..... 1,3-Dicyclohexylcarbodiimide

DCM..... Dichloromethane

DIPA..... Diisopropylamine

DMF ..... Dimethylformamide

DMP ..... Dess-Martin Periodinane

DPPA..... Diphenylphosphoryl azide

d..... Doublet

d.r..... Diasteriomeric ratio

EDCi..... 1-Ethyl-3-(3-dimethylaminopropyl)carbodiimide

EDG……..Electron Donating Group

e.e. ..... Enantiomeric excess

Eg ..... Examples

EICR..... Enamido Ireland-Claisen Rearrangement

eq ..... Mole equivalents

EWG..... Electron Withdrawing Group

HMPA ..... Hexamethylphosphoramide

ICR ..... Ireland-Claisen Rearrangement
KHMDS ..... Potassium Hexamethyl Disilazide
LAH ..... Lithium Aluminium Hydride
LDA ..... Lithium Diisopropyl Amide
LiCA ..... Lithium Cyclohexylisopropylamide
LiHMDS ..... Lithium Hexamethyl Disilazide
m ..... Multiplet
MHMDS ..... Metal Hexamethyl Disilazide
MS ..... Molecular sieves
na ..... Non-Applicable
pent ..... Pentet
PG ..... Protecting Group
PIVCl ..... Pivaloyl chloride
PhMe ..... Toluene
PMP 4-Methoxyphenyl
^{i}Pr ..... *Iso*Propyl
Pyr ..... Pyridine
q ..... Quartet
qn ..... Quintet
RSA ..... Retro Synthetic Analysis
RT ..... Room temperature
s ..... Singlet
SKA ..... Silyl Ketene Acetal
t ..... Triplet
Taddol ..... 4,5-Bis(diphenylhydroxymethyl)-2,2-dimethyldioxolane
TBAF ..... Tetrabutylammonium fluoride
TBDPS ..... ^{t}Butyl Diphenyl Silyl
TBS ..... ^{t}Butyl Dimethyl Silyl
TBSCl ..... ^{t}Butyl Dimethyl Silyl Chloride
Tf ..... Triflyl
TFA ..... Trifluoroacetic Acid
THF ..... Tetrahydrofuran
TIPSOTf ..... Triisopropylsilyl-trifluoromethanesulfonate

1. Introduction

1.1. β–Amino Acids

An amino acid is a compound that contains both an amine and a carboxylic acid functional group. β-amino acids differ from the more common proteinogenic α-amino acids in that a two carbon chain separates these functional groups as opposed to a one carbon link. In order to distinguish positional isomers of β-substituted amino acids, Seebach has proposed the terms β^2- and β^3-amino acid, where the superscripts indicate the α– or β–substitution with respect to the carboxyl group.[1] Seebach's notation shall be used throughout this report.

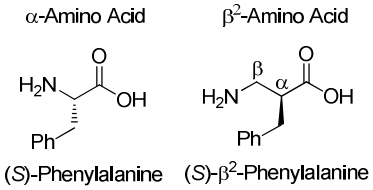

Fig. 1. α- & β-Amino Acids.

There are three general types of β-amino acids:

1) Acyclic – Where substitution takes place at the carbon bearing the carboxyl group (β^2-amino acid) e.g. (*R*)-β^2-homovaline **1**, the carbon bearing the amino portion (β^3-amino acid) e.g. iturnic acid **2**, or at both positions ($\beta^{2,3}$-amino acid) e.g. Amha (**3**) an important precursor to the Adda fragment in cytotoxic microcystins and nodularins.[2-3]

2) Carbocyclic – Where the $\beta^{2,3}$-amino acid substitution is presented in a carbocyclic ring, for example the antifungal antibiotic cispentacin **4**.[4]

3) Heterocyclic – Where the amino group is incorporated in a heterocyclic ring, for example methylphenidate (Ritalin®) **5**, which is used in the treatment of attention deficit hyperactivity disorder (ADHD) and narcolepsy.[5]

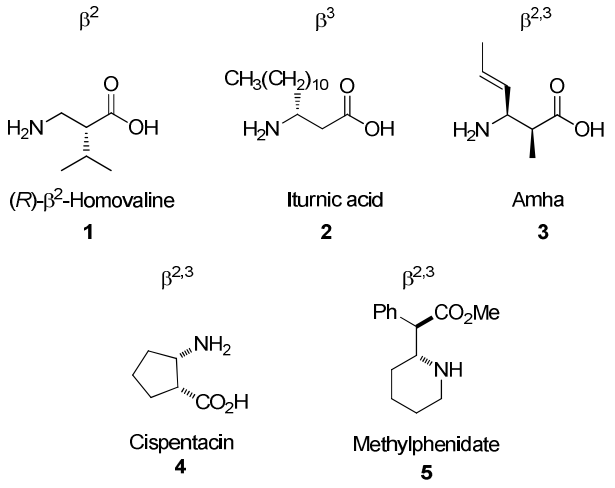

Fig. 2. General Types of β-Amino Acids.

To date there are eight natural occurring β-amino acids that are directly derived from the corresponding proteinogenic α-amino acids, either in free form, or as part of a larger molecule. These are: β-alanine **6**, β-leucine **7**, β-lysine **8**, β-glutamate **9**, β-glutamine **10**, β-arginine **11**, β-phenylalanine **12** and β-tyrosine **13**. Other β-amino acids that are not related to proteinogenic α-amino acids are classified as unusual β-amino acids. There are several classes of unusual β-amino acids, these being aliphatic, aliphatic hydroxyl, aliphatic with oxo groups, amino, alicyclic and heterocyclic.

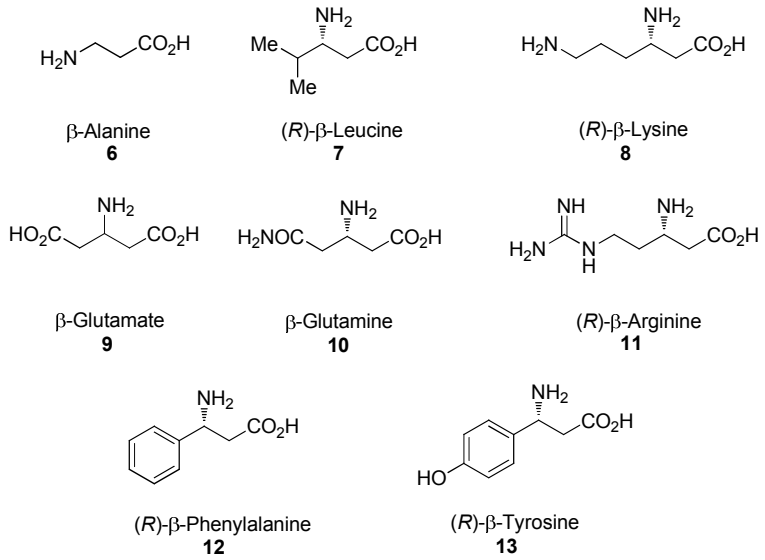

Fig. 3. Natural β-Amino Acids.

In general β-amino acids occur in all five kingdoms of living organisms, which are animals, plants, fungi, bacteria and protista.[6] Contrary to all other β-amino acids, β-alanine and β-amino*iso*butyric acid are present in all living organisms since they are directly involved in primary metabolism. To date it is thought that animals are not able to synthesise any β-amino acids except β-alanine **6** and β-amino*iso*butyric acid **14**.[7]

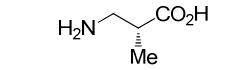

(*R*)-β-Amino*iso*butyric Acid
14

Fig. 4. Naturally Occuring β-Amino Acid.

Contrary to proteinogenic α-amino acids which are constituents of all enzymes controlling the metabolism in living matter and hence an essential prerequisite for life, most β-amino acids occur as constituents of distinct natural products, such as peptides, alkaloids or terpenoids.[8] Bacteria, cyanobacteria, fungi and plants often incorporate β-amino acids into secondary metabolites that serve as tools to secure their survival in competition with other organisms.[9-10] Therefore these compounds are often characterised by potent biological and physiological activities that are often crucially based on their β-amino acid substructures.[11] Moreover, the incorporation of β-amino acids into peptides as opposed to α–amino acids increases their stability against degradation by mammalian peptidases, caused by a lack of enzymes which allow cleavage of peptidic bonds between α-amino acids and β-amino acids.[12] Therefore β-amino acids are an important tool in the development of drugs capable of withstanding hydrolytic degradation for prolonged periods of time.

As a consequence, many natural products with a β-amino acid moiety are potential lead structures for the development of pharmaceutical and agro-chemicals and this still remains an area of extensive research. For instance, the disease lathyrism characterised by crippling of the bones is caused by consumption of seeds derived from plants such as the grass pea (*Lathyrus sativus*) that contain 3*N*-oxalyl-2,3-diamino propanoic acid (L-β-ODAP) **15**.[13] On the other hand, the outstanding cytotoxic effects of the cryptophycins **16** or the nodularins **19** might result in the development of new

anticancer drugs. Taxol® **17** and the derivative taxotere® **18** have already become important anticancer drugs, whereas penicillins such as **20** and related β-lactams have served for decades as prominent antibiotics.[14-19]

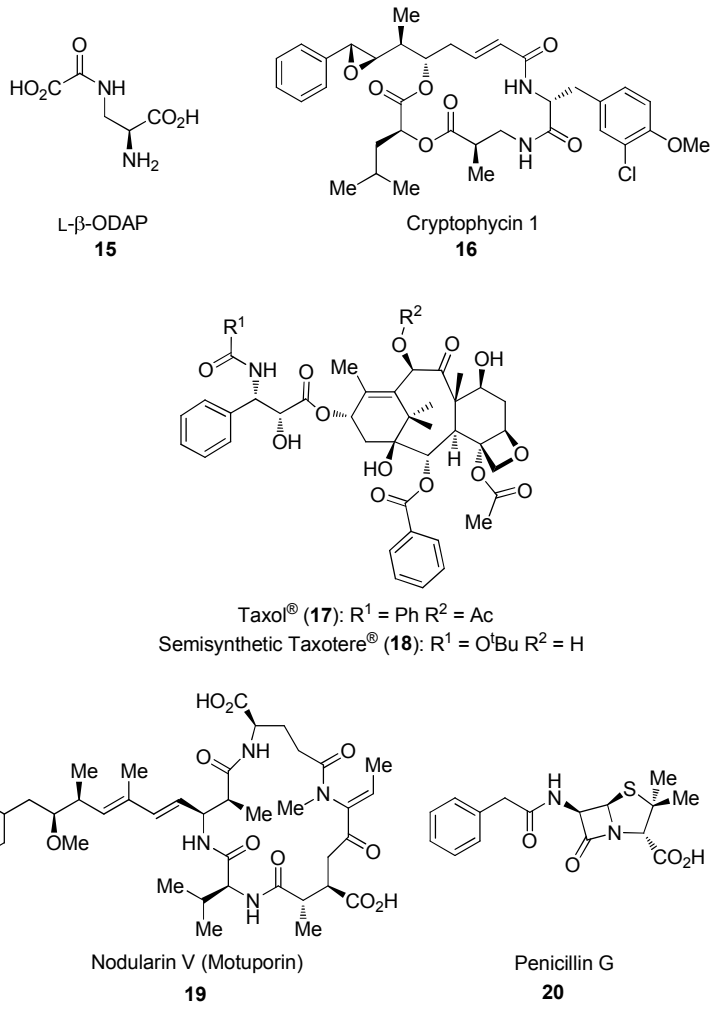

Fig. 5. β-Amino Acid Moiety in Natural Products.

In recent years β-peptide foldamers constructed from constrained carbocyclic β-amino acids like *trans*-2-aminocyclopentanecarboxylic acid (ACPC) **21** and *trans*-3-aminopyrrolidine-4-carboxylic acid (APC) **22** have gained significant interest as they adopt a robust helical conformation in aqueous solution with as few as six residues. This property makes these oligomers attractive scaffolds and antimicrobial activity paralleling that of host-defense peptides have been reported for a 12-helical β-peptide composed of ACPC and APC.[20-21]

ACPC **21** APC **22**

Fig. 6. Carbocyclic β-Amino Acids used in β-Peptide Foldamers.

1.2. Preparation of Enantiopure β-Amino Acids

1.2.1 Homologation of α-Amino Acids

Historically α-amino acids have been shown as excellent starting materials for the preparation of β-amino acids. This is not only due to the fact that there are a plethora of methods available for their synthesis, but also that there is a stereogenic centre present in these compounds that can be transferred to the homologated β-amino acid without significant racemisation.[22] There are two classical methods used for the homologation of α-amino acids to β-amino acids and these are-

1) Arndt-Eistert Homologation

In the late 1920's a method for the homologation of carboxylic acids was developed by Arndt, Eistert and Partale.[6] This procedure includes activation of the parent α-amino acid to either the acid chloride or the mixed anhydride, followed by treatment with diazomethane to give the diazoketone. Subsequent photolysis, thermolysis or treatment with catalytic amounts of silver salts in the presence of protic nucleophiles leads to a Wolff rearrangement resulting in loss of nitrogen and homologation of the starting substrate.[23,24] The original Arndt-Eistert homologation was subsequently adapted by Balenovic in 1947, allowing the formation of β-amino acids.[25] Initially, activation of the carboxylic acid was pursued with thionyl chloride, but later developments allowed milder activation methods utilising more suitable protecting groups for the amino function. α-Amino acids protected as carbamates **23** can be used as starting materials producing β^3 amino acids **24** in good yields (Scheme 1).[26-27]

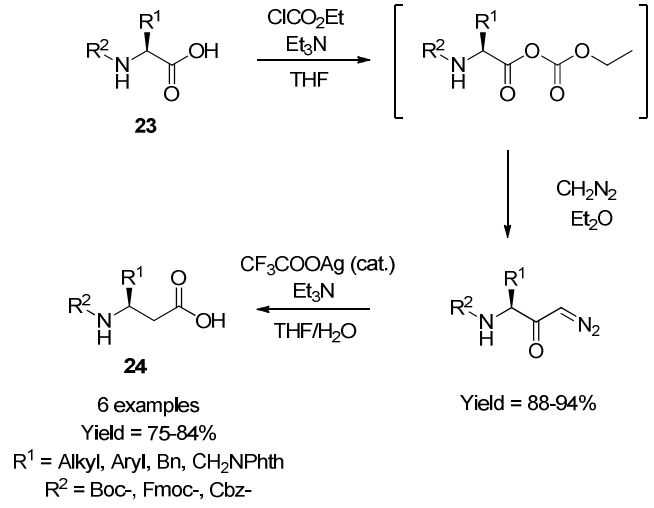

Scheme 1. Arndt-Eistert Homologation of α-Amino Acids.

2) Homologation of Amino Acids Using Cyanohydrins

Although the Wolff rearrangement is the most popular approach for the homologation of α-amino acids, another approach involves the transformation of amino acids **25** to β^2-hydroxy-amino acid derivatives **28**, *via* amino aldehydes **26**, which are converted to cyanohydrins **27** and subsequently hydrolysed. A major disadvantage with this approach are selectivities in cyanide addition are usually poor, resulting in mixtures of diastereoisomers (Scheme 2).[28,29]

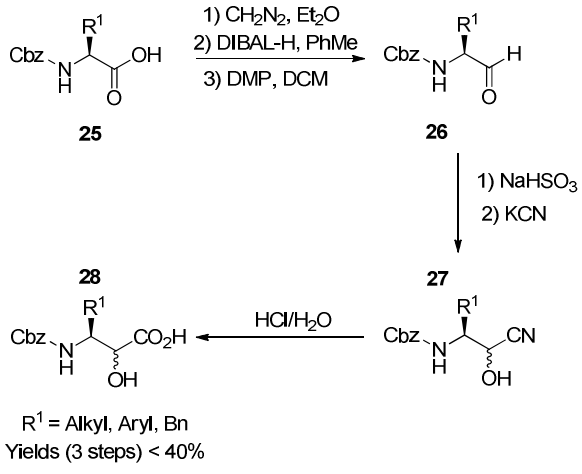

Scheme 2. Homologation of Amino Acids Using Cyanohydrins.

1.2.2. Hydrogenation of β-Amino Acrylates

Noyori was the first to publish an enantioselective route to β^3-amino acids *via* an asymmetric hydrogenation of *N*-acyl-β-(amino)acrylates utilising ruthenium complexes and (*R*)-BINAP, producing e.e.'s of >90%.[30] Since this intial report there have been countless publications based on improving yield and enantioselectivities with ruthenium and rhodium catalysed homogenous hydrogenations. An important breakthrough was presented by Hsiao in the realisation that chiral-ferrocenylphosphine ligand **30** could be used in the hydrogenation of unprotected (*Z*)-enamine esters **29** to yield the corresponding β^3-amino esters **31** with excellent yields and enantioselectivities.[31]

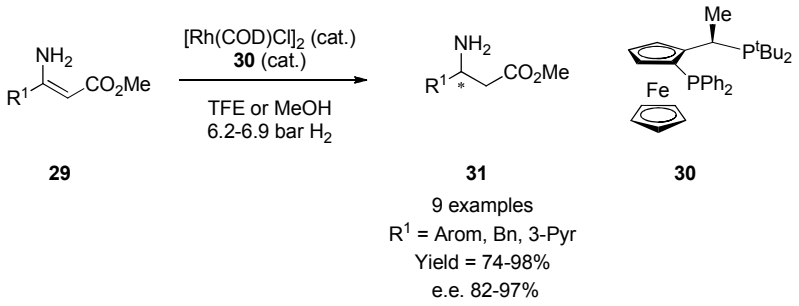

Scheme 3. Hydrogenation of β-Amino Acrylates using Hsiao's Protocol.

Holz has subsequently shown that MalPhos **32** is an effective ligand in the asymmetric hydrogenation of (*E*)- and (*Z*)-β-amino acrylates **31** providing β^2-amino acids **33** with enantioselectivities up to 99% and 90% respectively.[32]

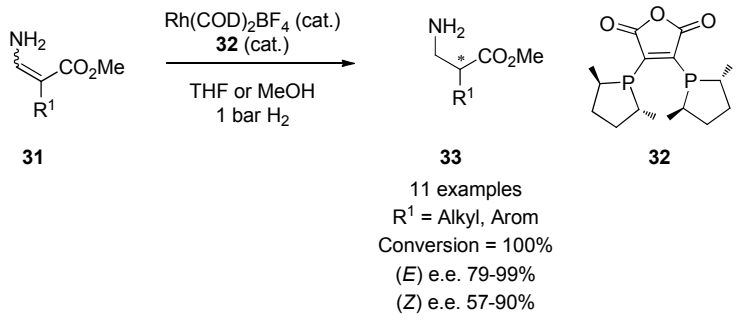

Scheme 4. Hydrogenation of β-amino Acrylates using Holz's Protocol.

Although the synthesis of multisubstituted β-amino acids by ruthenium or rhodium catalysis has yet to be accomplished, Zhang has reported the use of (*S*)-C3-TunaPhos **34** in the ruthenium catalysed synthesis of the $\beta^{2,3}$ carbocyclic amino acid derivative **35** of cispentacin **4**.[33]

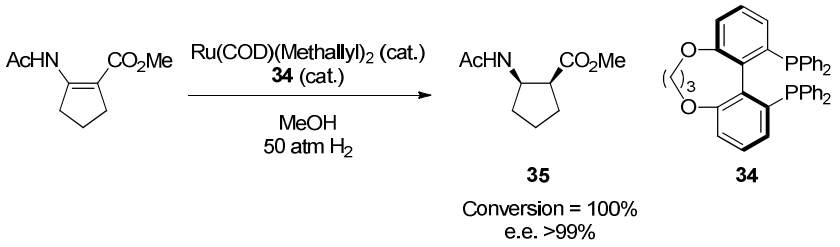

Scheme 5. Hydrogenation of β-Amino Acrylates using Zhang's Protocol.

1.2.3. Conjugate Addition

When applied to the synthesis of β-amino acids the catalytic asymmetric conjugate addition can be achieved by either the addition of carbon based nucleophiles, such as organometallics, cyanide and Michael donors, *or* by the addition of nitrogen nucleophiles such as amines, hydroxylamines and carbamates.[34]

The conjugate addition of carbon nucleophiles to a variety of α,β-unsaturated acceptors is an important *C*-*C* bond forming reaction, and in the context of synthesising β-amino acids, nitroolefins are versatile acceptors. Wendisch has shown the copper catalysed conjugate additions of organozinc species to nitropropenoates **36** utilising phosphoramidite **37** proceeds with excellent regio- and stereo-selectivities.[35] These β^{2}-amino acid precursors **38** can then be subjected to hydrogenation and saponification conditions to yield the required β^{2}-amino acids **39**.

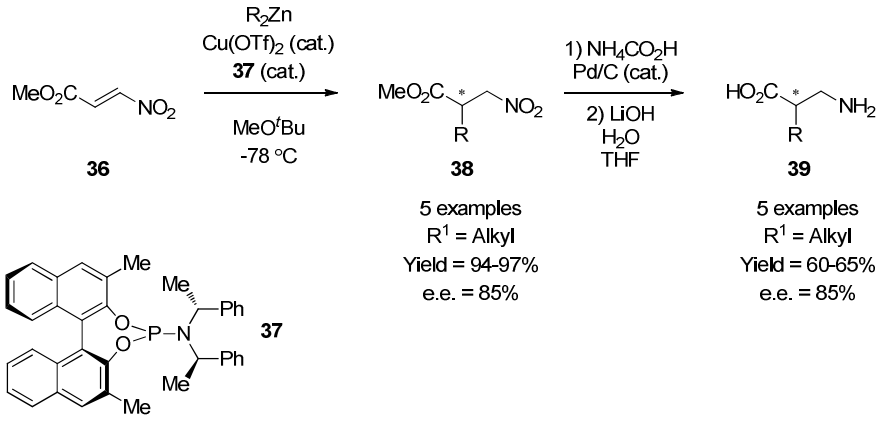

Scheme 6. Wendisch's Route to β²-Aliphatic Amino Acids.

Jacobsen has utilised the aluminium salen catalyst **41** for the conjugate addition of cyanide to α,β-unsaturated imides **40**.[36] The imide of the hydrocyanation adducts **42** are hydrolysed and subsequent Curtius rearrangement of acid **43** yields *N*-Boc protected cyano amides **44**. Subsequent hydrolysis of the nitrile in hydrochloric acid affords the β²-amino acid **45**, with only a small degree of racemisation (Scheme 7).

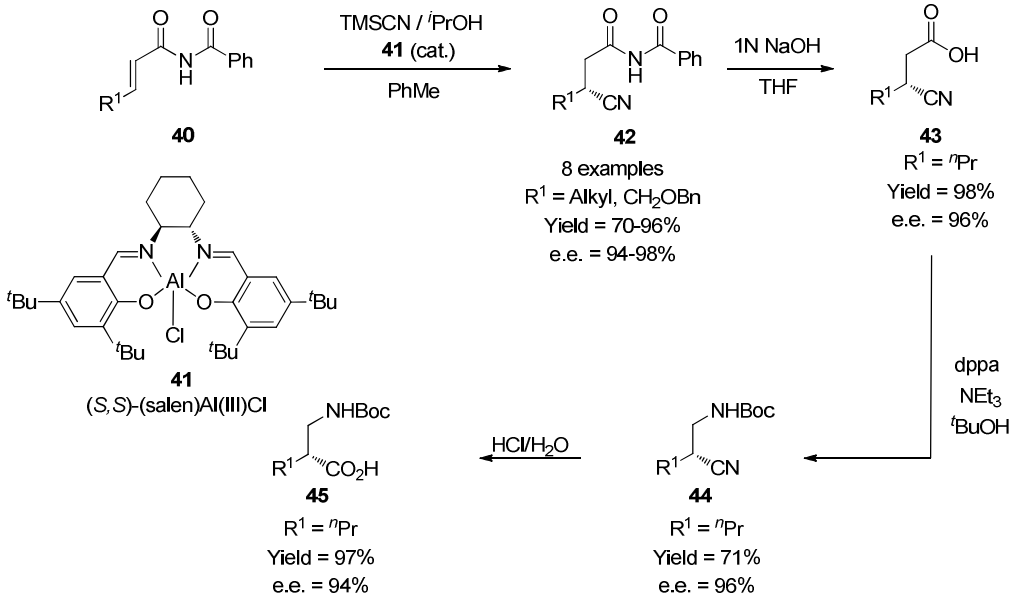

Scheme 7. Jacobsen Route to β²-Aliphatic Amino Acids.

Fillion has recently shown that Meldrum's acid derivatives **46** can be utilised with phosphoramidite **37** in synthesising β³,³-amino precursors **48**, post deprotection of adduct **47** and followed by a Curtius rearrangement.[37]

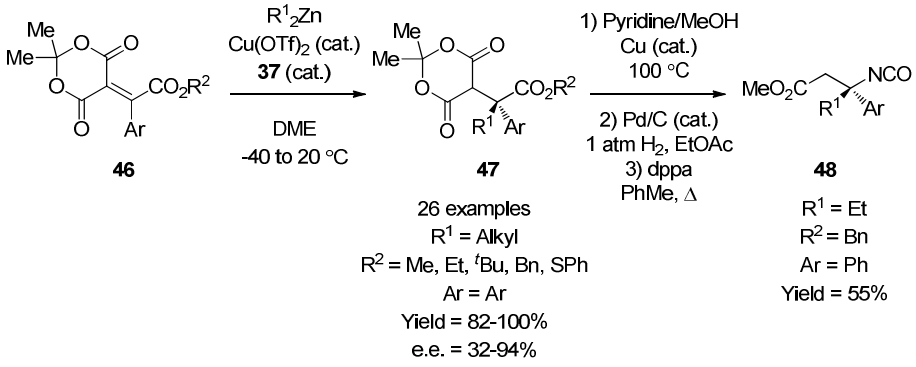

Scheme 8. Fillion's Route to $\beta^{3,3}$-Aliphatic Amino Acids.

Jacobsen has also reported the use of the salen catalyst **41** in the catalytic enantioselective conjugate addition of hydrazoic acid to α,β-unsaturated imides **49**, yielding the corresponding azides **50**.[38] Conversion to the corresponding β-amino acid was performed by a one pot azide hydrogenolysis/*N*-Boc protection sequence followed by regioselective cleavage of the imide group, allowing access to β^3-aliphatic amino acids **51** with excellent yields and enantioselectivities.[39]

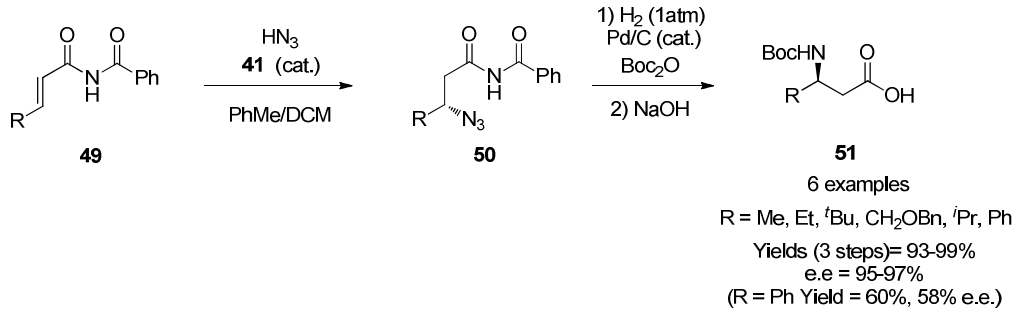

Scheme 9. Jacobsen Route to β^3-Amino Acids.

1.2.4. Catalytic Mannich Reactions

Asymmetric Mannich reactions provide useful direct routes for the synthesis of optically active β-amino acids. Two key features that render the Mannich reaction and its products very attractive, are that the reaction tolerates a large diversity of functionality and in cases where β-amino carbonyl products are formed, these can be

readily transformed into β-amino acids. Catalytic Mannich reactions rely on the utilisation of various Lewis and Brønsted acid catalysts.

Kobayashi has shown that Mannich reactions of imines **52** and silyl ketene acetals **53/54** in the presence of zirconium-based Lewis acid **55,** allows the synthesis of *syn*- **56** and *anti*-$\beta^{2,3}$-disubstituted-amino acids precursors **57**, in excellent yields, diastereoselectivities and enantioselectivities.[40,41] Full deprotection has been shown to yield the *syn*-$\beta^{2,3}$- amino acid **58** as the hydrochloride salt.

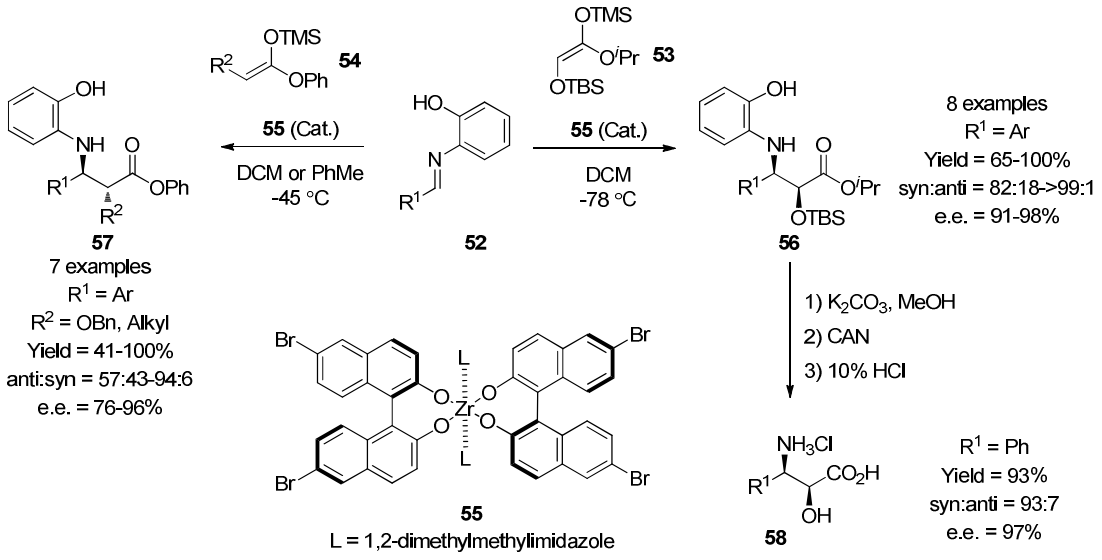

Scheme 10. Kobayashi's Route to syn- and anti-$\beta^{2,3}$-Amino Acids.

Hoveyda has shown the use of silver catalysed asymmetric additions of silyl ketene acetals **59** to alkynyl imines **60** in the presence of a Schiff base **61**, allows the synthesis of β^3-alkynyl amino esters **62**, in good yields and enantioselectivities.[42]

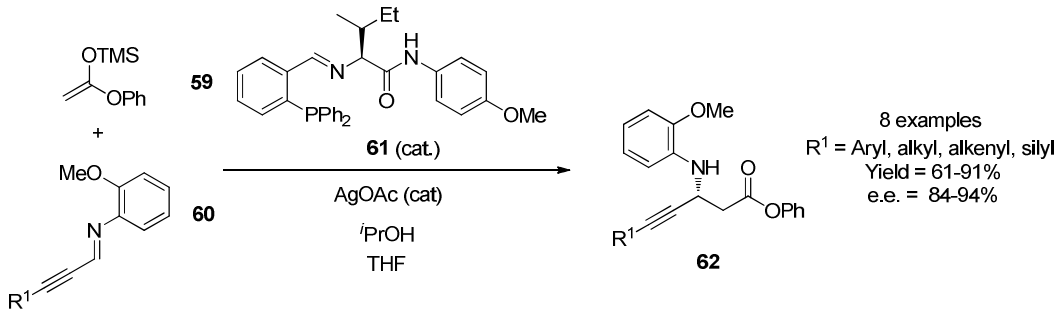

Scheme 11. Hoveyda's Route to β^3-Alkynyl Amino Acids.

The use of chiral Brønsted acids is ubiquitous in organocatalytic Mannich reactions and also allows a direct entry to the β-amino carbonyl moiety.[34] There are two general types of Brønsted acid, these being thiourea or (*L*)-proline derivatives, and stronger Brønsted acids such as binol or phosphoric acid derivatives. The mode of organocatalytic reaction follows a generic protocol, in which the electrophile becomes activated by hydrogen bond formation to the organocatalyst and a transition state ordering occurs prior to nucleophilic attack in a stereocontrolled fashion.[43-44]

Jacobsen has shown that access to β^3-aryl-amino acids **66** is possible *via* an asymmetric Mannich reaction of silyl ketene acetals **64** and imines **63**, catalysed by thiourea derivative **65**.[45]

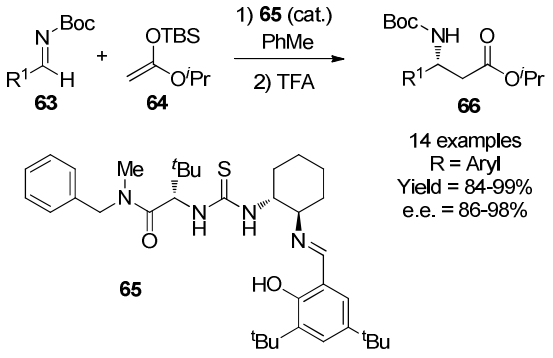

Scheme 12. Jacobsen's Route to β^3-Aryl-Amino Acids.

Barbas and Hayashi have shown that *syn*-$\beta^{2,3}$-aminoaldehydes **69** can be synthesised using the classical organocatalyst (*L*)-proline **68**.[46-47] This organocatalyst reacts with aldehyde **67** to form chiral nucleophilic enamines *in-situ*, which then react with electrophiles, such as aldimines and ketimines in a stereocontrolled manner. Advantages associated with this reaction are that it is atom economical, utilises relatively inexpensive readily available starting materials and preactivation of aldehydes (for example as silyl enol ethers) or preformation of enamines are not required. Higher yields, diastereoselectivities (*syn* selective) and enantioselectivities are often obtained when a three component reaction using aldehyde donors is utilised.

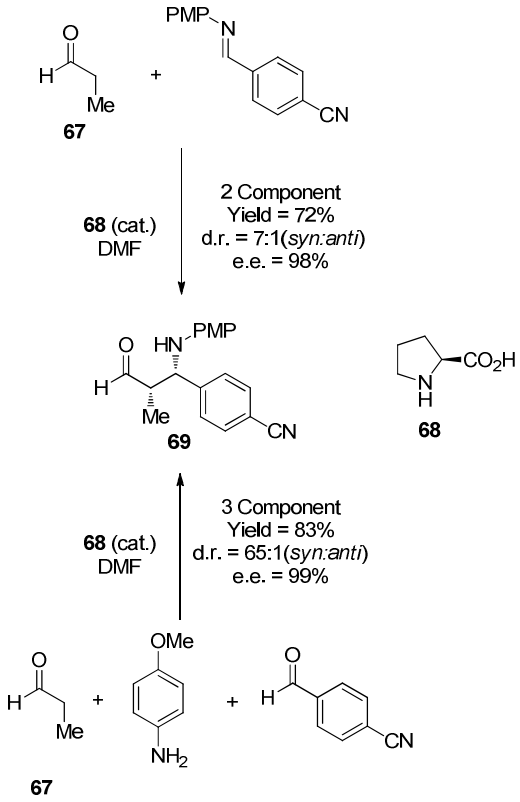

Scheme 13.Barbas & Hayashi Route to syn-$\beta^{2,3}$-Amino Acids.

Barbas has subsequently shown that all carbon quaternary stereocentres can be synthesised utilising the (*L*)-proline catalyst **68** and α,α–disubstituted aldehydes **70**, yielding β-formyl substituted α-amino acid derivatives **71** in excellent yield, diastereoselectivities and enantioselectivities.[48] Synthesis of spiro lactam **72** was accomplished by oxidation of the corresponding precursor **71** followed by a simple acid and base treatment.

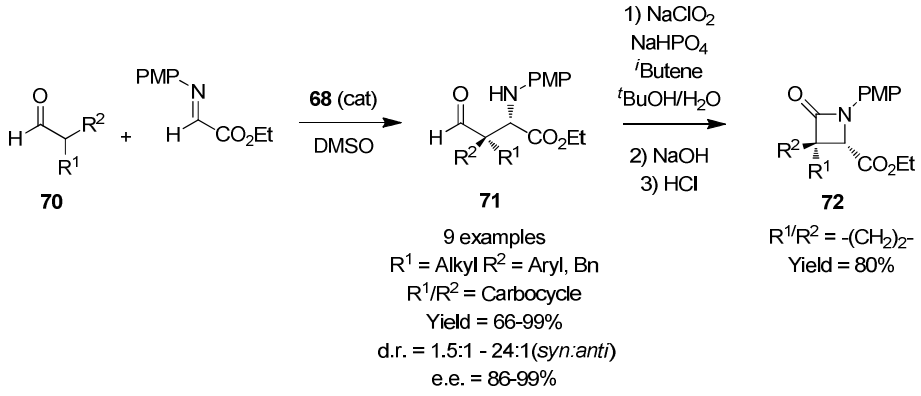

Scheme 14. Barbas's Route to syn-$\beta^{2,2,3}$-Lactam.

The mechanism for the direct asymmetric (*L*)-proline catalysed Mannich reaction has been extensively investigated by Houk.[49] The proposed transition state **73** explains the preferential formation of the *syn*-diastereomer, where (*L*)-proline directs the reaction between the *Si* face of the (*E*)-enamine of aldehyde and the *Si* face of the (*E*)-PMP-imine. The carboxylic acid proton is completely transferred to the imine and it is hypothesised that the interaction between the newly formed iminium and the carboxylate anion is retained even when water is present.

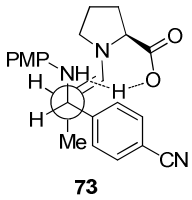

73

Fig. 7. (L)-Proline Catalysed Transition State.

Akiyama has shown that Taddol-derived phosphoric acid **76** can be used to catalyse the addition of silyl ketene acetals **75** to aromatic aldimines **74**, yielding $\beta^{2,2,3}$-amino acids **77** with good yields and excellent enantioselectivities.[50] Unfortunately, this chemistry was limited to the use of symmetric isobutyric derived silyl ketene acetals.

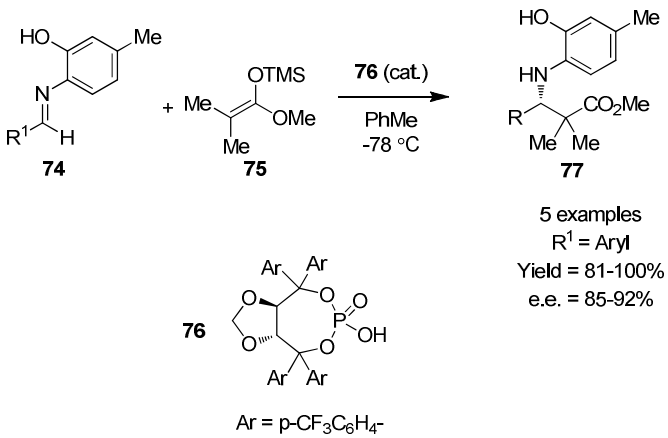

Scheme 15. Akiyama's Route to $\beta^{2,2,3}$Amino Acids

1.2.5. Organocatalytic Conjugate Addition

The synthesis of β-amino acids *via* organocatalytic C-N bond forming conjugate additions are a relatively recent development within the synthetic community and represent a fast and atom economic entry.

MacMillan's use of his second generation imidazolinone catalyst **80** with α,β-unsaturated aldehydes **78**, allows conjugate addition of his purpose designed nitrogen nucleophile **79**, to the *in-situ* formed α,β-unsaturated imminium ion.[51] The β^2-amino aldehyde products **81** were obtained in high yields and enantioselectivities, and were subsequently oxidised to *N*-protected amino acids **82**.

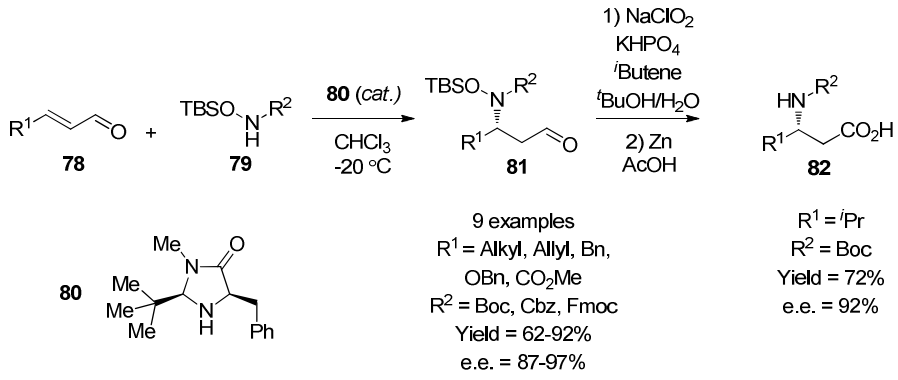

Scheme 16. Macmillan's Route to β^3-Amino Acids.

Córdova has subsequently followed a similar approach to synthesising analogous compounds to MacMillan, utilising a prolinol catalyst, producing the corresponding β^3-amino acids in lower yields but similar enantioselectivities.[52] These current results demonstrate that further optimization of the organocatalytic conjugate addition of nitrogen nucleophiles to α,β-unsaturated carbonyl compounds is required.

1.2.6. Enolate Addition to *N*-^{t}Butylsulfinyl Imines

Davis has shown the synthesis of $\beta^{3,3}$-amino acids **84** are possible by the addition of acetate ester enolates to a limited set of *N*-*p*-toluenesulfinyl imines **83** with good yields and excellent enantioselectivities.[53-55]

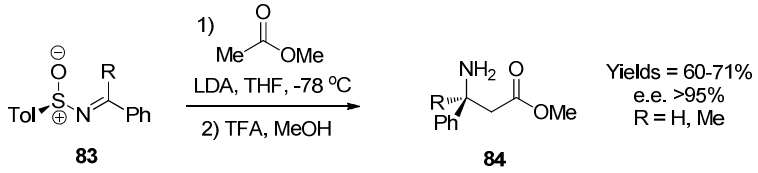

Scheme 17. Davis's Route to $\beta^{3,3}$-Amino Acids.

Prompted by this methodology, Ellman has extended this protocol to the more suitable *N*-^{t}butylsulfinyl imines **85**.[56-57] The additions of titanium enolates to various substituted-*N*-^{t}butanesulfinyl aldimines and ketimines were shown to proceed in good to excellent yields allowing access to *N*-^{t}butanesulfinyl-protected β^3, $\beta^{2,3}$, $\beta^{3,3}$, $\beta^{2,2,3}$, $\beta^{2,3,3}$ and $\beta^{2,2,3,3}$-amino esters **86** with diastereoselectivities of *anti:syn* between 9:1 and 99:1 with excellent enantioselectivities.

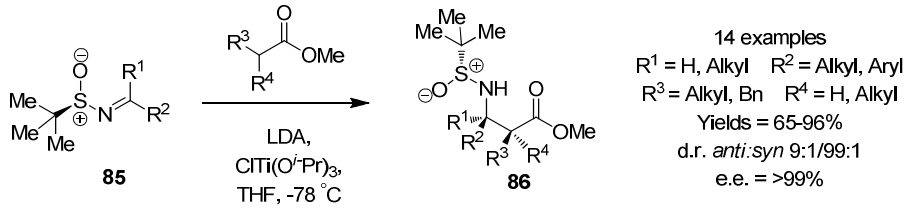

Scheme 18. Enolate Additions to N-^{t}Butylsulfinyl Imines.

The observed diastereoselectivity in the syntheses of these β-amino esters, regardless of substitution pattern, can be explained through a six-membered transition state **87**, where enolate addition occurs from the least hindered face of the imine.

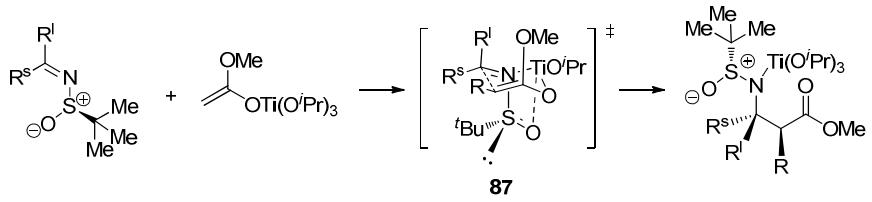

Scheme 19. Reaction Transition State.

In addition to the *N*-^{t}butylsulfinyl protecting group directing the reaction, it also serves as a versatile protecting group that parallels the reactivity of the Boc group. It is stable to basic conditions and is easily cleaved with one equivalent of HCl.

1.3. Pericylic reactions

Pericyclic reactions are a distinct class of reactions which possess cyclic transition structures, and in which all bond making and breaking occurs with a concerted movement of electrons, lacking formation of intermediates. There are four distinct subclasses of pericyclic reactions and these are:

Cycloadditions-

Cycloadditions are ring forming reactions between two conjugated π-systems and are classified by the net formation or loss (in the case of a retro-cycloaddition) of two σ-bonds. Diels–Alder reactions are ubiquitous in organic chemistry and the 6 π electron dimerization of cyclopentadiene *via* a [4+2]-cycloaddition is a common example, however the inherent reversibility is demonstrated by heating the dimer to afford the retro-cycloaddition products.

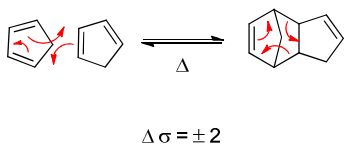

Scheme 20. Diels-Alder Cycloaddition Reaction.

Electrocyclic Reactions-

Electrocyclic reactions are invariably unimolecular ring forming reactions, derived from an open chain conjugated π-system. Electrocyclisations are classified by the net formation of a new σ-bond and the loss of 2π-orbitals or *vice-versa* in the case of an electrocyclic ring opening.

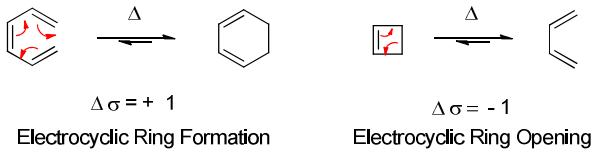

Scheme 21. Electrocyclic Ring Formation & Ring Opening.

Group Transfer Reactions-

Group transfer reactions are bimolecular reactions between an allylic group (ene) and a π-bond (enophile), and are classified by the formation of a new σ-bond with the migration of a hydrogen atom.

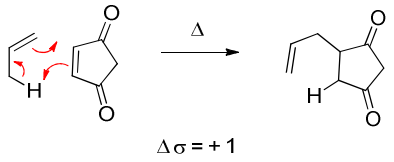

Scheme 22. Ene Reaction.

Sigmatropic Reactions-

Sigmatropic reactions are unimolecular reactions which involve the formation and simultaneous loss of a σ-bond, exemplified by the [3,3]-Cope rearrangement, where the [x,n] nomenclature refers to the number of carbon atoms on each fragment that the σ-bond migrates.

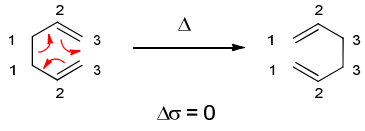

Scheme 23. Cope [3,3]-Rearrangement.

1.4. The Claisen Rearrangement

The Claisen [3,3] rearrangement was the first example of a sigmatropic rearrangement and was published in 1912 by Ludwig Claisen.[58] Historically the Claisen rearrangement is the thermal rearrangement of aliphatic **88** and aromatic allyl vinyl ethers **90** which occur through a suprafacial pericyclic process *via* a chair like transition state, to produce γ,δ-unsaturated aldehydes **89** and substituted phenols **91** (post rearomatisation) respectively.[59]

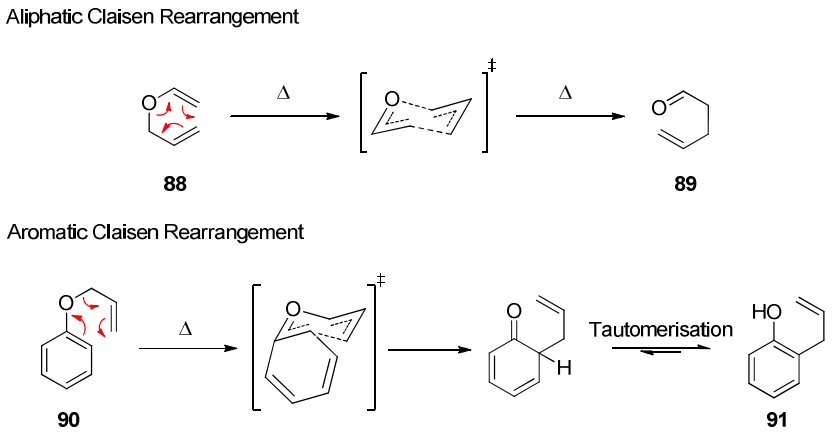

Scheme 24. Historical Claisen Rearrangements.

Since its introduction to the synthetic community the Claisen rearrangement has been utilised within the synthesis of a magnitude of carbon skeletons, for instance in the total synthesis of (-)-furodysinin, where a tandem Claisen rearrangement and an intramolecular ene reaction affords the bicyclic alcohol **92** in excellent yield and enantioselectivity.[60]

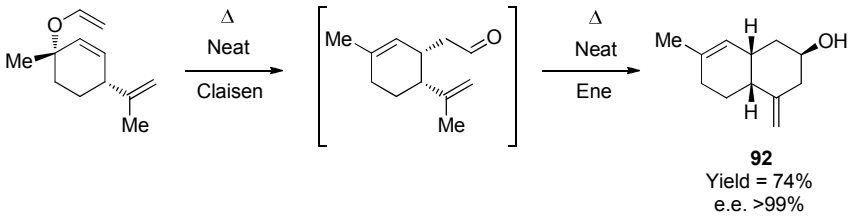

Scheme 25. Utilisation of Claisen Rearrangement in Natural Product Synthesis.

1.5. The Ireland–Claisen Rearrangement

The Ireland–Claisen [3,3]-sigmatropic rearrangement is the Ireland variant of the Claisen rearrangement and was first introduced to the synthetic community in 1972.[61] The reaction proceeds *via* the low temperature deprotonation of an allylic ester **93** by treatment with a lithium dialkylamide base in the presence of a silylating agent. The silyl ketene acetal **94** formed *in-situ* undergoes the [3,3]-sigmatropic rearrangement *via* a chair transition state **95** to generate the γ,δ-unsaturated carboxylic acid **96** in excellent yield, after acidic workup. Although the rearrangement was presumed to be diastereoselective, the diastereoselectivity was not reported in Ireland's seminal paper.

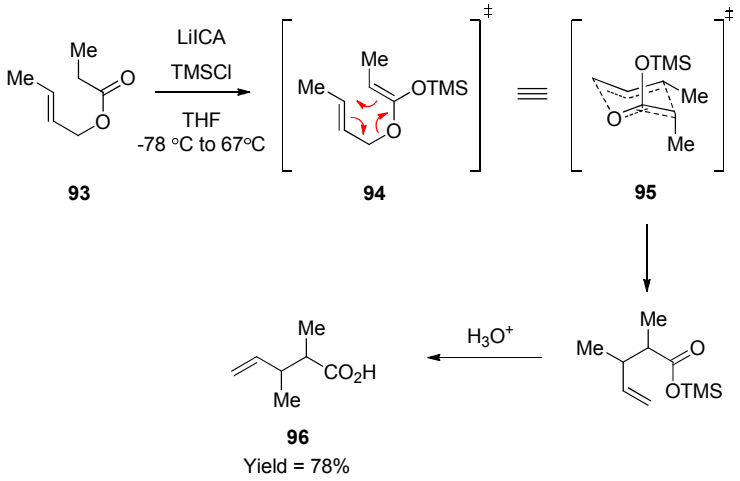

Scheme 26. The Ireland–Claisen Rearrangement. Relative Stereochemistry not Initally Reported.

Although Ireland reported the first successful rearrangement of allylic ester reactants, Wang reported the very first ester enolate Claisen rearrangement in 1937.[62] This protocol produced pent-4-enoic acid **98** in low yield, upon attempted acetoacetic ester **97** condensation using sodium metal.

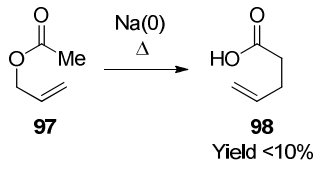

Scheme 27. First Ester Enolate Rearrangement.

There were subsequent scattered reports of ester enolate Claisen rearrangements that employed sodium metal, sodium hydride, mesityl-magnesium bromide and diethylamine magnesium bromide up to the point of Ireland's first publication, however these reactions all suffered low yields and high reaction temperatures.[63] Ireland's major contribution to this chemistry was the discovery that silylation of the ester enolate suppressed any side reactions, such as decomposition *via* the ketene pathway and Claisen type condensations.

Since Ireland's seminal work the Ireland-Claisen rearrangement has been incorporated into a wide variety of target-orientated syntheses and Ireland first exemplified his own chemistry within the synthesis of dihydrojasmone **99**.[61]

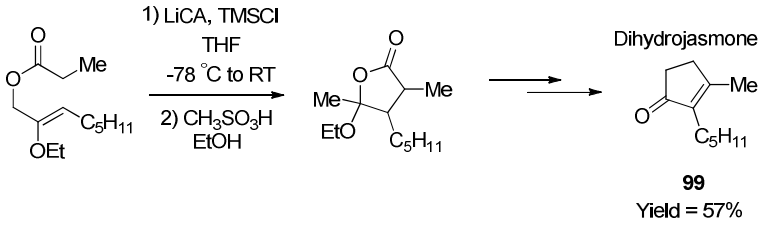

Scheme 28. Ireland–Claisen Rearrangement in the Synthesis of Dihydrojasmone.

Other examples of the inclusion of the Ireland-Claisen rearrangement have been seen within Angle's synthesis of the Pharoah' ant food trail pheromone (+)-monomorine I **100**, and within Zakarian's synthesis of the E-ring **101** of a spirolide C **102**, a marine toxin.[64,65]

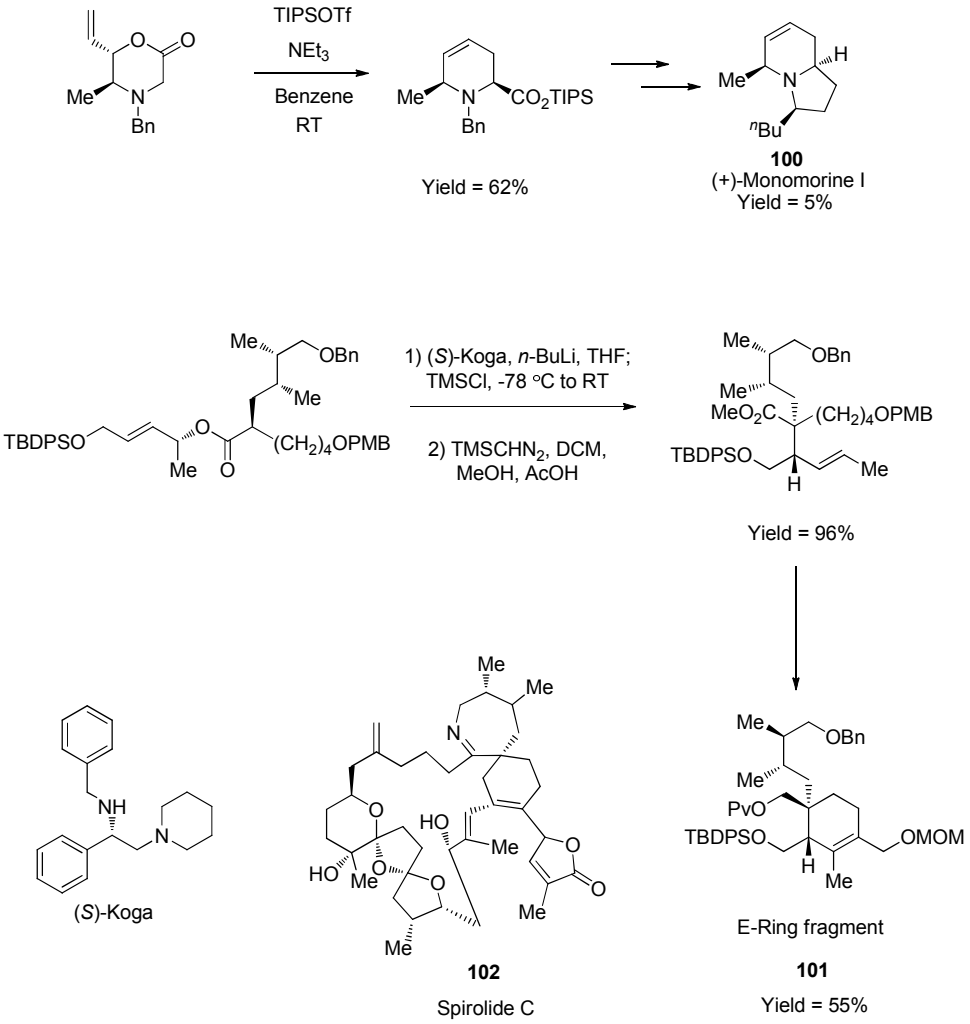

Scheme 29. Ireland-Claisen Rearrangement in Target Orientated Synthesis.

1.5.1. Stereochemical Aspects of the Ireland Claisen Rearrangement

An attractive feature of the Ireland-Claisen rearrangement lies in the ability to reliably transfer stereochemistry from appropriately substituted allyl silyl ketene acetals to either of the newly formed sp^3 stereocenters and the alkene, leading to the formation of *syn* or *anti* pentenoic acids. The stereochemical outcome of the reaction is determined by two features: (1) the geometry of the silyl ketene acetal and the allylic alkene, and (2) whether the rearrangement proceeds *via* a chair-like or boat like transition state.

Enolate and Silyl Ketene Acetal Geometry-

In 1975 Ireland reported ester enolates of propionates and related esters **103** could be stereoselectively generated to give either the (*E*)- **104** or the (*Z*)-silyl ketene acetal **105**, once trapped with TBSCl. When THF was used as the solvent, the (*E*)-silyl ketene acetal **104** predominates and selectivities were high, with the exception of the phenyl acetates, however when 23% HMPA/THF was used, (*Z*)-silyl ketene acetal **105** predominates.[66]

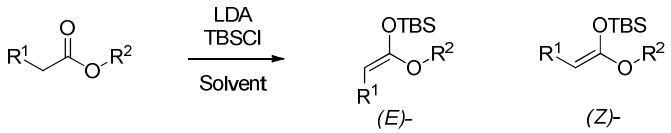

103 *(E)-* **104** *(Z)-* **105**

Entry	R^1	R^2	(*E*)-**104**:(*Z*)-**105** THF	(*E*)-**104**:(*Z*)-**105** 23 vol% HMPA,THF
1	Et	Me	91:9	16:84
2	^{t}Bu	Me	97:3	9:91
3	Et	^{t}Bu	95:5	23:77
4	Ph	Me	29:71	5:95

Table 1. Silyl Ketene Acetal Geometries

Acyclic Allyl Silyl Ketene Acetals-

Ireland demonstrated that relative diastereocontrol could be imparted into the synthesis of *anti*-2,3-dimethyl pentenoic acid **109** by rearrangement of the (*E*)-silyl ketene acetal **107** of (*E*)-crotyl propionate **106** or with the (*Z*)-silyl ketene acetal **111** of the (*Z*)-crotyl propionate **113** at comparable levels of diastereoselectivity.[61, 67-69] The analogous results for the *syn*-pentenoic acid **110** could be obtained using the (*Z*)-silyl ketene acetal **108** of (*E*)-crotyl propionate **106**, or with the (*E*)-silyl ketene acetal **112** with (*Z*)-crotyl propionate **113**, with diastereoselectivities varying from 5:1 to 8:1.

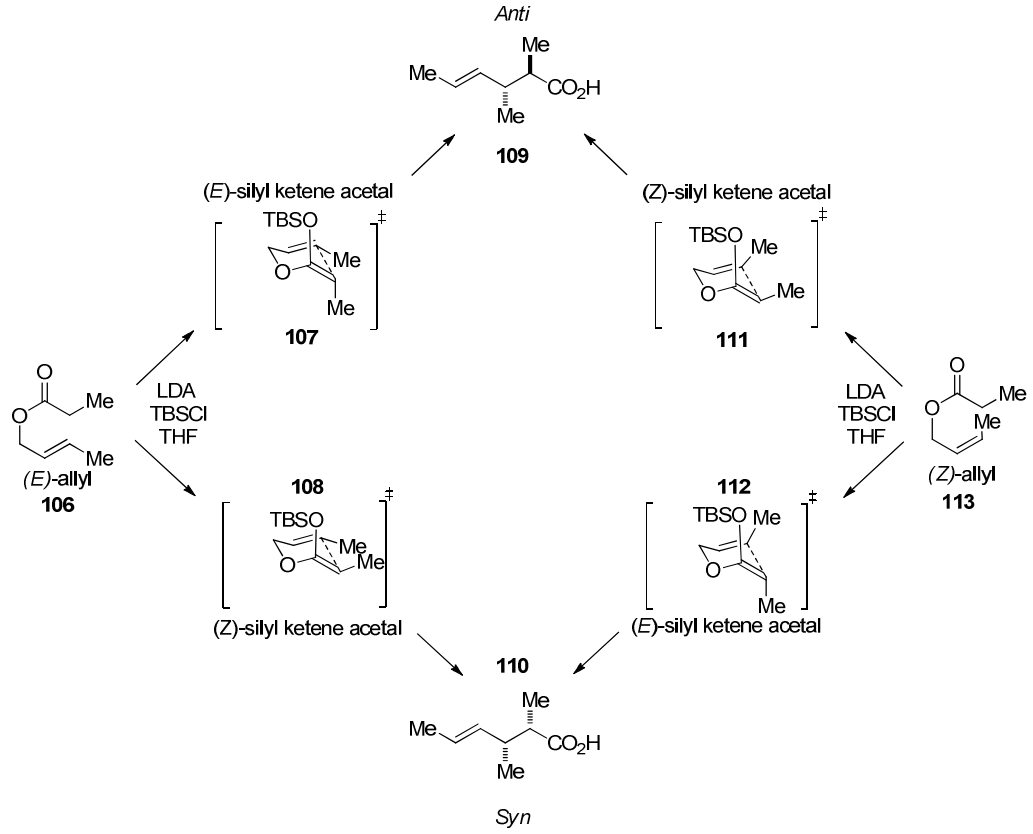

Scheme 30. Acyclic Allyl Silyl Ketene Acetals.

The stereochemical outcome of these rearrangements are consistent with preferential rearrangement *via* a chair like transition state, and computational analysis has confirmed that chair like transition states are favoured over the boat by 2-3 kcal/mol.[70]

Cyclic Allyl Silyl Ketene Acetals-

Ireland and others have shown that the rearrangement of cyclic substrates can preferentially rearrange *via* chair or boat transition states, however this is highly dependant on ring size, ring constitution and ring substituent stereochemistry.[71-72] Bartlett has also shown that the treatment of cyclohexenyl propionates under conditions for generation of (*E*)- or (*Z*)-silyl ketene acetals results in the formation of the same diastereoisomer **115** (Scheme 31).[73-74] It was subsequently concluded that the (*E*)-silyl ketene acetal **114** rearranges preferentially *via* a chair transition state, whereas the (*Z*)-silyl ketene acetal **116** rearranges *via* a boat transition state, a conclusion that was later supported by computational analysis.[70]

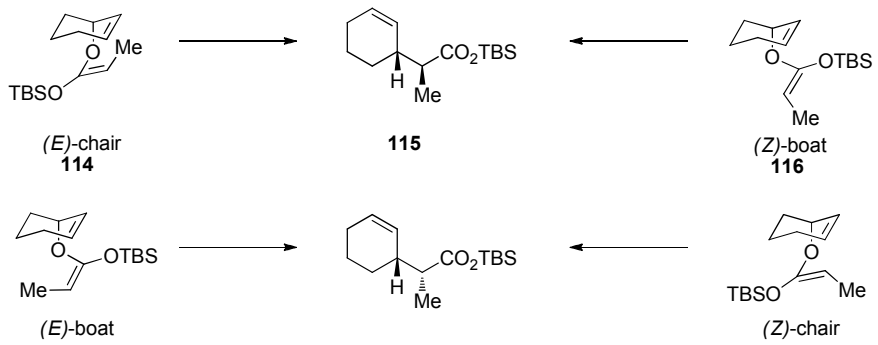

Scheme 31. Cyclic Allyl Silyl Ketene Acetals.

However, in the case of dihydropyran- and dihydrofuran-derived allylic esters the boat transition state is favoured, irrespective of the silyl ketene acetal geometry. Ireland has subsequently provided a pertinent explanation for this observation and this is based on the effect of the pyran/furan oxygen, which increases the level of C-O bond cleavage leading to a transition state that has more product like geometry.[71-72] This shift in the transition state relative to carbocyclic systems, leads to a more polarized transition state structure, which is better stabilised by the overlap of the two allyl moieties, hence rearrangement *via* a boat transition state is favoured (Scheme 32), however this postulation has yet to be computationally supported.

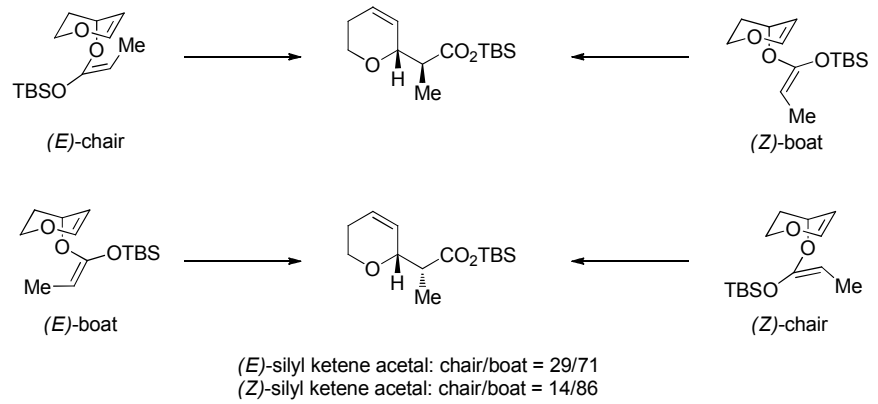

Scheme 32. Geometries of Dihydropyran Allylic Silyl Ketene Acetals.

Alkene Stereochemistry-

The rearrangement of allylic esters derived from primary alcohols affords terminal alkenes, however if the allylic ester is derived from secondary or tertiary alcohols, then the formation of geometrical alkene isomers may be an issue with the rearrangement. As acyclic systems possess a strong preference for chair-like transition states, the stereochemistry of the product alkene is highly predictable in the case of secondary carbinol derived esters. This is because the substituent is placed in a *pseudo*-equatorial position. This is exemplified in the synthesis of the butterfly pheromone **118**, in which the (*E*)-alkene **117** is selectively formed during the rearrangement.[75]

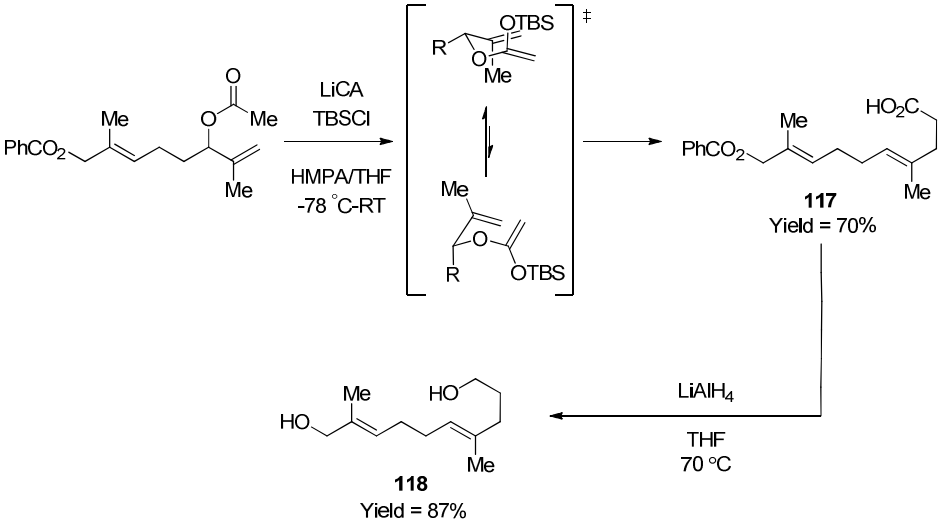

Scheme 33. Predictability of Alkene Geometry in Ireland-Claisen Rearrangement.

Allylic Esters Possessing One Stereocentre: Absolute Control-

Absolute stereocontrol in the Ireland-Claisen rearrangement can be accomplished through incorporating an enantiopure secondary carbinol derived allylic ester, which will allow transfer of chirality to the newly formed stereocenter(s) at the α– and/or β–postion of the pentenoic acid product. Ireland first demonstrated this by use of a bulky TBS crotyl propionate **119**.[76]

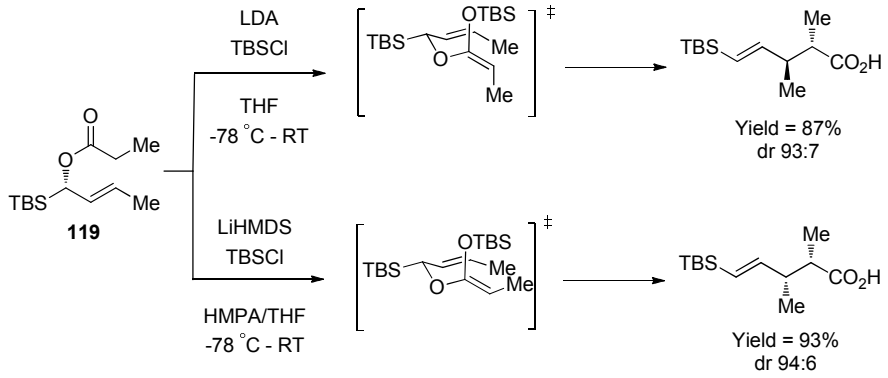

Scheme 34. Absolute Control in the Ireland-Claisen Rearrangement.

1.6. Other Variants of the Claisen Rearrangement

There are many other variations of the Claisen rearrangement, all of which have sub-classes of their own present in the literature. The most popular examples are:

Meerwein–Eschenmoser-Claisen Rearrangement-

This rearrangement involves the conversion of allylic,[77-79] benzylic, propargylic and allenyl carbinol systems to a ketene *N,O*-acetal, by treatment with dimethylacetamide dimethyl acetal under refluxing conditions, followed by a rapid [3,3]-sigmatropic rearrangement forming γ,δ-unsaturated amides (Scheme 35).[77-80]

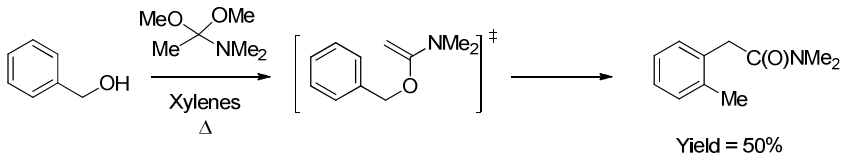

Scheme 35. Meerwein–Eschenmoser–Claisen Rearrangement.

Compared to the Ireland–Claisen, the Meerwein-Eschenmoser version is often found to proceed with higher yields and the neutral conditions required allows the use of sensitive substrates, provided they are not thermally labile.

The Johnson–Claisen Rearrangement-

This rearrangement proceeds *via* condensation of an *ortho*-ester and an allylic or propargylic alcohol, producing a mixed *ortho*-ester, which forms a ketene acetal by elimination of a low boiling alcohol.[81-82] The ketene acetal intermediate then rearranges *via* a [3,3]-sigmatropic process to produce γ,δ-unsaturated esters (Scheme 36).

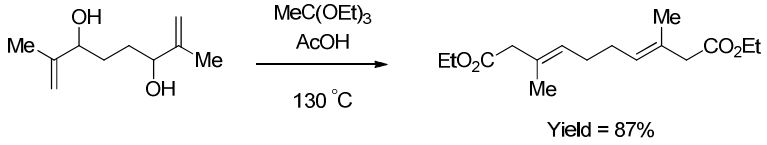

Scheme 36. The Johnson–Claisen Rearrangement.

The Overman Rearrangement-

This rearrangement involves the thermal or mercuric or palladium catalysed rearrangement of allylic trichloroacetimidates to afford the corresponding trichloroacetamides *via* a [3,3]-sigmatropic rearrangement.[83-84] The allylic trichloroacetimidates are easily prepared from reacting allylic alcohols with trichloroacetonitrile in the presence of catalytic amounts of base. Good levels of enantioselectivity have been accomplished through utilisation of chiral palladium sources (Scheme 37).

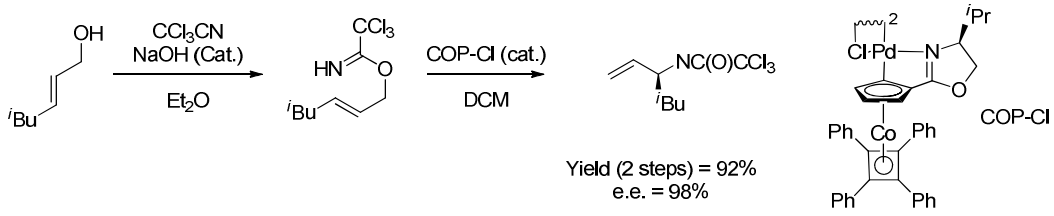

Scheme 37. The Overman Rearrangment.

The Carroll Rearrangement-

This involves the thermal or anionic [3,3]-sigmatropic rearrangement of β–keto-allylic esters to β-keto acids, which upon decarboxylation provides the corresponding γ,δ-unsaturated ketones. The overall transformation is equivalent to a Claisen rearrangement, but at the ketone oxidation state (Scheme 38).[67, 85]

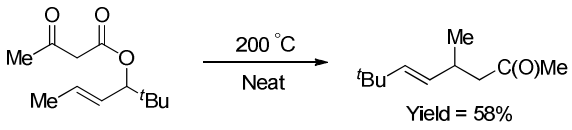

Scheme 38. The Carroll Rearrangement.

Craig has also reported a variant of the Carroll rearrangement, in which α-tosyl silyl ketene acetals formed from allylic tosylacetates or malonates, by bis(trimethylsilyl) acetamide (BSA) and catalytic potassium acetate undergo a [3,3]-sigmatropic rearrangemement.[86-87] Subsequent acetate-induced desilylation-decarboxylation provides homoallylic sulfones or α-tosyl-γ,δ-unsaturated esters (Scheme 39).

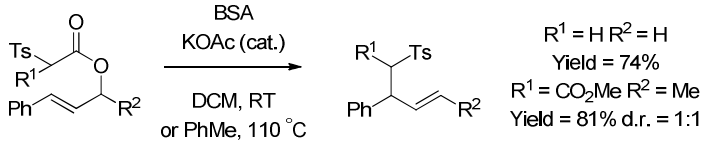

Scheme 39. The Craig Variant of the Carroll Rearrangement.

Aza–Claisen Rearrangement-

This sees the replacement of the oxygen atom in a simple Claisen rearrangement by a nitrogen atom. The rearrangement is a thermal process and incorporates the use of aliphatic and aromatic substrates, however product distributions may arise involving a subsequent Cope rearrangement on the aza–Claisen product (Scheme 40).[88]

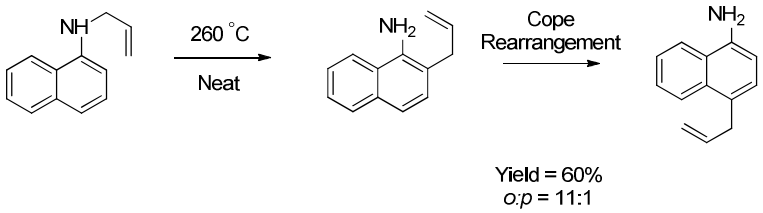

Scheme 40. Aza-Claisen Rearrangement.

A disadvantage of the aza-Claisen rearrangement is the high reaction temperatures that are required. However, introduction of zwitterionic Aza-Claisen rearrangements allows the reduction of these reaction temperatures to a more amenable range, through charge-accelerated ammonium or amide enolates (Scheme 41).[89-90]

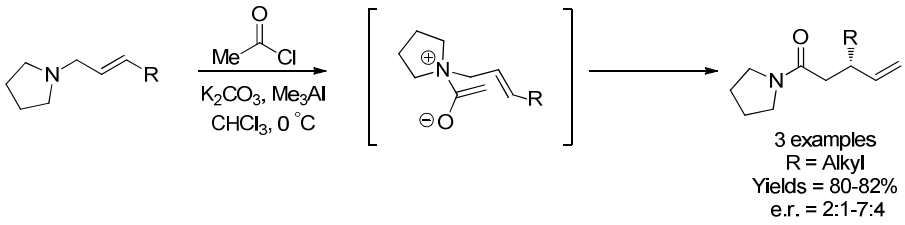

Scheme 41. The Zwitterionic Aza-Claisen Rearrangment

Thio–Claisen Rearrangement-

This sees the replacement of the oxygen atom in a simple Claisen rearrangement by a sulfur atom. The rearrangement is a thermal process and incorporates the use of aliphatic and aromatic substrates, but historically has been plagued by low yields due to product distributions and product instability. Considering the rearrangement of allyl phenyl sulfide, product distributions are seen to arise from the desired [3,3]-sigmatropic rearrangement, followed by prototropy and subsequent cyclization in 5-exo-trig 6-endo-trig fashion to yield 5 and 6 membered heterocycles (Scheme 42).[91]

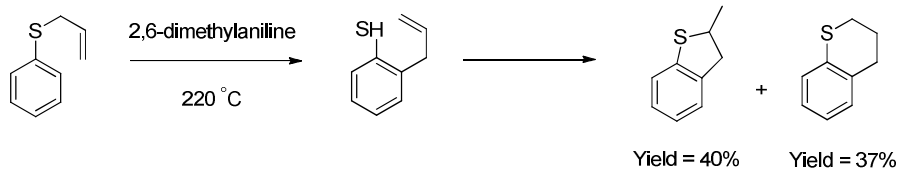

Scheme 42. The Thio–Claisen Rearrangement.

Bellus–Claisen Rearrangement-

The Bellus–Claisen rearrangement sees the reaction of allylic ethers, amines and thioethers with ketenes, which form a zwitterionic intermediate that subsequently undergoes a [3,3]-sigmatropic rearrangement, allowing the synthesis of γ,δ-unsaturated esters, amides and thioesters, after zinc dechlorination (Scheme 43).[92-93]

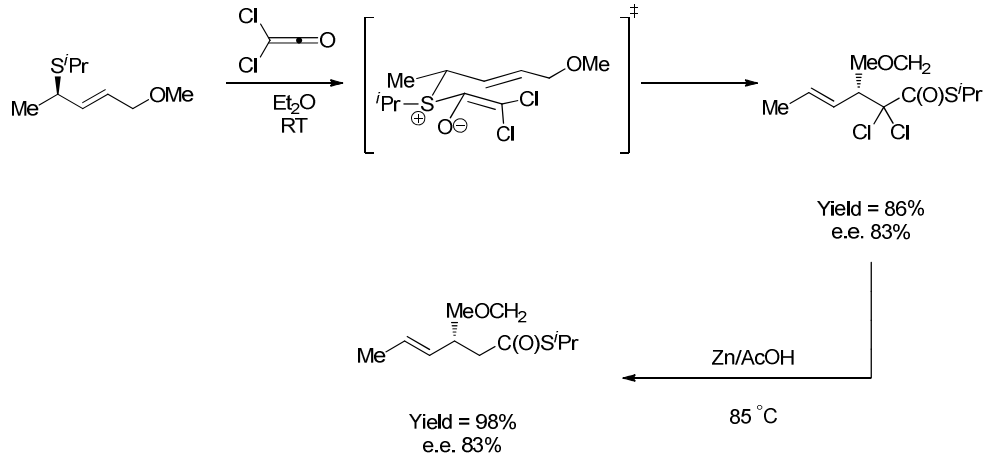

Scheme 43. The Bellus-Claisen Rearrangement.

Enamido–Claisen Rearrangement-

Recently Clive has published an enamido Claisen rearrangement in the synthesis of the marine alkaloid halichlorine **122**, where the distal terminus of the allylic double bond carries a protected Cbz-nitrogen fragment.[94] The rearrangement proceeds in one pot from the secondary cyclic alcohol **120** and butyl vinyl ether under mercuric catalysis to generate the β-amino-γ,δ-unsaturated aldehyde **121**.

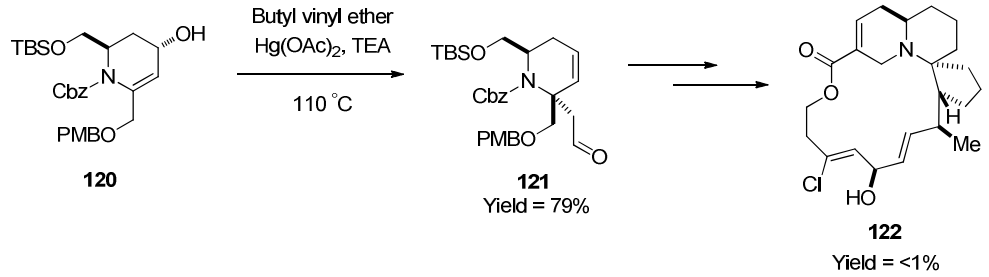

Scheme 44. The Enamido-Claisen Rearrangement.

1.7. Enamides

Enamides are tempered enamines which display significant chemical stability and nucleophilic reactivity, and are controlled by the electron withdrawing functionality upon the nitrogen centre. These molecules often react akin to simple olefins and allow *N*-functionality to be incorporated into complex systems. There are several classes of enamide **123** and an increasing level of interest in using these compounds has developed over the past decade, possibly due to the plethora of syntheses available offering substrate versatility and *E/Z* control.[95]

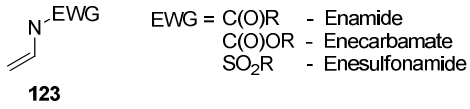

Fig. 8. Classes of Enamide.

There are a plethora of reactions involving the use of enamides within the literature, however some examples of each reaction type include:

Enamides as Nucleophiles-

As enamides can be viewed as tempered enamines, their nucleophilic properties are no surprise. The first enantioselective use of enamides as nucleophiles with aldimines using copper catalysis was reported by Kobayashi.[96] This use of enamides allows the synthesis of interesting α-amino acid precursor building blocks in excellent yield and enantioselectivities (Scheme 45).

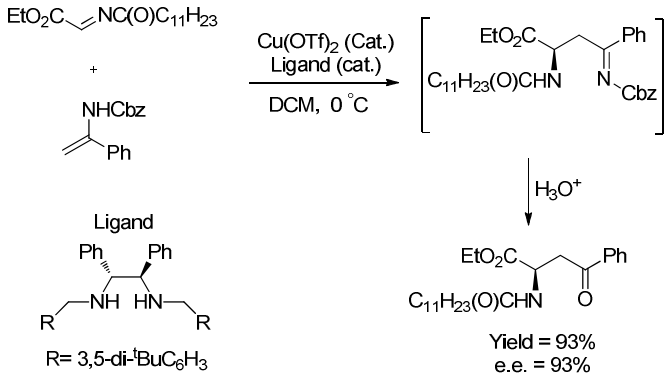

Scheme 45. Enamides Acting as Nucleophiles.

Gong has reported the H_8-BINOL derived phosphoric acid **124** catalysed alkylation of enamides with indolyl alcohols, allowing synthesis of β-aryl 3-(3-indolyl)propanones in excellent yields and enantioselectivities (Scheme 46).[97]

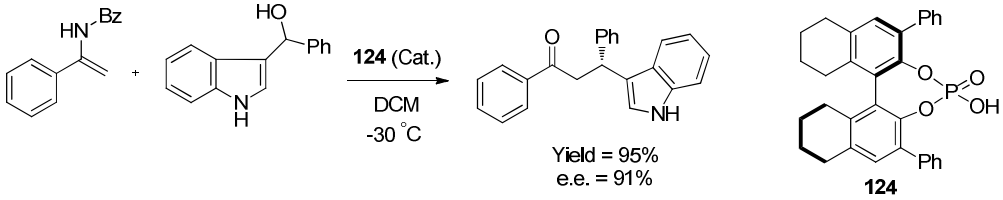

Scheme 46. Gong's Use of Enamides as Nucleophiles.

Enamides as Electrophiles-

The Tareda and Zhou groups have independently reported that chiral Brønsted acids **125** can promote the conversion of enamides to chiral iminium ion electrophiles, which can subsequently undergo Friedel-Crafts reactions (Scheme 47).[98,99]

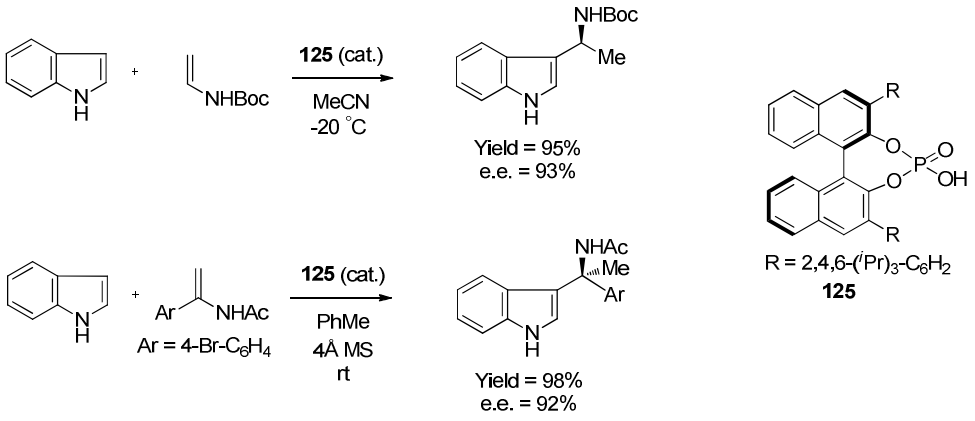

Scheme 47.Tareda & Zhou's Use of Enamides as Electrophiles.

Tsogoeva has shown that the BINOL phosphoric acid **126** can catalyse the formation of a quaternary carbon centre bearing a nitrogen atom, through the self coupling of enamides.[100] The β-amino ketone products are subsequently isolated in good yield and enantioselectivity (Scheme 48).

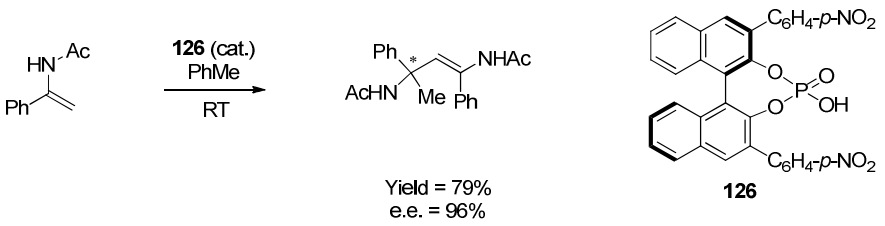

Scheme 48. Tsogoeva's Use of Enamides as a Simultaneous Electrophile & Nucleophile.

Enamides in Organocatalytic Reductions-

Carbery has reported the first use of a bridged flavinium organocatalyst **128** in the diimide reduction of enamide **127** with excellent conversion.[101]

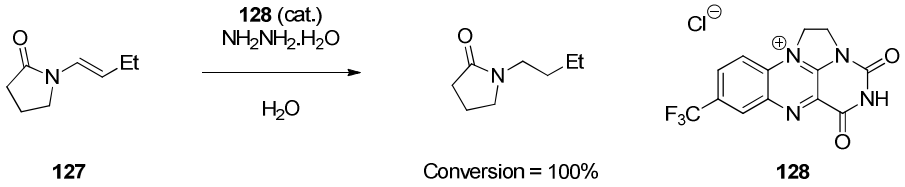

Scheme 49. Enamides in Organocatalytic Hydrogenation Reactions.

Antilla has also reported the highly enantioselective reduction of enamides catalysed by a dual chiral-achiral acid system. This sees catalytic amounts of chiral phosphoric acid **129** and acetic acid providing excellent yields and enantioselectivities of the reduction product.[102]

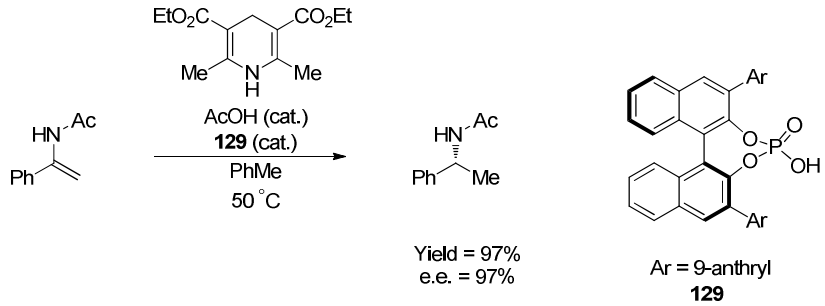

Scheme 50. Enamides in Organocatalytic Reductions.

Enamides in Transition Metal Catalysed Reactions-

Enamides can be viewed as attractive substrates in a number of transition metal mediated alkene transformations. The one reaction that is well developed for enamide substrates is alkene hydrogenation.[95] In contexts where incorporation of nitrogen functionality is important, ring closing metathesis has been utilised allowing the synthesis of cyclic enamides (Scheme 51).[103]

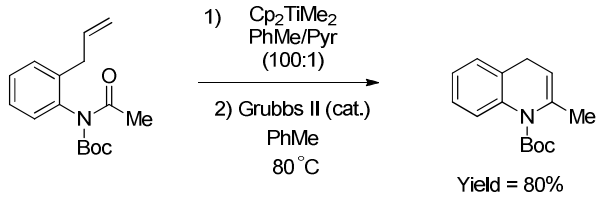

Scheme 51. Enamides in Transition Metal Catalysed Reactions.

Enamides in Pericyclic Reactions-

The use of enamide substrates in pericyclic reactions, such as cycloadditions, electrocyclisations and sigmatropic rearrangements has increased over the past several years.[95] For instance a highly efficient and stereoselective Diels-Alder reaction using a conjugated enamide **130** as the reactive diene has been reported, in the presence of chromium-salen catalyst **131** (Scheme 52).[104]

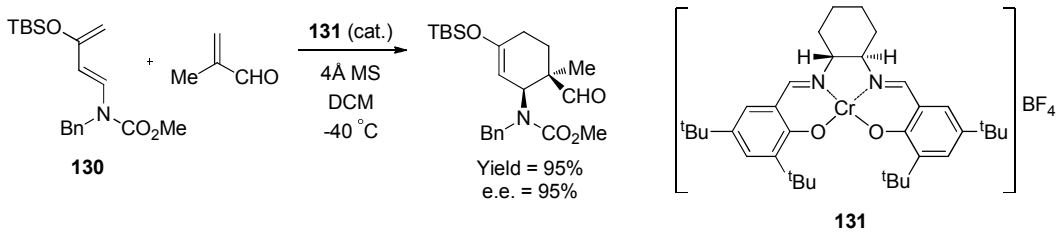

Scheme 52. Enamide in a Cycloaddition.

Funk has demonstrated the use of an enamide in the electrocyclisation of 2,3-pyrroline **132**, to yield the 6π-electrocyclic ring closure product **133** in good yield, allowing access to indole framework seen within trikentrin alkaloids (Scheme 53).[105]

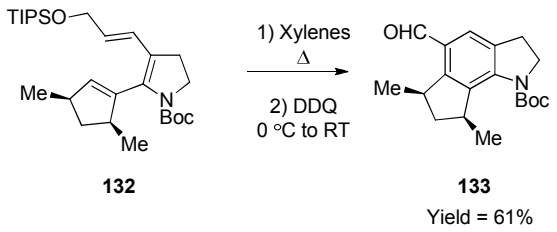

132 **133**

Yield = 61%

Scheme 53. Enamides in Electrocyclic Reactions.

Meyer has reported the first use of an enamide **134** in a sigmatropic rearrangement, that sees formation of amino alcohols **135** in excellent yield and diastereoselectivity, *via* a [2,3]-Wittig rearrangement.[106]

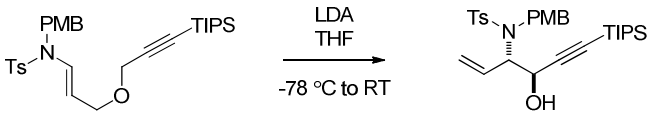

134 **135**

Yield = 93%
d.r. = 24:1

Scheme 54. Enamides in Sigmatropic Rearrangements.

Enamides in Radical Reactions-

The synthetic value of enamide substrates has recently been shown through the total synthesis of Lennoxamine **137**, as enamide **136** is observed to undergo a regioselective 7-*endo* cyclisation followed by subsequent homolytic aromatic substitution (Scheme 55).[107]

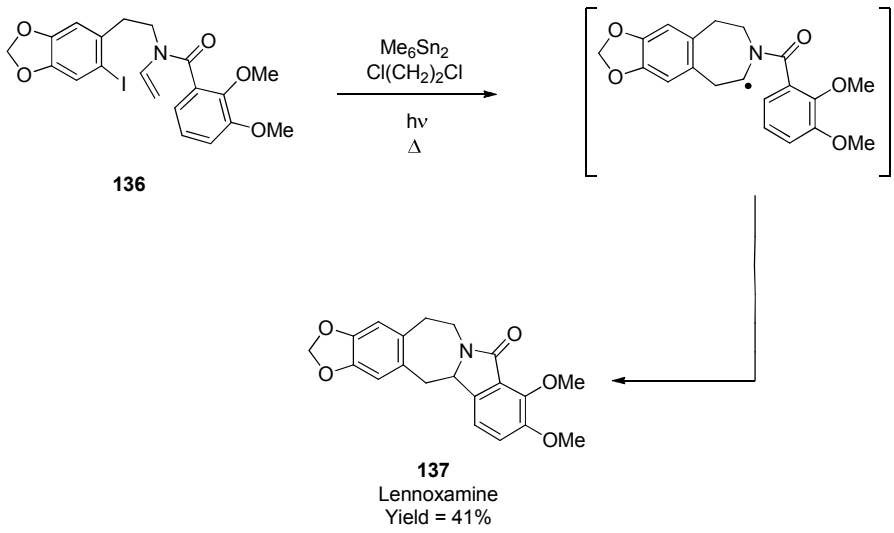

Scheme 55. Enamides in Radical Reactions.

Enamides in Heterocycle Synthesis-

Movassaghi has demonstrated a new synthesis of pyridines, whereby enamides are converted to *N*-vinyl iminium triflates *via* treatment with triflic anhydride, subsequently reacting with electron rich heterosubstituted alkynes or alkenes to form pyridines (Scheme 56).[108]

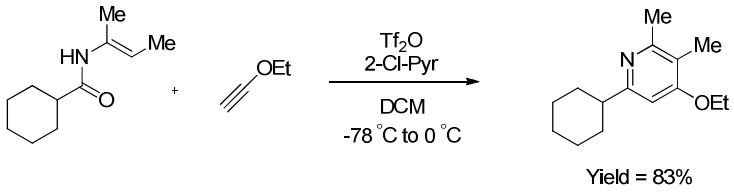

Scheme 56. Enamides in Heterocycle Synthesis.

2. The Enamido-Ireland-Claisen Rearrangement

2.1. Background

In spite of high demand for their availability, synthetic access to enantiopure β-amino acids relies on a variety of methods which are unique to the type and position of substitution required. Currently there is no single synthetic protocol allowing the synthesis of β-amino acids ranging from β- to $\beta^{2,2,3,3}$-amino acids. It was therefore envisaged that an Enamido-Ireland-Claisen rearrangement (EICR) could pose a versatile route, if the synthetic properties of the related Ireland-Claisen rearrangement (ICR) could be transposed. This EICR would allow the required substitution and stereochemical outcome of the β-amino acid be decided pre-reaction.

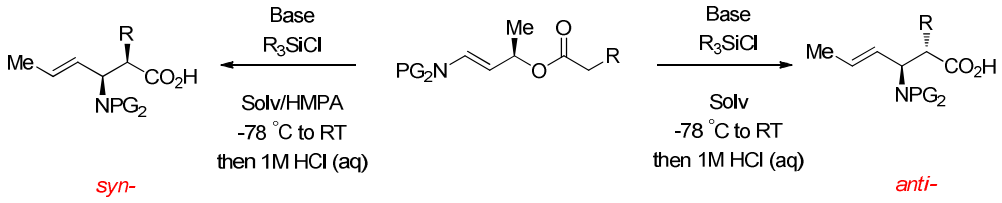

Scheme 57. Proposed [3,3]-Rearrangement of Enamides.

The key factors in making the EICR a useful transformation lie in:

1) A rapid preparation of enamido allylic ester substrates.
2) The potential to control the silyl ketene acetal (SKA) geometry and hence control relative stereochemistry in the product.
3) The potential for chirality transfer from the allylic stereocentre to the newly formed stereocenters in the product.
4) Alkene geometry of the allyl group can be built into synthesis of the substrate.
5) The rearrangements usually proceed at colder temperatures compared to the related Claisen rearrangement, hence allowing kinetic control to be achieved.
6) The predictability between chair and boat transition states.

The Carbery group has recently published a direct and novel route to complex β[2,3]-amino acid precursors.[109] This new methodology was based upon the use of enamido allylic esters **138** for use in an EICR and has been shown to proceed under similar conditions to the generic ICR. From the several examples published moderate to good yields and poor diastereoselectivities were observed for the rearrangement of alkyl derived enamido ester substrates. However the phenyl substrate displayed a good yield and excellent diastereoselectivity of rearranged β-amino ester precursor **144**.

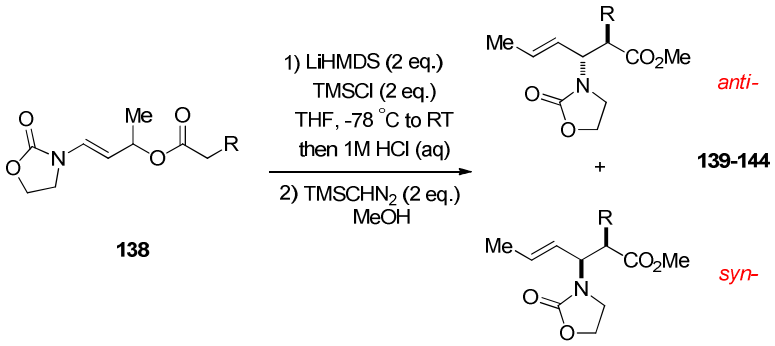

Entry	R	Product	Yield (%)	d.r. (*anti:syn*)
1	Me	**139**	55	2:1
2	H	**140**	Trace	na
3	^{i}Pr	**141**	48	3:2
4	Allyl	**142**	79	3:2
5	OBn	**143**	62	2:1
6	Phenyl	**144**	69	>95:5

Table 2. The EICR.

At the time of publication, relative stereochemistry was tentatively assigned based on the observed coupling constants of the allylic methine signal, within ^{1}H-NMR experiments. This proton was observed in both *anti*- and *syn*-diastereoisomers as a doublet of doublets, with the major diastereoisomer offering a larger coupling constant consistent with an *anti*-periplanar open chain of the product β-amino acid precursors and therefore assigned as the *anti*-diastereoisomer (Fig. 9.).

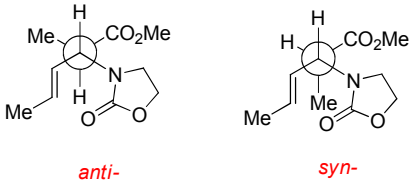

Fig. 9. Newman Projections of Syn- and Anti- Diastereoisomers.

Whilst the diastereoselectivity in the alkyl examples was disappointing it was also noticeably lower than many Ireland-Claisen reactions of propionates, where diastereomeric ratios of the order of 85:15 or better are often observed.[66] Several factors may be responsible for these observed reductions, including poor *E/Z* enolate geometry control, the enamide moiety affecting the preference of chair versus boat transition states and post-rearrangement enolisation all having deleterious effects.[110-111]

2.2. Initial Aim

The high diastereoselection observed with the phenylacetate was indeed intriguing. Following on from these initial results it was decided to first look at optimising the EICR of the phenylacetate, prior to probing the diastereoselection of the EICR through perturbing the electronic nature of the acyl fragment. Any differences in the observed diastereoselectivity may then offer insight into the stability of enolates, SKAs and conformational considerations of chair/boat transition states. Secondly, the use of enantiopure secondary carbinol derived enamido allylic esters may also provide useful information on the effect of electronic perturbations, as traditional Ireland-Claisen rearrangements have been shown to rearrange enantiopure starting materials to >95% e.e.[112]

2.3. Retrosynthesis

Two key requirements were identified for the synthesis of the desired enamido allylic ester substrates. Firstly, a cheap and simple synthesis that allows incorporation of the acyl moiety at late stage would be desirable, allowing multigram quantities of a key

intermediate to be synthesised. Secondly, investigations based on secondary allylic esters would offer potential for asymmetric control with enantiopure substrates during later studies. Retrosynthetic analysis (RSA) on enamido allylic ester **138**, provides a key oxazolidinone derived enamide **145** *via* ester C-O bond cleavage (Scheme 58).

138 **145**

Scheme 58. RSA of Generic Oxazolidinone Enamido Substrate.

Access to key intermediate **145** could then be based on a racemic and an enantiomerically pure basis, in which:

1) Racemic **145** could be accessed from vinylogous amide **146** under reduction conditions, subsequently produced from a conjugate addition of 2-oxazolidinone **147** to ynone **148** generated from alcohol **149**.

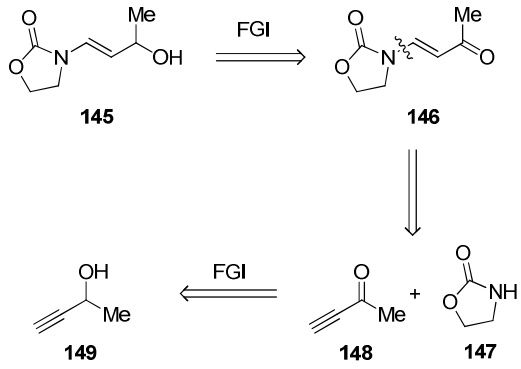

145 **146** **149** **148** **147**

*Scheme 59. RSA of Key Vinylogous Hemiaminal **145**.*

2) Enantiomerically pure ***(R)*-150** could be accessed *via* a selective reduction of ynamide ***(R)*-151**, synthesised *via* an Ullmann type coupling of 2-oxazolidinone **147** and bromoalkyne ***(R)*-152**. Bromoalkyne ***(R)*-152** could be synthesised from enantiomerically pure but-3-yn-2-ol ***(R)*-153** *via* *O*-protection and bromination (Scheme 60).

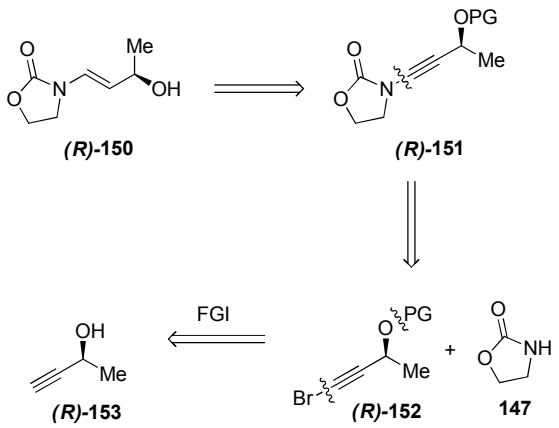

Scheme 60. RSA of Key Enantiomerically Pure Vinylogous Hemiaminal.

2.4. Synthesis of Racemic Enamido Allylic Esters

The synthetic route undertaken to racemic alcohol **145** followed a procedure reported by Carbery and Janey.[109,113] After further optimisation, the developed substrate synthesis is outlined in Scheme 61. Vinylogous amide **146** was synthesised in a markedly improved 58% yield, to that published.[109] This was accomplished by a two step procedure involving Jones oxidation of **149**, followed by the immediate conjugate addition of 2-oxazolidinone **147** in the presence of catalytic amounts of DABCO.[114] Subsequent sodium borohydride reduction cleanly and chemoselectively reduced the ketone moiety to form the key intermediate **145**, in quantitative yields and without the need for further purification.[115]

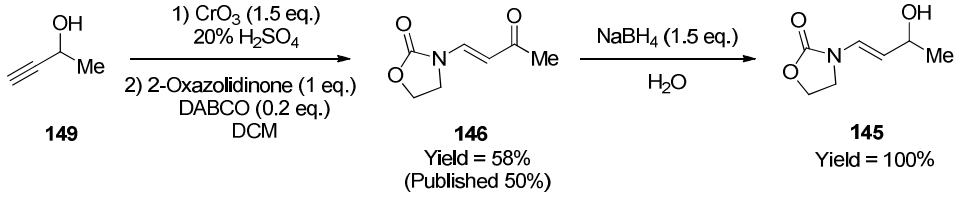

Scheme 61. Route to Key Racemic Intermediate.

Esterification of alcohol **145** was performed *via* the carbodiimide coupling reagent EDCi, and it is noted that significantly improved yields of phenylacetate **154** were observed to that published.[109]

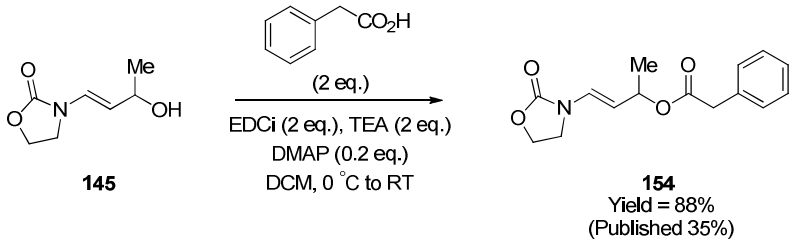

Scheme 62. EDCi Coupling.

The use of EDCi has been found to be optimal, as all by-products of the reaction can be easily removed during a weak acid-base extraction cycle, with the product isolable without need for further purification. The use of other esterification protocols which are reliant on or generate acidic conditions *in-situ,* such as the hydrochloric acid (generated from methanol/acetyl chloride) catalysed esterification of alcohol **145** and phenylacetic acid, or esterification of alcohol **145** with phenylacetyl chloride even in the presence of triethylamine, show complete degradation of **145** with no signs of product formation. Access to **154** *via* DCC was promising, however removal of the urea by-products by silica or alumina column chromatography was deleterious and degradation resulted. The degradation pathway for acid mediated esterification conditions can be envisaged to occur *via* dehydration of alcohol **145**, and that seen within chromatographic purification of phenyl acetate **154** could be envisaged to occur *via* elimination of phenylacetic acid facilitated by activation of the ester and ejection by the enamide. Both degradation pathways yield the same common iminium ion intermediate **155**, producing quantitative yields of 2-oxazolidinone **147** and phenyl acetic acid **156** after aqueous work up. Crotonaldehyde **157** has not been isolated post chromatographic separation, but its generation is based on ^{1}H NMR analysis of crude reaction mixtures for esterifications and by treatment of phenyl acetate **154** to 2M hydrochloric acid, followed by organic extraction.

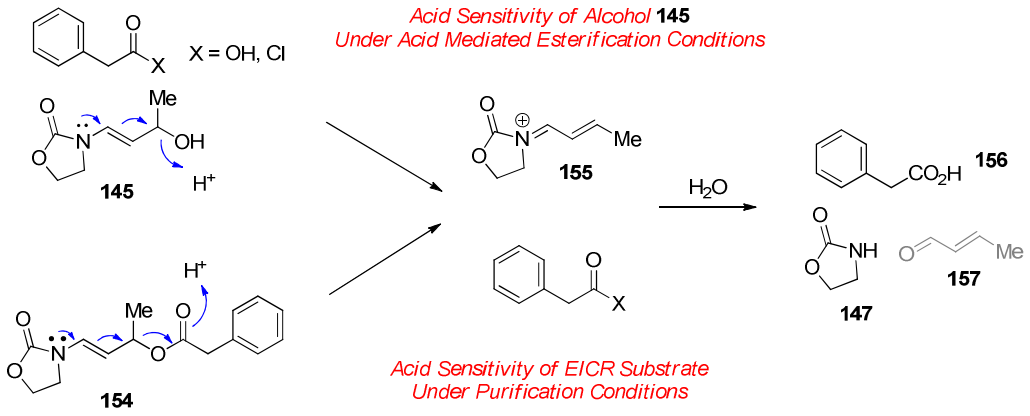

*Scheme 63. Sensitivity of Key Alcohol **145** & Substrate **154**.*

2.5. Optimisation of Phenylacetate EICR

Before investigation into the electronically differentiated phenylacetates, it was decided that optimisation of the EICR of the parent phenylacetate substrate **154** was required. This optimisation was envisaged to encompass all variables associated with this reaction and to compliment the published results.[109] These variables included the type and equivalents of base, solvent, reaction temperature, order of addition, quench and workup conditions. From the outset, the methylation of the $\beta^{2,3}$-amino acid precursors was accomplished by rapid treatment with diazomethane, as opposed to a published methanolic TMS diazomethane approach.[109] This approach was based on a thorough mechanistic elucidation made by Lloyd-Jones into the TMS diazomethane methylation of carboxylic acids.[116] This report highlighted product distributions seen using this protocol and exemplified the issues through the methylation of phenylacetic acid **156**, whereby methylated acid **158** and unwanted TMS-methyl acetate **159** were generated. Reductions in **159** were seen through increasing the methanol concentration and by the addition of a Brønsted acid.

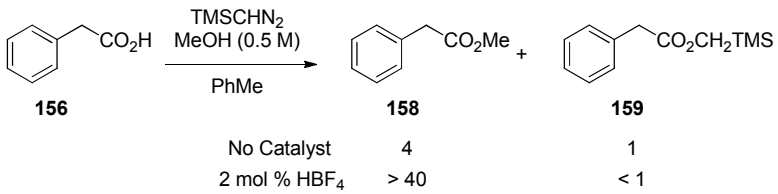

Scheme 64. Issues Observed with TMS Diazomethane Methylations.

Although there is certain dogma based on the use of diazomethane, such as its toxicity and explosive properties, its generation under a controlled environment allows a quick, easy and relatively safe methylation protocol, in absence of any other complications potentially seen with TMS diazomethane.[117]

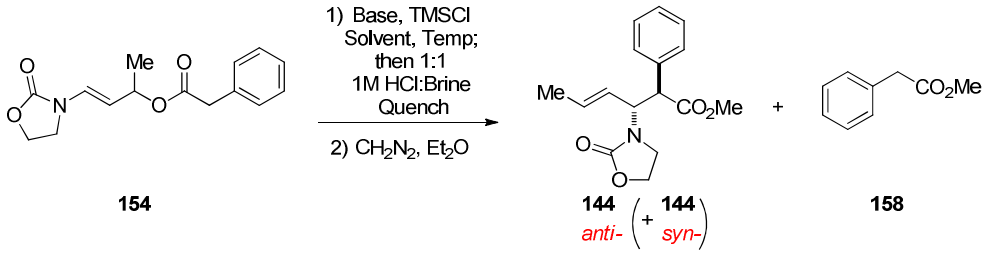

154 **144** *anti-* + **144** *syn-* **158**

Entry	Base	Eq.	Eq. TMSCl	Yield **144** / % (d.r.)[a]	Yield **158** / %
1	LiHMDS	1.1	1.1	74 (16:1)[bfj]	14
2	LiHMDS	1.3	1.3	80 (16:1)[bfj]	11
3	LiHMDS	1.5	1.5	85 (9:1)[bfj]	9
4	LiHMDS	1.3	1.3	72 (44:1)[cgj]	16
5	LiHMDS	1.3	1.3	80 (32:1)[chj]	14
6	LiHMDS	1.5	1.5	66 (32:1)[cgj]	21
7	LiHMDS	1.3	1.3	65 (32:1)[bgj]	26
8	NaHMDS	1.3	1.3	34 (2:1)[cgj]	26
9	KHMDS	1.3	1.3	na (na)[cgj]	na
10	LDA	1.3	1.3	na (na)[cgj]	na
11	LiHMDS	1.3	1.3	na(32:1)[cdgj]	na
12	LiHMDS	1.3	1.3	59 (32:1)[cegj]	21
13	LiHMDS	1.3	1.3	71 (41:1)[cgk]	14
14	LiHMDS	1.3	1.3	53 (32:1)[cgl]	27
15	LiHMDS	1.3	1.3	82 (32:1)[cij]	12

[a]d.r. measured by extended acquisition of crude on 500 MHz ^{1}H NMR [b]Reaction initiated at -78 °C [c]Reaction initiated at -95 °C [d]Reaction quenched by 10% citric acid (aq) [e]Reaction performed in toluene [f]Hand addition of substrate to base, TMSCl and THF [g]Addition of substrate at 4 ml/h to base and TMSCl and THF [h]Addition of substrate at 2 ml/h to base and TMSCl [i]Addition of base at 4 ml/h to substrate, TMSCl and THF [j]Warm to RT over 1 h [k]Reaction allowed to stir for 2 h [l]Warm to 0 °C over 1 h.

Table 3. Results from Optimisation of Phenylacetate EICR.

This optimisation has demonstrated that higher yields and diastereoselectivities are accomplished when reaction initiation was performed by slow addition of substrate to base and TMSCl (Entry 2, Table 3) and even better at the lower temperature of -95 °C (Entry 4, Table 3). The rearrangement displayed a striking dependence on the nature of the base used, where NaHMDS significantly reduced diastereocontrol (Entry 8, Table 3) and both KHMDS and LDA yielded intractable mixture of products (Entry 9 and 10, Table 3). The reaction was relatively insensitive to the choice of solvent, working well in toluene (Entry 12, Table 3). Furthermore, the manner of reaction quench was found to be important (Entry 11, Table 3), as methylation of residual citric acid present post work up was seen to co-elute with product during column chromatography leading to impure product. An inverse addition protocol was observed to have marginal reductions in diastereocontrol (Entry 15, Table 3).

To allow structural verification of the major diastereomer, **144** was successfully recrystallised allowing an X-ray structure be acquired (Figure 10). To ensure that the major diastereomer was correctly analysed, the single crystal and powder diffractions of bulk sample were compared (see appendix), verifying that the *anti*-relationship of these $\beta^{2,3}$-amino acid precursors predominates.

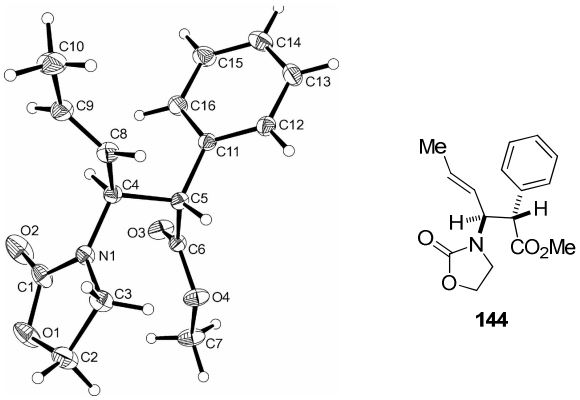

*Fig. 10. ORTEP Plot of Phenylacetate **144** (Ellipsoids Shown at 30% Probability).*

A general observation from these rearrangements was seen to be the recovery of variable amounts of methylated phenylacetic acid **158** in addition to the desired $\beta^{2,3}$-amino acid precursor, allowing near quantitative mass balance be accounted for. As the consumption of starting material can not be monitored by TLC, due to its inherent

sensitivity to acidic media, it was thought that the reaction may not be complete after 60 minutes and the acidic quench may play a deleterious effect by hydrolysing the unreacted enamido ester starting material. However, this was not considered to be a factor, as when the reaction time was increased (Entry 13, Table 3) comparable yields and diastereoselectivities were obtained. Other hypotheses for the generation of **158** are based on two possible degradation pathways involving the initial formation of the enolate **160**, from the enamido allylic ester starting material. It is postulated that either degradation occurs *via* a ketene type pathway in which the enolate **160** ejects the alkoxide **161** (Pathway A, Scheme 65), or alternatively through an enamide facilitated pathway, involving ejection of a doubly deprotonated carboxylic acid (Iwanov reagent) **162** and yielding iminium ion **155**. These intermediate degradation products would then yield the observed by-product **156**, post protic quench *via* either degradation pathway prior to methylation.

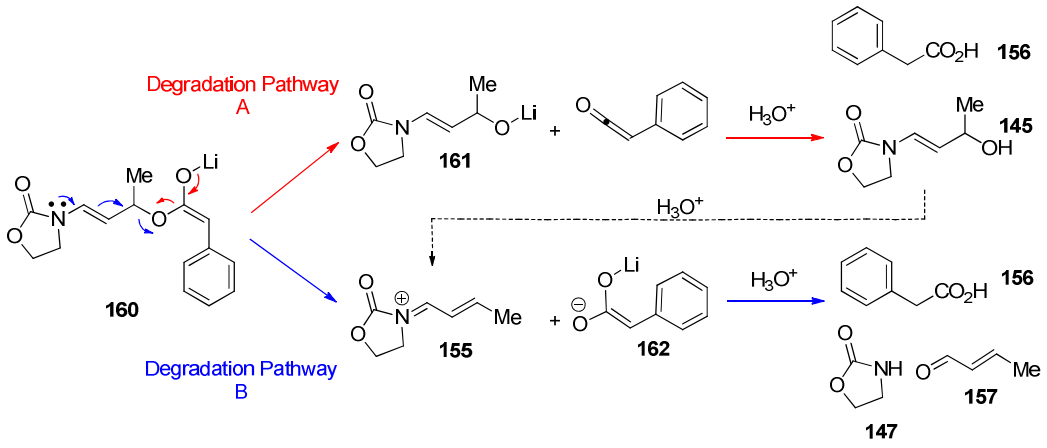

*Scheme 65. Possible Degradation Pathways for Enolate **160.***

Observation analytically and/or isolation physically of the enamido alcohol **145** from the reaction mixtures has not been acheived, perhaps an aspect of its strong sensitivity to protic environments such as the reaction quench. However, potential indications of the presence of aldehydic signals in the ^{1}H NMR spectra of crude reaction mixtures may allude to the presence of crotonaldehyde **157**. This observation, however, does not prove either degradation pathway, as separate treatment of alcohol **145** with 1M HCl:brine solution yields a complex reaction profile alluding to the formation of 2-oxazolidinone **147** and crotonaldehyde **157**.

2.6. Rearrangement of Electronically Differentiated Arylacetates

With improved rearrangement conditions in hand for the parent phenylacetate enamido ester, the level of diastereoselectivity relative to the electronic nature of the acyl moiety could now be investigated. A range of phenylacetates were prepared with electronically differentiated substituents, namely the electron rich methoxy, the electron poor nitro and the relatively electron neutral methyl group, each placed sequentially at the *ortho*-, *meta*- and *para*-positions. These substrates were synthesised utilising the now standard EDCi coupling conditions in excellent yields (Table 4).

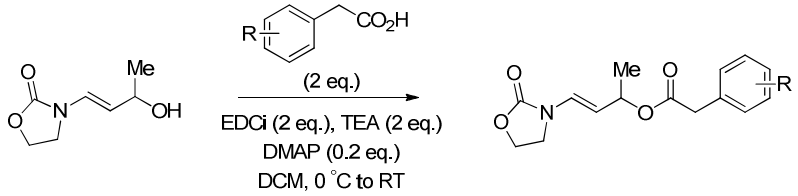

145 **163-171**

Entry	R	Product	Yield (%)
1	*o*-OMe	**163**	94
2	*m*-OMe	**164**	76
3	*p*-OMe	**165**	91
4	*o*-Me	**166**	71
5	*m*-Me	**167**	74
6	*p*-Me	**168**	88
7	*o*-NO_2	**169**	85
8	*m*-NO_2	**170**	92
9	*p*-NO_2	**171**	85

Table 4. Yields for EDCi Couplings.

Rearrangement and esterification of these substrates was then pursued using the newly optimised conditions, yielding the corresponding methyl esters in good yields and poor to excellent diastereoselectivities.

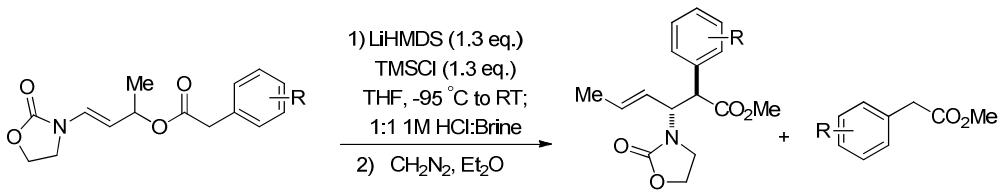

163-171 **172-180** *anti-* + **172-180** *syn-* **181-189**

Entry	R	Product	Yield (%)	d.r.[a,b] (*anti:syn*)	By-Product	Yield (%)[c]
1	*o*-OMe	**172**	79	22:1	**181**	13
2	*m*-OMe	**173**	73	19:1	**182**	15
3	*p*-OMe	**174**	77	24:1	**183**	13
4	*o*-Me	**175**	71	19:1	**184**	16
5	*m*-Me	**176**	74	43:1	**185**	14
6	*p*-Me	**177**	70	54:1	**186**	21
7	*o*-NO_2	**178**	73	5:1	**187**	17
8	*m*-NO_2	**179**	75	16:1	**188**	14
9	*p*-NO_2	**180**	76	9:1	**189**	13

[a]d.r. measured by extended acquisition of crude on 500 MHz ^{1}H NMR [b]Triplicates have been performed in each case. Measured d.r. is reproducible and reported as an average [c]Yield based on amount of EICR product that degradation product corresponds to.

Table 5. Results for Arylacetate EICR.

In all *ortho*-substituted systems a deterioration in diastereoselectivity was observed compared to the parent phenylacetate **144**, with a significant reduction seen for the *o*-NO_2 (Entry 9, Table 5). Consistent reductions in diastereoselectivity were seen for the *meta*-substituted analogues, however, the most interesting range of diastereoselectivities were observed for the *para*-substituted systems. Significant reductions in the diastereoselectivity were observed for the electron donating methoxy (Entry 3, Table 5) and the electron withdrawing nitro group (Entry 9, Table 5), but an increase in diastereoselectivity was observed for the relatively electron neutral methyl group (Entry 6, Table 5), compared to the parent phenylacetate **144**.

With the *ortho*-variants, the diminished diastereoselectivity observed can be attributed to dual steric and electronic effects within the rearrangement transition state. However,

the *para*-variants can be viewed on deconvoluted steric and electronic effects, as these groups are structurally remote from the site of reaction. Within these EICR reactions there are several possibilities that could lead to the diminished diastereoselectivity observed. These are-

1) Non-Selective Enolisation

It is well known within the Ireland-Claisen rearrangement that the enolisation by lithium amide bases occurs under kinetic control, yielding formation of the more favourable *Z*-enolate.[66-67] Therefore deprotonation of enamido allylic phenylacetate **144** would be expected to occur with a similar outcome through an analogous six-membered transition state, where 1,3-diaxial interactions predominate and a *pseudo*-equatorial positioning of the phenyl ring is favoured generating Z-enolate **160**.

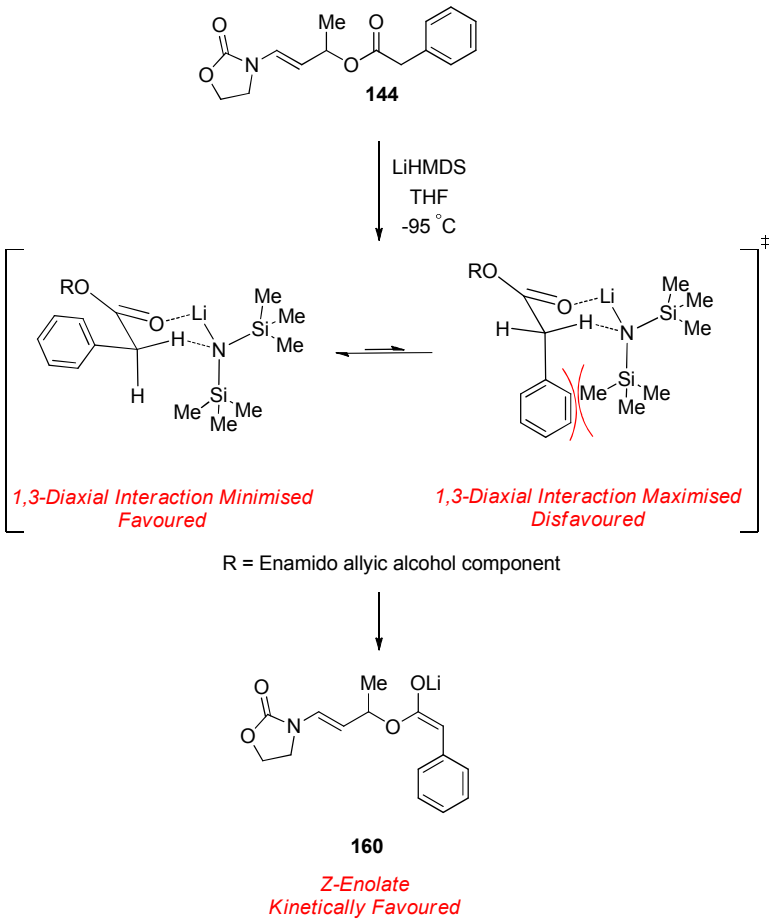

Scheme 66. Enolisation Transition States.

However, certainly in the presence of any *ortho*-arylsubstituents **190**, a 1,2-transannular effect may play a significant role, counteracting the strong 1,3-diaxial effect (Scheme 67).

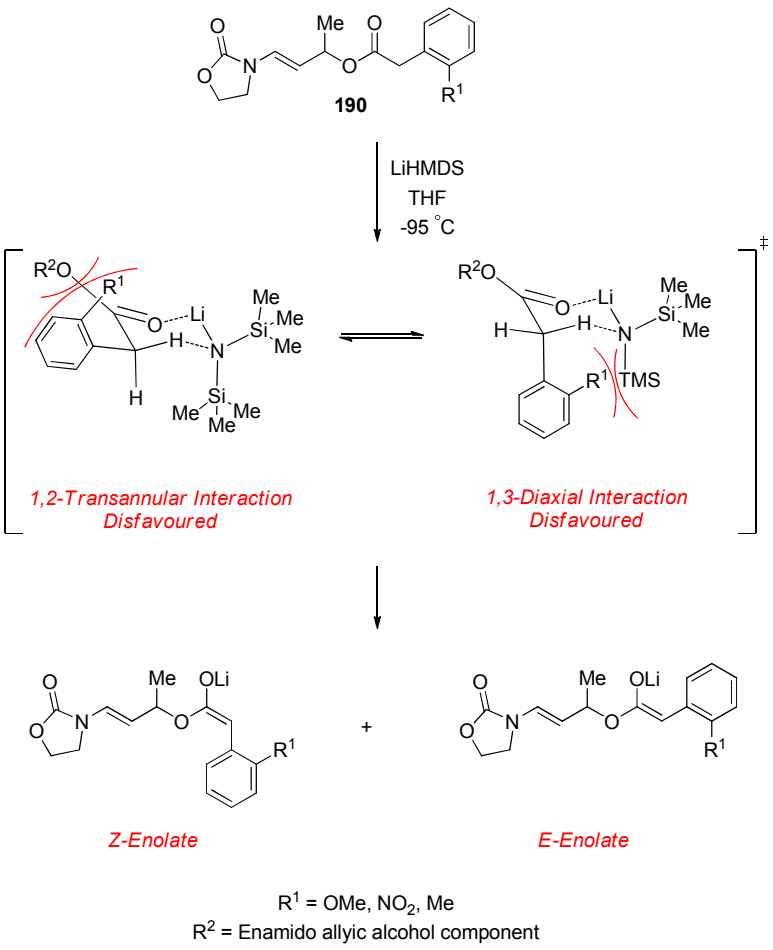

Scheme 67. Enolisation Transition States.

If this were the case, then poor *E/Z*-enolate control may be responsible for the poor diastereoselectivity seen, assuming that the rearrangement occurs, post silyation, through a reliable chair transition state. This argument is exemplified by the *ortho*- and *para*-methyl systems (**175** & **177**), as a notable reduction in diastereoselectivity is seen with the *ortho*-methyl variant, yet high diastereocontrol is observed with the *para*-methyl variant. However, the near identical reductions in diastereocontrol seen with the *ortho*- and *para*-nitro (**178** & **180**) and methoxy (**172** & **174**) systems respectively, may allude to the presence of an alternative stronger effect outweighing steric issues in these cases.

2) Enolate Isomerisation

An alternative to poor *E/Z*-enolate control *via* initial deprotonation could be seen through a post-enolisation isomerisation. This effect, perhaps most suited by the presence of a conjugated electron withdrawing or donating group, could mesomerically remove enolate character by either withdrawing electron density out of, or inserting electron density into the π-system. This mechanism, exemplified by the *para*-nitro **191** and methoxy **192** variants (Scheme 68), could subsequently erode any geometrical control of enolisation, as the enolate could isomerise prior to silylation and subsequent rearrangement.

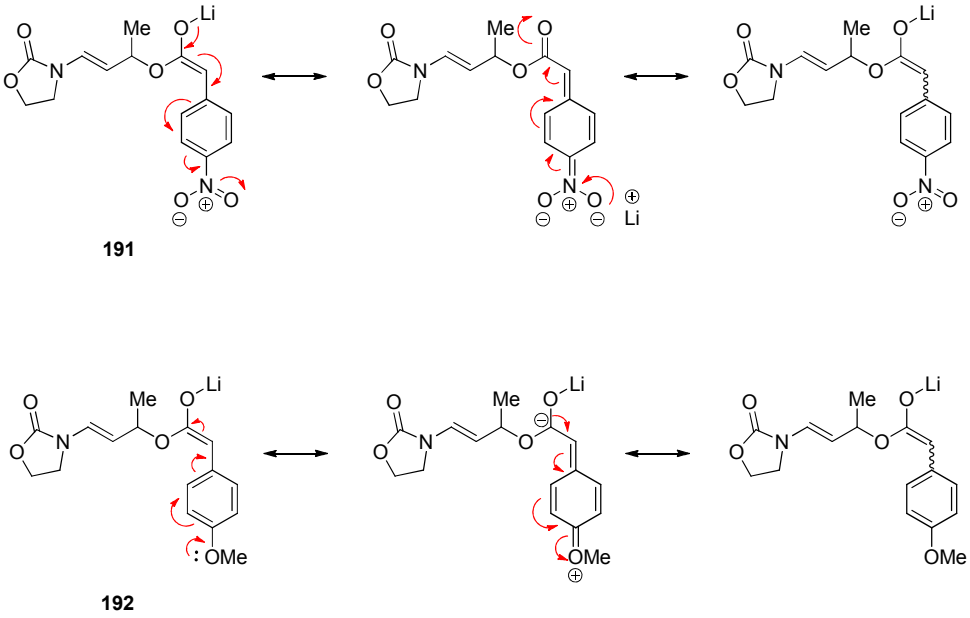

Scheme 68. Possible Explanation for Low d.r. with para-Nitro- and para-Methoxy-Substrates.

This argument may be more suited to electron withdrawing groups which can act as a resonance stabilised electron sink, exemplified in the above case through nitronate **191**.

3) Silyl Ketene Acetal Isomerisation

Providing that formation of the *E*-silyl ketene acetal is kinetically favoured, another variable that could result in poor diastereocontrol may be presented by silyl ketene acetal isomerisation. Dauben has computationally supported observed experimental results on *E/Z* silyl ketene acetal ratios of propionate derived systems, however inconsistencies are observed between the calculated *E/Z* ratios of phenylacetate

derived silyl ketene acetals to that observed experimentally.[118] The *E/Z* silyl ketene acetal ratios for the parent phenylacetate were calculated to be kinetically favoured and are in stark contrast to the observed ratio of 29:71 (*E:Z*) seen by Ireland.[66,67,68] Corset and Tanaka have both separately shown that Dauben's calculation for the selective formation of the *E*-silyl ketene acetal was correct.[119,120] The predominant formation of the *Z*-geometrical isomer is the result of a thermodynamic equilibration between the *E*- and *Z*-silyl ketene acetals under the reaction conditions and/or work up procedures, implying that silylation may be a poor technique for maintaining high *E/Z* ester enolate ratios. With these considerations in mind the thermodynamic isomerisation of the silyl ketene acetal may be responsible for the poor diastereoselectivity observed within the electron donating and withdrawing variants of the EICR.

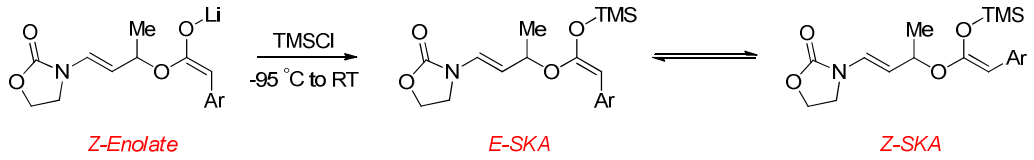

Scheme 69. Possible Thermodynamic Isomerisation of SKA.

4) Competition Amongst Alternative Transition States

Another consideration which may result in the observed diastereoselectivity could be energetically similar chair and boat transition states prior to rearrangement.[3] This factor combined with any thermodynamic aspects of SKA isomerisation could lead to a very complex situation where four diastereomeric transition states may coexist (Figure 11).[119,120] The formation of the *anti*-diastereomer is then not only consistent with an *E*-SKA rearranging *via* chair transition state **193**, but also a *Z*-SKA rearranging *via* boat transition state **194**. Simultaneously the *syn*-diastereomer could be accesed through rearrangement of a *Z*-SKA *via* chair transition state **196** or an *E*-SKA through boat transition state **195**.

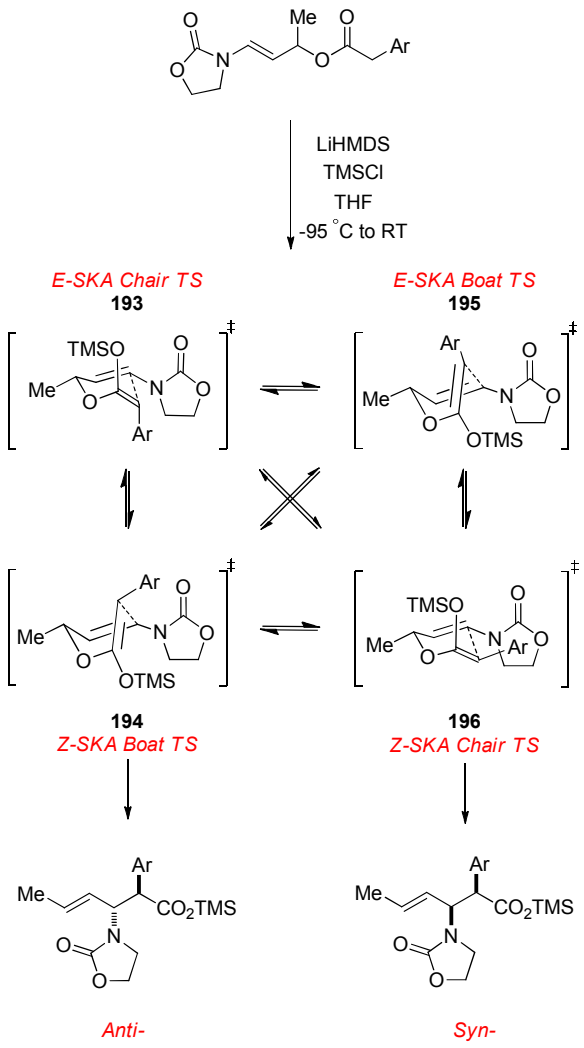

Scheme 70. Possible Transition States for the EICR.

5) Non-Concerted Character

The potential for pericyclic reactions to possess chameleonic transition states, where the mechanism skirts between a concerted intramolecular and a non-concerted intermolecular reaction, have proved an area of much discussion within the physical organic community.[121-123] A possible explanation for the observed trends in diastereoselectivity within the EICR may be presented by such a change in mechanism. A truly concerted, selective, one step mechanism may exist for the highly diastereoselective phenyl- **144** and tolylacetates **177**; however a non-concerted, non-selective, two step mechanism may result for the nitro- **180** and methoxyacetates **174**. The formation of intimate ion pairs could be facilitated by the enamide, causing cleavage of the C-Oσ ester bond and yielding iminium ion intermediate **155** in both

electron withdrawing nitro- and electron donating methoxy-cases. The recombination of these ion pairs could then occur *via* the nitronate **197**, or by the Iwanov reagent **198**, producing aldol type selectivity.

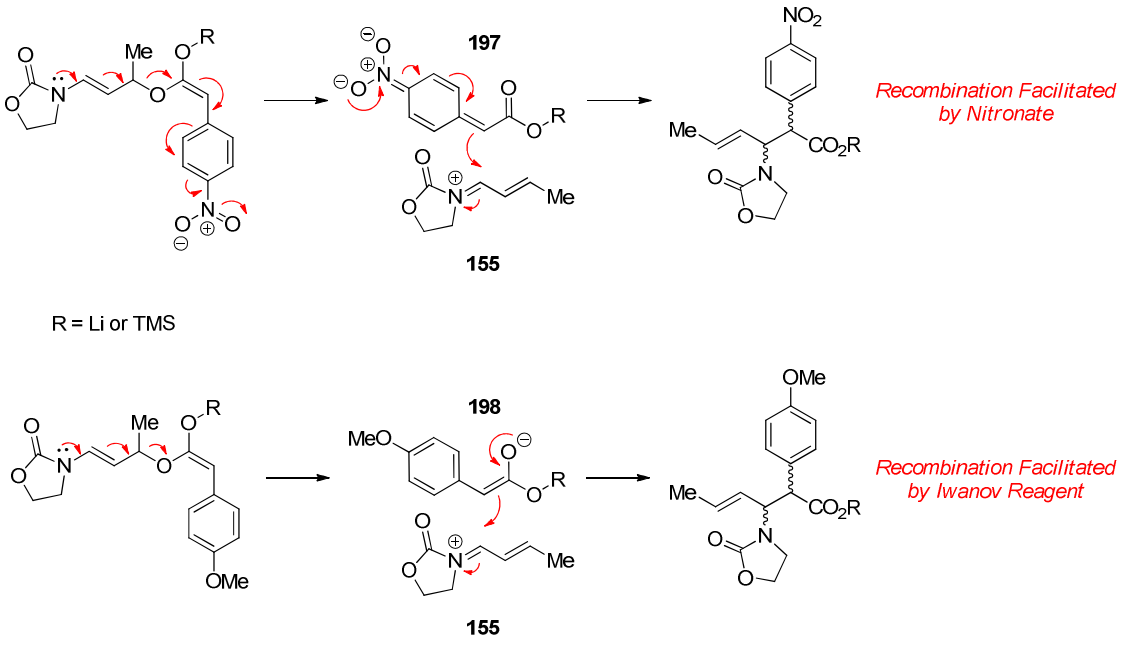

Scheme 71. Possible Non-Concerted Character of EICR.

6) Post Rearrangement Epimerisation

Post rearrangement enolisation was first reported in Ireland's seminal paper, where it was noted that 6% of *C*-silylated pentenoic acid **199** was isolated in addition to the desired product **96**.[61]

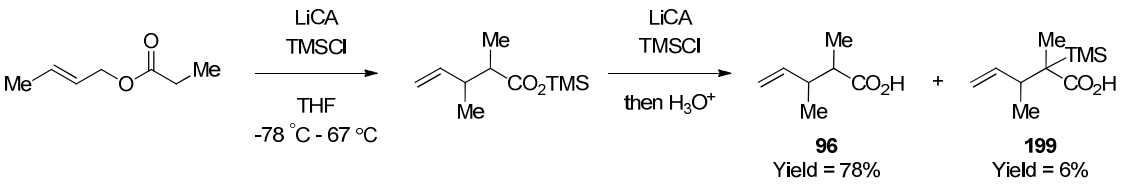

Scheme 72. C-Silyation in Ireland-Claisen Rearrangement.

The issue surrounding post rearrangement enolisation relies on the retention of a second enolisable proton within the pentenoic acid product. McIntosh has subsequently reported deleterious effects seen with post rearrangement epimerisation, in that, albeit

no C-silyation was noted, anomously low yields and variable diastereoselectivities were observed in the formation of **200** as a function of time.[110] These issues were circumvented *via* a cold quench with acetic acid, halting post rearrangement enolisation.

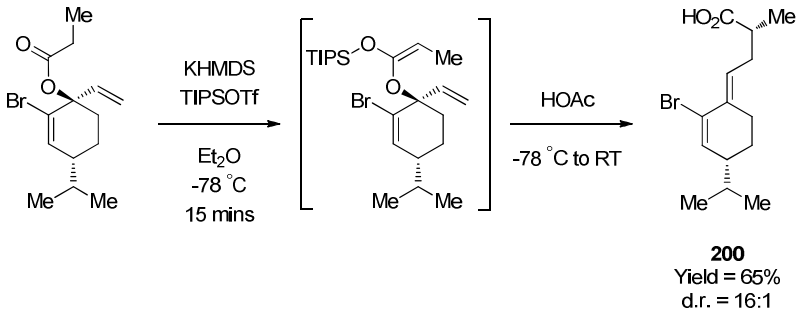

Scheme 73. McIntosh's Solution to Post Rearrangement Epimerisation.

Post rearrangement epimerisation may therefore be reponsible for the low diastereoselectivities seen within the EICR and in order to discount this variable a number of test reactions were performed. In order to test whether epimerisation of the product silyl ester was an issue, the rearrangement of **154** was monitored over 24 hours by extracting aliquots after 1, 3, 5, 11 and 24 hours. After treatment by diazomethane, the observed diastereoselectivity from these aliquots was seen to remain identical, subsequently demonstrating that erosions in diastereoselectivity are independent of reaction time. Also, the treatment of the isolated methyl ester **144** with LiHMDS and TMSCl lead to quantitative return of diene **201** *via* E1cB elimination of 2-oxazolidinone **147**.

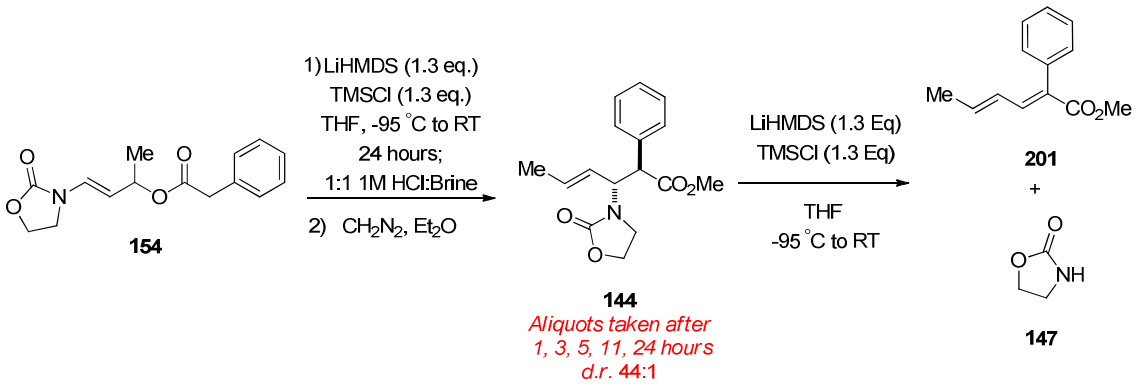

*Scheme 74. Time Study on EICR of Phenylacetate **154**.*

During the course of the EICR, the formation of by-products such as hexamethyldisilazane (HMDS) from enolisation, or lithium chloride from silyation of the enolate may prove important.

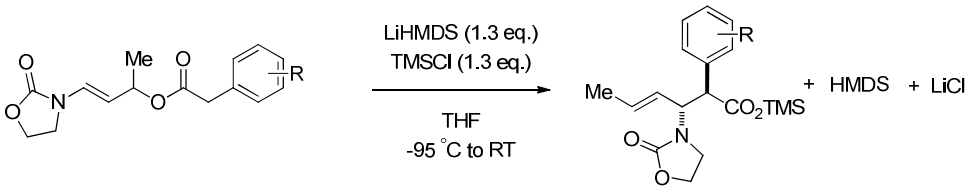

Scheme 75. By-Product Considerations.

These by-products may be reponsible for the low diastereoselectivity seen with the nitro-arylacetate silyl ester products, as these would be envisaged to be more susceptible to soft enolisation by the secondary amine HMDS in the presence of the Lewis acid, lithium chloride. In order to test this hypothesis, *syn*-**180** and *anti*-**180** were separately treated with HMDS and LiCl in THF at room temperature over 24 hours, no erosion of diastereomeric purity was observed in this experiment.

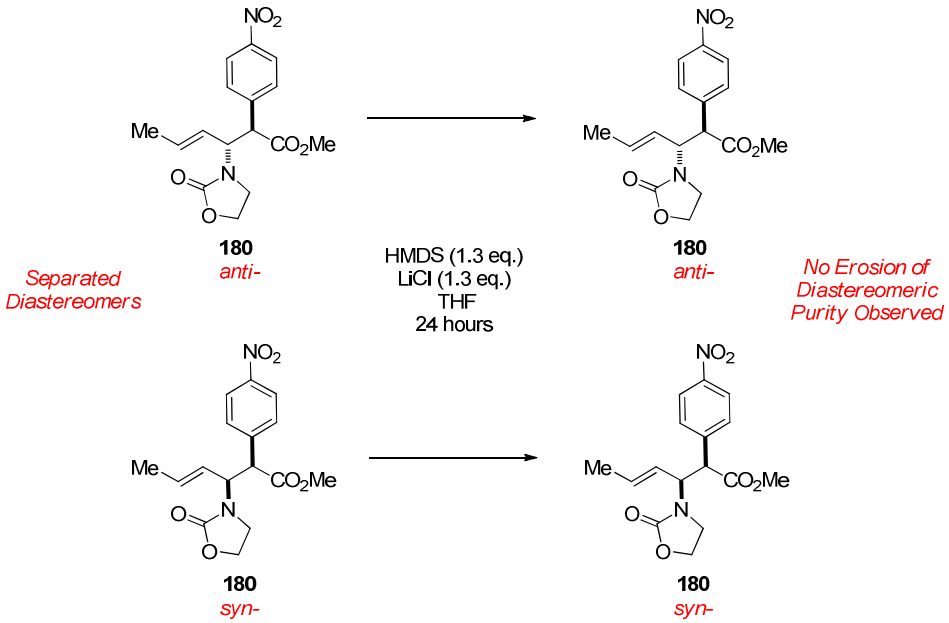

Scheme 76. Soft Enolisation Considerations.

2.7. Further Investigation into the Electronic Nature of *para*-Substitution

The striking range of diastereoselectivity observed with the *para*-nitro, methoxy and tolylarylacetates, strongly suggest that stereoelectronic effects play an important role in determining the diastereochemical outcome of the EICR. The sharp reductions in diastereoselectivity observed for the strongly electron withdrawing **180** and donating analogues **174**, compared to the relatively electron neutral tolyl **177** system, indicate that a fine balance between stereoelectronics and diastereoselectivity may exist. In order to probe this relationship a more comprehensive investigation into the nature of *para*-substitution was pursued, based on varying levels of electron withdrawing and donating capabilities. With this in mind seven other *para*-substituted arylacetate substrates were synthesised in high yields **202**-**208**. Additionally, the synthesis of the electron rich 2,4-dimethoxy arylacetate **209** was also accomplished in a high yield. Other substrates synthesised in high yields included the styryl **210**, 3-methylindolyl **211** and dioxolane **212** arylacetates, with the intention of probing electronics of substitution indirectly.

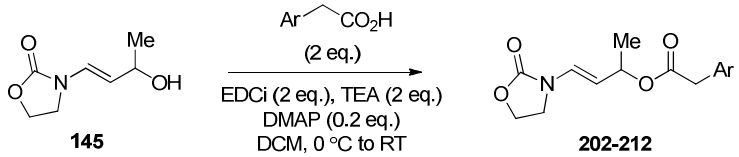

Entry	Ar	Product	Yield (%)	Entry	Ar	Product	Yield (%)
1	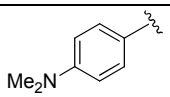	**202**	92	7	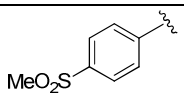	**208**	83
2	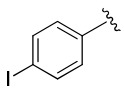	**203**	79	8	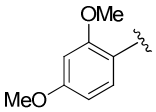	**209**	79
3	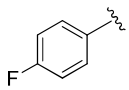	**204**	77	9	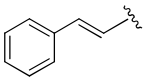	**210**	91
4	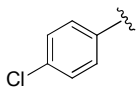	**205**	93	10	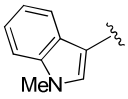	**211**	74[a]
5	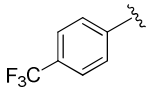	**206**	86	11	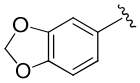	**212**	85
6	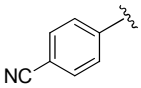	**207**	73				

[a]*Yield over 2 steps involving N-methylation of indole-3-acetic acid and subsequent esterification with* ***145****.*

Table 6. Yields for EDCi Couplings.

With these eleven other aryl acetates in hand, the rearrangement under optimised conditions provided the corresponding $\beta^{2,3}$-amino acid precursors in high yields and a range of diastereoselectivities.

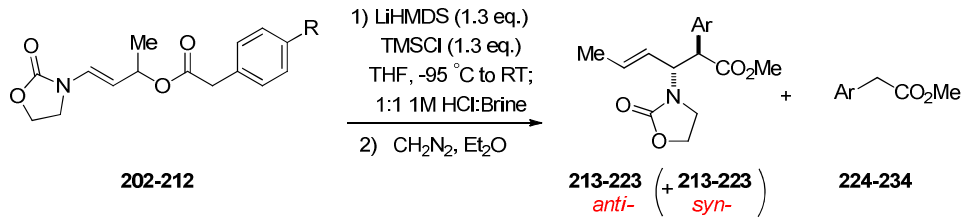

202-212 **213-223** (+ **213-223** *syn-*) *anti-* **224-234**

Entry	R	Product	Yield (%)	d.r.[a,b] (*anti:syn*)	By-Product	Yield[c] (%)
1	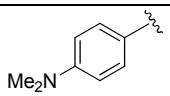	**213**[d]	58	6:1	**224**	24
2	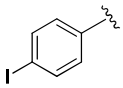	**214**	77	60:1	**225**	14
3	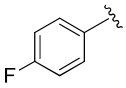	**215**	73	23:1	**226**	17
4	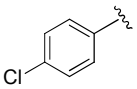	**216**	72	46:1	**227**	19
5	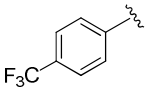	**217**	71	21:1	**228**	21
6	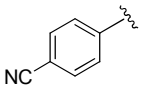	**218**	63	17:1	**229**	0[f]
7	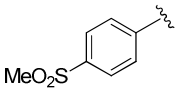	**219**[e]	67	>25:1	**230**	16
8	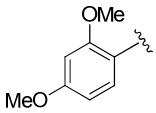	**220**	57	6:1	**231**	29
9	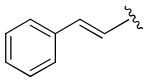	**221**	68	>25:1	**232**	19
10	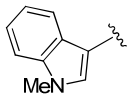	**222**	50	10:1	**233**	29
11	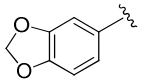	**223**	58	32:1	**234**	27

[a]d.r. measured by extended acquisition of crude on 500 MHz ^{1}H NMR NMR [b]Triplicates have been performed in each case. Measured dr is reproducible and reported as an average [c]Yield based on amount of EICR product that degradation product corresponds to. [d]LiHMDS added to a solution of substrate and TMSCl. [e]Substrate added as a solution in THF at 20 mg/mL, as opposed to standard 100 mg/mL. [f]Clean isolation not accomplished.

Table 7. Results for Substituted Arylacetate Substrate Rearrangements.

Over all eleven examples of *para*-substituted arylacetate rearrangements, capricious levels of diastereochemical control are observed varying from 6:1 for the electron rich *para*-dimethylamino **213**, to 60:1 for the *para*-iodo **214** and finally 9:1 for the *para*-nitro **180**. Whilst all *para*-arylacetate rearrangements seemed to fit into a scale of diastereoselectivity based on electron donating/withdrawing capability, it is worth while noting that the *para*-dimethylamino **213** and *para*-sulfone **219** could not be rearranged *via* the optimised protocol and thus cannot reliably be included in any discussions based around mechanistic evaluations. Issues surrounding injecting a solution of the *para*-dimethylamino substrate **202** to LiHMDS and TMSCl in THF were problematic, based on the substrate blocking the injection needle. This problem was circumvented by an inverse rearrangement protocol, in which a solution of LiHMDS was added to a solution of **202** and TMSCl in THF. Issues with the *para*-sulfone **208** were seen to be a general insolubility of the substrate. Following a modified procedure the rearrangement was accomplished *via* addition of sulfone **208** as a solution in THF at 20 mg/ml, as opposed to the standard 100 mg/ml, subsequently yielding an unexpectedly high diastereoselectivity based on its electron withdrawing capability. Rearrangement of the 2,4-dimethoxy arylacetate **220** was seen to occur with reduced diastereocontrol to that of even the *ortho*- **172** and *para*-methoxy arylacetate **174**, presumably a combination of increased electron density and the presence of *ortho*-substitution. The rearrangement of the vinylogous phenylacetate, to give styryl product **221** and also the incorporation of electron donating groups in the form of the dioxolane rearrangement **223** were seen to proceed with excellent levels of diastereocontrol. Marginal increase in diastereocontrol was noted for the rearrangement of the electron rich 3-methyl indole **222**. Again, nearly complete mass balance was recovered with the corresponding methylated arylacetates retrieved during column chromatography.

2.8. Hammett Relationship

The Hammett relationship and its extended forms have been one of the most widely used means for the study and interpretation of organic reaction mechanisms.[124] The relationship was developed by Hammett empirically, from the ionization equilibria of *meta*- and *para*-substituted benzoic acids in water at 25 ˚C.[125-128]

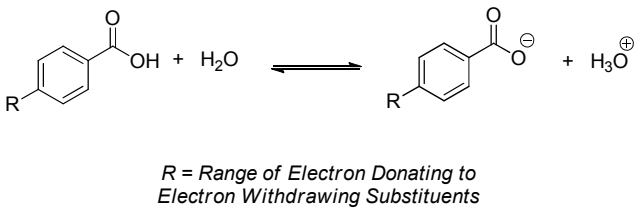

Scheme 77. Ionization of para-Substituted Benzoic Acids.

These values led Hammett to note the existence of a linear free energy relationship between the acidities of substituted benzoic acid derivatives and the rates of many chemical reactions through a simple formula-[129,130]

$$\log \frac{k}{k_0} = \sigma\rho = \log \frac{K}{K_0}$$

Equation 1. Hammett Equation.

From this, k and K refer to the rate constant and equilibrium constant respectively for a substituted reactant, k_0 and K_0 are the corresponding quantity for the unsubstituted reactant. The substituent constant, σ, is a value unique to the type of substituent and is a reflection on how electron-donating ($-\sigma$) or electron-withdrawing ($+\sigma$) that substituent is relative to hydrogen. The substituent constant σ, represents the sum of the total electrical effects of resonance R and field F, considerations of a substituent. The reaction constant, ρ, is dependant upon the reaction type but not on the substituent used and measures the susceptibility of the reaction to electronic effects. Graphical representation of the Hammett relationship allows clear indication of ρ, where a build

up of electrons towards (+ρ) or removal of electrons away from the aromatic ring (-ρ) may occur with in the rate determining step of the reaction.

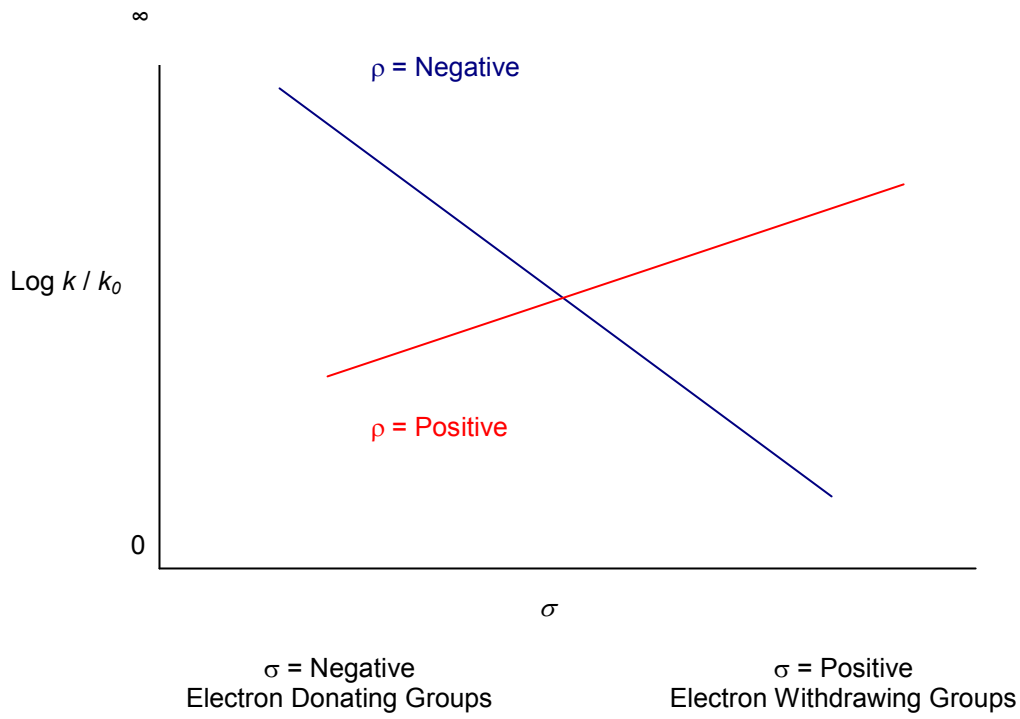

Fig. 11. Typical Hammett Plot.

Reactions that generate a positive ρ value typically involve nucleophilic attack on a carbonyl group, such as in the case of the alkaline hydrolysis of a variety of *meta*- and *para*-substituted ethyl benzoates where ρ = +2.5.[129] This value indicates that the reaction responds to substituent effects in the same way as the ionization of the corresponding benzoic acids, but is enhanced by a factor of 2.5. When ρ is positive the overall rate of reaction reduces with electron donating substituents. Reactions that generate a negative ρ value typically involve loss of electron density from the aryl ring and the overall rate of reaction decreases by the presence of electron withdrawing substituents. The S_N2 alkylation of *meta*- and *para*-substituted phenoxides with ethyl iodide leads to a ρ value of -1.0.[129]

In addition to linear Hammett plots, non-linear Hammett plots can also provide information about the mode of reaction through curvature of the plot. Generally a ‘‘concave-up’’ curve alludes to a change in the mechanism or transition state of the

reaction, however, the ‘‘concave-down’’ curve alludes to a single mechanism with a change in the rate determining step.[131]

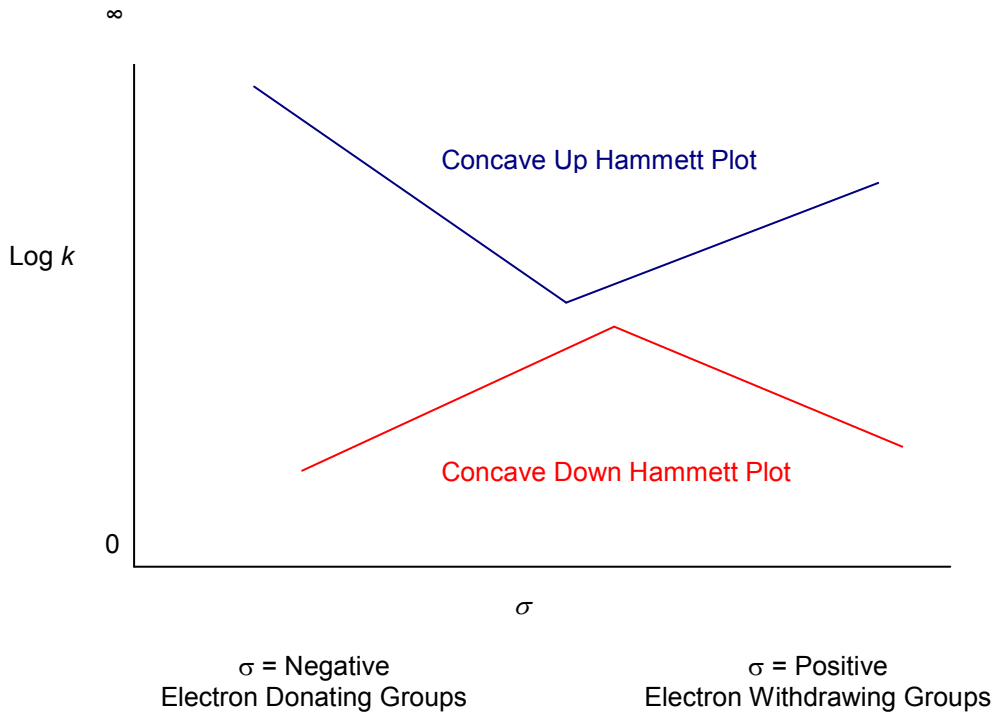

Fig. 12. Typical Non-Linear Hammett Plot.

Examples of a concave up Hammett plot include that of displacement reactions, involving a change between S_N1 and S_N2 for tertiary amine substitutions of *para*-substituted benzylhalides.[132]

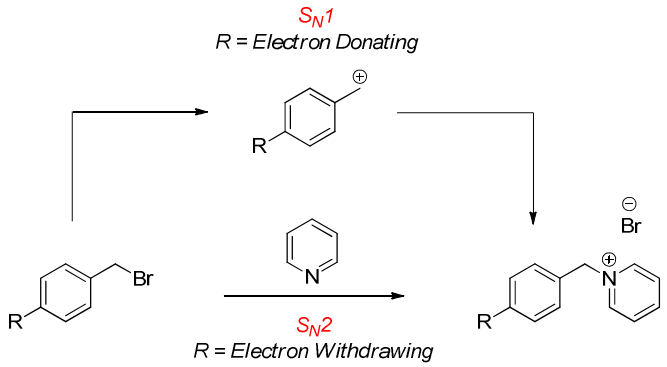

Scheme 78. Change in Mechanism between S_N1 and S_N2 Displacements, Concave Up Hammett Plots.

Examples of a concave down Hammett plot have been observed in the intramolecular Friedel-Crafts alkylation of 2-phenyltriarylcarbinols **235**. Here, formation of carbocation **236** is observed to be the rate determining step for electron withdrawing *para*-substitution and Friedel-Crafts alkylation is observed to be the rate determining step for electron donating *para*-substitution.[133]

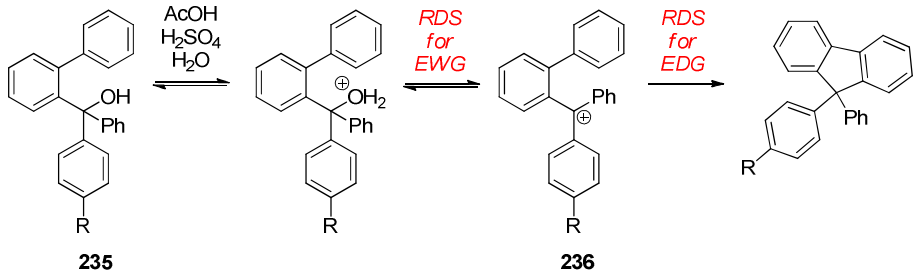

Scheme 79. Change in Rate Determining Step, Concave Down Hammett Plots.

Modifications to the Hammett Equation-

Hammett noted that deviations from his equation were seen for certain substituents within reactions producing a large value of ρ.[125,129,130] Notably, the *para*-nitro substituent was the most troublesome when combined with a reaction centre or group having a much stronger tendency than the carboxylate ion to supply electrons, such as aniline and phenol derivatives. It was noted that a unique σ value could not be used for this substituent and this led to the development of modified σ values for this, and other substituents that can enter into direct resonance with the reaction site in the transition state. From this two new sets of parameters were devised namely σ^-, developed by Hammett and σ^+ values developed by Brown.[125,129,130,134-135] For cases where an electron withdrawing group interacts with a developing negative charge in the transition state, the σ^- value would be best suited, and for cases where an electron donating group interacts with a developing positive charge in the transition state, the σ^+ value would suffice.

There have been a variety of further modifications to the Hammett equation, however the most pertinent are the Taft, Yukawa-Tsuno and the Swain-Lupton equations.[136-141] The Taft equation correlates field effects in the absence of resonance effects and was

generated from the assumption that steric and resonance effects were equal within the hydrolysis of propionate esters, catalysed by acid or base conditions.[136-138] This assumption led to the conclusion that rate differences would only be caused by the field effects of substitution of a propionate derived ester and the nature of the corresponding alcohol it is derived from. The field effects of substituents could therefore be determined by measuring the rates of acid- and base-catalysed hydrolysis of a series of propionate derived esters, providing the alcohol constituent remains constant. The observed rate constants lead to a new form of the Hammett equation based on a redefinition of σ as σ_I. Here $(k/k_0)_B$ is the rate constant for basic hydrolysis of the substituted propionate ester, divided by the unsubstituted propionate ester and $(k/k_0)_A$ is the rate constant for acidic hydrolysis of the substituted propionate ester divided by the unsubstituted propionate ester.

$$\log \frac{k}{k_0} = \sigma_I \rho_I$$

$$\text{where,} \quad \sigma_I = 0.181 \left[\log \left(\frac{k}{k_0} \right)_B - \left(\frac{k}{k_0} \right)_A \right]$$

Equation 2. The Taft Equation.

The major disadvantage of the Taft equation, even though it considers propionate esters in addition to the benzoic systems, are that steric and resonance effects (if possible) are not considered and if these are present then the equation fails. Taft has subsequently been able to isolate steric effects, E_s, but again only in cases where resonance interactions are absent, leading to a value that is proportional to the size of substituent. The modified Taft equation is –

$$\log \frac{k}{k_0} = E_s$$

Equation 3. Modified Taft Equation.

The Yukawa-Tsuno modification incorporates an enhanced resonance parameter *r*, that provides a measure of resonance stabilisation for positive or negative charge build up within the transition state structure.[141] The Yukawa-Tsuno equation independently utilises both σ^+ and σ^- values, depending on which substituent constant is under consideration.

$$\log \frac{k}{k_0} = \rho(\sigma + r(\sigma^{+/-} - \sigma)) = \log \frac{K}{K_0}$$

Equation 4. Yukawa-Tsuno Modified Hammett Equation.

The enhanced resonance parameter *r*, is determined *via* the ρ value for a given reaction. Calculation of *r* then allows the resonance considerations of a particular reaction be inferred. When $r = 0$ there are no resonance differences seen compared to that of the unsubstituted compound, however when $r > 0$ the reaction is more sensitive to resonance effects and when $r < 0$ the reaction is less sensitive to resonance effects than the unsubstituted compound.

The Swain-Lupton equation retains the idea of a practical distinction between the field, *F* and resonance, *R* contributions.[139-140] The substituent constant is therefore a combination of a numerical constant, *F* and *R*, which are independent of reaction, solvent and temperature.

$$\log \frac{k}{k_0} = \sigma\rho = \log \frac{K}{K_0}$$

$$\text{where } \sigma = 0.921F + R$$

Equation 5. Swain-Lupton Modified Hammett Equation.

Further modifications to the resonance parameter have been made in order to fully account for instances where strong resonance interaction occurs between reaction centre and substituent, of which *R* has been further optimised into R^+ and R^-, to coincide with σ^+ and σ^- constants.

2.9. Hammett Relationship & EICR

The Hammett relationship is an important tool that allows information about the mode and transition state structure of individual types of reactions be inferred. In order to explain the varied diastereoselectivity observed in the EICR of the electronically differentiated *para*-substituted arylacetates, we turned to the Hammett relationship. As rate constants for the EICR were lacking, utilisation of the observed diastereoselectivities were pursued in order to perform a Hammett type analysis. Although the use of diastereoselectivity is not purely Hammett based, its use has seen success within various types of reactions, including radical reactions, aminohydroxylations and Diels-Alder reactions.[142,143,144] It is important to note that log(d.r.) is under conditions of kinetic control and is proportional to the free energy difference between the two alternative transition states for formation of *anti*- and *syn*-diastereomers and is therefore considered a ratio of rate constants. Taking this in to account the Hammett equation takes the following form-

$$\log\left(\text{d.r.}\frac{anti}{syn}\right) = (\rho_{anti} - \rho_{syn})\sigma$$

Equation 6. Hammett Equation in Terms of d.r.

In order to examine any Hammett type relationships present, the log(d.r.) for all *para*-substituted rearrangements, except the *para*-dimethylamino **213** and the *para*-sulfone **219** were plotted against substituent constants σ, σ^+ and σ^- (see appendix). As these plots revealed no visible correlation, further investigation into the nature of the substituent constant σ, led us to probe the resonance *R* parameters, based on the Swain-Lupton modification.[124] Again poor correlations were observed with *R* and R^+ (see appendix), however utilisation of R^- demonstrated excellent correlation (Graph 1). Perhaps this result demonstrates that the diastereoselectivity of the EICR is purely dependant on the electron withdrawing resonance effects of substitution, independent of field effects, hence why poor correlations were observed for previous plots.

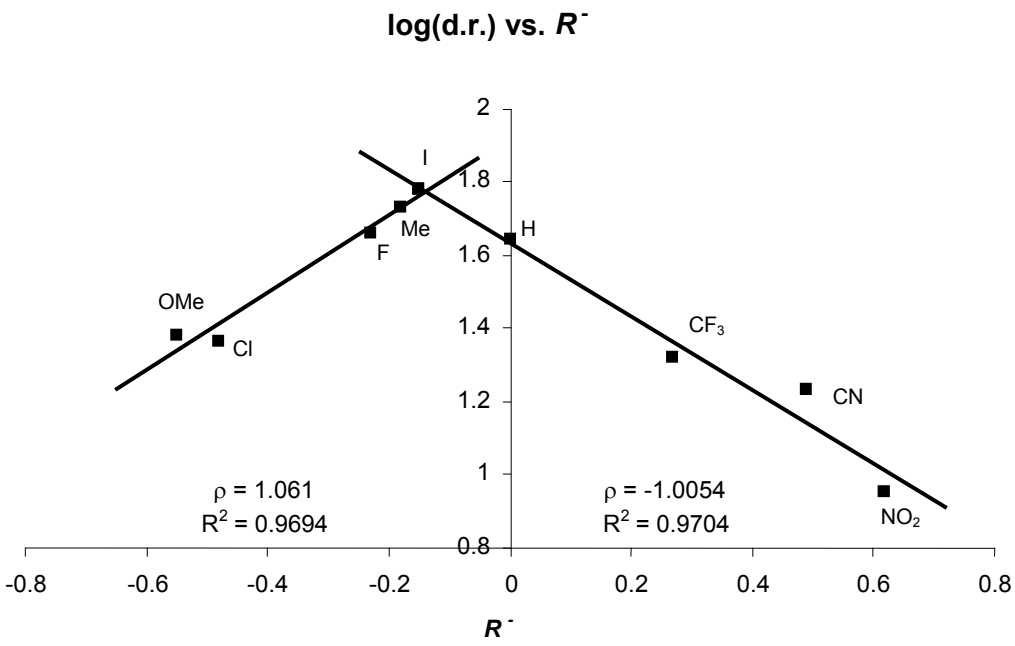

Graph 1. Log(d.r.) vs Resonance Parameter R^-.

The significance behind a non-linear Hammett plot arises when the mechanism of a reaction changes or when the measured rate constant is a combined quantity depending on the rate and equilibrium constant of several reaction steps. In the case of the varying diastereocontrol observed within the EICR, the non-linear relationship arises from the relative rates of reaction producing both the *syn*- and *anti*- diastereomers. This however, may arise from *either* a change in rate-determining step *or* a change in mechanism occurring for a particular diastereomer. Several viable scenarios are available to explain this break in Hammett type plot (Fig 13-17).

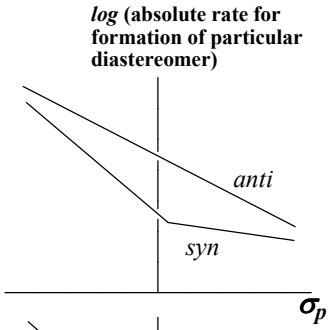

Fig. 13. *No change in RDS or mechanism occurs for the reaction producing the anti-diastereomer across the range of substituents considered; a change in mechanism occurs for electron withdrawing groups in the reaction producing the syn-diastereomer.*

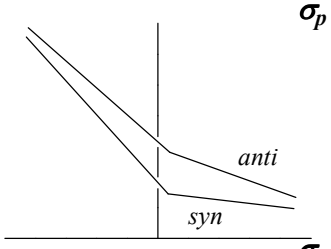

Fig. 14. *Change in mechanism occurs for reactions producing both syn- and anti-diastereomers.*

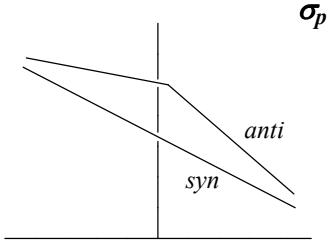

Fig. 15. *Change in RDS occurs for the mechanism producing the anti-diastereomer across the range of substituents considered; no change in RDS or mechanism occurs for the reaction producing the syn-diastereomer.*

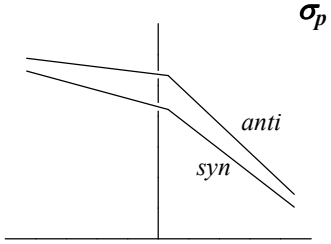

Fig. 16. *Change in RDS occurs for reactions producing both syn- and anti-diastereomers*

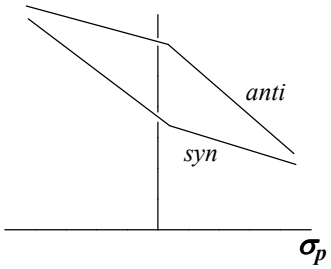

Fig. 17. *Change in RDS occurs for the reaction producing the anti-diastereomer; change in mechanism occurs for the reaction producing the syn-diastereomer.*

Perhaps the least likely scenarios are that resulting in figures 13, 15 and 17, as these require that diastereomeric transition states respond in fundamentally different fashions to electronic perturbations. Consequently we suppose that either a dual change in either the reaction mechanism (Fig. 14) or the rate-determining step (Fig. 16) for both diastereomeric transition states occurs. Assuming that we thus exclude scenarios resulting in figure 13, 15 and 17 from consideration then, in principle, we may distinguish between scenarios in figure 14 and 16 on the basis of absolute rate studies.

It is seen from the Hammett type plot (Graph 6.), that the overall preference of formation of the *anti*- over the *syn*-diastereomer decreases with increasing electron withdrawing substituents and is consistent with an observation made by Houk in studying similar effects in the related Claisen rearrangement.[145] If the absolute rates of reaction tended toward an increase with increasing electron withdrawing substituents on the aryl group, a change from a concerted mechanism to one involving the formation of an intimate ion pair may represent the change in mechanism giving rise to figure 14. However, it has been shown that electron withdrawing aryl groups in the related Claisen rearrangement retard the reaction, therefore the scenario in figure 16 may be best suited, reconfirming that a change in rate determining step of the EICR occurs.[85, 146-148]

2.10. Conclusions

From the experimental observations, the Enamido-Ireland-Claisen-Rearrangement of a range of electronically differentiated arylacetate enamido esters has proven intruiging. The conspicuous range of diastereoselectivities observed, certainly in the case of the *para*-substituents, has been postulated to be caused by a variety of factors, including issues surrounding initial enolisation, isomerisation of the enolate once formed, isomerisation of the silyl ketene acetal, chair/boat considerations of transition state structure, non-concerted character and post-rearrangement epimerization issues. The issues surrounding post-rearrangement epimerization have subsequently been discounted based on a range of control experiments performed. On consolidation of the residual factors which may be respnsible for the observed diastereoselectivity, this may be seen by thermodynamic issues of *E/Z*-silyl ketene acetal control, thus causing the observed diastereoselectivity assuming that the rearrangement occurs *via* a predictable chair transition state. A more complicated possibility may also involve contributions from all four diastereomic transition states (Scheme 70). In addition, the caveat observed by the concave down Hammett plot may be the result of a change in mechanism *or* a change in rate determining step. A change in mechanism may involve that of a concerted one-step mechanism for electron donating susbtituents and a non-concerted two-step mechanism for electron withdrawing substituents, whereas a change in the rate determining step may be due to either SKA formation or a diastereoselective rearrangement. Discussions surrounding the mechanistic evaluation of the EICR are to be focussed in Chapter 3.

3. Mechanistic Insight into the EICR of Arylacetates

With the intriguing range of diastereoselection observed for the electronically differentiated arylacetates, a range of mechanistic studies were performed in order to determine the origin of diastereoselection.

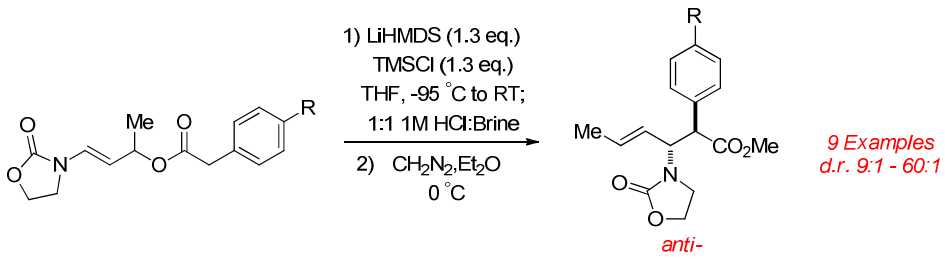

Scheme. 80. para-Substituted Substrates & Associated Diastereoselectivities from EICR.

These mechanistic studies were focussed on determining whether diastereoselection is an aspect of:

1) Initial formation of variable isomeric *E*- and *Z*-SKA mixtures, which rearrange through a chair transition state, *or*,
2) Rearrangement through competing chair and boat transition states, assuming selective *E*-SKA formation.

To probe these considerations, *in-situ* NMR studies were conducted. Initially, these studies involved the generation and *E/Z* monitoring of electronically differentiated model SKA's, designed to mimic the enamido ester substrate. Further studies then involved *in-situ* rearrangement monitoring of strongly electron deficient, electron rich and electron neutral enamido arylacetate substrates. It was envisaged that rearrangement monitoring would allow *E/Z*-SKA and *anti/syn* product distributions to be observed throughout the course of reaction and provide a rationale for the varied diastereoselectivities observed.

Other studies have included an *in-house* computational collaboration where-by the full range of electronically differentiated arylacetates have been modelled within the EICR, to examine the theoretical origins of diastereoselectivity.

3.1. Model SKA Studies

Silylketene acetals (SKAs) are themselves valuable nucleophiles and find widespread use within a broad range of *C*-*C* bond forming synthetic chemistry. In addition to use in the Ireland-Claisen rearrangement, they are frequently seen in a range of other reactions including the Mannich and aldol reactions, of which their geometric purity can affect the diastereo- and/or enantioselectivity obtained within the reaction (Scheme 81).[149-150]

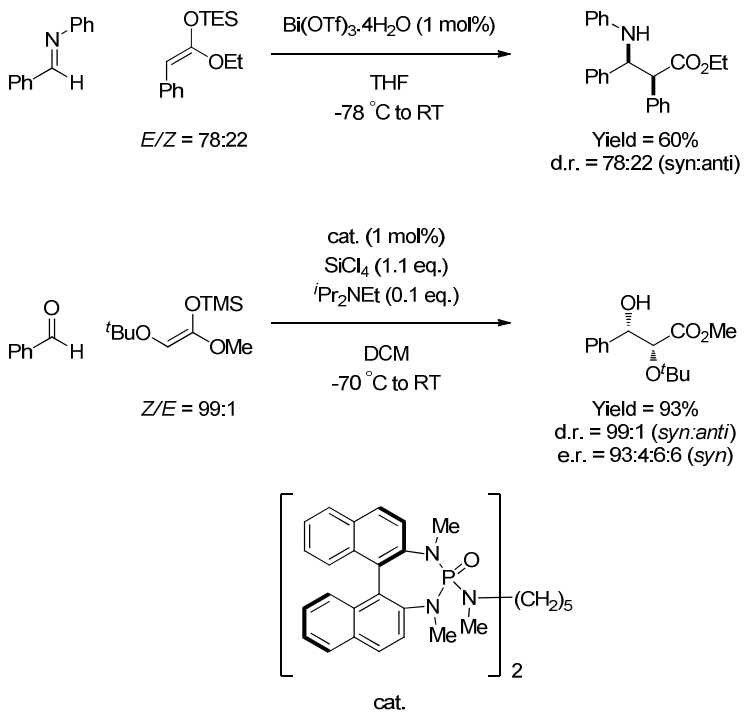

Scheme. 81. Stereoselective &Enantioselective Reactions Involving SKAs.

Recently, the Leighton group has demonstrated the use of an enantio- and diastereoselective Mannich reaction involving phenylacetate derived SKA **237**. This protocol allows synthesis of the β-amino acid precursor **238** in good yield with excellent enantio- and diastereoselectivity.[151]

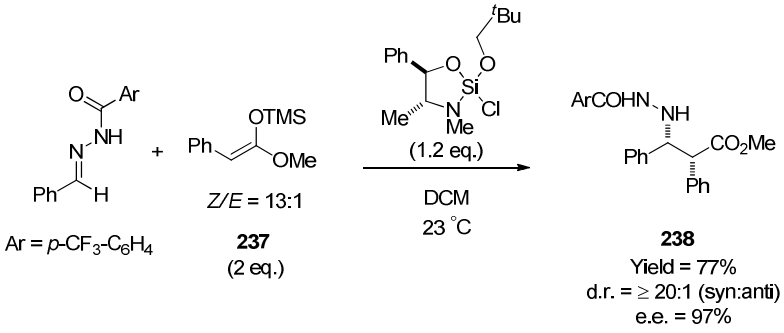

Scheme. 82. Enantio- & Diastereoselective Mannich Reaction.

To examine the issue of *E/Z* control during formation of arylacetate SKAs within our enamide substrates, efforts were focussed on the *in-situ* monitoring of model SKAs. Initial attempts were based on utilisation of the commercially available isopropyl phenylacetate **239**, as the EICR of the corresponding phenylacetate **154** was shown to produce high levels of diastereoselectivity and presumably generate high *E/Z*-SKA purity. Also, the secondary ester motif was chosen to mimic the secondary carbinol-derived center within enamido ester substrate.

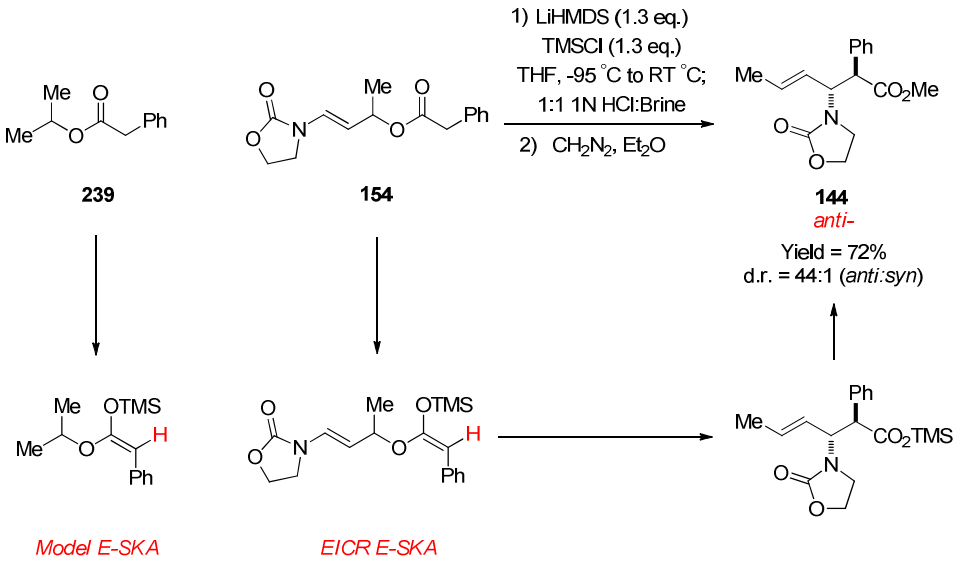

Scheme 83. Initial Model Substrate for SKA Investigation.

In order to follow the *in-situ* generation of SKAs by ^{1}H-NMR spectroscopy, it was important that this experimental protocol mirrored the standard laboratory procedure for the EICR as closely as possible. Initiation of these *in-situ* experiments therefore

relied on the use of an oven dried Young's tap NMR tube with the dropwise addition of a solution of substrate to LiHMDS and TMSCl at -95 ˚C, under 1 atmosphere of nitrogen. Once the NMR tube was sealed, it was then transferred to the 400 MHz spectrometer, precooled to -95 ˚C, prior to NMR experimentation.

As the consumption of **239** and formation of *E/Z*-SKA's were the main aim of this experiment, a range of temperatures for data acquisition were decided. As data were to be recorded at the intiation temperature (-95 °C) and room temperature (25 °C), an intermediary temperature was also required. Ideally, this intermediate temperature would represent the onset of rearrangement within the EICR and correspond to the stage where a ratio of generated *E/Z*-SKA's will be transferred to the observed diastereoselectivity in the product. In order to determine this temperature, several experiments were performed to estimate the onset of rearrangement of phenylacetate **154**. This was achieved by intiation of several phenylacetate EICR's prior to warming to a variety of temperatures over 1 hour. Quenching at these cryogenic temperatures was accomplished by methanol.

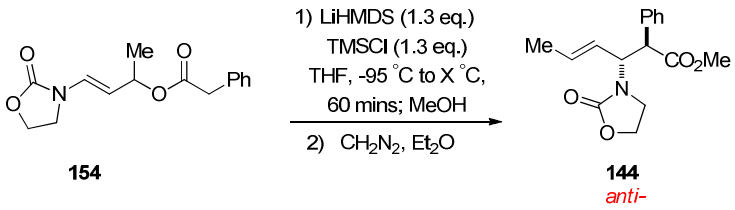

154 **144** *anti-*

Entry	Temperature (°C)	Yield (%)	d.r.[a] (*Anti:Syn*)
1	-95	12	n.d.[b]
2	-80	27	n.d.[b]
3	-60	40	41:1
4	-50	54	42:1
5	-40	56	39:1
6	-20	59	40:1

*[a]d.r. measured by extended acquisition of crude on 500 MHz ^{1}H NMR [b]d.r. not determined due to broad spectra and low conversion to **144**.*

*Table 8. Temperature Investigation into EICR of **154**.*

These results suggest that rearrangement is even observed at initiation temperature with diastereoselectivity relatively invariable across the quench temperatures tested (excluding Entries 1 & 2, Table **8**). From the variety of temperatures tested, -50 °C was chosen for data acquisition, as this demonstrated an adequate temperature where >50% of EICR product **144** was isolated.

With the range of temperatures for data recordal set, utilisation of isopropyl phenylacetate **239** was pursued. Initial experiments monitoring the consumption of **239** and formation of *E/Z*-SKA's **240** at -95 °C , -50 °C and 25 °C were shown to be entirely feasible. Furthermore, standard H_8-THF could be used within NMR experimentation. However, clean quantification of the minor *Z*-SKA became difficult due to its coincidence with the isopropyl methine signal as demonstrated in Scheme 84.

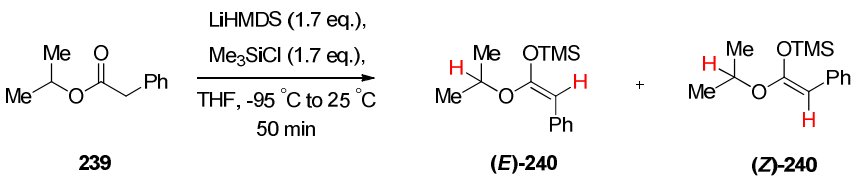

Scheme 84. Initial Attempts at SKA Reaction Monitoring.

It is noted that an increase in the loading of LiHMDS and TMSCl was required, as 40% of phenylacetate **239** remained when applying the standard 1.3 equivalents of base and silylating agent. Although an increase in the stoichiometry of reagents within the model SKA studies is in direct contravention to EICR conditions, the retrieval of methylated arylacetate degradation products post rearrangement (Chapter 2) may derive from an incomplete SKA formation and substrate hydrolysis on protic quench.

To counteract the problem of coincident ^{1}H resonances, it was decided to examine the use of $^2H_1$-isopropyl phenylacetate **^{2}H$_1$-239** instead, which was synthesised in good yield.

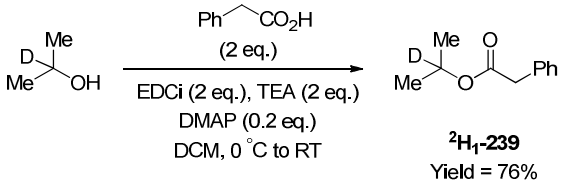

Scheme 85. Synthesis of $^{2}H_{1}$-Isopropyl Phenylacetate ***$^{2}H_{1}$-239****.*

With **$^{2}H_{1}$-239** in hand, *in-situ* SKA formation was pursued. The $^{2}H_{1}$ modification allowed succesful monitoring of *E*- and *Z*-SKA, with formation of Li-enolate not detected using this NMR analysis. The data obtained from this experiment demonstrated that a single *E*-SKA is observed at -95 °C, however on warming to -50 °C and 25 °C erosion of the *E/Z* purity occurs (*E/Z* = 61:1 and 30:1, Figure. 18).

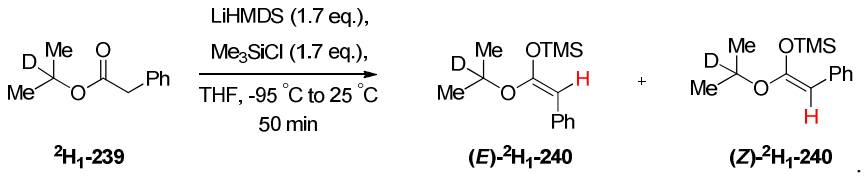

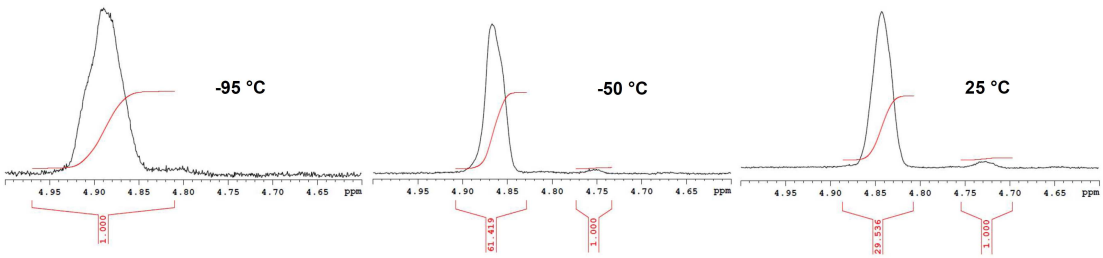

Figure 18. Variable Temperature ^{1}H-NMR study of E/Z-SKA Formation of Phenylacetate ***$^{2}H_{1}$-239****.*

As complete formation of SKA was only observed at 25 °C, an investigation into the formation and time dependance of the *E/Z* ratio was pursued at -50 °C. Interestingly, an initial fast, yet partial consumption of **$^{2}H_{1}$-239** was observed, associated with an intriguing inflexion, with **$^{2}H_{1}$-239** accumulating within the reaction mixture prior to its further consumption (Graph 2).

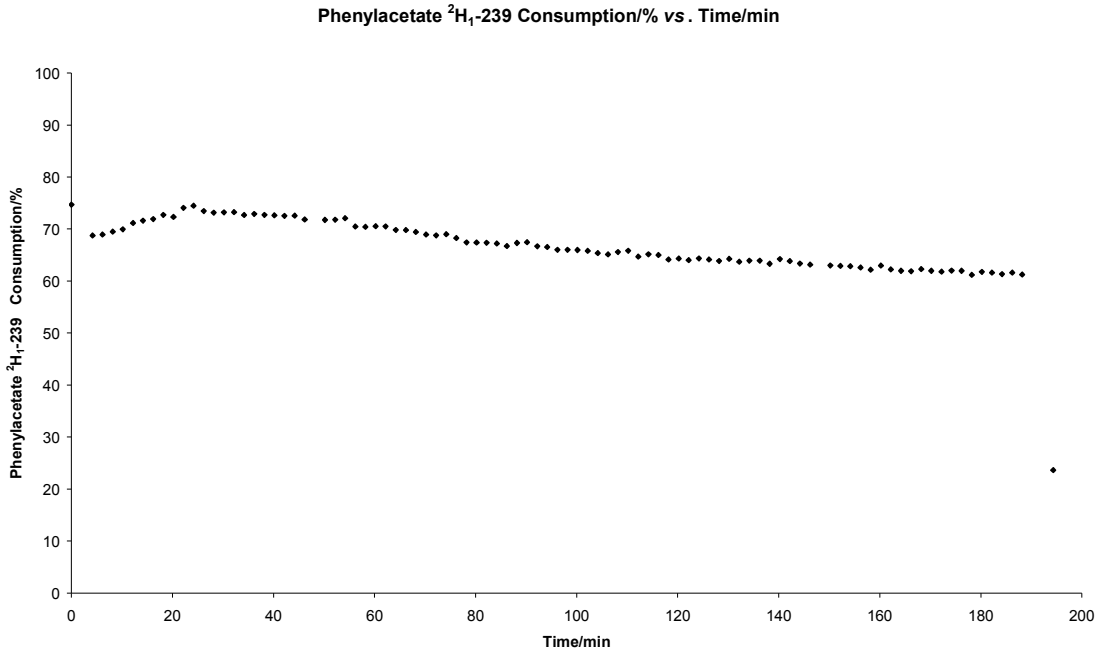

Graph 2. Time Dependence of ***$^2H_1$-239*** *Present in the Formation of SKA* ***$^2H_1$-240*** *at -50 °C. Initial & Final Data Point Refer to Monitoring at -95 °C & 25 °C.*

During this reaction, high levels of *E/Z*-SKA purity are observed and a plateau is evident at -50 °C. On warming to room temperature a drastic reduction in *E/Z* ratio results and is attributed to thermodynamic *E/Z*-SKA generation.

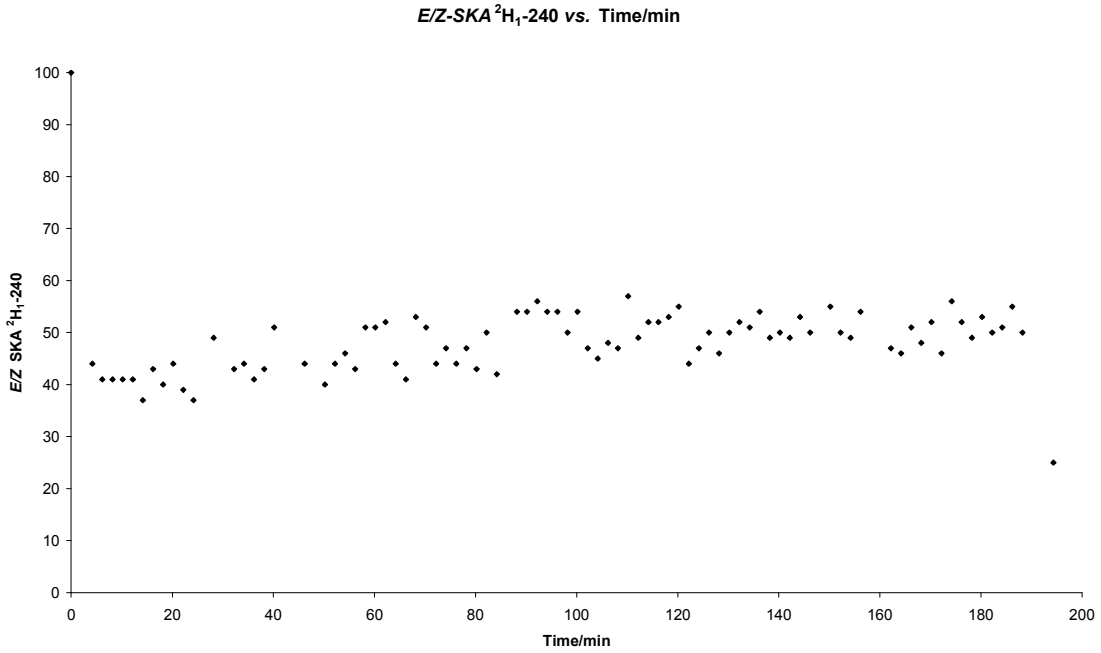

Graph 3. Time Dependence of E/Z-Purity in the Formation of ***(E)-$^2H_1$-240*** *at -50 °C. Initial & Final Data Point Refer to Monitoring at -95 °C & 25 °C.*

These *in-situ* observations concerning the high levels of *E/Z*-SKA purity obtained from phenylacetate $^{2}\mathbf{H_1}$**-239**, are in stark contrast to that previously reported in the literature. Attempts involving phenylacetate **239** with LDA and an external TMSCl quench 30 minutes after initiation at -78 °C and that involving **158** with LiHMDS and an internal TMSCl quench, generate isolated *E/Z*-SKAs of no greater than 4:1.[119-120, 152]

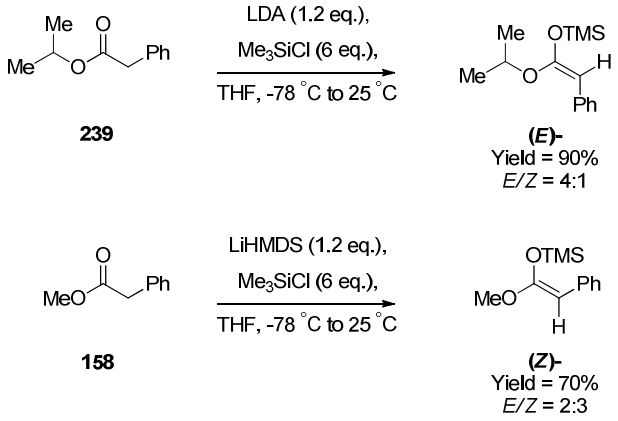

Scheme 86. Previous Attempts at Isolating Phenylacetate SKAs.

Subsequent studies have demonstrated that enolisation under kinetic conditions selectively forms the *Z*-enolate, however, difficulties in enolate trapping results in the generation of SKAs with poor *E/Z* control.[119-120, 152-155]

This dogma presented in the literature is intriguing, as our *in-situ* NMR experiments have clearly shown that SKA generation is accomplished with high *E/Z* purity. In order to discerne the key factors associated with generating high levels of *E*-SKA purity, a number of variables involving the type of amide base, stoichiometry of TMSCl and the nature of enolate quench were investigated (Table 9).

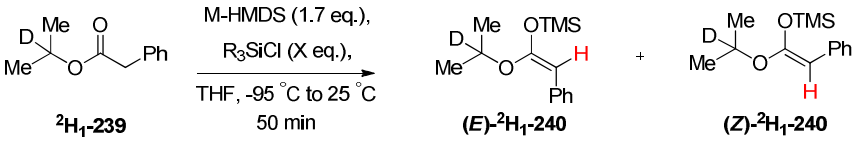

^{2}H$_1$-239 (*E*)-^{2}H$_1$-240 (*Z*)-^{2}H$_1$-240

Entry	M	R (equiv)	^{2}H$_1$-240 (*E*/*Z*)[a]		
			-95 °C	-50 °C	25 °C
1	Li	Me (1.7)	>100:1	61:1	30:1
2[b]	Li	Me (1.7)	71:1	42:1	16:1
3	Li	Me (6)	>100:1	>100:1	64:1
4[c]	Li	Me (6)	>100:1	>100:1[d]	56:1
5	Li	Me (1.7)[e]	>100:1	8:1	5:1
6	Li	Me (1.1)	>100:1	>100:1	33:1
7	Na	Me (6)	-	8:1	6:1
8	Li	^{i}Pr (6)	>100:1	10:1	4:1
9	Li	Et (6)	>100:1	>100:1	22:1
10	-[f]	Me (6)	4:1	4:1	4:1

[a]E/Z Ratio Measured by ^{1}H-NMR Integration of Appropriate SKA Signals. [b]Initiated at -78 °C [c]Observed at -65 °C for 60 mins. [d]Observed at -25 °C. [e]External Quench: TMSCl Added to Reaction Mixture 30 Minutes After Initiation of Enolate Generation [f]LDA Used as Base.

Table 9. Control Experiments

These results clearly demonstrate that the manner of reaction initiation, temperature control and enolate lifetime are key parameters in accessing high levels of *E*/*Z*-SKA purity. Reduced *E*/*Z* control was observed with intiation at higher temperatures (entry 2), the use of an external quench (entry 5) and lower loadings of TMSCl (entry 6). However, increasing the levels of TMSCl led to a more rapid silylation and reduced *E*/*Z* interconversion (entries 4 & 5) and it is noted that complete silylation was observed after 20 minutes at -50 °C. Other drastic reductions in *E*/*Z* purity were seen to occur when the use of bulkier silylating agents (entries 8 & 9) and alternative amide bases including NaHMDS and LDA (entries 7 & 10) were used. The generation of high *E*/*Z*-SKA purity (entry 3) was even observed to retain a significant excess of the *E*-geometrical isomer at room temperature (10:1) 48 hours after its formation.

The successful observations associated with *E/Z*-SKA formation and interconversions prompted us to return to the primary aim of this model SKA study, associated with examining SKA formation for a range of electronically differentiated *para*-substituted arylacetates. As these studies were designed to mimic formation of the SKA during EICR, it was hoped that indications into whether similar or varied *E/Z*-selectivities would be generated and potentially allude to whether diastereoselection in our rearrangement is a function of generated *E/Z*-SKA ratio. With this in mind, synthesis of a variety of model *para*-substituted arylacetates was acheived in excellent yield, *via* the familiar EDCi coupling conditions and monitoring SKA formation by *in-situ* NMR methods was subsequently pursued.

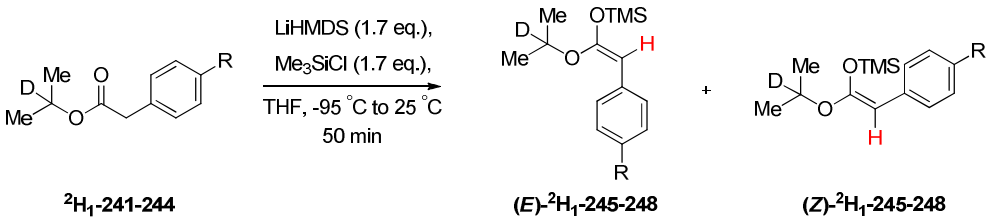

$^2H_1$-241-244 (*E*)-$^2H_1$-245-248 (*Z*)-$^2H_1$-245-248

Entry	Ester	R	SKA	*E/Z*			d.r. from EICR (*anti:syn*)
				-95 °C	-50 °C	25 °C	
1	**$^2H_1$-239**	H	**$^2H_1$-240**	>100:1	61:1	30:1	44:1
2	**$^2H_1$-241**	OMe	**$^2H_1$-245**	>100:1	>100:1	21:1	24:1
3	**$^2H_1$-242**	Me	**$^2H_1$-246**	>100:1	>100:1	39:1	54:1
4	**$^2H_1$-243**	CF_3	**$^2H_1$-247**	>100:1	>100:1	34:1	21:1
5	**$^2H_1$-244**	NO_2	**$^2H_1$-248**	>100:1	44:1	11:1	9:1

[a] Ester Added to TMSCl (1.7 eq.) and LiHMDS (1.7 eq.) in THF at -95 °C & Subsequent Transferral to the Cooled 400 MHz Spectrometer. [b] *E/Z* Ratio Measured by ^{1}H NMR Integration of Appropriate Signals. *E/Z* Geometrical Isomers Proven by 1D NOE Experiments on *para*-Tolyl ***$^2H_1$-246*** (See Appendix).

Table 10. Synthesis of para-Electronically Differentiated Ester Substrates and In-Situ Formation of Corresponding SKAs.

At the initiation temperature all substrates demonstrated selective formation of the *E*-SKA. On warming to -50 °C similar selectivities were observed, however a significant drop in geometric purity was noted for the nitro-substituted substrate (entry 5). Subsequent warming to 25 °C demonstrates a global erosion of *E/Z*-SKA

purities, all with varying levels. From these results it is obvious that the degree of *E/Z*-SKA purity generated depends strongly on the electronic nature of substitution. When comparing these *in-situ* SKA ratios to that of the diastereochemical outcome of the EICR for the same substituent, a similar ratio is observed, particularly so for the OMe and NO_2 substituents (entries 2 and 5). These results strongly suggest that *E/Z*-SKA formation may strongly influence the observed diastereomeric outcome of the associated EICR.

To further probe this electronic dependance of *E/Z*-SKA control we wanted to observe whether primary and teritiary derived arylacetates exhibited similar effects. With this in mind synthesis of a small range of model substrates based on electron withdrawing (-NO_2), electron donating (-OMe) and electron neutral (-Me) *para*-substitution was undertaken and subjection of these to *in-situ* SKA monitoring was pursued (Table 11). Interestingly, the range of methyl esters were seen to demonstrate similar dependancies to the isopropyl phenylacetates (entries 1-3). However, diminshed *E/Z* purity was observed for the tertiary arylacetates (entries 4-6), with the *p*-NO_2 substrate offering no selectivity at room temperature (entry 6).

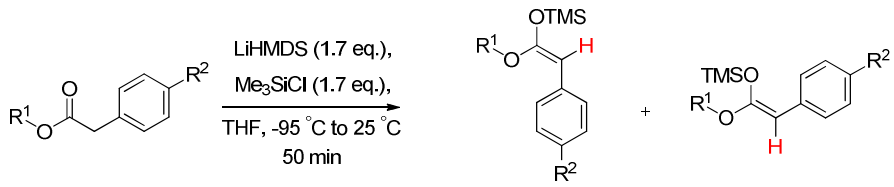

249-254 **(*E*)-255-260** **(*Z*)-255-260**

Entry	Ester	R^1	R^2	SKA	*E/Z* -95 °C	*E/Z* -50 °C	*E/Z* 25 °C
1	**249**	Me	OMe	**255**	>100:1	>100:1	25:1
2	**250**	Me	Me	**256**	>100:1	>100:1	26:1
3	**251**	Me	NO_2	**257**	>100:1	91:1	23:1
4	**252**	CMe_3	OMe	**258**	>100:1	14:1	8:1
5	**253**	CMe_3	Me	**259**	39:1	28:1	18:1
6	**254**	CMe_3	NO_2	**260**	>100:1	32:1	1:1

[a] Ester Added to TMSCl (1.7 eq.) and LiHMDS (1.7 eq.) in THF at -95 °C & Subsequent Transferral to the Cooled 400 MHz Spectrometer. [b] *E/Z* Ratio Measured by ^{1}H NMR Integration of Appropriate Signals. *E/Z* Geometrical Isomers Proven by 1D NOE Experiments on *p*-Tolyl **256** & **259** (See Appendix).

Table 11. Synthesis of para-Electronically Differentiated Methyl & ^{t}Butyl Ester Substrates and In-Situ Formation of Corresponding SKAs.

Considering the results from the primary, secondary and tertiary derived arylacetate SKAs, the influence of the aromatic substituent is clear. Although initial *E/Z*-SKA selectivity is high, the presence of strongly electron withdrawing or donating substituents appears to enhance the magnitude of geometrical isomerisation as the reaction warms to room temperature. In the case of the electron withdrawing nitro substituent, erosion of geometric purity could be facilitated by a reduction in C=C bond character *via* mesomeric withdrawal of electrons out of the SKA. In the case of the electron donating methoxy substituent it may be conceivable that electron donation into the SKA may occur, subsequently reducing C=C bond order.

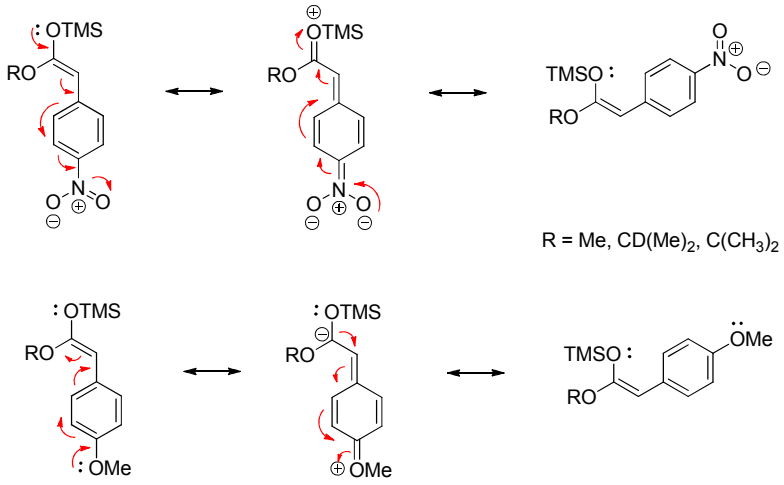

Scheme 87. Postulation for Reduced E/Z-SKA Purity in para-Nitro & para-Methoxy Substitution.

However, although significant reduction in *E/Z*-SKA geometric purity are observed for *para*-nitro and *para*-methoxy variants, their *in-situ* preparation has still been shown to be significantly higher than currently published results.[149, 156-159] As the utilisation of arylacetate SKA's are hindered by their isolation with low *E/Z* purity (≤4:1), the ability to isolate these compounds with the high levels of *E/Z*-control observed in our *in-situ* studies may be synthetically beneficial. With this in mind, utilisation of phenylacetate **^{2}H$_1$-239** was further investigated (Table 14).

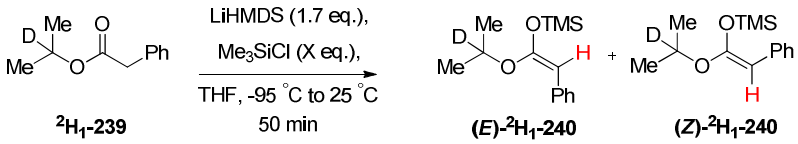

^{2}H$_1$-239 **(*E*)-^{2}H$_1$-240** **(*Z*)-^{2}H$_1$-240**

Entry	Method[a]	X eq.	(*E*/*Z*)[b]	Yield %[c]
1	(A)	1.7	68:1	81
2	(B)	1.7	17:1	88
3	(C)	6	>100:1	82

[a]Methods: (A): Ester added to base and TMSCl *via* syringe pump before warming to room temperature. (B): Ester added to base and TMSCl by hand before warming to room temperature (C): Ester added to base and TMSCl, holding at -95 °C for 30 minutes before warming to room temperature *via* syringe pump. [b]*E/Z* ratio measured by ^{1}H-NMR integration of appropriate SKA signals. [c]Isolated yield.

Table 12. Isolation of $^2H_1$-Phenylacetate-Derived SKA's.

To demonstrate that slow addition of a solution of **$^{2}H_{1}$-239** to LiHMDS and TMSCl was imperative for the generation of high *E/Z*-SKA selectivity, initiation by syringe pump and rapid injection was investigated. Isolation of the SKAs was achieved by rapid vacuum concentration of the reaction mixture and trituration with $CDCl_3$ subsequent to ^{1}H-NMR spectroscopy. In both cases excellent yields were obtained, however as expected, a reduced *E/Z*-SKA purity was obtained for the rapid injection protocol (entry 2) than the controlled addition by syringe pump (Entry 1). This observation corresponds well to the optimisation of the phenylacetate EICR (Chapter 2, Table 3), where the difference in diastereoselection for rapid injection compared to syringe pump addition was 16:1 to 44:1. The final initiation method relied on utilising the increased stoichiometry of TMSCl, as this demonstrated the highest *E/Z*-SKA purity *in-situ* (Chapter 3, Table 9, Entry 3). Employing this method within the generation and isolation of **$^{2}H_{1}$-240** demonstrated an excellent yield and by far the best *E/Z*-SKA selectivity (Entry 3).

With the successful isolation of the secondary phenylacetate ester SKA, isolation of primary and tertiary derived phenylacetate SKA's were also pursued. The synthesis of **158** and **261** were accomplished in good to excellent yields *via* similar carbodiimide coupling conditions and isolation of the corresponding SKA's were pursued utilising the increased stoichiometry of TMSCl (Table 13). In both instances, excellent yields were obtained, with excellent *E/Z* purity observed for the primary SKA (Entry 1) and good *E/Z* purity observed for the tertiary variant (Entry 2).

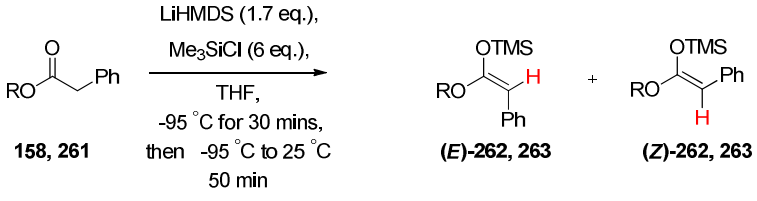

Entry	Ester	R	Product	(*E/Z*)[a]	Yield (%)[b]
1	**158**	Me	**262**	67:1	80
2	**261**	$C(Me)_3$	**263**	25:1	76

[a]*E/Z* ratio measured by ^{1}H-NMR integration of appropriate silylketene acetal signals. [b]Isolated yield.

Table 13. Synthesis of para-Substituted Arylacetates **158** & **261** and Isolation of Corresponding SKA's.

The isolation of these primary, secondary and tertiary derived SKAs in excellent yields and *E/Z* geometrical purities far surpasses any current syntheses.[160] The success observed with an increased loading of TMSCl are not to be ignored and would be expected to have a direct effect on increasing the rate of silyation, as viewed by *in-situ* ^{1}H-NMR studies. This subsequently allows generation and isolation of SKA's with enhanced *E/Z* purities, even compared to the high levels obtained by equimolar 1.7 equivalents of LiHMDS/TMSCl. With this in mind, the ability to improve the diastereomeric ratio of some EICR reactions may be possible. Indeed, subjection of the *para*-nitro and *para*-methoxy enamide substrates to rearrangement conditions involving 6 equivalents of TMSCl does significantly improve the diastereochemical outcome of the rearrangement reaction.

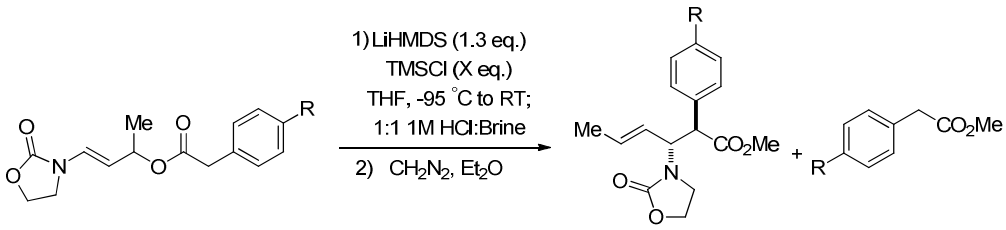

Entry	R	TMSCl (X eq.)	Product	Yield (%)	d.r.[a] (*anti:syn*)	By-Product	Yield (%)[b]
1	OMe	1.3	**174**	77	24:1	**183**	13
2		6		67	82:1		11
3	NO_2	1.3	**180**	76	9:1	**189**	13
4		6		66	16:1		13

[a]d.r. measured by extended acquisition of crude on 500 MHz ^{1}H-NMR [b]Yield based on amount of EICR product that degradation product corresponds to.

Table 14. Results for Improved Arylacetate EICR

3.2. *In-Situ* EICR Reaction Monitoring

The results generated from the model SKA studies have been informative, as they allude to the presence of a relationship between *E/Z*-SKA ratio and diastereoselection based upon electronic perturbation within the EICR. However, in order to prove any such relationship we require the ability to monitor the complete rearrangement, including consumption of substrate, generation of *E/Z*-SKAs and the *in-situ* formation of *anti*- and *syn*-β-amino silylesters. With this in mind, target substrates for investigation include phenylacetate **154**, the strongly electron donating *para*-methoxy arylacetate **165** and the strongly electron withdrawing *para*-nitro arylacetate **171**.

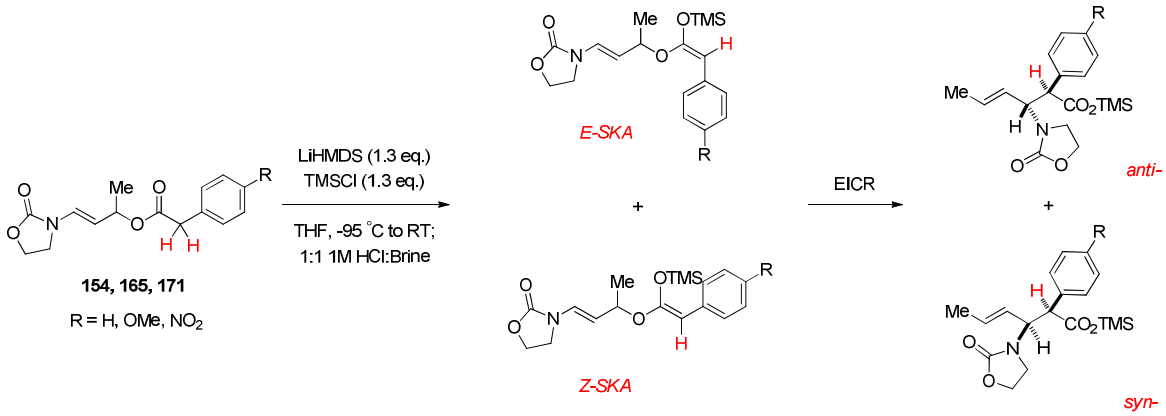

Scheme. 88. EICR Reaction Monitoring; Following the α-H.

Reaction monitoring of the EICR by ^{1}H-NMR spectroscopic analysis would prove logical, based on the successful model SKA studies and could be achieved by similiar monitoring of the α-H in substrate, SKA and rearranged product. However, as a $^{2}H_{1}$-modification was required for the model SKA substrates, the added structural complexity of the enamide substrates would also make tracking the α-H difficult due to coincident ^{1}H-NMR resonances. This consideration is highlighted in Figure 19, exemplifying the key spectral regions associated with phenylacetate **154**, model phenylacetate SKA **$^{2}H_{1}$-240** and β-amino ester **144**.

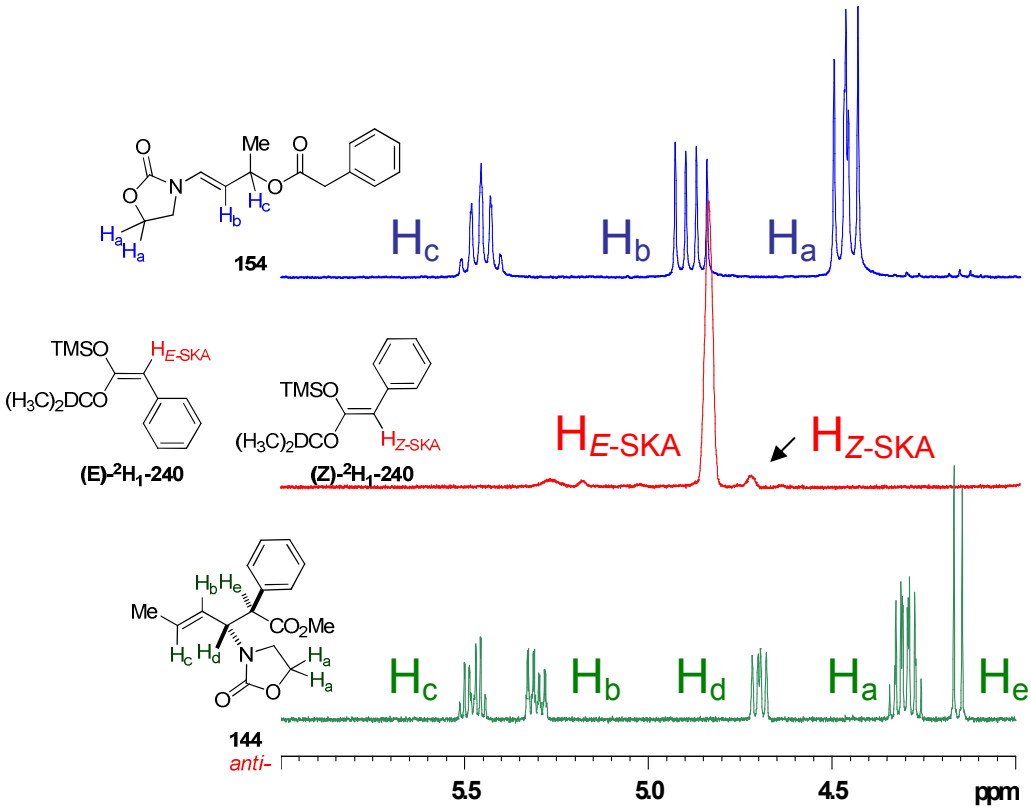

Fig. 19. Overlapping Resonances in EICR Reaction Monitoring.

With this issue in mind, three viable classes of bespoke enamide substrate were conceived, to allow *in-situ* reaction monitoring by ^{1}H-, ^{2}H- and ^{13}C-NMR spectroscopic analysis.

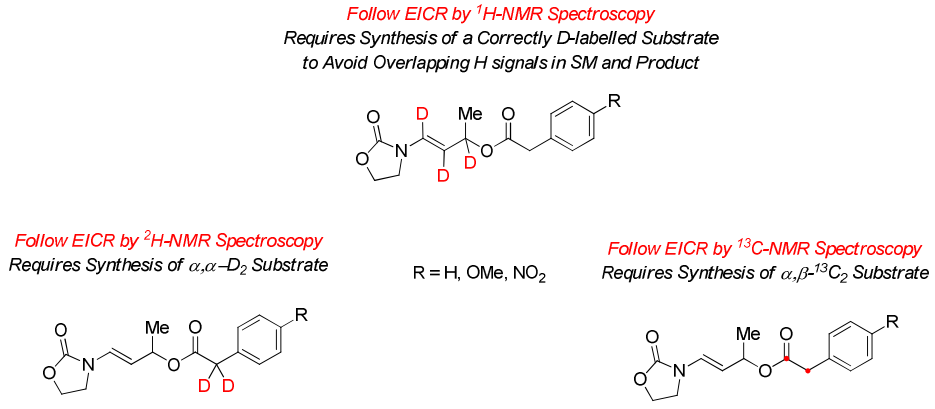

Fig. 20. Modified Enamido Substrates for EICR Reaction Monitoring.

3.2.1. EICR Reaction Monitoring by ^{1}H-NMR Spectroscopy

To overcome the issues associated with coincident ^{1}H-NMR resonances, access to correctly deuterium-labelled substrates were pursued, based on the synthesis of deuterated alcohol **$^{2}H_3$-145**.

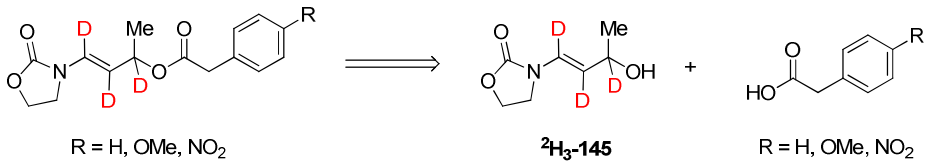

*Scheme 89. Deuterium Labelled Enamido Substrate and Key Intermediate **$^{2}H_3$-145**.*

From the outset, synthesis of **$^{2}H_3$-145** focussed on developing the familiar conditions for the non-deuterated analogue **145**. As formation of ketone **146** relies on a DABCO catalysed addition of 2-oxazolidinone **147** and ketone **148**, it was envisaged that the synthesis of deuterated ketone **$^{2}H_2$-146** could be achieved from deuterated ketone **$^{2}H_1$-148** and *N*-deuterated 2-oxazolidinone **$^{2}H_1$-147**.

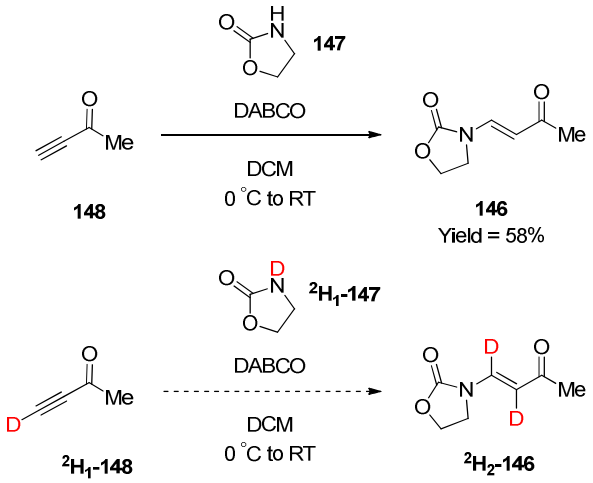

*Scheme 90. Route to Deutero Ketone **$^{2}H_2$-146**.*

Access to deuterated ketone **$^{2}H_2$-148** required synthesis of deuterated alcohol **$^{2}H_1$-149** prior to Jones oxidation. Attempted synthesis of **$^{2}H_1$-149** involved lithiation of

protected alcohol **264** and also double lithiation of alcohol **149**, both followed by deuterium oxide quench. However, variable and unpredictable levels of deuterium incorporation were observed.

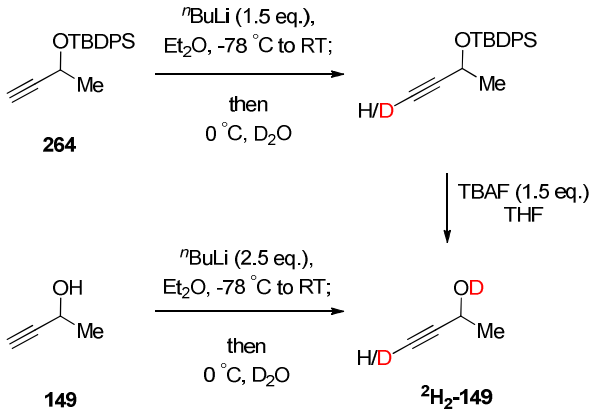

Scheme 91. Attempted Route to Deuterated Acetylenic Alcohol.

With facile acetylenic H/D exchange an issue, synthesis of deuterated ketone **$^2H_1$-146** was pursued directly from ketone **148**, by exchanging the solvent of the DABCO catalysed conjugate addition reaction for deuterium oxide. Analysis of the reaction by TLC demonstrated a complex reaction mixture, however careful column chromatography and recrystallisation allowed access to the required deuterated ketone **$^2H_2$-146**, but in poor yield.

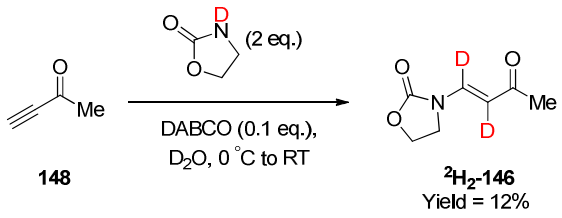

*Scheme 92. Route to Deutero Ketone **$^2H_2$-146**.*

Subsequent reduction of **$^2H_2$-146** was accomplished by $NaBD_4$ to yield the key deuterated alcohol **$^2H_3$-145** in excellent yield and synthesis of phenylacetate **$^2H_3$-154** was achieved under familiar EDCi coupling conditions, again in excellent yield.

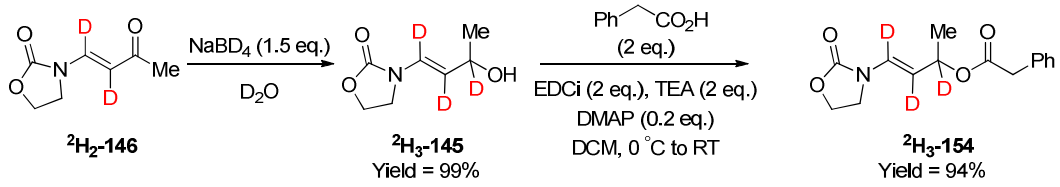

Scheme 93. Synthesis of Deuterated Phenylacetate ***^{2}H$_3$-154***.

With **^{2}H$_3$-154** in hand, rearrangement was pursued under the normal laboratory protocol prior to *in-situ* ^{1}H-NMR studies and was observed to produce comparable yields and diastereoselectivities to that observed for the non-deuterated phenylacetate analogue.

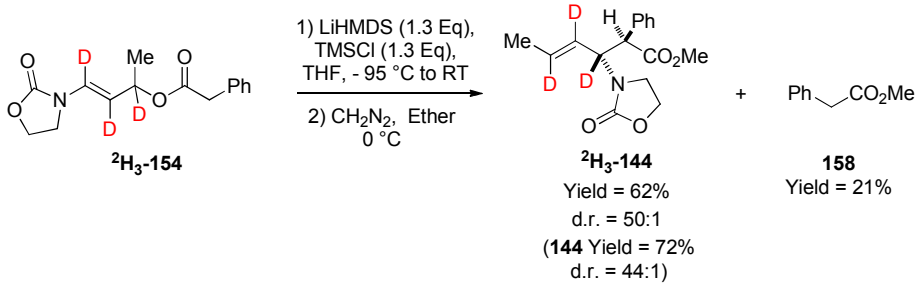

Scheme 94. EICR of ***^{2}H$_3$-154*** *Under Normal Laboratory Conditions.*

With successful rearrangement of **^{2}H$_3$-154** observed, subjection to reaction monitoring was pursued. Initiation of the rearrangement was performed under a similar protocol to the model SKA studies; however, the reaction was monitored at -50 ˚C over three hours prior to warming to 25 ˚C.

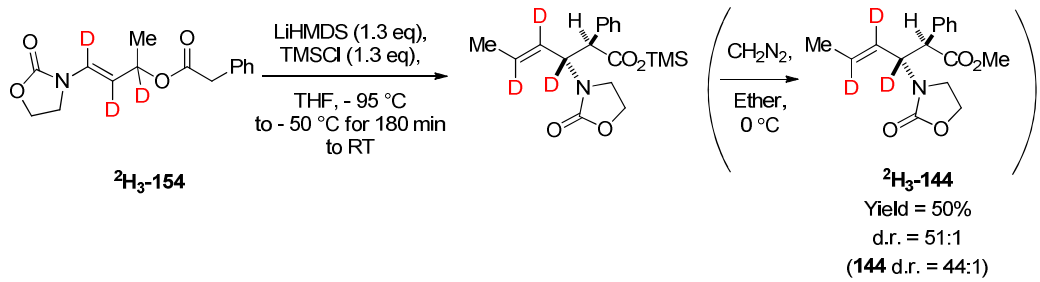

Scheme 95. In-Situ Attempt at Monitoring EICR of ***^{2}H$_3$-154***.

Unfortunately, observation of substrate consumption through monitoring the disappearance of the α-H's were masked by THF and formation of *E/Z*-SKAs were not cleanly observed due to signal broadening and coalescence. However, it is noted that an initial build-up of SKA was observed, which was rapidly consumed within the first 20 minutes of the experiment. Also, determination of the *in-situ* diastereoselectivity during EICR was not achievable as the ^{1}H-NMR resonances used in the silylester product, namely the vinylic methyl group and the α-H were masked by low field silyl by-products and THF respectively.

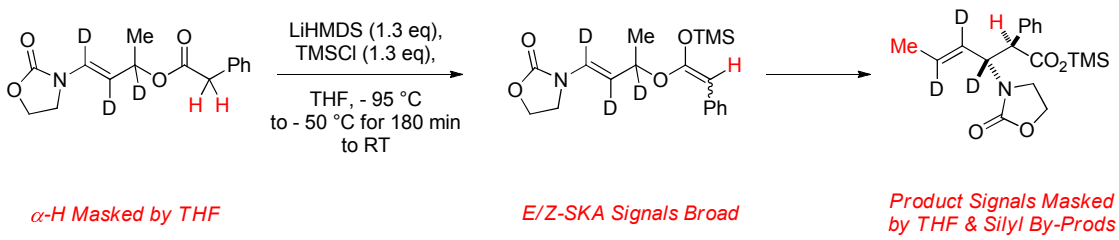

Scheme 96. Reaction Monitoring Issues of ***^{2}H$_3$-154***.

However, quenching and esterification of the *in-situ* reaction mixture yielded comparable diastereoselectivity to that observed with EICR of **154** however in a lower yield and clean isolation of methyl phenylacetate was not accomplished.

Although EICR reaction monitoring by ^{1}H-NMR spectroscopy has not been successful, it has at least verified the feasibility of studying this reaction by NMR. This is demonstrated by the similarities in the diastereomeric ratio and yield between the generic laboratory-based protocol and that conducted in an NMR tube.

3.2.2. EICR Reaction Monitoring by ^{2}H-NMR Spectroscopy

As subjection of phenylacetate **^{2}H$_3$-154** to *in-situ* ^{1}H-NMR studies was flawed by the inability to monitor the key α-H resonance in the substrate, *E/Z*-SKAs and the rearranged silylester, a solution to these issues may be found in ^{2}H-NMR analysis. As the spectral width of ^{2}H-NMR is identical to that of ^{1}H-NMR, similar chemical shifts would be anticipated for an α-D incorporated substrate, SKA and silylester product, as

compared to the α-H analogue.[161] As the chemical shifts of these three key signals are differentiated by at least 1 ppm, clean and distinguishable observation of these signals should be anticipated by ^{2}H-NMR spectroscopy.

With this in mind, it was envisaged that synthesis of α,α-$^{2}H_2$-substrates *via* esterification of α,α-$^{2}H_2$-carboxylic acids and key intermediate **145**, may provide a perfect solution to this issue, may also allow evaluation of alkylacetates. Initial focus therefore concentrated on utilisation of the commercially available α,α-$^{2}H_2$-phenylacetic- and α,α-$^{2}H_2$-propionic acids.

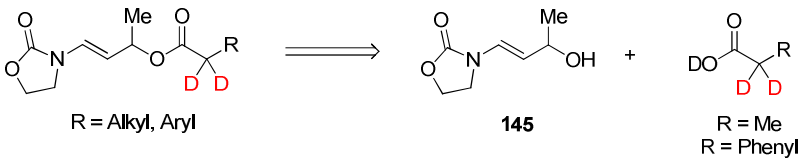

Scheme 97. Access to α,α-$^{2}H_2$-Aryl- & Alkylacetates.

Attempted synthesis of α,α-$^{2}H_2$-phenylacetate **$^{2}H_2$-154** proved problematic as substantial and unpredictable amounts of H/D exchange resulted. Efforts at limiting this exchange involved preparation of **$^{2}H_1$-145** utilisation of the free base of EDCi, performing the reaction in CD_2Cl_2 and also performing reaction workup with D_2O solutions of brine, citric acid and sodium bicarbonate, however to no avail.

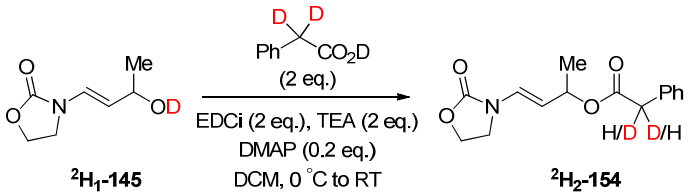

*Scheme 98. Attempted Synthesis of α,α-$^{2}H_2$-Phenylacetate **$^{2}H_2$-154**.*

With the unfavourable H/D exchange observed for synthesis of the α,α-$^2H_2$-phenylacetate, synthesis of α,α-$^2H_2$-propionate **$^2H_2$-265** was accomplished in excellent yield and isolated with complete deuterium incorporation.

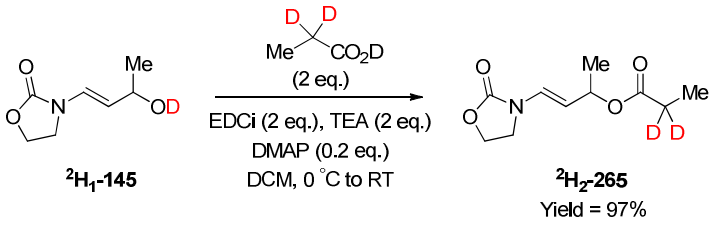

*Scheme 99. Synthesis of Deuterated Propionate **$^2H_2$-265**.*

With **$^2H_2$-265** hand, rearrangement under normal laboratory protocols was attempted, however no reaction was observed and complete mass return of substrate resulted.

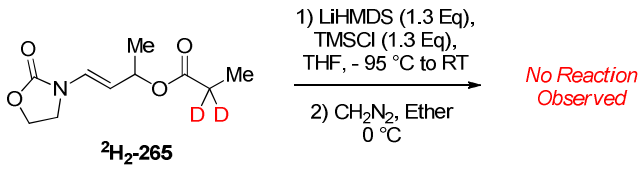

*Scheme 100. EICR of **$^2H_2$-265** Under Normal Laboratory Conditions.*

The stability of **$^2H_2$-265** to de-deuteration was demonstrated by an *in-situ* attempt at reaction monitoring of which the substrate remained intact in the reaction medium in excess of 40 days. This observed result is clearly an aspect of the kinetic isotope effect and it is unfortunate that the stability it confers on the substrate renders futile reaction monitoring by ^{2}H-NMR.

3.2.3. EICR Reaction Monitoring by ^{13}C-NMR Spectroscopy

With the unsuccessful monitoring of the EICR by both ^{1}H- and ^{2}H-NMR spectroscopy, monitoring by ^{13}C-NMR was subsequently pursued. Initial investigations focussed on synthesis of *ipso,alpha(ι,α)*-enriched phenylacetate **$^{13}C_2$-154**, accomplished in excellent yield under the familiar EDCi coupling conditions.

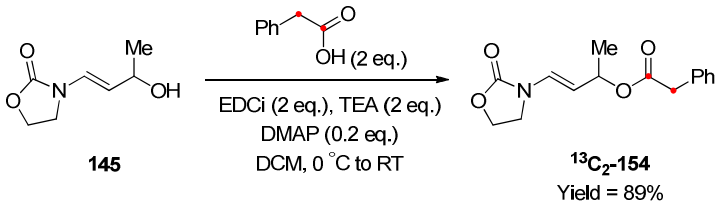

*Scheme 101. Synthesis of ^{13}C Enriched Phenylacetate Substrate **$^{13}C_2$-154**.*

Utilisation of a doubly ^{13}C enriched substrate possessing chemically and magnetically inequivalent carbon atoms, was envisaged to provide successful observation of *E*- and *Z*-SKA's and also *anti*- and *syn*-diastereomers during the *in-situ* rearrangement studies. With **$^{13}C_2$-154** in hand, rearrangement under optimised conditions (Chapter 2), prior to *in-situ* studies, demonstrated that β-amino ester **$^{13}C_2$-144** was obtained in similar yield and diastereoselectivity to that of the non-enriched analogue.

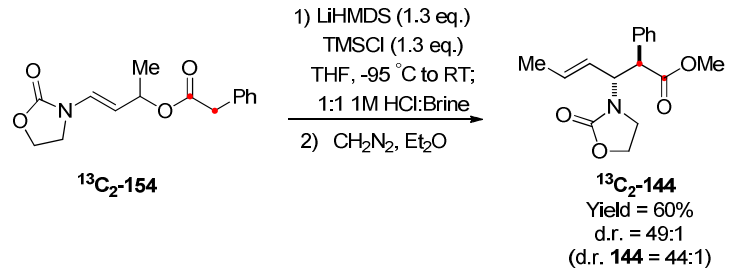

*Scheme. 102. EICR of ^{13}C Enriched Phenylacetate **$^{13}C_2$-154** under Standard Laboratory Conditions.*

With the successful rearrangement of **$^{13}C_2$-154** observed, subjection to *in-situ* reaction monitoring was pursued. The reaction was initiated in the reported fashion, injected into a pre-cooled 400 MHz NMR spectrometer at -95 ˚C and subsequently warmed to -65 ˚C where it was monitored in excess of 800 minutes prior to warming to 25 ˚C.

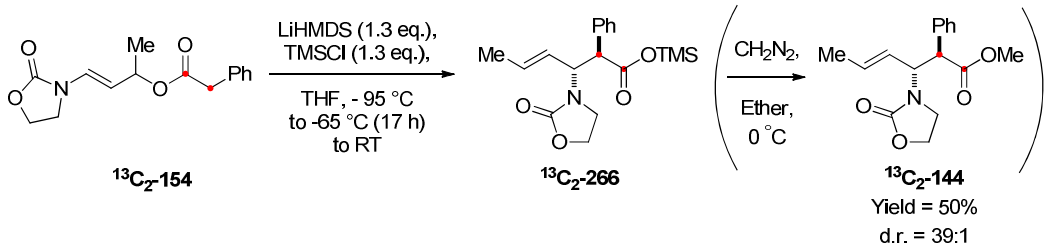

Scheme 103. In-Situ EICR Monitoring of ***$^{13}C_2$-154****; Equimolar 1.3 eq. LiHMDS & TMSCl.*

During the reaction monitoring, consumption of **$^{13}C_2$-154**, formation and consumption of *E/Z*-SKAs and formation of silylester product **$^{13}C_2$-266** were observed. The intermediary temperature of -65 ˚C was chosen, as the ability to clearly monitor SKAs at -50 ˚C was troublesome due to facile rearrangement at this temperature. Unfortunately, resolution of the *anti*- and *syn*-diastereomers of the silyl ester product were not observed, as the *ipso-(ι-)* and *alpha-(α-)*carbon resonances are coincidental in THF. However comparable diastereoselectivity was observed post reaction quench and esterification to that observed with the laboratory protocol. Plotting relative concentrations of species consumed and formed *versus* time demonstrates the progress of this *in-situ* reaction.

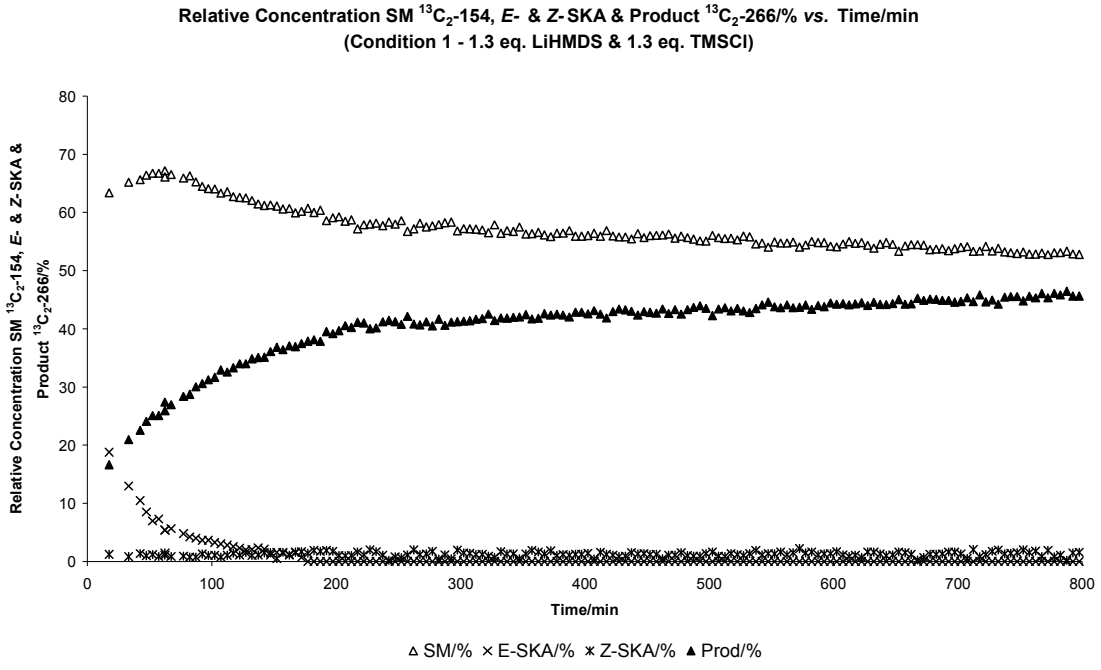

Graph 4. Consumption of ***$^{13}C_2$-154*** *& Formation of E/Z-SKA & Product* ***$^{13}C_2$-266****/% vs. Time/min at -65 ˚C (Condition 1 - 1.3 eq. LiHMDS & 1.3 eq. TMSCl).*

These intriguing results display certain resemblances to the model phenylacetate SKA studies (Graph 2). These include an initial return of starting material (SM) **$^{13}C_2$-154** prior to its further consumption, an initial fast, yet partial formation and subsequent consumption of the *E*-SKA and a constant low level concentration of the *Z*-SKA. This reaction also clearly demonstrates 2 key time regions. At t < 180 minutes, trends in the observed rates of phenylacetate **$^{13}C_2$-154** consumption (after 60 minutes) and product **$^{13}C_2$-266** formation are greater than when t > 180 minutes. This initial higher rate of product **$^{13}C_2$-266** formation is presumably based on consumption of the built-up *E*-SKA over this time period. It is noted that 50% consumption/formation of phenylacetate **$^{13}C_2$-154**/silylester **$^{13}C_2$-266** was observed after 900 minutes. As a mechanistic tool used to evaluate the origins of diastereoselection throughout the course of the EICR, the inability to monitor the formation of *anti*- and *syn*-silylesters **$^{13}C_2$-266** is unfortunate. However, the formation of high levels of *E*-SKA and subsequent consumption of the *E*-SKA strongly allude to this geometrical isomer rearranging, inferring the *anti*-diastereoselectivity observed in the rearrangement.

To further investigate the effects of reagent stoichiometry on the rearrangement of **$^{13}C_2$-154**, treatment with equimolar 1.7 equivalents of LiHMDS/TMSCl, and 1.3 equivalents LiHMDS and 6 equivalents of TMSCl was pursued. These conditions were chosen to compliment the findings from the earlier model phenylacetate SKA studies using **$^{2}H_1$-239**.

Condition 2 – Equimolar 1.7 Equivalents of LiHMDS/TMSCl-

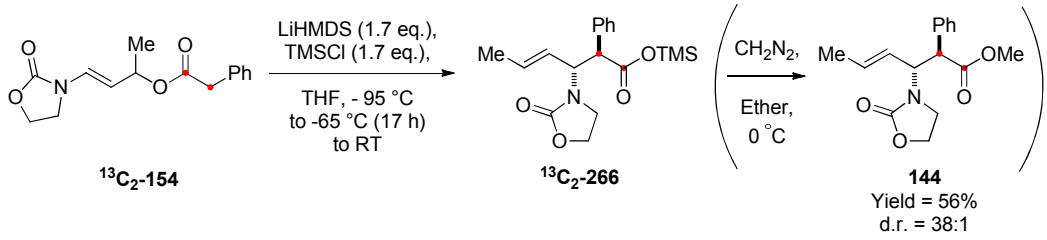

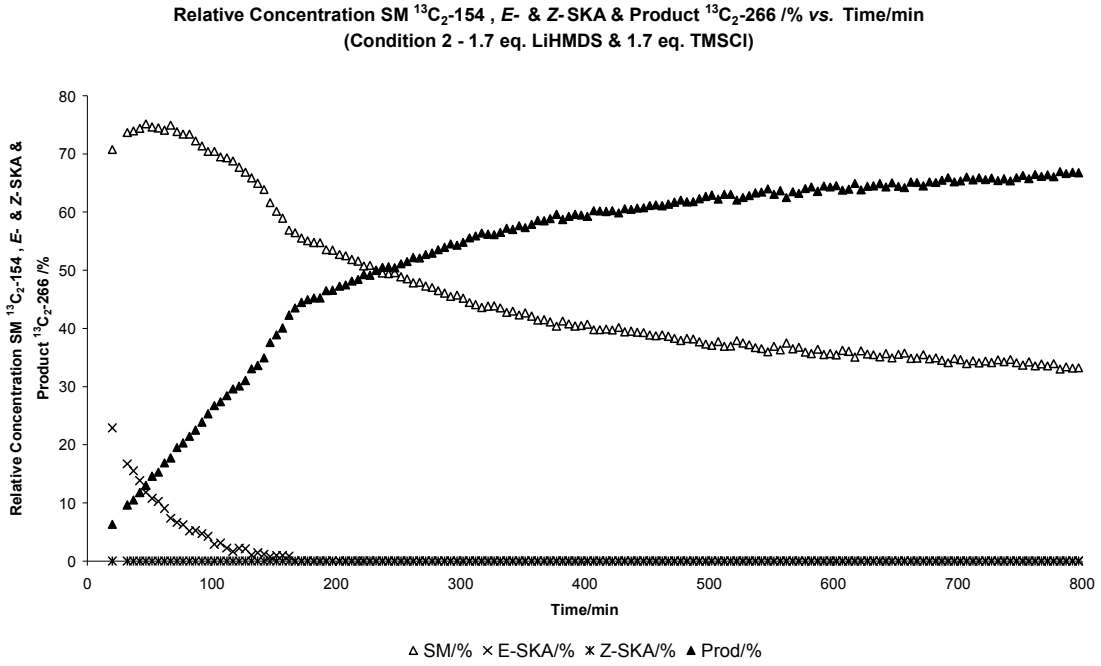

Graph 5. Consumption of ***$^{13}C_2$-154*** *& Formation of E/Z-SKA & Product* ***$^{13}C_2$-266****/% vs. Time/min at -65 °C (Condition 2 - 1.7 eq. LiHMDS & 1.7 eq. TMSCl).*

On subjecting **$^{13}C_2$-154** to equimolar 1.7 equivalents of LiHMDS and TMSCl it is noted that familiar trends are again observed, in that a similar inflection of SM **$^{13}C_2$-154** is seen and observation of the *E*-SKA is not detected post 180 minutes. There are 3 distinct time regions to consider, at t < 180 minutes the rate of formation of silylester **$^{13}C_2$-266** is highest, in concordance with consumption of *E*-SKA. Then reductions in the observed rate of **$^{13}C_2$-154** consumption and silylester **$^{13}C_2$-266** formation are seen to occur at 180 < t < 320 minutes and at t > 320 minutes. It is noted that 50% consumption/formation of phenylacetate **$^{13}C_2$-154**/silylester **$^{13}C_2$-266** is quicker, occurring under 230 minutes.

Condition 3 – 1.3 Equivalents of LiHMDS & 6 Equivalents TMSCl-

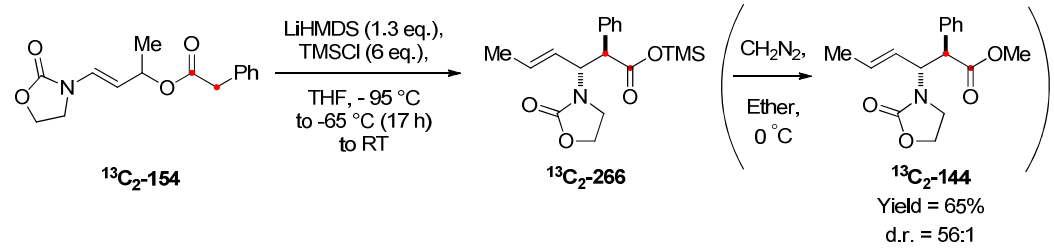

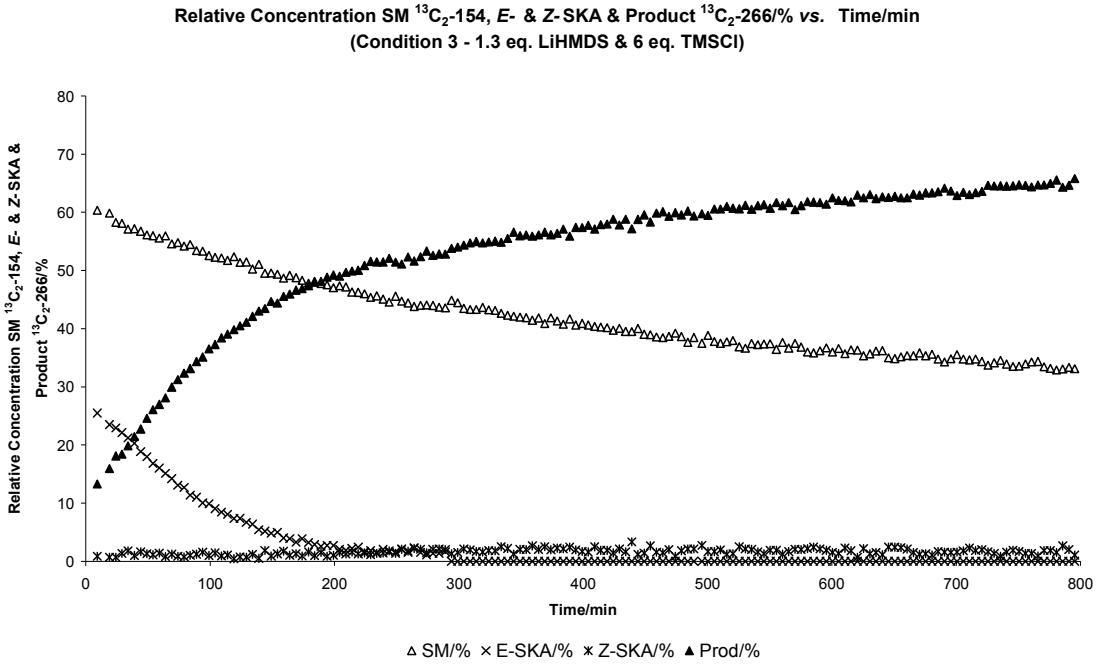

Graph 6. Consumption of ***$^{13}C_2$-154*** *& Formation of E/Z-SKA & Product* ***$^{13}C_2$-154****/% vs. Time/min at -65 ˚C (Condition 3 - 1.3 eq. LiHMDS & 6 eq. TMSCl).*

Interestingly, no inflection in the relative concentration of substrate **$^{13}C_2$-154** is observed in this instance. The time taken for 50% **$^{13}C_2$-154** consumption/silylester **$^{13}C_2$-266** formation is reduced relative to Condition 1, occurring after 190 minutes. The *E*-SKA is detected up to 280 minutes, after which trends in the observed relative rates of consumption **$^{13}C_2$-154**/formation **$^{13}C_2$-266** are again reduced.

As the model SKA studies had demonstrated that equimolar loadings of LiHMDS and TMSCl (1.3 equivalents) would not facilitate complete conversion of phenylacetate to SKA, these results demonstrate that higher concentrations of the silylester product **$^{13}C_2$-266** can be achieved by varying the stoichiometry of TMSCl. Although full conversion to the SKA has not been observed from the outset of these *in-situ* reactions, it was

decided to ascertain whether complete SKA formation would lead to full conversion to silylester **$^{13}C_2$-266**. As the results from Condition 1 demonstrated an initial formation of ca. 25% *E*-SKA, it was postulated that equimolar 5.2 equivalents LiHMDS/TMSCl may provide complete SKA formation and was thus pursued.

Condition 4 – Equimolar 5.2 Equivalents of LiHMDS/TMSCl-

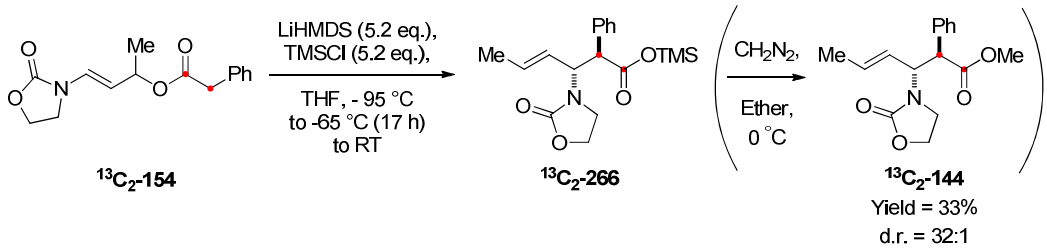

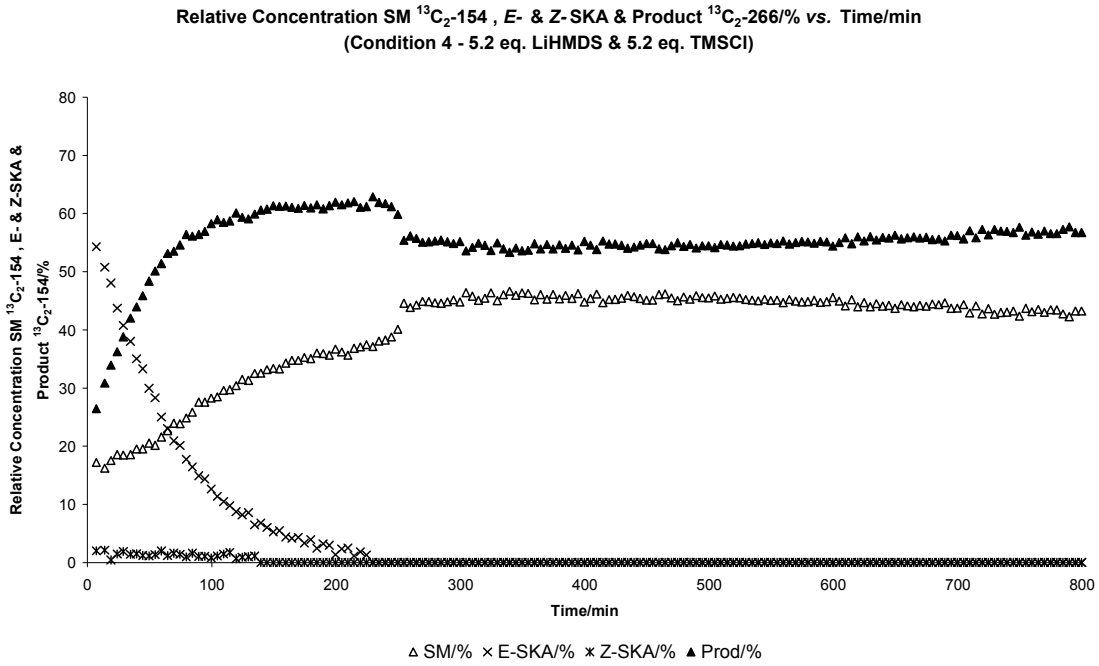

*Graph 7. Consumption of **$^{13}C_2$-154** & Formation of E/Z-SKA & Product **$^{13}C_2$-266**/% vs. Time/min at -65 ˚C (Condition 4 - 5.2 eq. LiHMDS & 5.2 eq. TMSCl).*

The results from this experiment are perhaps the most intriguing. As predicted, increasing the amount of LiHMDS and TMSCl leads to a higher initial concentration of the *E*-SKA which is consumed over a similar time period to the other experiments discussed (t = 220 minutes). Although full conversion to SKA is still not observed, a more rapid formation of silylester **$^{13}C_2$-266** results with 50% formation seen after 60 minutes and plateauing noted after 100 minutes. Curiously a reduction in **$^{13}C_2$-266** and

increase in **$^{13}C_2$-154** is noted at t = 250 minutes. Although E1cB elimination of **$^{13}C_2$-266** would not account for the sharp increase in **$^{13}C_2$-154** observed, another explanation may be a retro [3,3]-rearrangement. Unlike the other studied conditions, the trend in consumption of **$^{13}C_2$-154** was unexpected, as a prolonged inflection was observed throughout the course of reaction. It is also noted that recovery of β-amino ester **$^{13}C_2$-144** is markedly reduced as compared to previous *in-situ* experiments; this observation is in accordance with the results from the initial phenylacetate optimisation discussed in Chapter 2 (Table 3).

All though each reaction profile is different all are observed to possess the same generic trends-

Phenylacetate* $^{13}C_2$-154 *Consumption-

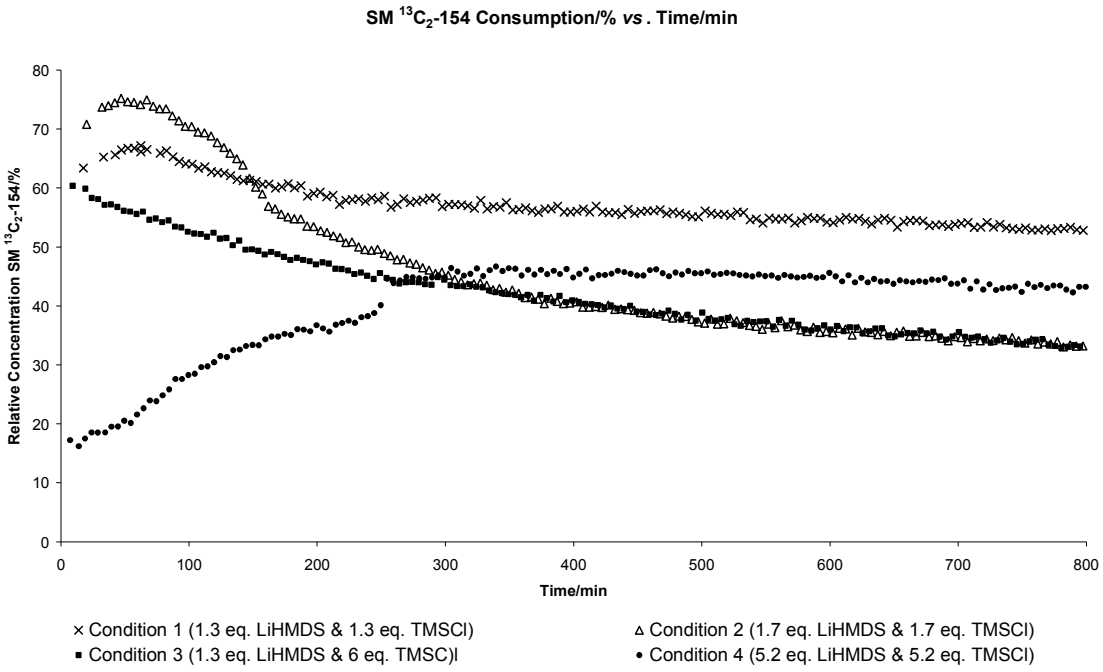

Graph 8. Consumption of ***$^{13}C_2$-154*** *vs. Time/min at -65 ˚C.*

With the exception of Condition 3, an inflection in the plot of **$^{13}C_2$-154** is observed prior to subsequent consumption, however all reactions tend toward a plateau at late stage indicating that the reaction is stalling. Although an inflection is observed for condition 2 and no inflection is observed for Condition 3, similar end-point conversions are observed. Condition 1 is observed to produce the lowest conversion, however Condition

4 demonstrates that increases in the stoichiometry of base and silylating agent does not ensure higher conversions.

E-SKA Formation/Consumption-

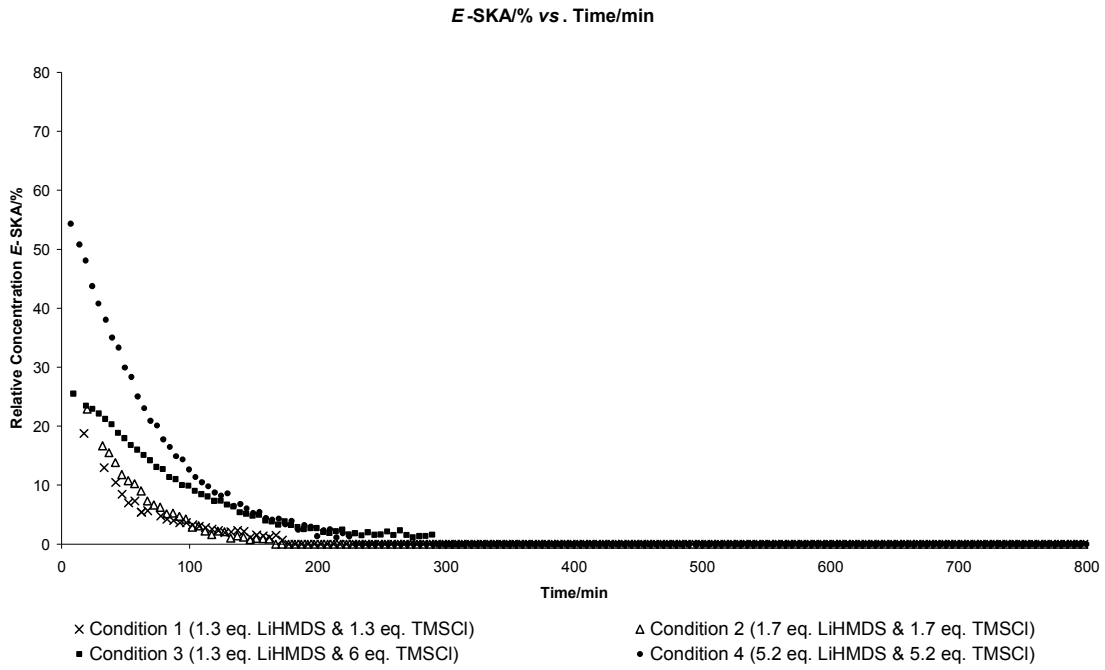

Graph 9. Consumption of E-SKA vs. Time/min at -65 ˚C.

From the outset of each reaction there is a high relative concentration of the *E*-SKA, with a markedly high initial concentration seen with Condition 4. Furthermore, it is noted that consumption of *E*-SKA occurs at $180 < t < 280$ minutes, irrespective of the initial conditions.

Z-SKA Formation/Consumption-

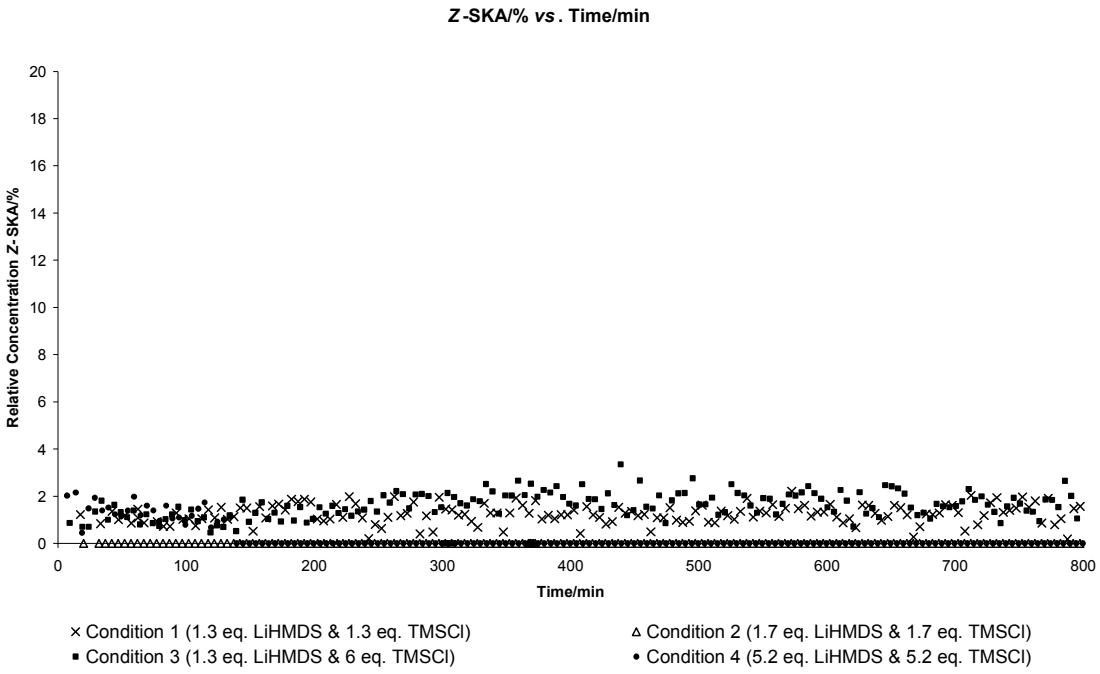

Graph 10. Consumption of Z-SKA vs. Time/min at -65 ˚C.

There remains a low yet steady relative concentration of the *Z*-SKA for condition 1 and 3, with an initial observation up to 140 minutes for Condition 4. However, it is noted that no *Z*-SKA is observed with condition 2.

Product Silylester $^{13}C_2$-266 Formation-

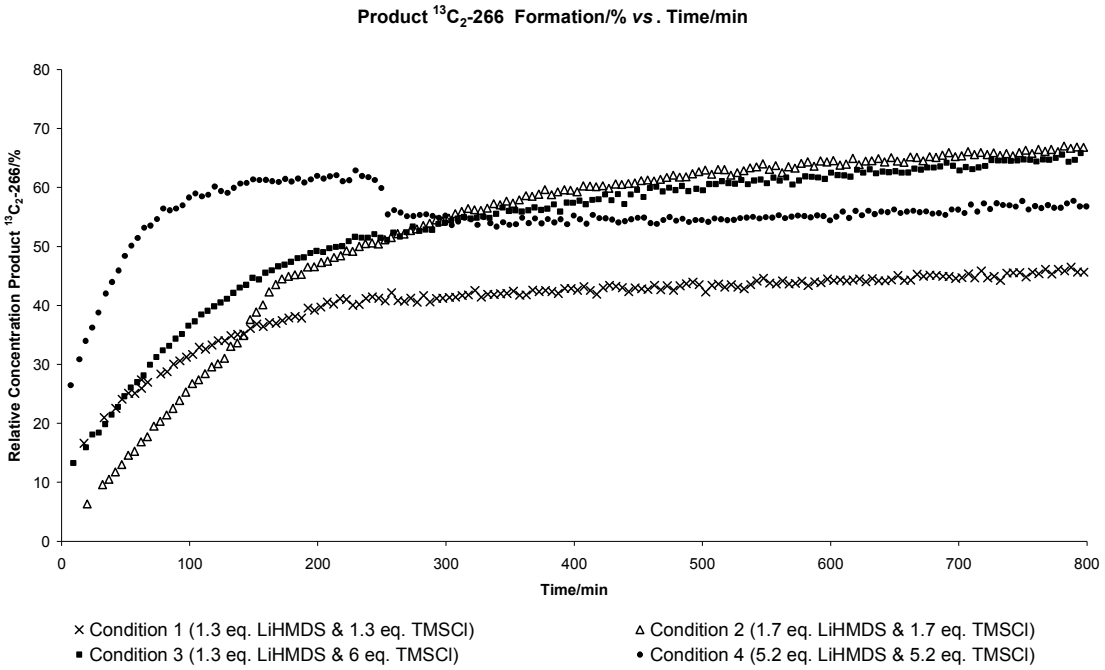

Graph 11. Formation of ***$^{13}C_2$-266*** *vs. Time/min at -65 ˚C.*

There are two key regions in the observed relative rates of product formation and involves a steep initial rise which tends towards plateau once the available *E*-SKA present has been consumed. For the first stage of reaction it is noted that the relative rate of product formation is by far the greatest for condition 4, where 50% is observed after 60 minutes. Curiously, Condition 3 appears to bear resemblance from the initial stage of Condition 1 and that of the late stage of condition 3. Here it is seen that the initial observed rate of product formation matches that of Condition 1, however although the reaction for Condition 2 appears slower, the end-point conversion is similar to that of Condition 3.

These observations are indeed intriguing and allude to important mechanistic ramifications. Although full consumption of **$^{13}C_2$-154** and formation of **$^{13}C_2$-266** is not obtained under any condition, the observed inflection of **$^{13}C_2$-154** and the formation of silyl derived by-products may not only provide an answer as to why complete conversion is not seen, but also the observed diastereoselectivity.

***Inflection in Phenylacetate* $^{13}C_2$-154-**

It has been known from the beginning of the Li-amide era, that the secondary amine generated from the enolisation of a carbonyl compound has an effect upon the reactivity of the newly formed enolate.[162] This maverick enolate reactivity in the presence of *in-situ* generated secondary amines, is highlighted by the addition of a deuterating reagent (MeOD) to the LDA generated enolate **267**.[163] From this, it is shown that the desired α-deutero ester **268** is recovered in minimal amounts, with the majority being that of diisopropylamine mediated re-protonated ester. In order to circumvent this scenario of 'Internal Proton Return (IPR)', it has been shown that addition of *n*butyllithium prior to addition of the electrophile allows isolation of the desired deuterated species in high yield.

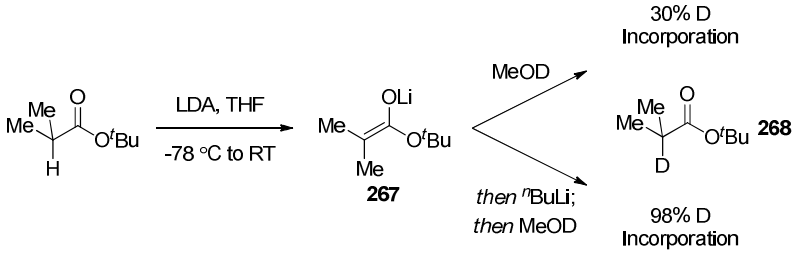

Scheme 104. Internal Proton Return (IPR) in LDA Mediated Enolisations.

With this in mind it was reasoned that the observed return of phenylacetate **$^{13}C_2$-154** may be due to HMDS mediated IPR to the enolate, the SKA or perhaps both. As detection of enolate is not observed during these NMR experiments, possibly an aspect of rapid silylation, it was felt that monitoring enolate formation would be highly desirable in order to distinguish the origins of IPR. Subjection of **$^{13}C_2$-154** to EICR conditions, excluding TMSCl did in fact allow us to observe the formation of enolate **$^{13}C_2$-160**, of which an initial inflection in the amount of phenylacetate **$^{13}C_2$-154** was detected.[119] On warming the reaction mixture to room temperature, complete

degradation of unreacted phenylacetate **$^{13}C_2$-154** and enolate **$^{13}C_2$-160** occurred, with no signs of Li-enolate [3,3]-rearrangement occurring.

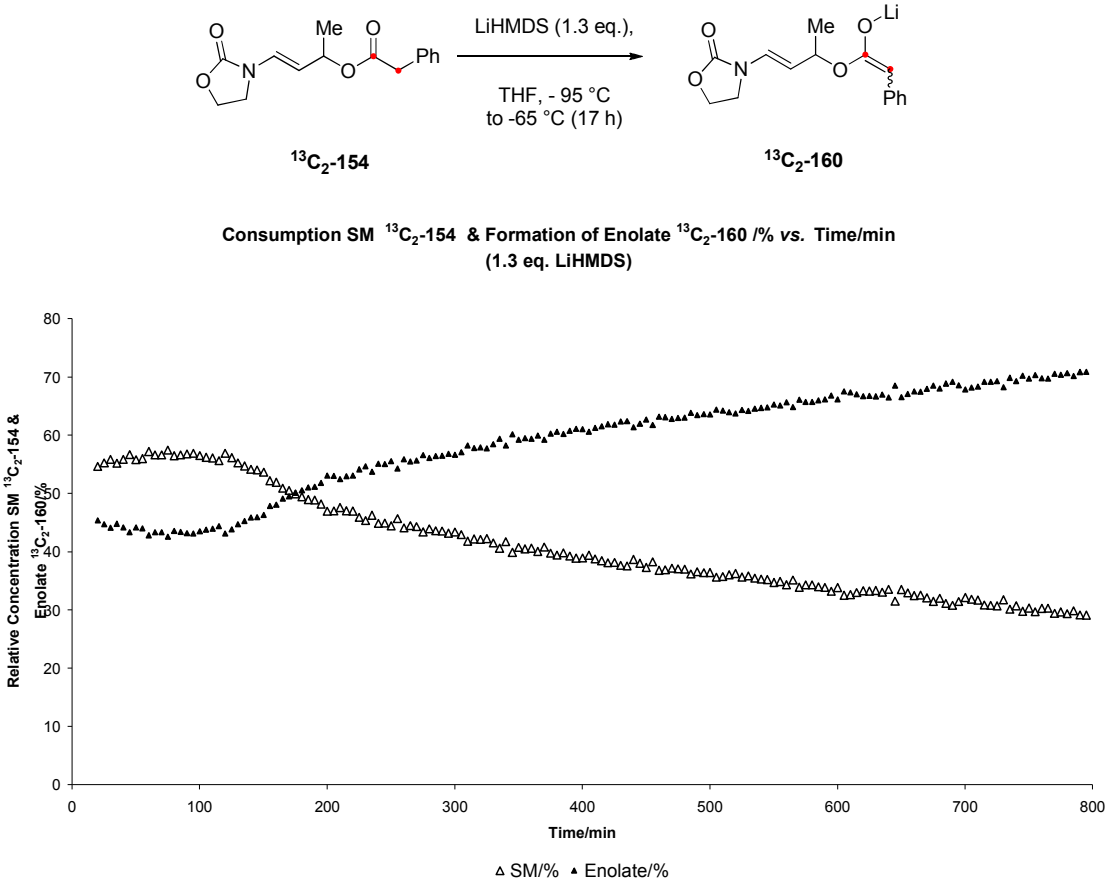

*Graph 12. Consumption of **$^{13}C_2$-154** & Formation of Enolate **$^{13}C_2$-160** /% vs. Time/min at -65 ˚C (1.3 eq. LiHMDS).*

It is noted that due to peak broadness, resolution of the *E*- and *Z*-enolate was not observed and evidence for enolate aggregates including monomeric and dimeric species were also detected, based on the reported monomeric **269** and dimeric **270** enolate species (Figure 21).[119]

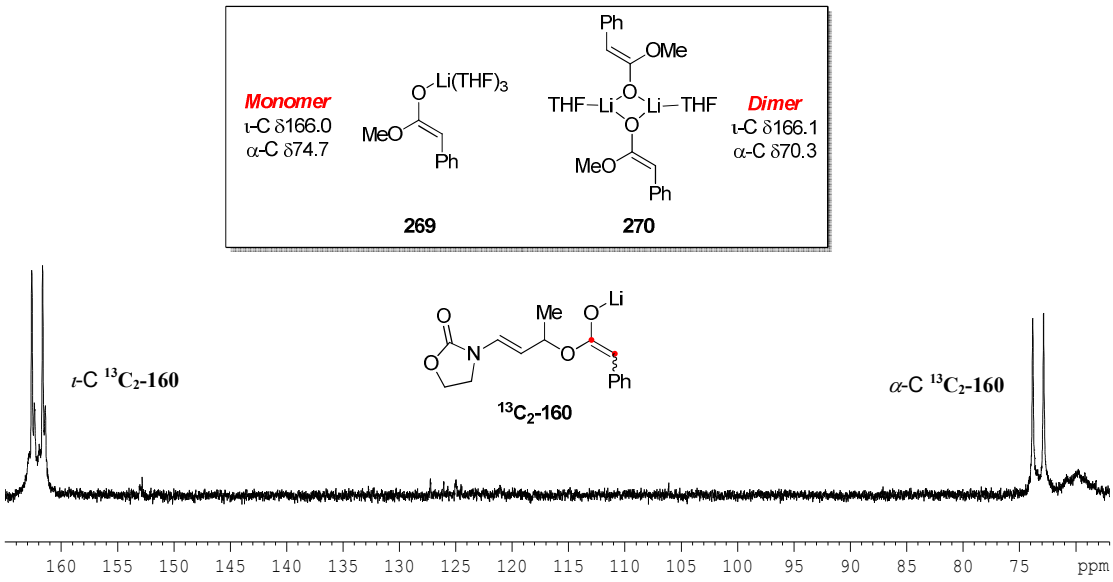

Fig. 21. Reported Monomeric/Dimeric Enolate Species & ι,α-C observed of Enolate ***$^{13}C_2$-160***.

Although IPR to the SKA cannot be ruled out, this study demonstrates that initial IPR to the enolate by HMDS may be responsible for the inflections associated with the observed return of phenylacetate **$^{13}C_2$-154**. This consideration is demonstrated with dimeric enolate species in Scheme 105.[162]

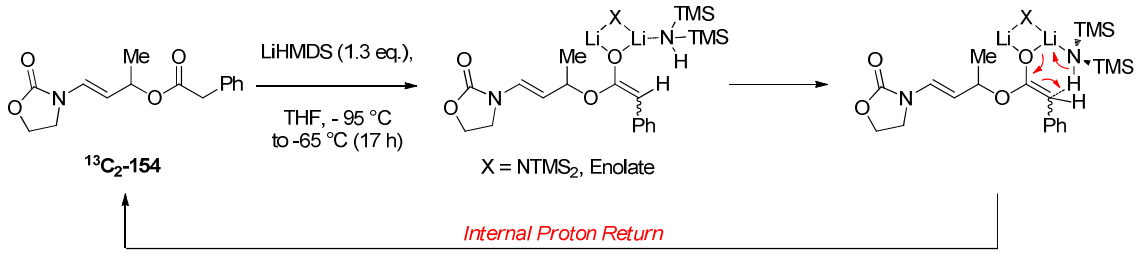

Scheme 105. Internal Proton Return (IPR) to Enolate by in-Situ Generated HMDS.

However, as no plateau is observed during late stage of enolate formation, reaction retardation within the *in-situ* EICR studies may be an aspect of deleterious effects associated with the formation of silyl by-products.

Silyl By-Products-

During the course of the EICR the expected by-products include HMDS and LiCl from enolisation and subsequent silylation. A re-examination of the *in-situ* reaction studies has allowed an insight into the formation of various silicon based species, by virtue of their α-silicon ^{13}C resonances, including TMSCl, HMDS, SKA and silylester product. It is noted that the TMS signals of *E*- and *Z*-SKA's appear coincidental as do the *syn*- and *anti*-silylester products. More importantly, observation of LiHMDS was not detected, however the formation of silanamine **271** is noted during these rearrangements.

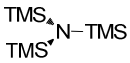

271

Scheme. 106. Silanamine.

This re-evaluation of the ^{13}C-NMR data in the context of mapping the distribution of silicon within these reactions, has allowed additional understanding of components not in the initial remit. To exemplify the silicon distribution in a typical reaction, it is shown from Condition 1 that product **$^{13}C_2$-266** only constitutes around 19% of total silicon. It is also demonstrated that there is a slight reduction of TMSCl during the course of reaction, presumably an aspect of SKA and silanamine formation; however the relative concentration of HMDS appears to remain constant. Although silanamine formation is only small its formation is deemed to be important.

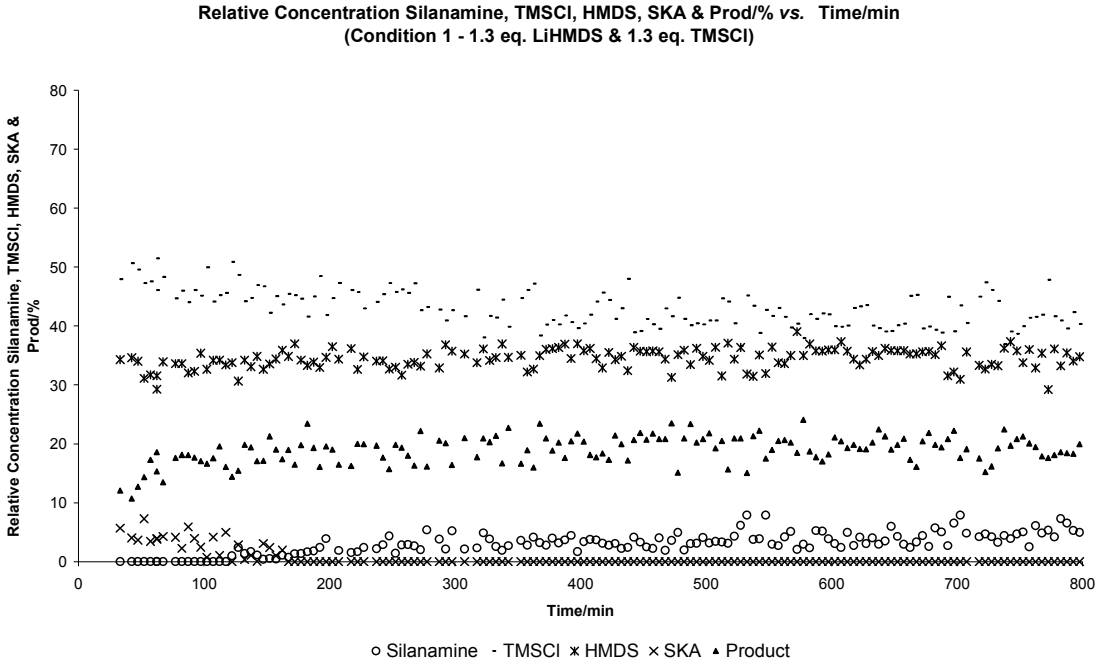

Graph 13. Silicon Distribution/% vs. Time/min at -65 ˚C (Condition 1 - 1.3 eq. LiHMDS & 1.3 eq. TMSCl).

Although different stoichiometries of LiHMDS/TMSCl are used within the other three reactions, similar trends in silicon distribution are undoubtedly observed. TMSCl is observed to be the major component followed by HMDS and although initial relative concentrations of product silylester and silanamine are different, these tend toward similar relative concentrations toward the end of reaction.

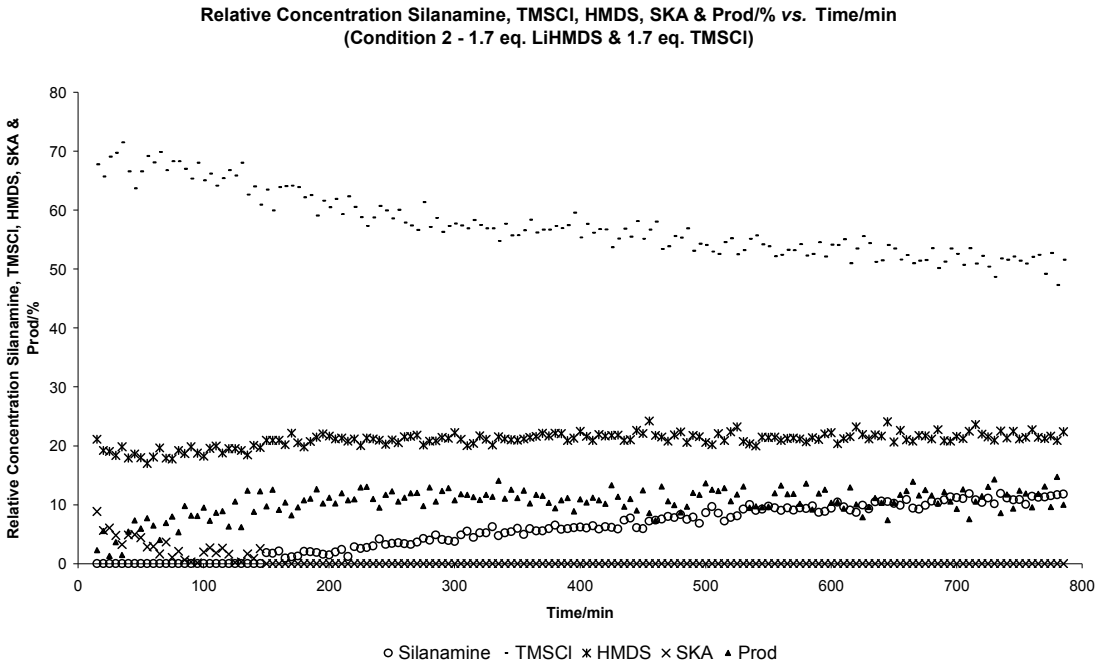

Graph 14. Silicon Distribution/% vs. Time/min at -65 ˚C (Condition 2 - 1.7 eq. LiHMDS & 1.7 eq. TMSCl).

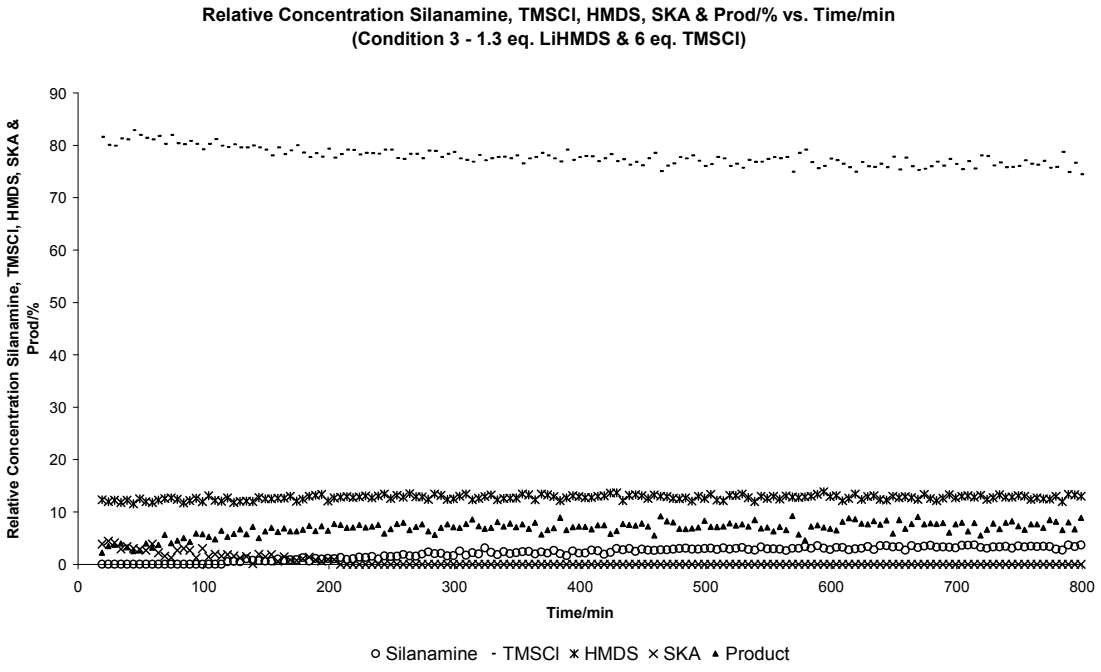

Graph 15. Silicon Distribution/% vs. Time/min at -65 ˚C (Condition 3 - 1.3 eq. LiHMDS & 6 eq. TMSCl).

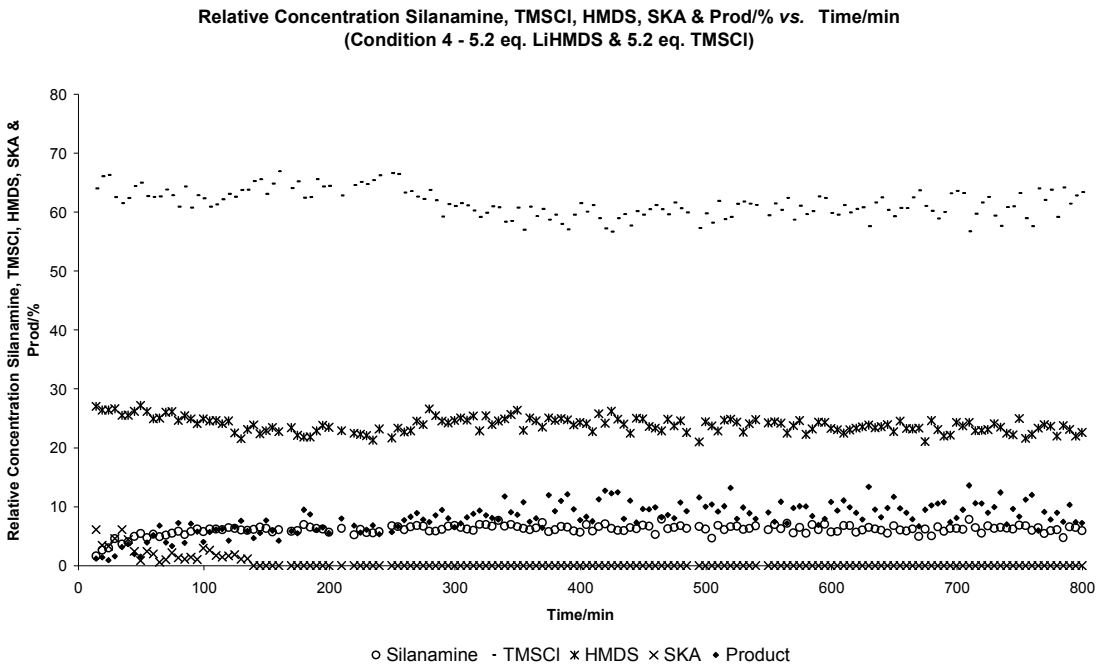

Graph 16. Silicon Distribution/% vs. Time/min at -65 ˚C (Condition 4 - 5.2 eq. LiHMDS & 5.2 eq. TMSCl).

On further consideration of the relative concentration of TMSCl, HMDS and silanamine within these 4 reactions, it is seen from-

TMSCl- A small degree of TMSCl consumption is observed (*ca*. 10%), which is more pronounced for condition 2 (*ca*. 20%). It is noted for condition 4 that an initial return of TMSCl is noted at t < 250 minutes, before its apparent consumption.

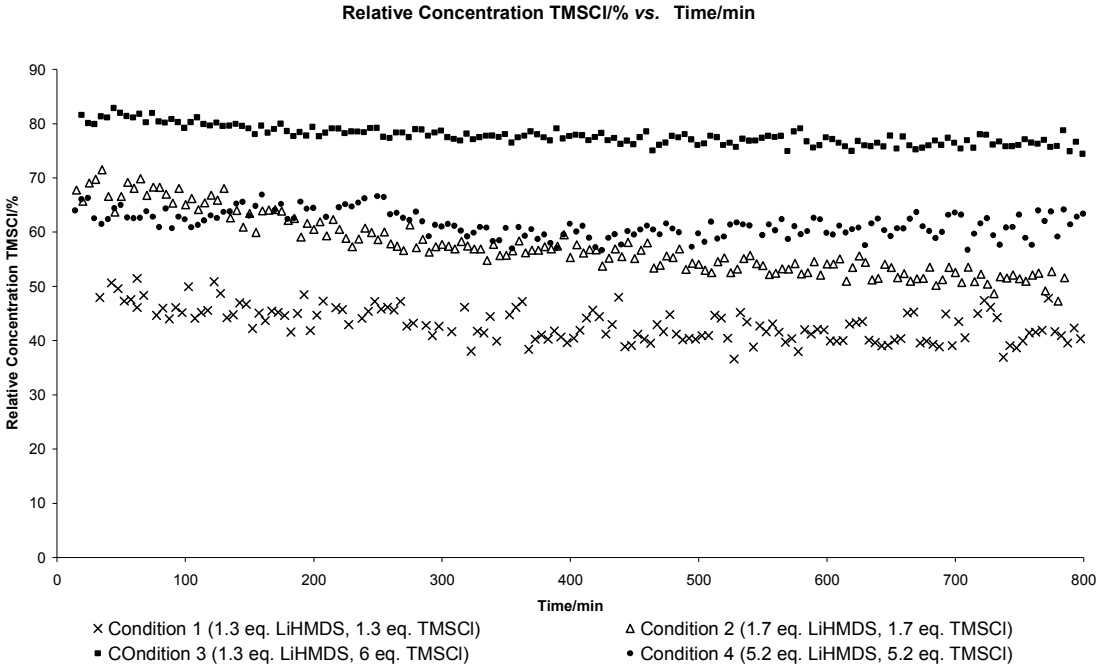

Graph 17. Relative Concentration of TMSCl vs. Time/min at -65 ˚C.

HMDS- The relative concentration of HMDS is observed to remain constant throughout each reaction, however a small negative inflection is observed for condition 2 (time < 50 minutes) with an elongated shallow inflection observed for condition 4. These negative inflections correspond to the time intervals associated with the inflections previously discussed with phenylacetate **$^{13}C_2$-154**.

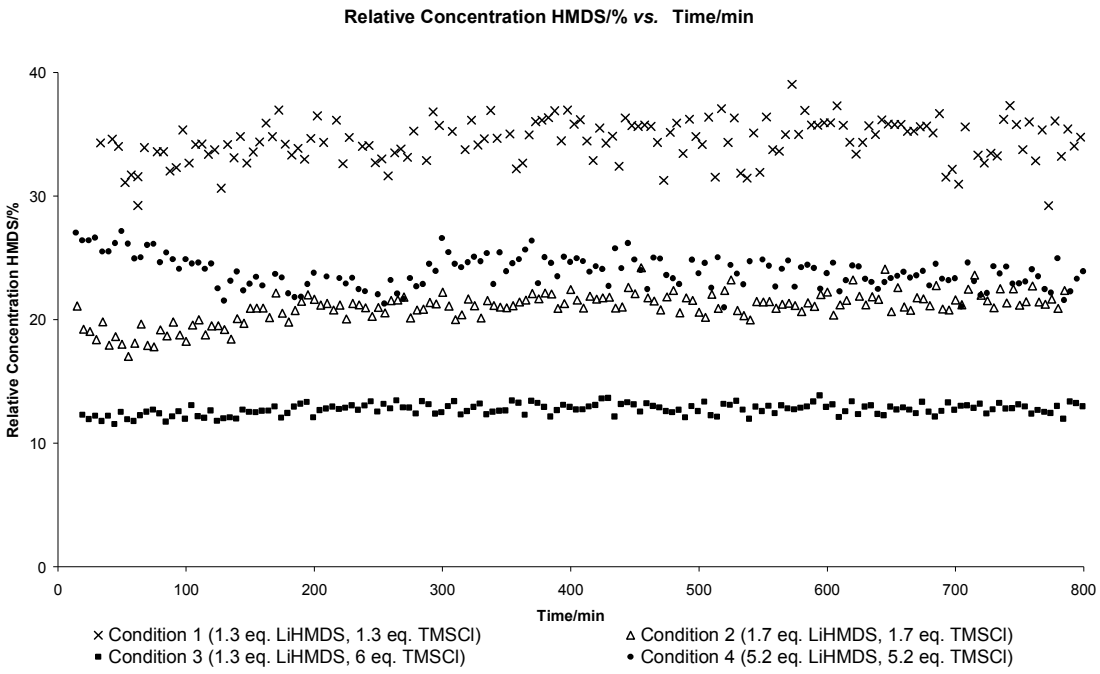

Graph 18. Relative Concentration of HMDS vs. Time/min at -65 ˚C.

This observed removal of HMDS from the system is proposed to be due to IPR to the SKA. As the largest degree of phenylacetate **$^{13}C_2$-154** return is observed for rearrangement under condition 4, deviations in the large relative concentrations of silyl species are easier to observe. It is noted that IPR to the SKA may also be facilitated by LiCl, as judged by coincidental TMSCl regeneration as HMDS is consumed during condition 4.

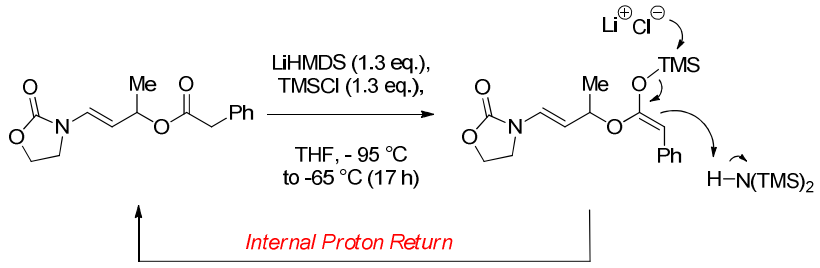

Scheme 106. Internal Proton Return (IPR) to SKA, Facilitated by LiCl & HMDS.

Silanamine- The changes in the observed trends of silanamine formation throughout each reaction are observed to vary the most. In most cases, detection of silanamine occurs after t = 100 minutes and once *E*-SKA is no longer detected, however in Condition 4 a sharp initial formation is observed which plateaus after t =

100 minutes. Interestingly the highest relative concentration of silanamine formation is observed with Condition 2 and the lowest is observed with Condition 3.

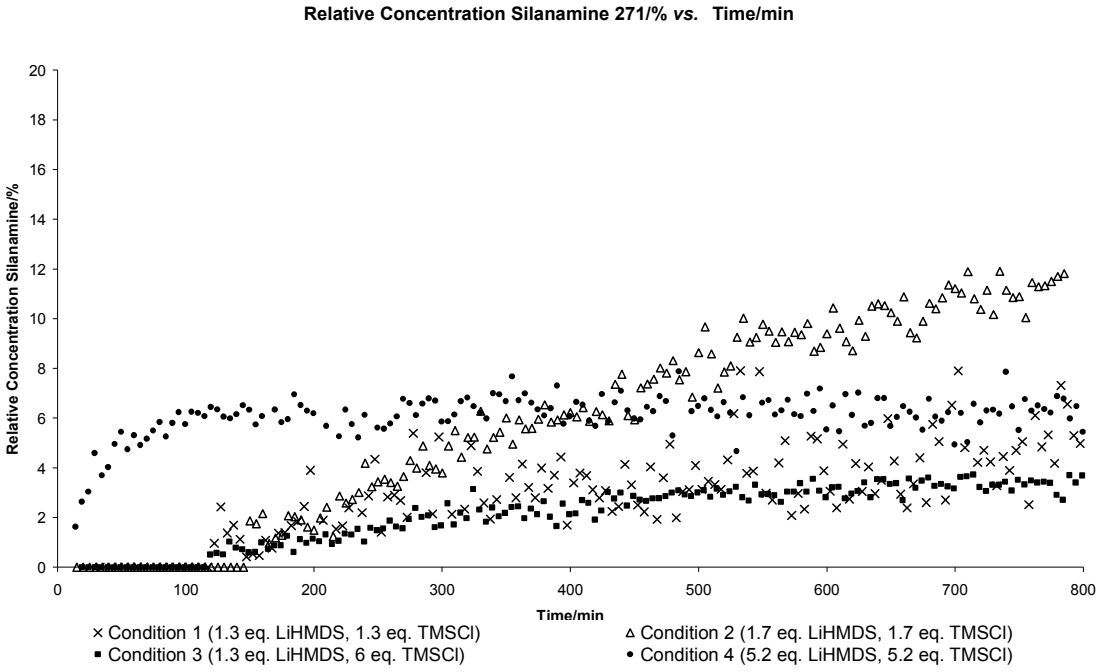

*Graph 19. Relative Concentration of Silanamine **271** vs. Time/min at -65 ˚C.*

The formation of silanamine is indeed intriguing and may originate from compatibility issues between HMDS and TMSCl, or between LiHMDS and TMSCl. As silanamine formation has no effect on the relative concentration of HMDS, its formation *via* this by-product is not thought to occur. However, Lipshutz has demonstrated that premixes of LDA and TMSCl at -78 ˚C generate silylated amine **272** and LiCl quantitatively.[164]

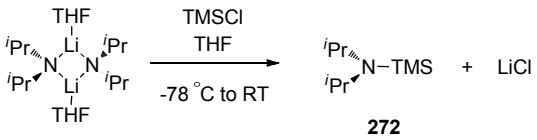

Scheme. 107. LDA & TMSCl Compatibility.

In order to test Lipshutz's observation, control experiments conducted with LiHMDS and TMSCl have subsequently demonstrated complete formation of silanamine **271** *in-*

situ; and it was also shown that combinations of HMDS and TMSCl yielded no reaction.

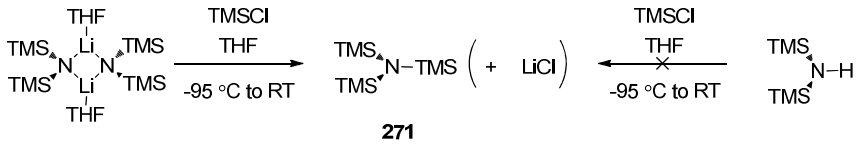

Scheme. 108. LiHMDS- & HMDS-TMSCl Compatibility.

The added benefit of being able to track the silicon content in addition to the pre-planned ι,α-^{13}C of phenylacetate **$^{13}C_2$-154**, *E/Z*-SKA and silylester product **$^{13}C_2$-266** has been mechanistically beneficial, as a more thorough insight into the EICR has been gained. One major draw back to this study has been the inability to observe formation of both the *syn*- and *anti*-diastereomers *via* the ^{13}C labels or the TMS signals. However, in order to rationalise this data in the context of examining the origins of diastereoselectivity within the EICR a number of key mechanistic observations can be made-

1) Throughout each reaction a large relative concentration of the *E*-SKA and rearranged product is observed from the outset of reaction monitoring. This observation alludes to a large initial formation of the *E*-SKA between initiation temperature (-95 ˚C) and whence reaction monitoring occurs (-65 ˚C), with rearrangement also being facile. Isolation of the *in-situ* rearranged products as the methyl esters yield similar diastereoselectivities to the standard laboratory based protocol and this initial high formation of the *E*-SKA may be responsible for the high diastereoselectivity observed.

2) Once the *E*-SKA is no longer detected, the trends in the observed relative rates of product **$^{13}C_2$-266** formation are much reduced and all tend toward plateau, indicating that phenylacetate **$^{13}C_2$-154** consumption and product **$^{13}C_2$-266** formation are stalling. It is noted throughout each reaction low concentrations of *Z*-SKA are present and are attributed to the observed diastereochemical outcome of the rearrangement, post quench and methylation.

3) Although detection of the Li-enolate **$^{13}C_2$-160** has not been observed during *in-situ* studies, it has been shown that IPR plays a role within the initial stages of enolate formation (Graph 12). As an inflection in phenylacetate **$^{13}C_2$-154** is observed for all rearrangements, bar Condition 3, IPR to the SKA is envisaged to be facilitated by LiCl and HMDS.

Although the formation of LiCl has not been followed experimentally, the *in-situ* generation of this salt is thought to exert strong underlying effects within the EICR. As the reaction proceeds, increases in the relative concentration of LiCl are expected due to SKA formation and silanamine formation. The presence of LiCl is known to exhibit an *auto*-catalytic effect within lithium amide enolisations and the pure LDA dimer **273** has been shown to form the more reactive mixed aggregate **274** upon exposure to LiCl.[165]

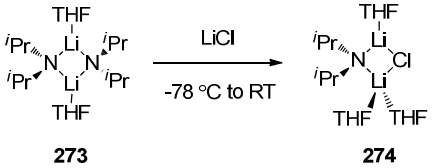

273 **274**

Scheme. 109. Origins of LiCl Auto-Catalysis.

Although formation of more reactive LiCl mixed aggregates can be advantageous in speeding up enolisations, the efficiency of Li-amide mediated reactions are known to be highly sensitive to varying concentrations of *in-situ* generated LiCl. It is known that *E/Z*-enolate selectivities are improved up to the addition of 0.3 equivalents of LiCl but are subsequently reduced with larger amounts.[165-168] It has also been shown that the presence of mixed halogen aggregates brings about facile *N*-alkylation of Li-amide bases, which becomes more favourable with increasing concentrations of Li-halide salt present.[17]

As there are 2 separate mechanisms allowing for LiCl production within the EICR, *auto*-catalysis may account for the observed inflection of phenylacetate **$^{13}C_2$-154**. From this concept it is reasoned that the apparent return of **$^{13}C_2$-154** is an aspect of an induction period allowing LiHMDS/LiCl mixed aggregates to form, in which time IPR

to the SKA is a faster process. The subsequent consumption of **$^{13}C_2$-154** is then observed once the relative rate of SKA formation begins to outweigh the relative rate of IPR. As silanamine formation is generally observed after observation of the *E*-SKA, the apparent stalling of phenylacetate **$^{13}C_2$-154** consumption/product **$^{13}C_2$-266** formation is attributed to a more favourable LiCl catalysed silanation of LiHMDS.

With these considerations in mind it is then possible to construct a reaction scheme considering the effects of by-products within the enamido Ireland-Claisen rearrangement (Scheme 110). Within this scheme there are three key mechanistic stages that would purport to the observed general trends observed with **$^{13}C_2$-154** consumption and **$^{13}C_2$-266** formation-

***Stage 1* -** The first pathway gives rise to the inflection in **$^{13}C_2$-154** concentration, in that enolisation by pure LiHMDS dimer **275** is expected to produce enolate **$^{13}C_2$-160**. As various aggregation states were observed in the enolisation studies (Graph 12), attempts at classifying the structure of enolate will not be pursued and a generic enolate shall be drawn. From the enolate IPR by HMDS may then regenerate **$^{13}C_2$-154**. However if enolate **$^{13}C_2$-160** is trapped as SKA **$^{13}C_2$-277**, it is envisaged that consumption is either by LiCl/HMDS facilitated IPR or rearrangement to product **$^{13}C_2$-266**.

***Stage 2*-** The onset of a new stage within the reaction is thought to occur when **$^{13}C_2$-154** consumption resumes. This is attributed to the start of LiCl autocatalysis, in that formation of mixed LiHMDS dimer **276** occurs, sequestering the use of LiCl within IPR and allowing rearrangement to occur. As formation of product **$^{13}C_2$-266** is still observed after *E*-SKA is no longer observable, enolisation *via* pure LiHMDS **275** or mixed aggregate **276** may occur, but it is thought that as the reaction proceeds increases in LiCl concentration will cause an increase in formation of mixed aggregate **276**. As Collum has demonstrated enolisation selectivities are compromised post 0.3 equivalents LiCl, reduction in diastereocontrol may result in rearrangement from the *Z*-SKA.

Stage 3- The third stage of the reaction is seen to occur by the onset of silanamine formation and reduction in the observed rates of phenylacetate **$^{13}C_2$-154** consumption/product **$^{13}C_2$-266** formation.

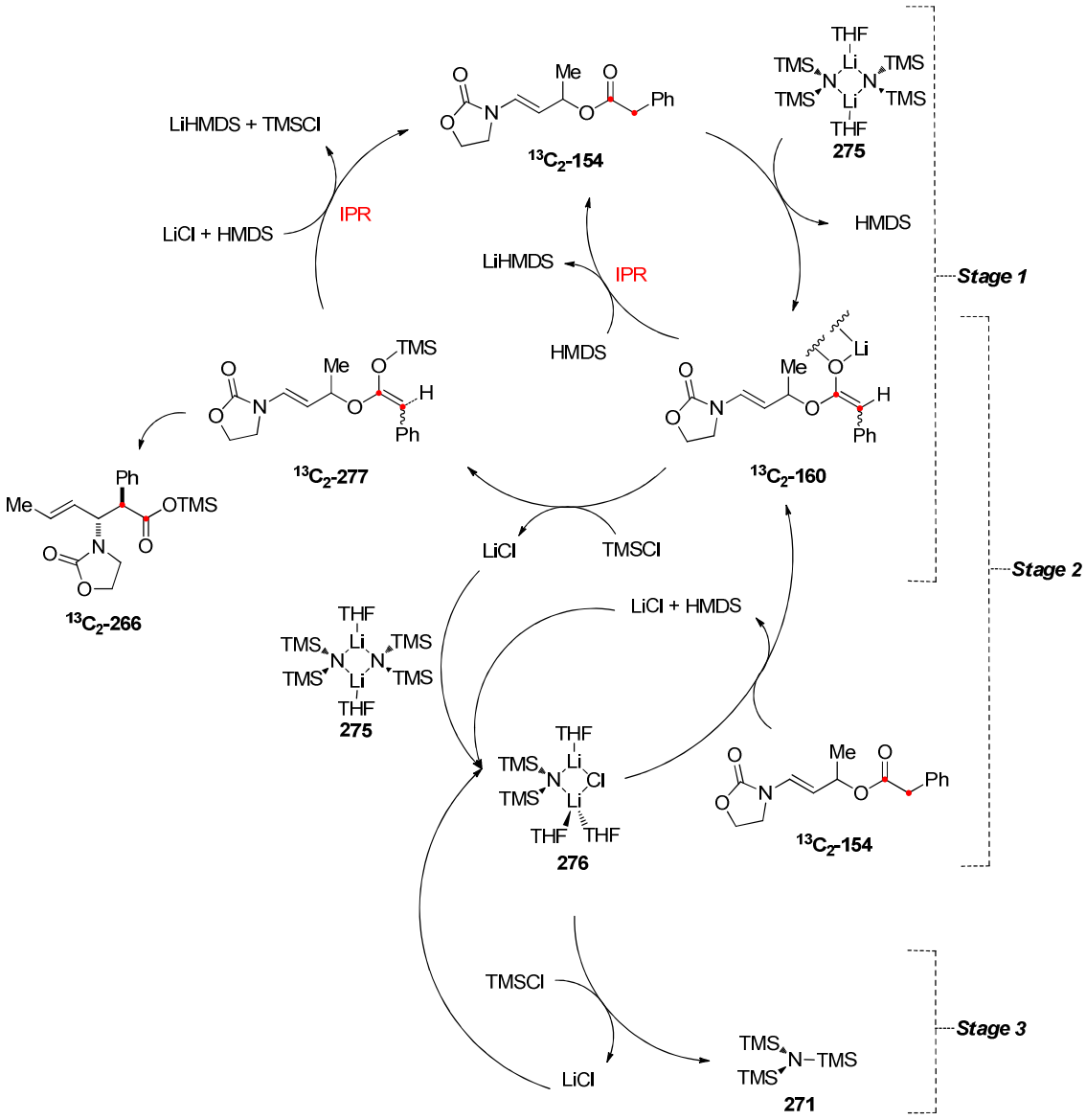

Scheme. 110. Three Postulated Stages within the EICR.

Synthesis & In-Situ Studies of Electronically Perturbed Phenylacetates-

As the main aim of the *in-situ* studies was to investigate the dependency of electronic perturbation on diastereoselectivity, efforts were redirected on synthesising a ^{13}C-incorporated electron donating (-methoxy) and withdrawing (-nitro) *para*-substituted enamido arylacetate. However, due to the lack of commercial availability for the corresponding ^{13}C enriched arylacetic acids, synthesis of these intermediate compounds was therefore required.

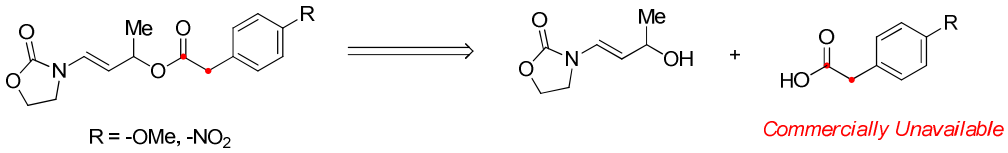

Scheme 111. Required ^{13}C Enriched para-Substituted Arylacetates.

Access to both *para*-methoxy and -nitro phenylacetic acids were based on the use of a common ^{13}C labelled starting material. Utilisation of α-bromo ester **278** in procedures reported by Gooßen and also by Hartwig has demonstrated a route to both methoxy-**280** and nitro-substituted **281** phenylacetates.[169-170] It was therefore envisaged that utilisation of an appropriately ^{13}C labelled α-bromo ester would allow similar access, generating the required α-labelled carboxylic acids post saponification. It is noted that mono-labelled **$^{13}C_1$-278** was used due to commercial availability.

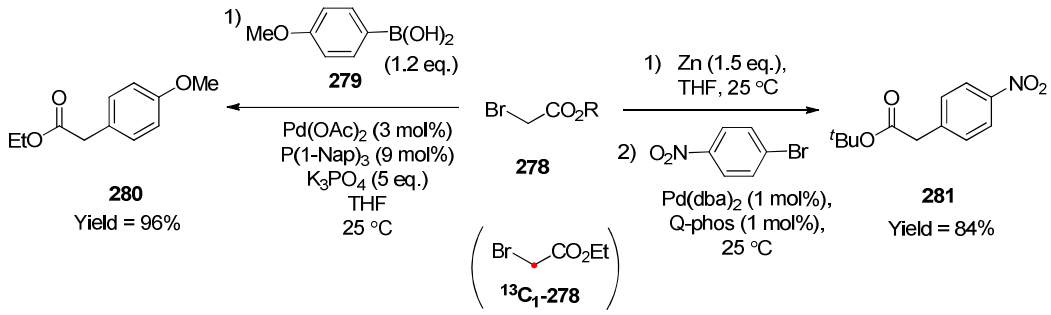

Scheme 112. Required ^{13}C Enriched para-Substituted Arylacetates.

Prior to using **$^{13}C_1$-278**, all initial reactions involved that of the non-labelled **278**. Initial attempts at synthesising methoxy-**280** were met with complex reaction mixtures with crude ^{1}H-NMR alluding to the formation of homocoupled **279**. However, after a

short optimisation synthesis of ^{13}C-*para*-methoxy phenylacetic acid **$^{13}C_1$-282** was accomplished in moderate yield over two steps and subsequent EDCi coupling allowed access to $^{13}C_1$-*para*-methoxy phenylacetate **$^{13}C_1$-165** in excellent yield.

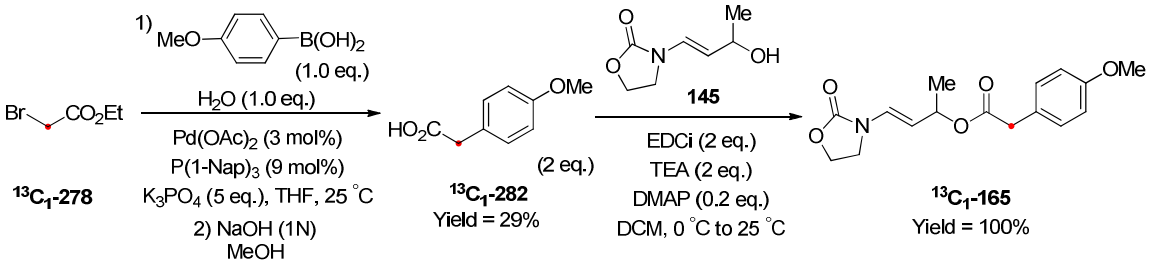

*Scheme 113. Synthesis of ^{13}C Enriched para-Methoxy Phenylacetate Substrate **$^{13}C_1$-165**.*

With *para*-methoxy phenylacetate **$^{13}C_1$-165** in hand synthesis of the electron withdrawn *para*-nitrophenylacetate **$^{13}C_1$-281** was pursued. However, attempts at following Hartwig's Reformatsky protocol were unsuccessful affording quantitative return of unreacted starting materials.

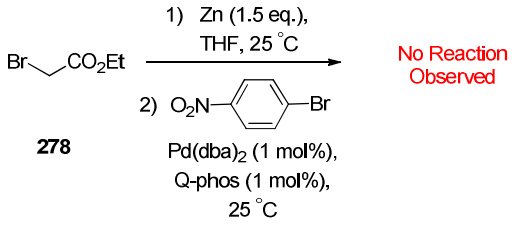

Scheme 114. Attempt at Hartwig's Route to para-Nitro Phenylacetate.

Other routes to **$^{13}C_1$-281**, involved utilisation of Gooßen's Suzuki protocol and after several attempts involving the required boronic acid and trifluororborate salt, no coupling was subsequently observed. As synthesis of *para*-nitrophenylacetate **$^{13}C_1$-281** was problematic, the nature of the electron withdrawing substituent was reconsidered. Subsequently, studies involving the trifluoromethyl substituent were envisaged to create a better mechanistic compliment to the methoxy variant, based on similar diastereoselectivities (*p*-OMe d.r. = 24:1, *p*-CF_3 d.r. = 21:1). With this in mind synthesis of **$^{13}C_1$-283** was accomplished in moderate yield over two steps and

subsequent EDCi coupling allowed synthesis of the labelled *p*-trifluoromethylphenylacetate **$^{13}C_1$-206** in excellent yield.

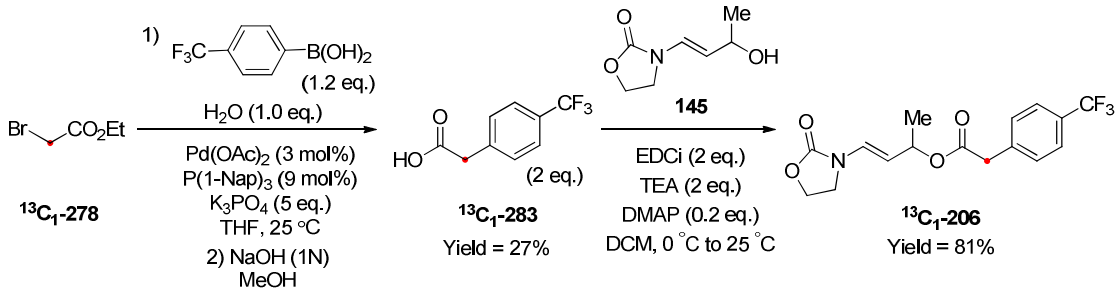

*Scheme 115. Synthesis of ^{13}C Enriched para-Trifluoromethyl Phenylacetate **$^{13}C_1$-206**.*

With only a limited amount of *para*-methoxy **$^{13}C_1$-165** and *para*-trifluoromethyl phenylacetate **$^{13}C_1$-206** available, subjection to *in-situ* rearrangement was subsequently pursued.

In-Situ Rearrangement of para-Methoxy Phenylacetate $^{13}C_1$-165 -

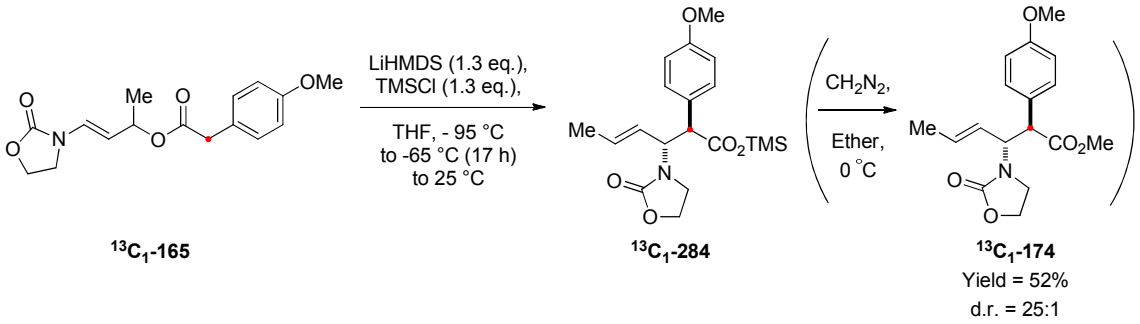

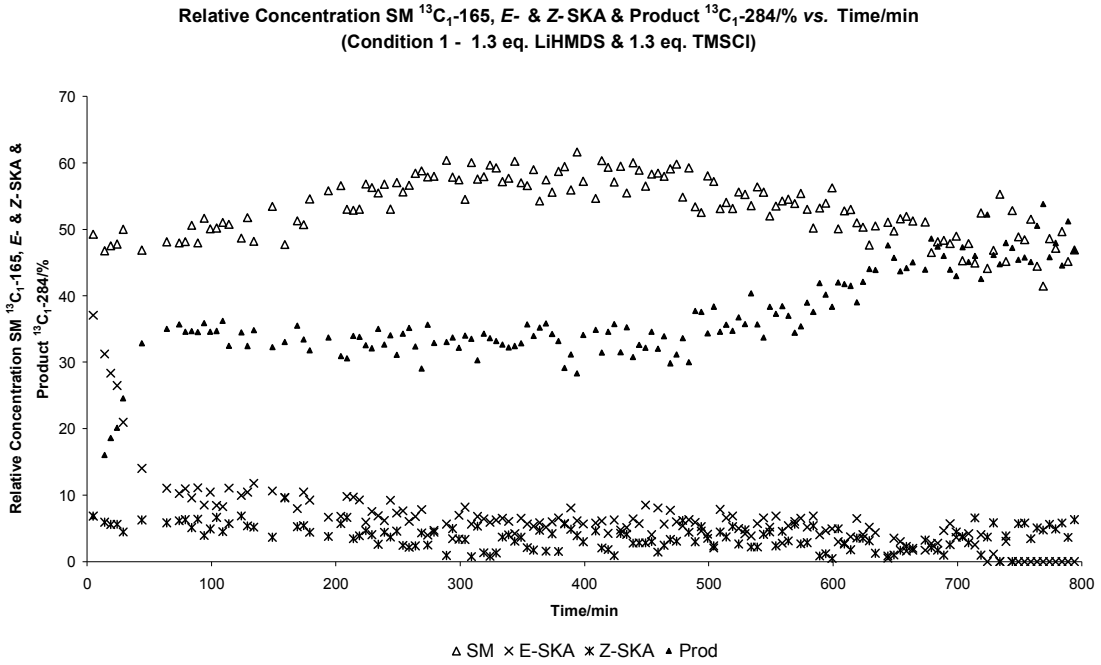

Graph 20. In-Situ EICR of $^{13}C_1$-165; Equimolar 1.3 eq. LiHMDS & TMSCl. Consumption of $^{13}C_1$-165 & Formation of E/Z-SKA & Product $^{13}C_1$-284/% vs. Time/min at -65 ˚C.

From this study it is shown that-

1) A large inflection of *para*-methoxy **$^{13}C_1$-165** occurs.
2) There is a large initial concentration of SKA, of which it is noted that the *E/Z* geometric purity is reduced compared to the phenylacetate **$^{13}C_2$-154** studies.
3) Throughout the experiment there remains a significant proportion of detectable *E*- and *Z*-SKA, unlike the *in situ* phenylacetate **$^{13}C_2$-154** studies.
4) There are 3 distinct regions of product **$^{13}C_1$-284** formation. Similar to the previous studies there is a fast initial relative rate of product formation which is mirrored by *E*-SKA consumption ($t < 50$ minutes). A plateau is later observed at $50 < t < 500$ minutes prior to its subsequent production at $t > 500$ minutes.
5) At $50 < t < 500$ minutes consumption of SKA is solely attributed to IPR.

In-Situ Rearrangement of para-Trifluoromethyl Phenylacetate $^{13}C_1$-206-

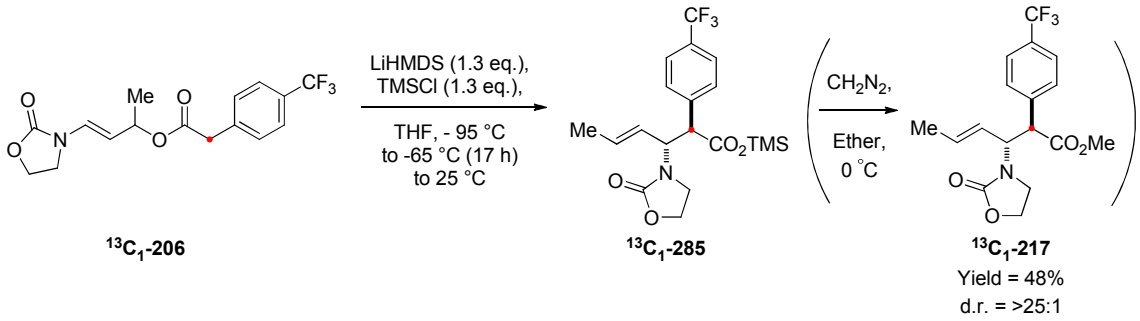

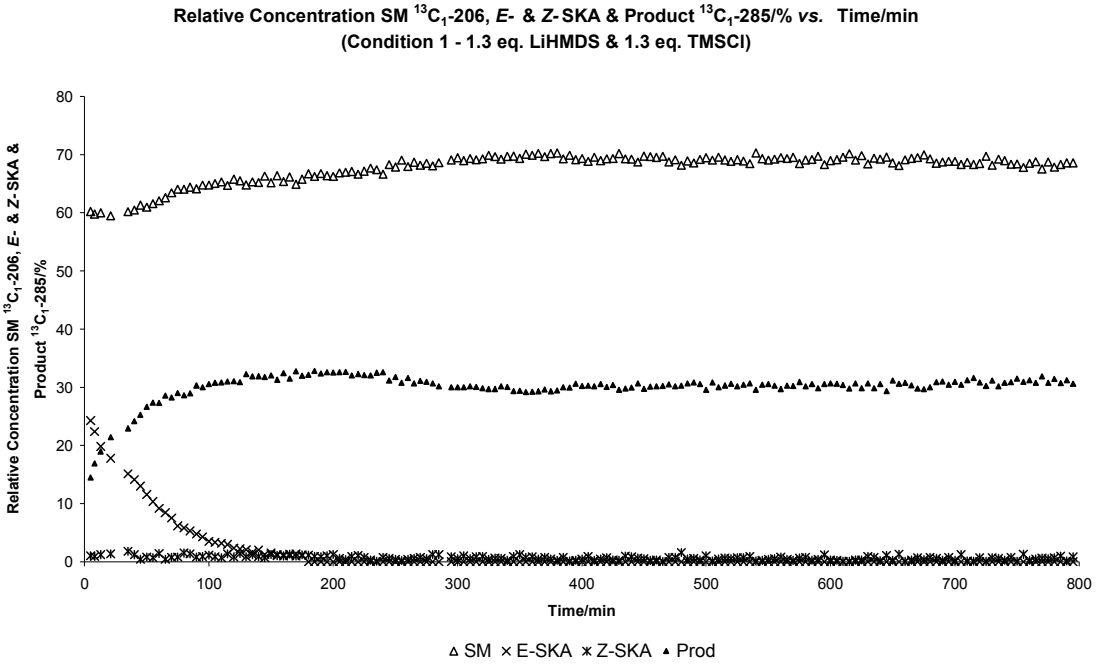

Graph 21. In-Situ EICR of $^{13}C_1$-206; Equimolar 1.3 eq. LiHMDS & TMSCl. Consumption of $^{13}C_1$-206 & Formation of E/Z-SKA & Product $^{13}C_1$-285/% vs. Time/min at -65 °C.

From this study it is shown that –

1) There is a shallow elongated inflection of *para*-trifluoromethyl **$^{13}C_1$-206** return.
2) Similar to the phenylacetate **$^{13}C_2$-154** studies there is a large initial formation of the *E*-SKA which is consumed either through IPR or *via* rearrangement.
3) There is a low steady relative concentration of the Z-SKA throughout and is similar to the *in-situ* phenylacetate **$^{13}C_2$-154** studies.
4) The observed relative rate of product formation is initially high followed by a plateau, mirroring *E*-SKA consumption at t < 100 minutes.
5) The reaction appears to stall after *E*-SKA is no longer detected.

Unfortunately, the ability to monitor the formation of the *syn*- and *anti*-diastereomers within the rearrangement of *para*-methoxy **$^{13}C_1$-165** and *para*-trifluoromethyl **$^{13}C_1$-206** are again plagued by coincident resonances. Also due to an electrical fault within the NMR, analysis of the silyl by-products during these reactions was not achievable. However, in order to rationalise the acquired data in the context of explaining our structure-diastereoselectivity trend, significant insights into the mechanism have been gained. Comparisons of SM, SKA and product concentrations for the EICR of phenylacetate **$^{13}C_2$-154**, *para*-methoxy **$^{13}C_1$-165** and *para*-trifluoromethyl **$^{13}C_1$-206** allude to the electronic dependencies responsible for varied diastereoselection-

SM (Ph-$^{13}C_2$-154/p-MeO-$^{13}C_1$-165/p-CF_3-$^{13}C_1$-206) Consumption-

It is seen that the greatest consumption of SM is observed for the *para*-methoxy substrate, with the lowest levels observed with the *para*-trifluoromethyl system. An inflection in SM return is observed for all substrates; however these are more extreme for *p*-OMe and *p*-CF_3 insinuating that IPR is a major issue in the EICR of these substrates.

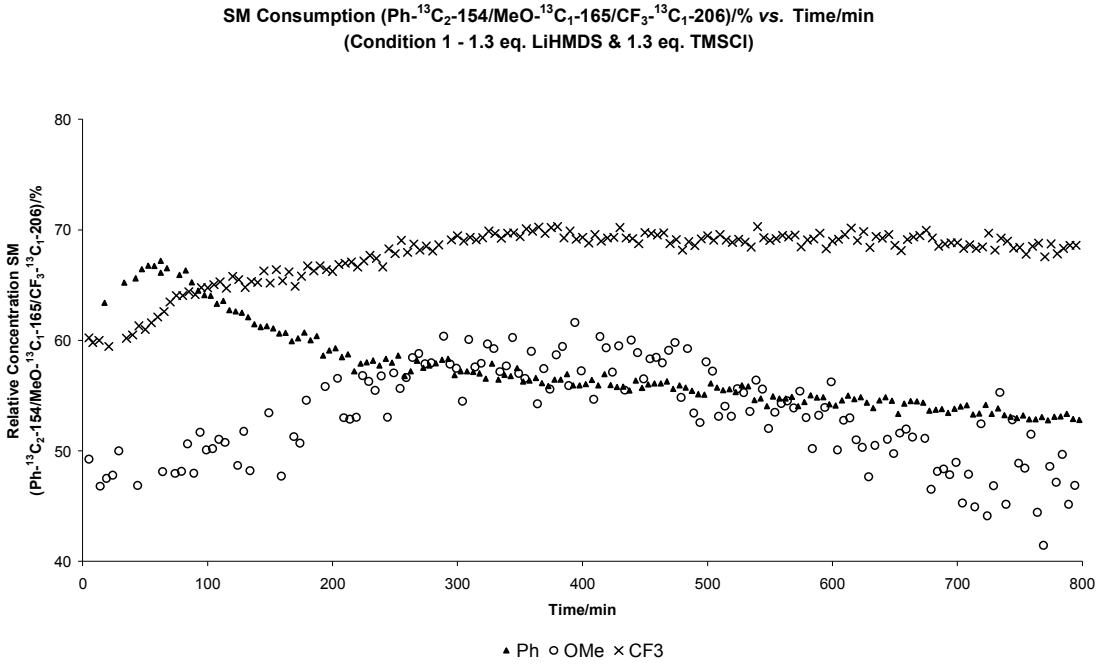

*Graph 22. Consumption of **$^{13}C_2$-154**, **$^{13}C_1$-165** & **$^{13}C_1$-206** /% vs. Time/min at -65 ˚C (Condition 1 - 1.3 eq. LiHMDS & 1.3 eq. TMSCl).*

From the outset of the reaction, most starting material consumption is seen for *para*-methoxy **$^{13}C_1$-165** which also demonstrates the largest inflection. It is rationalised that IPR to the SKA may be more facile as electron density on the α-carbon will be further enhanced by the electron donating substituent and the larger, longer inflection is the result of a fierce competition of SKA consumption *via* IPR and rearrangement. Intriguingly a shallow, longer inflection with the least SM consumption is observed for the *para*-trifluoromethyl **$^{13}C_1$-206**. At first consideration this appears counterintuitive as a greater degree of enolisation would be anticipated for systems which possess lower *pKa* values. However, although enolisation isn't a consideration in the associated Claisen rearrangement, mechanistic studies have demonstrated that electron withdrawing groups retard substrate consumption, whilst electron donating groups speed it up.[85, 146-148]

E-SKA Formation/Consumption (Ph-/MeO-/CF_3-)-

A large presence of the *E*-SKA is observed from the outset of each reaction, of which similarities in relative concentrations and consumption times are present for phenylacetate and *para*-trifluoromethyl. Intriguingly a marked increase for the initial concentration of *para*-methoxy is noted where its consumption is rapid at t < 70 minutes and gradual consumption of the residual *E*-SKA is observed until t < 750 minutes.

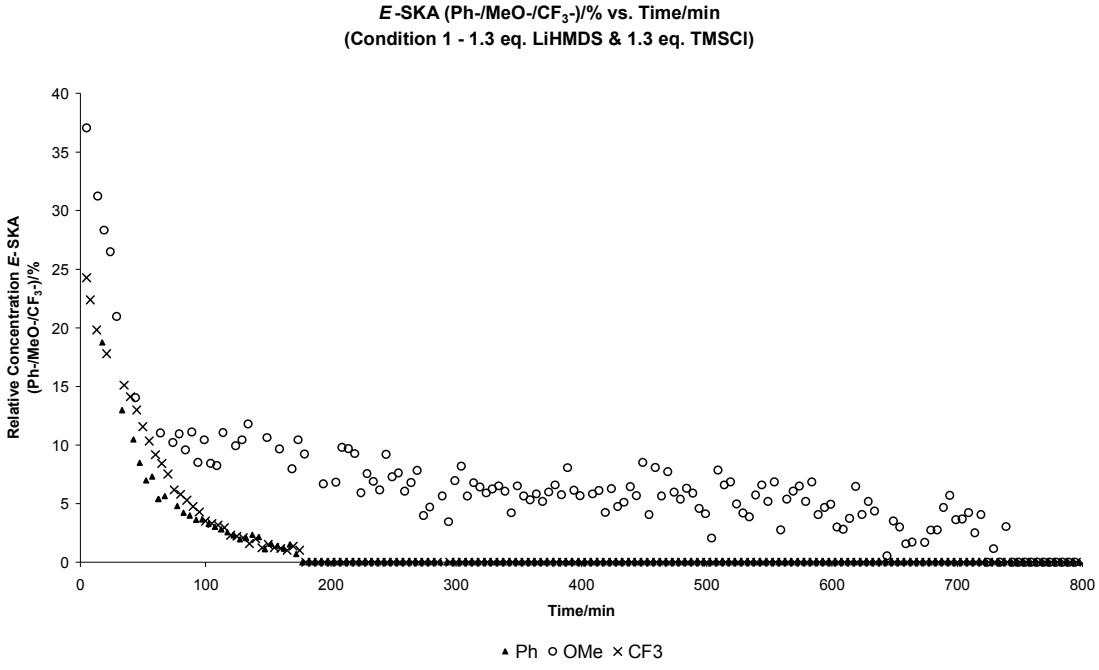

*Graph 23. Consumption of E-SKA from **$^{13}C_2$-154**, **$^{13}C_1$-165** & **$^{13}C_1$-206**/% vs. Time/min at -65 ˚C (Condition 1 - 1.3 eq. LiHMDS & 1.3 eq. TMSCl).*

Z-SKAFormation/Consumption (Ph-/MeO-/CF_3-)-

Again similarities are present for phenylacetate and *para*-trifluoromethyl in that a low steady concentration of *Z*-SKA is observed. However a marked increase is observed for the *para*-methoxy.

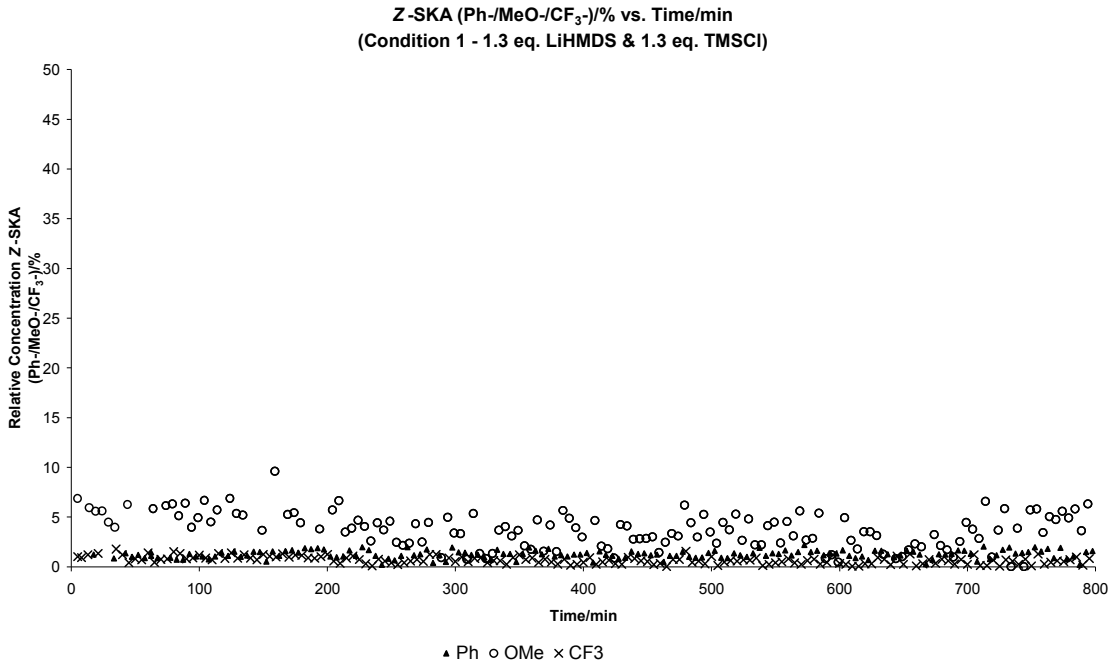

Graph 24. Consumption of Z-SKA from ***$^{13}C_2$-154***, ***$^{13}C_1$-165*** *&* ***$^{13}C_1$-206****/% vs. Time/min at -65 ˚C (Condition 1 - 1.3 eq. LiHMDS & 1.3 eq. TMSCl).*

These results concerning SKA formation may pertain to the origins of diastereoselection within the EICR and explain the change in rate determining step as alluded to by the Hammett type plot (Chapter 2). As phenylacetate **$^{13}C_2$-154** and *para*-trifluoromethyl **$^{13}C_1$-206** display similar trends in SKA formation/consumption and the *para*-methoxy **$^{13}C_1$-165** demonstrates a significantly different profile, perhaps this change in rate determining step between electron donating and withdrawing substitution is based on –

1) A reduced geometric selectivity of *E/Z*-SKA generation for electron donating substitution, which subsequently rearranges through a chair transition state.
2) A selective formation of the *E*-SKA for electron withdrawing substitution, which subsequently rearranges through chair and boat transition states.

Product (Ph-$^{13}C_2$-266/p-MeO-$^{13}C_1$-284/p-CF_3-$^{13}C_1$-285) Formation-

Similarities are yet again present between phenylacetate and *para*-trifluoromethyl in that a sharp initial formation is followed by a plateau, in which higher concentrations are ultimately observed for phenylacetate over *para*-trifluoromethyl. The *para*-methoxy displays the most intriguing behaviour in that the highest relative rate of formation is observed (t < 50 minutes) before the reaction appears to stall (50 < t < 500 minutes) and product formation resumes (t > 500 minutes). This curious behaviour associated with the mid plateau in formation of *para*-methoxy **$^{13}C_2$-284** is attributed to the selective IPR to the SKA, as observed through the extreme inflection in *para*-methoxy **$^{13}C_2$-165** return.

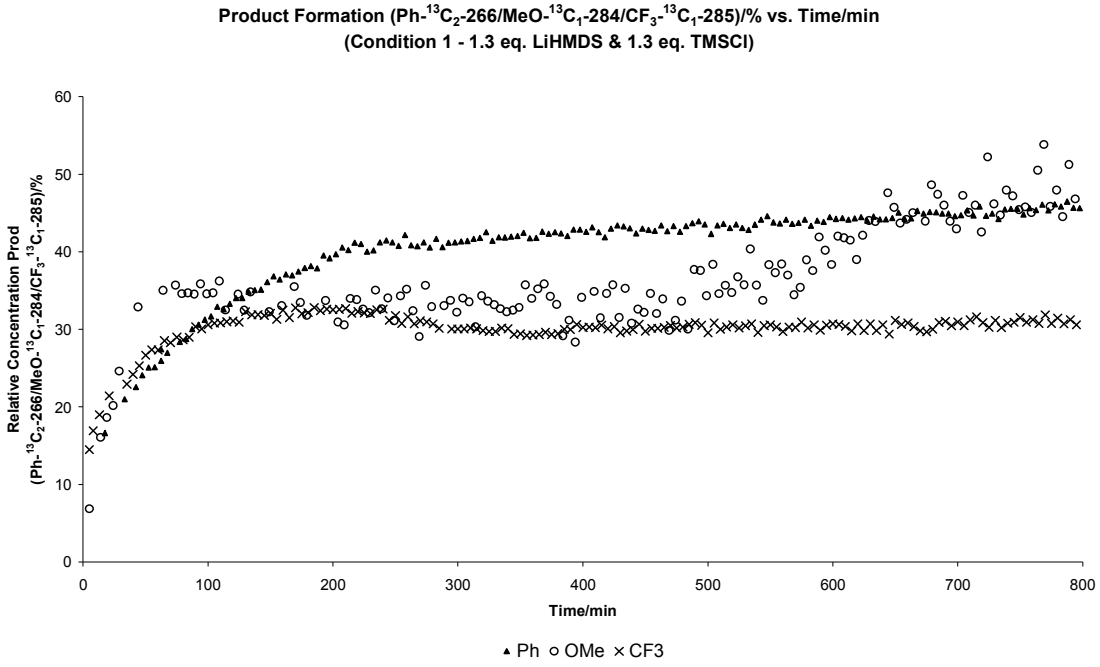

Graph 25. Product Formation from $^{13}C_2$-266, $^{13}C_1$-284 & $^{13}C_1$-285/% vs. Time/min at -65 ˚C (Condition 1 - 1.3 eq. LiHMDS & 1.3 eq. TMSCl).

It is shown that the relative concentrations of product formation are observed to be higher for *para*-methoxy with the lowest obtained for *para*-trifluoromethyl. This observation corresponds well to computational studies involving the related Claisen rearrangement, as product formation is reduced with electron withdrawing substitution on the terminal vinyl position of allyl vinyl ether reactants.[85, 146-148]

3.4. Conclusions

These mechanistic studies have allowed an in-depth insight into the electronic dependance of aryl substitution upon diastereoselection within the enamido-Ireland-Claisen rearrangement. Initial studies focussed on the *in-situ* formation and monitoring of *E/Z*-SKA selectivity derieved from electronically perturbed phenylacetate esters. Their formation was found to be highly *E*-selective but geometrical interconversion was facile under duress of remote electronic effects and the nature of the ester alkoxy moiety. These model SKA studies demonstrated that *E/Z*-SKA geometry may be responsible for diastereoselectivity within the associated EICR. In addition it has been shown that isolation of phenyl derieved SKA's are now obtainable with high levels of *E*-geometric purity and eclipse all current methodologies for their synthesis.

With a greater understanding of phenylacetate SKA's, the *in-situ* monitoring of the EICR by ^{13}C-NMR was pursued and involved the prior synthesis of ^{13}C-labelled phenylacetate **$^{13}C_2$-154**, *para*-methoxy **$^{13}C_1$-165** and *para*-trifluoromethyl **$^{13}C_1$-206** substrates. Although these *in-situ* studies have allowed a significant understanding into the EICR based on data associated with the ^{13}C label and also the silyl by-products, all reactions were plagued by the inability to monitor the formation of the *anti*- and *syn*-diastereomers of the silyester products as they are formed. However, diastereoselection within the *in-situ* rearrangements was found to correspond to the non-labelled analogues, post quench and methylation of the reaction mixture. These studies have demonstrated the complexity of the EICR through complications involving internal proton return to the enolate and SKA, and also interferences from other by-products including LiCl *auto*-catalysis and silanamine formation. The studies involving *para*-methoxy **$^{13}C_1$-165** and *para*-trifluoromethyl **$^{13}C_1$-206** substrates have aided the understanding of the varied diastereoselectivity based upon electronic perturbation. It is thought that the Hammett plot alludes to, the occurrence of a single mechanism with a change in rate determining step and it is postulated that reductions in diastereoselectivity observed for –

1) Electron donating substitution, are brought about *via* generation of poor *E/Z*-SKA geometric purity which subsequently rearranges through a chair transition state, *and*

2) Electron withdrawing susbtitution, are brought about *via* competing chair and boat transition states from the selectively formed *E*-SKA.

In addition to the NMR studies a computational collaboration has been initiated *in-house*, in order to corroborate the origins of diastereoselection. These *in-silico* studies have involved modelling the rearrangement for the 9 *para*-substituted substrates, assuming that they proceed from either the *E*- or *Z*-SKA or if a rapid interconversion of the *E/Z*-SKA's occurs. Initial results from this study have indicated that correspondence to experimental results are best suited to the occurrence of an *E/Z*-SKA interconversion and rate studies have alluded to faster rates of rearrangement for electron rich substitution.

4. Alternative *N*-Protection in the EICR

As thorough investigations into the EICR of arylacetate enamides have been conducted, attention was now redirected towards alkylacetate substrates, as previous results have shown that their rearrangement occurs with poor diastereoselectivity.[109]

4.1. Propionate EICR

Initial investigation focussed on the EICR of the propionate **265**, synthesised in good yield *via* the standard EDCi coupling of **145** with propionic acid.

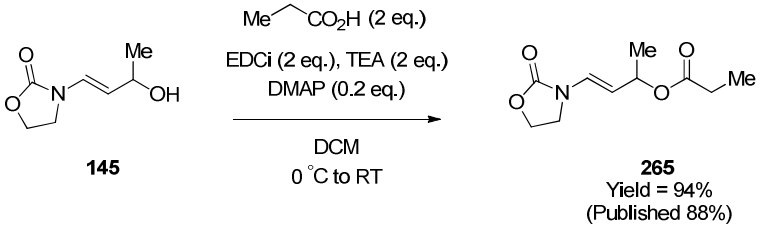

Scheme 116. Synthesis of Propionate 265.

Initial investigations with propionate **265** focussed on utilising the optimised conditions developed for the phenylacetate EICR (Chapter 2) and that involving the increased loading of TMSCl (Chapter 3). Utilisation of these conditions produced **139** with an improved yield, however no improvement in diastereocontrol was observed (Entry 1 and 2, Table 15). Recovery of mass balance through isolation of methylated propionic acid **286** was not accomplished due to volatility, however ^{1}H-NMR analysis of crude reaction mixtures alludes to its presence.

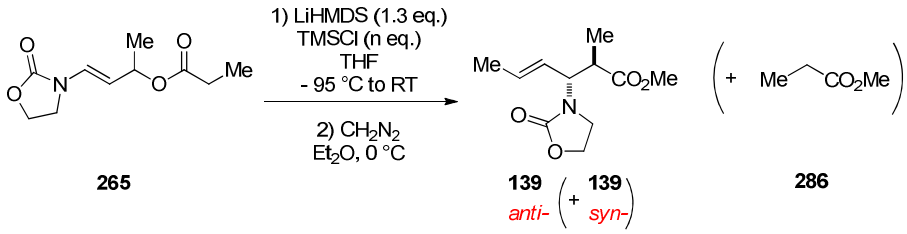

Entry	TMSCl (n eq.)	Yield **139** (%)	d.r.[b] (*anti:syn*)
1	1.3	72	2:1
2	6	70	2:1

[a]*d.r. measured by* ^{1}*H NMR*

*Table 15. EICR of **265** under Optimised Conditions.*

Further investigations involved probing the effect of amide base used, where utilisation of NaHMDS resulted in a quantitative return of alcohol **145**, however KHMDS, $Mg(HMDS)_2$ and LDA all yielded intractable mixtures of products.

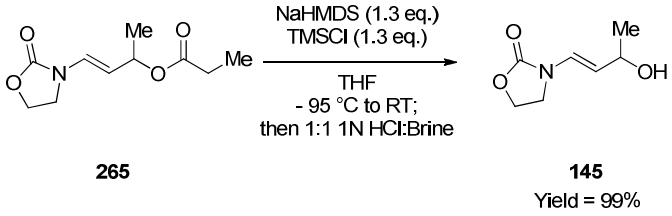

*Scheme 117. Subjection of **265** to NaHMDS Mediated EICR.*

Alternative investigations have involved the use of soft enolisation conditions as that reported by Angle in the synthesis of $\Delta^{4,5}$-pipecolic esters, which saw the Ireland-Claisen rearrangement of lactone **287** by triethylamine and triisopropylsilyl triflate.[171]

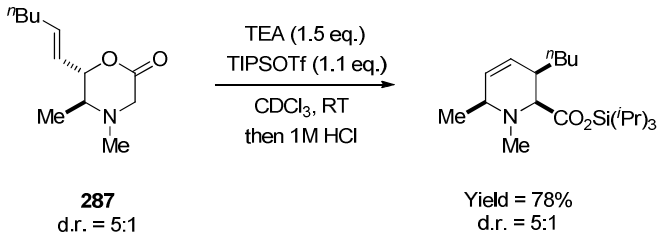

Scheme 118. Angle's Soft Enolisation Conditions.

Unfortunately, subjection of propionate **265** to these reaction conditions resulted in the formation of intractable mixtures of products.

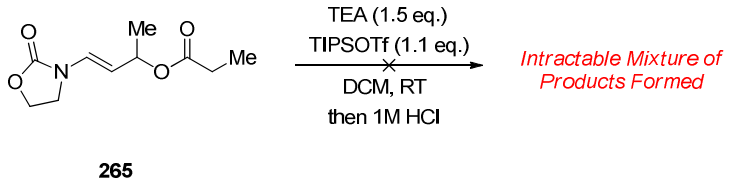

Scheme 119. Application of Angle's Soft Enolisation Conditions.

Other alternatives have included investigations into alternative enolate trapping agents. Funk reported the use of diethoxyphosphinyl chloride, allowing generation of enol phosphates **288** after LDA deprotonation.[172] Subsequent rearrangement of **288** generates the mixed carboxylic diethoxyphosphoric anhydrides **289**, which have been shown to be useful acylating agents allowing generation of esters and Weinreb reagents **290**. Funk noted that the diastereoselection obtained matched that of the traditional Ireland-Claisen protocol.

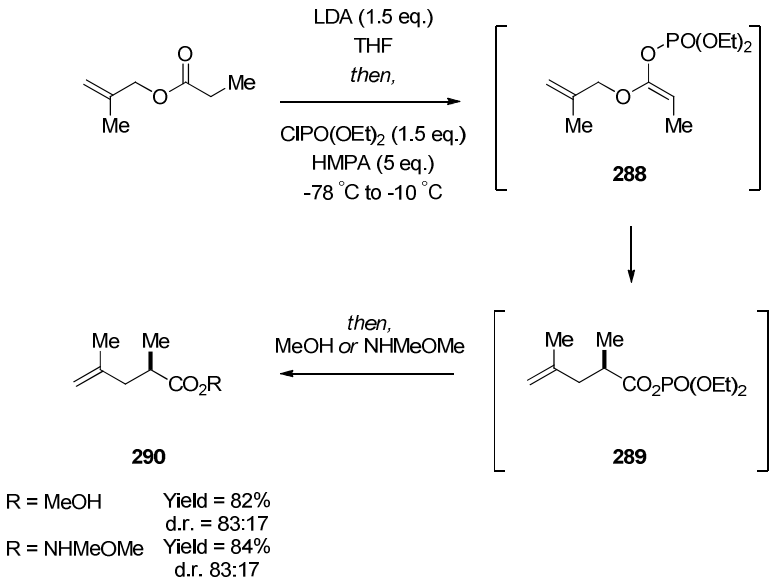

Scheme 120. Funk's Alternative Trapping Reagent.

Unfortunately, treatment of propionate **265** yielded intractable mixtures of products.

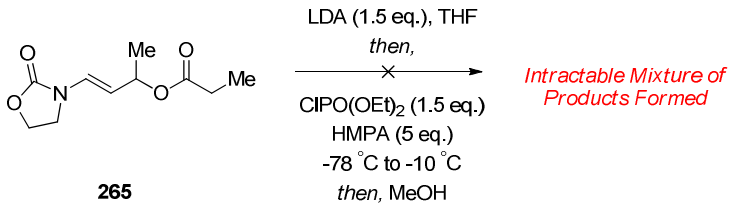

Scheme 121. Attempt at Funk's Alternative Trapping Conditions.

Although Funk's protocol proved to have detrimental effects on the rearrangement of **265**, the use of HMPA in this context was intriguing. It is well known that the geometrical outcome of SKA generation *via* traditional Ireland-Claisen protocols can be controlled by the presence or absence of certain additives and HMPA is classically used to allow selective formation of the Li-(*E*)-enolate and subsequently the *Z*-SKA.[66] The mechanism in which the *E*-enolate is formed relies on premixing the lithium base and HMPA, allowing the Lewis basic HMPA to co-ordinate to lithium subsequently reducing its Lewis acidity, prior to addition of substrate. The reduction in the electrophilicity of lithium yields a looser six-membered transition state for enolisation, of which 1,2-transannular effects become more important than 1,3-diaxial effects, resulting in the *E*-enolate. This aspect of enolate control is highlighted by Ireland-Claisen rearrangement of **119** in Scheme 122.[76]

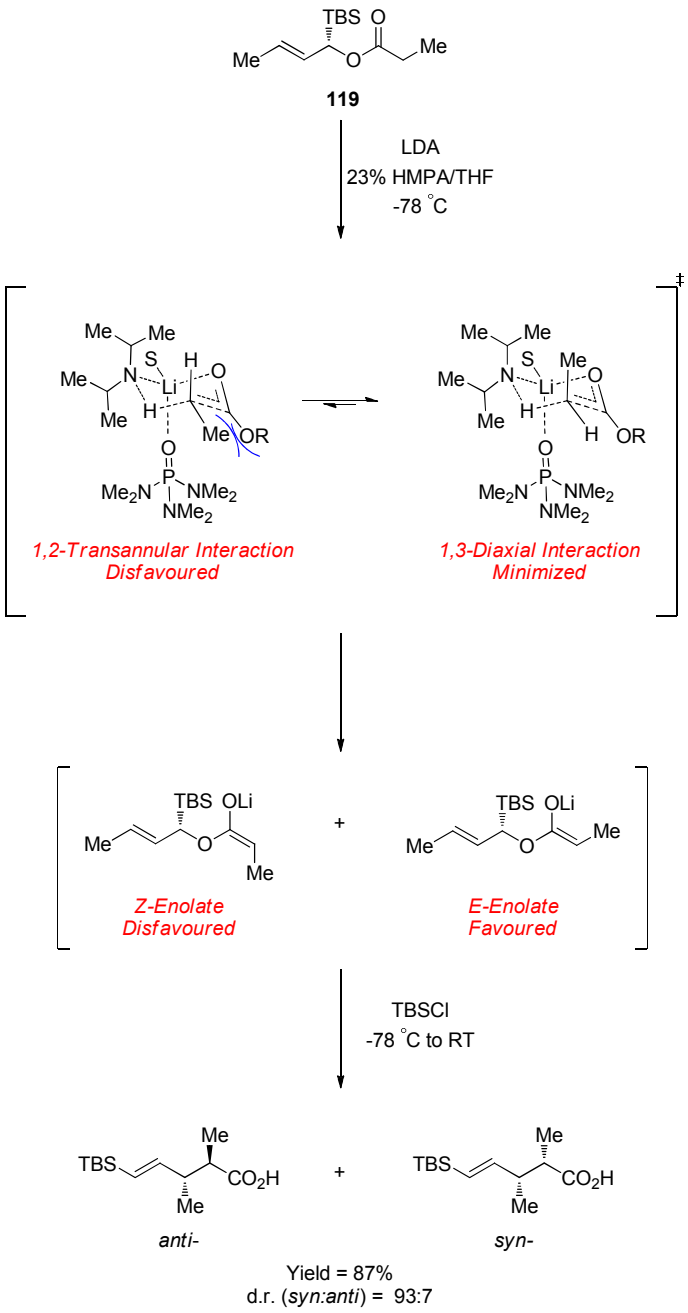

Scheme 122. Mechanistic Considerations for syn-Selective Ireland–Claisen Rearrangement.

As the selective formation of either *E*- or Z-SKA's offers diastereocontrol, this prompted us to ascertain whether the *syn*-diastereomer could be formed using the EICR protocol. Subjection of propionate **265** to rearrangement conditions containing 23 vol% HMPA/THF yielded an intractable mixture of products. However repeating the reaction and replacing the hydrochloric acid quench with methanol, allowed the quantitative isolation of the alcohol **145**. Isolation of **145** by this modified quench protocol insinuates that the presence of HMPA may favour decomposition of the

enolate formed, possibly resulting in a degradation *via* a ketene pathway (Chapter 2, Scheme 65).

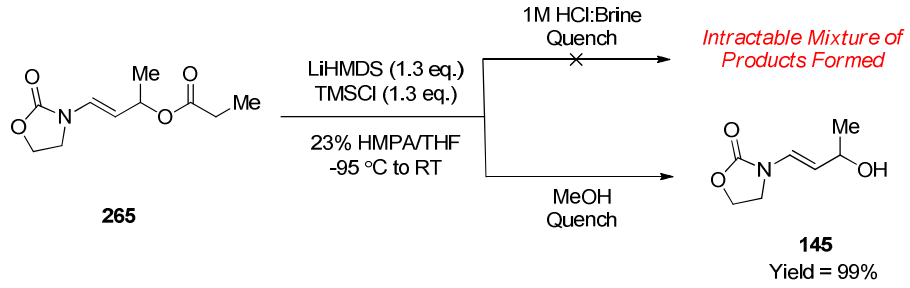

Scheme 123. Attempt at syn-Selective EICR

Whilst studies concerning **265** where ongoing, Collum reported the first example of a TMSCl-free, LiHMDS-mediated Ireland-Claisen rearrangement.[173] The key to the success of this reaction was replacement of the Lewis basic solvent, THF, for a toluene/triethylamine solvent mixture. Collum reported that the LiHMDS/triethylamine mediated enolisation of **291** affords **292** rapidly and selectively, with subsequent rearrangement producing **293** in excellent yield, diastereoselectivity and was also twenty times faster than the corresponding reaction conducted in THF.

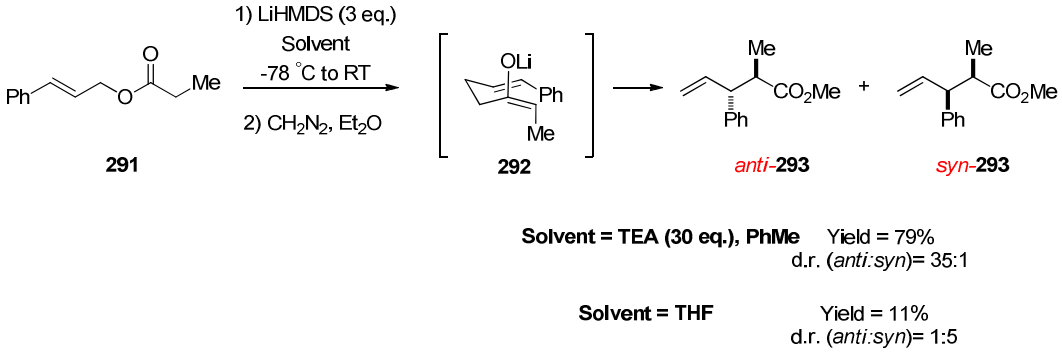

Scheme 124. Collum's LiHMDS/TEA Ireland-Claisen Rearrangement Protocol.

Unfortunately, mechanistic studies involving the nature of LiHMDS/triethylamine ester enolisation and subsequent Ireland–Claisen rearrangement are reported to be published in due course. However, Collum has currently proposed an explanation for the rapid and selective enolisation observed, through analytical techniques such as

React-IR and ^{6}Li- and ^{15}N-NMR spectroscopic studies involving enolisation of ketone **294**.[173]

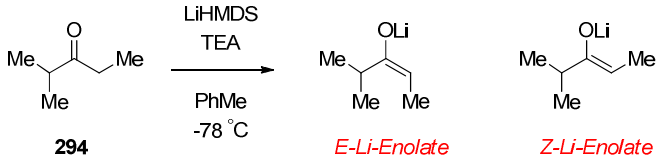

Scheme 125. Ketone Used for Collum's Enolisation Mechanistic Studies.

Primarily the reaction proceeds under kinetic control, however, the analytical observations revealed some interesting subtleties (Scheme 126). Notably the toluene/triethylamine mediated enolisation occurs *via* a dimer based mechanism **298** in contrast to a monomer based mechanism associated with THF **299**.[174,175] Subjection of ketone **294** to LiHMDS/triethylamine (3:30 equivalents) revealed the lithium enolate-LiHMDS mixed dimer **300** with an *E/Z* selectivity of 100:1. However, when the equivalents of LiHMDS are lowered (<2) significant reductions in *E/Z*-enolate purity are observed, resulting from a facile equilibration and consequent formation of mixed *E/Z*-**300** dimers. When LiHMDS loading is lowered to 1 equivalent, enolisation is not observed and the substrate autoinhibits the reaction, leading to the formation of the unreactive bis-complexed dimer **297**.

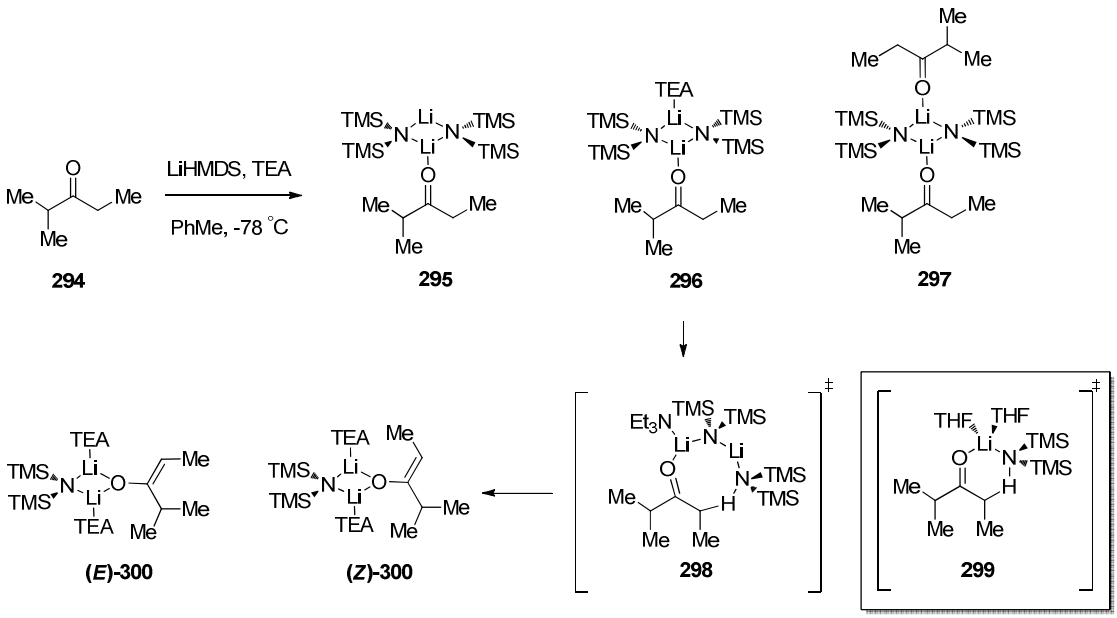

Scheme 126. Solvation Structures of Reactant, Transition Structures & Enolates.

The excellent geometric selectivity associated with the triethylamine mediated enolisation, stems from the selective stabilisation of the rate-limiting transition structures, relative to the reactants. Therefore solvents which display little or no affinity for the reactants and a high affinity for the transition structure maximise reaction rates. It has been shown that triethylamine mediated enolisations are typically 150 times faster than when performed in neat THF.[174] This rate acceleration derives from the destabilising steric affects associated with solvation of the LiHMDS dimer **295**, producing **296**. Alleviation of these unfavourable steric interactions is subsequently accomplished through generation of dimeric transition structure **298** allowing enolisation. With this exciting protocol reported by Collum in hand, rearrangement of propionate **265** was attempted using this procedure.

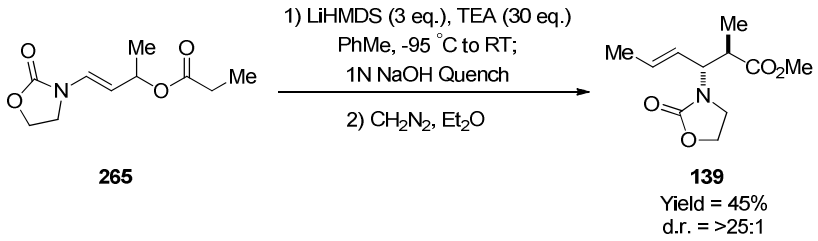

Scheme 126. EICR Using Collum's Protocol.

Encouragingly, the isolation of **139** in moderate yield and excellent diastereoselectivity is in stark contrast to previous attempts. However, accounting for mass balance of this reaction became difficult. Analysis of the crude reaction mixture by ^{1}H-NMR pre-methylation, alluded to the selective formation of the *anti*-diastereomer **301** and **302**, presumably generated by an E1cB type elimination of the rearranged lithium carboxylate.[176] Methylation of the crude reaction mixture was pursued and although isolation of **139** was accomplished, isolation of **303** was not. Attempts at isolating **302** was subsequently attempted by column chromatography and recrystallisation post rearrangement, however co-elution and recrystallisation with **301** resulted in both cases.

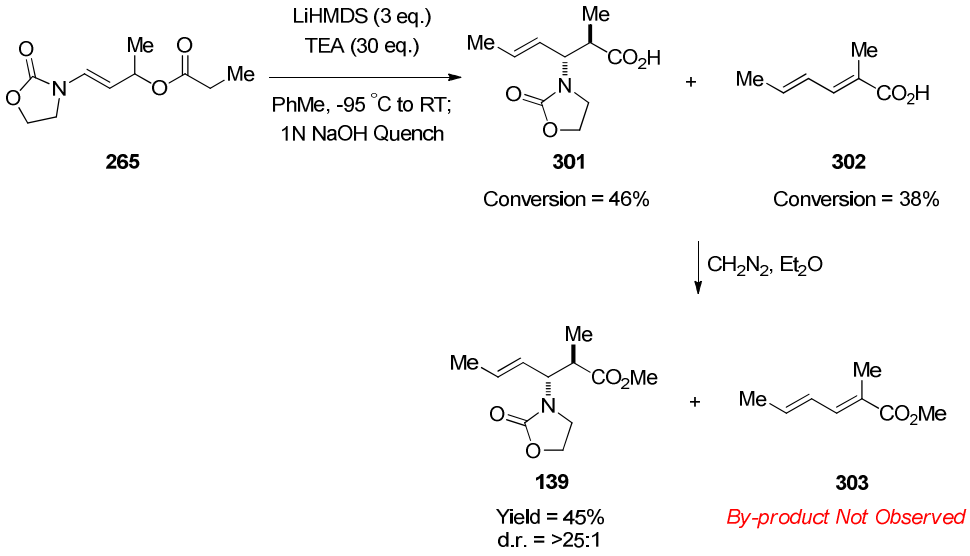

Scheme 127. By-product Observation.

To rationalise the generation of **302**, it was reasoned its formation may occur *via* post-rearrangement enolisation of Li-carboxylate **304** by either the presence of excess LiHMDS *and/or* the 1N NaOH reaction quench.

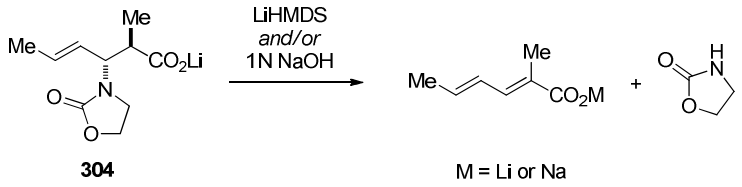

Scheme 128. Possible Degradation of Rearranged Li-Carboxylate via E1cB Elimination.

Quenching the rearrangement with the non-nucleophilic $NaHCO_3$ resulted in identical product distributions to that seen with the 1N NaOH quench. The generation of **302** was subsequently attributed to the large excess of LiHMDS required with Collum's protocol and is in conjunction with observations previously reported (Chapter 2).

The use of LiHMDS/triethylamine (3 eq./30 eq.) has been found to be optimal for enolisations of esters and ketones. However, in order to ascertain whether Collum's protocol can be adapted to the EICR, optimisation of this procedure was pursued. In order to counteract the issue of excess LiHMDS within the reaction protocol, any attempts at reducing the amount of LiHMDS and triethylamine resulted in complex

intractable reaction mixtures, with limited if any signs of product or by-product formation by ^{1}H-NMR. Unsurprisingly, increasing the amount of LiHMDS (4 eq.) led to a reduced yield of **301** with an increase in **302**.

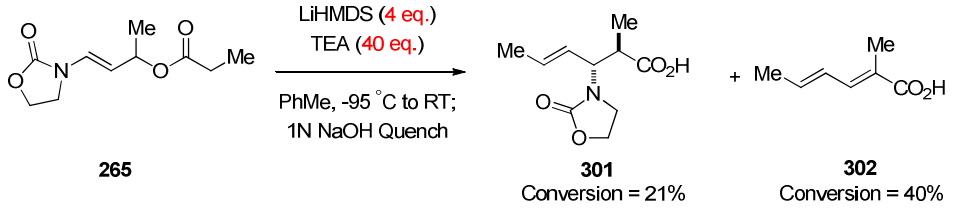

Scheme 129. Increasing LiHMDS in Propionate EICR.

Investigations into solvent exchange demonstrated the importance of a non-Lewis basic media. Hexane displayed analogous results to toluene; however the use of THF and ^{t}butylmethylether displayed complex and intractable reaction mixtures, with no product **301** or by-product **302** observed.

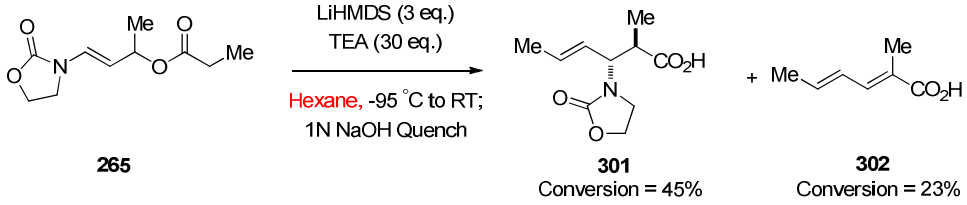

Scheme 130. Solvent Exchange in Propionate EICR.

Investigations into alternative bases including NaHMDS and KHMDS yielded varying amounts of unreacted starting propionate **265** (Entries 1 & 2, Table 16) with no signs of any rearrangement occurring.

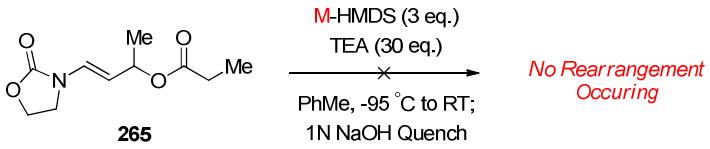

Entry	M	Yield **265** (%)
1	Na	67
2	K	51

Table 16. Amide Base Exchange in Propionate EICR.

In order to improve the reaction efficiency, the addition of TMSCl was pursued, following *in-situ* (Entry 1, Table 17) and *ex-situ* (Entry 2, Table 17) quench protocols. Incorporation of this additive demonstrated near complete formation of the E1cB by-product **302**, with trace amounts of product **301** being observed. Presumably this enhanced degradation arises from generation of the Lewis acid, LiCl within the reaction mixture.

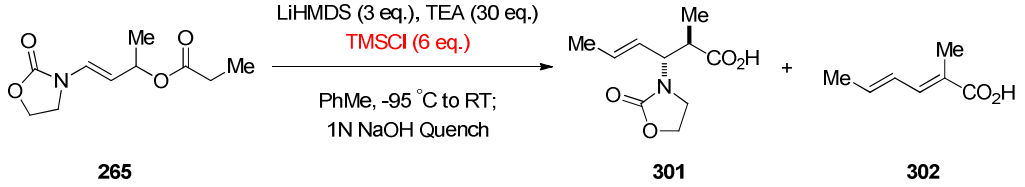

Entry	Addition of TMSCl	Yield **301** (%)	Yield **302**[a] (%)
1	*In-situ*	2	80
2	*Ex-situ*	3	80

[a]*Based on ^{1}H-NMR Conversion.*

Table 17. Additive Effects in Propionate EICR.

As these initial optimisation attempts were shown to be unfavourable, attention was now turned to product **301** and by-product **302** distributions. A notable observation was that formation of **301** was never acheived in a yield >45%, with mass balance being accounted for by formation of **302**. Further to this, the addition of TMSCl (Table 20) yielded near quantitative formation of **302**, presumably caused by the formation of the familiar Lewis acid, LiCl (as discussed in Chapter 3). In relation to our enamido

ICR, the *in-situ* formation of LiCl could either allow E1cB degradation to occur on a diastereoselective or a non-diastereoselective rearrangement product. It was subsequently realised that a non-diastereoselective rearrangement may be occurring under Collum's protocol and the formation of a single diastereomer in 45% yield may be the result of a *pseudo*-kinetic resolution of one diastereomer (*syn*-) compared to the other (*anti*-). In order to determine if this is the case, quenching the reaction prior to the onset of E1cB elimination would be advantageous. It is noted that during warming of the reaction a colour change was noted at 0 ˚C and was ascribed to the possible onset of E1cB elimination. With this in mind the reaction was repeated and an arbitrary temperature of -10 ˚C was chosen to warm the reaction to, where it was subsequently quenched after an identical reaction time. Analysis of the crude reaction mixture by ^{1}H-NMR alluded to no formation of **302** with **139** generated in a non-diastereoselective fashion. Although the yield for this reaction was low the majority of the mass balance was obtained by re-isolation of the starting propionate **265**.

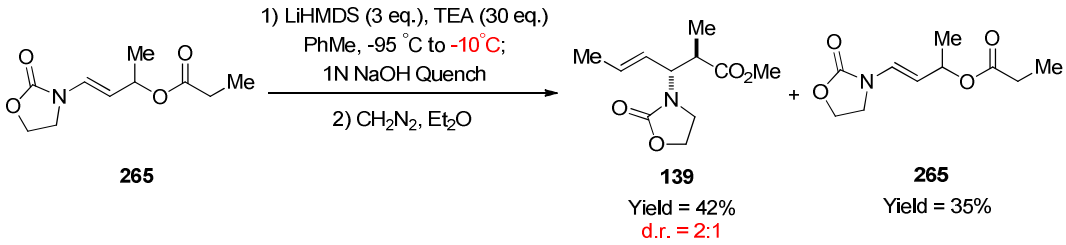

Scheme 131. Investigating Diastereoselectivity of EICR.

To demonstrate that the *syn*-diastereomer is more susceptible to E1cB type elimination than the *anti*-diastereomer, subjection of carboxylic acid **301** (d.r. = 2:1) to LiHMDS (3 eq.) and triethylamine (30 eq.) was pursued. The subjection of **301** to standard Collum protocols was envisaged to mirror post rearrangement concentrations of LiHMDS and triethylamine, as one equivalent of LiHMDS would generate a lithium carboxylate. This study demonstrated the selective elimination of *syn*- over the *anti*-diastereomer and it is noted that conversion to *anti*-**301** in 59% is marginally lower than that expected for a 2:1 mix of diastereomers, where 66% would be the theoretical maximum yield. It is therefore suggested that elimination of *syn*-**301** is more facile, but this does not mean that *anti*-**301** is completely unsusceptible.

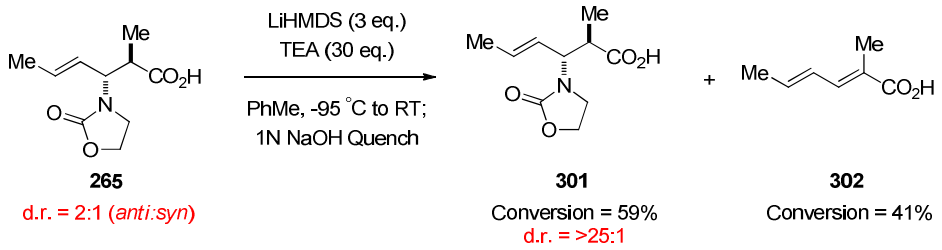

Scheme 132. Investigating the Selectivity of the E1cB Type Elimination.

The utilisation of the Collum protocol in the EICR of propionate **265** allows clean access to a single *anti*-diastereomer in 45% yield. This contrasts favourably with our previous report.[109] However the inherent issues associated with the unselective reaction and the reliance of a *pseudo*-kinetic resolution to generate high *anti*-diastereoselectivities are not ideal and led us to pursue alternative enamide nitrogen protection.

4.2. Investigation into Alternative *N*-Protection

The successful EICR of propionate and arylacetate enamido allylic esters in generating β-amino acid precursors would allow access to a wide variety of natural and non-natural targets. Such targets could involve the prescribed stimulant methylphenidate (Ritalin®) **5** and the antimicrobial β-peptide unit key to β-foldamers, such as *trans*-2-aminocyclpentanecarboxylic acid (ACPC) **21** and derivatives thereof.[5, 20-21] Other larger targets could involve that of the cytotoxic motuporin **19**.[14]

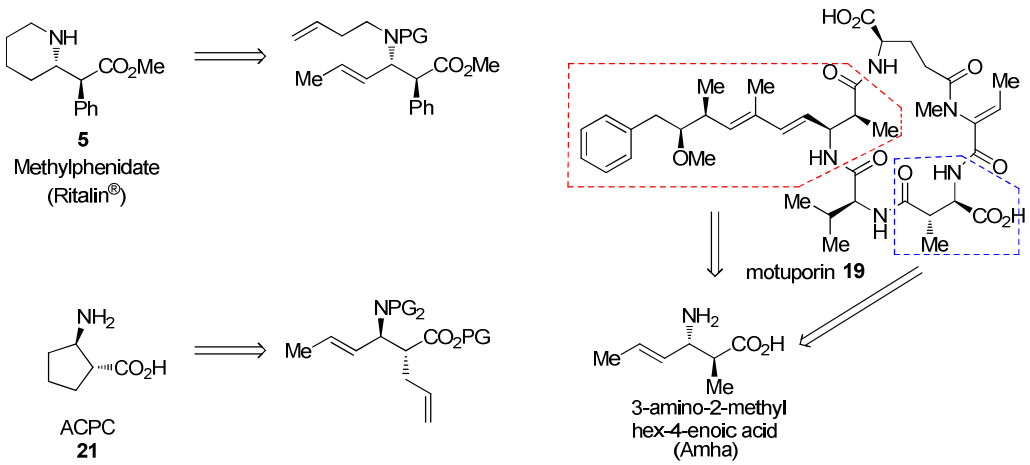

Scheme 133. RSA of Potential Target Molecules

Access to any target molecule using the EICR strategy relies on the use of a suitable enamide with reliable protecting groups. In an attempt to enhance the utility of the EICR, alternative enamides were investigated to probe any structure-reactivity trends. A number of potential enamides were identified based on the ability to modulate the electron donating capability of the enamine nitrogen but also to serve as readily cleavable protecting groups. The use of *p*-tolylsulfonamide (cleaved by Mg/MeOH) the use of *N*-Boc (cleaved by trifluoroacetic acid) and *N*-phthalimide (cleaved by hydrazine) were chosen for investigation.[177-179] Other orthogonal components, in addition to the required electron withdrawing group, could be satisfied by use of *N*-alkyl derivatives such as the allyl group (cleaved by Wilkinson's catalyst) or the benzyl group (cleaved by hydrogenolysis).[180-181] With these protecting groups in mind several, target EICR substrates were identified, subsequently allowing synthesis of a variety of protected β-amino acid precursors, including the phthalimide **305**, diBoc **306**, allylBoc **307**, benzylsulfonamide **308** and the allylsulfonamide **309**.

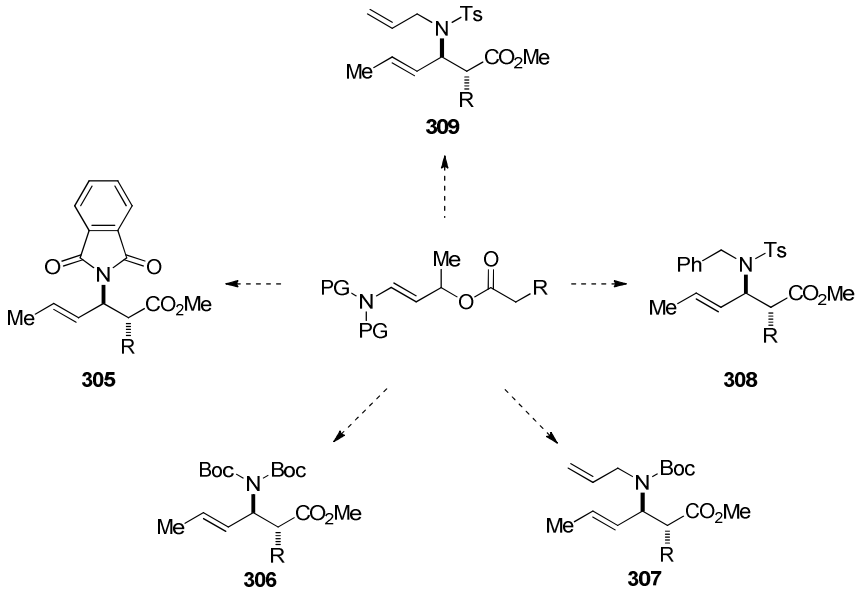

Scheme 134. Enamide Substrates for Evaluation.

4.2.1. Enecarbamates

Initial investigations surrounding the use of *N*-Phth and *N*-Boc protection proved problematic. Access to racemic *N*-Phth and *N*-Boc enamido secondary alcohols were attempted by the standard protocol, involving Jones oxidation of **149** and subsequent addition of the appropriate nitrogen nucleophile in good yields.

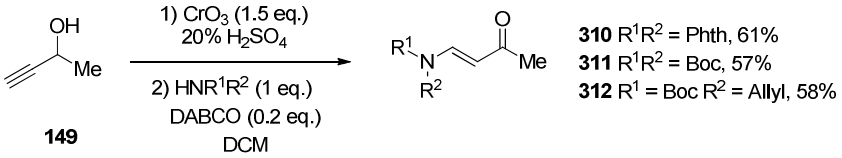

Scheme 134. Route to Alternative N-Protected Enamides.

Subsequent chemoselective reduction of the ketone proved to be problematic for the *N*-phthalimide **310**, as competition between reduction of the imide functionality was seen in addition to reduction of the ketone. Reduction of **310** with 1 equivalent of $NaBH_4$ offered no advantage, with intractable mixtures of products resulting.

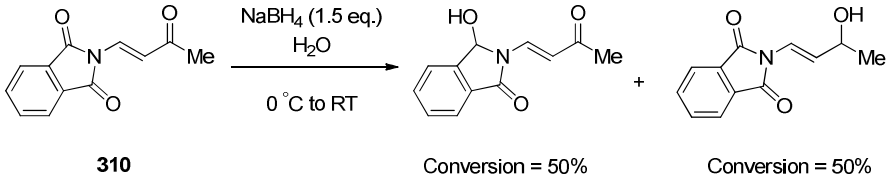

Scheme 135. Route to N-Phth Protected Enamides.

Reduction of the *N*-Boc systems **311** and **312** also appeared challenging as the alcohols **313** and **314** proved more facile to dehydration and observation of crotonaldehyde **157** and parent *N*-Boc amine **315** signals by ^{1}H-NMR spectroscopy resulted.

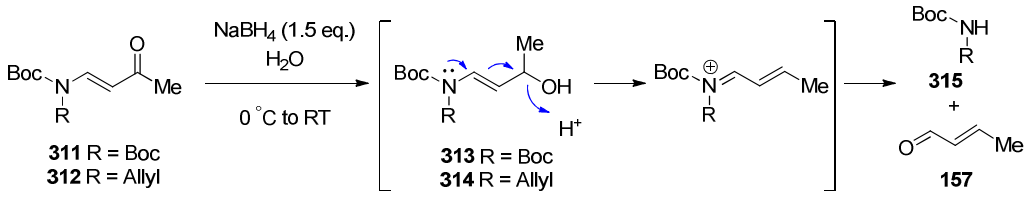

Scheme 136. Route to N-Boc Protected Enamides.

4.2.2. Enesulfonamides

With unsuccessful access to *N*-Boc and *N*-Phth secondary alcohols, attention was turned to the stereoselective synthesis of secondary sulfonamide alcohols adapted from a procedure reported by Meyer.[106, 182] This approach was initially shown to allow selective access to primary propargylic *E*- and *Z*-enesulfonamides, *via* copper-catalysed coupling between sulfonamide **316** and bromoalkyne **317**. Alkyne, **319** was then reduced with geometrical control to produce the *E*-**322** or *Z*-**321** isomer. Meyer has subsequently demonstrated that the synthesis can also be applied to generating the secondary *N*-benzylsulfonamide alcohol **323** in high yield.

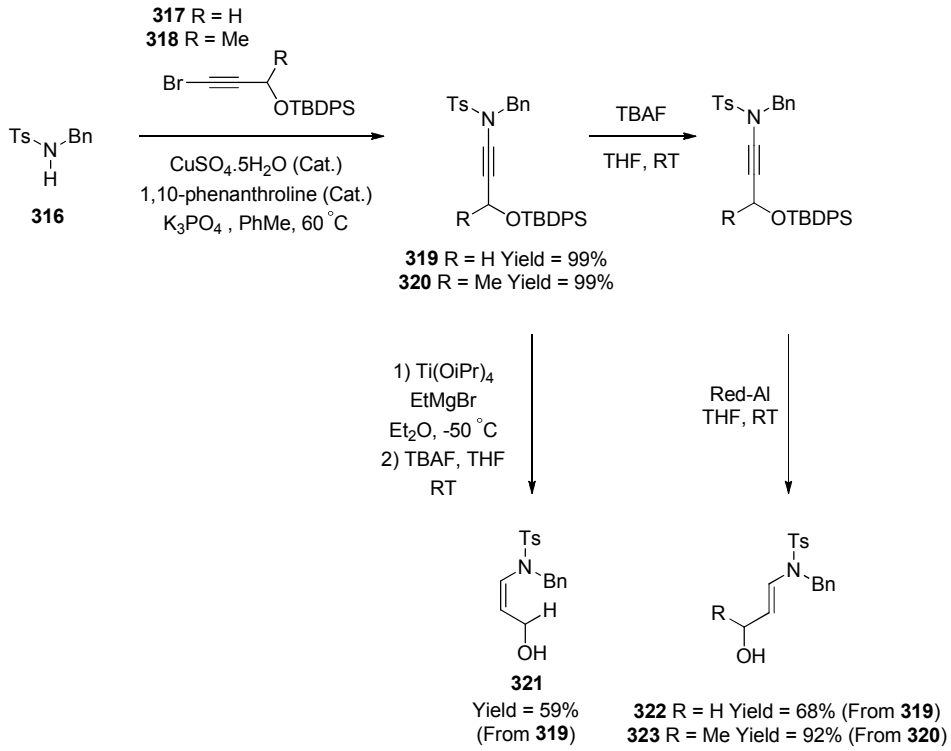

Scheme 137. Meyer's Synthesis of N-Protected Vinylogous Alcohols.

The added benefit of utilising Meyer's protocol is that the synthesis can offer access to enantiomerically pure secondary enesulfonamide alcohols. This synthetic route should then allow chirality transfer within the EICR, providing rearrangement of the sulfonamide allylic ester substrates occurs efficiently. Therefore a unique entry into carbocyclic and heterocyclic β-amino acids, such as ACPC **21** and β-proline **324** or iminosugar analogues **325** should be possible.

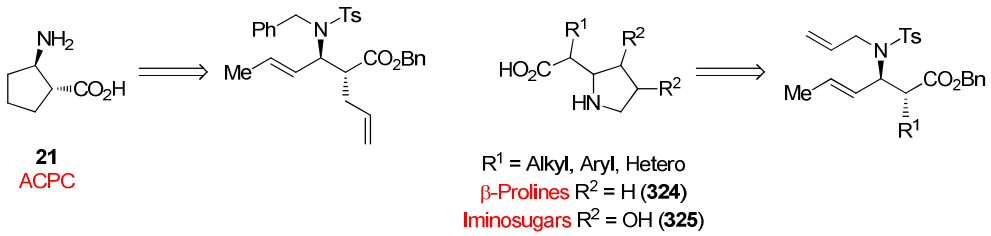

Scheme 138. RSA of Potential Target Molecules.

To allow rapid investigation into the EICR of these enesulfonamides, the synthetic route undertaken again relied on the reported procedure by Carbery and Janey.[109,113] The synthesis of racemic **329** and **323** involved the two step procedure involving Jones oxidation of **149**, followed by the immediate conjugate addition of the appropriate sulfonamide **326** or **316** in the presence of catalytic amounts of DABCO.[114] Reduction of ketone **327**/**328** was achieved by a modified protocol where higher loadings of sodium borohydride and a dual THF/MeOH solvent system were required.[183] Key sulfonamides **329** and **323** were afforded in good yields and importantly, the acid sensitive compounds were isolated by simple aqueous work-up, without the need for further purification.

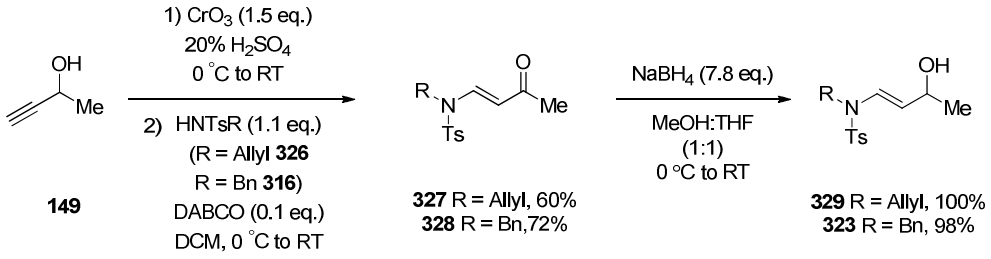

Scheme 139. Route to Racemic AllylTs & BnTs Secondary Alcohol.

4.2.3. EICR Optimisation of Propionate & Phenylacetate *N*-Allylsulfonamides

With a rapid and efficient route to multigram quantities of both racemic *N*-allylsulfonamide **329** and racemic *N*-benzylsulfonamide **323** alcohols in hand, synthesis of rearrangement substrates was subsequently pursued. Initial investigations involved synthesis of the propionate-**330** and phenylacetate-allylsulfonamide **331**, both in excellent yields *via* the standard esterification protocol using EDCi.

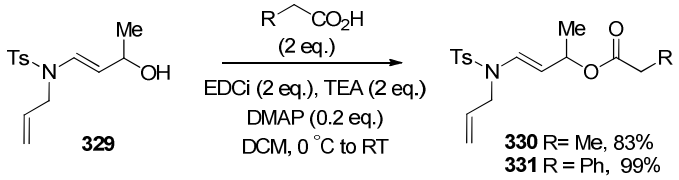

Scheme 140. Synthesis of Racemic Propionate & Phenylacetate Sulfonamide Substrates.

With the required alkyl and phenylacetate substrates in hand, investigations surrounding the EICR of these substrates could now be pursued. Both substrates were subjected to optimised rearrangement conditions detailed in Chapter 3 (LiHMDS 1.3 eq., TMSCl 6 eq.). Subjection of the propionate allylsulfonamide **330** to these conditions led to quantitative return of the alcohol precursor **329**, presumably resulting from instability of enolate or SKA. It is further noted that isolation of methyl propionate **332** would be expected, but due to volatility issues this was never accomplished. However subjection of phenylacetate **331** to rearrangement conditions was mildly successful, generating the rearranged β-amino acid precursor **333** in poor yield but excellent diastereoselectivity. Near quantitative mass balance for this rearrangement was recovered by isolation of methyl phenylacetate **158**.

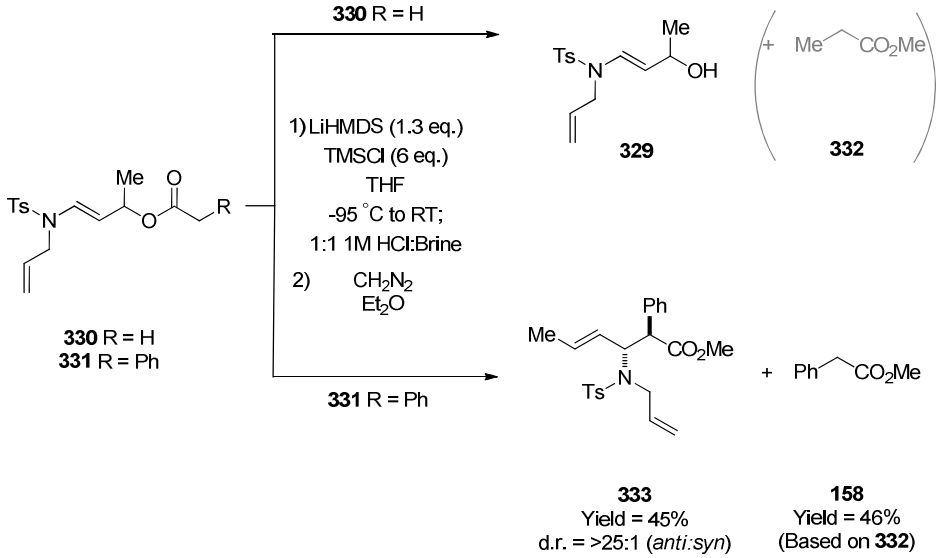

Scheme 141. EICR of Racemic Propionate & Phenylacetate Sulfonamide Substrates.

With encouraging results seen by the rearrangement of the phenylacetate **331**, an optimisation of rearrangement conditions was performed on this substrate. A possible consideration as to why the reaction may produce a poor yield, is that lithiation of the *N*-allyl group and subsequent formation of a sulfonamide co-ordinated 5-membered ring may be a competing process.[184]

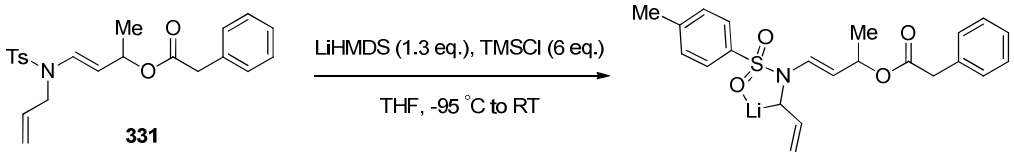

Scheme 142. Possible Formation of 5-membered Ring.

If this were the case then simply increasing the number of equivalents of LiHMDS should circumvent this issue. With this in mind a small optimisation involving investigations into the equivalents of LiHMDS was pursued, with 2, 2.25, 2.5 and 3 equivalents all demonstrating increased yields of **333** and reductions in **158**. As an optimal yield was obtained for use of 2.5 equivalents of LiHMDS (Entry 3, Table 18), all future rearrangements of arylacetate sulfonamides were subjected to this condition.

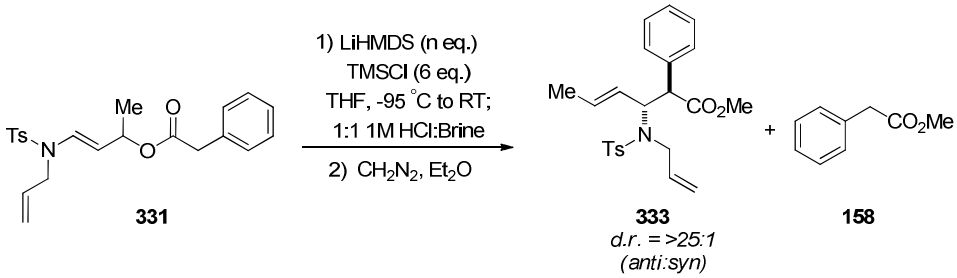

Entry	LiHMDS (n eq.)	Yield **333** (%)	Yield **158** (%)[a]
1	2	59	18
2	2.25	60	31
3	2.5	67	27
4	3	60	31

[a] *Yield refers to **333** that **158** would correspond to.*

Table 18. Optimisation of Phenylacetate Allylsulfonamide EICR.

With the successful rearrangement of the phenylacetate **331** in hand, efforts were then redirected to the rearrangement of the propionate **330**. Subjection of **330** to the newly optimised rearrangement conditions yielded an intractable mixture of products, however analysis of crude ^{1}H-NMR spectra indicated limited signs of **334** with a diastereomeric ratio of 1:1.

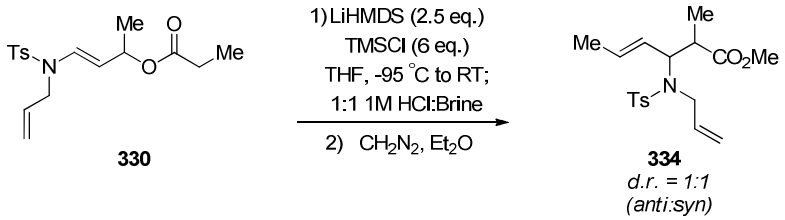

Scheme 143. EICR of Racemic Propionate Sulfonamide Substrate.

With the EICR of the propionate **330** still being problematic, the use of Collum's conditions was revisited.[173] Subjection of **330** to the standard conditions involving 3 equivalents of LiHMDS and 30 equivalents of triethylamine led to the formation of intractable reaction mixtures. However, following a swift investigation into increasing the stoichiometry of the base and co-solvent, clean formation of **334** was only

observed with 4.5 equivalents of LiHMDS and 45 equivalents of triethylamine. In an attempt to account for mass balance, it is noted that formation of E1cB degradation product was not observed, but the presence of methyl propionate **332** signals within the crude ^{1}H-NMR alludes to the familiar degradation of enolate.

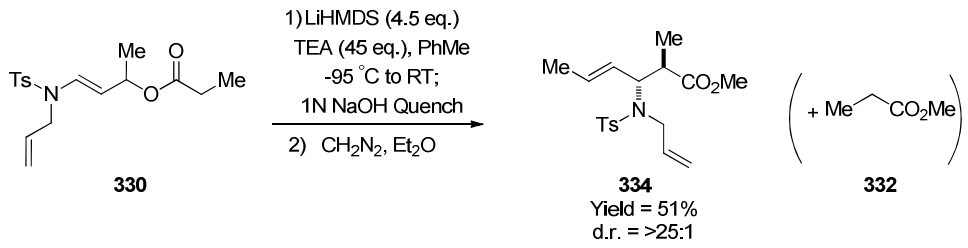

Scheme 144. EICR of Racemic Propionate Allylsulfonamide Using Collum Conditions.

4.2.4. EICR of Alkyl & Arylacetate *N*-Allylsulfonamides

With the optimisation of the phenylacetate **331** and propionate **330** rearrangements completed, a number of alkyl- and aryl-substrates were synthesised using the standard EDCi coupling conditions in excellent yields. It is noted however, that heteroatom substitution (Entry 3 & 4, Table 19) was extremely sensitive and subjection of these substrates to EICR conditions was required immediately. Synthesis of an *N*-phthalimide substrate (Entry 5, Table 19) was not accomplished as intractable mixtures of products resulted post work-up.

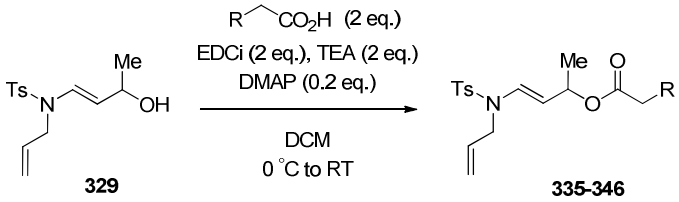

Entry	R	Product	Yield (%)	Entry	R	Product	Yield (%)
1	^{i}Pr	**335**	87	7	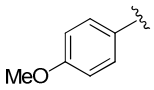	**341**	89
2		**336**	99	8	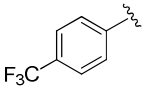	**342**	86
3	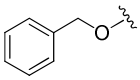	**337**	87	9	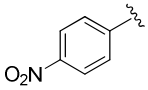	**343**	86
4	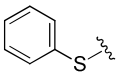	**338**	92	10	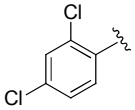	**344**	82
5	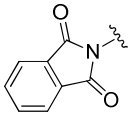	**339**	-	11	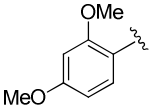	**345**	86
6	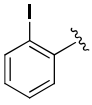	**340**	86	12	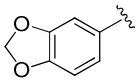	**346**	85

Table 19. Yields for EDCi Couplings.

With several substrates in hand, rearrangement was then pursued using the newly optimised conditions. For alkyl derivatives the newly modified Collum conditions were utilised and for the aryl derivatives the newly optimised LiHMDS/TMSCl conditions were used. The heteroatom substrates, **337** and **338**, were subjected to both sets of rearrangement conditions.

The rearrangement of the alkyl substrates (Entries 1-3, Table 20) were observed to proceed in moderate to good yields and excellent diastereoselectivities, with a reduction in diastereoselectivity seen for rearrangement of pentenoicacetate (Entry 3, Table 20). The results obtained from the successful rearrangement of these alkylacetate

sulfonamide rearrangements are in stark contrast to that observed for the propionate oxazolidinone system **256** seen previously. This result presumably signifies the onset of a selective enolisation and efficient rearrangement. It is also noted that no E1cB degradation product was observed during rearrangement of these alkylsulfonamides. Rearrangement of the heteroatom substrates (Entries 4 & 5, Table 20) under these conditions provided a different outcome, with complex reaction mixtures resulting. Analysis of crude ^{1}H-NMR spectra alluded to no signs of desired rearrangement, however careful purification of these reaction mixtures allowed the isolation of the familiar E1cB degradation product **353** and **354**.

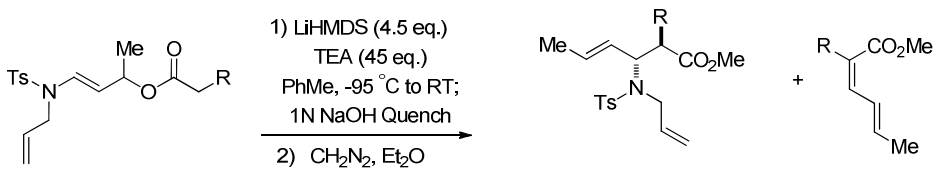

330, 335-338 **334-350** *anti-* **302, 351-354**

Entry	R	Product	Yield (%)	d.r.[a,b] (*anti:syn*)	By-Product	Yield (%)[c]
1	Me	**334**	51	>25:1	**302**	0
2	^{i}Pr	**347**	65	>25:1	**351**	0
3		**348**	70	10:1	**352**	0
4	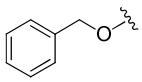	**349**	0	na	**353**	41
5	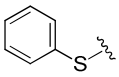	**350**	0	na	**354**	43

[a]d.r. measured of crude on 250 MHz ^{1}H NMR [b]Triplicates have been performed in each case. Measured dr is reproducible and reported as an average [c]Yield refers to product that E1cb product corresponds to.

Table 20. Results for Alkyl- & Heteroacetate EICR.

Rearrangement of aryl substrates (Table 21) has also been shown to occur in good yield and generally excellent diastereoselectivities. A significant observation is that rearrangement of systems that have previously shown poor diastereoselectivity

(Chapter 2) including *ortho*-substituents and the electron withdrawing *para*-nitro and electron donating *para*-methoxy now possess excellent diastereoselectivity. Of notable interest is the reduced diastereocontrol observed with the *p*-CF_3 substrate (Entry 3, Table 21), which is now less than that obtained for the oxazolidinone variant (Chapter 2, **217**, d.r. = 21:1). Near quantitative mass balance was returned by isolation of the corresponding methyl arylacetates. Attempted rearrangement of the hetereoatom substrates **349** and **350** yielded complex intractable reaction mixtures.

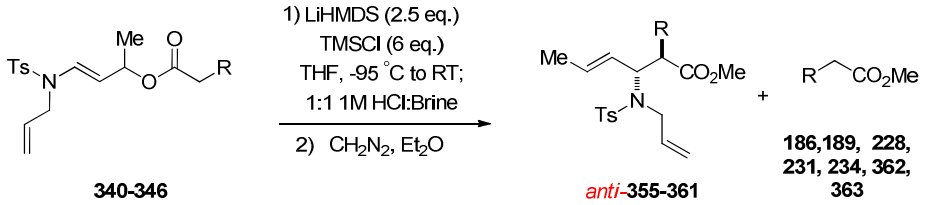

340-346 *anti*-**355-361** **186,189, 228, 231, 234, 362, 363**

Entry	R	Product	Yield (%)	d.r.[a,b] (*anti:syn*)	By-Product	Yield (%)[c]
1		**355**	67	>25:1	**362**	21
2	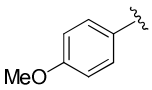	**356**	73	>25:1	**186**	18
3	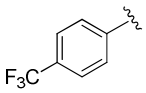	**357**	54	12:1	**228**	18
4	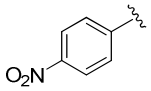	**358**	40	20:1	**189**	15
5	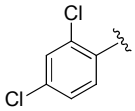	**359**	68	>25:1	**363**	22
6	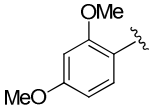	**360**	72	20:1	**231**	15
7	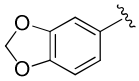	**361**	55	>25:1	**234**	25

[a]d.r. measured by acquisition of crude on 250 MHz ^{1}H NMR [b]Duplicates have been performed in each case. Measured dr is reproducible and reported as an average [c]Yield refers to prod that by-prod corresponds to.

Table 21. Results for Arylacetate EICR

In order to rationalise the improved diastereoselectivity seen by rearrangement of alkyl- and arylsulfonamides compared to the oxazolidinone examples, considerations surrounding the electronic nature of these enamide substrates were pursued. Based on the observed ^{13}C-NMR resonances it is seen that C1 in the sulfonamides are more deshielded than the corresponding carbamates. Whilst resonances are similar for C2 and C3, subtle differences are observed with C4 and C5 in that the sulfonamides are more shielded than the corresponding carbamates.

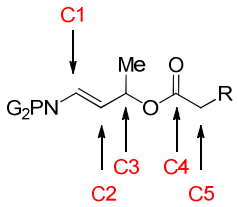

Entry	Substrate	NPG_2	R	δC				
				C1	C2	C3	C4	C5
1	**330**	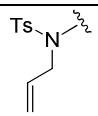	Me	129.5	110.1	69.8	173.5	27.9
2	**256**		Me	127.1	110.1	69.5	174.1	28.3
3	**331**	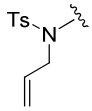	Ph	129.9	109.7	70.7	170.8	41.7
4	**154**		Ph	127.0	110.1	70.3	171.2	42.0

Table 22. Comparing δC for Sulfonamides & Carbamates.

These differences in δC allude to the degree of nitrogen involvement within these substrates. The more deshielded C1 and more shielded C4 of the sulfonamides indicate that this *N*-protection allows a greater degree of electron release into the enamide, purporting to more iminium character and an elongated C-Oσ bond **364** as compared to the corresponding carbamate.

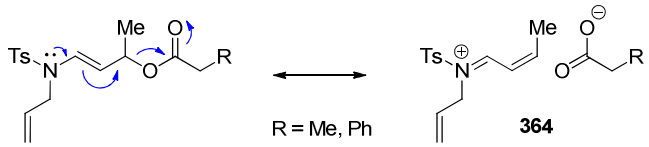

Scheme 145. Structural Depiction of Sulfonamide Substrates.

The increased diastereoselectivity observed with the more electron releasing sulfonamide substrates may be an aspect of a faster rearrangement, with issues such as Li-enolate and SKA isomerisation, or chair/boat interconversion no longer contributing to the diastereochemical outcome. It has been well documented in the related Cope rearrangement, that rate accelerations are observed with electron releasing terminal allyl substituents.[85, 146-148, 185]

The successful rearrangement of alkyl sulfonamides under Collum's protocol is markedly improved to that involving propionate oxazolidinone **256**, in that a diastereoselective rearrangement occurs with no E1cB degradation. This apparent resistance may be due to conformational constraints and a steric in-accessibility of LiHMDS to the α-H of the rearranged Li-carboxylate. During rearrangement of the sulfonamide and oxazolidinone systems it is envisaged that each Li-carboxylate exists as a mixed dimer **365** and **366** respectively. However, steric considerations of the sulfonamide may possess another factor hindering post-rearrangement enolisation, anticipated to be the formation of the 5-membered lithiated-allylsulfonamide ring

.

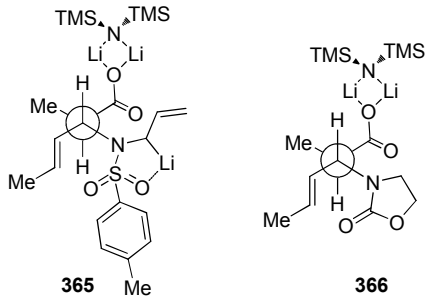

Fig. 22. In-Solution Considerations of Rearrangement Li-Carboxylates.

4.2.5. Derivatisation of *N*-Allylsulfonamide Rearrangement Products

With the successful rearrangement of alkyl- and arylacetate β-amino acid precursors of allylsulfonamide in hand, utilisation of the synthetic handles was pursued. Elaboration heavily focused on utilising the bis-olefin functionality present within the EICR products, with the sole aim of gaining access to heterocyclic β-amino acid precursors through means of a simple ring closing metathesis (RCM). In a similar protocol reported by Moreno-Mañas involving the RCM of bis-allylic sulfonamides, subjection of the sulfonamide EICR products to RCM conditions allowed access to the hetereocyclic β-amino acid precursors in high to excellent yield.[186] It is noted that substrates possessing *ortho*-substitution required a toluene solvent exchange and subjection to mild heating.

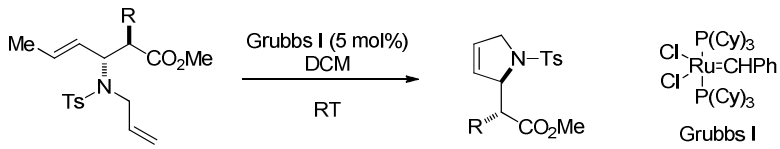

333, 334, 347, 355-361 **366-375**

Entry	R	Product	Yield (%)	Entry	R	Product	Yield (%)
1	Me	**367**	71	6	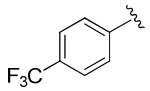	**372**	91
2	^{i}Pr	**368**	86	7	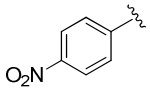	**373**	96
3	Ph	**369**	92	8	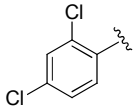	**374**	83[a]
4		**370**	51[a]	9	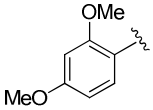	**375**	90[a]
5	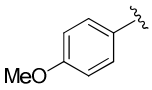	**371**	89	10	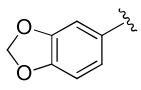	**376**	89

[a]*Conducted in toluene at 65 ˚C*

Table 23. Results for Grubbs I RCM of Sulfonamide EICR Products.

With a variety of heterocyclic β-amino acid precursors in hand, this opens up possible synthetic access to β-proline derivatives and may also allow access to iminosugar analogues. With this in mind a variety of transformations on **369** have been pursued, of which hydrogenation **377** and saponification **378** have successfully been achieved. Brief attempts at sulfonamide deprotection using Mg/MeOH and epoxide formation by treatment with *m*CPBA yielded intractable mixtures of products.

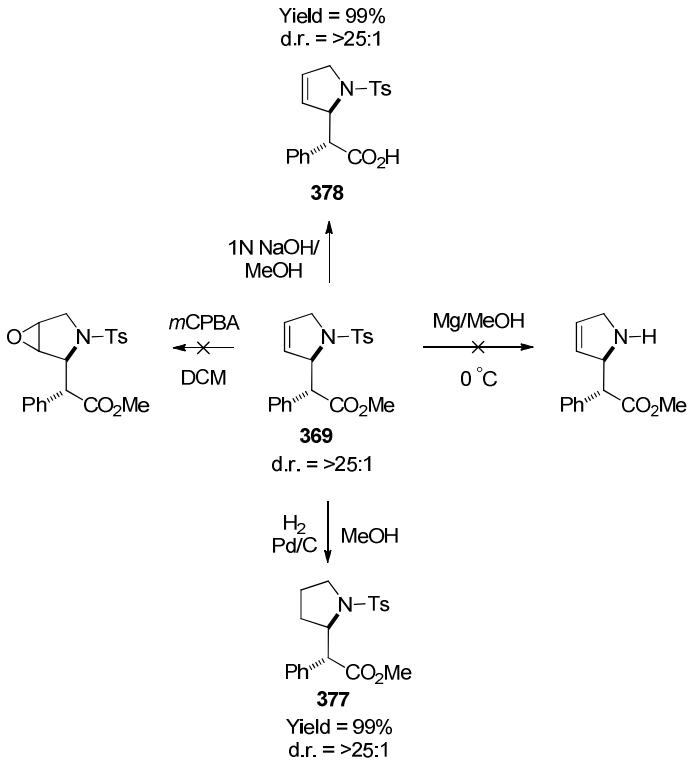

Scheme 146. Derivitisation of Phenylacetate Heterocyclic β-Amino Acid Precursor.

The synthetic handle presented by *ortho*-iodo heterocyclic β-amino acid precursor **370** provides an excellent substrate for the synthesis of an interesting 6,5,5-fused heterocyclic β-amino ester **379**. Following a protocol reported by Fürstner for intramolecular Heck reactions, the synthesis of **379** was accomplished in an excellent yield.[187]

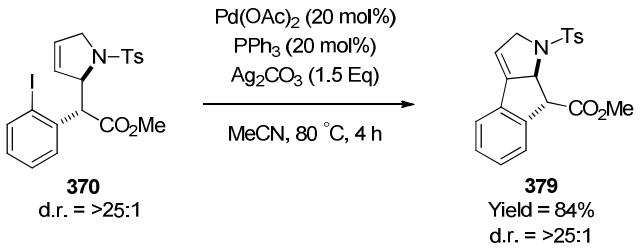

370
d.r. = >25:1

379
Yield = 84%
d.r. = >25:1

*Scheme 147. Heck Derivitisation of ortho-Iodo Heterocyclic β-Amino Acid Precursor **370**.*

4.2.6. EICR of *N*-Benzylsulfonamides

With the success seen in derivatising *N*-allylsulfonamide rearrangement products as heterocyclic β-amino esters, it was hoped access to carbocyclic β-amino acids such as ACPC **21** could be achieved *via* rearrangement of *N*-benzyl protected sulfonamides. With this in mind esterification of **323** with pentenoic acid yielded **380** in excellent yield.

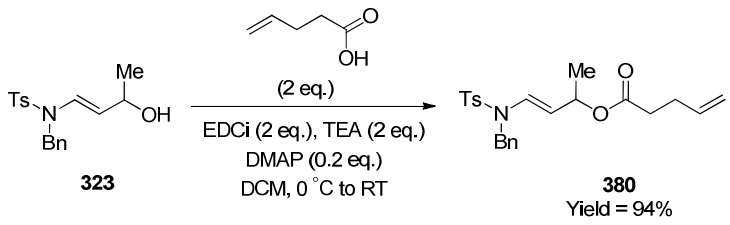

323

380
Yield = 94%

Scheme 148. Route to Racemic BnTs Secondary Allylic Ester.

Rearrangement of **380** under modified Collum conditions yielded **381** in excellent diastereoselectivity but very poor yield, however with no indication of E1cB degradation.

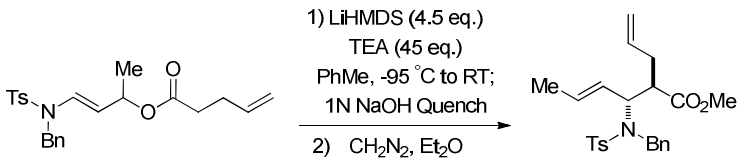

380

381
Yield = 10%
d.r. = >25:1

*Scheme 149. EICR of BnTs Secondary Allylic Ester **380**.*

Subsequent attempts at increasing the efficiency of this rearrangement have included varying the stoichiometry of the reagents used and performing cold reaction quenches, however these attempts have been unsuccessful. Subjection of **380** to LiHMDS and TMSCl rearrangement conditions yields similar results, however no diastereoselection is obtained in product **381**. However, to demonstrate that carbocyclic β-amino acid precursors can be accessed from **381** (generated within scheme 149), subjection to RCM conditions produced **382** in excellent yield.

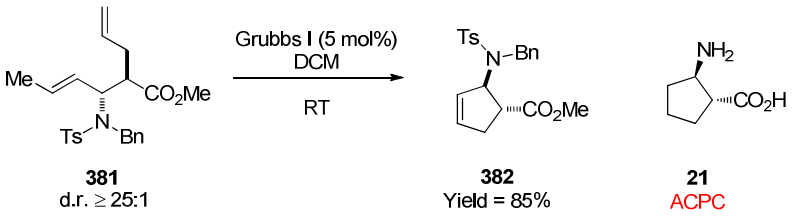

*Scheme 150. Generation of Carbocyclic β-Amino Acid Precursor **382**.*

4.2.7. Chirality Transfer within the EICR of *N*-Allylsulfonamides

With the success seen in the yield and diastereoselectivities of the EICR of the alkyl- and aryl allylsulfonamides, it was decided to pursue an enantiopure synthesis of this class of substrate. It was hoped that rearrangement of an enantiopure substrate would allow the synthesis of optically active β-amino esters, *via* the reliable chirality transfer apparent in the Ireland-Claisen rearrangement.[76] With this in mind, it was decided that this study shall focus on the synthesis and rearrangent of the (*S*)-phenylacetate **(*S*)-331**, based on an adaptation of Meyer's reported synthesis.[106, 182]

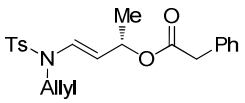

(*S*)-331

*Fig. 23. (S)-Phenylacetate **(S)-331**.*

The synthesis of **(*S*)-331** first involved silyl protection and bromination of alcohol **(*S*)-149**, followed by Ullmann coupling of **(*S*)-383** with allylsulfonamide **326** to afford ynamide **(*S*)-384** in good yield. Subsequent TBAF deprotection afforded **(*S*)-385** in good yield, however reduction and isolation of **(*S*)-329** proved problematic.

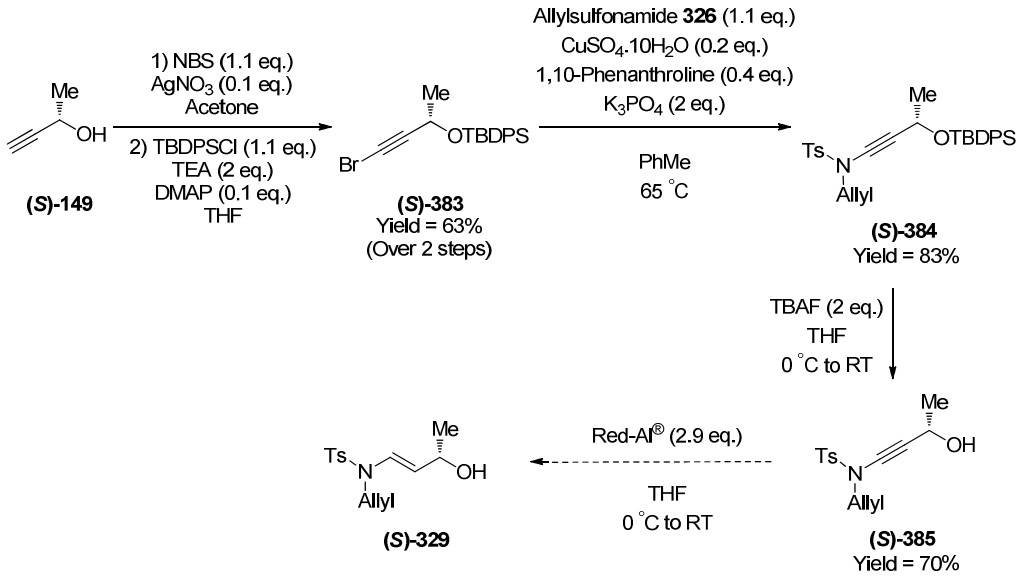

Scheme 151. Attempted Synthesis of ***(S)-329****.*

Meyer's synthesis involved the reduction of an anologous *N*-benzylsulfonamide, with purification achieved by an aqueous Rochelle's salt quench and subsequent column chromatography. The reduction of **(*S*)-385** under Meyer's protocol initially proved succesful, however the purification of **(*S*)-329** presented issues. Superficially the aqueous Rochelle's salt quench appeared to cleanly provide **(*S*)-329** without the need for column chromatography. However attempted esterification with phenylacetic acid led to unpurifiable mixtures of phenylacetate **(*S*)-331** and unreacted alcohol **(*S*)-329**, possibly due to the presence of residual aluminium salt impurities.

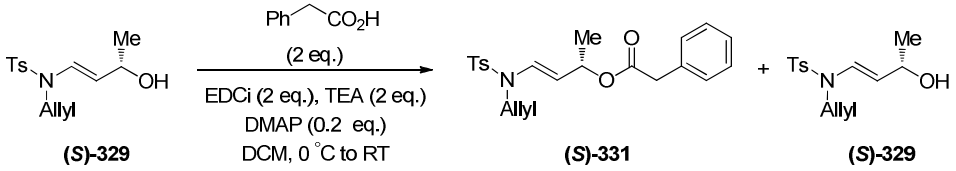

Scheme 152. Attempt at Synthesising (S)-Phenylacetate ***(S)-331****.*

Attempted purification of **(*S*)-329** *via* column chromatography using silica or grade V alumina unfortunately led to degradation, with spectroscopic analysis aluding to the formation of familiar crotonaldehyde **157** and allylsulfonamide **326** dehydration products.

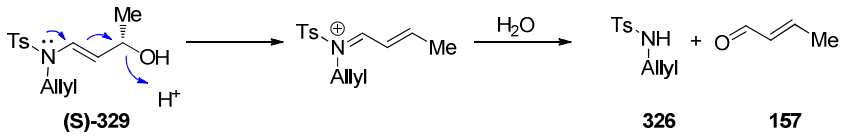

*Scheme 153. Sensitivity of **(S)-329** to Purification Conditions.*

This difference in stability between the *N*-benzyl and *N*-allylsulfonamide alcohols to purification is indeed unfortunate. However, to allow clean synthesis of **(*S*)-329** without recourse to column chromatography a number of variables were investigated. Investigations surrounding the stoichiometry of Red-Al® were initially pursued, where reduction to 1.5 equivalents allowed complete conversion to **(*S*)-329**, however issues with its subsequent esterification were still observed. Similar issues were also observed with the use of $LiAlH_4$. In an attempt to solve the purification issues of **(*S*)-329**, an alternative work-up protocol was pursued. Tomooka noted that the use of a 'pea crystal' ($Na_2SO_4.10H_2O$) quench can efficiently remove aluminium hydrides and their by-products.[188] Reduction of **(*S*)-385** following this protocol was found to be succesful and subsequent esterification yielded **(*S*)-329** in high yield.

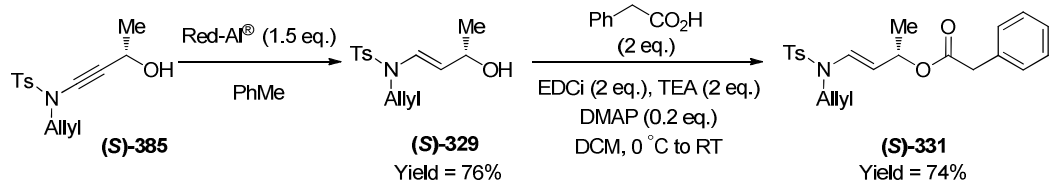

*Scheme 154. Synthesis of **(S)-331**.*

With the desired enantiopure substrate **(S)-331** in hand, subjection to rearrangement yielded the β-amino acid precursor (***2R,3R*)-333** in high yield and excellent diastereoselectivity. Importantly, excellent levels of enantiocontrol were observed within the rearrangement, however efforts at obtaining an absolute value of enantiomeric excess have not yet been successful, based on an inability to gain total baseline resolution by HPLC. An important observation associated with rearrangement of this enantiopure substrate has demonstrated that the minor *Z*-SKA appears to display no chirality transfer, as enantioselection is not observed in formation of the *syn*-product and may be attributed to a non-concerted bimolecular recombination reaction.

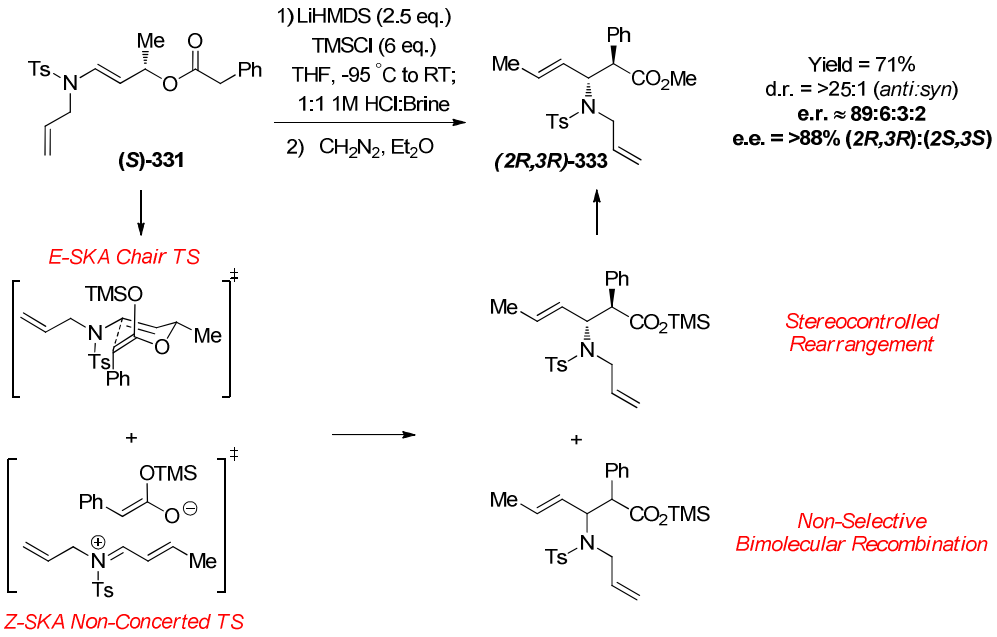

Scheme 154. EICR of (S)-Phenylacetate ***(S)-331***

4.3. Conclusions

Although superficial improvements within the diastereoselectivity for rearrangement of *N*-oxazolidinone-propionate **265** were achieved by Collum's protocol, poor yields resulted.[173] Subsequent investigation demonstrated that the EICR under these conditions was non-selective and 2:1 mixtures of *anti:syn* diastereomers were generated. The superficial appearance of a selective rearrangement was the result of a more facile E1cB type elimination of the *syn*-diastereomer compared to the *anti*-.

In an attempt to observe successful rearrangement of both alkyl- and arylacetate substrates, investigations into the use of alternative *N*-protected enamides were pursued to probe any structure reactivity trends. The use of *N*-Phthalimide and *N*-Boc protection was non-profitable based on substrate instabilities, however the use of sulfonamide protection was observed to allow the successful rearrangement of both alkyl-and aryl-substrates. Further derivitisation of these N-allylsulfonamide rearrangement products was seen within the derivitisation as heterocyclic β-amino acid precursors. Also the synthesis of an enantiopure phenylacetate substrate allowed excellent chirality transfer within the EICR be demonstrated.

5. Conclusions & Future Work

The initial remit of the enamido Ireland-Claisen rearrangement was to harness the synthetic properties associated with the related Ireland-Claisen rearrangement and allow access to multi substituted β-amino acids with high levels of stereocontrol. Initial efforts focussed on developing the preliminary results involving the rearrangement of *N*-oxazolidinone substrates.[109] After a reaction optimisation further investigation into the variation of diastereoselectivity based upon the nature of electronic perturbation in α-arylacetates was pursued. This study demonstrated a conspicuous range of diastereoselectivity whereby a free energy relationship was realised for the *para*-substituted analogues and allowed diastereoselection be examined in terms of deconvoluted steric and electronic effects.

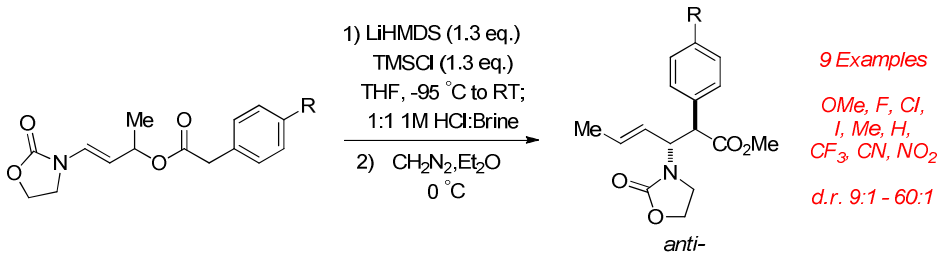

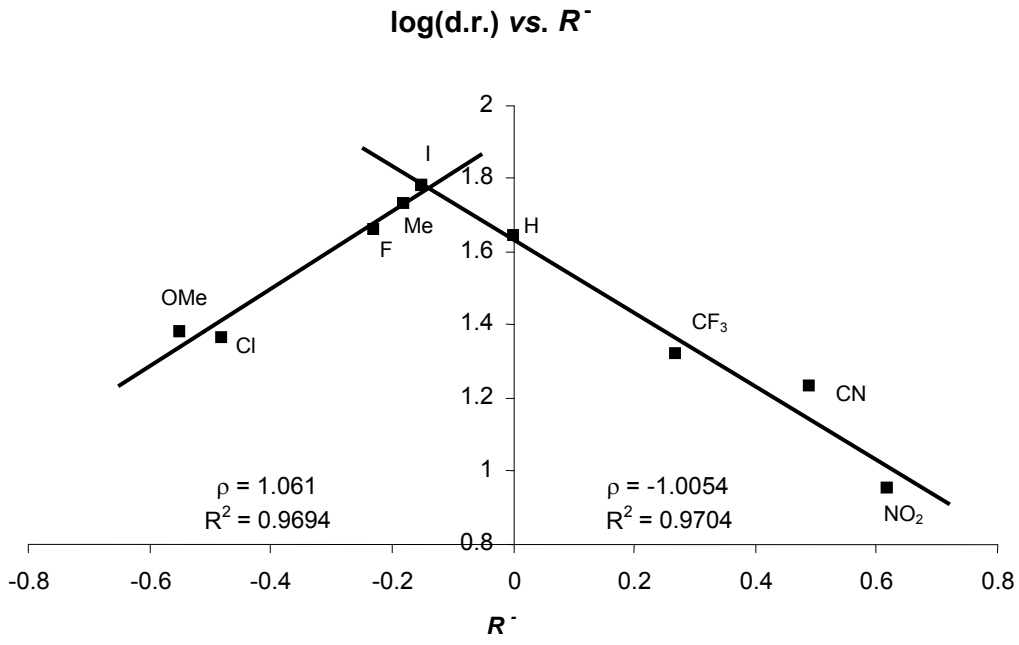

Fig. 24. EICR of Para-Substituted Substrates & Associated Log(d.r.) vs Resonance Parameter R⁻.

As this non-linear Hammett type plot alludes to a change within the rate determining step of the mechanism, it was clear that the EICR was sensitive to electronic perturbation as reductions in diastereocontrol were observed with increasing electron withdrawal and donation.[131] In order to evaluate the origins of diastereoselection mechanistic studies were undertaken. It was rationalised that 2 key stages within the EICR may be responsible for the varied diastereoselectivity, this being from initially generated mixtures of *E/Z*-SKAs which rearrange through a predictable chair transition state or from selective formation of the *E*-SKA which then rearranges through competing chair and boat transition states. With these considerations in mind, *in-situ* NMR experimentation was pursued with the aim of being able to monitor the EICR of an electron withdrawing, neutral and donating substrate. Initial studies involved the ^{1}H-NMR monitoring of model α-aryl SKA formation, designed to mimic the secondary ester of the enamide substrates. From this study it was shown that SKA formation was in fact sensitive to the nature of electronic substitution, with reduced geometric control observed for the strongly electron withdrawing and electron donating systems.[160] These results were indeed important as they demonstrated that generation of varied *E/Z*-SKAs may influence the diastereochemical outcome of the associated EICR.

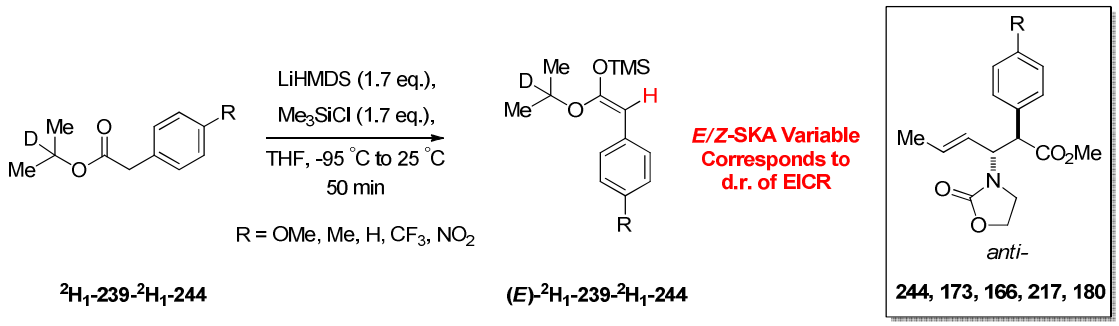

$^{2}H_1$-239-$^{2}H_1$-244 **(*E*)-$^{2}H_1$-239-$^{2}H_1$-244**

Scheme 155. Comparing Aryl SKAs to d.r. of EICR

Although varied degrees of geometric control were observed for the *in-situ* formation of the model SKAs, they were shown to be much higher than previous literature isolations.[149, 156-159] With this in mind a protocol for the formation and isolation of α-aryl *E*-SKAs was developed, where **(*E*)-$^{2}H_1$-240** was isolated essentially as a single geometric product.[160]

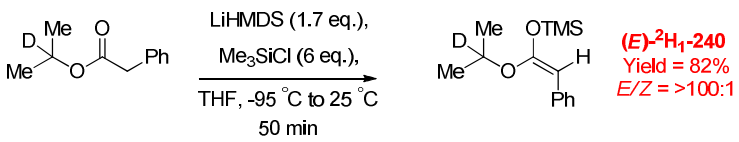

Scheme 156. Isolation of Phenylacetate SKA.

The success observed within the monitoring of SKA formation then led us to follow the *in-situ* reaction monitoring of the EICR. After several attempts at synthesising a viable class of substrate, synthesis of ^{13}C-labelled phenyl-, *para*-methoxy- and *para*-trifluoromethylphenylacetates were accomplished. The *in-situ* reaction monitoring by ^{13}C-NMR allowed observation of *E/Z*-SKA formation/consumption and subsequent β-silylester formation.

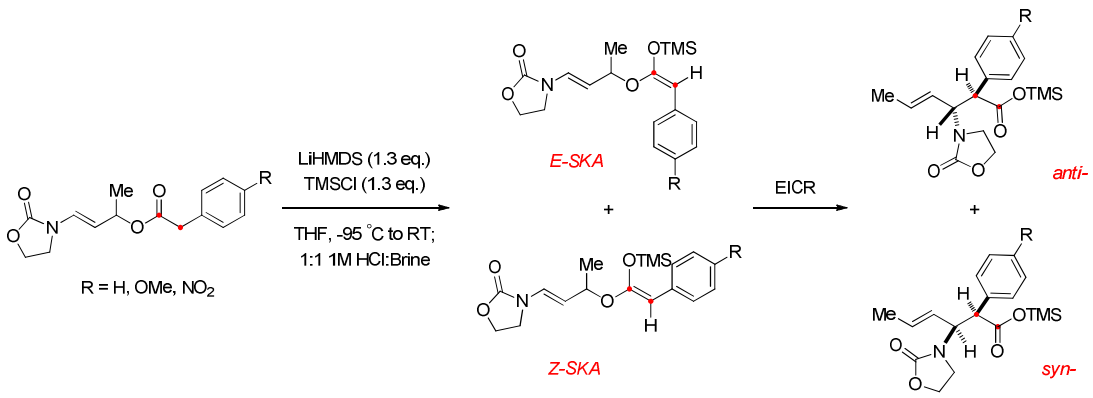

Scheme. 157. EICR Reaction Monitoring by ^{13}C-NMR.

Unfortunately, the inability to detect both the *syn*- and *anti*-diastereomers of product were plagued by coincident resonances. However the results from this study were informative in that the origins of diastereoselection are attributed to-

1) Poor *E/Z*-SKA control which rearranges through a chair transition state for electron donating substitution.
2) Selective formation of the *E*-SKA which rearranges through competing chair and boat transition states for electron withdrawing substitution.

In addition the results generated from these studies have also allowed a major insight into the effects of silyl by-products generated within the reaction. Throughout each *in-*

situ reaction, inflections in the return of substrates were observed and this is attributed to a facile 'Internal Proton Return' mechanism to the enolate and SKA.[162,163] Generation of LiCl is also thought to play a major role within the observed reaction profile as it exhibits *auto*-catalytic effects, speeding up the rate of enolisation and reducing that of IPR, resulting in consumption of substrate.[165] The formation of silanamine within these reactions has also alluded to the observed stalling of the EICR, as silylation of LiHMDS becomes more facile compared to enolisation of substrates and is attributed to an ever increasing concentration of LiCl exhibiting deleterious effects.

In addition to the mechanistic studies, other areas of research have involved improvement of the alkylacetate EICR, in which alternative reaction conditions were investigated. The most promising conditions for *N*-oxazolidinone substrates were seen to be that offered by Collum, involving a TMSCl-free protocol.[173] However, even after a comprehensive optimisation the reaction was seen to demonstrate poor diastereoselectivity, masked by a *pseudo*-kinetic resolution involving a preferential E1cB degradation of the *syn*-diastereomer. To allow the successful EICR of alkylacetates alternative *N*-protection was sought. This resulted in the synthesis of *N*-allylsulfonamide substrates and encouragingly successful rearrangement of both alkyl- and arylacetates was obtained. Utilisation of these rearrangement products has subsequently been demonstrated in the synthesis of β-proline analogues.

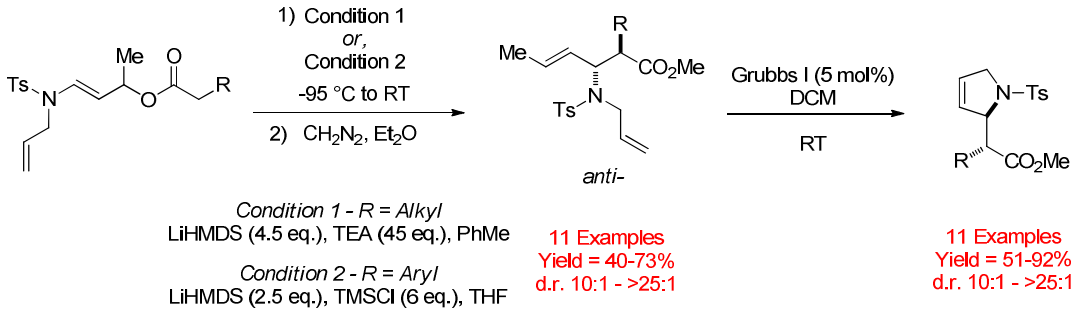

Scheme 158. Allylsulfonamide EICR and Subsequent Ring Closing Metathesis.

In addition the successful rearrangement associated with *N*-allylsulfonamide protection has also allowed access to enantiomerically enriched substrates and rearrangement has shown high levels of chirality transfer (>88% e.e).

Future Work- This research has created several viable areas for future exploration, both within the EICR and external to it. First and foremost the mechanistic studies have allowed an interesting insight into the nature of the EICR; however they have also demonstrated the complexities associated with it. The inability to monitor the formation of both *syn*- and *anti*-diastereomers throughout any *in-situ* reaction has been a limiting factor in the discussions surrounding the origins of diastereoselectivity. The presence of HMDS and the presumably ever increasing concentration of LiCl are envisaged to both play major roles within the EICR and other curiosities are observed with the inability to detect LiHMDS and the formation of silanamine throughout each reaction. Therefore in order to allow further mechanistic rationale other NMR techniques involving isotopically enriched reagents could entail:[173]

1) **^{7}Li-NMR** – To allow tracking of total lithium content, including various Li-incorporated aggregates and build up of LiCl.
2) **^{15}N-NMR** – To allow tracking of total nitrogen content of reagent and reactant, including LiHMDS, HMDS, silanamine and also oxazolidinone of substrate.
3) **^{29}Si-NMR –** To allow tracking of total silicon content, with the main aim of being able to distinguish *E/Z*-SKAs and also *syn*- and *anti*-β-silylester products.

As further mechanistic studies would allow a greater understanding of the electronic effects of substitution within the EICR, we would also gain a further insight into the *in-situ* compatibilities between LiHMDS/TMSCl. These observations could then be transposed into other similarly mediated reactions.

In addition to the mechanistic studies, the potential synthetic benefits of the EICR have been demonstrated by the successful rearrangement in high diastereo- and enantioselectivity of the *N*-allylsulfonamides. Although further exploitation of these synthetic intermediates has only incorporated the synthesis of β-proline analogues, the further development of this chemistry may allow a novel route into ACPC **21** derived β-foldamers, β-proline organocatalysts **324** and iminosugars **325**.[20-21]

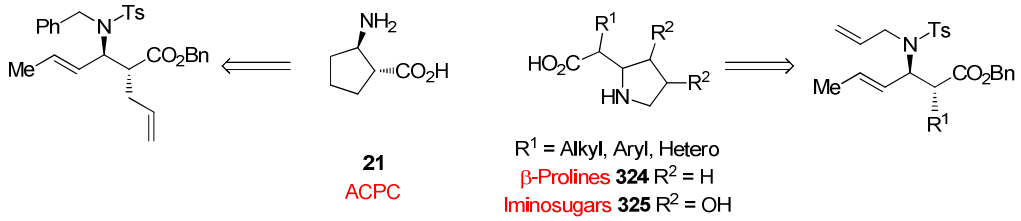

Scheme 159. RSA of Potential Target Molecules.

Also, the formation and isolation with high *E*-SKA purity of phenylacetate derived SKAs creates a new topical area of interest. For instance, the involvement in Mannich reactions previously inhibited by a non-selective *E*-SKA formation, or where only the selectively formed *Z*-SKA was used, *may* now allow selective access into both *syn*- and *anti*-β-amino acid precursors by utilisation of our selectively formed *E*-SKA.[149,151]

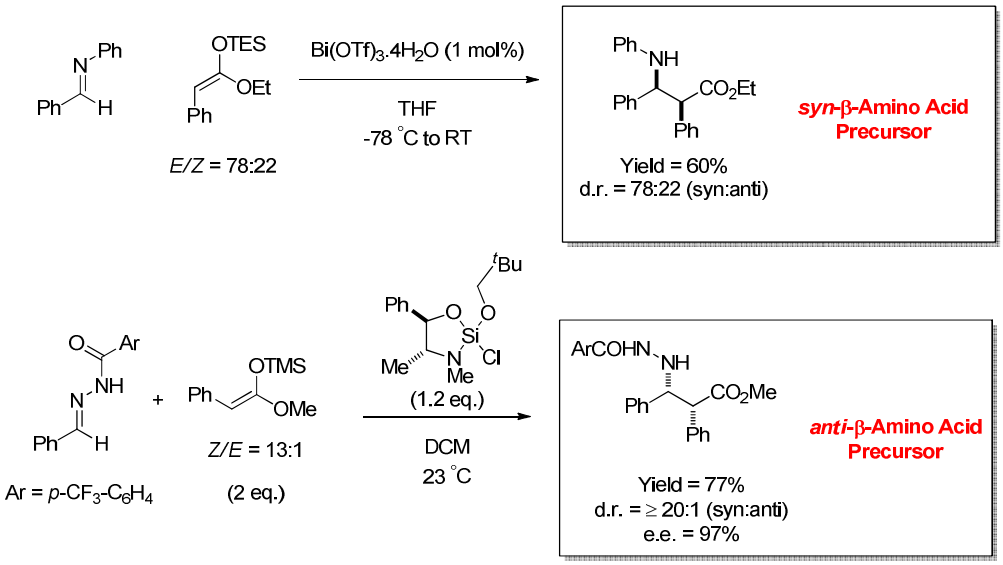

Scheme. 160. Potential Mannich Reactions for Exploitation with Selective Formation of E-SKA.

The use of our developed synthesis of α-aryl-*E*-SKAs and their subsequent use within various Mannich reactions, may then serve as a back-up route to compliment the enamido-Ireland-Claisen rearrangement in the synthesis of β-amino acids.

6. Experimental

6.1. General Experimental Information

Reactions were conducted in flame dried vessels using anhydrous solvents and under an inert atmosphere of nitrogen. In all cases, solvents were obtained by passing through anhydrous alumina columns using an Innovative Technology Inc. PS-400-7 solvent purification system. All reagents were purchased from commercial suppliers: Acros Organics, Alfa Aesar, Sigma Aldrich or Novabiochem and used without purification. Triethylamine was freshly distilled alone and chlorotrimethylsilane was freshly distilled from 10 % quinoline. All distilled materials were stored under nitrogen at 4 ^{o}C or less. All reactions were monitored by thin layer chromatography (TLC) using pre-coated MN Alugram Sil G/UV_{254} silica gel 60 aluminium backed plates. Plates were developed using UV light followed by a chemical dip, usually $KMnO_4$ and gentle heating. Flash chromatography was performed on chromatography grade, silica 60Å particle size 35-70 micron from Fisher Scientific using the solvent system as stated.

^{1}H and ^{13}C NMR were performed on a Brüker Avance 250 (250 MHz), Brüker Avance 300 (300 MHz), Brüker Avance 400 (400 MHz) and Brüker Avance 500 (500 MHz) as stated. Chemical shifts are reported in parts per million (ppm) relative to tetramethylsilane (TMS) (δ = 0.00). Coupling constants are reported in Hertz (Hz) and signal multiplicity is denoted as singlet (s), doublet (d), triplet (t), quartet (q), doublet of doublets (dd), doublet of triplets (dt), doublet of quartets (dq), quartet of triplets (qt), triplet of doublets (td), multiplet (m), quintet (quin) and broad (br). C-H assignments in ^{1}H-NMR spectra are quoted for compounds that have received 2D-NMR analysis. Mass spectroscopy was performed on a Brüker μTOF using electrospray ionisation (ESI) in either positive or negative ionisation as stated. Infra-red spectroscopy was carried out using a Perkin Elmer Spectrum RX FT-IR system with KBr plates, using a thin film. Melting points were determined by recrystallisations of substrates from DCM/petroleum ether 60–80° using a Bibby Scientific Melting point apparatus Stuart SMP10 digital. X-ray data was collected at 150 K on a Nonius KappaCCD area diffractometer using Mo-

Kα radiation (λ = 0.71073 Å) and all structures were solved by direct methods and refined on all *F2* data using SHELXL-97 suite of programs, with hydrogen atoms included in idealised positions and refined using the riding model.

6.2. General Experimental Procedures

General Procedure 1 –

Synthesis of Enamido Esters

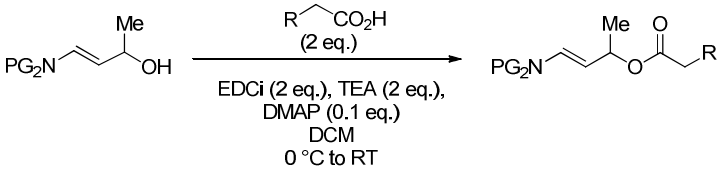

To a solution of EDCi (2 eq.) in DCM was added triethylamine (2 eq.), DMAP (0.1 eq.), and the required carboxylic acid (2 eq.). The resulting solution was cooled to 0 °C and the vinylogous enamido alcohol (1 eq.) was added as a solution in DCM. The reaction mixture was allowed to stir before slowly warming to room temperature. The reaction was quenched by addition of 10 % citric acid (30 ml), washed with further 10 % citric acid (2 × 30 ml), washed with $NaHCO_3$ (sat, 3 × 30 ml), washed with brine (30 ml) and the combined organics were dried over $MgSO_4$, filtered and concentrated *in vacuo* to yield the desired enamido esters.

General Procedure 2 –

Rearrangement & Esterification of Enamido Esters

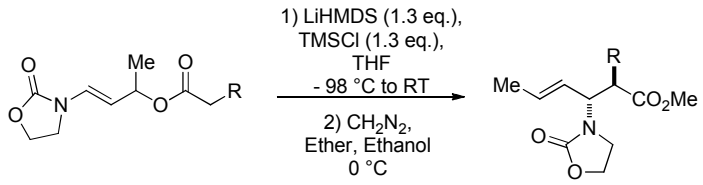

To a solution of LiHMDS (1M in THF, 1.3 eq.) and TMSCl (1.3 eq.) at -95 °C was added a solution of enamide (1 eq.) in THF by syringe pump (4 ml/h) down the side of the reaction vessel. On complete addition the reaction mixture was allowed to warm to

RT over 1 hour and was then quenched with HCl (1M)/Brine (1:1, 5 ml). The organics were extracted with EtOAc (5 × 15 ml), dried over $MgSO_4$, filtered, concentrated *in vacuo* and the crude acid product was subjected to esterification with diazomethane following general procedure 5, to yield the desired crude methyl esters, of which d.r's were assigned by extended aquistion (100 scans) on the 500 MHz ^{1}H NMR. Each ester was then subjected to purification by silica gel chromatography, using gradient elution ethyl acetate/petroleum ether 40-60°/triethylamine (20:80:1–40:60:1), to yield pure β-amino esters. Data is subsequently reported on the major diastereoisomer, unless resolution has been achieved.

General Procedure 3 –

Rearrangement & Esterification of Enesulfonamido Esters

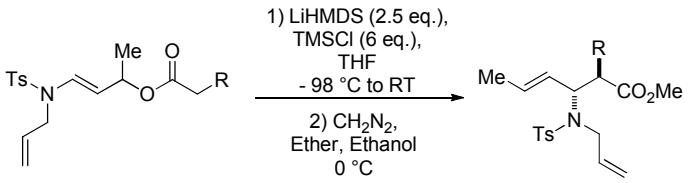

To a solution of LiHMDS (1M in THF, 2.5 eq.) and TMSCl (6 eq.) at -95 °C was added a solution of enamide (1 eq.) in THF by syringe pump (4 ml/h) down the side of reaction vessel. On complete addition the reaction mixture was allowed to warm to RT over 1 hour and was then quenched with HCl (1M)/Brine (1:1, 5 ml). The organics were extracted with Et_2O (3 × 15 ml) and the crude acid product was subjected to esterification with diazomethane following general procedure 5, to yield the desired crude methyl esters, of which d.r's were assigned by ^{1}H NMR. Each ester was then subjected to purification by silica gel chromatography, using gradient elution ethyl acetate/petroleum ether 40-60°/triethylamine (20:80:1–40:60:1), to yield pure β-amino esters. Data is subsequently reported on the major diastereoisomer.

General Procedure 4 -

Rearrangement & Esterification of Enesulfonamido Esters

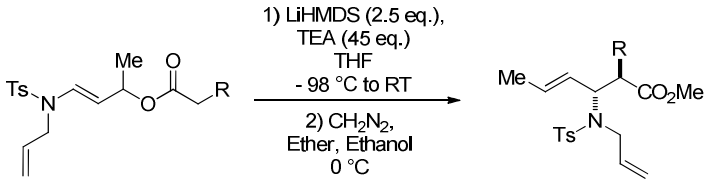

To a solution of LiHMDS (1M in THF, 4.5 eq.) and TEA (45 eq.) at -95 °C was added a solution of enamide (1 eq.) in THF by syringe pump (4 ml/h) down the side of the reaction vessel. On complete addition the reaction mixture was allowed to warm to RT over 1 hour and was then quenched with HCl (1M)/Brine (1:1, 5 ml). The organics were extracted with Et_2O (5 × 15 ml) and the crude acid product was subjected to esterification with diazomethane following general procedure 5, to yield the desired crude methyl esters, of which d.r's were assigned by ^1H NMR. Each ester was then subjected to purification by silica gel chromatography, using gradient elution ethyl acetate/petroleum ether 40-60°/triethylamine (20:80:1–40:60:1), to yield pure β-amino esters. Data is subsequently reported on the major diastereoisomer.

General Procedure 5 –

Diazomethane Methylation

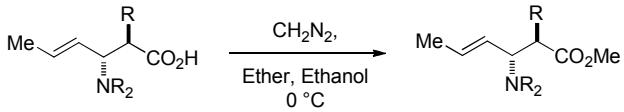

To a solution of the crude acid in diethylether/ethanol (99:1) at 0 °C was added diazomethane generated from *N*-nitrosomethyl urea (50 mg) and 37% KOH (5 ml). Once esterification complete (yellow colour persists), the mix was quenched with glacial acetic acid then basified with $NaHCO_3$ (sat). The organics were extracted with EtOAc (5 × 15 ml), dried over $MgSO_4$, filtered and concentrated *in vacuo.*

General Procedure 6 –

RCM of Allyl Sulfonamide β-Amino Esters

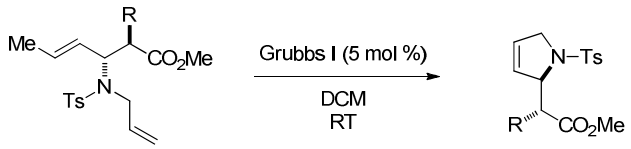

To a solution of rearranged allyl sulfonamide β-amino ester in DCM was added Grubbs I catalyst (5 mol%). The reaction mixture was allowed to stir at room temperature and once the reaction was complete by TLC, the reaction mixture was concentrated in vacuo and then subjected to purification by silica gel chromatography, using gradient elution ethyl acetate/petroleum ether 40-60° (10:90–20:80), to yield pure RCM material.

General Procedure 7 –

RCM of Allyl Sulfonamide β-Amino Esters

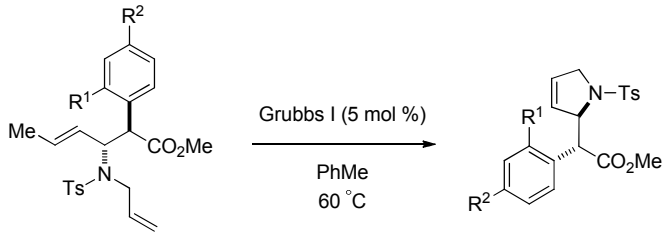

R^1/R^2 = I/H, Cl/Cl, OMe/OMe

To a solution of rearranged allyl sulfonamide β-amino ester in toluene was added Grubbs I catalyst (5 mol%). The reaction mixture was allowed to stir at 60 °C and once the reaction was complete by TLC, the reaction mixture was concentrated in vacuo and purified by silica gel chromatography, using gradient elution ethyl acetate/petroleum ether 40-60° (10:90–20:80), to yield pure RCM material.

General Procedure 8 –

For the *in-situ* NMR study of SKA Formation & Isomerisation

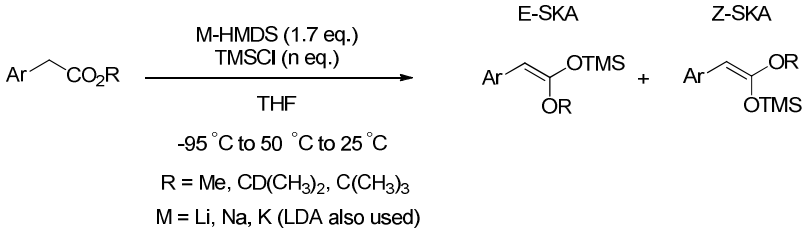

To an oven dried Young's tap NMR tube, inserted into a Dewar at -95 °C and under an atmosphere of nitrogen, was added a solution of M-HMDS (1M in THF, 1.7 eq.) and TMSCl (n eq). Thermal equilibration was allowed (5 minutes) and then a solution of substrate (50 mg, 1 eq.) was added in THF (0.5 ml). The cooled NMR tube was rapidly lowered into the pre-cooled NMR machine at -95 °C. From this point ^{1}H- and ^{13}C-NMR spectroscopy were recorded, and the sample was subsequently warned to -50 °C and 25 °C allowing the sample to equilibrate for five minutes before recording data.

General Procedure 9 –

For the Synthesis and Isolation of *E*-selective Phenyl Derived SKA's

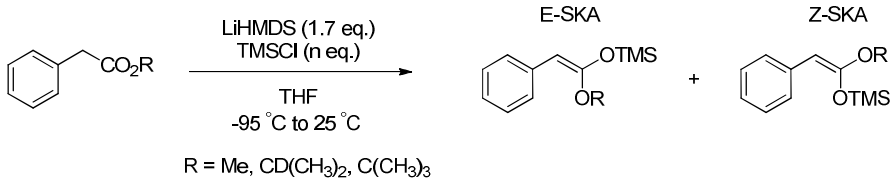

Method A-To a stirred solution of LiHMDS (1M in THF, 1.7 eq.) and TMSCl (1.7 eq.) at -95 °C was added a solution of phenyl ester (1 eq.) in THF by syringe pump at rate of 4 ml/h.

Method B- To a stirred solution of LiHMDS (1M in THF, 1.7 eq.) and TMSCl (1.7 eq.) at -95 °C was added a solution of phenyl ester (1 eq.) in THF by fast hand addition.

Method C- To a stirred solution of LiHMDS (1M in THF, 1.7 eq.) and TMSCl (6 eq.) at -95 °C was added a solution of phenyl ester (1 eq.) in THF by syringe pump at rate of 4 ml/h.

All three methods were then subjected to a standardised workup protocol-
Once addition complete the reaction mixture was allowed to stir at room temperature for 1 hour before rapid vacuum concentration at 4 mbar. The crude SKA was then dissolved in $CDCl_3$ (stored over magnesium sulfate and potassium carbonate) and filtered through cotton wool into a Young's tap NMR tube for analysis. Post analysis the product was then re-concentrated to constant dryness to allow yield be determined.

6.3. Compound Characterisation

6.3.1. *N*-Oxazolidinone Substrates

(*E*)-3-(3-oxobut-1-enyl)oxazolidin-2-one 146

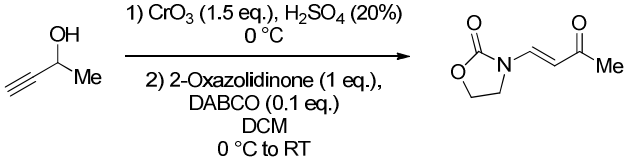

To a solution of chromium (VI) trioxide (42.8 g, 428 mmol, 1.5 eq.) in 20% H_2SO_4 (250 ml) was added dropwise a solution of 3-butyn-2-ol (25.5 ml, 285 mmol, 1 eq.) in 20% H_2SO_4 (250 ml). The reaction mixture was stirred at 0 °C for 6 hours and a colour change from orange to green was observed. The reaction was quenched by addition of $NaHCO_3$ (sat.) (200 ml) and the organics were extracted with DCM (3 x 300 ml) and dried over $MgSO_4$. The crude butynone was chilled to 0 °C before 2-oxazolidinone (24.84 g, 285.34 mmol, 1 Eq) and DABCO (3.20 g, 28.53 mmol, 0.1 Eq) were added. The reaction mixture was allowed to stir for 12 hours whilst slowly warming to room temperature and a colour change to a deep maroon was observed. The reaction mixture was washed with $NaHCO_3$ (sat, 3 × 200 ml), brine (3 × 200 ml) before the combined organics were dried over $MgSO_4$, filtered and concentrated *in vacuo* to afford (*E*)-3-(3-oxobut-1-enyl)oxazolidin-2-one **146** as a cream solid (25.8 g, 58%). M.p. 91–93 °C; FTIR (film/cm^{-1}) υ_{max}: 2923 (s), 2853 (s), 1754 (s), 1622 (s); ^1H NMR (250 MHz, $CDCl_3$) δ: 2.27 (s, 3H), 3.78 (m, 2H), 4.54 (m, 2H), 5.47 (d, 1H, *J* = 14.5 Hz), 7.81 (d,

1H, *J* = 14.5 Hz); ^{13}C NMR (62 MHz, $CDCl_3$) δ: 26.8, 42.1, 62.6, 111.0, 137.9, 154.7, 196.7. HRMS (ESI, +ve) *m/z* calcd. for $C_7H_{10}NO_3$ 156.0660, found 156.0650 $(M+H)^+$.

3-(3-Oxo-d^1-d^2-but-1-enyl)-oxazolidin-2-one $^2H_2$-146

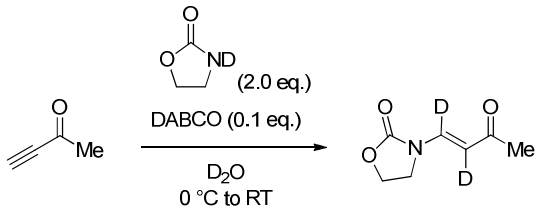

To 2-oxazolidinone (1.28 g, 14.7 mmol, 2.0 eq.) was added D_2O (10 ml) and the resulting solution was concentrated *in vacuo*. The resulting *N*-deuterated 2-oxazolidinone was redissolved in D_2O (20 ml) at 0 ˚C then DABCO (0.08 g, 0.7 mmol, 0.1 eq.) and but-3-yn-2-one (0.50 g, 7.35 mmol, 1.0 eq.) was added dropwise. The reaction mixture was allowed to stir for 3 hours, then DCM (50 ml) and brine (50 ml) was added and the organics were extracted with DCM (3 × 50 ml), dried over magnesium sulphate and concentrated *in vacuo* to yield the crude product which was further purified by flash column chromatography, using ethyl acetate/petroleum ether 40-60˚ (80:20) to yield 3-(3-oxo-d^1-d^2-but-1-enyl)-oxazolidin-2-one **$^2H_2$-146** as a faint brown solid (0.14 g, 12 %). M.p. 91–93 ˚C; FTIR (film/cm^{-1}) υ_{max}: 2992 (w), 2918 (w), 1762 (s), 1656 (s), 1589 (s), 1572 (s); ^{1}H NMR (250 MHz, $CDCl_3$) δ: 2.20 (s, 3H), 3.72 (app. t, 2H, *J* = 7.7 Hz), 4.50 (app. t, 2H, *J* = 7.7 Hz). ^{13}C NMR (125 MHz, $CDCl_3$) δ: 26.8, 42.0, 62.6, 110.5 (t, *J* = 24.3 Hz), 137.6 (t, *J* = 27.5 Hz), 154.7, 198.7; HRMS (ESI, +ve) *m/z* calcd. for $C_7H_8D_2NO_3$ 158.0786, found 158.0772 $(M+H)^+$.

(*E*)-3-(3-Hydroxybut-1-enyl)oxazolidin-2-one 145

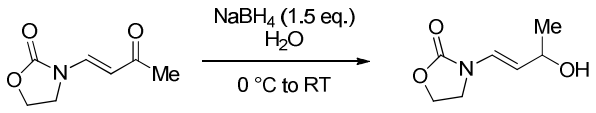

To a solution of (*E*)-3-(3-oxobut-1-enyl)oxazolidin-2-one **146** (5.00 g, 32.2 mmol, 1 eq.) in water (250 ml) at 0 ˚C was slowly added $NaBH_4$ (1.83 g, 48.4 mmol, 1.5 eq.). The reaction mixture was allowed to stir for 12 hours whilst slowly warming to room

temperature and before quenching with brine (100 ml). The organics were extracted with DCM (5 × 50 ml), dried over $MgSO_4$, filtered and concentrated *in vacuo* to give (*E*)-3-(3-hydroxybut-1-enyl)oxazolidin-2-one **145** (5.10 g, 100%) as a yellow oil. FTIR (film/cm^{-1}) υ_{max}: 3321 (bs), 2971 (s), 1732 (s), 1668 (s); ^{1}H NMR (500 MHz, $CDCl_3$) δ: 1.31 (d, 3H, *J* = 6.9 Hz), 1.92 (br s, 1H), 3.6–3.72 (m, 2H), 4.32 (app. quin, 1H, *J* = 6.9 Hz), 4.44 (app. t, 2H, *J* = 8.2 Hz), 4.92 (dd, 1H, *J* = 14.3, 6.9 Hz), 6.84 (d, 1H, *J* = 14.3 Hz); ^{13}C NMR (125 MHz, $CDCl_3$) δ: 23.4, 42.5, 62.2, 67.1, 114.9, 124.9, 155.5; HRMS (ESI, +ve) *m/z* calcd. for $C_7H_{11}NNaO_3$ 180.0636, found 180.0632 $(M+Na)^+$.

3-(3-Hydroxy-d^1-d^2-d^3-but-1-enyl)-oxazolidin-2-one $^2H_3$-145

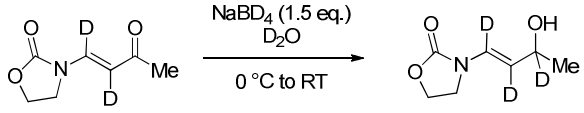

To a solution of 3-(3-hydroxy-d^1-d^2-d^3-but-1-enyl)-oxazolidin-2-one **$^2H_2$-146** (0.07 g, 0.42 mmol, 1 eq.) in D_2O (10 ml) at 0 °C was slowly added $NaBD_4$ (0.03 g, 0.63 mmol, 1.5 eq.). The reaction mixture was allowed to stir for 12 hours whilst slowly warming to room temperature and was then quenched with brine (20 ml). The organics were extracted with DCM (5 × 20 ml), dried over $MgSO_4$, filtered and concentrated *in vacuo* to give 3-(3-hydroxy-d^1-d^2-d^3-but-1-enyl)-oxazolidin-2-one **$^2H_3$-145** (0.07 g, 99%) as a clear oil. FTIR (film/cm^{-1}) υ_{max}: 3422 (br s), 3058 (m), 2973 (m), 2928 (m), 1744 (s), 1630 (s); ^{1}H NMR (250 MHz, $CDCl_3$) δ: 1.28 (s, 3H), 1.76 (br S, 1H), 3.65 (app. t, 2H, *J* = 7.6 Hz), 4.40 (app. t, 2H, *J* = 7.6 Hz); ^{13}C NMR (100 MHz, $CDCl_3$) δ: 23.8, 42.2, 62.3, 66.3 (t, *J* = 21.0 Hz), 114.5 (t, *J* = 22.9 Hz), 124.2 (t, *J* = 24.9 Hz), 155.6; HRMS (ESI, +ve) *m/z* calcd. for $C_7H_8D_3NNaO_3$ 183.0825, found 183.0820 $(M+Na)^+$.

(*E*)-4-(2-Oxooxazolidin-3-yl)but-3-en-2-yl phenylacetate 154

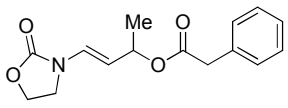

EDCi (0.73 g, 3.81 mmol) in DCM (100 ml), triethylamine (0.53 ml, 3.81 mmol), DMAP (0.03 g, 0.19 mmol), phenylacetic acid (0.52 g, 3.81 mmol) and (*E*)-3-(3-

hydroxybut-1-enyl)oxazolidin-2-one **145** (0.30 g, 1.91 mmol) in DCM (20 ml) were combined according to general procedure 1 (reaction time: 15 hours). Purification was achieved by reported procedure to afford (*E)*-4-(2-oxooxazolidin-3-yl)but-3-en-2-yl phenylacetate **154** as a white solid (0.46 g, 88%). M.p. 94–96 °C; FTIR (film/cm^{-1}) υ_{max}: 2981 (s), 1747 (s), 1731 (s), 1672 (s); ^{1}H NMR (300 MHz, $CDCl_3$) δ: 1.30 (d, 3H, *J* = 6.7 Hz, C*H*$_3$CH(CH)O-), 3.60 (s, 2H, -C(O)C*H*$_2$C$_6$H$_5$), 3.62–3.72 (m, 2H, -N(CH-)C*H*$_2$-), 4.40–4.48 (m, 2H, -OC*H*$_2$-), 4.86 (dd, 1H, *J* = 14.4, 6.7 Hz, -NCHC*H*-), 5.43 (app. quin, 1H, *J* = 6.7 Hz, CH$_3$C*H*(CH-)O-), 6.93 (d, 1H, *J* = 14.4 Hz, -NC*H*CH-), 7.21–7.36 (m, 5H, C$_6$*H*$_5$-); ^{13}C NMR (62 MHz, $CDCl_3$) *δ*: 21.0, 42.0, 42.7, 62.6, 70.3, 110.2, 127.4, 127.5, 129.0, 129.6, 124.4, 155.7, 171.2; HRMS (ESI, +ve) *m/z* calcd. for $C_{15}H_{17}NNaO_4$ 298.1055, found 298.1050 $(M+Na)^+$.

Phenyl-acetic acid d^1-d^2-d^3-1-methyl-3-(2-oxo-oxazolidin-3-yl)-allyl ester ^{2}H$_3$-154

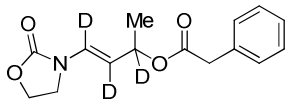

EDCi (0.33 g, 1.72 mmol) in DCM (100 ml), triethylamine (0.24 ml, 1.72 mmol), DMAP (0.01 g, 0.09 mmol), phenylacetic acid (0.23 g, 1.72 mmol) and 3-(3-Hydroxy-d^1-d^2-d^3-but-1-enyl)-oxazolidin-2-one **^{2}H$_3$-145** (0.14 g, 0.86 mmol) in DCM (20 ml) were combined according to general procedure 1 (reaction time: 15 hours). Purification was achieved by reported procedure to afford phenyl-acetic acid d^1-d^2-d^3-1-methyl-3-(2-oxo-oxazolidin-3-yl)-allyl ester **^{2}H$_3$-154** as a cream solid (0.38 g, 94%). M.p. 97–100 °C; FTIR (film/cm^{-1}) υ_{max}: 3054 (m), 2990 (m), 2919 (m), 1740 (s), 1691 (s), 1670 (s), 1633 (m); ^{1}H NMR (500 MHz, $CDCl_3$) δ: 1.39 (s, 3H), 3.62 (s, 2H), 3.63 (app. t, 2H, *J* = 7.6 Hz), 4.41 (app. t, 2H, *J* = 7.6 Hz); ^{13}C NMR (125 MHz, $CDCl_3$) δ: 20.4, 41.6, 42.2, 62.2, 69.4 (t, *J* = 22.9 Hz), 109.2 (t, *J* = 22.9 Hz), 126.6 (t, *J* = 27.0 Hz), 127.0, 128.5, 129.2, 134.0, 155.2, 170.8; HRMS (ESI, +ve) *m/z* calcd. for $C_{15}H_{14}D_3NNaO_4$ 301.1244, found 301.1245 $(M+Na)^+$.

Phenyl-acetic acid-$^{13}C_2$ 1-methyl-3-(2-oxo-oxazolidin-3-yl)-allyl ester $^{13}C_2$-154

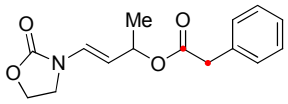

EDCi (0.69 g, 3.62 mmol) in DCM (100 ml), triethylamine (0.50 ml, 3.62 mmol), DMAP (0.02 g, 0.18 mmol), $^{13}C_2$-phenyl-acetic acid (0.50 g, 3.62 mmol) and (*E*)-3-(3-hydroxybut-1-enyl)oxazolidin-2-one **145** (0.28 g, 1.81 mmol) in DCM (20 ml) were combined according to general procedure 1 (reaction time: 15 hours). Purification was achieved by reported procedure to afford phenyl-acetic acid-$^{13}C_2$ 1-methyl-3-(2-oxo-oxazolidin-3-yl)-allyl ester **$^{13}C_2$-154** as a white solid (0.48 g, 89%). M.p. 98–101 ^{o}C. FTIR (film/cm^{-1}) υ_{max}: 2991 (m), 2918 (m), 1739 (s), 1691 (s), 1669 (s). ^{1}H NMR (400 MHz, $CDCl_3$) δ: 1.40 (d, 3H, *J* = 6.6 Hz), 3.65 (dd, 2H, *J* = 129.6, 7.8 Hz), 3.74 (app. t, 2H, *J* = 7.9 Hz), 4.48 (app. t, 2H, *J* = 7.9 Hz), 4.91 (dd, 1H, *J* = 14.3, 7.1 Hz), 5.48 (pd, 1H, *J* = 6.6, 3.0 Hz), 6.97 (d, 1H, *J* = 14.3 Hz), 7.27–7.40 (m, 5H). ^{13}C NMR (100 MHz, $CDCl_3$) *δ*: 20.6, 41.6 (d, *J* 57.4 Hz), 42.3, 62.2, 69.9 (d, *J* 1.4 Hz), 109.8 (d, *J* 1.1 Hz), 127.0, 127.1, 128.5 (d, *J* 3.5 Hz), 129.3 (t, *J* 2.3 Hz), 134.0 (dd, *J* 43.7, 2.95 Hz), 155.3, 170.8 (d, *J* 57.4 Hz). HRMS (ESI, +ve) *m/z* calcd. for $C_{13}C^{13}{}_2H_{17}NNaO_4$ 300.1212, found 300.1115 $(M+Na)^+$.

(*E*)-4-(2-Oxooxazolidin-3-yl)but-3-en-2-yl 2-(*o*-methoxyphenyl)acetate 163

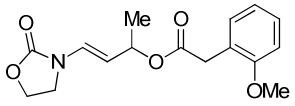

EDCi (0.73 g, 3.81 mmol) in DCM (100 ml), triethylamine (0.53 ml, 3.81 mmol), DMAP (0.03 g, 0.19 mmol), *o*-methoxyphenylacetic acid (0.63 g, 3.81 mmol) and (*E*)-3-(3-hydroxybut-1-enyl)oxazolidin-2-one **145** (0.30 g, 1.91 mmol) in DCM (20 ml) were combined according to general procedure 1 (reaction time: 15 hours). Purification was achieved by reported procedure to afford (*E*)-4-(2-oxooxazolidin-3-yl)but-3-en-2-yl 2-(*o*-methoxyphenyl)acetate **163** as an off white solid (0.55 g, 94%). M.p. 92–93 $^{\circ}$C; FTIR (film/cm^{-1}) υ_{max}: 2925 (s), 2850 (w), 1755 (s), 1676 (s), 1603 (w), 1590 (w); ^{1}H NMR (300 MHz, $CDCl_3$) δ: 1.35 (d, 3H, *J* = 6.7 Hz), δ 3.59 (s, 2H), 3.63 (app. t, 2H, *J*

= 8.3 Hz), 3.79 (s, 3H), 4.39 (app. t, 2H, *J* = 8.3 Hz), 4.86 (dd, 1H, *J* = 14.3, 6.7 Hz), 5.49 (app. quin, 1H, *J* = 6.7 Hz), 6.83–6.93 (m, 2H), 7.16 (d, 1H, *J* = 14.3 Hz), 7.23 (td, 1H, *J* = 8.0, 1.6 Hz); ^{13}C NMR (75 MHz, $CDCl_3$) δ: 21.1, 36.7, 42.7, 55.8, 62.6, 69.9, 110.5, 110.9, 120.8, 123.5, 127.0, 128.9, 131.2, 155.7, 157.9, 171.5; HRMS (ESI, +ve) *m/z* calcd. for $C_{16}H_{19}NNaO_5$ 328.1161, found 328.1155 $(M+Na)^+$.

(*E*)-4-(2-Oxooxazolidin-3-yl)but-3-en-2-yl 2-(*m*-methoxyphenyl)acetate 164

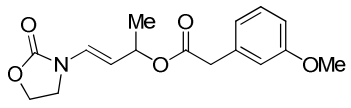

EDCi (0.73 g, 3.81 mmol) in DCM (100 ml), triethylamine (0.53 ml, 3.81 mmol), DMAP (0.03 g, 0.19 mmol), *m*-methoxyphenylacetic acid (0.63 g, 3.81 mmol) and (*E*)-3-(3-hydroxybut-1-enyl)oxazolidin-2-one **145** (0.30 g, 1.91 mmol) in DCM (20 ml) were combined according to general procedure 1 (reaction time: 15 hours). Purification was achieved by reported procedure to afford (*E*)-4-(2-oxooxazolidin-3-yl)but-3-en-2-yl 2-(*m*-methoxyphenyl)acetate **164** as an off white solid (0.44 g, 76%). M.p. 90–91 °C. FTIR (film/cm^{-1}) υ_{max}: 3498 (w), 2978 (m), 2933 (m), 1757 (s), 1670 (s), 1601 (s); ^{1}H NMR (250 MHz, $CDCl_3$) δ: 1.34 (d, 3H, *J* = 6.7 Hz), 3.55 (s, 2H), 3.57–3.68 (m, 2H), 3.78 (s, 3H), 4.35–4.45 (m, 2H), 4.84 (dd, 1H, *J* = 14.3, 6.7 Hz), 5.42 (app. quin, 1H, *J* = 6.7 Hz), 6.81–6.90 (m, 3H), 6.90 (d, 1H, *J* = 14.3 Hz), 7.22 (td, 1H, *J* = 7.6, 1.2 Hz). ^{13}C NMR (75 MHz, $CDCl_3$) δ: 19.6, 40.6, 41.3, 54.2, 61.2, 69.0, 108.8, 111.5, 113.8, 120.6, 126.0, 128.5, 134.4, 154.3, 158.6, 169.7. HRMS (ESI, +ve) *m/z* calcd. for $C_{16}H_{19}NNaO_5$ 328.1161, found 328.1155 $(M+Na)^+$.

(*E*)-4-(2-Oxooxazolidin-3-yl)but-3-en-2-yl 2-(*p*-methoxyphenyl)acetate 165

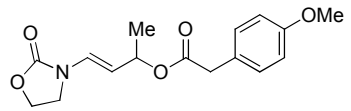

EDCi (0.73 g, 3.81 mmol) in DCM (100 ml), triethyalmine (0.53 ml, 3.81 mmol), DMAP (0.03 g, 0.19 mmol), para-methoxyphenylacetic acid (0.63 g, 3.81 mmol) and (*E*)-3-(3-hydroxybut-1-enyl)oxazolidin-2-one **145** (0.30 g, 1.91 mmol) in DCM (20 ml)

were combined according to general procedure 1 (reaction time: 15 hours). Purification was achieved by reported procedure to afford (*E*)-4-(2-oxooxazolidin-3-yl)but-3-en-2-yl 2-(*p*-methoxyphenyl)acetate **165** as an off white solid (0.53 g, 91%). M.p. 89–91 °C; FTIR (film/cm^{-1}) υ_{max}: 2980 (m), 2932 (m), 2838 (w), 1755 (s), 1671 (s), 1613 (m), 1585 (m), 1514 (s); ^{1}H NMR (300 MHz, $CDCl_3$) δ: 1.34 (d, 3H, *J* = 6.7 Hz), 3.52 (s, 2H), 3.61–3.69 (m, 2H), 3.77 (s, 3H), 4.37–4.45 (m, 2H), 4.85 (dd, 1H, *J* = 14.4, 6.7 Hz), 5.40 (app. quin, 1H, *J* = 6.7 Hz), 6.84 (app. d, 2H, *J* = 8.6 Hz), 6.89 (d, 1H, *J* = 14.4 Hz), 7.17 (app. d, 2H, *J* = 8.6 Hz); ^{13}C NMR (75 MHz, $CDCl_3$) *δ*: 21.0, 41.1, 42.7, 55.7, 62.6, 70.2, 110.3, 114.4, 126.5, 127.3, 130.7, 155.7, 159.1, 171.6; HRMS (ESI, +ve) *m/z* calcd. for $C_{16}H_{19}NNaO_5$ 328.1161, found 328.1155 $(M+Na)^+$.

$^{13}C_1$-(4-Methoxyphenyl)acetic acid ($^{13}C_1$-282)

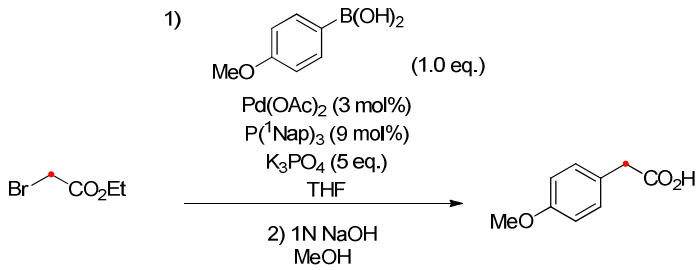

To a degassed solution of $Pd(OAc)_2$ (0.02 g, 0.07 mmol, 3 mol%), $P(^1Nap)_3$ (0.09 mg, 0.21 mmol, 9 mol%), and finely ground K_3PO_4 (2.53 g, 11.90 mmol, 5 eq.) in THF (20 ml) was added ^{13}C-ethylbromo acetate (0.26 ml, 2.38 mmol, 1.0 eq.). The reaction mixture was allowed to stir for 5 minutes and then a solution of 4-methoxyphenyl boronic acid (0.36g, 2.38 mmol, 1.0 eq.) and H_2O (0.09 ml, 4.76 mmol, 2.0 eq.) in THF (10 ml) was added. The reaction mixture was allowed to stir at room temperature over 16 hours and was then quenched by addition to water and extraction with DCM (3 × 20 ml), dried over magnesium sulphate and concentrated *in vacuo* to yield the crude product. The crude ester was then saponified by dissolution in 1N NaOH (20 ml) in methanol (20 ml) and allowed to stir at room temperature over 12 hours. The target compound was isolated by extraction of the organics with 5% NaOH (3 × 20 ml), acidifying the aqueous by 6N HCl (30 ml), extracting the organics with DCM (3 × 20 ml), concentration *in-vacuo* and subsequent purification by flash column chromatography, using ethyl acetate/petroleum ether 40-60° (10:90) to yield $^{13}C_1$-(4-

methoxyphenyl)acetic acid **$^{13}C_1$-282** as a white solid (0.12 g, 29 %). M.p. 90–92 ^{o}C; FTIR (film/cm^{-1}) υ_{max}: 3006 (m), 3000 (br s), 2915 (m), 2835 (m), 1687 (s), 1614 (s), 1586 (w), 1512 (s); ^{1}H NMR (400 MHz, $CDCl_3$) δ: 3.64 (d, 2H, *J* = 129.0 Hz), 3.85 (s, 3H), 6.93 (app. d, 2H, *J* = 8.5 Hz), 7.25 (app. dd, 2H, *J* = 8.5, 4.2 Hz), 11.6 (br s, 1H); ^{13}C NMR (100 MHz, $CDCl_3$) δ: 40.0, 55.3, 114.1 (d, *J* = 4.3 Hz), 125.4 (d, *J* = 44.4 Hz), 130.4 (d, *J* = 3.3 Hz), 158.9, 178.4 (d, *J* = 57.1 Hz); HRMS (ESI, +ve) *m/z* calcd. for $C_8{}^{13}C_1H_{10}Na_2O_3$ 213.0504, found 213.0411 $(M+2Na)^{2+}$.

(*E*)-4-(2-Oxooxazolidin-3-yl)but-3-en-2-yl 2-^{13}C$_1$-(4-methoxyphenyl)acetate $^{13}C_1$-165

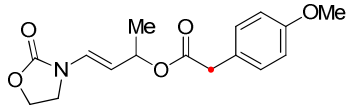

EDCi (0.13 g, 0.68 mmol) in DCM (50 ml), triethylamine (0.10 ml, 0.68 mmol), DMAP (0.01 g, 0.03 Eq), ^{13}C$_1$-(4-methoxyphenyl)acetic acid **$^{13}C_1$-282** (0.11 g, 0.68 mmol) and (*E*)-3-(3-hydroxybut-1-enyl)oxazolidin-2-one (0.05 g, 0.34 mmol) in DCM (10 ml) were combined according to general procedure 1 (reaction time: 15 hours). Purification was achieved by reported procedure to afford (*E*)-4-(2-oxooxazolidin-3-yl)but-3-en-2-yl 2-^{13}C$_1$-(4-methoxyphenyl)acetate **$^{13}C_1$-165** as a yellow oil (0.10 g, 100%). FTIR (film/cm^{-1}) υ_{max}: 2970 (m), 2991 (m), 2923 (m), 2840 (m), 1745 (s), 1726 (s), 1668 (s), 1603 (m), 1590 (m); ^{1}H NMR (400 MHz, $CDCl_3$) δ: 1.39 (d, 3H, *J* = 6.6 Hz), 3.56 (d, 2H, *J* = 129.0 Hz), 3.68 (app. t, 2H, *J* = 7.9 Hz), 3.83 (s, 3H), 4.45 (app. t, 2H, *J* = 7.9 Hz), 4.89 (dd, 1H, *J* = 14.2, 6.9 Hz), 5.45 (app. quin, 1H, *J* = 6.6 Hz), 6.89 (app. d, 2H, *J* = 8.5 Hz), 6.94 (d, 1H, *J* = 14.2 Hz), 7.22 (app. dd, 1H, *J* = 8.5 Hz); ^{13}C NMR (100 MHz, $CDCl_3$) *δ*: 20.6, 40.7, 42.3, 55.2, 62.2, 69.8, 109.8, 114.0 (d, *J* = 4.0 Hz), 126.1 (d, *J* = 45.8 Hz), 126.9, 130.3 (d, *J* = 3.3 Hz), 155.3, 158.6, 171.2 (d, *J* = 48.9 Hz); HRMS (ESI, +ve) *m/z* calcd. for $C_{15}{}^{13}C_1H_{19}NNaO_5$ 329.1239, found 329.1177 $(M+Na)^{+}$.

(*E*)-4-(2-Oxooxazolidin-3-yl)but-3-en-2-yl 2-*o*-tolylacetate 166

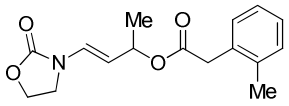

EDCi (0.73 g, 3.81 mmol) in DCM (100 ml), triethylamine (0.53 ml, 3.81 mmol), DMAP (0.03 g, 0.19 mmol), *o*-tolylphenylacetic acid (0.57 g, 3.81 mmol) and (*E*)-3-(3-hydroxybut-1-enyl)oxazolidin-2-one **145** (0.30 g, 1.91 mmol) in DCM (20 ml) were combined according to general procedure 1 (reaction time: 15 hours). Purification was achieved by reported procedure to afford (*E*)-4-(2-oxooxazolidin-3-yl)but-3-en-2-yl 2-*o*-tolylacetate **166** as a white solid (0.39 g, 71%). M.p. 83–85 °C; FTIR (film/cm^{-1}) υ_{max}: 2999 (s), 2924 (s), 1756 (s), 1670 (s); ^{1}H NMR (250 MHz, $CDCl_3$) δ: 1.35 (d, 3H, *J* = 6.7 Hz), 2.30 (s, 3H), 3.60 (s, 2H), 3.69–3.77 (m, 2H), 4.46–4.54 (m, 2H), 4.85 (dd, 1H, *J* = 14.6, 6.7 Hz), 5.42 (app quin, 1H, *J* = 6.7 Hz), 6.90 (d, 1H, *J* = 14.6 Hz), 7.10–7.20 (m, 4H); ^{13}C NMR (75 MHz, $CDCl_3$) *δ*: 20.0, 21.0, 39.9, 42.7, 62.6, 70.3, 110.2, 126.5, 127.4, 127.7, 130.5, 130.7, 133.2, 137.2, 135.7, 171.1; HRMS (ESI, +ve) *m/z* calcd. for $C_{16}H_{19}NNaO_4$ 312.1212, found 312.1206 $(M+Na)^+$.

(*E*)-4-(2-Oxooxazolidin-3-yl)but-3-en-2-yl 2-*m*-tolylacetate 167

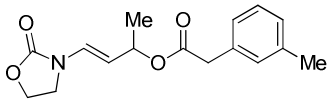

EDCi (0.73 g, 3.81 mmol) in DCM (100 ml), triethylamine (0.53 ml, 3.81 mmol), DMAP (0.03 g, 0.19 mmol), *m*-tolylphenylacetic acid (0.57 g, 3.81 mmol) and (*E*)-3-(3-hydroxybut-1-enyl)oxazolidin-2-one **145** (0.30 g, 1.91 mmol) in DCM (20 ml) were combined according to general procedure 1 (reaction time: 15 hours). Purification was achieved by reported procedure to afford (*E*)-4-(2-oxooxazolidin-3-yl)but-3-en-2-yl 2-*m*-tolylacetate **167** as a white solid (0.41 g, 74%). M.p. 82–84 °C; FTIR (film/cm^{-1}) υ_{max}: 3050 (w), 2980 (s), 2919 (s), 1761 (s), 1670 (s), 1609 (w), 1590 (w); ^{1}H NMR (250 MHz, $CDCl_3$) δ: 1.40 (d, 3H, *J* = 6.7), 2.33 (s, 3H), 3.55 (s, 2H), 3.55–3.64 (m, 2H), 4.38–4.48 (m, 2H), 4.86 (dd, 1H, *J* = 14.2, 6.7 Hz), 5.42 (app. quin, 1H *J* = 6.7 Hz), 6.92 (d, 1H, *J* = 14.2 Hz), 7.03–7.11 (m, 3H), 7.16–7.24 (m, 1 H); ^{13}C NMR (75

MHz, $CDCl_3$) δ: 21.0, 21.8, 41.9, 42.7, 62.6, 70.2, 110.2, 126.6, 127.3, 128.2, 128.8, 130.4, 134.3, 138.6, 155.6, 171.3; HRMS (ESI, +ve) *m/z* calcd. for $C_{16}H_{19}NNaO_4$ 312.1212, found 312.1206 $(M+Na)^+$.

(*E*)-4-(2-Oxooxazolidin-3-yl)but-3-en-2-yl 2-*p*-tolylacetate 168

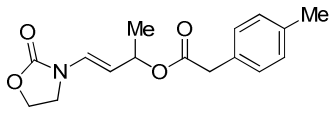

EDCi (0.73 g, 3.81 mmol) in DCM (100 ml), triethylamine (0.53 ml, 3.81 mmol), DMAP (0.03 g, 0.19 mmol), *p*-tolylphenylacetic acid (0.57 g, 3.81 mmol) and (*E*)-3-(3-hydroxybut-1-enyl)oxazolidin-2-one **145** (0.30 g, 1.91 mmol) in DCM (20 ml) were combined according to general procedure 1 (reaction time: 15 hours). Purification was achieved by reported procedure to afford (*E*)-4-(2-oxooxazolidin-3-yl)but-3-en-2-yl 2-*p*-tolylacetate **168** as a white solid (0.49 g, 88%). M.p. 86–89 °C; FTIR (film/cm^{-1}) υ_{max}: 3051 (w), 2981 (s), 2924 (s), 1766 (s), 1670 (s), 1516 (s); ^{1}H NMR (250 MHz, $CDCl_3$) δ: 1.35 (d, 3H, *J* = 7.0 Hz), 2.32 (s, 3H), 3.55 (s, 2H), 3.61–3.71 (m, 2H), 4.38–4.48 (m, 2H), 4.86 (dd, 1H, *J* = 14.3, 7.0 Hz), 5.41 (app. quin, 1H, *J* = 7.0 Hz), δ 6.92 (d, 1H, *J* = 14.3 Hz), δ 7.08–7.19 (m, 4H); ^{13}C NMR (75 MHz, $CDCl_3$) δ: 21.0, 21.5, 41.6, 42.7, 62.6, 70.3, 110.2, 127.3, 129.5, 129.6, 131.4, 137.0, 155.7, 171.5. HRMS (ESI, +ve) *m/z* calcd. for $C_{16}H_{19}NNaO_4$ 312.1212, found 312.1206 $(M+Na)^+$.

(*E*)-4-(2-Oxooxazolidin-3-yl)but-3-en-2-yl 2-(*o*-nitrophenyl)acetate 169

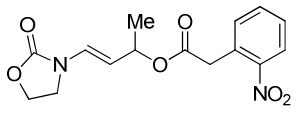

EDCi (0.73 g, 3.81 mmol) in DCM (100 ml), triethylamine (0.53 ml, 3.81 mmol), DMAP (0.03 g, 0.19 mmol), *o*-nitrophenylacetic acid (0.69 g, 3.81 mmol) and (*E*)-3-(3-hydroxybut-1-enyl)oxazolidin-2-one **145** (0.30 g, 1.91 mmol) in DCM (20 ml) were combined according to general procedure 1 (reaction time: 15 hours). Purification was achieved by reported procedure to afford (*E*)-4-(2-oxooxazolidin-3-yl)but-3-en-2-yl 2-(*o*-nitrophenyl)acetate **169** as a yellow oil (0.52 g, 85%). FTIR (film/cm^{-1}) υ_{max}: 2982

(m), 2928 (m), 1756 (s), 1671 (s), 1613 (m), 1580 (m), 1526 (s); ^{1}H NMR (300 MHz, $CDCl_3$) δ: 1.35 (d, 3H, *J* = 6.7 Hz), 3.68 (app. t, 2H, *J* = 8.0 Hz), 3.94 (d, 1H, *J* = 17.1 Hz), 4.00 (d, 1H, *J* = 17.1 Hz),4.42 (app. t, 2H *J* = 8.0 Hz), 4.85 (dd, 1H, *J* = 14.4, 6.7 Hz), 5.41 (app. quin, 1H, *J* = 6.7 Hz), 6.87 (d, 1H, *J* = 14.4 Hz), 7.33 (dd, 1H, *J* = 7.8, 1.2 Hz), 7.45 (td, 1H, *J* = 7.8, 1.2 Hz), 7.58 (td, 1H, *J* = 7.8, 1.2 Hz), 8.07 (dd, 1H, *J* = 7.8, 1.2 Hz); ^{13}C NMR (75 MHz, $CDCl_3$) *δ*: 20.8, 40.6, 42.7, 62.7, 71.0, 110.2, 125.7, 127.5, 129.0, 130.2, 133.8, 134.0, 149.1, 155.7, 169.6; HRMS (ESI, +ve) *m/z* calcd. for $C_{15}H_{16}N_2NaO_6$ 343.0906, found 343.0901 $(M+Na)^+$.

(*E*)-4-(2-Oxooxazolidin-3-yl)but-3-en-2-yl 2-(*m*-nitrophenyl)acetate 170

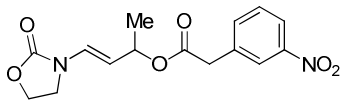

EDCi (0.73 g, 3.81 mmol) in DCM (100 ml), triethylamine (0.53 ml, 3.81 mmol), DMAP (0.03 g, 0.19 mmol), *m*-nitrophenylacetic acid (0.69 g, 3.81 mmol) and (*E*)-3-(3-hydroxybut-1-enyl)oxazolidin-2-one **145** (0.30 g, 1.91 mmol) in DCM (20 ml) were combined according to general procedure 1 (reaction time: 15 hours). Purification was achieved by reported procedure to afford (*E*)-4-(2-oxooxazolidin-3-yl)but-3-en-2-yl 2-(*m*-nitrophenyl)acetate **170** as an orange oil (0.56 g, 92%). FTIR (film/cm^{-1}) υ_{max}: 2983 (w), 2927 (w), 1755 (s), 1669 (s), 1529 (s); ^{1}H NMR (250 MHz, $CDCl_3$) δ: 1.37 (d, 3H, *J* = 6.9 Hz), 3.64–3.68 (m, 2H), 3.70 (s, 2H), 4.45 (app. t, 2H, *J* = 8.1 Hz), 4.85 (dd, 1H, *J* = 14.4, 6.9 Hz), 5.44 (app. quin, 1H, *J* = 6.9 Hz), 6.93 (d, 1H, *J* = 14.4 Hz), 7.48–7.55 (m, 1H), 7.58–7.65 (m, 1H), 8.1–8.2 (m, 2H); ^{13}C NMR (75 MHz, $CDCl_3$) *δ*: 21.0, 41.4, 42.7, 62.7, 71.1, 109.7, 122.7, 124.6, 127.9, 129.9, 136.0, 136.3, 148.7, 155.7, 170.0; HRMS (ESI, +ve) *m/z* calcd. for $C_{15}H_{16}N_2NaO_6$ 343.0906, found 343.0901 $(M+Na)^+$.

(*E*)-4-(2-Oxooxazolidin-3-yl)but-3-en-2-yl 2-(*p*-nitrophenyl)acetate 171

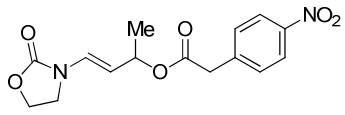

EDCi (0.73 g, 3.81 mmol) in DCM (100 ml), triethylamine (0.53 ml, 3.81 mmol), DMAP (0.03 g, 0.19 mmol), *p*-nitrophenylacetic acid (0.69 g, 3.81 mmol) and (*E*)-3-(3-hydroxybut-1-enyl)oxazolidin-2-one **145** (0.30 g, 1.91 mmol) in DCM (20 ml) were combined according to general procedure 1 (reaction time: 15 hours). Purification was achieved by reported procedure to afford (*E*)-4-(2-oxooxazolidin-3-yl)but-3-en-2-yl 2-(*p*-nitrophenyl)acetate **171** as a red oil (0.50 g, 85%). FTIR (film/cm^{-1}) υ_{max}: 3081 (w), 2982 (m), 2928 (m), 1757 (s), 1670 (s), 1606 (m), 1521 (s); ^{1}H NMR (250 MHz, $CDCl_3$) δ: 1.35 (d, 3H, *J* = 6.9 Hz), 3.62–3.71 (m, 2H), 3.70 (s, 2H), 4.44 (app. t, 2H, *J* = 8.1 Hz), 4.83 (dd, 1H, *J* = 14.4, 6.9 Hz), 5.42 (app. quin, 1H, *J* = 6.9 Hz), 6.92 (app. d, 1H, *J* = 14.4 Hz), 7.44 (app. d, 2H, *J* = 8.7 Hz), 8.17 (d, 2H, *J* = 8.7 Hz); ^{13}C NMR (75 MHz, $CDCl_3$) *δ*: 21.0, 41.7, 42.7, 62.6, 71.1, 109.7, 124.1, 127.8, 130.7, 141.8, 147.6, 155.6, 169.8; HRMS (ESI, +ve) *m/z* calcd. for $C_{15}H_{16}N_2NaO_6$ 343.0906, found 343.0901 $(M+Na)^+$.

(*E*)-4-(2-Oxooxazolidin-3-yl)but-3-en-2-yl 2-(4-(dimethylamino)phenyl)acetate 202

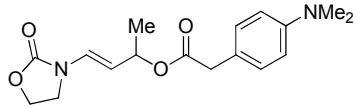

EDCi (0.82 g, 4.28 mmol) in DCM (100 ml), triethylamine (0.60 ml, 4.28 mmol), DMAP (0.03 g, 0.21 mmol), *p*-dimethyl amino phenyl acetic acid (0.77 g, 4.28 mmol) and (*E*)-3-(3-hydroxybut-1-enyl)oxazolidin-2-one **145** (0.34 g, 2.14 mmol) in DCM (20 ml) were combined according to general procedure 1 (reaction time: 15 hours). Purification was achieved by reported procedure to afford (*E*)-4-(2-oxooxazolidin-3-yl)but-3-en-2-yl 2-(4-(dimethylamino)phenyl)acetate **202** as a brown solid (0.62 g, 92%). M.p. 101–103 °C; FTIR (film/cm^{-1}) υ_{max}: 2978.7 (w), 2918.3 (w), 2803.7 (w), 1764.5 (s), 1731.6 (s), 1670.1 (m), 1615.8 (m), 1523.8 (s). ^{1}H NMR (250 MHz, $CDCl_3$) δ: 1.39 (d, 3H, *J* = 6.8 Hz), 2.93 (s, 6H), 3.49 (s, 2H), 3.62 (app. t, 2H, *J* = 7.7 Hz), 4.41

(app. t, 2H, *J* = 7.7 Hz), 4.87 (dd, 1H, *J* = 14.4, 6.8 Hz), 5.41 (app. quin, 1 H, *J* = 6.8 Hz), 6.70 (d, 2H, *J* = 8.8 Hz), 6.92 (d, 1 H, *J* = 14.4 Hz), 7.14 (d, 2H, *J* = 8.8 Hz) ^{13}C NMR (75 MHz, $CDCl_3$) δ: 19.6, 39.5, 41.3, 52.5, 61.2, 68.6, 109.0, 111.8, 120.8, 125.8, 128.8, 148.7, 154.3, 170.4. HRMS (ESI, +ve) *m/z* calcd. For $C_{17}H_{22}N_2NaO_4$ 341.1477, found 341.1472 $(M+Na)^+$.

(*E*)-4-(2-Oxooxazolidin-3-yl)but-3-en-2-yl 2-(*p*-iodophenyl)acetate 203

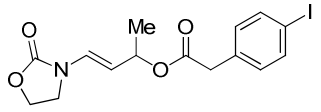

EDCi (0.73 g, 3.81 mmol) in DCM (100 ml), triethylamine (0.53 ml, 3.81 mmol), DMAP (0.03 g, 0.19 mmol), *p*-iodophenylacetic acid (1.00 g, 3.81 mmol) and (*E*)-3-(3-hydroxybut-1-enyl)oxazolidin-2-one **145** (0.30 g, 1.91 mmol) in DCM (20 ml) were combined according to general procedure 1 (reaction time: 15 hours). Purification was achieved by reported procedure to afford (*E*)-4-(2-oxooxazolidin-3-yl)but-3-en-2-yl 2-(*p*-iodophenyl)acetate **203** as a white solid (0.61 g, 79%). M.p. 97–98 °C; FTIR (film/cm^{-1}) υ_{max}: 2979 (w), 2928 (w), 1757 (s), 1670 (s); ^{1}H NMR (500 MHz, $CDCl_3$) δ: 1.34 (d, 3H, *J* = 6.4 Hz), 3.51 (s, 2H), 3.60 (app. t, 2H, *J* = 6.7 Hz), 4.37–4.44 (m, 2H), 4.82 (dd, 1H, *J* = 14.2, 6.4 Hz), 5.40 (app. quin, 1 H, *J* = 6.4 Hz), 6.89 (d, 1H, *J* = 14.2 Hz), 7.01 (app. d, 2H, *J* = 6.5 Hz), 7.62 (app. d, 2H, *J* = 6.5 Hz); ^{13}C NMR (125 MHz, $CDCl_3$) δ: 20.6, 41.1, 42.3, 62.2, 70.2, 92.6, 109.6, 127.1, 131.3, 133.7, 137.6, 155.3, 170.2. HRMS (ESI, +ve) *m/z* calcd. for $C_{15}H_{16}INNaO_4$ 424.0022, found 424.0016 $(M+Na)^+$.

(*E*)-4-(2-Oxooxazolidin-3-yl)but-3-en-2-yl 2-(*p*-fluorophenyl)acetate 204

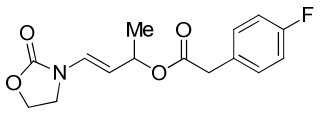

EDCi (0.73 g, 3.81 mmol) in DCM (100 ml), triethylamine (0.53 ml, 3.81 mmol), DMAP (0.03 g, 0.19 mmol), *p*-fluorophenylacetic acid (0.59 g, 3.81 mmol) and (*E*)-3-(3-hydroxybut-1-enyl)oxazolidin-2-one **145** (0.30 g, 1.91 mmol) in DCM (20 ml) were

combined according to general procedure 1 (reaction time: 15 hours). Purification was achieved by reported procedure to afford (*E*)-4-(2-oxooxazolidin-3-yl)but-3-en-2-yl 2-(*p*-fluorophenyl)acetate **204** as an off white solid (0.43 g, 77%). M.p. 94–96 °C; FTIR (film/cm^{-1}) υ_{max}: 2983 (w), 1760 (s), 1670 (s), 1510 (s); ^{1}H NMR (500 MHz, $CDCl_3$) δ: 1.32 (d, 3H, *J* = 6.7 Hz), 3.53 (s, 2H), 3.62 (app. t, 2H, *J* = 8.1 Hz), 4.38 (app. t, 2H, *J* = 8.1 Hz), 4.82 (dd, 1H, *J* = 14.4, 6.7 Hz), 5.39 (app. quin, 1 H, *J* = 6.7 Hz), 6.87 (d, 1H, *J* = 14.4 Hz), 6.96 (app t, 2H, *J* = 8.5 Hz), 7.17–7.23 (m, 2H); ^{13}C NMR (125 MHz, $CDCl_3$) δ: 20.6, 40.7, 42.3, 62.3, 70.1, 110.0, 115.3 (d, J = 20.6 Hz), 127.0, 129.8 (d, J = 3.5 Hz), 130.8, (d, J = 7.3 Hz), 155.3, 161.9 (d, J = 245 Hz), 170.6; HRMS (ESI, +ve) *m/z* calcd. For $C_{15}H_{16}FNNaO_4$ 316.0961, found 316.0956 $(M+Na)^+$.

(*E*)-4-(2-Oxooxazolidin-3-yl)but-3-en-2-yl 2-(*p*-chlorophenyl)acetate 205

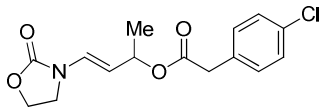

EDCi (0.73 g, 3.81 mmol) in DCM (100 ml), triethylamine (0.53 ml, 3.81 mmol), DMAP (0.03 g, 0.19 mmol), *p*-chlorophenylacetic acid (0.65 g, 3.81 mmol) and (*E*)-3-(3-hydroxybut-1-enyl)oxazolidin-2-one **145** (0.30 g, 1.91 mmol) in DCM (20 ml) were combined according to general procedure 1 (reaction time: 15 hours). Purification was achieved by reported procedure to afford (*E*)-4-(2-oxooxazolidin-3-yl)but-3-en-2-yl 2-(*p*-chlorophenyl)acetate **205** as a yellow solid (0.55 g, 93%). M.p. 91–93 °C; FTIR (film/cm^{-1}) υ_{max}: 2982 (w), 2928 (w), 1759 (s), 1671 (s), 1599 (w); ^{1}H NMR (500 MHz, $CDCl_3$) δ: 1.34 (d, 3H, *J* = 6.8 Hz), 3.55 (s, 2H), 3.70 (app. t, 2H, *J* = 8.0 Hz), 4.42 (app. t, 2H, *J* = 8.0 Hz), 4.83 (dd, 1H, *J* = 14.4, 6.8 Hz), 5.41 (app. quin, 1 H, *J* = 6.8 Hz), 6.91 (d, 1H, *J* = 14.4 Hz), 7.19 (app. d, 2H, *J* = 8.4 Hz), 7.28 (app. d, 2H, *J* = 8.4 Hz); ^{13}C NMR (125 MHz, $CDCl_3$) δ: 20.6, 40.9, 42.3, 62.2, 70.2, 109.6, 127.1, 128.7, 130.6, 132.5, 133.0, 155.2, 170.4; HRMS (ESI, +ve) *m/z* calcd. for $C_{15}H_{16}ClNNaO_4$ 332.0660, found 332.0653 $(M+Na)^+$.

(*E*)-4-(2-Oxooxazolidin-3-yl)but-3-en-2-yl 2-(*p*-(trifluoromethyl)phenyl)acetate 206

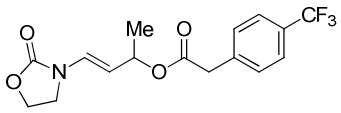

EDCi (0.73 g, 3.81 mmol) in DCM (100 ml), triethylamine (0.53 ml, 3.81 mmol), DMAP (0.03 g, 0.19 mmol), *p*-trifluoromethylphenylacetic acid (0.78 g, 3.81 mmol) and (*E*)-3-(3-hydroxybut-1-enyl)oxazolidin-2-one **145** (0.30 g, 1.91 mmol) in DCM (20 ml) were combined according to general procedure 1 (reaction time: 15 hours). Purification was achieved by reported procedure to afford (*E*)-4-(2-oxooxazolidin-3-yl)but-3-en-2-yl 2-(*p*-(trifluoromethyl)phenyl)acetate **206** as a yellow oil (0.56 g, 86%). FTIR (film/cm^{-1}) υ_{max}: 2984 (w), 1757 (s), 1671 (m), 1619 (w); ^{1}H NMR (500 MHz, $CDCl_3$) δ: 1.34 (d, 3H, *J* = 7.0 Hz), 3.63 (s, 2H), 3.63 (app. t, 2H, *J* = 8.1 Hz), 4.40 (app. t, 2H, *J* = 8.1 Hz), 4.83 (dd, 1H, *J* = 14.4, 7.0 Hz), 5.41 (app. quin, 1 H, *J* = 7.0 Hz), 6.90 (d, 1H, *J* = 14.4 Hz), 7.34 (app. d, 2H, *J* = 8.0 Hz), 7.55 (app. d, 2H, *J* = 8.0 Hz); ^{13}C NMR (125 MHz, $CDCl_3$) δ: 20.6, 41.3, 42.3, 62.2, 70.4, 109.5 124.1 (q, *J* = 273.0 Hz), 125.4 (q, *J* = 3.7 Hz), 127.2, 129.4 (q, *J* = 32.6 Hz), 129.6, 138.0, 155.3, 170.0; HRMS (ESI, +ve) *m/z* calcd. for $C_{16}H_{16}F_3NNaO_4$ 366.0929, found 366.0924 $(M+Na)^+$.

$^{13}C_1$-2-(4-(trifluoromethyl)phenyl)acetic acid ($^{13}C_1$-283)

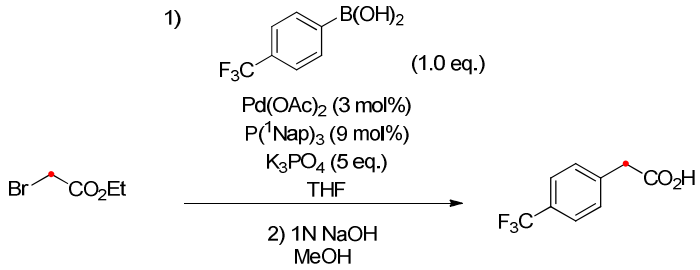

To a degassed solution of $Pd(OAc)_2$ (0.01 g, 0.06 mmol, 3 mol%), $P(^{1}Nap)_3$ (0.07 mg, 0.17 mmol, 9 mol%), and finely ground K_3PO_4 (1.96 g, 9.25 mmol, 5 eq.) in THF (20 ml) was added ^{13}C-ethylbromo acetate (0.31 mg, 1.85 mmol, 1.0 eq.). The reaction mixture was allowed to stir for 5 minutes and then a solution of 4-trifluorophenyl boronic acid (0.35 g, 1.85 mmol, 1.0 eq.) and H_2O (0.07 ml, 3.70 mmol, 2.0 eq.) in THF (10 ml) was added. The reaction mixture was allowed to stir at room temperature over

16 hours and was then quenched by addition to water and extraction with DCM (3 × 20 ml), dried over magnesium sulphate and concentrated *in vacuo* to yield the crude product. The crude ester was subjected to flash column chromatography using ethyl acetate/petroleum ether 40-60° (10:90) and was then saponified by dissolution in 1N NaOH (20 ml) in methanol (20 ml) and allowed to stir at room temperature over 12 hours. The target compound was isolated by extraction of the organics with 5% NaOH (3 × 20 ml), acidifying the aqueous by 6N HCl (30 ml), extracting the organics with DCM (3 × 20 ml), concentration *in vacuo* and subsequent purification by flash column chromatography, using ethyl acetate/petroleum ether 40-60° (10:90) to yield $^{13}C_1$-2-(4-(trifluoromethyl)phenyl)acetic acid **$^{13}C_1$-283** as a white solid (0.10 g, 27 %). M.p. 89–91 °C; FTIR (film/cm^{-1}) υ_{max}: 3018 (m), 2919 (br s), 1694 (s), 1619 (m), 1588 (w); ^{1}H NMR (500 MHz, $CDCl_3$) δ: 3.74 (d, 2H, *J* = 129.9 Hz), 7.39–7.48 (m, 2H), 7.64 (app. d, 2H, *J* = 8.5 Hz), 11.77 (br s, 1H); ^{13}C NMR (125 MHz, $CDCl_3$) δ: 40.8, 124.0 (q, *J* = 266.3 Hz), 125.6 (quin, *J* = 125.6 Hz), 129.8 (q, *J* = 30.8 Hz), 129.8 (d, *J* = 2.9 Hz), 137.1 (d, *J* = 45.2 Hz), 177.4 (d, *J* = 58.3 Hz); HRMS (ESI, +ve) *m/z* calcd. for $C_8{}^{13}C_1H_6O_2F_3$ 204.0398, found 204.0343 $(M-H)^-$.

(*E*)-4-(2-oxooxazolidin-3-yl)but-3-en-2-yl 2-$^{13}C_1$-(4-(trifluoromethyl)phenyl)acetate

$^{13}C_1$-206

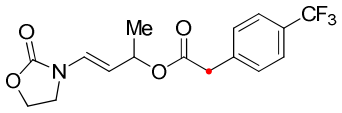

EDCi (0.09 g, 0.49 mmol) in DCM (30 ml), triethylamine (0.07 ml, 0.49 mmol), DMAP (2.44 mg, 0.02 eq.), $^{13}C_1$-2-(4-(trifluoromethyl)phenyl)acetic acid **$^{13}C_1$-283** (0.10 g, 0.49 mmol) and (*E*)-3-(3-hydroxybut-1-enyl)oxazolidin-2-one (0.04 g, 0.24 mmol) in DCM (10 ml) were combined according to general procedure 1 (reaction time: 15 hours). Purification was achieved by reported procedure to afford (*E*)-4-(2-oxooxazolidin-3-yl)but-3-en-2-yl 2-$^{13}C_1$-(4-(trifluoromethyl)phenyl)acetate **$^{13}C_1$-206** as a yellow oil (0.06 g, 81%). FTIR (film/cm^{-1}) υ_{max}: 3096 (m), 2978 (m), 2927 (m), 1702 (s), 1664 (m), 1590 (m), 1561 (m); ^{1}H NMR (500 MHz, $CDCl_3$) δ: 1.37 (d, 3H, *J* = 6.5 Hz), 3.66 (d, 2H, *J* = 130.0 Hz), 3.67 (app. t, 2H, *J* = 8.1 Hz), 4.45 (app. t, 2H, *J* = 8.1 Hz), 4.85 (dd, 1H, *J* = 14.1, 7.1 Hz), 5.44 (app. quin, 1H, *J* = 7.1 Hz), 6.94 (d, 2H, *J* = 14.1 Hz), 7.34–7.45 (m, 2H), 7.59 (app. d, 2H, *J* = 7.6 Hz); ^{13}C NMR (125 MHz, $CDCl_3$) *δ*: 20.6,

41.3, 42.3, 62.2, 70.4, 109.5, 123.1 (q, J = 272.4 Hz), 125.5 (quin, J = 4.3 Hz), 127.2, 129.5 (d, J = 33.3 Hz), 129.7 (d, J = 3.5 Hz), 138.0 (d, J = 46.2 Hz), 155.2, 170.0 (d, J = 58.2 Hz); HRMS (ESI, +ve) *m/z* calcd. for $C_{15}C^{13}H_{16}F_3NO_4$ 343.1031, found 343.1002 $(M-H)^-$.

(*E*)-4-(2-Oxooxazolidin-3-yl)but-3-en-2-yl 2-(*p*-cyanophenyl)acetate 207

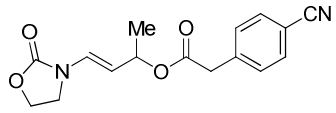

EDCi (0.73 g, 3.81 mmol) in DCM (100 ml), triethylamine (0.53 ml, 3.81 mmol), DMAP (0.03 g, 0.19 mmol), *p*-cyanophenylacetic acid (0.62 g, 3.81 mmol) and (*E*)-3-(3-hydroxybut-1-enyl)oxazolidin-2-one **145** (0.30 g, 1.91 mmol) in DCM (20 ml) were combined according to general procedure 1 (reaction time: 15 hours). Purification was achieved by reported procedure to afford (*E*)-4-(2-oxooxazolidin-3-yl)but-3-en-2-yl 2-(*p*-cyanophenyl)acetate **207** as a yellow oil (0.42 g, 73%). FTIR (film/cm^{-1}) υ_{max}: 2982 (w), 2929 (w), 2230 (s), 1753 (s), 1670 (s), 1610 (w); ^{1}H NMR (500 MHz, $CDCl_3$) δ: 1.33 (d, 3H, J = 6.8 Hz), 3.63 (s, 2H), 3.67 (app. t, 2H, J = 8.1 Hz), 4.42 (app. t, 2H, J = 8.1 Hz), 4.82 (dd, 1H, J = 14.4, 6.8 Hz), 5.40 (app. quin, 1 H, J = 6.8 Hz), 6.89 (d, 1H, J = 14.4 Hz), 7.37 (app. d, 2H, J = 7.9 Hz), 7.59 (app. d, 2H, J = 7.9 Hz); ^{13}C NMR (125 MHz, $CDCl_3$) δ: 20.7, 41.5, 42.3, 62.3, 70.6, 109.4, 111.1, 118.7, 127.3, 130.2, 132.3, 139.4, 155.3, 169.5; HRMS (ESI, +ve) *m/z* calcd. For $C_{16}H_{16}N_2NaO_4$ 323.1008, found 323.1002 $(M+Na)^+$.

(*E*)-4-(2-Oxooxazolidin-3-yl)but-3-en-2-yl 2-(4-(methylsulfonyl)phenyl)acetate 208

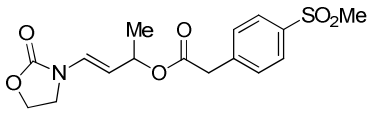

EDCi (0.73 g, 3.81 mmol) in DCM (100 ml), triethylamine (0.53 ml, 3.81 mmol), DMAP (0.03 g, 0.19 mmol), *p*-methane sulfunyl phenyl acetic acid (0.81 g, 3.81 mmol) and (*E*)-3-(3-hydroxybut-1-enyl)oxazolidin-2-one **145** (0.30 g, 1.91 mmol) in DCM (20

ml) were combined according to general procedure 1 (reaction time: 15 hours). Purification was achieved by reported procedure to afford the pure enamido ester substrate, but a further toluene trituration was required to yield (*E*)-4-(2-oxooxazolidin-3-yl)but-3-en-2-yl 2-(4-(methylsulfonyl)phenyl)acetate **208** as a white solid (0.60 g, 83%). M.p. 108–110 °C; FTIR (film/cm^{-1}) υ_{max}: 2983.4 (w), 2928.7 (w), 2931.5 (w), 1756.0 (s), 1670.8 (m), 1600.1 (w). ^{1}H NMR (500 MHz, $CDCl_3$) δ: 1.33 (d, 3H, *J* = 6.6 Hz), 3.02 (s, 3H), 3.62 (s, 2H), 3.62 (app. t, 2H, *J* = 8.2 Hz), 4.41 (app. t, 2H, *J* = 8.2 Hz), 4.81 (dd, 1H, *J* = 14.0, 6.6 Hz), 5.40 (app. quin, 1 H, *J* = 6.6 Hz), 6.86 (d, 1 H, *J* = 14.0 Hz), 7.46 (d, 2 H, *J* = 8.8 Hz), 7.86 (d, 2 H, *J* = 8.8 Hz). ^{13}C NMR (125 MHz, $CDCl_3$) δ: 20.7, 41.4, 42.3, 44.5, 62.3, 70.6, 109.4, 127.2, 127.6, 130.4, 139.3, 140.3, 155.3, 169.6. HRMS (ESI, +ve) *m/z* calcd. for $C_{16}H_{20}NO_6S$ 354.1011, found 354.1025 $(M+H)^+$.

(*E*)-4-(2-Oxooxazolidin-3-yl)but-3-en-2-yl 2-(2,4-dimethoxyphenyl)acetate 209

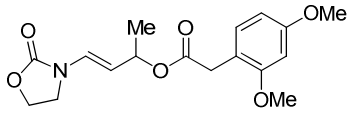

EDCi (0.73 g, 3.81 mmol) in DCM (100 ml), triethylamine (0.53 ml, 3.81 mmol), DMAP (0.03 g, 0.19 mmol), 2,4-dimethoxy phenyl acetic acid (0.74 g, 3.81 mmol) and (*E*)-3-(3-hydroxybut-1-enyl)oxazolidin-2-one **145** (0.30 g, 1.91 mmol) in DCM (20 ml) were combined according to general procedure 1 (reaction time: 15 hours). Purification was achieved by reported procedure to afford (*E*)-4-(2-oxooxazolidin-3-yl)but-3-en-2-yl 2-(2,4-dimethoxyphenyl)acetate **209** as a clear oil (0.50 g, 79%). FTIR (film/cm^{-1}) υ_{max}: 2935.8 (w), 1756.9 (s), 1670.5 (m), 1615.0 (w). ^{1}H NMR (300 MHz, $CDCl_3$) δ: 1.63 (d, 3H, *J* = 6.6 Hz), 3.53 (s, 2H), 3.62 (app. t, 2H, *J* = 8.2 Hz), 3.79 (s, 3H), 3.80 (s 3H), 4.41 (app. t, 2H, *J* = 8.2 Hz), 4.89 (dd, 1H, *J* = 14.3, 6.6 Hz), 5.44 (app. quin, 1 H, *J* = 6.6 Hz), 6.44 (d, 1 H, *J* = 7.9 Hz), 6.46 (s, 1 H), 6.90 (d, 1 H, *J* = 14.3 Hz), 7.07 (d, 1H, *J* = 7.9 Hz). ^{13}C NMR (75 MHz, $CDCl_3$) δ: 21.0, 36.0, 42.8, 55.8, 55.9, 62.6, 69.8, 99.0, 104.5, 110.6, 115.9, 126.9, 131.5, 155.6, 158.8, 160.6, 171.8. HRMS (ESI, +ve) *m/z* calcd. For $C_{17}H_{21}NNaO_6$ 358.1267, found 358.1261 $(M+Na)^+$.

(*E*)-((*E*)-4-(2-Oxooxazolidin-3-yl)but-3-en-2-yl) 4-phenylbut-3-enoate 210

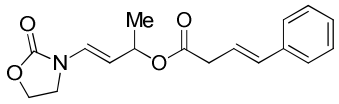

EDCi (0.97 g, 5.06 mmol) in DCM (100 ml), triethylamine (0.70 ml, 5.06 mmol), DMAP (0.03 g, 0.25 mmol), *E*-styryl acetic acid acid (0.82 g, 5.06 mmol) and (*E*)-3-(3-hydroxybut-1-enyl)oxazolidin-2-one **145** (0.40 g, 2.53 mmol) in DCM (20 ml) were combined according to general procedure 1 (reaction time: 15 hours). Purification was achieved by reported procedure to afford (*E*)-((*E*)-4-(2-oxooxazolidin-3-yl)but-3-en-2-yl) 4-phenylbut-3-enoate **210** as a yellow oil (0.76 g, 91%). FTIR (film/cm^{-1}) υ_{max}: 3027.2 (w), 2980.7 (w), 2928.9 (w), 1756.6 (s), 1670.3 (m), 1619.2 (w). ^{1}H NMR (500 MHz, $CDCl_3$) δ: 1.38 (d, 3H, *J* = 6.9 Hz), 3.21 (dd, 2H, *J* = 7.1, 0.9 Hz), 3.65 (app. t, 2H, *J* = 8.1 Hz), 4.40 (app. t, 2H, *J* = 8.1 Hz), 4.88 (dd, 1H, *J* = 14.2, 6.9 Hz), 5.45 (app. quin, 1 H, *J* = 6.9 Hz), 6.28 (dt, 1 H, *J* = 15.5, 7.1 Hz), 6.48 (d, 1 H, *J* = 15.5 Hz), 6.90 (d, 1H, *J* = 14.2 Hz), 7.21 (app. d, 1H, *J* = 7.3 Hz), 7.29 (app. t, 2H, *J* = 7.3 Hz), 7.36 (d, 2H, *J* = 7.3 Hz). ^{13}C NMR (125 MHz, $CDCl_3$) δ: 20.6, 38.7, 42.3, 62.3, 69.9, 109.8, 121.7, 126.3, 127.1, 127.6, 128.5, 133.4, 136.9, 155.3, 170.8. HRMS (ESI, +ve) *m/z* calcd. For $C_{17}H_{19}NNaO_4$ 324.1212, found 324.1206 $(M+Na)^+$.

(*E*)-4-(2-Oxooxazolidin-3-yl)but-3-en-2-yl 2-(1-methyl-1H-indol-3-yl)acetate 211

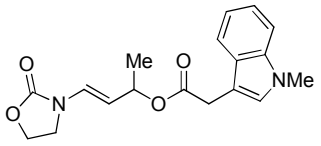

Part 1- Synthesis of methyl 2-(1-methyl-1H-indol-3-yl)acetate

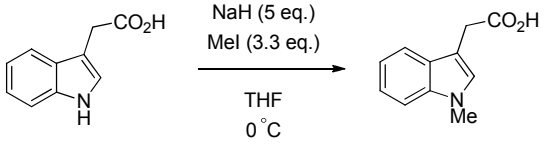

To stirred suspension of NaH (1.39 g, 57.9 mmol, 5 eq.) in THF (100 ml) at 0 °C was added a solution of indole-3-acetic acid (2.00 g, 11.6 mmol, 1 eq.) in THF (50 ml) and the reaction mixture was allowed to stir for 30 mins, before the addition of a solution of iodomethane (2.41 ml, 38.22 mmol, 3.3 eq.) as a solution in THF (50 ml). The reaction mixture was allowed to stir for 15 hours and quenched by the addition of aqueous methanol until a clear yellow solution resulted. The resulting mixture was acidified by the addition of 6N HCl (100 ml), and the organics were extracted by DCM (3 × 100 ml), dried over $MgSO_4$, filtered and concentrated in vacuo to yield methyl 2-(1-methyl-1H-indol-3-yl)acetate as a brown solid (1.65 g, 76 %). M.p. 128–130 °C; FTIR (film/cm^{-1}) υ_{max}: 3433.2 (br s), 1705.3 (s). ^{1}H NMR (500 MHz, $CDCl_3$) δ: 3.77 (s, 3H), 3.81 (d, 2H, *J* = 0.6 Hz), 7.05 (s, 1H), 7.13 (td, 1H, *J* = 7.8, 0.9 Hz), 7.22-7.26 (m, 1H), 7.30 (d, 1H, *J* = 7.8 Hz), 7.59 (d, 1H, *J* = 7.8 Hz), ^{13}C NMR (125 MHz, $CDCl_3$) δ: 31.0, 32.7, 106.1, 109.4, 119.0, 119.3, 121.9, 127.6, 127.9, 136.9, 178.5. HRMS (ESI, +ve) *m/z* calcd. For $C_{11}H_{11}NNaO_2$ 212.0867, found 212.0682 $(M+Na)^+$.

Part 2- EDCi (0.50 g, 2.61 mmol) in DCM (100 ml), triethylamine (0.36 ml, 2.61 mmol), DMAP (0.02 g, 0.13 mmol), methyl 2-(1-methyl-1H-indol-3-yl)acetate (0.50 g, 2.61 mmol) and (*E*)-3-(3-hydroxybut-1-enyl)oxazolidin-2-one **145** (0.20 g, 1.31 mmol) in DCM (20 ml) were combined according to general procedure 1 (reaction time: 15 hours). Purification was achieved by reported procedure to afford (*E*)-4-(2-oxooxazolidin-3-yl)but-3-en-2-yl 2-(1-methyl-1H-indol-3-yl)acetate **211** as an orange

oil (0.42 g, 97%). FTIR (film/cm^{-1}) υ_{max}: 3053.5 (w), 2980.1 (w), 2931.5 (w), 1756.5 (s), 1670.3 (m), 1616.3 (w), 1552.9 (w). ^{1}H NMR (500 MHz, $CDCl_3$) δ: 1.38 (d, 3H, *J* = 6.8 Hz), 3.45 (app. t, 2H, *J* = 8.1 Hz), 3.71 (s, 3H), 3.75 (s, 2H), 4.27 (app. t, 2H, *J* = 8.1 Hz), 4.82 (dd, 1H, *J* = 14.6, 6.8 Hz), 5.46 (app. quin, 1 H, *J* = 6.8 Hz), 6.88 (d, 1 H, *J* = 14.6 Hz), 7.03 (s, 1 H), 7.11 (td, 1H, *J* = 7.8, 1.0 Hz), 7.22 (td, 1H, *J* = 7.8, 1.0 Hz), 7.28 (d, 1H, *J* = 7.8 Hz), 7.60 (d, 1H, *J* = 7.8 Hz). ^{13}C NMR (125 MHz, $CDCl_3$) δ: 20.7, 31.7, 32.7, 42.2, 62.3, 69.8, 106.8, 109.3, 110.0, 119.0, 119.1, 121.7, 126.8, 127.7, 127.9, 136.9, 155.4, 171.4. HRMS (ESI, +ve) *m/z* calcd. For $C_{18}H_{20}N_2NaO_4$ 351.1321, found 351.1315 $(M+Na)^+$.

(*E*)-4-(2-Oxooxazolidin-3-yl)but-3-en-2-yl 2-(benzo[d][1,3]dioxol-5-yl)acetate 212

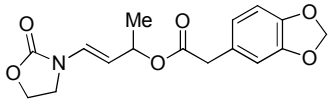

EDCi (0.73 g, 3.81 mmol) in DCM (100 ml), triethylamine (0.53 ml, 3.81 mmol), DMAP (0.03 g, 0.19 mmol), benzodioxole phenyl acetic acid (0.69 g, 3.81 mmol) and (*E*)-3-(3-hydroxybut-1-enyl)oxazolidin-2-one **145** (0.30 g, 1.91 mmol) in DCM (20 ml) were combined according to general procedure 1 (reaction time: 15 hours). Purification was achieved by reported procedure to afford (*E*)-4-(2-oxooxazolidin-3-yl)but-3-en-2-yl 2-(benzo[d][1,3]dioxol-5-yl)acetate **212** as a clear oil (0.52 g, 85%). FTIR (film/cm^{-1}) υ_{max}: 2922.9(m), 1750.9(s) 1670.4(s), 1503.6(s). ^{1}H NMR (250 MHz, $CDCl_3$) δ: 1.34 (d, 3H, *J* = 6.9 Hz), 3.49 (s, 2H), 3.66 (app. t, 2H, *J* = 7.9 Hz), 4.43 (app. t, 2H, *J* = 7.9 Hz), 4.85 (dd, 1H, *J* = 14.4, 6.9), 5.40 (app. quin, 1H, *J* = 6.9 Hz), 5.93 (s, 2H), 6.66–6.78 (m, 3H), 6.90 (d, 1H, *J* = 14.4 Hz). ^{13}C NMR (75 MHz, $CDCl_3$) δ: 21.0, 41.6, 42.7, 62.6, 70.3, 101.4, 108.7, 110.0, 110.1, 122.8, 127.4, 128.0, 147.1, 148.1, 155.7, 171.4. HRMS (ESI, +ve) *m/z* calcd. For $C_{16}H_{17}NNaO_6$ 342.0954, found 342.0948 $(M+Na)^+$.

(*E*)-4-(2-Oxooxazolidin-3-yl)but-3-en-2-yl propionacetate 265

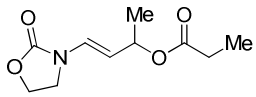

EDCi (0.73 g, 3.81 mmol) in DCM (100 ml), triethylamine (0.53 ml, 3.81 mmol), DMAP (0.03 g, 0.19 mmol), propionic acid (0.28 g, 3.81 mmol) and (*E*)-3-(3-hydroxybut-1-enyl)oxazolidin-2-one **145** (0.30 g, 1.91 mmol) in DCM (20 ml) were combined according to general procedure 1 (reaction time: 15 hours). Purification was achieved by reported procedure to afford (*E*)-4-(2-oxooxazolidin-3-yl)but-3-en-2-yl propionacetate **265** as a white solid (0.38 g, 94%). M.p. 89–91 °C. FTIR (film/cm^{-1}) υ_{max}: 2977 (s), 2956 (s), 2852 (s), 1747 (s), 1726 (s), 1665 (w), 1479 (w); ^{1}H NMR (250 MHz, $CDCl_3$) δ: 1.11 (t, 3H, *J* = 7.6 Hz, C*H*$_3$CH$_2$-), 1.35 (d, 3H, *J* = 6.7 Hz, C*H*$_3$CH-), 2.29 (q, 2H, *J* = 7.6 Hz, CH$_3$C*H*$_2$-), 3.64–3.73 (m, 2H, -N(C*H*$_2$-)CH-), 4.39–4.48 (m, 2H, -OC*H*$_2$-), 4.87 (dd, 1H, *J* = 14.4, 6.7 Hz, -NCHC*H*-), 5.41 (app. quin, 1H, *J* = 6.7 Hz, CH$_3$C*H*(CH-)O-), 6.92 (d, 1H, *J* = 14.4 Hz, -NC*H*CH-); ^{13}C NMR (75 MHz, $CDCl_3$) *δ*: 9.5, 21.1, 28.3, 42.7, 62.6, 69.5, 110.5, 127.1, 155.7, 174.1; HRMS (ESI, +ve) *m/z* calcd. for $C_1H_{15}NNaO_4$ 236.0898, found 236.0893 $(M+Na)^+$.

α,α-^{2}H$_2$-Propionic acid 1-methyl-3-(2-oxo-oxazolidin-3-yl)-allyl ester ^{2}H$_2$-265

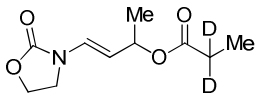

EDCi (0.60 g, 3.82 mmol) in CD_2Cl_2 (100 ml), triethylamine (0.53 ml, 3.82 mmol), DMAP (0.05 g, 0.19 mmol), α,α-d^2-propionic acid (0.28 g, 3.82 mmol) and (*E*)-3-(3-hydroxybut-1-enyl)oxazolidin-2-one (0.30 g, 1.91 mmol) **145** in CD_2Cl_2 (20 ml) were combined according to general procedure 1 (reaction time: 15 hours). Purification was achieved by reported procedure, with solutions of citric acid (10%) and sat. sodium bicarbonate made as solutions in D_2O, to afford α,α-d^2-propionic acid 1-methyl-3-(2-oxo-oxazolidin-3-yl)-allyl ester **^{2}H$_2$-265** as a cream solid (0.29 g, 71%). M.p. 89–92 °C; FTIR (film/cm^{-1}) υ_{max}: 2990 (m), 2975 (m), 2937 (m), 1743 (s), 1721 (s), 1662 (s), 1475 (s); ^{1}H NMR (250 MHz, $CDCl_3$) δ: 1.04 (s, 3H), 1.29 (d, 3H, *J* = 6.7 Hz), 3.64 (app. t,

2H, *J* = 8.2 Hz), 4.39 (app. t, 3H, *J* = 8.2 Hz), 4.82 (dd, 1H, *J* = 14.4, 6.7 Hz), 5.35 (app. pent, 1H, *J* = 6.7 Hz), 6.85 (d, 1H, *J* = 6.7 Hz); ^{13}C NMR (100 MHz, $CDCl_3$) *δ*: 8.8, 20.7, 27.2 (quin, *J* = 19.8 Hz), 42.3, 62.3, 69.1, 110.1, 126.7, 155.3, 173.6; HRMS (ESI, +ve) *m/z* calcd. for $C_{10}H_{13}D_2NNaO_4$ 238.1022, found 238.1020 $(M+Na)^+$.

6.3.2. *N*-Oxazolidinone Rearrangement Products

<u>*anti*-2-Methyl-3-(2-oxo-oxazolidin-3-yl)-hex-4-enoic acid methyl ester</u> 139

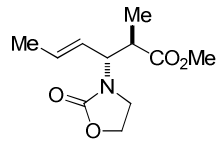

LiHMDS (0.61 ml, 0.61 mmol), TMSCl (0.08 ml, 0.61 mmol) and (*E)*-4-(2-oxooxazolidin-3-yl)but-3-en-2-yl propionacetate **256** (0.10 g, 0.46 mmol) in THF (1 ml) were combined according to general procedure 2 (reaction time : 75 minutes). Treatment with diazomethane and purification by flash chromatography afforded *anti*-2-methyl-3-(2-oxo-oxazolidin-3-yl)-hex-4-enoic acid methyl ester **139** as a white solid (0.06 g, 60%, d.r. 2:1). M.p. 89–90 °C; FTIR (film/cm^{-1}) υ_{max}: 2922 (s), 1754 (s), 1726 (s) 1658 (m), 1572 (m); ^{1}H NMR (250 MHz, $CDCl_3$) *anti* δ: 1.12 (d, 3H, *J* = 7.0 Hz), 1.65–1.75 (m, 3H), 2.74–2.93 (m, 1H), 3.36–3.63 (m, 2H), 3.66 (s, 3H), 4.15–4.38 (m, 3H), 5.34–5.54 (m, 1H), 5.64–5.86 (m, 1H, *J* = 15.3 Hz); *syn* δ: 1.16 (d, 3H, *J* = 7.0 Hz), 1.65–1.75 (m, 3H), 2.74–2.93 (m, 1H), 3.36–3.63 (m, 2H), 3.64 (s, 3H), 4.15–4.38 (m, 3H), 5.34–5.54 (m, 1H), 5.64–5.86 (m, 1H, *J* = 15.3 Hz); ^{13}C NMR (62 MHz, $CDCl_3$) *anti δ*: 14.7, 17.9, 41.9, 42.5, 51.9, 59.1, 62.2, 124.9, 131.6, 158.1, 174.8; *syn δ*: 14.2, 14.8, 41.4, 42.3, 51.8, 58.1, 62.1, 125.0, 132.4, 157.6, 174.5. HRMS (ESI, +ve) *m/z* calcd. For $C_{11}H_{17}NNaO_4$ 250.1055, found 250.1065 $(M+Na)^+$.

(*anti-E*)-Methyl 3-(2-oxooxazolidin-3-yl)-2-phenylhex-4-enoate 144

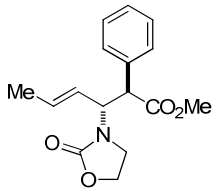

LiHMDS (0.47 ml, 0.47 mmol), TMSCl (0.06 ml, 0.47 mmol) and *(E)*-4-(2-oxooxazolidin-3-yl)but-3-en-2-yl phenylacetate **154** (0.10 g, 0.36 mmol) in THF (1 ml) were combined according to general procedure 2 (reaction time : 75 minutes). Treatment with diazomethane and purification by flash chromatography afforded (*anti-E*)-methyl 3-(2-oxooxazolidin-3-yl)-2-phenylhex-4-enoate **144** as a white solid (0.08 g, 72%, d.r. 44:1). M.p. 98–99 °C; FTIR (film/cm^{-1}) υ_{max}: 3062 (m), 3031 (m), 2952 (m), 2918 (m), 1738 (s); ^{1}H NMR (500 MHz, $CDCl_3$) δ: 1.49 (dd, 3H, J = 6.5, 1.3 Hz, CH_3CHCH-), 3.55–3.64 (m, 2H, -N(CH)CH_2-), 3.65 (s, 3H, -CO_2CH_3), 4.14 (d, 1H, J = 11.4 Hz, -C$H$$CO_2CH_3$), 4.24–4.33 (m, 2H, -OC$H_2$-), 4.69 (dd, 1H, J = 11.4, 7.9 Hz, -CHCH(C_6H_5)CO_2CH_3), 5.29 (ddq, 1H, J = 15.3, 7.9, 1.3 Hz, CH_3CHCH-), 5.42 (dqd, 1H, J = 15.3, 6.5, 0.7 Hz, CH_3CHCH-), 7.23–7.34 (m, 5H, C_6H_5-); ^{13}C NMR (125 MHz, $CDCl_3$) δ: 17.7, 42.7, 52.3, 54.3, 58.7, 62.6, 124.3, 127.9, 128.7, 128.9, 131.5, 135.1, 157.6, 172.4; HRMS (ESI, +ve) *m/z* calcd. For $C_{16}H_{20}NO_4$, 290.1392, found 290.1385 $(M+H)^+$.

(*anti-E*)-methyl 3-(2- d^{2-}oxooxazolidin-3-yl)-2-phenylhex-4- d^4d^5-enoate $^2H_3$-144

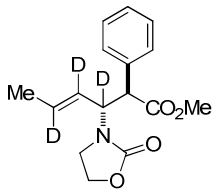

To an oven dried Young's tap NMR tube, inserted into a Dewar at -95 °C and under an atmosphere of nitrogen, was added a solution of LiHMDS (1 M in THF, 0.24 ml, 0.23 mmol, 1.3 eq.), and TMSCl (0.03 ml, 0.23 mmol, 1.3 eq.). Thermal equilibration was allowed (5 minutes) and then a solution of phenyl-acetic acid d^1-d^2-d^3-1-methyl-3-(2-oxo-oxazolidin-3-yl)-allyl ester **$^2H_3$-154** (0.05 g, 0.18 mmol, 1 eq.) in THF (0.5 ml) was

added. The cooled NMR tube was rapidly lowered into the pre-cooled NMR machine at -95 °C. From this point ^{1}H and ^{13}C NMR spectroscopy were recorded utilising solvent suppression techniques, and the sample was subsequently warmed to -50 °C and 25 °C allowing the sample to equilibrate for five minutes before recording data. After *in-situ* reaction monitoring the reaction mixture was quenched following general procedure 2 and treatment with diazomethane and purification by flash column chromatography afforded (*anti-E*)-methyl 3-(2- d^{2}-oxooxazolidin-3-yl)-2-phenylhex-4- $d^{4}d^{5}$-enoate **$^{2}H_3$-144** as an amorphous yellow solid (0.03 g, 59%, d.r. 51:1). FTIR (film/cm^{-1}) υ_{max}: 3015 (m), 3001 (m), 2955 (m), 2919 (m), 1748 (s), 1519 (m); ^{1}H NMR (500 MHz, $CDCl_3$) δ: 1.51 (s, 3H), 3.57–3.67 (m, 2H), 3.68 (s, 3H), 4.16 (s, 1H), 4.26–4.36 (m, 2H), 7.25–7.37 (5H, m); ^{13}C NMR (125 MHz, $CDCl_3$) δ: 17.6, 42.6, 52.3, 54.2, 58.3 (t, J = 20.6 Hz), 62.3, 123.8 (t, J = 23.5 Hz), 127.9, 128.7, 128.9, 131.1 (t, J = 23.5 Hz), 135.1, 157.5, 172.3 HRMS (ESI, +ve) *m/z* calcd. for $C_{16}H_{17}D_3NO_4$ 293.1581, found 293.1582$(M+H)^{+}$.

$^{13}C_2$-(*anti-E*)-Methyl 3-(2-oxooxazolidin-3-yl)-2-phenylhex-4-enoate $^{13}C_2$-144

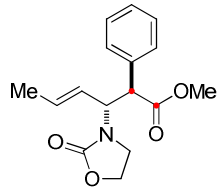

To an oven dried Young's tap NMR tube, inserted into a Dewar at -95 °C and under an atmosphere of nitrogen, was added a solution of LiHMDS (1 M in THF, n eq.), and TMSCl (m eq.). Thermal equilibration was allowed (5 minutes) and then a solution of $^{13}C_2$-*(E)*-4-(2-oxooxazolidin-3-yl)but-3-en-2-yl phenylacetate **$^{13}C_2$-154** (0.05 g, 0.17 mmol, 1 eq.) in THF (0.5 ml) was added. The cooled NMR tube was rapidly lowered into the pre-cooled NMR machine at -95 °C. From this point ^{13}C NMR spectroscopy was recorded at -95 °C and then the machine was allowed to warm to -65 °C, where it was then kept for the rest of the experiment (ca. 12 hours) and ^{13}C data was recorded every 5 minutes. After *in-situ* reaction monitoring the reaction mixture was quenched following general procedure 2 and treatment with diazomethane and purification by flash chromatography afforded $^{13}C_2$-(*anti-E*)-methyl 3-(2-oxooxazolidin-3-yl)-2-phenylhex-4-enoate **$^{13}C_2$-144** as a white solid.

Entry	LiHMDS (n eq.)	TMSCl (m eq.)	Yield $^{13}C_2$-144 (%)	d.r. (*anti:syn*)
1	1.3	1.3	50	39:1
2	1.7	1.7	56	38:1
3	1.3	6	65	56:1
4	5.2	5.2	33	32:1

Table 24. In-Situ EICR of ***$^{13}C_2$-154****.*

M.p. 98–100 °C; FTIR (film/cm^{-1}) υ_{max}: 3031 (m), 2951 (m), 2920 (m), 1739 (s), 1669 (s), 1482 (m); ^{1}H NMR (500 MHz, $CDCl_3$) δ: 1.52 (d, 3H, *J* = 6.3 Hz), 3.58–3.67 (m, 2H), 3.68 (s, 3H, *J* = 3.9 Hz), 4.03 (dd, 1H, *J* = 11.5, 7.1 Hz), 4.25–4.36 (m, 2H), 4.67–4.75 (m, 1H), 5.31 (dd, 1H, *J* = 15.2, 7.8 Hz), 5.49 (dq, 1H, *J* = 15.2, 6.3 Hz), 7.25–7.38 (m, 5H); ^{13}C NMR (125 MHz, $CDCl_3$) δ: 17.7, 42.6, 52.3, 54.3 (d, *J* = 61.7 Hz), 58.7 (d, *J* = 46.1 Hz), 62.2, 124.3 (d, *J* = 5.4 Hz), 127.8, 128.6 (d, *J* = 5.4 Hz), 128.9, 131.4 (d, *J* = 2.8 Hz), 135.1 (d, *J* = 38.9 Hz), 157.5, 172.3 (d, *J* = 61.7 Hz); HRMS (ESI, +ve) *m/z* calcd. for $C_{14}C^{13}{}_2H_{19}NNaO_4$, 314.1368, found 314.1400 $(M+Na)^+$.

(*anti-E*)-Methyl 2-(*o*-methoxyphenyl)-3-(2-oxooxazolidin-3-yl)hex-4-enoate 172

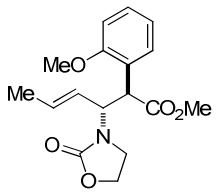

LiHMDS (0.43 ml, 0.43 mmol), TMSCl (0.06 ml, 0.43 mmol) and (*E*)-4-(2-oxooxazolidin-3-yl)but-3-en-2-yl 2-(*o*-methoxyphenyl)acetate **163** (0.10 g, 0.33 mmol) in THF (1 ml) were combined according to general procedure 2 (reaction time : 75 minutes). Treatment with diazomethane and purification by flash chromatography afforded (*anti-E*)-methyl 2-(*o*-methoxyphenyl)-3-(2-oxooxazolidin-3-yl)hex-4-enoate **172** as a white solid (0.08 g, 79%, d.r. 22:1). M.p. 95–96 °C; FTIR (film/cm^{-1}) υ_{max}: 2919 (m), 1747 (s), 1600 (w), 1495 (m); ^{1}H NMR (250 MHz, $CDCl_3$) δ: 1.50 (dd, 3H, *J*

= 6.3, 1.2 Hz), 3.60–3.68 (m, 2H), 3.64 (s, 3H), 3.83 (s, 3H), 4.21–4.37 (m, 2H), 4.67 (d, 1H, *J* = 11.0 Hz), 4.78 (dd, 1H, *J* = 11.0, 7.3 Hz), 5.30 (ddq, 1H, *J* = 15.3, 7.3, 1.2 Hz), 5.50 (dq, 1H, *J* = 15.3, 7.3 Hz), 6.85 (dd, 1H, *J* = 7.8, 1.0 Hz), 6.93 (td, 1H, *J* = 7.8, 1.0 Hz), 7.24 (td, 1H, *J* = 8.2, 1.6 Hz), 7.42 (dd, 1H, *J* = 7.8, 1.6 Hz). ^{13}C NMR (75 MHz, $CDCl_3$) δ: 17.7, 42.2, 45.7, 52.2, 55.6, 57.9, 62.2, 110.7, 120.8, 123.8, 124.8, 128.8, 129.3, 130.8, 157.1, 157.6, 172.5; HRMS (ESI, +ve) *m/z* calcd. For $C_{17}H_{22}NO_5$, 320.1498, found 320.1490 $(M+H)^+$.

(*anti-E*)-Methyl 2-(*m*-methoxyphenyl)-3-(2-oxooxazolidin-3-yl)hex-4-enoate 173

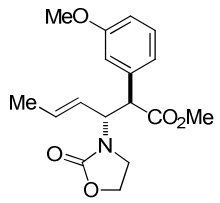

LiHMDS (0.43 ml, 0.43 mmol), TMSCl (0.06 ml, 0.43 mmol) and (*E*)-4-(2-oxooxazolidin-3-yl)but-3-en-2-yl 2-(*m*-methoxyphenyl)acetate **164** (0.10 g, 0.33 mmol) in THF (1 ml) were combined according to general procedure 2 (reaction time : 75 minutes). Treatment with diazomethane and purification by flash chromatography afforded (*anti-E*)-methyl 2-(*m*-methoxyphenyl)-3-(2-oxooxazolidin-3-yl)hex-4-enoate **173** as a white solid (0.08 g, 73%, d.r. 19:1). M.p. 98–99 °C; FTIR (film/cm^{-1}) υ_{max}: 2922 (m), 1746 (s), 1600 (m); ^{1}H NMR (300 MHz, $CDCl_3$) δ: 1.52 (dd, 3H, *J* = 6.4, 1.2 Hz), 3.61 (td, 2H, *J* = 7.9, 2.1 Hz), 3.67 (s, 3H), 3.80 (s, 3H), 4.12 (d, 1H, *J* = 11.4 Hz) 4.30 (td, 2H, *J* = 7.9, 2.1 Hz), 4.68 (dd, 1H, *J* = 11.4, 7.7 Hz), 5.31 (ddq, 1H, *J* = 15.3, 7.7, 1.2 Hz), 5.50 (dqd, 1H, *J* = 15.3, 6.4, 0.7 Hz), 6.81 (dd, 1H, *J* = 8.1, 2.4 Hz), 6.87–6.91 (m, 1H), 6.91–6.94 (m, 1H), 7.22 (t, 1H, *J* = 8.1 Hz); ^{13}C NMR (75 MHz, $CDCl_3$) δ: 16.7, 41.7, 51.3, 53.2, 54.3, 57.6, 61.2, 112.4, 113.5, 120.3, 123.2, 128.6, 130.3, 135.5, 156.5, 158.7, 171.3; HRMS (ESI, +ve) *m/z* calcd. for $C_{17}H_{21}NNaO_5$, 342.1317, found 342.1304 $(M+Na)^+$.

(*anti-E*)-Methyl 2-(*p*-methoxyphenyl)-3-(2-oxooxazolidin-3-yl)hex-4-enoate 174

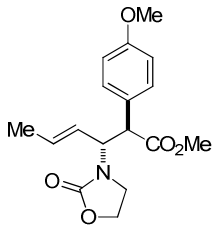

LiHMDS (0.43 ml, 0.43 mmol), TMSCl (0.06 ml, 0.43 mmol) and (*E*)-4-(2-oxooxazolidin-3-yl)but-3-en-2-yl 2-(*p*-methoxyphenyl)acetate **165** (0.10 g, 0.33 mmol) in THF (1 ml) were combined according to general procedure 2 (reaction time : 75 minutes). Treatment with diazomethane and purification by flash chromatography afforded (*anti-E*)-methyl 2-(*p*-methoxyphenyl)-3-(2-oxooxazolidin-3-yl)hex-4-enoate **174** as a white solid (0.08 g, 77%, d.r. 24:1). M.p. 101–103 °C; FTIR (film/cm^{-1}) υ_{max}: 2922 (m), 1747 (s), 1611 (w), 1514 (m); ^{1}H NMR (300 MHz, $CDCl_3$) δ: 1.52 (dd, 3H, *J* = 6.4, 1.1 Hz), 3.53–3.66 (m, 2H), 3.66 (s, 3H), 3.79 (s, 3H), 4.08 (d, 1H, *J* = 11.5 Hz) 4.23–4.36 (m, 2H), 4.67 (dd, 1H, *J* = 11.5, 7.7 Hz), 5.23 (ddq, 1H, *J* = 15.4, 7.7, 1.1 Hz), 5.49 (dqd, 1H, *J* = 15.4, 6.4, 0.7 Hz), 6.84 (app. d, 2H, *J* = 8.8 Hz), 7.25 (app. d, 2H, *J* = 8.8 Hz); ^{13}C NMR (75 MHz, $CDCl_3$) *δ:* 18.2, 42.9, 52.7, 53.9, 55.6, 59.1, 62.7, 114.4, 124.8, 127.5, 130.4, 131.8, 157.9, 159.6, 173.0; HRMS (ESI, +ve) *m/z* calcd. for $C_{17}H_{21}NNaO_5$, 342.1317, found 342.1321 $(M+Na)^+$.

$^{13}C_1$-(*anti-E*)-Methyl 2-(4-methoxyphenyl)-3-(2-oxooxazolidin-3-yl)hex-4-enoate $^{13}C_1$-174

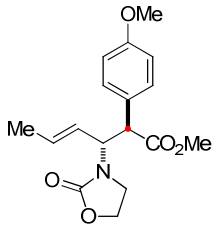

To an oven dried Young's tap NMR tube, inserted into a Dewar at -95 °C and under an atmosphere of nitrogen, was added a solution of LiHMDS (1 M in THF, 0.21 ml, 0.21 mmol, 1.3 eq.), and TMSCl (0.03 ml, 0.21 mmol, 1.3 eq.). Thermal equilibration was allowed (5 minutes) and then a solution of (*E*)-4-(2-Oxooxazolidin-3-yl)but-3-en-2-yl 2-

$^{13}C_1$-(4-methoxyphenyl)acetate **$^{13}C_1$-165** (0.05 g, 0.16 mmol, 1.0 eq.) in THF (0.5 ml) was added. The cooled NMR tube was rapidly lowered into the pre-cooled NMR machine at -95 °C. From this point ^{13}C NMR spectroscopy was recorded at -95 °C and then the machine was allowed to warm to -65 °C, where it was then kept for the rest of the experiment (ca. 12 hours) and ^{13}C data was recorded every 5 minutes. After in-situ reaction monitoring the reaction mixture was quenched following general procedure 2 and treatment with diazomethane and purification by flash chromatography to afford $^{13}C_1$-(*anti-E*)-methyl 2-(4-methoxyphenyl)-3-(2-oxooxazolidin-3-yl)hex-4-enoate **$^{13}C_1$-174** as a white solid (0.03 g, 52%, d.r. 25:1). M.p. 103–104 °C; FTIR (film/cm^{-1}) υ_{max}: 3012 (m), 2985 (m), 2937 (m), 1710 (s), 1671 (m), 1596 (m), 1566 (m); ^1H NMR (500 MHz, $CDCl_3$) δ: 1.53 (d, 3H, *J* = 6.5 Hz), 3.56–3.65 (m, 2H), 3.67 (s, 3H), 3.80 (s, 3H), 4.10 (dd, 1H, *J* = 132.9, 11.3 Hz) 4.26–4.36 (m, 2H), 4.64–4.73 (m, 1H), 5.30 (app. dd, 1H, *J* = 15.1, 8.2 Hz), 5.50 (app. dq, 1H, *J* = 15.1, 6.5 Hz), 6.86 (app. d, 2H, *J* = 8.8 Hz), 7.24 (m, 2H); ^{13}C NMR (125 MHz, $CDCl_3$) δ: 17.8, 42.6, 52.3, 53.5, 55.2, 58.7 (d, *J* = 24.9 Hz), 62.2, 114.0 (d, *J* = 2.6 Hz), 124.4, 127.1 (d, *J* = 30.0 Hz), 130.0 (d, *J* = 1.7 Hz), 131.4 (d, *J* = 2.6 Hz), 157.6, 159.2, 172.6 (d, *J* = 39.5 Hz); HRMS (ESI, +ve) *m/z* calcd. for $C_{16}{}^{13}C_1H_{21}NNaO_5$, 343.1395, found 343.1377 $(M+Na)^+$.

(*anti-E*)-Methyl 3-(2-oxooxazolidin-3-yl)-2-*o*-tolylhex-4-enoate 175

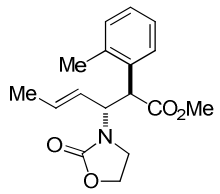

LiHMDS (0.45 ml, 0.45 mmol), TMSCl (0.06 ml, 0.45 mmol) and (*E*)-4-(2-oxooxazolidin-3-yl)but-3-en-2-yl 2-*o*-tolylacetate **166** (0.10 g, 0.35 mmol) in THF (1 ml) were combined according to general procedure 2 (reaction time : 75 minutes). Treatment with diazomethane and purification by flash chromatography afforded (*anti-E*)-methyl 3-(2-oxooxazolidin-3-yl)-2-*o*-tolylhex-4-enoate **175** as a white solid (0.08 g, 71%, d.r. 19:1). M.p. 100–102 °C; FTIR (film/cm^{-1}) υ_{max}: 2923 (w), 1745 (s), 1484 (m); ^1H NMR (250 MHz, $CDCl_3$) δ: 1.48 (d, 3H, *J* = 5.7 Hz), 2.40 (s, 3H), 3.60–3.71 (m, 2H), 3.63 (s, 3H), 4.30 (app. t, 2H, *J* = 7.88 Hz), 4.55–4.69 (m, 2H), 5.30 (dd, 1H, *J*

= 15.7, 5.7 Hz), 5.41 (dq, 1H, *J* = 15.7, 5.7 Hz), 7.12–7.21 (m, 3H), 7.34–7.40 (m, 1H); ^{13}C NMR (75 MHz, $CDCl_3$) δ: 16.7, 19.1, 42.4, 47.6, 51.2, 58.3, 61.2, 122.9, 125.3, 126.4, 126.5, 129.5, 130.0, 132.8, 136.0, 156.6, 171.8. HRMS (ESI, +ve) *m/z* calcd. for $C_{17}H_{22}NO_4$, 304.1549, found 304.1546 $(M+H)^+$.

(*anti-E*)-Methyl 3-(2-oxooxazolidin-3-yl)-2-*m*-tolylhex-4-enoate 176

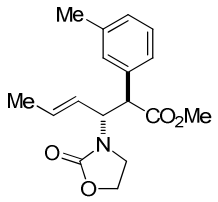

LiHMDS (0.45 ml, 0.45 mmol), TMSCl (0.06 ml, 0.45 mmol) and (*E*)-4-(2-oxooxazolidin-3-yl)but-3-en-2-yl 2-*m*-tolylacetate **167** (0.10 g, 0.35 mmol) in THF (1 ml) were combined according to general procedure 2 (reaction time : 75 minutes). Treatment with diazomethane and purification by flash chromatography afforded (*anti-E*)-methyl 3-(2-oxooxazolidin-3-yl)-2-*m*-tolylhex-4-enoate **176** as an off white solid (0.08 g, 74%, d.r. 43:1). M.p. 95–97 °C; FTIR (film/cm^{-1}) υ_{max}: 2919 (m), 1746 (s), 1607 (m), 1484 (m); ^{1}H NMR (300 MHz, $CDCl_3$) δ: 1.51 (d, 3H, *J* = 6.4 Hz), 2.33 (s, 3H), 3.60 (td, 2H, *J* = 8.0, 3.4 Hz), 3.66 (s, 3H), 4.09 (d, 1H, *J* = 11.4 Hz), 4.22–4.37 (m, 2H), 4.71 (dd, 1H, *J* = 11.4, 7.5 Hz), 5.28 (ddq, 1H, *J* = 15.4, 7.5, 1.5 Hz), 5.48 (dq, 1H, *J* = 15.4, 6.4 Hz), 7.04–7.23 (m, 4H); ^{13}C NMR (75 MHz, $CDCl_3$) δ: 16.7, 20.4, 41.5, 51.3, 53.2, 57.4, 61.2, 123.3, 124.9, 127.5, 127.6, 128.5, 130.2, 133.9, 137.4, 156.6, 171.4; HRMS (ESI, +ve) *m/z* calcd. for $C_{17}H_{22}NO_4$, 304.1549, found 304.1537 $(M+H)^+$.

(*anti-E*)-Methyl 3-(2-oxooxazolidin-3-yl)-2-*p*-tolylhex-4-enoate 177

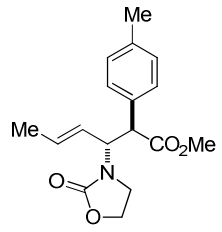

LiHMDS (0.45 ml, 0.45 mmol), TMSCl (0.06 ml, 0.45 mmol) and (*E*)-4-(2-oxooxazolidin-3-yl)but-3-en-2-yl 2-*p*-tolylacetate **168** (0.10 g, 0.35 mmol) in THF (1 ml) were combined according to general procedure 2 (reaction time : 75 minutes). Treatment with diazomethane and purification by flash chromatography afforded (*anti-E*)-methyl 3-(2-oxooxazolidin-3-yl)-2-*p*-tolylhex-4-enoate **177** as a white solid (0.07 g, 70%, d.r. 54:1). M.p. 101–102 °C; FTIR (film/cm^{-1}) υ_{max}: 2920 (m), 1746 (s), 1666 (m), 1612 (m), 1514 (m), 1483 (m); ^{1}H NMR (300 MHz, $CDCl_3$) δ: 1.52 (d, 3H, *J* = 6.2 Hz), 2.32 (s, 3H), 3.60 (td, 2H, *J* = 8.2, 2.0 Hz), 3.65 (s, 3H), 4.09 (d, 1H, *J* = 11.4 Hz), 4.21–4.37 (m, 2H), 4.70 (dd, 1H, *J* = 11.4, 7.7 Hz), 5.29 (ddq, 1H, *J* = 15.3, 7.7, 1.4 Hz), 5.50 (dq, 1H, *J* = 15.3, 6.2 Hz), 7.12 (app. d, 2H, *J* = 7.9 Hz), 7.22 (app. d, 2H, *J* = 7.9 Hz); ^{13}C NMR (75 MHz, $CDCl_3$) *δ*: 18.2, 21.5, 42.9, 52.7, 54.4, 58.9, 62.6, 124.8, 129.2, 129.8, 131.7, 132.4, 138.0, 157.9, 172.9; HRMS (ESI, +ve) *m/z* calcd. for $C_{17}H_{22}NO_4$, 304.1549, found 304.1538 $(M+H)^+$.

(*anti-E*)-Methyl 2-(*o*-nitrophenyl)-3-(2-oxooxazolidin-3-yl)hex-4-enoate *anti*-178

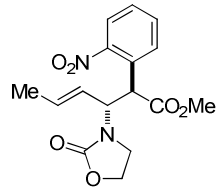

LiHMDS (0.41 ml, 0.41 mmol), TMSCl (0.05 ml, 0.41 mmol) and (*E*)-4-(2-oxooxazolidin-3-yl)but-3-en-2-yl 2-(*o*-nitrophenyl)acetate **169** (0.10 g, 0.32 mmol) in THF (1 ml) were combined according to general procedure 2 (reaction time : 75 minutes). Treatment with diazomethane and purification by flash chromatography afforded (*anti-E*)-methyl 2-(*o*-nitrophenyl)-3-(2-oxooxazolidin-3-yl)hex-4-enoate **178**

as a yellow solid (0.06 g, 60%). M.p. 134–135 °C; FTIR (film/cm^{-1}) υ_{max}: 2955 (m), 2918 (m), 1748 (s), 1529 (m); ^{1}H NMR (500 MHz, $CDCl_3$) δ: 1.45 (dd, 3H, *J* = 6.6, 1.4 Hz), 3.66–3.70 (m, 2H), 3.67 (s, 3H), 4.25–4.40 (m, 2H), 4.78 (d, 1H, *J* = 10.4 Hz), 4.84 (dd, 1H, *J* = 10.4, 8.4 Hz), 5.29 (ddq, 1H, *J* = 15.4, 8.4, 1.4 Hz), 5.48 (dq, 1H, *J* = 15.4, 6.6 Hz), 7.42 (td, 1H, *J* = 8.0, 1.1 Hz), 7.59 (td, 1H, *J* = 8.0, 1.1 Hz), 7.74 (dd, 1H, *J* = 8.0, 1.1 Hz), 7.85 (dd, 1H, *J* = 8.0, 1.1 Hz); ^{13}C NMR (125 MHz, $CDCl_3$) *δ:* 17.7, 42.0, 47.9, 52.6, 58.6, 62.3, 124.0, 124.6, 128.7, 129.9, 131.5, 132.5, 133.1, 149.7, 157.6, 170.8; HRMS (ESI, +ve) *m/z* calcd. for $C_{16}H_{18}N_2NaO_6$, 357.1063, found 357.1071 $(M+Na)^+$.

(*syn*-*E*)-Methyl 2-(*o*-nitrophenyl)-3-(2-oxooxazolidin-3-yl)hex-4-enoate *syn*-178

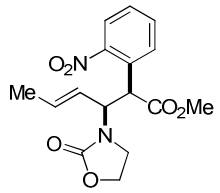

LiHMDS (0.41 ml, 0.41 mmol), TMSCl (0.05 ml, 0.41 mmol) and (*E*)-4-(2-oxooxazolidin-3-yl)but-3-en-2-yl 2-(*o*-nitrophenyl)acetate **169** (0.10 g, 0.32 mmol) in THF (1 ml) were combined according to general procedure 2 (reaction time : 75 minutes). Treatment with diazomethane and purification by flash chromatography afforded (*syn*-*E*)-methyl 2-(*o*-nitrophenyl)-3-(2-oxooxazolidin-3-yl)hex-4-enoate **178** as a yellow solid (0.01 g, 12%). M.p. 133–134 °C; FTIR (film/cm^{-1}) υ_{max}: 2954 (m), 2918 (m), 1747 (s), 1529 (s); ^{1}H NMR (500 MHz, $CDCl_3$) δ: 1.74 (d, 3H, *J* = 6.4 Hz), 3.34 (dt, 1H, *J* = 8.8, 5.0 Hz), 3.47 (q, 1H, *J* = 8.9 Hz), 3.64 (s, 3H), 3.94 (q, 1H, *J* = 8.9 Hz), 4.17 (dt, 1H, *J* = 8.8, 5.0 Hz), 4.66 (d, 1H, *J* = 11.4 Hz), 5.17 (dd, 1H, *J* = 11.4, 7.8 Hz), 5.53 (ddq, 1H, *J* = 15.4, 7.8, 1.2 Hz), 5.90 (dq, 1H, *J* = 15.4, 6.4 Hz), 7.43 (t, 1H, *J* = 7.8 Hz), 7.62 (t, 1H, *J* = 7.8 Hz), 7.76 (d, 1H, *J* = 7.8 Hz), 7.87 (d, 1H, *J* = 7.8 Hz); ^{13}C NMR (125 MHz, $CDCl_3$) *δ:* 17.9, 40.6, 47.5, 52.6, 56.4, 62.1, 124.2, 124.6, 128.5, 128.9, 130.6, 132.5, 133.0, 150.5, 157.7, 170.5; HRMS (ESI, +ve) *m/z* calcd. For $C_{16}H_{18}N_2NaO_6$, 357.1063, found 357.1069 $(M+Na)^+$.

(*anti-E*)-Methyl 2-(*m*-nitrophenyl)-3-(2-oxooxazolidin-3-yl)hex-4-enoate 179

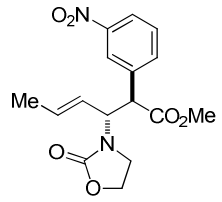

LiHMDS (0.41 ml, 0.41 mmol), TMSCl (0.05 ml, 0.41 mmol) and (*E*)-4-(2-oxooxazolidin-3-yl)but-3-en-2-yl 2-(*m*-nitrophenyl)acetate **170** (0.10 g, 0.32 mmol) in THF (1 ml) were combined according to general procedure 2 (reaction time : 75 minutes). Treatment with diazomethane and purification by flash chromatography afforded (*anti-E*)-methyl 2-(*m*-nitrophenyl)-3-(2-oxooxazolidin-3-yl)hex-4-enoate **179** as an orange solid (0.08 g, 75%, d.r. 16:1). M.p. 97–99 °C; FTIR (film/cm^{-1}) υ_{max}: 2953 (m), 1746 (s), 1531 (s), 1482 (w); ^{1}H NMR (500 MHz, $CDCl_3$) δ: 1.50 (dd, 3H, *J* = 6.4, 1.4 Hz), 3.60–3.68 (m, 2H), 3.70 (s, 3H), 4.30–4.35 (m, 2H), 4.35 (d, 1H, *J* = 11.3 Hz), 4.64 (dd, 1H, *J* = 11.3, 8.6 Hz), 5.34 (ddq, 1H, *J* = 15.4, 8.7, 1.4 Hz), 5.50 (dqd, 1H, *J* = 15.4, 6.4, 0.6 Hz), 7.51 (t, 1H, *J* = 7.8 Hz), 7.71 (d, 1H, *J* = 7.8, 1.2 Hz), 8.14 (d, 1H, *J* = 7.8 Hz), 8.20 (s, 1H); ^{13}C NMR (75 MHz, $CDCl_3$) *δ:* 18.1, 43.4, 53.1, 54.1, 59.6, 62.8, 123.4, 124.2, 124.3, 130.1, 133.3, 135.6, 137.7, 148.8, 157.9, 171.8; HRMS (ESI, +ve) *m/z* calcd. for $C_{16}H_{18}N_2NaO_6$, 357.1063, found 357.1063 $(M+Na)^+$.

(*anti-E*)-Methyl 2-(*p*-nitrophenyl)-3-(2-oxooxazolidin-3-yl)hex-4-enoate 180

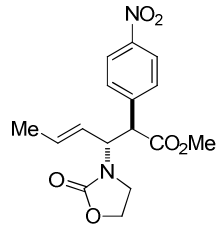

LiHMDS (0.41 ml, 0.41 mmol), TMSCl (0.05 ml, 0.41 mmol) and (*E*)-4-(2-oxooxazolidin-3-yl)but-3-en-2-yl 2-(*p*-nitrophenyl)acetate **171** (0.10 g, 0.32 mmol) in THF (1 ml) were combined according to general procedure 2 (reaction time : 75 minutes). Treatment with diazomethane and purification by flash chromatography afforded (*anti-E*)-methyl 2-(*p*-nitrophenyl)-3-(2-oxooxazolidin-3-yl)hex-4-enoate **anti-**

180 as a red solid (0.07 g, 69%). M.p. 101–103 °C; FTIR (film/cm^{-1}) υ_{max}: 2954 (m), 1739 (s), 1607 (w), 1522 (m); ^{1}H NMR (500 MHz, $CDCl_3$) δ: 1.51 (dd, 3H, *J* = 6.5, 1.2 Hz), 3.62 (app. t, 2H, *J* = 8.0 Hz), 3.67 (s, 3H), 4.27–4.34 (m, 2H), 4.35 (d, 1H, *J* = 11.3 Hz), 4.62 (dd, 1H, *J* = 11.3, 8.5 Hz), 5.31 (ddq, 1H, *J* = 15.3, 8.5, 1.5 Hz), 5.47 (dq, 1H, *J* = 15.3, 6.5 Hz), 7.51 (app. d, 2H, *J* = 8.7 Hz), 8.16 (app. d, 1H, *J* = 8.7 Hz); ^{13}C NMR (125 MHz, $CDCl_3$) *δ:* 17.7, 43.0, 52.7, 53.8, 59.2, 62.3, 123.7, 123.8, 129.9, 132.7, 142.5, 147.6, 157.5, 171.3; HRMS (ESI, +ve) *m/z* calcd. for $C_{16}H_{18}N_2NaO_6$, 357.1063, found 357.1075 $(M+Na)^+$. (*syn-E*)-methyl 2-(*p*-nitrophenyl)-3-(2-oxooxazolidin-3-yl)hex-4-enoate **syn-180** as a red solid (0.01 g, 7%). M.p. 101–102 °C; FTIR (film/cm^{-1}) υ_{max}: 2954 (m), 1740 (s), 1607 (w), 1521 (s); ^{1}H NMR (500 MHz, $CDCl_3$) δ: 1.74 (dd, 3H, *J* = 6.6, 1.3 Hz), 3.31 (app. t, 2H, *J* = 8.0 Hz), 3.66 (s, 3H), 4.02 (dt, 1H, J = 8.2, 2.9 Hz), 4.70 (dt, 1H, J = 8.2, 2.9 Hz), 4.27 (d, 1H, *J* = 11.2 Hz), 4.76 (dd, 1H, *J* = 11.2, 8.0 Hz), 5.63 (ddq, 1H, *J* = 15.3, 8.0, 1.6 Hz), 5.87 (dq, 1H, *J* = 15.3, 6.6 Hz), 7.62 (d, 2H, *J* = 8.7 Hz), 8.12 (d, 1H, *J* = 8.7 Hz); ^{13}C NMR (125 MHz, $CDCl_3$) *δ:* 17.9, 42.5, 52.6, 53.9, 58.2, 61.9, 123.9, 124.3, 129.5, 132.4, 142.4, 147.7, 157.4, 170.8; HRMS (ESI, +ve) *m/z* calcd. for $C_{16}H_{18}N_2NaO_6$, 357.1063, found 357.1058 $(M+Na)^+$.

(*anti-E*)-Methyl 2-(4-(dimethylamino)phenyl)-3-(2-oxooxazolidin-3-yl)hex-4-enoate 213

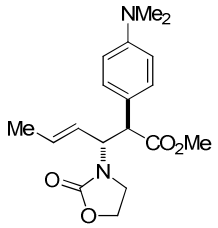

LiHMDS (1.02 ml, 1.02 mmol), TMSCl (0.13 ml, 1.02 mmol) and (*E*)-4-(2-oxooxazolidin-3-yl)but-3-en-2-yl 2-(4-(dimethylamino)phenyl)acetate **202** (0.25 g, 0.78 mmol) in THF (2.5 ml) were combined according to a modified general procedure 2, in which LiHMDS was added by syringe pump at 4 ml/h to a solution of (*E*)-4-(2-oxooxazolidin-3-yl)but-3-en-2-yl 2-(4-(dimethylamino)phenyl)acetate **202**, TMSCl and THF (reaction time : 75 minutes). Treatment with diazomethane and purification by flash chromatography afforded (*anti-E*)-methyl 2-(4-(dimethylamino)phenyl)-3-(2-

oxooxazolidin-3-yl)hex-4-enoate **213** as a brown solid (0.15 g, 58%, d.r. 6:1); M.p. 130–132 °C; FTIR (film/cm^{-1}) υ_{max}: 2950 (m), 2916 (m), 2805 (m), 1748 (s), 1612 (w), 1613 (m), 1523 (m); ^{1}H NMR (500 MHz, $CDCl_3$) *Major* δ: 1.52 (d, 3H, *J* = 6.4 Hz), 2.91 (s, 3H), 3.52–3.60 (m, 2H), 3.67 (s, 3H), 3.97 (d, 1H, *J* = 11.4 Hz), 4.20–4.32 (m, 2H), 4.70 (dd, 1H, *J* = 11.4, 7.4 Hz), 5.27 (ddq, 1H, *J* = 15.3, 7.4, 0.9 Hz), 5.50 (dqd, 1H, *J* = 15.3, 6.4, 0.8 Hz), 6.63 (app. d, 2H, *J* = 8.9 Hz), 7.19 (app. d, 2H, *J* = 8.9 Hz). *Minor* δ: 1.69 (d, 3H, *J* = 6.5 Hz), 2.90 (s, 3H), 3.20–3.32 (m, 2H), 3.59 (s, 3H), 3.84 (d, 1H, *J* = 11.4 Hz), 3.88–4.12 (m, 2H), 4.84 (dd, 1H, *J* = 11.4, 7.6 Hz), 5.57 (ddq, 1H, *J* = 15.3, 7.6, 1.6 Hz), 5.79 (dqd, 1H, *J* = 15.3, 6.5, 0.6 Hz), 6.63–6.65 (m, 2H), 7.22 (app. d, 2H, *J* = 8.6 Hz); ^{13}C NMR (75 MHz, $CDCl_3$) *Major* δ: 17.8, 40.3, 42.2, 52.0, 53.4, 58.2, 62.2, 112.4, 122.3, 124.7, 129.5, 130.8, 150.0, 157.6, 127.8; *Minor* δ: 17.9, 40.3, 41.5, 52.0, 53.3, 56.9, 61.9, 112.4, 122.1, 125.6, 128.9, 130.4, 150.1, 157.6, 172.3; HRMS (ESI, +ve) *m/z* calcd. For $C_{18}H_{24}NaN_2O_4$ 355.1634, found 355.1628 $(M+Na)^+$.

(*anti-E*)-Methyl 2-(4-iodophenyl)-3-(2-oxooxazolidin-3-yl)hex-4-enoate 214

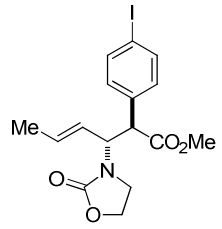

LiHMDS (0.32 ml, 0.32 mmol), TMSCl (0.04 ml, 0.32 mmol) and (*E*)-4-(2-oxooxazolidin-3-yl)but-3-en-2-yl 2-(*p*-iodophenyl)acetate **203** (0.10 g, 0.25 mmol) in THF (1 ml) were combined according to general procedure 2 (reaction time : 75 minutes). Treatment with diazomethane and purification by flash chromatography afforded (*anti-E*)-methyl 2-(4-iodophenyl)-3-(2-oxooxazolidin-3-yl)hex-4-enoate **214** as a yellow solid (0.08 g, 77%, d.r. 60:1); M.p. 108–110 °C; FTIR (film/cm^{-1}) υ_{max}: 2951 (w), 1745 (s) 1485 (m); ^{1}H NMR (500 MHz, $CDCl_3$) δ: 1.53 (dd, 3H, *J* = 6.5, 1.4 Hz), 3.56–3.63 (m, 2H), 3.66 (s, 3H), 4.13 (d, 1H, *J* = 11.2 Hz), 4.25–4.34 (m, 2H), 4.62 (dd, 1H, *J* = 11.2, 8.1 Hz), 5.29 (ddq, 1H, *J* = 15.3, 8.1, 1.4 Hz), 5.49 (dq, 1H, *J* = 15.3, 6.5 Hz), 7.08 (app. d, 2H, *J* = 8.3 Hz), 7.64 (app. d, 2H, *J* = 8.3 Hz); ^{13}C NMR (125 MHz, $CDCl_3$) *δ*: 17.8, 42.8, 52.4, 53.8, 58.7, 62.3, 93.6, 124.1, 130.8, 132.0, 134.8,

137.8, 157.5, 171.9; HRMS (ESI, +ve) *m/z* calcd. For $C_{16}H_{18}INNaO_4$ 438.0178, found 438.0173 $(M+Na)^+$.

(*anti-E*)-Methyl 2-(*p*-fluorophenyl)-3-(2-oxooxazolidin-3-yl)hex-4-enoate 215

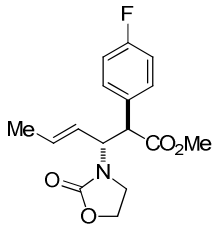

LiHMDS (0.42 ml, 0.42 mmol), TMSCl (0.06 ml, 0.42 mmol) and (*E*)-4-(2-oxooxazolidin-3-yl)but-3-en-2-yl 2-(*p*-fluorophenyl)acetate **204** (0.10 g, 0.32 mmol) in THF (1 ml) were combined according to general procedure 2 (reaction time : 75 minutes). Treatment with diazomethane and purification by flash chromatography afforded (*anti-E*)-methyl 2-(*p*-fluorophenyl)-3-(2-oxooxazolidin-3-yl)hex-4-enoate **215** as a yellow solid (0.08 g, 73%, d.r. 23:1). M.p. 95–97 °C; FTIR (film/cm^{-1}) υ_{max}: 2954 (w), 2918 (w), 1748 (s) 1605 (m), 1510 (s); ^{1}H NMR (500 MHz, $CDCl_3$) δ: 1.51 (dd, 3H, *J* = 6.6, 1.3 Hz), 3.53–3.64 (m, 2H), 3.67 (s, 3H), 4.16 (d, 1H, *J* = 11.4 Hz), 4.25–4.34 (m, 2H), 4.61 (dd, 1H, *J* = 11.4, 8.2 Hz), 5.29 (ddq, 1H, *J* = 15.4, 8.2, 1.3 Hz), 5.47 (dq, 1H, *J* = 15.4, 6.6 Hz), 7.00 (app. t, 2H, *J* = 8.6 Hz), 8.30 (dd, 1H, *J* = 4.6, 4.2 Hz); ^{13}C NMR (125 MHz, $CDCl_3$) *δ*: 17.7, 42.8, 52.4, 53.4, 59.0, 62.2, 115.6 (d, *J* = 22.1 Hz), 124.1, 130.5 (d, *J* = 8.2 Hz), 131.0, 131.9, 157.5, 163.5, 172.3; HRMS (ESI, +ve) *m/z* calcd. for $C_{16}H_{18}FNNaO_4$, 330.1118, found 330.1112 $(M+Na)^+$.

(*anti-E*)-Methyl 2-(*p*-chlorophenyl)-3-(2-oxooxazolidin-3-yl)hex-4-enoate 216

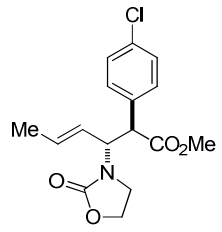

LiHMDS (0.42 ml, 0.42 mmol), TMSCl (0.05 ml, 0.42 mmol) and (*E*)-4-(2-oxooxazolidin-3-yl)but-3-en-2-yl 2-(*p*-chlorophenyl)acetate **205** (0.10 g, 0.32 mmol) in THF (1 ml) were combined according to general procedure 2 (reaction time : 75 minutes). Treatment with diazomethane and purification by flash chromatography afforded (*anti-E*)-methyl 2-(*p*-chlorophenyl)-3-(2-oxooxazolidin-3-yl)hex-4-enoate **216** as a yellow solid (0.07 g, 72%, d.r. 46:1). M.p. 107–108 °C; FTIR (film/cm^{-1}) υ_{max}: 2953 (w), 1746 (s), 1492 (m); ^{1}H NMR (500 MHz, $CDCl_3$) δ: 1.51 (dd, 3H, *J* = 6.6, 1.4 Hz), 3.57–3.62 (m, 2H), 3.66 (s, 3H), 4.15 (d, 1H, *J* = 11.3 Hz), 4.25–4.33 (m, 2H), 4.61 (dd, 1H, *J* = 11.3, 8.1 Hz), 5.29 (ddq, 1H, *J* = 15.4, 8.1, 1.4 Hz), 5.48 (dq, 1H, *J* = 15.4, 6.6 Hz), 7.24–7.30 (m, 4H); ^{13}C NMR (125 MHz, $CDCl_3$) *δ*: 17.7, 42.8, 52.4, 53.6, 58.9, 62.3, 124.1, 128.9, 130.2, 131.9, 133.6, 133.8, 157.5, 172.0; HRMS (ESI, +ve) *m/z* calcd. for $C_{16}H_{18}ClNNaO_4$, 346.0822, found 346.0832 $(M+Na)^+$.

(*anti-E*)-Methyl 3-(2-oxooxazolidin-3-yl)-2-(*p*-(trifluoromethyl)phenyl)hex-4-enoate 217

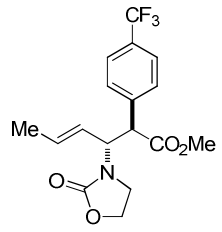

LiHMDS (0.36 ml, 0.36 mmol), TMSCl (0.05 ml, 0.36 mmol) and (*E*)-4-(2-oxooxazolidin-3-yl)but-3-en-2-yl 2-(*p*-trifluoromethylphenyl)acetate **206** (0.10 g, 0.28 mmol) in THF (1 ml) were combined according to general procedure 2 (reaction time : 75 minutes). Treatment with diazomethane and purification by flash chromatography afforded (*anti-E*)-methyl 3-(2-oxooxazolidin-3-yl)-2-(*p*-(trifluoromethyl)phenyl)hex-4-

enoate **217** as a yellow solid. (0.07 g, 71%, d.r. 21:1); M.p. 103–104 °C; FTIR (film/cm^{-1}) υ_{max}: 2955 (w), 2917 (w), 2850 (w), 1747 (s), 1671 (w), 1620 (w); ^{1}H NMR (500 MHz, $CDCl_3$) δ: 1.51 (dd, 3H, *J* = 6.6, 1.5 Hz), 3.58–3.65 (m, 2H), 3.68 (s, 3H), 4.26–4.34 (m, 3H), 4.65 (dd, 1H, *J* = 11.2, 8.2 Hz), 5.31 (ddq, 1H, *J* = 15.3, 8.2, 1.5 Hz), 5.48 (dq, 1H, *J* = 15.3, 6.6 Hz), 7.46 (app. d, 2H, *J* = 8.2 Hz), 7.58 (app. d, 2H, *J* = 8.2 Hz); ^{13}C NMR (125 MHz, $CDCl_3$) *δ*: 17.8, 42.9, 52.5, 53.9, 58.9, 62.3, 123.8, 124.0 (q, *J* = 272.1 Hz), 125.6 (q, *J* = 3.4 Hz), 129.3, 130.1 (q, *J* = 32.8 Hz), 132.3, 139.2, 157.5, 171.7; HRMS (ESI, +ve) *m/z* calcd. For $C_{17}H_{18}F_3NNaO_4$ 380.1086, found 380.1080 $(M+Na)^+$.

$^{13}C_1$-(*anti-E*)-methyl 3-(2-oxooxazolidin-3-yl)-2-(4-(trifluoromethyl)phenyl)hex-4-enoate $^{13}C_1$-217

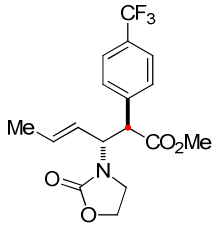

To an oven dried Young's tap NMR tube, inserted into a Dewar at -95 °C and under an atmosphere of nitrogen, was added a solution of LiHMDS (1 M in THF, 0.23 ml, 0.23 mmol, 1.3 eq.), and TMSCl (0.03 ml, 0.23 mmol, 1.3 eq.). Thermal equilibration was allowed (5 minutes) and then a solution of (*E*)-4-(2-oxooxazolidin-3-yl)but-3-en-2-yl 2-$^{13}C_1$-(4-(trifluoromethyl)phenyl)acetate **$^{13}C_1$-206** (0.06 g, 0.18 mmol, 1.0 eq.) in THF (0.6 ml) was added. The cooled NMR tube was rapidly lowered into the pre-cooled NMR machine at -95 °C. From this point ^{13}C NMR spectroscopy was recorded at -95 °C and then the machine was allowed to warm to -65 °C, where it was then kept for the rest of the experiment (ca. 12 hours) and ^{13}C data was recorded every 5 minutes. After *in-situ* reaction monitoring the reaction mixture was quenched following general procedure 2 and treatment with diazomethane and purification by flash chromatography to afford $^{13}C_1$-(*anti-E*)-methyl 3-(2-oxooxazolidin-3-yl)-2-(4-(trifluoromethyl)phenyl)hex-4-enoate **$^{13}C_1$-217** as a white solid (0.02 g, 48%, d.r. >25:1). M.p. 104–106 °C; FTIR (film/cm^{-1}) υ_{max}: 2998 (m), 2915 (m), 2948 (m), 1737 (s), 1657 (m);^{1}H NMR (500 MHz, $CDCl_3$) δ: 1.52 (d, 3H, *J* = 6.6 Hz), 3.60–3.66 (m, 2H), 3.69 (s, 3H), 4.29 (dd, 1H, *J* = 135.0, 11.7 Hz) 4.32 (app. dt, 2H, *J* = 23.5, 8.7

Hz), 4.63–4.70 (m, 1H), 5.32 (app. dd, 1H, *J* = 15.2, 8.3 Hz), 5.49 (app. dq, 1H, *J* = 15.2, 6.6 Hz), 7.48 (app. dd, 2H, *J* = 8.1, 3.5 Hz), 7.59 (app. d, 2H, *J* = 8.1 Hz); ^{13}C NMR (125 MHz, $CDCl_3$) δ: 17.7, 42.9, 52.5, 53.9, 59.0 (d, *J* = 35.6 Hz), 62.3, 125.6 (q, *J* = 270.6 Hz), 125.0, 125.7 (quin, *J* = 3.6 Hz), 129.7 (d, *J* = 2.3 Hz), 130.4 (q, *J* = 37.9 Hz), 132.2, 139.2 (d, *J* = 42.2 Hz), 157.5, 171.7 (d, *J* = 59.7 Hz); HRMS (ESI, +ve) *m/z* calcd. for $C_{16}{}^{13}C_1H_{19}F_3N_1O_4$, 359.1344, found 359.1311 $(M+H)^+$.

(*anti-E*)-Methyl 2-(*p*-cyanophenyl)-3-(2-oxooxazolidin-3-yl)hex-4-enoate 218

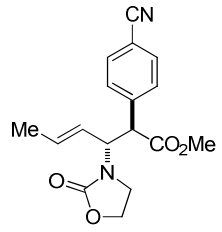

LiHMDS (0.43 ml, 0.43 mmol), TMSCl (0.06 ml, 0.43 mmol) and (*E*)-4-(2-oxooxazolidin-3-yl)but-3-en-2-yl 2-(*p*-cyanophenyl)acetate **207** (0.10 g, 0.33 mmol) in THF (1 ml) were combined according to general procedure 2 (reaction time : 75 minutes). Treatment with diazomethane and purification by flash chromatography afforded (*anti-E*)-methyl 2-(*p*-cyanophenyl)-3-(2-oxooxazolidin-3-yl)hex-4-enoate **218** as a cream solid (0.07 g, 63%, d.r. 17:1); M.p. 106–109 °C; FTIR (film/cm^{-1}) υ_{max}: 2954 (m), 2918 (w), 2851 (w), 1747 (s), 1672 (w), 1608 (w), 1505 (w). ^{1}H NMR (500 MHz, $CDCl_3$) δ: 1.50 (dd, 3H, *J* = 6.4, 1.2 Hz), 3.58–3.63 (m, 2H), 3.67 (s, 3H), 4.26–4.35 (m, 3H), 4.59 (dd, 1H, *J* = 11.0, 8.4 Hz), 5.30 (ddq, 1H, *J* = 15.3, 8.4, 1.2 Hz), 5.46 (dq, 1H, *J* = 15.3, 6.4 Hz), 7.45 (app d, 2H, *J* = 8.3 Hz), 7.61 (app. d, 2H, *J* = 8.3 Hz); ^{13}C NMR (125 MHz, $CDCl_3$) *δ*: 17.7, 43.0, 52.6, 54.0, 59.2, 62.3, 111.9, 118.4, 123.8, 129.8, 132.4, 132.6, 140.5, 157.5, 171.4; HRMS (ESI, +ve) *m/z* calcd. For $C_{17}H_{18}N_2NaO_4$ 337.1164, found 337.1159. $(M+Na)^+$.

(*anti-E*)-Methyl-2-(4-(methylsulfonyl)phenyl)-3-(2-oxooxazolidin-3-yl)hex-4-enoate 219

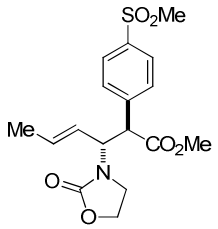

LiHMDS (0.18 ml, 0.18 mmol), TMSCl (0.02 ml, 0.18 mmol) and (*E*)-4-(2-oxooxazolidin-3-yl)but-3-en-2-yl 2-(4-(methylsulfonyl)phenyl)acetate **208** (0.05 g, 0.47 mmol) in THF (5 ml) were combined according to general procedure 2 (reaction time : 75 minutes). Treatment with diazomethane and purification by flash chromatography afforded (*anti-E*)-methyl 2-(4-(methylsulfonyl)phenyl)-3-(2-oxooxazolidin-3-yl)hex-4-enoate **219** as a white solid (0.03 g, 67%, d.r. >25:1); M.p. 138–140 °C; FTIR (film/cm^{-1}) υ_{max}: 2998 (m), 2954 (m), 2924 (m), 1744 (s), 1598 (m); ^{1}H NMR (500 MHz, $CDCl_3$) δ: 1.50 (d, 3H, *J* = 6.5 Hz), 3.04 (s, 3H), 3.57–3.64 (m, 2H), 3.68 (s, 3H), 4.25–4.37 (m, 3H), 4.63 (app. t, 1H, *J* = 9.0 Hz), 5.30 (app. dd, 1H, *J* = 15.5, 9.0 Hz), 5.48 (app. dq, 1H, *J* = 15.5, 6.5 Hz), 7.54 (app. d, 2H, *J* = 8.4 Hz), 7.89 (app. d, 2H, *J* = 8.4 Hz); ^{13}C NMR (125 MHz, $CDCl_3$) *δ*: 17.7, 43.0, 44.4, 52.6, 53.9, 59.1, 62.3, 123.7, 127.7, 130.0, 132.7, 140.0, 141.4, 157.5, 171.4; HRMS (ESI, +ve) *m/z* calcd. For $C_{17}H_{21}NaNO_6S$ 390.0987, found 390.0973 $(M+Na)^+$.

(*anti-E*)-Methyl 2-(2,4-dimethoxyphenyl)-3-(2-oxooxazolidin-3-yl)hex-4-enoate 220

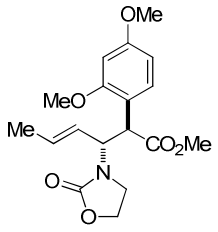

LiHMDS (0.39 ml, 0.39 mmol), TMSCl (0.05 ml, 0.39 mmol) and (*E*)-4-(2-oxooxazolidin-3-yl)but-3-en-2-yl 2-(2,4-dimethoxyphenyl)acetate **209** (0.10 g, 0.30 mmol) in THF (1 ml) were combined according to general procedure 2 (reaction time : 75 minutes). Treatment with diazomethane and purification by flash chromatography afforded (*anti-E*)-methyl 2-(2,4-dimethoxyphenyl)-3-(2-oxooxazolidin-3-yl)hex-4-

enoate **220** as a clear oil (0.06 g, 57%, d.r. 6:1); FTIR (film/cm^{-1}) υ_{max}: 2951 (m), 2840 (m), 1747 (s), 1612 (s), 1587 (m), 1508 (m); ^{1}H NMR (500 MHz, $CDCl_3$) δ: 1.51 (dd, 3H, *J* = 6.4, 1.0 Hz), 3.58–3.68 (m, 5H), 3.78 (s, 3H), 3.79 (s, 3H), 4.21–4.33 (m, 2H), 4.55 (d, 1H, *J* = 11.1 Hz), 4.74 (dd, 1H, *J* = 11.1, 7.7 Hz), 5.28 (ddq, 1H, *J* = 15.4, 7.7, 1.0 Hz), 5.50 (app. dq, 1H, *J* = 15.4, 6.4 Hz), 6.41 (d, 1H, *J* = 2.4 Hz), 6.46 (dd, 1H, *J* = 8.4, 2.3 Hz), 7.31 (d, 1H, *J* = 8.4 Hz); ^{13}C NMR (125 MHz, $CDCl_3$) *δ*: 17.7, 42.1, 45.1, 52.1, 55.2, 55.6, 57.9, 62.1, 98.5, 104.5, 116.1, 124.8, 129.8, 130.7, 157.6, 158.1, 160.1, 172.6; HRMS (ESI, +ve) *m/z* calcd. For $C_{18}H_{23}NaNO_6$ 372.1423, found 372.1418 $(M+Na)^+$.

((*anti-E*)-Methyl 3-(2-oxooxazolidin-3-yl)-2-((*E*)-styryl)hex-4-enoate 221

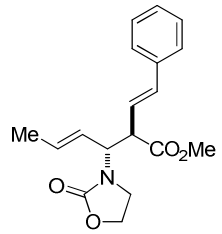

LiHMDS (0.43 ml, 0.43 mmol), TMSCl (0.06 ml, 0.43 mmol) and (*E*)-((*E*)-4-(2-oxooxazolidin-3-yl)but-3-en-2-yl) 4-phenylbut-3-enoate **210** (0.10 g, 0.33 mmol) in THF (1 ml) were combined according to general procedure 2 (reaction time : 75 minutes). Treatment with diazomethane and purification by flash chromatography afforded ((*anti-E*)-methyl 3-(2-oxooxazolidin-3-yl)-2-((*E*)-styryl)hex-4-enoate **221** as an amorphous orange oil (0.07 g, 68%, d.r. >25:1); FTIR (film/cm^{-1}) υ_{max}: 3010 (m), 2992 (m), 2853 (m), 1745 (s); ^{1}H NMR (500 MHz, $CDCl_3$) δ: 1.78 (d, 3H, *J* = 6.4 Hz), 3.52–3.59 (m, 3H), 3.71 (s, 3H), 4.22–4.33 (m, 2H), 4.59 (app. t, 1H, *J* = 9.1 Hz), 5.45 (app. dd, 1H, *J* = 15.3, 9.1 Hz), 5.75 (app. dq, 1H, *J* = 15.3, 6.4 Hz), 6.10 (dd, 1H, *J* = 15.7, 9.4 Hz), 6.52 (d, 1H, *J* = 15.7 Hz), 7.23–7.28 (m, 1H), 7.29–7.38 (m, 4H); ^{13}C NMR (125 MHz, $CDCl_3$) *δ*: 17.8, 41.8, 52.2, 52.8, 57.5, 62.2, 123.6, 124.6, 126.4, 127.9, 128.6, 132.0, 134.6, 136.3, 157.6, 172.0; HRMS (ESI, +ve) *m/z* calcd. For $C_{18}H_{21}NNaO_4$ 338.1368, found 338.1368 $(M+Na)^+$.

((*anti-E*)-Methyl 2-(1-methyl-1H-indol-3-yl)-3-(2-oxooxazolidin-3-yl)hex-4-enoate 222

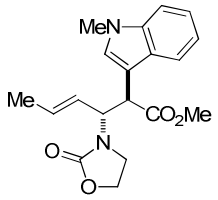

LiHMDS (0.40 ml, 0.40 mmol), TMSCl (0.05 ml, 0.40 mmol) and (*E*)-4-(2-oxooxazolidin-3-yl)but-3-en-2-yl 2-(1-methyl-1H-indol-3-yl)acetate **211** (0.10 g, 0.31 mmol) in THF (1 ml) were combined according to general procedure 2 (reaction time : 75 minutes). Treatment with diazomethane and purification by flash chromatography afforded ((*anti-E*)-methyl 2-(1-methyl-1H-indol-3-yl)-3-(2-oxooxazolidin-3-yl)hex-4-enoate **222** as an amorphous brown oil (0.05 g, 50%, d.r. 10:1); FTIR (film/cm^{-1}) υ_{max}: 3057 (m), 2958 (m), 2917 (m), 2850 (m), 1732 (s), 1667 (s), 1613 (m), 1548 (w); ^1H NMR (500 MHz, $CDCl_3$) δ: 1.50 (d, 3H, *J* = 6.4 Hz), 3.52–3.63 (m, 2H), 3.66 (s, 3H), 3.77 (s, 3H), 4.23 (app. q, 1H, *J* = 8.1 Hz), 4.30 (dt, 1H, *J* = 8.1, 6.1 Hz), 4.39 (d, 1H, *J* = 10.6 Hz), 4.92 (dd, 1H, *J* = 10.6, 7.3 Hz), 5.37 (ddq, 1H, *J* = 15.4, 10.6, 1.6 Hz), 5.56 (dqd, 1H, *J* = 15.4, 6.4, 0.9 Hz), 7.12 (s, 1H), 7.13 (t, 1H, *J* = 7.9 Hz), 7.23 (t, 1H, *J* = 7.9 Hz), 7.29 (t, 1H, *J* = 7.9 Hz), 7.69 (t, 1H, *J* = 7.9 Hz); ^{13}C NMR (125 MHz, $CDCl_3$) *δ*: 17.7, 32.9, 41.9, 45.9, 52.1, 57.7, 62.2, 109.1, 109.3, 119.1, 119.4, 121.8, 124.9, 127.3, 128.2, 130.7, 136.7, 157.7, 172.7; HRMS (ESI, +ve) *m/z* calcd. For $C_{19}H_{23}N_2O_4$ 343.1657, found 343.1637 $(M+H)^+$.

(*anti-E*)-Methyl 2-(benzo[d][1,3]dioxol-5-yl)-3-(2-oxooxazolidin-3-yl)hex-4-enoate 223

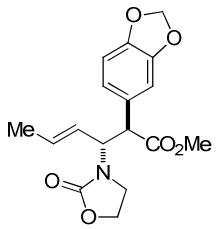

LiHMDS (0.39 ml, 0.39 mmol), TMSCl (0.05 ml, 0.39 mmol) and (*E*)-4-(2-oxooxazolidin-3-yl)but-3-en-2-yl 2-(benzo[d][1,3]dioxol-5-yl)acetate **212** (0.10 g, 0.30mmol) in THF (2 ml) were combined according to general procedure 2 (reaction

time : 75 minutes). Treatment with diazomethane and purification by flash chromatography afforded (*anti-E*)-methyl 2-(benzo[d][1,3]dioxol-5-yl)-3-(2-oxooxazolidin-3-yl)hex-4-enoate **223** as a white solid (0.06 g, 58%, d.r. 32:1); M.p. 122–125 °C; FTIR (film/cm^{-1}) υ_{max}: 2999 (m), 2917 (m), 1744 (s), 1505 (m); ^{1}H NMR (250 MHz, $CDCl_3$) δ: 1.55 (dd, 3H, *J* = 6.4, 0.9 Hz), 3.54–3.65 (m, 2H), 3.67 (s, 3H), 4.06 (d, 1H, *J* = 11.3 Hz), 4.22–4.37 (m, 2H), 4.60 (dd, 1H, *J* = 11.3, 7.7 Hz), 5.30 (ddq, 1H, *J* = 15.3, 7.7, 0.9 Hz), 5.52 (app. dq, 1H, *J* = 15.3, 6.4 Hz), 5.94–5.97 (m, 2H), 6.71–6.79 (m, 2H), 6.87 (d, 1H, *J* = 1.2 Hz); ^{13}C NMR (75 MHz, $CDCl_3$) δ: 18.2, 43.0, 52.7, 54.2, 59.1, 62.6, 101.5, 108.7, 109.2, 122.9, 124.6, 129.0, 131.9, 147.6, 148.3, 157.9, 172.8; HRMS (ESI, +ve) *m/z* calcd. For $C_{17}H_{20}NO_6$ 334.1291, found 334.1292 $(M+H)^+$.

6.3.3. *N*-Sulfonamide Substrates

<u>*N*-Allyl-4-methylbenzenesulfonamide</u> 326

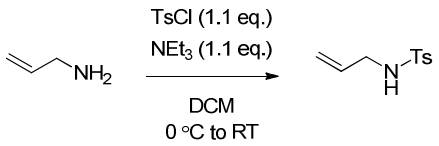

To a solution of *p*-toluenesulfonyl chloride (18.4 g, 96.3 mmol, 1.1 eq.) and triethylamine (13.4 ml, 96.3 mmol, 1.1 eq.) in DCM (70 ml) at 0 °C was added allylamine (5.00 g, 87.6 mmol, 1.0 eq.) by dropwise addition. The reaction mixture was stirred for 1.5 hours under nitrogen at 0 °C, poured onto brine and washed with brine (3 × 100 ml), the organics were dried over $MgSO_4$ and concentrated *in vacuo* to yield a white solid which was subjected to flash column chromatography (15% EtOAc/Petrol 40-60°) to yield *N*-allyl-4-methylbenzenesulfonamide **326** as a white crystalline solid (14.8 g, 80%). M.p. 60–63 °C; ^{1}H NMR (250MHz, $CDCl_3$) δ: 2.42 (s, 3H), 3.57 (app. t, 2H, *J* = 6.0 Hz), 4.69 (bt, 1H *J* = 5.8 Hz), 5.10 (dq, 1H, *J* = 10.2, 1.1 Hz), 5.19 (dq, 1H, *J* = 17.2, 1.4 Hz), 5.74 (ddt, 1H, *J* = 17.2, 10.2, 6.0 Hz), 7.31 (app. d, 2H, *J* = 17.2, 1.4 Hz), 7.75 (app. d, 2H, *J* = 17.2, 1.4 Hz); ^{13}C NMR (250MHz, $CDCl_3$) δ 21.5, 45.7, 117.6, 127.1, 129.7, 133.0, 136.9, 143.5. All analytical data in accordance with commercial sources.

***(E)*-*N*-Allyl-4-methyl-*N*-(3-oxobut-1-enyl)benzenesulfonamide 327**

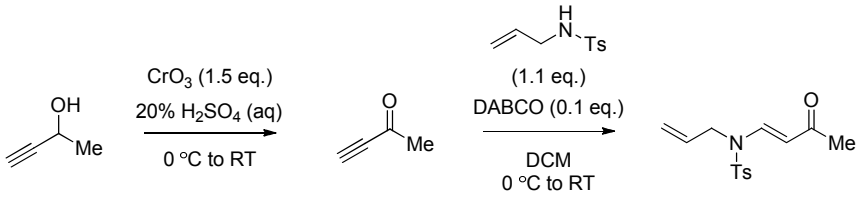

To a solution of Cr(VI)O_3 (10.3 g, 103 mmol, 1.5 eq.) in 20% H_2SO_4 (180 ml) at 0 ^oC under a nitrogen atmosphere was added a solution of 3-butyn-2-ol (5.00 g, 71.3 mmol, 1.0 eq.) in 20% H_2SO_4 (180 ml) by dropwise addition. The reaction mixture was stirred at 0 ^oC for 12 hours and a colour change from orange to green was noted, saturated aqueous sodium bicarbonate was added and the organics were extracted with DCM (3 × 450 ml) and dried over $MgSO_4$. The crude butynone was chilled to 0 ^oC then *N*-allyl-4-methylbenzenesulfonamide **326** (15.0 g, 78.4 mmol, 1.1 eq.) and DABCO (0.80 g, 7.13 mmol, 0.1 eq.) were added. The reaction mixture was allowed to stir for 12 hours whilst slowly warming to room temperature and a colour change from a clear to a deep maroon solution was noted. The reaction mixture was washed with 5% NaOH (3 × 500 ml), brine and then the organics were dried over $MgSO_4$ and concentrated *in vacuo* to give a red oil which was subjected to flash column chromatography (25% EtOAc/Petrol 40-60^o) to give the desired *(E)*-*N*-allyl-4-methyl-N-(3-oxobut-1-enyl)benzenesulfonamide **327** (10.5 g, 53%) as well as the –(*Z*) (0.79 g, 4%) as a brown oil in both cases.

(*E*)-327 product- FTIR (film/cm^{-1}) υ_{max}: 3082(s), 2980(s), 2879(s), 1682(s), 1586(s); ^{1}H NMR (250MHz, $CDCl_3$) δ 2.22 (s, 3H), 2.44 (s, 3H), 4.07 (dt, 2H, *J* = 5.24, 1.59 Hz), 5.13 (dm, 1H, *J* = 9.2 Hz), 5.19 (m, 1H), 5.48 (d, 1H, *J* = 14.3 Hz), 5.56 (ddt, 1H, *J* = 17.2, 10.6, 5.3 Hz), 7.34 (m, 2H), 7.71 (m, 2H), 8.03 (d, 1H, *J* = 14.3 Hz); ^{13}C NMR (250MHz, $CDCl_3$) *δ* 21.7, 27.6, 48.3, 109.0, 118.9, 127.3, 129.9, 130.2, 135.3, 141.2, 145.1, 196.6; HRMS (ESI, +ve) *m/z* calcd. for $C_{14}H_{18}NO_3S$ 280.1007, found 280.0990 $(M+H)^+$.

(*Z*)-327 product- FTIR (film/cm^{-1}) υ_{max}: 3100(s), 2925(s), 1679(s), 1595(s); ^{1}H NMR (250MHz, $CDCl_3$) δ 2.03 (s, 3H), 2.33 (s, 3H), 4.41 (dt, 2H, *J* = 5.7, 1.3 Hz,), 4.86 (dq, 1H, J = 29.0, 1.5 Hz), 4.91 (dq, 1H, *J* = 22.3, 1.4 Hz), 5.21 (ddq, 1H, *J* = 17.9, 10.3, 5.6 Hz), 5.35 (d, 1H, J = 10.3 Hz), 6.71 (d, 1H, *J* = 10.4 Hz), 7.23 (m, 2H), 7.62 (m, 2H);

^{13}C NMR (250MHz, $CDCl_3$) δ: 21.5, 30.9, 49.67, 108.5, 118.4, 127.2, 130.0, 131.3, 133.3, 135.6, 144.7, 196.2; HRMS (ESI, +ve) *m/z* calcd. for $C_{14}H_{18}NO_3S$ 280.1007, found 280.0990 $(M+H)^+$. Formation of the minor *Z*-ene-sulfonamide was not observed on subsequent repeats of this reaction and yields in the order of 60% were obtained.

<u>*(E)*-*N*-Allyl-*N*-(3-hydroxybut-1-enyl)-4-methylbenzenesulfonamide</u> 329

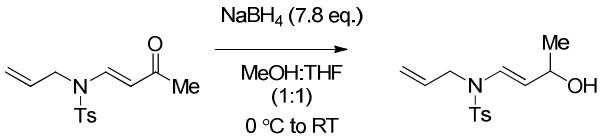

To a solution of *(E)*-*N*-allyl-4-methyl-*N*-(3-oxobut-1-enyl)benzenesulfonamide **327** (1.00 g, 3.58 mmol, 1.0 eq.) in THF:MeOH (20 ml:20 ml) at 0 ^oC was added $NaBH_4$ (1.03 g, 27.8 mmol, 7.8 eq.) by portionwise addition. The reaction mixture was allowed to stir whilst slowly warming to RT over 12 hours and then was poured onto sat. NaCl (100 ml) and extracted with DCM (3 × 100 ml), dried over $MgSO_4$, filtered and concentrated *in vacuo* to give *(E)*-*N*-allyl-N-(3-hydroxybut-1-enyl)-4-methylbenzenesulfonamide **329** as a colourless oil (1.00 g, 100%). FTIR (film/cm^{-1}) υ_{max}: 3392 (bs), 3086 (s), 2971(s), 2925 (s), 2871(s), 1708 (s), 1657 (s), 1597 (s); ^{1}H NMR (250MHz, $CDCl_3$) δ 1.27 (d, 3H), 2.42 (s, 3H), 4.00 (dt, 2H, *J* = 5.2, 1.6 Hz), 4.32 (m, 1H), 4.87 (dd, 1H, *J* = 14.2, 7.5Hz), 5.18 (dm, 2H, *J* = 9.9Hz), 5.32 (ddt, 1H, *J* = 17.4, 10.3, 5.2 Hz), 6.89 (d, 1H, *J* = 14.2 Hz), 7.30 (m, 2H), 7.67 (m, 2H); ^{13}C NMR (250MHz, $CDCl_3$) *δ* 21.9, 24.4, 48.5, 68.1, 115.3, 118.3, 127.4, 127.5, 130.2, 131.9, 136.6, 144.3; HRMS (ESI, +ve) *m/z* calcd. for $C_{14}H_{19}NNaO_3S$ 304.0983, found 304.0978 $(M+Na)^+$.

(*S*)-(4-Bromobut-3-yn-2-yloxy)(*tert*-butyl)diphenylsilane (*S*)-383

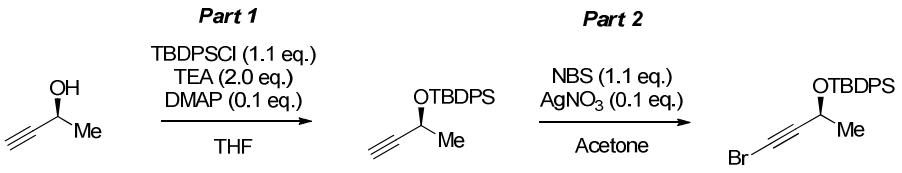

Part 1 - To a stirred solution of 3-butyn-2-ol (15.0 g, 214 mmol, 1.0 eq.) in THF (200 ml) was added DMAP (2.61 g, 21.4 mmol, 0.1 eq.), TEA (59.1 ml, 428 mmol, 2.0 eq.) and TBDPSCl (64.7 g, 235, 1.1 eq.). The reaction mixture was stirred for 15 hours and then poured onto saturated ammonium chloride (200 ml). The organics were extracted with heptane (3 × 200 ml), concentrated *in vacuo* and the crude product was subjected to flash column chromatography (0-5% EtOAc/Petrol 40-60^{o}) to give (but-3-yn-2-yloxy)(*tert*-butyl)diphenylsilane as a clear oil (66.0 g, 100%). $[\alpha]_D^{20}$ = +65 .0 (*c* 1, DCM); Other data as previously reported.

Part 2 - To a stirred solution of but-3-yn-2-yloxy)(*tert*-butyl)diphenylsilane (66.0 g, 214 mmol, 1.0 eq.) in acetone (200 ml) was added NBS (41.9 g, 235 mmol, 1.1 eq.) and silver nitrate (3.63 g, 21.4 mmol, 0.1 eq.). The reaction mixture was stirred for 15 hours and then poured onto saturated sodium chloride (100 ml). The organics were extracted with diethyl ether (3 × 200 ml), dried over magnesium sulphate and concentrated *in vacuo* to yield a yellow oil which was triturated with heptane and the insolubilities were filtered off and the mother liquir was concentrated in vacuo to yield (4-bromobut-3-yn-2-yloxy)(*tert*-butyl)diphenylsilane **(*S*)-383** as an orange oil (65.0 g, 78%). $[\alpha]_D^{20}$ = +10.3 (*c* 1, DCM); Other data as previously reported.

(*S*)-*N*-Allyl-*N*-(3-(*tert*-butyldiphenylsilyloxy)but-1-ynyl)-4-methylbenzenesulfonamide (*S*)-384

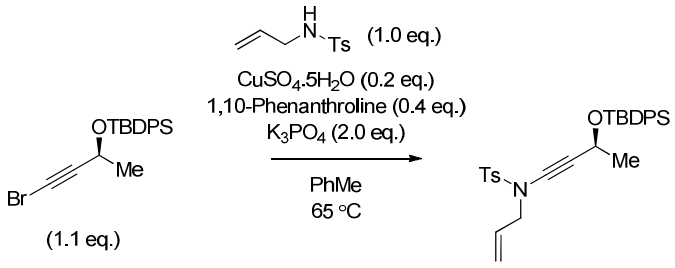

To a solution of *N*-allyl-4-methylbenzenesulfonamide **326** (2.46 g, 11.6 mmol, 1.0 eq.) in toluene (200 ml) was added (*S*)-(4-bromobut-3-yn-2-yloxy)(*tert*-butyl)diphenylsilane **(*S*)-383** (5.00 g, 12.9 mmol, 1.1 eq.), $CuSO_4.5H_2O$ (0.58 g, 2.34 mmol, 0.2 eq.), 1,10-phenanthroline (0.84 g, 4.68 mmol, 0.4 eq.) and finely ground K_3PO_4 (4.97 g, 23.2 mmol, 2 eq.). The reaction mixture was allowed to stir at 65 ^oC for 48 hours, after which was concentrated *in vacuo* and subjected to flash column chromatography (5-10% EtOAc/Petrol 40-60^o) to give (*S*)-*N*-allyl-*N*-(3-(*tert*-butyldiphenylsilyloxy)but-1-ynyl)-4-methylbenzenesulfonamide **(*S*)-384** as a colourless oil (5.05 g, 83%). $[\alpha]_D^{20} = +20.0$ (*c* 1, DCM); FTIR (film/cm^{-1}) υ_{max}: 3036 (m), 3105 (m), 2961 (m), 2932 (m), 1681 (m), 1647 (m), 1619 (s), 1582 (s); ^{1}H NMR (500 MHz, $CDCl_3$) δ: 1.06 (s, 9H), 1.41 (d, 3H, *J* = 6.4 Hz), 2.44 (s, 3H), 3.79 (ddt, 1H, *J* = 14.6, 6.3, 1.3 Hz), 3.85 (ddt, 1H, *J* = 14.6, 6.3, 1.3 Hz), 4.61 (app. quin, 1H, *J* = 6.4 Hz), 5.11–5.17 (m, 2H), 5.62 (ddt, 1H, *J* = 17.3, 10.2, 6.3 Hz), 7.28–7.46 (m, 7H), 7.66–7.72 (m, 4H), 7.72–7.77 (m, 2H); ^{13}C NMR (100 MHz, $CDCl_3$) δ: 19.1, 21.6, 25.3, 26.5, 26.8, 54.0, 60.1, 73.2, 119.6, 127.4, 127.6, 127.8, 129.6, 131.0, 133.7, 134.8, 135.7, 135.9, 144.4; HRMS (ESI, +ve) *m/z* calcd. for $C_{30}H_{35}NNaO_3SSi$ 540.2005, found 540.2209 $(M+Na)^+$.

_N_-Allyl-_N_-(3-hydroxy-but-1-ynyl)-4-methyl-benzenesulfonamide (_S_)-385

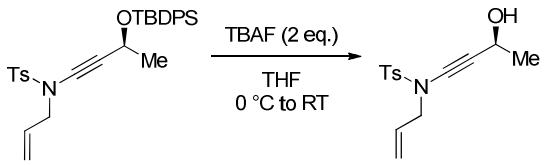

To a solution of *N*-allyl-*N*-(3-(*tert*-butyldiphenylsilyloxy)but-1-ynyl)-4-methylbenzenesulfonamide **(*S*)-384** (3.72 g, 7.20 mmol, 1.0 eq.) in THF (200 ml) at 0 ^{o}C was added TBAF (1M soln. in THF, 14.4 ml, 14.4 mmol, 2.0 eq.). The reaction mixture was allowed to stir for 2 hours whilst slowly warming to RT, until complete by TLC, followed by concentration in vacuo and subjection to flash column chromatography (10% EtOAc/Petrol 40-60^{o}) to give *N*-allyl-*N*-(3-hydroxy-but-1-ynyl)-4-methyl-benzenesulfonamide **(*S*)-385** as a faint yellow oil (1.40 g, 70%). $[\alpha]_D^{20} = -38.0$ (*c* 1, DCM); FTIR (film/cm^{-1}) υ_{max}: 2978 (m), 2929 (m), 1697 (m), 1596 (w). ^{1}H NMR (400 MHz, $CDCl_3$) δ: 1.47 (d, 3H, *J* = 6.6 Hz), 2.03 (d, 1H, *J* = 5.2 Hz), 2.49 (s, 3H), 3.93–4.04 (m, 2H), 4.67 (app quin, 1H, *J* = 6.6 Hz), 5.22–5.31 (m, 4H), 5.71 (ddt, 1H, *J* = 17.1, 10.2, 6.4 Hz), 7.39 (d, 2H, *J* = 8.3 Hz), 7.83 (d, 2H, *J* = 8.3 Hz); ^{13}C NMR (100 MHz, $CDCl_3$) δ: 21.6, 24.4, 26.5, 54.1, 58.5, 73.1, 120.0, 127.7, 129.7, 130.8, 134.6, 144.8; HRMS (ESI, +ve) *m/z* calcd. for $C_{14}H_{18}NO_3S$ 280.1007, found 280.1004 $(M+H)^+$.

(_S_)-(_E_)-_N_-Allyl-_N_-(3-hydroxybut-1-enyl)-4-methylbenzenesulfonamide (_S_)-329

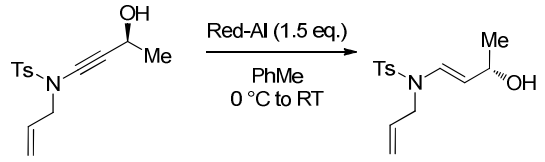

To a solution of (*S*)-*(E)*-*N*-allyl-4-methyl-*N*-(3-oxobut-1-enyl)benzenesulfonamide **(*S*)-385** (0.10 g, 0.36 mmol, 1.0 eq.) in toluene (5 ml) at 0 ^{o}C was added Vitride® (0.11 μl, 0.53 mmol, 1.5 eq.) by portionwise addition. The reaction mixture was allowed to stir whilst slowly warming to RT over 4 hours and then was quenched by the addition of Na2SO4.10H2O. After the solution cleared the reaction mixture was filtered through

celite and concentrated in vacuo to yield (*S*)-(*E*)-*N*-allyl-*N*-(3-hydroxybut-1-enyl)-4-methylbenzenesulfonamide **(*S*)-329** as a colourless oil (0.07 g, 76%). $[\alpha]_D^{20} = -11.0$ (*c* 1, DCM); Other data as previously reported for racemic compound.

(*E*)-4-(*N*-Allyl-4-methylphenylsulfonamido)but-3-en-2-yl propionate 330

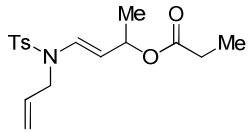

EDCi (0.54 g, 2.81 mmol) in DCM (100 ml), triethylamine (0.39 ml, 2.81 mmol), DMAP (0.02 g, 0.14 mmol), propionic acid (0.22 ml, 2.81 mmol) and (*E*)-*N*-allyl-*N*-(3-hydroxybut-1-enyl)-4-methylbenzenesulfonamide **329** (0.40 g, 1.41 mmol) in DCM (10 ml) were combined according to general procedure 1 (reaction time: 15 hours). Purification was achieved by reported procedure to afford (*E*)-4-(*N*-allyl-4-methylphenylsulfonamido)but-3-en-2-yl propionate **330** as a yellow oil (0.40 g, 84%). FTIR (film/cm^{-1}) υ_{max}: 3082 (m), 3039 (m), 2980 (m), 2931 (m), 2861 (m), 1727 (s), 1656 (s), 1597 (s); ^{1}H NMR (500 MHz, $(CD_3)_2CO$) δ: 1.10 (t, 3H, *J* = 7.6 Hz, C*H*$_3$CH$_2$-), 1.29 (d, 3H, *J* = 6.6 Hz, C*H*$_3$CH(CH-)O-), 2.25 (q, 2H, *J* = 7.6 Hz, CH$_3$C*H*$_2$-), 2.45 (s, 3H, -C$_6$H$_4$C*H*$_3$), 3.96 (qd, 2H, *J* = 15.0, 5.4 Hz, -NC*H*$_2$CHCH$_2$), 4.80 (dd, 1H, *J* = 14.2, 6.6 Hz, -NCHC*H*-), 5.09–5.17 (m, 2H, C*H*$_2$CHCH$_2$N-), 5.34 (app. quin, 1H, *J* = 6.6 Hz, CH$_3$C*H*(CH-)O-), 5.79 (ddt, 1H, *J* = 17.0, 10.3, 5.4 Hz, -NCH$_2$C*H*CH$_2$), 6.96 (d, 1H, *J* = 14.2 Hz, -NC*H*CH-), 7.29 (app. d, 2H, *J* = 7.6 Hz, Ar*H* Ts), 7.65 (d, 2H, *J* = 7.6 Hz, Ar*H* Ts) ; ^{13}C NMR (125 MHz, $(CDCl_3)$ δ: 9.1, 21.0, 21.5, 27.9, 48.0, 69.8, 110.1, 117.9, 127.0, 129.5, 129.8, 131.3, 136.1, 143.9, 173.6; HRMS (ESI, +ve) *m/z* calcd. for $C_{23}H_{27}NNaO_4S$ 436.1558, found 436.1679 $(M+Na)^+$.

(*E*)-4-(*N*-Allyl-4-methylphenylsulfonamido)but-3-en-2-yl 2-phenylacetate 331

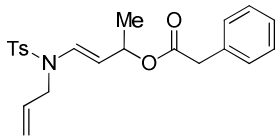

EDCi (0.68 g, 3.55 mmol) in DCM (100 ml), triethylamine (0.49 ml, 3.55 mmol), DMAP (0.02 g, 0.18 mmol), phenylacetic acid (0.48 g, 3.55 mmol) and (*E*)-*N*-allyl-*N*-(3-hydroxybut-1-enyl)-4-methylbenzenesulfonamide **329** (0.50 g, 1.78 mmol) in DCM (20 ml) were combined according to general procedure 1 (reaction time: 15 hours). Purification was achieved by reported procedure to afford (*E*)-4-(*N*-allyl-4-methylphenylsulfonamido)but-3-en-2-yl 2-phenylacetate **331** as a yellow oil (0.70 g, 98%). FTIR (film/cm^{-1}) υ_{max}: 3051 (m), 2977 (m), 2922 (m), 1727 (s), 1655 (s), 1597 (m); ^{1}H NMR (250 MHz, $(CD_3)_2CO$) δ: 1.29 (d, 3H, *J* = 6.5 Hz, C*H*$_3$CH(CH-)O-), 2.40 (s, 3H, C*H*$_3$C$_6$H$_4$-), 3.60 (s, 2H, -C*H*$_2$C$_6$H$_5$), 3.93–4.10 (m, 2H, -NC*H*$_2$CHCH$_2$), 4.88 (dd, 1H, *J* = 14.2, 6.5 Hz, -NC*H*CH-), 5.05–5.24 (m, 2H, -NCH$_2$CHC*H*$_2$), 5.37 (app quin, 1H, *J* = 6.5 Hz, CH$_3$C*H*(CH-)O-), 5.62 (ddt, 1H, *J* = 17.3, 10.4, 5.2 Hz, -NCH$_2$C*H*CH$_2$), 7.03 (d, 1H, *J* = 14.2 Hz, -NC*H*CH-), 7.23–7.37 (m, 5H, CH$_2$C$_6$*H*$_5$), 7.39 (app. d, 2H, *J* = 8.3 Hz, Ar*H*), 7.71 (app. d, 2H, *J* = 8.3 Hz, Ar*H*); ^{13}C NMR (100 MHz, CD_3Cl) *δ*: 20.9, 21.5, 41.7, 48.0, 70.7, 109.7, 117.9, 127.0 (x2), 128.5, 129.2, 129.8 (x2), 131.2, 134.2, 136.1, 143.9, 170.7; HRMS (ESI, +ve) *m/z* calcd. for $C_{22}H_{25}NNaO_4S_1$ 422.1411, found 422.1375 $(M+Na)^+$.

(*S,E*)-4-(*N*-allyl-4-methylphenylsulfonamido)but-3-en-2-yl 2-phenylacetate (*S*)-331

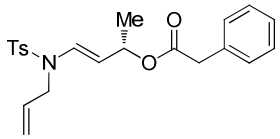

EDCi (0.68 g, 3.55 mmol) in DCM (100 ml), triethylamine (0.49 ml, 3.55 mmol), DMAP (0.02 g, 0.18 mmol), phenylacetic acid (0.48 g, 3.55 mmol) and (*S*)-(*E*)-*N*-allyl-*N*-(3-hydroxybut-1-enyl)-4-methylbenzenesulfonamide **(*S*)-329** (0.50 g, 1.78 mmol) in DCM (20 ml) were combined according to general procedure 1 (reaction time: 15 hours). Purification was achieved by reported procedure to afford (*S,E*)-4-(*N*-allyl-4-

methylphenylsulfonamido)but-3-en-2-yl 2-phenylacetate **(*S*)-331** as a yellow oil (0.53 g, 74%); $[\alpha]_D^{20}$ = -8.0 (*c* 1, DCM). All data as previously recorded for racemic compound.

(*E*)-4-(*N*-Allyl-4-methylphenylsulfonamido)but-3-en-2-yl 3-methylbutanoate 335

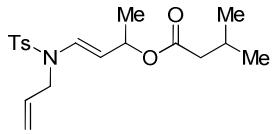

EDCi (0.54 g, 2.81 mmol) in DCM (100 ml), triethylamine (0.39 ml, 2.81 mmol), DMAP (0.02 g, 0.14 mmol), isovaleric acid (0.31 ml, 2.81 mmol) and (*E*)-*N*-allyl-*N*-(3-hydroxybut-1-enyl)-4-methylbenzenesulfonamide **329** (0.40 g, 1.41 mmol) in DCM (10 ml) were combined according to general procedure 1 (reaction time: 15 hours). Purification was achieved by reported procedure to afford (*E*)-4-(*N*-allyl-4-methylphenylsulfonamido)but-3-en-2-yl 3-methylbutanoate **335** as a yellow oil (0.45 g, 87%). FTIR (film/cm^{-1}) υ_{max}: 2960 (m), 2931 (m), 1725 (s), 1655 (s), 1597 (m); ^{1}H NMR (500 MHz, CD_2Cl_2) δ: 0.92–0.96 (m, 6H), 1.32 (d, 3H, *J* = 6.6 Hz), 2.01–2.10 (m, 1H), 2.14 (d, 2H, *J* = 6.7 Hz), 2.44 (s, 3H), 3.94–4.06 (m, 2H), 4.83 (dd, 1H, *J* = 14.1, 6.6 Hz), 5.15 (d, 1H, *J* = 11.0 Hz), 5.18 (d, 1H, *J* = 17.6 Hz), 5.38 (app. quin, 1H, *J* = 6.6 Hz), 5.64 (ddt, 1H, *J* = 17.6, 11.0, 6.3 Hz), 7.02 (d, 1H, *J* = 14.1 Hz), 7.35 (app. d, 2H, *J* = 7.7 Hz), 7.69 (app. d, 2H, *J* = 7.7 Hz); ^{13}C NMR (125 MHz, CD_2Cl_2) *δ*: 20.8, 21.2, 22.1, 25.7, 43.6, 47.9, 69.6, 110.2, 117.5, 126.9, 129.6, 129.8, 131.4, 136.0, 144.1, 172.0; HRMS (ESI, +ve) *m/z* calcd. for $C_{19}H_{27}NNaO_4S$ 388.1558, found 388.1567 $(M+Na)^+$.

(*E*)-4-(*N*-Allyl-4-methylphenylsulfonamido)but-3-en-2-yl pent-4-enoate 336

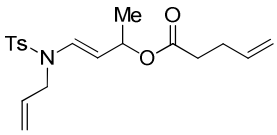

EDCi (0.54 g, 2.81 mmol) in DCM (100 ml), triethylamine (0.39 ml, 2.81 mmol), DMAP (0.02 g, 0.14 mmol), penteneoic acid (0.28 g, 2.81 mmol) and (*E*)-*N*-allyl-*N*-(3-

hydroxybut-1-enyl)-4-methylbenzenesulfonamide **329** (0.40 g, 1.41 mmol) in DCM (20 ml) were combined according to general procedure 1 (reaction time: 15 hours). Purification was achieved by reported procedure to afford (*E*)-4-(*N*-allyl-4-methylphenylsulfonamido)but-3-en-2-yl pent-4-enoate **336** as a yellow oil (0.51 g, 99%). FTIR (film/cm^{-1}) υ_{max}: 3054 (m), 2981 (m), 2918 (m), 1718 (s), 1655 (s), 1597 (m); ^{1}H NMR (500 MHz, $(CD_3)_2CO$) δ: 1.28 (d, 3H, *J* = 6.8 Hz), 2.29–2.37 (m, 4H), 2.44 (s, 3H), 3.98–4.11 (m, 2H), 4.90 (dd, 1H, *J* = 14.4, 6.7 Hz), 4.94 (dd, 1H, *J* = 10.1, 1.2 Hz), 5.04 (dd, 1H, *J* = 17.1, 1.4 Hz), 5.13 (dd, 1H, *J* = 10.1, 1.2 Hz), 5.21 (dd, 1H, *J* = 17.1, 1.2 Hz), 5.35 (app. quin, 1H, *J* = 6.8 Hz), 5.66 (ddt, 1H, *J* = 17.1, 10.1, 5.4 Hz), 5.78–5.92 (m, 1H), 7.01 (d, 1H, *J* = 14.4 Hz), 7.44 (app. d, 2H, *J* = 8.2 Hz), 7.74 (app. d, 2H, *J* = 8.2 Hz); ^{13}C NMR (125 MHz, $(CD_3)_2CO$) *δ*: 20.4, 20.5, 33.4, 34.0, 47.6, 69.7, 110.3, 114.7, 117.1, 127.0, 129.7, 129.8, 131.8, 136.3, 137.0, 144.1, 171.4; HRMS (ESI, +ve) *m/z* calcd. for $C_{19}H_{25}NNaO_4S$ 386.1402, found 386.1480 $(M+Na)^+$.

Benzyloxy-acetic acid 3-[allyl-(toluene-4-sulfonyl)-amino]-1-methyl-allyl ester 337

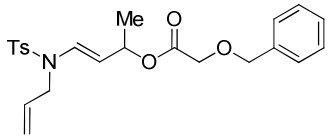

EDCi (0.54 g, 2.81 mmol) in DCM (100 ml), triethylamine (0.39 ml, 2.81 mmol), DMAP (0.02 g, 0.14 mmol), benzyloxyacetic acid (0.41 ml, 2.81 mmol) and (*E*)-*N*-allyl-*N*-(3-hydroxybut-1-enyl)-4-methylbenzenesulfonamide **329** (0.40 g, 1.41 mmol) in DCM (20 ml) were combined according to general procedure 1 (reaction time: 15 hours). Purification was achieved by reported procedure to afford benzyloxy-acetic acid 3-[allyl-(toluene-4-sulfonyl)-amino]-1-methyl-allyl ester **337** as a yellow oil (0.54 g, 87%). FTIR (film/cm^{-1}) υ_{max}: 3051 (m), 2971 (m), 2934 (m), 1744 (s), 1655 (s), 1597 (m); ^{1}H NMR (500 MHz, $(CD_3)_2CO$) δ: 1.32 (d, 3H, *J* = 6.8 Hz), 2.40 (s, 3H), 3.98–4.15 (m, 4H), 4.60 (s, 2H), 4.93 (dd, 1H, *J* = 14.3, 6.8 Hz), 4.93 (dq, 1H, *J* = 10.5, 1.4 Hz), 5.21 (dq, 1H, *J* = 17.2, 1.5 Hz), 5.46 (app. quin, 1H, *J* = 6.8 Hz), 5.65 (ddt, 1H, *J* = 17.2, 10.5, 5.2 Hz), 7.08 (d, 1H, *J* = 14.3 Hz), 7.28–7.43 (m, 7H), 7.74 (app. d, 2H, *J* = 8.1 Hz); ^{13}C NMR (125 MHz, $(CD_3)_2CO$) *δ*: 20.4, 20.5, 47.6, 67.3, 70.5, 72.6,

109.9,117.1, 127.0, 127.5, 127.7, 128.2, 129.8, 130.2, 131.7, 136.3, 138.1, 144.1, 169.3; HRMS (ESI, +ve) *m/z* calcd. for $C_{23}H_{27}NNaO_5S$ 452.1508, found 452.1543 $(M+Na)^+$.

Phenylsulfanyl-acetic acid 3-[allyl-(toluene-4-sulfonyl)-amino]-1-methyl-allyl ester 338

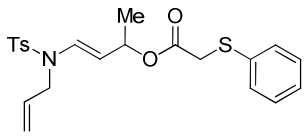

EDCi (0.54 g, 2.81 mmol) in DCM (100 ml), triethylamine (0.39 ml, 2.81 mmol), DMAP (0.02 g, 0.14 mmol), thiophenylacetic acid (0.47 g, 2.81 mmol) and (*E*)-*N*-allyl-*N*-(3-hydroxybut-1-enyl)-4-methylbenzenesulfonamide **329** (0.40 g, 1.41 mmol) in DCM (20 ml) were combined according to general procedure 1 (reaction time: 15 hours). Purification was achieved by reported procedure to afford phenylsulfanyl-acetic acid 3-[allyl-(toluene-4-sulfonyl)-amino]-1-methyl-allyl ester **338** as a yellow oil (0.56 g, 92%). FTIR (film/cm^{-1}) υ_{max}: 3079 (m), 2980 (m), 2919 (m), 1726 (s), 1655 (s), 1597 (m); ^{1}H NMR (500 MHz, $(CD_3)_2CO$) δ: 1.24 (d, 3H, *J* = 7.2 Hz), 2.40 (s, 3H), 3.90–4.07 (m, 2H), 4.83 (dd, 1H, *J* = 14.3, 7.2 Hz), 5.09 (dq, 1H, *J* = 10.4, 1.5 Hz), 5.17 (dq, 1H, *J* = 17.1, 1.5 Hz), 5.34 (app. quin, 1H, *J* = 7.2 Hz), 5.62 (ddt, 1H, *J* = 17.1, 10.4, 5.2 Hz), 7.03 (d, 1H, *J* = 14.3 Hz), 7.17–7.24 (m, 1H), 7.25–7.34 (m, 2H), 7.35–7.45 (m, 4H), 7.71 (app. d, 2H, *J* = 8.2 Hz); ^{13}C NMR (125 MHz, $(CD_3)_2CO$) *δ*: 25.5, 30.4, 41.0, 52.8, 72.3, 76.4, 114.7, 122.3, 131.6, 132.1, 134.3, 135.0, 135.4, 136.9, 140.8, 141.5, 149.3, 173.6; HRMS (ESI, +ve) *m/z* calcd. for $C_{22}H_{25}NNaO_4S_2$ 454.1123, found 454.1126 $(M+Na)^+$.

(*E*)-4-(*N*-Allyl-4-methylphenylsulfonamido)but-3-en-2-yl 2-(2-iodophenyl)acetate 340

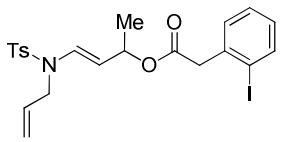

EDCi (0.54 g, 2.81 mmol) in DCM (100 ml), triethylamine (0.39 ml, 2.81 mmol), DMAP (0.02 g, 0.14 mmol), 2-Iodo phenylacetic acid (0.74 g, 2.81 mmol) and (*E*)-*N*-allyl-*N*-(3-hydroxybut-1-enyl)-4-methylbenzenesulfonamide **329** (0.40 g, 1.41 mmol) in

DCM (20 ml) were combined according to general procedure 1 (reaction time: 15 hours). Purification was achieved by reported procedure to afford (*E*)-4-(*N*-allyl-4-methylphenylsulfonamido)but-3-en-2-yl 2-(2-iodophenyl)acetate **340** as a yellow oil (0.64 g, 86%). FTIR (film/cm^{-1}) υ_{max}: 2978 (m), 2922 (m), 1727 (s), 1655 (s), 1596 (w); ^{1}H NMR (500 MHz, $(CD_3)_2CO$) δ: 1.31 (d, 3H, *J* = 6.6 Hz), 2.44 (s, 3H), 3.77 (app. d, 2H), 3.97–4.08 (m, 2H), 4.91 (dd, 1H, *J* = 14.2, 6.6 Hz), 5.12 (app. dq, 1H, *J* = 10.4, 1.4 Hz), 5.20 (app. dq, 1H, *J* = 17.3, 1.7 Hz), 5.39 (app. quin, 1H, *J* = 6.6 Hz), 5.65 (ddt, 1H, *J* = 17.3, 10.4, 5.0 Hz), 7.00–7.08 (m, 2H), 7.35–7.43 (m, 4H), 7.72 (app. d, 2H, *J* = 8.2 Hz), 7.88 (d, 1H, *J* = 7.8 Hz); ^{13}C NMR (125 MHz, $(CD_3)_2CO$) *δ*: 20.4, 20.5, 46.0, 47.6, 70.6, 100.6, 109.9, 117.1, 127.0, 128.4, 128.8, 129.8, 129.9, 131.0, 131.8, 136.4, 138.5, 139.2, 144.0, 169.0; HRMS (ESI, +ve) *m/z* calcd. for $C_{22}H_{24}INNaO_4S$ 548.0368, found 548.0407 $(M+Na)^+$.

(*E*)-4-(*N*-Allyl-4-methylphenylsulfonamido)but-3-en-2-yl 2-(4-methoxyphenyl)acetate 341

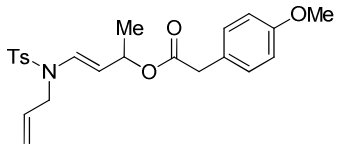

EDCi (0.54 g, 2.81 mmol) in DCM (100 ml), triethylamine (0.39 ml, 2.81 mmol), DMAP (0.02 g, 0.14 mmol), 4-methoxy phenylacetic acid (0.47 g, 2.81 mmol) and (E)-*N*-allyl-*N*-(3-hydroxybut-1-enyl)-4-methylbenzenesulfonamide **329** (0.40 g, 1.41 mmol) in DCM (20 ml) were combined according to general procedure 1 (reaction time: 15 hours). Purification was achieved by reported procedure to afford (*E*)-4-(*N*-allyl-4-methylphenylsulfonamido)but-3-en-2-yl 2-(4-methoxyphenyl)acetate **341** as a yellow oil (0.54 g, 81%). FTIR (film/cm^{-1}) υ_{max}: 2978 (m), 2943 (m), 1726 (s), 1655 (s), 1613 (m), 1597 (w); ^{1}H NMR (250 MHz, $(CD_3)_2CO$) δ: 1.27 (d, 3H, *J* = 6.5 Hz), 2.42 (s, 3H), 3.50 (2H, s), 3.77 (s, 3H), 3.92–4.05 (m, 2H), 4.86 (dd, 1H, *J* = 14.1, 6.5 Hz), 5.09 (dd, 1H, *J* = 10.7, 1.5 Hz), 5.16 (dd, 1H, *J* = 17.1, 1.5 Hz), 5.37 (app. quin, 1H, *J* = 6.5 Hz), 5.59 (ddt, 1H, *J* = 17.1, 10.7, 5.4 Hz), 6.85 (d, 2H, *J* = 8.5 Hz), 6.99 (d, 1H, *J* = 14.1 Hz), 7.17 (app. d, 2H, *J* = 8.3 Hz), 7.37 (app. d, 2H, *J* = 8.2 Hz), 7.68 (d, 2H, *J* = 8.2 Hz); ^{13}C NMR (125 MHz, $(CD_3)_2CO$) *δ*: 21.3, 21.4, 41.0, 48.4, 55.4, 71.0, 111.0, 114.5,

118.0, 127.4, 127.8, 127.9, 130.7, 131.0, 132.6, 137.2, 144.9, 159.6, 171.3; HRMS (ESI, +ve) *m/z* calcd. for $C_{23}H_{27}NNaO_5S_1$ 452.1508, found 452.1463 $(M+Na)^+$.

(*E*)-4-(*N*-Allyl-4-methylphenylsulfonamido)but-3-en-2-yl 2-(4-(trifluoromethyl)phenyl)acetate 342

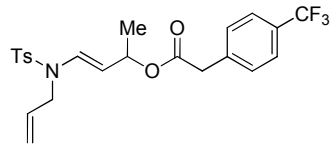

EDCi (0.54 g, 2.81 mmol) in DCM (100 ml), triethylamine (0.39 ml, 2.81 mmol), DMAP (0.02 g, 0.14 mmol), 4-trifluoro tolyl phenylacetic acid (0.57 g, 2.81 mmol) and (*E*)-*N*-allyl-*N*-(3-hydroxybut-1-enyl)-4-methylbenzenesulfonamide **329** (0.40 g, 1.41 mmol) in DCM (20 ml) were combined according to general procedure 1 (reaction time: 15 hours). Purification was achieved by reported procedure to afford (*E*)-4-(*N*-allyl-4-methylphenylsulfonamido)but-3-en-2-yl 2-(4-(trifluoromethyl)phenyl)acetate **342** as a yellow oil (0.57 g, 86%). FTIR (film/cm^{-1}) υ_{max}: 3015 (w), 2988 (m), 2937 (m), 1727 (s), 1699 (s), 1656 (m), 1596 (w); ^{1}H NMR (500 MHz, $(CD_3)_2CO$) δ: 1.30 (d, 3H, *J* = 6.8 Hz), 2.42 (s, 3H), 3.74 (2H, s), 3.95–4.06 (m, 2H), 4.88 (dd, 1H, *J* = 14.3, 6.8 Hz), 5.09 (app. d, 1H, *J* = 10.7 Hz), 5.17 (app. d, 1H, *J* = 17.2 Hz), 5.38 (app. quin, 1H, *J* = 6.8 Hz), 5.61 (ddt, 1H, *J* = 17.2, 10.7, 5.1 Hz), 7.03 (d, 1H, *J* = 14.3 Hz), 7.39 (app. d, 2H, *J* = 8.3 Hz), 7.52 (app. d, 2H, *J* = 8.3 Hz), 7.66 (app. d, 2H, *J* = 8.3 Hz), 7.71 (app. d, 2H, *J* = 8.3 Hz); ^{13}C NMR (125 MHz, $(CD_3)_2CO$) *δ*: 20.2, 20.4, 40.5, 47.4, 70.6, 109.6, 116.9, 124.3 (q, *J* = 271.4 Hz), 124.9 (q, *J* = 3.6 Hz), 126.8, 128.3 (q, *J* = 32.0 Hz), 129.6, 129.8, 129.9, 131.4, 136.1, 139.1, 143.9, 169.3; HRMS (ESI, +ve) *m/z* calcd. for $C_{23}H_{23}F_3NO_4S$ 466.1299, found 466.1311 $(M+H)^+$.

(*E*)-4-(*N*-Allyl-4-methylphenylsulfonamido)but-3-en-2-yl 2-(4-nitrophenyl)acetate 343

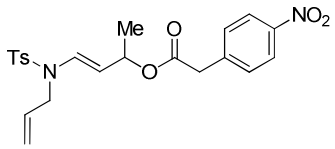

EDCi (0.54 g, 2.81 mmol) in DCM (100 ml), triethylamine (0.39 ml, 2.81 mmol), DMAP (0.02 g, 0.14 mmol), 4-nitro phenylacetic acid (0.51 g, 2.81 mmol) and (*E*)-*N*-allyl-*N*-(3-hydroxybut-1-enyl)-4-methylbenzenesulfonamide **329** (0.40 g, 1.41 mmol) in DCM (20 ml) were combined according to general procedure 1 (reaction time: 15 hours). Purification was achieved by reported procedure to afford (*E*)-4-(*N*-allyl-4-methylphenylsulfonamido)but-3-en-2-yl 2-(4-nitrophenyl)acetate **343** as an orange oil (0.54 g, 86%). FTIR (film/cm^{-1}) υ_{max}: 3018 (w), 2988 (m), 2967 (m), 1727 (s), 1698 (s), 1656 (m), 1599 (w), 1522 (m); ^{1}H NMR (500 MHz, $(CD_3)_2CO$) δ: 1.29 (d, 3H, *J* = 6.7 Hz), 2.41 (s, 3H), 3.80 (2H, s), 3.95–4.05 (m, 2H), 4.87 (dd, 1H, *J* = 14.5, 6.7 Hz), 5.08 (dq, 1H, *J* = 10.7, 1.95 Hz), 5.15 (dq, 1H, *J* = 17.2, 1.3 Hz), 5.38 (app. quin, 1H, *J* = 6.7 Hz), 5.59 (ddt, 1H, *J* = 17.2, 10.7, 5.1 Hz), 7.00 (d, 1H, *J* = 14.5 Hz), 7.38 (app. d, 2H, *J* = 7.9 Hz), 7.57 (app. d, 2H, *J* = 8.7 Hz), 7.69 (app. d, 2H, *J* = 7.9 Hz), 8.18 (app. d, 2H, *J* = 8.7 Hz); ^{13}C NMR (100 MHz, $(CD_3)_2CO$) *δ*: 20.3, 20.5, 40.6, 47.5, 70.9, 109.6, 117.1, 123.3, 126.9, 129.8, 130.1, 130.5, 131.6, 136.3, 142.5, 144.1, 147.0, 169.2; HRMS (ESI, +ve) *m/z* calcd. for $C_{44}H_{48}N_4NaO_{12}S_2$ 911.2613, found 911.2604 $(2M+Na)^+$.

(*E*)-4-(*N*-Allyl-4-methylphenylsulfonamido)but-3-en-2-yl 2-(2,4-dichlorophenyl)acetate 344

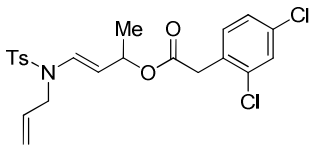

EDCi (0.54 g, 2.81 mmol) in DCM (100 ml), triethylamine (0.39 ml, 2.81 mmol), DMAP (0.02 g, 0.14 mmol), 2,4-dichlorophenylacetic acid (0.58 g, 2.81 mmol) and (*E*)-*N*-allyl-*N*-(3-hydroxybut-1-enyl)-4-methylbenzenesulfonamide **329** (0.40 g, 1.41 mmol)

in DCM (20 ml) were combined according to general procedure 1 (reaction time: 15 hours). Purification was achieved by reported procedure to afford (*E*)-4-(*N*-allyl-4-methylphenylsulfonamido)but-3-en-2-yl 2-(2,4-dichlorophenyl)acetate **344** as a yellow oil (0.55 g, 82%). FTIR (film/cm^{-1}) υ_{max}: 3091 (m), 2978 (m), 2937 (m), 1729 (s), 1655 (s), 1614 (s), 1591 (s), 1509 (s); ^{1}H NMR (500 MHz, $(CD_3)_2CO$) δ: 1.29 (d, 3H, *J* = 6.7 Hz), 2.44 (s, 3H), 3.76 (2H, s), 3.97–4.07 (m, 2H), 4.89 (dd, 1H, *J* = 14.2, 6.7 Hz), 5.12 (app d, 1H, *J* = 10.3 Hz), 5.19 (app d, 1H, *J* = 17.2 Hz), 5.38 (app. quin, 1H, *J* = 6.7 Hz), 5.63 (ddt, 1H, *J* = 17.2, 10.3, 5.1 Hz), 7.01 (d, 1H, *J* = 14.2 Hz), 7.32–7.47 (m, 4H), 7.50 (d, 1H, *J* = 1.9 Hz), 7.71 (app. d, 2H, *J* = 8.2 Hz); ^{13}C NMR (125 MHz, $(CD_3)_2CO$) *δ*: 20.4, 20.5, 38.4, 47.6, 70.8, 109.7, 117.1, 126.9, 127.2, 128.7, 129.8, 129.9, 131.7, 132.2, 133.0, 133.1, 135.1, 136.4, 144.0, 168.7; HRMS (ESI, +ve) *m/z* calcd. for $C_{22}H_{23}Cl_2N_1NaO_4S_1$ 490.0617, found 490.0614 $(M+Na)^+$.

(*E*)-4-(*N*-Allyl-4-methylphenylsulfonamido)but-3-en-2-yl 2-(2,4-dimethoxyphenyl)acetate 345

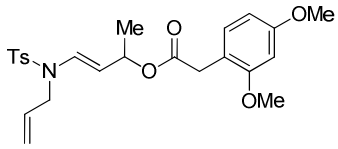

EDCi (0.54 g, 2.81 mmol) in DCM (100 ml), triethylamine (0.39 ml, 2.81 mmol), DMAP (0.02 g, 0.14 mmol), 2,4-dimethoxyphenylacetic acid (0.56 g, 2.81 mmol) and (*E*)-*N*-allyl-*N*-(3-hydroxybut-1-enyl)-4-methylbenzenesulfonamide **329** (0.40 g, 1.41 mmol) in DCM (20 ml) were combined according to general procedure 1 (reaction time: 15 hours). Purification was achieved by reported procedure to afford (*E*)-4-(*N*-allyl-4-methylphenylsulfonamido)but-3-en-2-yl 2-(2,4-dimethoxyphenyl)acetate **345** as a clear oil (0.56 g, 86%). FTIR (film/cm^{-1}) υ_{max}: 3061 (w), 2988 (m), 2937 (m), 2838 (m), 1728 (s), 1656 (s), 1614 (s), 1590 (s), 1509 (s); ^{1}H NMR (500 MHz, $(CD_3)_2CO$) δ: 1.27 (d, 3H, *J* = 6.6 Hz), 2.43 (s, 3H), 3.47 (2H, s), 3.76 (3H, s), 3.79 (3H, s), 3.94–4.09 (m, 2H), 4.89 (dd, 1H, *J* = 14.2, 6.6 Hz), 5.17 (dq, 1H, *J* = 10.3, 1.4 Hz), 5.21 (dq, 1H, *J* = 17.1, 1.4 Hz), 5.34 (app. quin, 1H, *J* = 6.6 Hz), 5.65 (ddt, 1H, *J* = 17.1, 10.3, 5.1 Hz), 6.44–6.49 (m, 1H), 6.51–6.57 (m, 1H), 6.98 (d, 1H, *J* = 14.2 Hz), 7.07 (d, 1H, *J* = 8.3 Hz), 7.39 (app. d, 2H, *J* = 8.3 Hz), 7.71 (app. d, 2H, *J* = 8.3 Hz); ^{13}C NMR (125 MHz,

$(CD_3)_2CO$) δ: 20.5 (x2), 35.0, 47.6, 54.6, 54.9, 69.7, 98.2, 104.2, 110.3, 115.7, 117.1, 127.0, 129.4, 129.8, 130.9, 131.8, 136.3, 144.0, 158.5, 160.3, 170.5; HRMS (ESI, +ve) *m/z* calcd. for $C_{24}H_{29}NNaO_6S$ 482.1613, found 482.1653 $(M+Na)^+$.

(*E*)-4-(*N*-Allyl-4-methylphenylsulfonamido)but-3-en-2-yl 2-(benzo[d][1,3]dioxol-5-yl)acetate 346

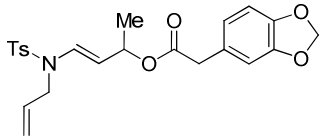

EDCi (0.54 g, 2.81 mmol) in DCM (100 ml), triethylamine (0.39l, 2.81 mmol), DMAP (0.02 g, 0.14 mmol), 3,4-methylenedioxyphenylacetic acid (0.51 g, 2.81 mmol) and (*E*)-*N*-allyl-*N*-(3-hydroxybut-1-enyl)-4-methylbenzenesulfonamide **329** (0.40 g, 1.41 mmol) in DCM (20 ml) were combined according to general procedure 1 (reaction time: 15 hours). Purification was achieved by reported procedure to afford (*E*)-4-(*N*-allyl-4-methylphenylsulfonamido)but-3-en-2-yl 2-(benzo[d][1,3]dioxol-5-yl)acetate **346** as a yellow oil (0.54 g, 86%). FTIR (film/cm^{-1}) υ_{max}: 3049 (m), 2916 (m), 1729 (s), 1655 (s), 1503 (s); ^1H NMR (500 MHz, CD_3Cl) δ: 1.30 (d, 3H, J = 6.6 Hz), 2.41 (s, 3H), 3.46 (2H, s), 3.89–4.01 (m, 2H), 4.76 (dd, 1H, J = 14.3, 6.6 Hz), 5.10 (app. d, 1H, J = 10.3 Hz), 5.10 (app. d, 1H, J = 17.0 Hz), 5.32 (app. quin, 1H, J = 6.6 Hz), 5.50 (ddt, 1H, J = 17.0, 10.3, 5.3 Hz), 5.91 (s, 2H), 6.65–6.75 (m, 3H), 6.97 (d, 1H, J = 14.3 Hz), 7.26 (app. d, 2H, J = 7.8 Hz), 7.63 (app. d, 2H, J = 7.8 Hz); ^{13}C NMR (125 MHz, CD_3Cl) δ: 20.9, 21.5, 30.9, 41.2, 47.9, 70.6, 100.9, 108.2, 109.6 (x2), 117.8, 122.2, 127.0, 127.1, 127.7, 129.7, 129.8, 131.2, 136.0, 143.9, 146.6, 147.7, 170.7; HRMS (ESI, +ve) *m/z* calcd. for $C_{23}H_{25}NNaO_6S$ 466.1300, found 466.1295 $(M+Na)^+$.

<u>*N*-Benzyl-4-methylbenzenesulfonamide</u> 316

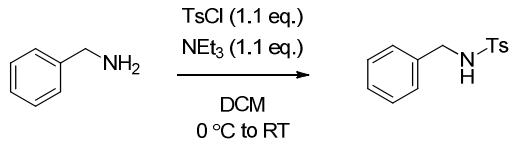

To a solution of *p*-toluenesulfonyl chloride (6.12 g, 32.1 mmol, 1.1 eq.) and triethylamine (4.46 ml, 32.1 mmol, 1.1 eq.) in DCM (70 ml) at 0 ^{o}C was added benzylamine (5.00 g, 29.2 mmol, 1.0 eq.) by dropwise addition. The reaction mixture was stirred for 1.5 hours under nitrogen at 0 ^{o}C, poured onto brine and washed with brine (3 × 100 ml), the organics were dried over $MgSO_4$ and concentrated *in vacuo* to yield a white solid which was subjected to flash column chromatography (15% EtOAc/Petrol 40-60^{o}) to yield *N*-benzyl-4-methylbenzenesulfonamide **316** as a white crystalline solid (6.71 g, 88%). M.p. 111–114 °C; ^{1}H NMR (250 MHz, $CDCl_3$) δ: 2.47 (s, 3H), 4.15 (s, 2H), 4.81 (br s, 1H), 7.10–7.48 (m, 7H), 7.78 (app. d, 1H, J = 8.3 Hz); ^{13}C NMR (250 MHz, $CDCl_3$) δ 21.5, 47.8, 127.2, 127.8, 127.9, 128.7, 129.7, 136.3, 136.8, 143.5. All analytical data in accordance with commercial sources.

<u>(*E*)-*N*-Benzyl-4-methyl-*N*-(3-oxobut-1-enyl)benzenesulfonamide</u> 328

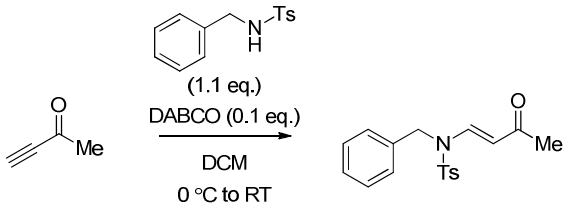

To a solution of *N*-benzyl-4-methylbenzenesulfonamide **316** (6.90 g, 26.4 mmol, 1.0 eq.), DABCO (0.37 g, 0.26 mmol, 0.1 Eq) in DCM (200 ml) at 0 ^{o}C was added butyn-3-one (2.00 g, 29.41 mmol, 1.1 Eq) and the reaction mixture was stirred for 15 hours whilst slowly warming to RT. The reaction mixture was then extracted with 3N HCl (3 × 200 ml) and then 5% NaOH (3 × 200 ml), dried over $MgSO_4$ and concentrated in vacuo to give an amorphous orange oil which was triturated with EtOAc/Petrol 40-60^{o} to give (*E*)-*N*-benzyl-4-methyl-*N*-(3-oxobut-1-enyl)benzenesulfonamide **328** as a cream solid (total yield after a second trituration of mother liquor = 7.10 g, 72%). M.p. 91–93

°C; FTIR (film/cm^{-1}) υ_{max}: 3069 (m), 3039 (m), 2970 (m), 2925 (m); ^{1}H NMR (500 MHz, $CDCl_3$) δ: 2.16 (s, 3H), 2.46 (s, 3H), 4.62 (s, 2H), 5.36 (d, 1H, *J* = 14.9 Hz), 7.14–7.40 (m, 7H), 7.72 (d, 2H, *J* = 8.6 Hz), 8.10 (d, 1H, *J* = 14.9 Hz); ^{13}C NMR (500 MHz, $CDCl_3$) δ: 21.6, 27.6, 49.7, 109.7, 126.7, 127.2, 127.8, 128.8, 130.2, 133.8, 135.2, 141.3, 145.0, 196.4; HRMS (ESI, +ve) *m/z* calcd. for $C_{18}H_{20}NO_3S$ 330.1164, found 330.1297 $(M+H)^+$.

(*E*)-*N*-Benzyl-*N*-(3-hydroxybut-1-enyl)-4-methylbenzenesulfonamide 323

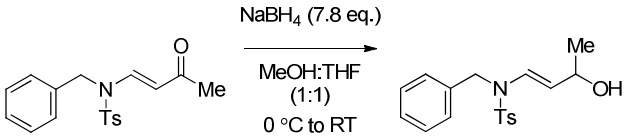

To a solution of (*E*)-*N*-benzyl-4-methyl-*N*-(3-oxobut-1-enyl)benzenesulfonamide **328** (2.00 g, 6.07 mmol, 1.0 eq.) in THF:MeOH (50 ml:50 ml) at 0 °C was added $NaBH_4$ (1.75 g, 47.4 mmol, 7.8 eq.) by portionwise addition. The reaction mixture was allowed to stir whilst slowly warming to RT over 12 hours and then was poured onto sat. NaCl (200 ml) and extracted with DCM (3 × 150 ml), dried over $MgSO_4$, filtered and concentrated *in vacuo* to give (*E*)-*N*-benzyl-*N*-(3-hydroxybut-1-enyl)-4-methylbenzenesulfonamide **323** as an orange oil (1.97 g, 98%). FTIR (film/cm^{-1}) υ_{max}: 3375 (b), 3033 (m), 2971 (m), 2924 (m), 1656 (s), 1597 (s), 1542 (w); ^{1}H NMR (500 MHz, $(CD_3)_2CO$) δ: 1.03 (3H, d, *J* = 6.4 Hz), 2.44 (3H, s), 3.66 (3H, d, *J* = 4.3 Hz), 4.14–4.22 (1H, m), 4.49–4.60 (2H, m), 4.87 (1H, dd, *J* = 14.2, 6.4 Hz), 6.90 (1H, d, *J* = 14.2 Hz), 7.21–7.28 (1H, m), 7.28–7.38 (4H, m), 7.44 (2H, d, *J* = 8.2 Hz), 7.76 (2H, d, *J* = 8.2 Hz); ^{13}C NMR (500 MHz, $CDCl_3$) δ: 21.4, 24.8, 50.0, 66.8, 118.2, 126.7, 127.8 (x2), 128.0, 129.1, 130.7, 137.2 (x2), 144.8; HRMS (ESI, +ve) *m/z* calcd. for $C_{18}H_{21}NNaO_3S$ 354.1140, found 354.1323 $(M+Na)^+$.

(*E*)-4-(*N*-Benzyl-4-methylphenylsulfonamido)but-3-en-2-yl pent-4-enoate 380

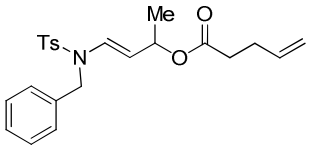

EDCi (0.46 g, 2.40 mmol) in DCM (100 ml), triethylamine (0.33 ml, 2.81 mmol), DMAP (0.02 g, 0.12 mmol), pentenoic acid (0.24 ml, 2.81 mmol) and (*E*)-*N*-benzyl-*N*-(3-hydroxybut-1-enyl)-4-methylbenzenesulfonamide **323** (0.40 g, 1.20 mmol) in DCM (20 ml) were combined according to general procedure 1 (reaction time: 15 hours). Purification was achieved by reported procedure to afford (*E*)-4-(*N*-benzyl-4-methylphenylsulfonamido)but-3-en-2-yl pent-4-enoate **380** as a white solid (0.47 g, 94%). M.p. 100–103 ˚C; FTIR (film/cm^{-1}) υ_{max}: 3082 (m), 3039 (m), 2980 (m), 2931 (m); ^{1}H NMR (500 MHz, $(CD_3)_2CO$) δ: 1.15 (d, 3H, *J* = 6.6 Hz), 2.17–2.34 (m, 4H), 2.45 (s, 3H), 4.58 (d, 1H, *J* = 16.1 Hz), 4.60 (d, 1H, *J* = 16.1 Hz), 4.80 (app. dd, 1H, *J* = 14.2, 6.6 Hz), 4.93 (app. dd, 1H, *J* = 9.7, 1.7 Hz), 5.01 (app. dd, 1H, *J* = 17.0, 1.7 Hz), 5.28 (app. quin, 1H, *J* = 6.6 Hz), 5.79 (ddt, 1H, *J* = 17.0, 9.7, 7.1 Hz), 7.05 (d, 1H, *J* = 14.2 Hz), 7.23–7.30 (m, 1H), 7.30–7.37 (m, 4H), 7.46 (app. d, 2H, *J* = 8.2 Hz), 7.78 (app. d, 2H, *J* = 8.2 Hz); ^{13}C NMR (125 MHz, CD_3Cl) *δ*: 19.7, 20.5, 27.8, 32.8, 48.3, 68.7, 109.9, 114.3, 125.8, 126.0, 126.3, 127.4, 128.5, 128.8, 134.0, 134.8, 135.6, 142.9, 171.0; HRMS (ESI, +ve) *m/z* calcd. for $C_{23}H_{27}NNaO_4S$ 436.1558, found 436.1679 $(M+Na)^+$.

6.3.4. *N*-Sulfonamide Rearrangement Products

(*anti-E*)-Methyl 3-(*N*-allyl-4-methylphenylsulfonamido)-2-phenylhex-4-enoate 333

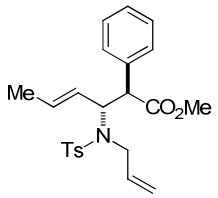

LiHMDS (1M in toluene, 0.63 ml, 0.63 mmol), TMSCl (0.19 ml, 2.91 mmol) and (*E*)-4-(*N*-allyl-4-methylphenylsulfonamido)but-3-en-2-yl 2-phenylacetate **331** (0.10 g, 0.48 mmol) in THF (1 ml) was combined according to general procedure 3 (reaction time : 75 minutes). Treatment with diazomethane and purification by flash chromatography afforded (*anti-E*)-methyl 3-(*N*-allyl-4-methylphenylsulfonamido)-2-phenylhex-4-enoate **333** as a white solid (0.06 g, 57%, d.r. >25:1). M.p. 103–104 ˚C; FTIR (film/cm^{-1}) υ_{max}: 3032 (m), 2950 (m), 2855 (m), 1734 (s), 1668 (w), 1598 (m); ^{1}H NMR (500 MHz, CD_3Cl) δ: 1.28 (d, 3H, *J* = 4.8 Hz, C*H*$_3$CH-), 2.33 (s, 3H, C*H*$_3$C$_6$H$_4$-), 3.55 (s, 3H, -CO$_2$C*H*$_3$), 3.62–3.87 (m, 2H, -NC*H*$_2$CHCH$_2$), 4.19 (d, 1H, *J* = 11.2 Hz, -C*H*CO$_2$CH$_3$), 4.68 (dd, 1H, *J* = 11.2, 7.4 Hz, -NC*H*(CH-)CH-), 4.99–5.30 (m, 4H, C*H*$_2$C*H*CH$_2$N(Ts)CH(CH-)CHC*H*CH$_3$), 5.63 (ddt, 1H, *J* = 17.0, 10.3, 6.5 Hz, -NCH(CH-)C*H*-), 7.08–7.30 (m, 7H, Ar*H*), 7.65 (app. d, 2H, *J* = 8.2 Hz, ArH Ts); ^{13}C NMR (125 MHz, CD_3Cl) *δ*: 17.6, 21.4, 50.1, 52.0, 55.7, 63.7, 118.1, 125.9, 127.7, 127.8, 128.5, 128.9, 129.2, 131.8, 134.9, 135.8, 137.8, 143.1, 172.5; HRMS (ESI, +ve) *m/z* calcd. for $C_{23}H_{28}NO_4S$ 414.1739, found 414.1734 $(M+H)^+$.

(*2R,3R,E*)-methyl 3-(*N*-allyl-4-methylphenylsulfonamido)-2-phenylhex-4-enoate (*S*)-333

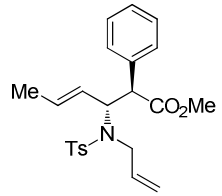

LiHMDS (1M in toluene, 0.63 ml, 0.63 mmol), TMSCl (0.19 ml, 2.91 mmol) and (*S,E*)-4-(*N*-allyl-4-methylphenylsulfonamido)but-3-en-2-yl 2-phenylacetate **(*S*)-331** (0.10 g, 0.48 mmol) in THF (1 ml) was combined according to general procedure 3 (reaction time : 75 minutes). Treatment with diazomethane and purification by flash chromatography afforded (*2R,3R,E*)-methyl 3-(*N*-allyl-4-methylphenylsulfonamido)-2-phenylhex-4-enoate **(*S*)-333** as a white solid (0.08 g, 71%, d.r. >25:1). M.p. 105–107 ˚C; $[\alpha]_D^{20}$ = -15.0 (*c* 1, DCM). All other data as previously recorded for racemic compound.

(*anti-E*)-Methyl 3-(*N*-allyl-4-methylphenylsulfonamido)-2-methylhex-4-enoate 334

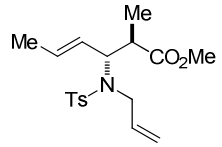

LiHMDS (1M in toluene, 1.34 ml, 1.34 mmol), triethylamine (1.81 ml, 13.4 mmol) and (*E*)-4-(*N*-allyl-4-methylphenylsulfonamido)but-3-en-2-yl propionate **330** (0.10 g, 0.30 mmol) in THF (1 ml) was combined according to general procedure 4 (reaction time : 75 minutes). Treatment with diazomethane and purification by flash chromatography afforded (*anti-E*)-methyl 3-(*N*-allyl-4-methylphenylsulfonamido)-2-methylhex-4-enoate **334** as a white solid (0.06 g, 55%, d.r. >25:1). M.p. 88–90 ˚C; FTIR (film/cm^{-1}) υ_{max}: 2966 (m), 2916 (m), 1735 (s), 165s (m); ^{1}H NMR (500 MHz, CD_3Cl) δ: 1.06 (d, 3H, *J* = 6.9 Hz), 1.51 (dd, 3H, *J* = 6.4, 1.5 Hz), 2.39 (3H, s), 3.02 (ddt, 2H, *J* = 10.1, 7.8, 6.9 Hz), 2.83 (s, 3H), 3.69–3.85 (s, 2H), 4.27 (app. t, 1H, *J* = 10.1 Hz), 5.07–5.18 (m, 2H), 5.41 (ddq, 1H, *J* = 15.1, 10.1, 1.5 Hz), 5.55 (dq, 1H, *J* = 15.1, 6.4 Hz), 5.71 (ddt, 1H, *J*

= 17.3, 10.2, 6.5 Hz), 7.26 (app. d, 2H, *J* = 8.2 Hz), 7.69 (app. d, 2H, *J* = 8.2 Hz); ^{13}C NMR (125 MHz, CD_3Cl) *δ*: 15.6, 17.7, 21.4, 43.4, 49.4, 51.7, 64.1, 117.6, 126.2, 127.7, 129.1, 132.1, 135.3, 137.8, 142.9, 175.0; HRMS (ESI, +ve) *m/z* calcd. for $C_{18}H_{25}NO_4S$ 352.1582, found 352.1577 $(M+H)^+$.

(*anti-E*)-Methyl 3-(*N*-allyl-4-methylphenylsulfonamido)-2-(4-(trifluoromethyl)phenyl)hex-4-enoate 342

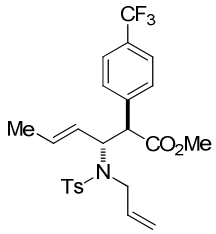

LiHMDS (1M in toluene, 1.07 ml, 1.07 mmol), TMSCl (0.33 ml, 4.94 mmol) and (I)-4-(*N*-allyl-4-methylphenylsulfonamido)but-3-en-2-yl 2-(4-(trifluoromethyl)phenyl)acetate **357** (0.20 g, 0.82 mmol) in THF (2 ml) was combined according to general procedure 3 (reaction time : 75 minutes). Treatment with diazomethane and purification by flash chromatography afforded (*anti-E*)-methyl 3-(*N*-allyl-4-methylphenylsulfonamido)-2-(4-(trifluoromethyl)phenyl)hex-4-enoate **342** as a yellow solid (0.11 g, 54%, d.r. 12:1). M.p. 104–106 ˚C; FTIR (film/cm^{-1}) υ_{max}: 3034 (w), 2951 (m), 2922 (m), 1735 (s), 1669 (w), 1598 (m), 1512 (m); ^{1}H NMR (500 MHz, CD_3Cl) δ: 1.37 (d, 3H, *J* = 4.5 Hz), 2.41 (s, 3H), 3.66 (s, 3H), 3.74–3.89 (m, 2H), 4.39 (d, 1H, *J* = 11.3 Hz), 4.73 (dd, 1H, *J* = 11.3, 8.8 Hz), 5.15 (app. d, 1H, *J* = 10.1 Hz), 5.22 (app. d, 1H, *J* = 17.0 Hz), 5.19–5.36 (m, 2H), 5.70 (ddt, 1H, *J* = 17.0, 10.1, 6.4 Hz), 7.27 (app. d, 2H, *J* = 8.1 Hz), 7.44 (app. d, 2H, *J* = 8.1 Hz), 7.54 (app. d, 2H, *J* = 8.1 Hz), 7.73 (app. d, 2H, *J* = 8.1 Hz); ^{13}C NMR (125 MHz, CD_3Cl) *δ*: 17.5, 21.4, 50.3, 52.2, 55.6, 63.7, 118.4, 124.1 (q, *J* = 272.0 Hz), 125.4 (q, *J* = 3.5 Hz), 125.5, 127.8, 129.3 (x2), 129.9 (q, *J* = 32.4 Hz), 132.5, 134.6, 137.6, 139.9, 143.3, 171.9; HRMS (ESI, +ve) *m/z* calcd. for $C_{24}H_{26}F_3NO_4S$ 481.1535, found 481.1400 $(M+H)^+$.

(*anti-E*)-Methyl 3-(*N*-allyl-4-methylphenylsulfonamido)-2-isopropylhex-4-enoate 347

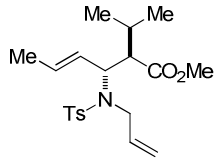

LiHMDS (1M in toluene, 2.47 ml, 2.47 mmol), triethylamine (3.42 ml, 24.7 mmol) and (*E*)-4-(*N*-allyl-4-methylphenylsulfonamido)but-3-en-2-yl 3-methylbutanoate **335** (0.20 g, 0.55 mmol) in THF (2 ml) was combined according to general procedure 4 (reaction time : 75 minutes). Treatment with diazomethane and purification by flash chromatography afforded (*anti-E*)-methyl 3-(*N*-allyl-4-methylphenylsulfonamido)-2-isopropylhex-4-enoate **347** as a white solid (0.14 g, 65%, d.r. >25:1). M.p. 105–107 ˚C; FTIR (film/cm^{-1}) υ_{max}: 3082 (m), 3021 (m), 2985 (m), 2958 (m), 1730 (s), 1655 (m), 1615 (m), 1597 (m), 1509 (m); ^{1}H NMR (400 MHz, CD_3Cl) δ: 0.90 (d, 3H, J = 6.7 Hz), 0.99 (d, 3H, J = 6.7 Hz), 1.67 (d, 3H, J = 5.8 Hz), 1.78–1.94 (1H, m), 2.43 (s, 3H), 3.08 (dd, 2H, J = 11.3, 2.7 Hz), 3.65 (s, 3H), 3.67–3.86 (m, 2H), 4.45 (app. t, 1H, J = 11.3 Hz), 5.07–5.28 (m, 1H), 5.48–5.80 (m, 1H), 7.27 (app. d, 2H, J = 8.1 Hz), 7.72 (app. d, 2H, J = 8.1 Hz); ^{13}C NMR (125 MHz, CD_3Cl) δ: 16.0, 17.8, 21.4, 21.9, 27.6, 51.1, 54.2, 61.9, 117.8, 126.9, 127.9, 129.1, 131.5, 135.2, 137.9, 142.9, 172.8; HRMS (ESI, +ve) *m/z* calcd. for $C_{20}H_{30}NO_4S$ 380.1895, found 380.1900 $(M+H)^+$.

(*anti-E*)-Methyl 2-allyl-3-(*N*-allyl-4-methylphenylsulfonamido)hex-4-enoate 348

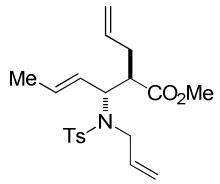

LiHMDS (1M in toluene, 2.48 ml, 2.48 mmol), triethylamine (3.43 ml, 24.80 mmol) and (*E*)-4-(*N*-allyl-4-methylphenylsulfonamido)but-3-en-2-yl pent-4-enoate **336** (0.20 g, 0.55 mmol) in THF (2 ml) was combined according to general procedure 4 (reaction time : 75 minutes). Treatment with diazomethane and purification by flash

chromatography afforded (*anti-E*)-methyl 2-allyl-3-(*N*-allyl-4-methylphenylsulfonamido)hex-4-enoate **348** as a yellow oil (0.15 g, 70%, d.r. 10:1). FTIR (film/cm^{-1}) υ_{max}: 3012 (m), 2983 (m), 2934 (m), 1729 (s), 1655 (s), 1616 9 (s), 1596 (s), 1509 (m); ^{1}H NMR (400 MHz, CD_3Cl) δ: 1.66 (d, 3H, *J* = 6.3 Hz), 2.12–2.29 (2H, m), 2.43 (s, 3H), 3.08 (td, 1H, *J* = 10.6, 4.5 Hz), 3.66 (s, 3H), 3.74 (dd, 1H, *J* = 15.8, 6.7 Hz), 3.83 (dd, 1H, *J* = 16.0, 6.7 Hz), 4.33 (app. t, 1H, *J* = 10.6 Hz), 4.98–5.22 (m, 4H), 5.48 (dd, 1H, *J* = 15.5, 9.9 Hz), 5.60 (dq, 1H, *J* = 14.2, 6.3 Hz), 5.65–5.77 (m, 2H), 7.28 (app. d, 2H, *J* = 8.1 Hz), 7.73 (app. d, 2H, *J* = 8.1 Hz); ^{13}C NMR (125 MHz, CD_3Cl) *δ*: 17.8, 21.4, 34.9, 49.4, 49.5, 51.5, 63.2, 117.1, 117.8, 126.4, 127.8, 129.2, 132.4, 134.5, 135.1, 137.7, 143.0, 173.6; HRMS (ESI, +ve) *m/z* calcd. for $C_{20}H_{28}NO_4S$ 378.1739, found 378.1699 $(M+H)^+$.

(*anti-E*)-Methyl 3-(*N*-allyl-4-methylphenylsulfonamido)-2-(2-iodophenyl) hex-4-enoate 355

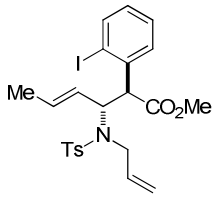

LiHMDS (1M in toluene, 0.34 ml, 0.34 mmol), TMSCl (0.10 ml, 1.57 mmol) and (*E*)-4-(*N*-allyl-4-methylphenylsulfonamido)but-3-en-2-yl 2-(2-iodophenyl)acetate **340** (0.07 g, 0.26 mmol) in THF (0.7 ml) was combined according to general procedure 3 (reaction time : 75 minutes). Treatment with diazomethane and purification by flash chromatography afforded (*anti-E*)-methyl 3-(*N*-allyl-4-methylphenylsulfonamido)-2-(2-iodophenyl)hex-4-enoate **355** as a white solid (0.05 g, 67%, d.r. >25:1). M.p. 97–99 ˚C; FTIR (film/cm^{-1}) υ_{max}: 3179 (w), 2953 (m), 2922 (m), 1734 (s), 1597 (m); ^{1}H NMR (500 MHz, CD_3Cl) δ: 1.35 (d, 3H, *J* = 6.5 Hz), 2.41 (s, 3H), 3.63 (s, 3H), 3.83 (app. d, 1H, *J* = 17.3, 6.7 Hz), 3.93 (app. d, 1H, *J* = 17.3, 6.7 Hz), 4.75 (d, 1H, *J* = 11.7 Hz), 4.91 (d, 1H, *J* = 11.7 Hz), 5.14–5.23 (m, 2H), 5.25–5.37 (m, 2H), 5.79 (ddt, 1H, *J* = 17.0, 10.8, 6.7 Hz), 6.92 (app. t, 1H, *J* = 7.9 Hz), 7.26 (app. d, 2H, *J* = 8.7 Hz), 7.27–7.33 (m, 1H), 7.51 (app d, 1H, *J* = 7.9 Hz), 7.74 (app. d, 2H, *J* = 8.7 Hz), 7.82 (d, 1H, *J* = 7.9 Hz); ^{13}C NMR (125 MHz, CD_3Cl) *δ*: 17.6, 21.4, 49.2, 52.2, 57.8, 64.2, 118.1,

124.7, 127.9, 128.5, 128.9, 129.0, 129.2, 129.3, 132.1, 135.0, 137.7, 138.9, 139.6, 143.1, 171.8; HRMS (ESI, +ve) *m/z* calcd. for $C_{25}H_{32}NO_6S$ 474.1950, found 474.1948 $(M+H)^+$.

(*anti-E*)-Methyl 3-(*N*-allyl-4-methylphenylsulfonamido)-2-(4-methoxyphenyl)hex-4-enoate 356

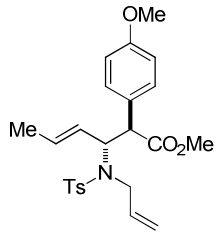

LiHMDS (1M in toluene, 1.16 ml, 1.16 mmol), TMSCl (0.35 ml, 5.35 mmol) and (*E*)-4-(*N*-allyl-4-methylphenylsulfonamido)but-3-en-2-yl 2-(4-methoxyphenyl)acetate **341** (0.20 g, 0.89 mmol) in THF (2 ml) was combined according to general procedure 3 (reaction time : 75 minutes). Treatment with diazomethane and purification by flash chromatography afforded (*anti-E*)-methyl 3-(*N*-allyl-4-methylphenylsulfonamido)-2-(4-methoxyphenyl)hex-4-enoate **356** as a white solid (0.15 g, 73%, d.r. >25:1). M.p. 109–110 ˚C; FTIR (film/cm^{-1}) υ_{max}: 3039 (w), 2952 (m), 2919 (m), 1734 (s), 1670 (w), 1608 (m), 1598 (m), 1522 (m), 1512 (m); ^{1}H NMR (500 MHz, CD_3Cl) δ: 1.39 (d, 3H, *J* = 4.5 Hz), 2.41 (s, 3H), 3.62 (s, 3H), 3.77 (s, 3H), 3.75–3.88 (m, 2H), 4.21 (d, 1H, *J* = 11.5 Hz), 4.73 (dd, 1H, *J* = 11.5, 7.44 Hz), 5.12 (app. d, 1H, *J* = 10.3 Hz), 5.20 (app d, 1H, *J* = 17.1 Hz), 5.23–5.33 (m, 2H), 5.70 (ddt, 1H, *J* = 17.1, 10.3, 6.5 Hz), 6.81 (app. d, 2H, *J* = 8.7 Hz), 7.22 (app. d, 2H, *J* = 8.7 Hz), 7.26 (app. d, 2H, *J* = 8.4 Hz), 7.73 (app. d, 2H, *J* = 8.4 Hz); ^{13}C NMR (125 MHz, CD_3Cl) *δ*: 17.6, 21.4, 50.0, 51.9, 54.9, 55.1, 63.6, 113.9, 118.0, 126.0, 127.8 (x2), 129.2, 129.9, 131.7, 134.9, 137.9, 143.0, 159.0, 172.8; HRMS (ESI, +ve) *m/z* calcd. for $C_{24}H_{30}NO_5S$ 444.1844, found 444.1857 $(M+H)^+$.

(*anti-E*)-Methyl 3-(*N*-allyl-4-methylphenylsulfonamido)-2-(4-nitrophenyl) hex-4-enoate 358

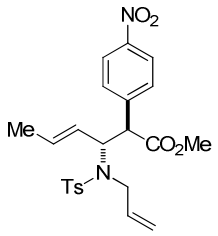

LiHMDS (1M in toluene, 1.13 ml, 1.13 mmol), TMSCl (0.34 ml, 5.22 mmol) and (*E*)-4-(*N*-allyl-4-methylphenylsulfonamido)but-3-en-2-yl 2-(4-nitrophenyl)acetate **343** (0.20 g, 0.87 mmol) in THF (2 ml) was combined according to general procedure 3 (reaction time : 75 minutes). Treatment with diazomethane and purification by flash chromatography, recrystallisation and a two subsequent recrystallisations of the mother liquor afforded (*anti-E*)-methyl 3-(*N*-allyl-4-methylphenylsulfonamido)-2-(4-nitrophenyl)hex-4-enoate **358** as an off white solid (0.10 g, 53%, d.r. 20:1). M.p. 128–130 ˚C; FTIR (film/cm^{-1}) υ_{max}: 3018 (w), 2988 (m), 2952 (m) 2925 (m), 1736 (s), 1669 (w), 1598 (m), 1521 (s); ^{1}H NMR (500 MHz, CD_3Cl) δ: 1.38 (dd, 3H, *J* = 6.2, 1.0 Hz), 2.42 (s, 3H), 3.69 (s, 3H), 3.78 (dd, 1H, *J* = 16.0, 6.8 Hz), 3.86 (dd, 1H, *J* = 16.0, 6.8 Hz), 4.49 (d, 1H, *J* = 11.2 Hz), 4.69 (app. t, 1H, *J* = 11.2 Hz), 5.17 (app. d, 1H, *J* = 10.2 Hz), 5.23 (app. d, 1H, *J* = 17.0 Hz), 5.20–5.38 (m, 2H), 5.69 (ddt, 1H, *J* = 17.0, 10.2, 6.8 Hz), 7.28 (app. d, 2H, *J* = 8.2 Hz), 7.51 (app. d, 2H, *J* = 8.2 Hz), 7.73 (app. d, 2H, *J* = 8.2 Hz), 8.16 (app. d, 2H, *J* = 8.2 Hz); ^{13}C NMR (125 MHz, CD_3Cl) *δ*: 17.5, 21.4, 50.5, 52.5, 55.6, 63.8, 118.6, 123.7, 125.4, 127.8, 129.3, 129.9, 132.9, 134.5, 137.5, 143.2, 143.4, 147.4, 171.5; HRMS (ESI, +ve) *m/z* calcd. for $C_{23}H_{26}N_2O_6S$ 481.1409, found 481.1715 $(M+Na)^+$.

(*anti-E*)-Methyl 3-(*N*-allyl-4-methylphenylsulfonamido)-2-(2,4-dichlorophenyl)hex-4-enoate 359

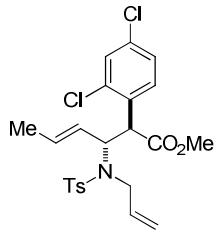

LiHMDS (1M in toluene, 1.07 ml, 1.07 mmol), TMSCl (0.33 ml, 4.94 mmol) and (*E*)-4-(*N*-allyl-4-methylphenylsulfonamido)but-3-en-2-yl 2-(2,4-dichlorophenyl)acetate **344** (0.20 g, 0.82 mmol) in THF (2 ml) was combined according to general procedure 3 (reaction time : 75 minutes). Treatment with diazomethane and purification by flash chromatography afforded (*anti-E*)-methyl 3-(*N*-allyl-4-methylphenylsulfonamido)-2-(2,4-dichlorophenyl)hex-4-enoate **359** as a yellow oil (0.14 g, 68%, d.r. >25:1). FTIR (film/cm^{-1}) υ_{max}: 3034 (w), 2950 (m), 2919 (m), 1736 (s), 1669 (m), 1598 (m), 1523 (m), 1512 (m); ^{1}H NMR (500 MHz, CD_3Cl) δ: 1.37 (d, 3H, *J* = 5.8 Hz), 2.41 (s, 3H), 3.65 (s, 3H), 3.80 (dd, 1H, *J* = 15.9, 6.9 Hz), 3.92 (dd, 1H, *J* = 15.9, 6.9 Hz), 4.79 (dd, 1H, *J* = 11.5, 8.6 Hz), 4.90 (d, 1H, *J* = 11.5 Hz), 5.15 (app. d, 1H, *J* = 10.2 Hz), 5.18–5.33 (m, 3H), 5.71 (ddt, 1H, *J* = 16.9, 10.3, 6.9 Hz), 7.21 (dd, 2H, *J* = 8.3, 2.3 Hz), 7.26 (app. d, 2H, *J* = 8.2 Hz), 7.36 (d, 1H, *J* = 2.3 Hz), 7.51 (d, 1H, *J* = 8.3 Hz), 7.72 (app. d, 2H, *J* = 8.2 Hz); ^{13}C NMR (125 MHz, CD_3Cl) *δ*: 17.6, 21.4, 49.5, 49.6, 52.3, 63.9, 118.2, 124.7, 127.4, 127.8, 129.2, 129.3, 130.3, 132.4, 132.5, 133.9, 134.9, 135.2, 137.6, 143.2, 171.5; HRMS (ESI, +ve) *m/z* calcd. for $C_{23}H_{26}Cl_2NO_4S$ 482.0959, found 482.0971 $(M+H)^+$.

(*anti-E*)-Methyl 3-(*N*-allyl-4-methylphenylsulfonamido)-2-(2,4-dimethoxyphenyl)hex-4-enoate 360

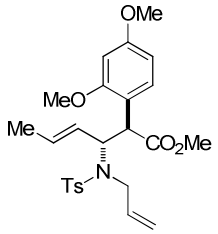

LiHMDS (1M in toluene, 1.09 ml, 1.09 mmol), TMSCl (0.33 ml, 5.03 mmol) and (*E*)-4-(*N*-allyl-4-methylphenylsulfonamido)but-3-en-2-yl 2-(2,4-dimethoxyphenyl)acetate **345** (0.20 g, 0.84 mmol) in THF (2 ml) was combined according to general procedure 3 (reaction time : 75 minutes). Treatment with diazomethane and purification by flash chromatography afforded (*anti-E*)-methyl 3-(*N*-allyl-4-methylphenylsulfonamido)-2-(2,4-dimethoxyphenyl)hex-4-enoate **360** as a yellow oil (0.15 g, 72%, d.r. 20:1). FTIR (film/cm^{-1}) υ_{max}: 3033 (w), 2950 (m), 2919 (m), 1734 (s), 1608 (m), 1522 (m), 1507 (m); ^{1}H NMR (500 MHz, CD_3Cl) δ: 1.35 (d, 3H, *J* = 4.3 Hz), 2.39 (s, 3H), 3.59 (s, 3H), 3.77 (s, 3H), 3.78 (s, 3H), 3.77–3.91 (m, 2H), 4.70 (d, 1H, *J* = 11.0 Hz), 4.77–4.85 (m, 1H), 5.10 (d, 1H, *J* = 10.0 Hz), 5.17–5.25 (m, 3H), 5.74 (ddt, 1H, *J* = 16.9, 10.0, 6.9 Hz), 6.36–6.40 (m, 1H), 6.40–6.48 (m, 1H), 7.24 (app. d, 2H, *J* = 8.4 Hz), 7.32 (d, 1H, *J* = 8.5 Hz), 7.72 (app. d, 2H, *J* = 8.4 Hz); ^{13}C NMR (125 MHz, CD_3Cl) *δ*: 17.6, 21.4, 45.7, 49.2, 51.8, 55.2, 55.6, 63.5, 98.4, 104.6, 116.8, 117.6, 125.9, 127.9, 129.1, 129.3, 130.8, 135.3, 138.0, 142.9, 158.0, 160.1, 172.8; HRMS (ESI, +ve) *m/z* calcd. for $C_{25}H_{32}NO_6S$ 474.1950, found 474.1948 $(M+H)^+$.

(*anti-E*)-Methyl 3-(*N*-allyl-4-methylphenylsulfonamido)-2-(benzo[d][1,3]dioxol-5-yl)hex-4-enoate 361

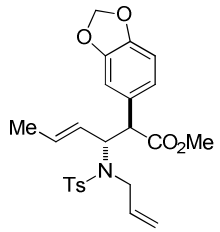

LiHMDS (1M in toluene, 0.55 ml, 0.55 mmol), TMSCl (0.17 ml, 2.53 mmol) and (*E*)-4-(*N*-allyl-4-methylphenylsulfonamido)but-3-en-2-yl 2-(benzo[d][1,3]dioxol-5-yl)acetate **340** (0.10 g, 0.42 mmol) in THF (1 ml) was combined according to general procedure 3 (reaction time : 75 minutes). Treatment with diazomethane and purification by flash chromatography afforded (*anti-E*)-methyl 3-(*N*-allyl-4-methylphenylsulfonamido)-2-(benzo[d][1,3]dioxol-5-yl)hex-4-enoate **361** as a white solid (0.06 g, 55%, d.r. >25:1). M.p. 119–121 ˚C; FTIR (film/cm^{-1}) υ_{max}: 3020 (w), 2952 (m), 2928 (m), 1733 (s), 1597 (m), 1504 (s); ^{1}H NMR (500 MHz, CD_3Cl) δ: 1.42 (d, 3H, *J* = 4.8 Hz), 2.41 (s, 3H), 3.17 (s, 3H), 3.77 (dd, 1H, *J* = 16.0, 6.9 Hz), 3.84 (dd, 1H, *J* = 16.0, 6.9 Hz), 4.19 (d, 1H, *J* = 11.3 Hz), 4.66 (dd, 1H, *J* = 11.3 Hz), 5.13 (app. d, 1H, *J* = 10.1 Hz), 5.20 (app. d, 1H, *J* = 17.1 Hz), 5.27–5.35 (m, 2H), 5.69 (ddt, 1H, *J* = 17.1, 10.1, 6.9 Hz), 5.92–5.95 (m, 2H), 6.68–6.77 (m, 2H), 6.85 (d, 1H, *J* = 1.7 Hz), 7.26 (app. d, 2H, *J* = 8.3 Hz), 7.72 (app. d, 2H, *J* = 8.3 Hz); ^{13}C NMR (125 MHz, CD_3Cl) *δ*: 17.7, 21.4, 50.2, 52.0, 55.3, 63.6, 101.0, 108.1, 108.8, 118.1, 122.6, 125.9, 127.8, 129.2, 129.5, 131.8, 134.8, 137.8, 143.1, 147.0, 147.8, 172.6; HRMS (ESI, +ve) *m/z* calcd. for $C_{24}H_{28}NO_6S$ 458.1637, found 458.1649 $(M+H)^+$.

(*anti-E*)-Methyl 2-allyl-3-(*N*-benzyl-4-methylphenylsulfonamido)hex-4-enoate 381

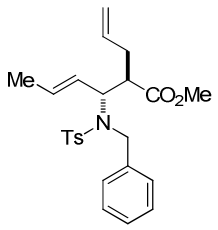

LiHMDS (1M in toluene, 2.16 ml, 2.16 mmol), triethylamine (3.00 ml, 21.60 mmol) and (*E*)-4-(N-benzyl-4-methylphenylsulfonamido)but-3-en-2-yl pent-4-enoate **380** (0.20 g, 0.48 mmol) in THF (2 ml) was combined according to general procedure 4 (reaction time : 75 minutes). Treatment with diazomethane and purification by flash chromatography (× 2) afforded (*anti-E*)-methyl 2-allyl-3-(*N*-benzyl-4-methylphenylsulfonamido)hex-4-enoate **381** as a white solid (0.02 g, 10%, d.r. >25:1). M.p. 92–94 ˚C; FTIR (film/cm^{-1}) υ_{max}: 3045 (m), 2971 (m), 2934 (m), 1708 (s), 1601 (m), 1508 (s); ^{1}H NMR (500 MHz, CD_3Cl) δ: 1.61 (d, 3H, *J* = 5.7 Hz), 1.96–2.08 (m, 1H), 2.10–2.21 (m, 1H), 2.42 (s, 3H), 3.10 (td, 1H, *J* = 10.7, 4.2 Hz), 3.48 (s, 3H), 4.13–4.34 (m, 3H), 4.94 (app. d, 1H, *J* = 12.8 Hz), 5.33–5.49 (m, 2H), 5.55–5.68 (m, 1H), 7.11–7.18 (m, 2H), 7.20–7.31 (m, 5H), 7.70 (app. d, *J* = 8.18 Hz); ^{13}C NMR (125 MHz, CD_3Cl) *δ*: 17.7, 21.4, 35.1, 48.8, 50.6, 51.4, 63.6, 117.0, 126.6, 127.6, 127.8, 128.1, 129.2 (x2), 132.0, 134.4, 136.6, 138.0, 143.0, 173.6; HRMS (ESI, +ve) *m/z* calcd. for $C_{24}H_{30}NO_4S$ 428.1895, found 428.1856 $(M+H)^+$.

6.3.5. Derivatisation of *N*-Sulfonamide Rearrangement Products

Methyl 2-(1-tosyl-2,5-dihydro-1H-pyrrol-2-yl)propanoate 367

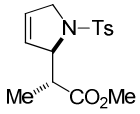

anti-(*E*)-Methyl 3-(*N*-allyl-4-methylphenylsulfonamido)-2-methylhex-4-enoate **334** (0.02 g, 0.05 mmol), catalytic Grubbs I and DCM (5 ml) were combined according to general procedure 6 (reaction time: 6 hours). Purification was achieved by the reported

procedure to yield the methyl 2-(1-tosyl-2,5-dihydro-1H-pyrrol-2-yl)propanoate **367** as a white solid (0.01 g, 79%). M.p. 95–97 ˚C; FTIR (film/cm^{-1}) υ_{max}: 2960 (m), 2928 (m), 2878 (m), 1730 (s), 1597 (m); ^{1}H NMR (500 MHz, CD_3Cl) δ: 1.12 (d, 3H, *J* = 7.1 Hz), 2.44 (s, 3H), 3.31 (qd, 1H, *J* = 7.13, 3.96 Hz), 3.72 (s, 3H), 4.06–4.19 (m, 2H), 4.84–4.89 (m, 1H), 5.55 (app dq, 1H, *J* = 5.5, 2.2 Hz), 5.72 (app. dq, 1H, *J* = 5.5, 2.2 Hz), 7.33 (app. d, 2H, *J* = 8.1 Hz), 7.74 (app. d, 2H, *J* = 8.1 Hz); ^{13}C NMR (125 MHz, CD_3Cl) *δ*: 10.1, 21.5, 43.9, 51.8, 56.1, 67.9, 126.5, 126.8, 127.4, 129.8, 134.1, 143.6, 174.5; HRMS (ESI, +ve) *m/z* calcd. for $C_{15}H_{20}NO_4S$ 310.113, found 310.1108 $(M+H)^+$.

Methyl 3-methyl-2-(1-tosyl-2,5-dihydro-1H-pyrrol-2-yl)butanoate 368

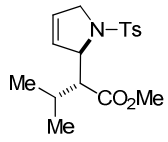

anti-(*E*)-Methyl 3-(*N*-allyl-4-methylphenylsulfonamido)-2-isopropylhex-4-enoate **347** (0.05 g, 0.13 mmol), catalytic Grubbs I and DCM (5 ml) were combined according to general procedure 6 (reaction time: 13 hours). Purification was achieved by the reported procedure to yield the methyl 3-methyl-2-(1-tosyl-2,5-dihydro-1H-pyrrol-2-yl)butanoate **368** as an amorphous white solid (0.04 g, 86%). FTIR (film/cm^{-1}) υ_{max}: 2994 (m), 2956 (m), 2878 (m), 1727 (s), 1598 (m); ^{1}H NMR (500 MHz, CD_3Cl) δ: 0.86 (d, 3H, *J* = 6.0 Hz), 1.10 (d, 3H, *J* = 6.0 Hz), 1.96–2.06 (m, 1H), 2.42 (s, 3H), 3.03 (app. t, 1H, *J* = 6.0 Hz), 3.72 (s, 3H), 4.08–4.18 (m, 2H), 4.68–4.73 (m, 1H), 5.66 (app. dq, 1H, *J* = 6.4, 2.1 Hz), 5.86 (app. dq, 1H, *J* = 6.4, 2.1 Hz), 7.31 (app. d, 2H, *J* = 8.1 Hz), 7.70 (app. d, 2H, *J* = 8.1 Hz); ^{13}C NMR (125 MHz, CD_3Cl) *δ*: 20.0, 21.5, 22.7, 26.3, 51.2, 56.0, 67.6, 125.5, 127.5, 128.5, 129.7, 134.0, 143.6, 173.9; HRMS (ESI, +ve) *m/z* calcd. for $C_{17}H_{24}NO_4S$ 338.1426, found 338.1426 $(M+H)^+$.

Methyl 2-phenyl-2-(1-tosyl-2,5-dihydro-1H-pyrrol-2-yl)acetate 369

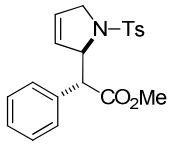

anti-(*E*)-Methyl 3-(*N*-allyl-4-methylphenylsulfonamido)-2-phenylhex-4-enoate **333** (0.10 g, 0.24 mmol), catalytic Grubbs I and DCM (10 ml) were combined according to general procedure 6 (reaction time: 13 hours). Purification was achieved by the reported procedure to yield the methyl 2-phenyl-2-(1-tosyl-2,5-dihydro-1H-pyrrol-2-yl)acetate **369** as a white solid (0.08 g, 92%). M.p. 98–100 ˚C. FTIR (film/cm^{-1}) υ_{max}: 3024 (m), 2950 (m), 2931 (m), 1730 (s), 1657 (m), 1615 (m), 1596 (m), 1510 (m); ^{1}H NMR (500 MHz, CD_3Cl) δ: 2.43 (s, 3H), 3.39–3.45 (m, 1H), 3.73 (s, 3H), 3.85 (app. dq, 1H, *J* = 15.2, 2.1 Hz), 4.48 (d, 1H, *J* = 4.4 Hz), 5.06–5.06 (m, 1H), 5.43 (app. dq, 1H *J* = 6.4, 2.0 Hz), 5.80 (app. dq, 1H *J* = 6.4, 2.0 Hz), 7.23–7.30 (m, 5H), 7.32 (app. d, 2H, *J* = 8.2 Hz), 7.73 (app. d, 2H, *J* = 8.2 Hz); ^{13}C NMR (125 MHz, CD_3Cl) *δ*: 21.5, 52.0, 55.5, 56.2, 68.3, 129.9, 127.3 (x2), 127.6, 127.8, 129.8, 130.0, 134.0, 134.3, 143.6, 172.9; HRMS (ESI, +ve) *m/z* calcd. for $C_{20}H_{22}NO_4S$ 372.1269, found 372.1238 $(M+H)^+$.

Methyl 2-(2-iodophenyl)-2-(1-tosyl-2,5-dihydro-1H-pyrrol-2-yl)acetate 370

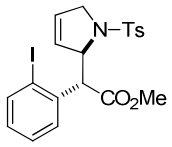

anti-(*E*)-methyl 3-(*N*-allyl-4-methylphenylsulfonamido)-2-(2-iodophenyl)hex-4-enoate **355** (0.09 g, 0.17 mmol), catalytic Grubbs I and toluene (5 ml) were combined according to general procedure 7 (reaction time : 5 hours). Purification was achieved by the reported procedure to yield the methyl 2-(2-iodophenyl)-2-(1-tosyl-2,5-dihydro-1H-pyrrol-2-yl)acetate **370** as a white solid (0.04 g, 51%). M.p. 186–188 ˚C; FTIR (film/cm^{-1}) υ_{max}: 3026 (m), 2952 (m), 2878 (m), 1728 (s), 1597 (m); ^{1}H NMR (500 MHz, CD_3Cl) δ: 2.42 (s, 3H), 3.66–3.75 (m, 1H), 3.75 (s, 3H), 3.97 (app. dq, 1H *J* = 15.7, 1.9 Hz), 4.78 (d, 1H, *J* = 5.6 Hz), 5.19–5.24 (m, 1H), 5.50–5.59 (m, 2H), 6.95

(app. t, 1H, *J* = 7.4 Hz), 7.24–7.34 (m, 4H), 7.73 (app. d, 2H, *J* = 8.3 Hz), 7.89 (app. d, 1H, *J* = 7.4 Hz); ^{13}C NMR (125 MHz, CD_3Cl) *δ*: 21.5, 52.3, 55.5, 59.9, 68.7, 127.5, 127.6 (x2), 127.7, 129.1, 129.7, 129.9, 134.2, 136.3, 138.0, 140.2, 143.6, 172.2; HRMS (ESI, +ve) *m/z* calcd. for $C_{22}H_{21}INO_4S$ 498.0235, found 498.0259 $(M+H)^+$.

Methyl 2-(4-methoxyphenyl)-2-(1-tosyl-2,5-dihydro-1H-pyrrol-2-yl)acetate 371

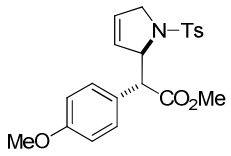

anti-(*E*)-Methyl 3-(*N*-allyl-4-methylphenylsulfonamido)-2-(4-methoxyphenyl)hex-4-enoate **356** (0.05 g, 0.11 mmol), catalytic Grubbs I and DCM (5 ml) were combined according to general procedure 6 (reaction time: 13 hours). Purification was achieved by the reported procedure to yield the methyl 2-(4-methoxyphenyl)-2-(1-tosyl-2,5-dihydro-1H-pyrrol-2-yl)acetate **371** as a clear oil (0.04 g, 89%). FTIR (film/cm^{-1}) υ_{max}: 3035 (m), 2953 (m), 2884 (m), 1727 (s), 1597 (m), 1512 (m); ^{1}H NMR (500 MHz, CD_3Cl) δ: 2.42 (s, 3H), 3.44 (ddt, 1H, *J* = 15.0, 5.4, 2.0 Hz), 3.72 (s, 3H), 3.79 (s, 3H), 3.85 (app. dq, 1H, *J* = 15.0, 2.0 Hz), 4.42 (d, 1H, *J* = 4.3 Hz), 4.97–5.02 (m, 1H), 5.44 (app. dq, 1H *J* = 6.4, 2.0 Hz), 5.80 (app. dq, 1H *J* = 6.4, 2.0 Hz), 6.82 (app. d, 2H, *J* = 8.6 Hz), 7.17 (app. d, 2H, *J* = 8.6 Hz), 7.31 (app. d, 2H, *J* = 8.6 Hz), 7.72 (app. d, 2H, *J* = 8.6 Hz); ^{13}C NMR (125 MHz, CD_3Cl) *δ*: 21.5, 52.0, 55.1, 55.4, 55.5, 68.4, 113.3, 126.0, 127.0, 127.3, 127.6, 129.8, 131.1, 134.4, 143.6, 158.8, 173.1; HRMS (ESI, +ve) *m/z* calcd. for $C_{21}H_{24}NO_5S$ 402.1375, found 402.1366 $(M+H)^+$.

Methyl 2-(1-tosyl-2,5-dihydro-1H-pyrrol-2-yl)-2-(4-(trifluoromethyl)phenyl)acetate 372

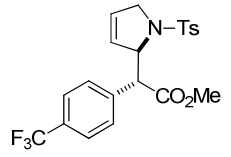

anti-(*E*)-Methyl 3-(*N*-allyl-4-methylphenylsulfonamido)-2-(4-(trifluoromethyl) phenyl) hex-4-enoate **357** (0.05 g, 0.11 mmol), catalytic Grubbs I and DCM (5 ml) were

combined according to general procedure 6 (reaction time: 13 hours). Purification was achieved by the reported procedure to yield the methyl 2-(1-tosyl-2,5-dihydro-1H-pyrrol-2-yl)-2-(4-(trifluoromethyl)phenyl)acetate **372** as a yellow solid (0.04 g, 91%). M.p. 114–115 ˚C; FTIR (film/cm^{-1}) υ_{max}: 3010 (m), 2948 (m), 2897 (m), 1730 (s), 1597 (m), 1504 (m); ^{1}H NMR (500 MHz, CD_3Cl) δ: 2.44 (s, 3H, C*H*$_3$C$_6$H$_4$-), 3.38 (ddt, 1H, *J* = 15.1, 5.4, 2.3 Hz, -NCH*H*CH-), 3.74 (s, 3H, -CO$_2$C*H*$_3$), 3.84 (app. dq, 1H, *J* = 15.1, 2.3 Hz, -NCH*H*CH-), 4.60 (d, 1H, *J* = 4.4 Hz, -C*H*CO$_2$CH$_3$), 5.03–5.07 (m, 1H, -NC*H*(CH-)CH-), 5.48 (app. dq, 1H *J* = 6.5, 2.3 Hz, -NCH$_2$C*H*CH-), 5.81 (app. dq, 1H *J* = 6.5, 2.3 Hz, -NCH$_2$CHC*H*-), 7.33 (app. d, 2H, *J* = 8.2 Hz, Ar*H* Ts), 7.39 (app. d, 2H, *J* = 8.2 Hz, Ar*H* *p*-CF$_3$), 7.55 (app. d, 2H, *J* = 8.2 Hz, Ar*H* *p*-CF$_3$), 7.72 (app. d, 2H, *J* = 8.2 Hz, Ar*H* Ts); ^{13}C NMR (125 MHz, CD_3Cl) *δ*: 21.5, 52.2, 55.5, 55.8, 68.2, 124.1 (q, *J* = 272.0 Hz), 124.3 (q, *J* = 3.6 Hz), 127.0, 127.3, 127.5, 129.6 (q, *J* = 32.6 Hz), 129.9, 130.5, 134.0, 138.0, 143.9, 172.1; HRMS (ESI, +ve) *m/z* calcd. for $C_{21}H_{21}F_3NO_4S$ 440.1143, found 440.1140 $(M+H)^+$.

Methyl 2-(4-nitrophenyl)-2-(1-tosyl-2,5-dihydro-1H-pyrrol-2-yl)acetate 373

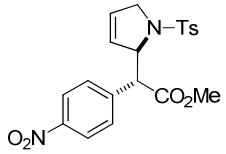

anti-(*E*)-Methyl 3-(*N*-allyl-4-methylphenylsulfonamido)-2-(4-nitrophenyl)hex-4-enoate **358** (0.03 g, 0.07 mmol), catalytic Grubbs I and DCM (5 ml) were combined according to general procedure 6 (reaction time : 13 hours). Purification was achieved by the reported procedure to yield the methyl 2-(4-nitrophenyl)-2-(1-tosyl-2,5-dihydro-1H-pyrrol-2-yl)acetate **373** as an off white solid (0.03 g, 96%). M.p. 178–180 ˚C; FTIR (film/cm^{-1}) υ_{max}: 3030 (m), 2954 (m), 1732 (s), 1599 (s), 1521 (s); ^{1}H NMR (500 MHz, CD_3Cl) δ: 2.44 (s, 3H), 3.34–3.42 (m, 1H), 3.76 (s, 3H), 3.84 (app. d, 1H, *J* = 15.6 Hz), 4.69 (d, 1H, *J* = 4.2 Hz), 5.03–5.09 (m, 1H), 5.48–5.54 (m, 1H), 5.80–5.85 (m, 1H), 7.34 (app. d, 2H, *J* = 8.1 Hz), 7.45 (app. d, 2H, *J* = 8.4 Hz), 7.72 (app. d, 2H, *J* = 8.1 Hz), 8.16 (app. d, 2H, *J* = 8.4 Hz); ^{13}C NMR (125 MHz, CD_3Cl) *δ*: 21.5, 52.4, 55.6, 55.7, 68.2, 122.8, 126.7, 127.4, 127.8, 129.9, 131.2, 133.7, 141.5, 144.0, 147.3, 171.6; HRMS (ESI, +ve) *m/z* calcd. for $C_{20}H_{21}N_2O_6S$ 417.1120, found 417.1123 $(M+H)^+$.

Methyl 2-(2,4-dichlorophenyl)-2-(1-tosyl-2,5-dihydro-1H-pyrrol-2-yl)acetate 374

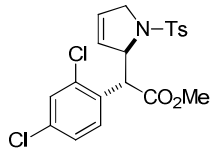

anti-(*E*)-Methyl 3-(*N*-allyl-4-methylphenylsulfonamido)-2-(2,4-dichlorophenyl)hex-4-enoate **359** (0.04 g, 0.08 mmol), catalytic Grubbs I and toluene (5 ml) were combined according to general procedure 7 (reaction time : 5 hours). Purification was achieved by the reported procedure to yield the methyl 2-(2,4-dichlorophenyl)-2-(1-tosyl-2,5-dihydro-1H-pyrrol-2-yl)acetate **374** as a white solid (0.03 g, 83%). M.p. 147–148 ˚C; FTIR (film/cm^{-1}) υ_{max}: 3039 (m), 2953 (m), 2931 (m), 2876 (m), 1734 (s), 1589 (m), 1542 (w), 1524 (w); ^{1}H NMR (500 MHz, CD_3Cl) δ: 2.43 (s, 3H), 3.52 (ddt, 1H, *J* = 15.4, 5.2, 2.2 Hz), 3.74 (s, 3H), 3.84 (app. dq, 1H, *J* = 15.4, 2.2 Hz), 4.83 (d, 1H, *J* = 4.5 Hz), 5.14–5.23 (m, 1H), 5.50 (app. dq, 1H *J* = 6.3, 2.2 Hz), 5.79 (app. dq, 1H *J* = 6.3, 2.2 Hz), 7.21 (d, 1H, *J* = 2.1 Hz), 7.29–7.36 (m, 3H), 7.38 (app. d, 1H, *J* = 2.1 Hz), 7.72 (app. d, 2H, *J* = 8.2 Hz); ^{13}C NMR (125 MHz, CD_3Cl) *δ*: 21.5, 52.3, 53.2, 55.4, 68.5, 126.6, 127.0, 127.2, 127.4, 129.7, 129.8, 131.1, 133.4, 133.9, 134.0, 135.7, 143.8, 171.8; HRMS (ESI, +ve) *m/z* calcd. for $C_{20}H_{20}Cl_2NO_5S$ 440.0490, found 440.0686 $(M+H)^+$.

Methyl 2-(2,4-dimethoxyphenyl)-2-(1-tosyl-2,5-dihydro-1H-pyrrol-2-yl)acetate 375

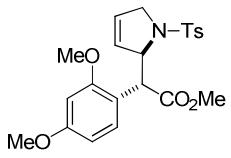

anti-(*E*)-methyl 3-(*N*-allyl-4-methylphenylsulfonamido)-2-(2,4-dimethoxyphenyl)hex-4-enoate **360** (0.07 g, 0.15 mmol), catalytic Grubbs I and toluene (5 ml) were combined according to general procedure 7 (reaction time : 5 hours). Purification was achieved by the reported procedure to yield the methyl 2-(2,4-dimethoxyphenyl)-2-(1-tosyl-2,5-dihydro-1H-pyrrol-2-yl)acetate **375** as a clear oil (0.06 g, 90%). FTIR (film/cm^{-1}) υ_{max}: 3000 (m), 2950 (m), 2867 (m), 2840 (m), 1731 (s), 1611 (s), 1587 (s), 1542 (w), 1508

(m); ^{1}H NMR (500 MHz, CD_3Cl) δ: 2.42 (s, 3H), 3.41 (ddt, 1H, *J* = 14.7, 5.4, 2.3 Hz), 3.68 (s, 3H), 3.70 (s, 3H), 3.80 (s, 3H), 3.76–3.88 (m, 1H), 4.47 (d, 1H, *J* = 4.1 Hz), 5.10–5.15 (m, 1H), 5.33 (app. dq, 1H *J* = 6.4, 2.3 Hz), 5.76 (app. dq, 1H *J* = 6.4, 2.3 Hz), 6.38 (d, 1H, *J* = 2.8 Hz), 6.48 (d, 1H, *J* = 8.5, 2.8 Hz), 7.27–7.33 (d, 3H), 7.72 (app. d, 2H, *J* = 7.9 Hz); ^{13}C NMR (125 MHz, CD_3Cl) *δ*: 21.5, 51.5, 51.7, 55.1, 55.2, 55.3, 68.5, 98.6, 104.1, 115.5, 124.9, 127.3, 127.8, 129.7. 133.4, 134.5, 143.4, 158.2, 160.3, 173.4; HRMS (ESI, +ve) *m/z* calcd. for $C_{22}H_{25}NNaO_6S$ 454.1300, found 454.1533 $(M+Na)^+$.

Methyl 2-(benzo[d][1,3]dioxol-5-yl)-2-(1-tosyl-2,5-dihydro-1H-pyrrol-2-yl)acetate 376

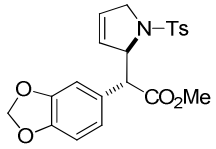

anti-(*E*)-Methyl 3-(*N*-allyl-4-methylphenylsulfonamido)-2-(benzo[d][1,3]dioxol-5-yl)hex-4-enoate **361** (0.05 g, 0.11 mmol), catalytic Grubbs I and DCM (5 ml) were combined according to general procedure 6 (reaction time : 5 hours). Purification was achieved by the reported procedure to yield methyl 2-(benzo[d][1,3]dioxol-5-yl)-2-(1-tosyl-2,5-dihydro-1H-pyrrol-2-yl)acetate **376** as a white solid (0.04 g, 89%). M.p. 134–136 °C; FTIR (film/cm^{-1}) υ_{max}: 2994 (m), 2946 (m), 2909 (m), 1728 (s), 1598 (m), 1504 (s); ^{1}H NMR (500 MHz, CD_3Cl) δ: 2.43 (s, 3H), 3.56 (app. ddt, 1H, *J* = 15.0, 5.3, 2.0 Hz), 3.73 (s, 3H), 3.89 (app. dq, 1H, *J* = 15.0, 2.4 Hz), 4.38 (d, 1H, *J* = 4.4 Hz), 4.95–4.99 (m, 1H), 5.49 (app. dq, 1H, *J* = 6.3, 2.1 Hz), 5.77 (app. dq, 1H, *J* = 6.3, 2.1 Hz), 5.94 (app. d, 2H, *J* = 4.7 Hz), 6.70–6.76 (m, 3H), 7.32 (app. d, 2H, *J* = 8.5 Hz), 7.72 (app. d, 2H, *J* = 8.9 Hz); ^{13}C NMR (125 MHz, CD_3Cl) *δ*: 21.5, 52.1, 55.6, 55.8, 68.3, 101.0, 107.9, 110.1, 123.7, 127.0, 127.3, 127.6 (x2), 129.8, 134.2, 143.7, 146.9, 147.0, 172.9; HRMS (ESI, +ve) *m/z* calcd. for $C_{21}H_{22}NO_6S$ 416.1167, found 416.1168 $(M+H)^+$.

(*R*)-methyl 2-phenyl-2-((*R*)-1-tosylpyrrolidin-2-yl)acetate 377

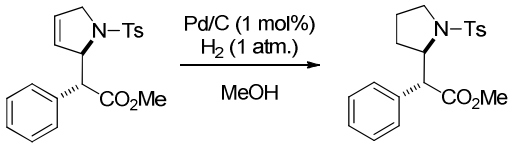

To a solution of methyl 2-phenyl-2-(1-tosyl-2,5-dihydro-1H-pyrrol-2-yl)acetate **369** (10.0 mg, 0.03 mmol, 1.0 eq.) in methanol (5 ml) was added Pd/C (1.00 mg, 2.00×10^{-4} mmol, 1 mol%) and the reaction mixture was allowed to stir at room temperature for 4 hours. The reaction mixture was filtered through a short pad of silica and concentrated *in vacuo* to yield (*R*)-methyl 2-phenyl-2-((*R*)-1-tosylpyrrolidin-2-yl)acetate **377** as an amorphous white solid (10.0 mg, 100%). FTIR (film/cm^{-1}) υ_{max}: 3037 (m), 2952 (m), 2925 (m), 1731 (s), 1598 (m); ^{1}H NMR (500 MHz, CD_3Cl) δ: 0.81–0.96 (m, 1H), 1.14–1.25 (m, 1H), 1.53–1.65 (m, 1H), 1.69–1.80 (m, 1H), 2.45 (s, 3H), 3.00–3.13 (m, 1H), 3.74 (s, 3H), 4.26 (q, 1H, J = 4.7 Hz), 4.38 (d, 1H, J = 4.7 Hz), 7.28–7.39 (m, 7H), 7.78 (app. d, 2H, J = 8.2 Hz); ^{13}C NMR (125 MHz, CD_3Cl) δ: 21.5, 23.6, 28.3, 49.1, 52.0, 55.4, 61.2, 127.6, 127.7, 128.4, 129.7 (× 2), 134.2, 134.9, 143.6, 173.2; HRMS (ESI, +ve) *m/z* calcd. for $C_{20}H_{24}N_1O_4S_1$ 374.1426, found 374.1469 $(M+H)^+$.

***anti*-methyl 1-tosyl-1,2,8,8a-tetrahydroindeno[2,1-b]pyrrole-8-carboxylate 379**

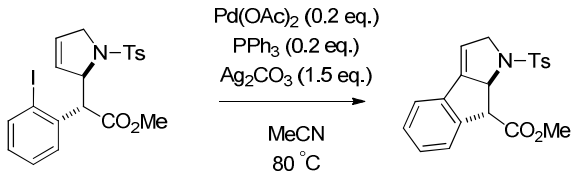

To a solution of $Pd(OAc)_2$ (3.00 mg, 0.01 mmol, 0.2 eq.), PPh_3 (3.67 mg, 0.01 mmol, 0.2 eq.), Ag_2CO_3 (29.1 mg, 0.11 mmol, 1.5 eq.) in MeCN was added methyl 2-(2-iodophenyl)-2-(1-tosyl-2,5-dihydro-1H-pyrrol-2-yl)acetate **370** (35.0 mg, 0.07 mmol, 1.0 eq.). The reaction mixture was refluxed for 4 hours and then concentrated *in vacuo* and subjected to flash column chromatography using ethyl acetate/petroleum ether 40-60° (20:80) to yield *anti*-methyl 1-tosyl-1,2,8,8a-tetrahydroindeno[2,1-b]pyrrole-8-carboxylate **379** as an amorphous clear solid (22.0 mg, 84%). FTIR (film/cm^{-1}) υ_{max}: 2958 (m), 2919 (m), 2849 (m), 1734 (s), 1597 (m); ^{1}H NMR (500 MHz, CD_3Cl) δ: 2.47

(s, 3H, -$C_6H_4CH_3$), 3.80 (s, 3H, -CO_2CH_3), 4.92 (br. d, 1H, *J* = 9.5 Hz, -NCH*H*CH-), 4.63 (br. s, 1H, -C*H*CO_2CH_3), 4.90 (dd, 1H, *J* = 9.5, 2.0 Hz, -NCH*H*CH-), 5.31 (app. dd, 1H, *J* = 4.1, 2.8 Hz, -NC*H*(CH-)CH-), 6.36 (app. dd, 1H, *J* = 4.1, 2.8 Hz, -NCH_2CH-), 7.10–7.15 (m, 1H, Ar*H*), 7.23–7.27 (m, 2H, Ar*H*), 7.36 (app. d, 2H, *J* = 8.2 Hz, Ar*H*, Ts), 7.45–7.51 (m, 1H, Ar*H*), 7.75 (app. d, 2H, *J* = 8.2 Hz, Ar*H*, Ts); ^{13}C NMR (125 MHz, CD_3Cl) δ: 21.6, 52.5, 54.5, 58.3, 66.1, 112.9, 125.1, 126.1, 127.8, 127.9, 128.6, 129.9, 130.5, 132.9, 137.8, 142.9, 144.2, 172.3; HRMS (ESI, +ve) *m/z* calcd. for $C_{20}H_{20}N_1O_4S_1$ 370.1148, found 370.1113 $(M+H)^+$.

<u>*anti*-methyl 2-(*N*-benzyl-4-methylphenylsulfonamido)cyclopent-3-enecarboxylate</u>

382

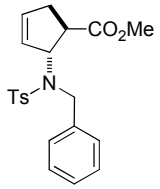

(*anti*,*E*)-methyl 2-allyl-3-(*N*-benzyl-4-methylphenylsulfonamido)hex-4-enoate **381** (0.02 g, 0.05 mmol), catalytic Grubbs I and DCM (5 ml) were combined according to general procedure 6 (reaction time : 12 hours). Purification was achieved by the reported procedure to yield *anti*-methyl 2-(*N*-benzyl-4-methylphenylsulfonamido)cyclopent-3-enecarboxylate **382** as a clear oil (0.02 g, 85%). FTIR (film/cm^{-1}) υ_{max}: 3031 (m), 2952 (m), 2925 (m), 1731 (s), 1598 (m); ^{1}H NMR (500 MHz, CD_3Cl) δ: 2.34–2.51 (m, 2H, -CH_2CH(CH-)CO_2Me), 2.45 (s, 3H, -$C_6H_4CH_3$), 2.77 (dt, 1H, *J* = 9.1, 4.9 Hz, -CH_2C*H*(CH-)CO_2Me), 3.66 (s, 3H, -CO_2CH_3), 4.18 (d, 1H, *J* = 16.1 Hz, -N(Ts)C*H*HPh), 4.49 (d, 1H, *J* = 16.1 Hz, -N(Ts)CH*H*Ph), 5.19–5.26 (m, 1H, NC*H*(CHCO_2Me)CH-), 5.33–5.39 (m, 1H, NCH(CHCO_2Me)C*H*-), 5.75–5.82 (m, 1H, NCH(CHCO_2Me)CHC*H*), 7.22–7.37 (m, 7H, Ar*H*), 7.73 (app. d, 2H, *J* = 8.2 Hz, Ar*H*, Ts); ^{13}C NMR (125 MHz, CD_3Cl) δ: 21.5, 35.9, 46.7, 48.2, 52.1, 68.0, 127.3, 127.4, 127.8, 128.3, 128.4, 129.7, 133.9, 137.5, 138.1, 143.3, 174.9; HRMS (ESI, +ve) *m/z* calcd. for $C_{12}H_{23}N_1Na_1O_4S_1$ 408.1245, found 408.1401 $(M+Na)^+$.

6.3.6 SKA Precursors & Products

Phenyl-acetic acid methyl ester 158

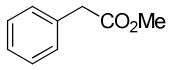

EDCi (1.40 g, 7.30 mmol) in DCM (200 ml), triethylamine (1.02 ml, 7.30 mmol), DMAP (0.05 g, 0.37 mmol), phenylacetic acid (1.00 g, 7.30 mmol) and methanol (3.02 ml, 3.65 mmol) in DCM (50 ml) were combined according to general procedure 1 (reaction time: 15 hours). Purification was achieved by reported procedure and further purification by column chromatography using gradient elution ethyl acetate/petroleum ether 40-60° (5–15 %) yielded phenyl-acetic acid methyl ester **158** as a pale yellow oil (1.10 g, 100%). FTIR (film/cm^{-1}) υ_{max}: 3032 (m), 2953 (s), 1734 (s), 1603 (s); ^{1}H NMR (250 MHz, $CDCl_3$) δ: 3.68 (s, 2H), 3.74 (s, 3H), 7.25–7.49 (m, 5H); ^{13}C NMR (63 MHz, $CDCl_3$) δ: 41.2, 52.0, 127.1, 128.6, 129.2, 134.0, 172.0; HRMS (ESI, +ve) *m/z* calcd. for $C_9H_{11}O_2$ 151.0759, found 151.0769 $(M+H)^+$.

Phenyl-acetic acid isopropyl-2-d_1 ester $^{2}H_1$-239

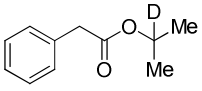

EDCi (1.24 g, 6.47 mmol) in DCM (200 ml), triethylamine (0.91 ml, 6.47 mmol), DMAP (0.04 g, 0.32 mmol), phenyl-acetic acid (0.89 g, 6.47 mmol) and 2-propanol-2-d_1 (0.20 g, 3.23 mmol) as a solution in DCM (30 mL) were combined according to general procedure 1 (reaction time: 15 hours). Purification was achieved by reported procedure to yield phenyl-acetic acid isopropyl-2-d_1 ester **$^{2}H_1$-239** as a yellow oil (0.46 g, 76%). FTIR (film/cm^{-1}) υ_{max}: 3032 (m), 2976 (m), 1731 (s), 1604 (m), 1497 (s); ^{1}H NMR (250 MHz, $CDCl_3$) δ: 1.26 (s, 6H), 3.62 (s, 2H), 7.24–7.42 (m, 5H); ^{13}C NMR (75 MHz, $CDCl_3$) δ: 20.3, 41.8, 67.8 (t, J = 24.3 Hz), 127.0, 128.5, 129.2, 134.4, 171.1; HRMS (GC-EI, +ve) *m/z* calcd. for $C_{11}H_{17}DO_2N_1$ 197.1395, found 197.1391 $(M+NH_4)^+$.

$^{13}C_2$-Phenyl-acetic acid isopropyl-D^1-ester $^2H_1$-$^{13}C_2$-239

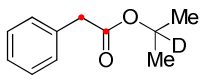

EDCi (0.28 g, 1.44 mmol) in DCM (100 ml), triethylamine (0.20 ml, 1.44 mmol), DMAP (0.01 g, 0.07 mmol), $^{13}C_2$-phenyl-acetic acid (0.20 g, 1.44 mmol) and d^1-isopropanol (0.04 ml, 0.72 mmol) were combined according to general procedure 1 (reaction time: 15 hours). Purification was achieved by reported procedure, with an additional chloroform (20 ml) trituration to afford $^{13}C_2$-phenyl-acetic acid isopropyl-d^1-ester **$^2H_1$-$^{13}C_2$-239** as a yellow oil (0.09 g, 34%). FTIR (film/cm^{-1}) υ_{max}: 2978 (m), 2934 (m), 1686 (s), 1496 (m); ^{1}H NMR (400 MHz, $CDCl_3$) δ: 1.28 (s, 6H), 3.64 (dd, 2H, *J* = 129.8, 7.6 Hz), 7.27–7.42 (m, 5H); ^{13}C NMR (100 MHz, $CDCl_3$) δ: 21.6 (d, *J* = 2.0 Hz), 41.8 (d, *J* = 57.2 Hz), 67.8 (td, *J* = 23.5, 2.5 Hz), 126.9, 128.5 (d, *J* = 4.1 Hz), 129.2 (t, *J* = 2.0 Hz), 134.4 (dd, *J* = 43.9, 3.0 Hz), 171.1 (d, *J* = 57.2 Hz); HRMS (ESI, +ve) *m/z* calcd. for $C_{11}C^{13}{}_2H_{17}D_1N_1O_2$ 223.1556, found 223.1797 $(M+ACN+H)^+$.

(1-d$_1$-Isopropoxy-2-phenyl-*E*-vinyloxy)-trimethyl-silane (*E*)-$^2H_1$-240

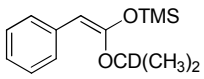

LiHMDS (0.47 ml, 0.47 mmol, 1M in THF), TMSCl (0.10 ml, 1.68 mol) and phenyl-acetic acid isopropyl-2-d$_1$ ester **$^2H_1$-239** (0.05 g, 0.28 mmol) were combined according to general procedure 9c and purification was achieved by reported procedure to afford (1-d$_1$-isopropoxy-2-phenyl-*E*-vinyloxy)-trimethyl-silane **(*E*)-$^2H_1$-240** as a yellow oil (0.05 g, 82%, *E/Z* >100:1). ^{1}H NMR (400 MHz, $CDCl_3$) δ: 0.31 (s, 9H), 1.29 (s, 6H), 2.29 (s, 3H), 4.72 (s, 1H), 7.04 (app. d, 2H, *J* = 7.8 Hz), 7.36 (app. d, 2H, *J* = 7.8 Hz); ^{13}C NMR (100 MHz, $CDCl_3$) δ: 5.5, 21.0, 22.2, 69.2 (t, *J* = 22.3 Hz), 88.1, 126.5, 128.7, 133.1, 134.0, 153.0. IR and HRMS not obtainable. Data in accordance with related non-deuterated analogue.[152]

(4-Methoxy-phenyl)-acetic acid isopropyl-2-d_1 ester $^2H_1$-241

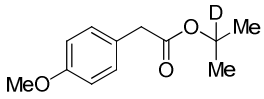

EDCi (1.24 g, 6.47 mmol) in DCM (200 ml), triethylamine (0.91 ml, 6.47 mmol), DMAP (0.04 g, 0.32 mmol), (4-methoxy-phenyl)-acetic acid (1.08 g, 6.47 mmol) and 2-propanol-2-d_1 (0.20 g, 3.23 mmol) as a solution in DCM (30 mL) were combined according to general procedure 1 (reaction time: 15 hours). Purification was achieved by reported procedure to yield (4-methoxy-phenyl)-acetic acid isopropyl-2-d_1 ester **$^2H_1$-241** as a yellow oil (0.68 g, 100%). FTIR (film/cm^{-1}) υ_{max}: 2978 (m), 2934 (m), 2837 (m), 1723 (s), 1613 (w), 1512 (s); ^{1}H NMR (250 MHz, $CDCl_3$) δ: 1.22 (s, 6H), 3.51 (s, 2H), 3.78 (s, 3H), 6.85 (app. d, 2H, *J* = 8.8 Hz), 7.19 (app. d, 2H, *J* = 8.8 Hz); ^{13}C NMR (63 MHz, $CDCl_3$) δ: 21.7, 40.8, 55.2, 67.7 (t, *J* = 24.2 Hz), 113.9, 126.4, 130.2, 158.6, 171.5; HRMS (GC-EI, +ve) *m/z* calcd. for $C_{12}H_{19}D_1O_3N_1$ 227.1500, found 227.1499 $(M+NH_4)^+$.

***p*-Tolyl-acetic acid isopropyl-2-d_1 ester $^2H_1$-242**

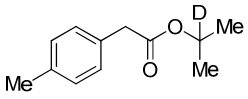

EDCi (1.24 g, 6.47 mmol) in DCM (200 ml), triethylamine (0.91 ml, 6.47 mmol), DMAP (0.04 g, 0.33 mmol), *p*-tolyl-acetic acid (0.98 g) and 2-propanol-2-d_1 (0.20 g, 3.23 mmol) as a solution in DCM (30 mL) were combined according to general procedure 1 (reaction time: 15 hours). Purification was achieved by reported procedure to yield *p*-tolyl-acetic acid isopropyl-2-d_1 ester **$^2H_1$-242** as a yellow oil (0.63 g, 100%). FTIR (film/cm^{-1}) υ_{max}: 2979 (m), 2932 (m), 1720 (s), 1516 (m); ^{1}H NMR (250 MHz, $CDCl_3$) δ: 1.23 (s, 6H), 2.34 (s, 3H), 3.55 (s, 2H), 7.07–7.23 (m, 4H); ^{13}C NMR (75 MHz, $CDCl_3$) δ: 21.1, 21.7, 41.3, 67.7 (t, *J* = 23.2 Hz), 129.1, 129.2, 131.3, 136.5, 171.3; HRMS (GC-EI, +ve) *m/z* calcd. for $C_{12}H_{19}D_1O_2N_1$ 211.1551, found 211.1551 $(M+NH_4)^+$.

(4-Trifluoromethyl-phenyl)-acetic acid isopropyl-2-d_1 ester $^2H_1$-243

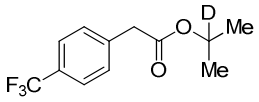

EDCi (1.24 g, 6.47 mmol) in DCM (200 ml), triethylamine (0.91 ml, 6.47 mmol), DMAP (0.04 g, 0.32 mmol), (4-trifluoromethyl-phenyl)-acetic acid (1.33 g, 6.47 mmol) and 2-propanol-2-d_1 (0.20 g, 3.23 mmol) as a solution in DCM (30 mL) were combined according to general procedure 1 (reaction time: 15 hours). Purification was achieved by reported procedure to yield (4-trifluoromethyl-phenyl)-acetic acid isopropyl-2-d_1 ester **$^2H_1$-243** as a yellow amorphous solid (0.67 g, 83%). FTIR (film/cm^{-1}) υ_{max}: 2980 (m), 2937 (m), 1732 (s), 1620 (m); ^{1}H NMR (250 MHz, $CDCl_3$) δ: 1.22 (s, 6H), 3.63 (s, 2H), 7.39 (app. d, J = 8.0 Hz), 7.52 (app. d, J = 8.0 Hz); ^{13}C NMR (75 MHz, $CDCl_3$) δ: 22.0, 41.8, 68.7 (t, J = 24.2 Hz), 124.6 (q, J = 272 Hz), 125.8 (q, J = 3.8 Hz), 129.7 (q, J = 32.0 Hz), 130.0, 138.9, 170.7; HRMS (GC-EI, +ve) *m/z* calcd. for $C_{12}H_{12}D_1F_3O_2$ 247.0925, found 247.0925 $(M)^+$.

(4-Nitro-phenyl)-acetic acid isopropyl-2-d_1 ester $^2H_1$-244

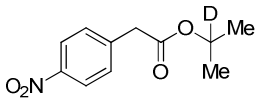

EDCi (1.24 g, 6.47 mmol) in DCM (200 ml), triethylamine (0.91 ml, 6.47 mmol), DMAP (0.04 g, 0.65 mmol), (4-nitro-phenyl)-acetic acid (1.18 g, 6.47 mmol) and 2-propanol-2-d_1 (0.20 g, 3.23 mmol) as a solution in DCM (30 mL) were combined according to general procedure 1 (reaction time: 15 hours). Purification was achieved by reported procedure to yield (4-nitro-phenyl)-acetic acid isopropyl-2-d_1 ester **$^2H_1$-244** as an orange/red oil (0.73 g, 100%). FTIR (film/cm^{-1}) υ_{max}: 3081 (m), 2979 (m), 2934 (m), 1726 (s), 1601 (w), 1518 (s); ^{1}H NMR (250 MHz, $CDCl_3$) δ: 1.21 (s, 6H), 3.68 (s, 2H), 7.44 (app. d, 2H, J = 8.7 Hz), 8.17 (app. d 2H, J = 8.7 Hz); ^{13}C NMR (63 MHz, $CDCl_3$) δ: 21.6, 41.4, 68.6 (t, J = 22.4 Hz), 123.7, 130.2, 141.7, 147.2, 169.7; HRMS (GC-EI, -ve) *m/z* calcd. for $C_{11}H_{11}D_1N_1O_4$ 223.0835, found 223.0836 $(M-H)^-$.

<u>*tert*-Butyl 2-(4-methoxyphenyl)acetate</u> 252

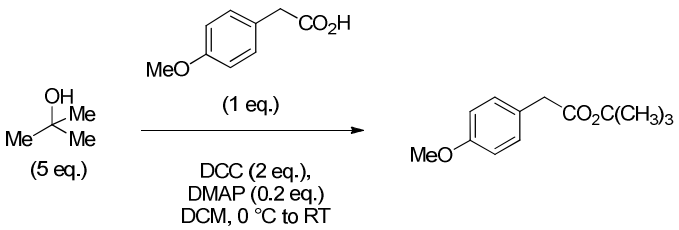

To a solution of DCC (2.75 g , 13.3 mmol, 2.0 eq.) in DCM (100 ml) at 0 °C was added DMAP (0.16 g, 1.33 mmol, 0.2 eq.) and (4-methoxy-phenyl)-acetic acid (1.11 g, 6.66 mmol, 1.0 eq.). To the resulting suspension was then added *tert*-butyl alcohol (33.3 mmol, 5.0 eq.). The reaction mixture was allowed to stir whilst slowly warming to room temperature over 15 hours. The reaction was concentrated in *vacuo*, washed with ether (150 ml), filtered through celite, washed with 1N NaOH (100 ml), washed with 1N HCl (100 ml), dried over magnesium sulfate, concentrated *in vacuo* and subjected to purification by preparative HPLC (acetonitrile/water with 3% trifluoroacetic acid) to afford *tert*-butyl 2-(4-methoxyphenyl)acetate **252** as a yellow oil (0.57 g, 42%). FTIR (film/cm^{-1}) υ_{max}: 2978 (s), 2934 (m), 2836 (m), 1732 (s), 1613 (s), 1513 (s); ^{1}H NMR (300 MHz, $CDCl_3$) δ: 1.35 (s, 9H), 3.37 (s, 2H), 3.70 (s, 3H), 6.71 (app. d 2H, J = 8.7 Hz), 7.10 (app. d 2H, J = 8.7 Hz); ^{13}C NMR (63 MHz, $CDCl_3$) δ: 28.0, 41.7, 55.2, 80.7, 113.9, 126.8, 130.2, 158.5, 171.3; HRMS (GC-EI, +ve) *m/z* calcd. for $C_{13}H_{22}O_3N_1$ 240.1594, found 240.1594 $(M+NH_4)^+$.

<u>*tert*-Butyl 2-*p*-tolylacetate</u> 253

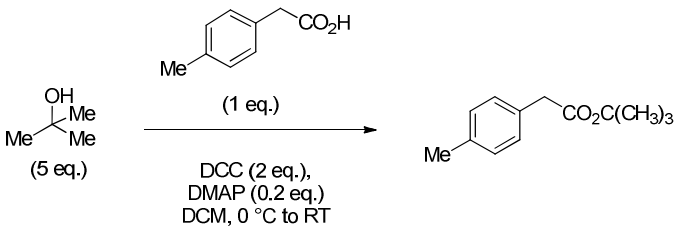

To a solution of DCC (2.75 g, 13.3 mmol, 2.0 eq.) in DCM (100 ml) at 0 °C was added DMAP (0.16 g, 1.33 mmol, 0.2 eq.) and *p*-tolyl-acetic acid (1.00 g, 6.66 mmol, 1.0 eq.). To the resulting suspension was then added *tert*-butyl alcohol (2.47 g, 33.3 mmol, 5.0

eq.). The reaction mixture was allowed to stir whilst slowly warming to room temperature over 15 hours. The reaction was concentrated *in vacuo*, washed with ether (150 ml), filtered through celite, washed with 1N NaOH (100 ml), washed with 1N HCl (100 ml), dried over magnesium sulfate, concentrated in vacuo and subjected to purification by preparative HPLC (acetonitrile/water with 3% trifluoroacetic acid) to afford *tert*-butyl 2-*p*-tolylacetate **253** as a yellow oil (0.45 g, 33%). FTIR (film/cm^{-1}) υ_{max}: 2978(m), 2928 (m), 1734 (s), 1515 (s); ^{1}H NMR (300 MHz, $CDCl_3$) δ: 1.39 (s, 9H), 2.26 (s, 3H), 3.41 (s, 2H), 7.00–7.11 (m, 4H); ^{13}C NMR (63 MHz, $CDCl_3$) δ: 21.1, 28.1, 42.2, 80.7, 129.1, 129.2, 131.7, 136.4, 171.2; HRMS (GC-EI, +ve) *m/z* calcd. for $C_{13}H_{22}O_2N_1$ 224.1645, found 224.1644 $(M+NH_4)^+$.

<u>*tert*-Butyl 2-(4-nitrophenyl)acetate</u> 254

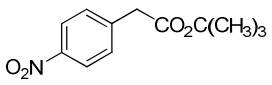

EDCi (5.17 g, 27.07 mmol) in DCM (400 ml), triethylamine (3.75 ml, 22.07 mmol), DMAP (0.08 g, 1.35 mmol), (4-nitro-phenyl)-acetic acid (4.89 g, 27.07 mmol) and *tert*-butyl alcohol (1.00 g, 13.54 mmol) as a solution in DCM (30 mL) were combined according to general procedure 1 (reaction time: 15 hours). The reaction was concentrated *in vacuo*, washed with ether (150 ml), filtered through celite, washed with 1N NaOH (100 ml), washed with 1N HCl (100 ml), dried over magnesium sulfate, concentrated *in vacuo* and subjected to purification by preparative HPLC (acetonitrile/water with 3% trifluoroacetic acid) to afford *tert*-butyl 2-(4-nitrophenyl)acetate **254** as a yellow oil (1.01 g, 31%). FTIR (film/cm^{-1}) υ_{max}: 3084 (w), 2981 (m), 2932 (m), 1728 (s), 1606 (w), 1519 (s); ^{1}H NMR (250 MHz, $CDCl_3$) δ: 1.43 (s, 9H), 3.63 (s, 2H), 7.34 (app. d, 2H, J = 8.8 Hz), 8.18 (app. d, 2H, J = 8.8 Hz); ^{13}C NMR (63 MHz, $CDCl_3$) δ: 28.2, 42.5, 81.9, 123.8, 130.3, 142.2, 147.2, 169.5; HRMS (ESI, -ve) *m/z* calcd. for $C_{12}H_{14}N_1O_4$ 236.0928, found 236.0927 $(M-H)^-$.

***tert*-Butyl 2-phenylacetate 261**

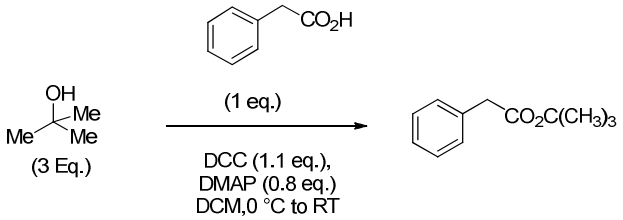

Utilising a protocol reported by Hofmann.[189] To a solution of DCC (8.32 g , 40.4 mmol, 1.1 eq.) in DCM (200 mL) at 0 °C was added DMAP (3.58 g, 29.4 mmol, 0.8 eq.) and phenylacetic acid (5.00 g, 36.8 mmol, 1 eq.). To the resulting suspension was then added *tert*-butyl alcohol (8.20 g, 110 mmol, 3 eq.). The reaction mixture was allowed to stir whilst slowly warming to room temperature over 15 hours. The reaction was concentrated *in vacuo*, washed with ether (150 ml), filtered through celite, washed with 1N NaOH (100 ml), washed with 1N HCl (100 ml), dried over magnesium sulfate, concentrated *in vacuo* and subjected to subjected to column chromatography using gradient elution ethyl acetate/petroleum ether 40-60° (5–10 %) to yield *tert*-butyl 2-phenylacetate **261** as a pale yellow oil (4.90 g, 70%). FTIR (film/cm^{-1}) υ_{max}: 3032 (m), 2979 (m), 2933 (m), 1729 (s), 1604 (s), 1497 (s); ^{1}H NMR (250 MHz, $CDCl_3$) δ: 1.47 (s, 9H), 3.56 (s, 3H), 7.23–7.42 (m, 5H);. ^{13}C NMR (63 MHz, $CDCl_3$) δ: 28.0, 42.7, 80.8, 126.8, 128.4, 129.2, 134.7, 170.9; HRMS (ESI, +ve) *m/z* calcd. for $C_{12}H_{16}NaO_2$ 215.1047, found 215.1042 $(M+Na)^+$.

(1-Methoxy-2-phenyl-*E*-vinyloxy)-trimethyl-silane (*E*)-$^{2}H_1$-262

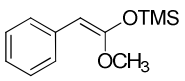

LHMDS (0.57 ml, 0.57 mmol, 1M in THF), TMSCl (0.25 ml, 2.00 mmol) and phenyl-acetic acid methyl ester **158** (50 mg, 0.33 mmol) were combined according to general procedure 9c and purification was achieved by reported procedure to afford (1-methoxy-2-phenyl-*E*-vinyloxy)-trimethyl-silane **(*E*)-$^{2}H_1$-262** as a yellow oil (0.06 g, 80%, *E/Z* = 67:1). ^{1}H NMR (400 MHz, $CDCl_3$) δ: 0.38 (s, 9H), 3.76 (s, 3H), 4.74 (s, 1H), 7.01–7.13 (m), 7.21–7.36 (m, 2H), 7.40–7.51 (m, 2H). ^{13}C NMR (100 MHz,

$CDCl_3$) δ: 0.0, 54.2, 86.0, 124.2, 126.9, 128.5, 136.9, 155.0. IR and HRMS not obtainable. Spectral data in accordance with literature.[190]

(1-tert-Butoxy-2-phenyl-*E*-vinyloxy)-trimethyl-silane (*E*)-$^2H_1$-263

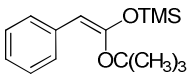

LiHMDS (0.44 ml, 0.44 mmol, 1M in THF), TMSCl (0.20 ml, 1.56 mmol) and *tert*-butyl 2-phenylacetate **261** (0.05 g, 0.26 mmol) were combined according to general procedure 9c and purification was achieved by reported procedure to afford (1-tert-butoxy-2-phenyl-*E*-vinyloxy)-trimethyl-silane **(*E*)-$^2H_1$-263** s a yellow oil (0.05 g, 76%, *E/Z* = 34:1). ^{1}H NMR (400 MHz, $CDCl_3$) δ: 0.39 (s, 9H), 1.51 (s, 9H), 4.90 (s, 1H), 7.09 (app. t 1H, *J* = 7.7 Hz), 7.26–7.32 (m, 2H), 7.53 (app. d, 2H, *J* = 8.1 Hz). ^{13}C NMR (100 MHz, $CDCl_3$) δ: 0.1, 29.4, 80.3, 91.7, 124.0, 126.8, 128.0, 137.1, 153.6. IR and HRMS not obtainable. Data for *E*-SKA in accordance with literature, however *Z*-SKA is not, see NOE spectral assignments of similar compound in appendix.[119]

6.3.7 Isolated Arylacetate Degradation Products

Methyl 2-(2-methoxyphenyl)acetate 181

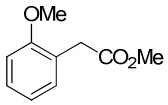

Methyl 2-(2-methoxyphenyl)acetate **181** obtained as a yellow oil. ^{1}H NMR (500 MHz, $CDCl_3$) δ: 3.67 (s, 2H), 3.71 (s, 3H), 3.84 (s, 3H), 6.90 (app. d, 1H, *J* = 7.7 Hz), 6.95 (app. t, 1H, *J* = 7.7 Hz), 7.21 (app. td, 1H, *J* = 7.7 Hz), 7.28 (app. t, 1H, *J* = 7.7 Hz); ^{13}C NMR (125 MHz, $CDCl_3$) δ: 35.7, 51.9, 55.5, 110.5, 120.5, 123.0, 128.6, 130.9, 157.5, 172.3. All analytical data in accordance with literature values.[191]

Methyl 2-(3-methoxyphenyl)acetate 182

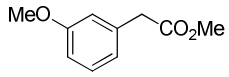

Methyl 2-(3-methoxyphenyl)acetate **182** obtained as a yellow oil. ^{1}H NMR (500 MHz, $CDCl_3$) δ: 3.62 (s, 2H), 3.71 (s, 3H), 3.82 (s, 3H), 6.81–6.91 (m, 3H), 7.25 (t, 1H, *J* = 7.5 Hz); ^{13}C NMR (125 MHz, $CDCl_3$) δ: 41.2, 52.0, 55.1, 112.6, 114.9, 121.6, 129.6, 135.4, 159.7, 171.9. All analytical data in accordance with literature values.[192]

(4-Methoxy-phenyl)-acetic acid methyl ester 183

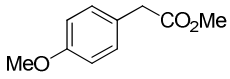

EDCi (1.24 g, 6.47 mmol) in DCM (200 ml), triethylamine (0.91 ml, 6.47 mmol), DMAP (0.04 g, 0.32 mmol), (4-methoxy-phenyl)-acetic acid (1.09 g, 6.47 mmol) and methanol (0.27 ml, 3.23 mmol) were combined according to general procedure 1 (reaction time: 15 hours). Purification was achieved by reported procedure and further purification by column chromatography using gradient elution ethyl acetate/petroleum ether 40-60° (5–15 %) yielded (4-methoxy-phenyl)-acetic acid methyl ester **183** as a clear oil (0.50 g, 84%). FTIR (film/cm^{-1}) υ_{max}: 3000 (m), 2953 (m), 2838 (m), 1733 (s), 1612 (m), 1512 (s); ^{1}H NMR (250 MHz, $CDCl_3$) δ: 3.57 (s, 2H), 3.69 (s, 3H), 3.79 (s, 3H), 6.86 (app. d, 2H, *J* = 8.54 Hz), 7.20 (app. d, 2H, *J* = 8.54 Hz); ^{13}C NMR (63 MHz, $CDCl_3$) δ: 40.3, 52.0, 55.3, 114.0, 126.1, 130.3, 158.7, 172.4; HRMS (ESI, +ve) *m/z* calcd. for $C_{10}H_{16}O_3N_1$ 198.1125, found 198.1121 $(M+NH_4)^+$.

Methyl 2-(*o*-tolyl)acetate 184

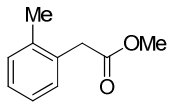

Methyl 2-(o-tolyl)acetate **184** obtained as a yellow oil. ^{1}H NMR (500 MHz, $CDCl_3$) δ: 2.34 (s, 3H), 3.67 (s, 2H), 3.71 (s, 3H), 7.14–7.25 (m, 4H); ^{13}C NMR (125 MHz, $CDCl_3$) δ: 19.6, 39.0, 52.0, 126.1, 127.4, 130.2, 130.4, 132.7, 136.9, 172.0. All analytical data in accordance with literature values.[193]

Methyl 2-(*m*-tolyl)acetate 185

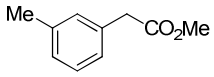

Methyl 2-(m-tolyl)acetate **185** obtained as a yellow oil. ^{1}H NMR (500 MHz, $CDCl_3$) δ: 2.36 (s, 3H), 3.61 (s, 2H), 3.71 (s, 3H), 7.07–7.13 (m, 3H), 7.23 (app. t, 1H, J = 7.6 Hz); ^{13}C NMR (125 MHz, $CDCl_3$) δ: 21.4, 41.2, 52.0, 126.3, 127.9, 128.5, 130.0, 133.9, 138.2, 172.2. All analytical data in accordance with literature values.[194]

***p*-Tolyl-acetic acid methyl ester 186**

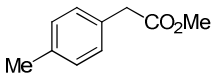

EDCi (1.24 g, 6.47 mmol) in DCM (200 ml), triethylamine (0.91 ml, 6.47 mmol), DMAP (0.04 g, 0.32 mmol), *p*-tolyl acetic acid (0.98 g, 6.47 mmol) and methanol (0.27 ml, 3.23 mmol) were combined according to general procedure 1 (reaction time: 15 hours). Purification was achieved by reported procedure and further purification by column chromatography using gradient elution ethyl acetate/petroleum ether 40-60° (5–15 %) yielded *p*-tolyl-acetic acid methyl ester **186** as an orange oil (0.43 g, 80%). FTIR (film/cm^{-1}) υ_{max}: 3004 (m), 2952 (s), 2924 (m), 1735 (s); ^{1}H NMR (250 MHz, $CDCl_3$) δ: 2.35 (s, 3H), 3.60 (s, 2H), 3.70 (s, 3H), 7.11–7.22 (m, 4H); ^{13}C NMR (63 MHz, $CDCl_3$)

δ: 21.1, 40.8, 52.0, 129.1, 129.3, 130.9, 136.7, 172.2; HRMS (GC-EI, +ve) *m/z* calcd. for $C_{10}H_{12}O_2$ 165.0910, found 165.0908 $(M)^+$.

Methyl 2-(2-nitrophenyl)acetate 187

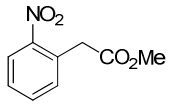

Methyl 2-(2-nitrophenyl)acetate **187** obtained as a yellow oil. ^{1}H NMR (500 MHz, $CDCl_3$) δ: 3.78 (s, 3H), 4.05 (s, 2H), 7.37 (app. d, 1H, *J* = 7.8 Hz), 7.49 (app. t, 1H, *J* = 7.8 Hz), 7.62 (app. t, 1H, *J* = 7.8 Hz), 8.14 (app. d, 1H, *J* = 7.8 Hz); ^{13}C NMR (125 MHz, $CDCl_3$) δ: 39.6, 52.3, 125.3, 128.6, 129.7, 133.3, 133.6, 148.9, 170.4. All analytical data in accordance with literature values.[195]

Methyl 2-(3-nitrophenyl)acetate 188

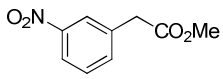

Methyl 2-(3-nitrophenyl)acetate **188** obtained as a yellow oil. ^{1}H NMR (500 MHz, $CDCl_3$) δ: 3.74 (s, 3H), 3.76 (s, 2H), 7.54 (app. t, 1H, *J* = 8.0 Hz), 7.64 (app. d, 1H, *J* = 8.0 Hz), 8.13–8.20 (m, 2H); ^{13}C NMR (125 MHz, $CDCl_3$) δ: 40.5, 52.4, 122.3, 124.4, 129.5, 135.6, 135.8, 148.3, 170.8. All analytical data in accordance with literature values.[196]

(4-Nitro-phenyl)-acetic acid methyl ester 189

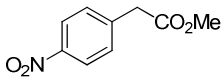

EDCi (1.24 g, 6.47 mmol) in DCM (200 ml), triethylamine (0.91 ml, 6.47 mmol), DMAP (0.04 g, 0.32 mmol), 4-nitro-phenyl)-acetic acid (1.20 g, 6.47 mmol) and methanol (0.27 ml, 3.23 mmol) were combined according to general procedure 1 (reaction time: 15 hours). Purification was achieved by reported procedure and further

purification by column chromatography using gradient elution ethyl acetate/petroleum ether 40-60° (5–15 %) yielded (4-nitro-phenyl)-acetic acid methyl ester **189** as an amorphous solid (0.53 g, 84%). FTIR (film/cm^{-1}) υ_{max}: 2994 (m), 2955 (m), 1736 (s), 1607 (m), 1515 (s); ^{1}H NMR (250 MHz, $CDCl_3$) δ: 3.72 (s, 3H), 3.74 (s, 2H), 7.46 (app.d, 2H, *J* = 8.79 Hz), 8.19 (app.d, 2H, *J* = 8.79 Hz); ^{13}C NMR (75 MHz, $CDCl_3$) δ: 40.9, 52.6, 124.0, 130.7, 141.9, 147.4, 171.0; HRMS (GC-EI, +ve) *m/z* calcd. for $C_9H_9N_1O_4$ 195.0526, found 195.0526 $(M)^+$.

Methyl 2-(4-(dimethylamino)phenyl)acetate 224

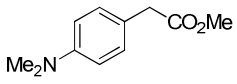

Methyl 2-(4-(dimethylamino)phenyl)acetate **224** as a brown solid. M.p. 54–57 °C; ^{1}H NMR (500 MHz, $CDCl_3$) δ: 2.94 (s, 6H), 3.54 (s, 2H), 3.69 (s, 3H), 6.71 (app.d, 2H, *J* = 8.4 Hz), 7.16 (app.d, 2H, *J* = 8.4 Hz); ^{13}C NMR (125 MHz, $CDCl_3$) δ: 40.2, 40.6, 51.9, 112.7, 121.8, 129.9, 149.8, 172.7. All analytical data in accordance with literature values.[197]

Methyl 2-(4-iodophenyl)acetate 225

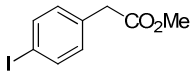

Methyl 2-(4-iodophenyl)acetate **225** obtained as a yellow oil. ^{1}H NMR (500 MHz, $CDCl_3$) δ: 3.58 (s, 2H), 3.71 (s, 3H), 7.04 (app. d, 2H, *J* = 8.0 Hz), 7.66 (app. d, 1H, *J* = 8.0 Hz); ^{13}C NMR (125 MHz, $CDCl_3$) δ: 40.6, 52.2, 92.6, 131.3, 133.6, 137.7, 171.5. All analytical data in accordance with literature values.[198]

Methyl 2-(4-fluorophenyl)acetate 226

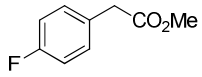

Methyl 2-(4-fluorophenyl)acetate **226** obtained as a yellow oil. ^{1}H NMR (500 MHz, $CDCl_3$) δ: 3.60 (s, 2H), 3.69 (s, 3H), 6.98–7.04 (m, 2H), 7.21–7.27 (m, 2H); ^{13}C NMR (125 MHz, $CDCl_3$) δ: 40.2, 52.0, 115.4 (d, J = 21.3 Hz), 129.6 (d, J = 3.3 Hz), 130.8 (d, J = 7.9 Hz), 161.5 (d, J = 244 Hz), 171.9. All analytical data in accordance with literature values.[199]

Methyl 2-(4-chlorophenyl)acetate 227

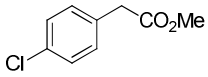

Methyl 2-(4-chlorophenyl)acetate **227** obtained as a yellow oil. ^{1}H NMR (500 MHz, $CDCl_3$) δ: 3.61 (s, 2H), 3.71 (s, 3H), 7.22 (app. d, 2H, J = 8.4 Hz), 7.31 (app. d, 1H, J = 8.4 Hz); ^{13}C NMR (125 MHz, $CDCl_3$) δ: 40.4, 52.1, 128.7, 130.6, 132.4, 133.1, 171.6. All analytical data in accordance with literature values.[200]

Methyl 2-(4-(trifluoromethyl)phenyl)acetate 228

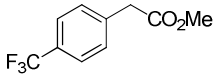

Methyl 2-(4-(trifluoromethyl)phenyl)acetate **228** obtained as a yellow oil. ^{1}H NMR (500 MHz, $CDCl_3$) δ: 3.70 (s, 2H), 3.72 (s, 3H), 7.41 (app. d, 2H, J = 8.2 Hz), 7.59 (app. d, 2H, J = 8.2 Hz); ^{13}C NMR (125 MHz, $CDCl_3$) δ: 40.8, 52.2, 124.2 (q, J = 271.4 Hz), 125.5 (q, J = 3.8 Hz), 129.5 (q, J = 32.7 Hz), 129.7, 137.9, 171.2. All analytical data in accordance with literature values.[199]

Methyl 2-(4-(methylsulfonyl)phenyl)acetate 230

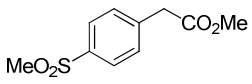

Methyl 2-(4-(methylsulfonyl)phenyl)acetate **230** obtained as an amorphous white solid. FTIR (film/cm^{-1}) υ_{max}: 3003 (m), 2953 (m), 2931 (m), 1735 (s), 1592 (m), 1562 (m); ^{1}H NMR (500 MHz, $CDCl_3$) δ: 3.06 (s, 2H), 3.74 (s, 3H), 3.76 (s, 2H), 7.51 (app. d, 2H, *J* = 8.2 Hz), 7.92 (app. d, 2H, *J* = 8.2 Hz); ^{13}C NMR (125 MHz, $CDCl_3$) δ: 40.9, 44.5, 52.4, 127.7, 130.4, 139.5, 140.2, 170.8; HRMS (ESI, +ve) *m/z* calcd. for $C_{10}H_{12}Na_1O_4S_1$ 251.0349, found 251.0347 $(M+Na)^+$.

(2,4-Dimethoxy-phenyl)-acetic acid methyl ester 231

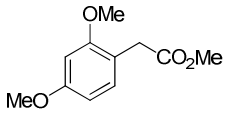

(2,4-Dimethoxy-phenyl)-acetic acid methyl ester **231** obtained as a clear oil. ^{1}H NMR (500 MHz, $CDCl_3$) δ: 3.58 (s, 2H), 3.69 (s, 3H), 3.80 (s, 3H), 3.81 (s, 3H), 6.45–6.49 (m, 2H), 7.09 (app. d, 1H, *J* = 7.9 Hz); ^{13}C NMR (125 MHz, $CDCl_3$) δ: 35.1, 51.9, 55.4, 55.5, 98.7, 104.1, 115.5, 131.1, 158.4, 160.2, 172.6. All analytical data in accordance with literature values.Charabarty.[201]

(*E*)-Methyl 4-phenylbut-3-enoate 232

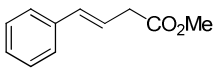

(*E*)-Methyl 4-phenylbut-3-enoate **232** obtained as a yellow oil. ^{1}H NMR (500 MHz, $CDCl_3$) δ: 3.27 (dd, 3H, *J* = 7.1, 1.1 Hz), 3.73 (s, 3H), 6.31 (dt, 1H, *J* = 15.9, 7.1 Hz), 6.51 (d, 1H, *J* = 15.9 Hz),7.23–7.27 (m, 1H), 7.32 (app. t, 2H, *J* = 7.2 Hz), 7.36–7.41 (m, 2H); ^{13}C NMR (125 MHz, $CDCl_3$) δ: 29.7, 38.2, 116.7, 121.7, 126.3, 126.6, 128.5, 133.5, 172.0. All analytical data in accordance with literature values.[202]

Methyl 2-(1-methyl-1H-indol-3-yl)acetate 233

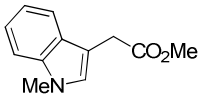

Methyl 2-(1-methyl-1H-indol-3-yl)acetate **233** obtained as a red oil. ^{1}H NMR (500 MHz, $CDCl_3$) δ: 3.71 (s, 3H), 3.78 (s, 3H), 3.79 (s, 2H), 7.06 (s, 1H), 7.14 (app. t, 1H, *J* = 7.6 Hz), 7.25 (app. d, 1H, *J* = 7.6 Hz), 7.31 (app. d, 1H, *J* = 7.6 Hz), 7.61 (app. d, 1H, *J* = 7.6 Hz); ^{13}C NMR (125 MHz, $CDCl_3$) δ: 31.0, 32.7, 51.9, 106.8, 109.3, 118.9, 119.2, 121.8, 127.6, 127.7, 136.9, 172.7. All analytical data in accordance with literature values.[203]

Benzo[1,3]dioxol-5-yl-acetic acid methyl ester 234

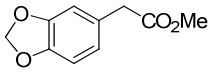

Benzo[1,3]dioxol-5-yl-acetic acid methyl ester **234** obtained as a yellow oil. ^{1}H NMR (500 MHz, $CDCl_3$) δ: 3.52 (s, 2H), 3.67 (s, 3H), 5.91 (s, 2H), 6.66–6.79 (m, 3H); ^{13}C NMR (125 MHz, $CDCl_3$) δ: 40.7, 52.0, 101.0, 108.2, 109.7, 122.4, 127.6, 146.7, 147.8, 172.1. All analytical data in accordance with literature values.[204]

(2-Iodo-phenyl)-acetic acid methyl ester 362

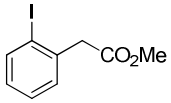

(2-Iodo-phenyl)-acetic acid methyl ester **362** obtained as a yellow oil. ^{1}H NMR (500 MHz, $CDCl_3$) δ: 3.73 (s, 3H), 3.82 (s, 2H), 6.97 (td, 1H, *J* = 7.7, 1.6 Hz), 7.26–7.36 (m, 2H), 7.85 (dd, 1H, *J* = 7.7, 1.6 Hz); ^{13}C NMR (125 MHz, $CDCl_3$) δ: 46.1, 52.2, 101.0, 128.5, 128.9, 130.7, 137.7, 139.5, 171.0. All analytical data in accordance with literature values.[205]

(2,4-Dichloro-phenyl)-acetic acid methyl ester 363

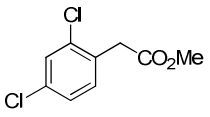

(2,4-Dichloro-phenyl)-acetic acid methyl ester **363** obtained as a faint yellow oil. FTIR (film/cm^{-1}) υ_{max}: 3009 (w), 2954 (m), 1736 (s), 1592 (m), 1562 (m); ^{1}H NMR (500 MHz, $CDCl_3$) δ: 3.70 (s, 3H), 3.73 (s, 2H), 7.16–7.23 (m, 2H), 7.36–7.39 (m, 1H); ^{13}C NMR (125 MHz, $CDCl_3$) δ: 38.3, 52.2, 127.2, 129.3, 131.0, 132.2, 133.8, 135.2, 170.5; HRMS (ESI, +ve) *m/z* calcd. for $C_9H_8Cl_2NaO_2$ 240.9794, found 240.9786 $(M+Na)^+$.

6.3.8. E1cB Degradation Products

2-Phenyl-hexa-2,4-dienoic acid methyl ester 201

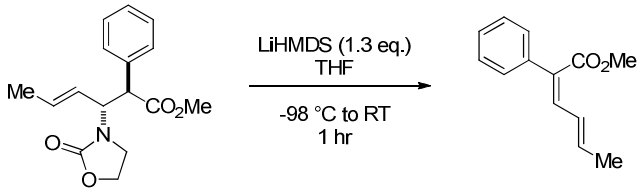

To a solution of (*anti-E*)-methyl 3-(2-oxooxazolidin-3-yl)-2-phenylhex-4-enoate **144** (0.20 g, 0.53 mmol, 1.0 eq.) in THF (2 ml) at –98 °C was added LiHMDS (1 M in THF, 0.68 ml, 0.68 mmol, 1.3 eq.) by hand addition. On complete addition the reaction mixture was allowed to warm to RT over 1 hour and was then quenched with HCl (1M)/Brine (1:1, 5 ml). The organics were extracted with EtOAc (5 × 15 ml), dried over $MgSO_4$, filtered and then concentrated *in vacuo* to yield the crude reaction mixture, which was purified by flash column chromatography using gradient elution ethyl acetate/petroleum ether 40-60°/triethylamine (5:95:1–50:60:1), to yield 2-phenyl-hexa-2,4-dienoic acid methyl ester **201** as a yellow oil (0.06 g, 57%). FTIR (film/cm^{-1}) υ_{max}: 2921 (m), 2255 (w), 1705 (s), 1519 (s), 1436 (m); ^{1}H NMR (250 MHz, $CDCl_3$) δ: 1.71 (d, 3H, J = 6.3 Hz), 3.68 (s, 3H), 5.93–6.24 (m, 2H), 7.17–7.24 (m, 2H), 7.30–7.49 (m, 4H); ^{13}C NMR (100 MHz, $CDCl_3$) δ: 18.9, 52.1, 127.5, 128.0, 128.2, 130.1, 130.2,

135.4, 139.9, 141.2, 168.2; HRMS (ESI, +ve) *m/z* calcd. for $C_{13}H_{14}NaO_2$, 225.0891, found 225.0886 $(M+Na)^+$.

2-Benzyloxy-hexa-2,4-dienoic acid methyl ester 353

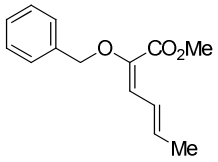

LiHMDS (1M in toluene, 3.15 ml, 3.15 mmol), triethylamine (4.37 ml, 31.5 mmol) and (*E*)-4-(*N*-benzyl-4-methylphenylsulfonamido)but-3-en-2-yl pent-4-enoate **337** (0.30 g, 0.70 mmol) in THF (3 ml) was combined according to general procedure 4 (reaction time : 75 minutes). Treatment with diazomethane and purification by flash chromatography afforded 2-benzyloxy-hexa-2,4-dienoic acid methyl ester **353** as a yellow oil (0.16 g, 90%). FTIR (film/cm^{-1}) υ_{max}: 3020 (m), 2961 (m), 1713 (s), 1643 (m); ^{1}H NMR (500 MHz, CD_3Cl) δ: 1.81 (dd, 3H, *J* = 7.0, 1.4 Hz), 3.81 (s, 3H), 4.90 (s, 3H), 6.02 (dq, 1H, *J* = 14.8, 7.0 Hz), 6.40 (ddq, 1H, *J* = 14.8, 11.4, 1.4 Hz), 6.76 (d, 1H, *J* = 11.4 Hz), 7.31–7.46 (m, 5H); ^{13}C NMR (125 MHz, CD_3Cl) *δ*: 18.8, 51.9, 74.6, 124.8, 127.4, 128.1, 128.4 (x2), 136.5, 137.0, 141.7, 164.8; HRMS (ESI, +ve) *m/z* calcd. for $C_{14}H_{16}NaO_3$ 255. 0997, found 255.0999 $(M+Na)^+$.

2-Phenylsulfanyl-hexa-2,4-dienoic acid methyl ester 354

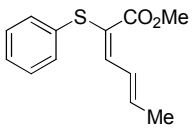

LiHMDS (1M in toluene, 2.61 ml, 2.61 mmol), triethylamine (3.62 ml, 26.1 mmol) and (*E*)-4-(*N*-benzyl-4-methylphenylsulfonamido)but-3-en-2-yl pent-4-enoate **338** (0.25 g, 0.58 mmol) in THF (2.5 ml) was combined according to general procedure 4 (reaction time : 75 minutes). Treatment with diazomethane and purification by flash chromatography afforded 2-phenylsulfanyl-hexa-2,4-dienoic acid methyl ester **354** as a yellow oil (0.13 g, 93%). FTIR (film/cm^{-1}) υ_{max}: 3085 (m), 3021 (m), 2982 (m), 2937 (m), 1730 (s), 1656 (s), 1615 (m), 1596 (m), 1509 (m); ^{1}H NMR (500 MHz, CD_3Cl) δ:

1.93 (dd, 3H, J = 7.0, 1.1 Hz), 3.70 (s, 3H), 6.39 (dq, 1H, J = 14.8, 7.0 Hz), 6.80–6.90 (m, 1H), 7.10–7.54 (m, 5H), 7.80 (d, 1H, J = 11.0 Hz); ^{13}C NMR (125 MHz, CD_3Cl) δ: 19.2, 52.6, 121.1, 125.8, 127.6, 128.9, 129.9, 136.2, 143.1, 149.7, 166.5; HRMS (ESI, +ve) *m/z* calcd. for $C_{13}H_{15}O_2S$ 235.0792, found 235.0767 $(M+H)^+$.

7. Appendix

7.1. X-Ray Data for $\beta^{2,3}$-Amino Acid Precursor 144

Identification code	k08dc4
Empirical formula	C16 H19 N O4
Formula weight	289.32
Temperature	150(2) K
Wavelength	0.71073 Å
Crystal system	Monoclinic
Space group	P21/c
Unit cell dimensions	a = 15.0780(2)Å $\alpha = 90^o$
	b = 6.2840(1)Å $\beta = 105.097(1)^o$
	c = 16.5130(3)Å $\gamma = 90^o$
Volume	1510.61(4) $Å^3$
Z	4
Density (calculated)	1.272 Mg/m^3
Absorption coefficient	0.091 mm^{-1}
F(000)	616
Crystal size	0.50 x 0.40 x 0.35 mm
Theta range for data collection	3.63 to 29.13^o
Index ranges	-20<=h<=20; -8<=k<=8; -22<=l<=22
Reflections collected	28323
Independent reflections	4056 [R(int) = 0.0452]
Reflections observed (>2σ)	3110
Data Completeness	0.994
Absorption correction	Semi-empirical from equivalents
Max. and min. transmission	0.96 and 0.90
Refinement method	Full-matrix least-squares on F^2
Data / restraints / parameters	4056 / 0 / 193
Goodness-of-fit on F^2	1.018
Final R indices [I>2σ(I)]	R1 = 0.0485 wR2 = 0.1193
R indices (all data)	R1 = 0.0668 wR2 = 0.1327
Largest diff. peak and hole	0.454 and -0.242 $eÅ^{-3}$

*Table 25. Crystal Data and Structure Refinement for **144**. Notes: Potential for C-H···O interactions leading to 1-D hydrogen-bonded chains in the lattice. Crystal structure representative of the batch according PXRD analysis*

Atom	x	y	z	U(eq)
O(1)	6104(1)	4741(2)	3039(1)	53(1)
O(2)	7027(1)	6146(2)	2307(1)	66(1)
O(3)	6308(1)	3486(2)	391(1)	43(1)
O(4)	5494(1)	1248(2)	963(1)	38(1)
N(1)	6977(1)	2554(2)	2539(1)	28(1)
C(1)	6743(1)	4597(2)	2594(1)	39(1)
C(2)	5870(1)	2640(3)	3261(1)	49(1)
C(3)	6533(1)	1140(2)	3007(1)	37(1)
C(4)	7615(1)	1892(2)	2054(1)	28(1)
C(5)	7094(1)	623(2)	1268(1)	26(1)
C(6)	6272(1)	1951(2)	819(1)	27(1)
C(7)	4691(1)	2534(3)	599(1)	44(1)
C(8)	8416(1)	644(2)	2579(1)	34(1)
C(9)	9211(1)	1504(3)	2943(1)	42(1)
C(10)	10026(1)	349(4)	3483(1)	60(1)
C(11)	7685(1)	118(2)	677(1)	27(1)
C(12)	7695(1)	-1945(2)	369(1)	33(1)
C(13)	8182(1)	-2386(2)	-224(1)	41(1)
C(14)	8668(1)	-809(3)	-497(1)	46(1)
C(15)	8673(1)	1225(3)	-184(1)	45(1)
C(16)	8184(1)	1693(2)	397(1)	37(1)

Table 26. Atomic coordinates (x 10^4) and equivalent isotropic displacement parameters ($Å^2$ x 10^3) for 1.U(eq) is defined as one third of the trace of the orthogonalized Uij tensor.

O(1)-C(1)	1.3589(18)	O(1)-C(2)	1.438(2)
O(2)-C(1)	1.2082(18)	O(3)-C(6)	1.2051(16)
O(4)-C(6)	1.3304(15)	O(4)-C(7)	1.4501(16)
N(1)-C(1)	1.3413(17)	N(1)-C(3)	1.4509(16)
N(1)-C(4)	1.4629(16)	C(2)-C(3)	1.510(2)
C(2)-H(2A)	0.9900	C(2)-H(2B)	0.9900
C(3)-H(3A)	0.9900	C(3)-H(3B)	0.9900
C(4)-C(8)	1.5100(18)	C(4)-C(5)	1.5502(17)
C(4)-H(4)	1.0000	C(5)-C(11)	1.5174(17)
C(5)-C(6)	1.5188(16)	C(5)-H(5)	1.0000
C(7)-H(7A)	0.9800	C(7)-H(7B)	0.9800
C(7)-H(7C)	0.9800	C(8)-C(9)	1.310(2)
C(8)-H(8)	0.9500	C(9)-C(10)	1.503(2)
C(9)-H(9)	0.9500	C(10)-H(10A)	0.9800
C(10)-H(10B)	0.9800	C(10)-H(10C)	0.9800
C(11)-C(16)	1.3924(18)	C(11)-C(12)	1.3937(18)
C(12)-C(13)	1.396(2)	C(12)-H(12)	0.9500
C(13)-C(14)	1.376(2)	C(13)-H(13)	0.9500
C(14)-C(15)	1.378(2)	C(14)-H(14)	0.9500
C(15)-C(16)	1.386(2)	C(15)-H(15)	0.9500
C(16)-H(16)	0.9500		
C(1)-O(1)-C(2)	109.39(11)	C(6)-O(4)-C(7)	114.89(10)

C(1)-N(1)-C(3)	112.59(11)	C(1)-N(1)-C(4)	122.09(11)
C(3)-N(1)-C(4)	125.32(10)	O(2)-C(1)-N(1)	128.17(14)
O(2)-C(1)-O(1)	122.18(13)	N(1)-C(1)-O(1)	109.65(12)
O(1)-C(2)-C(3)	106.20(12)	O(1)-C(2)-H(2A)	110.5
C(3)-C(2)-H(2A)	110.5	O(1)-C(2)-H(2B)	110.5
C(3)-C(2)-H(2B)	110.5	H(2A)-C(2)-H(2B)	108.7
N(1)-C(3)-C(2)	101.31(11)	N(1)-C(3)-H(3A)	111.5
C(2)-C(3)-H(3A)	111.5	N(1)-C(3)-H(3B)	111.5
C(2)-C(3)-H(3B)	111.5	H(3A)-C(3)-H(3B)	109.3
N(1)-C(4)-C(8)	112.01(10)	N(1)-C(4)-C(5)	110.05(10)
C(8)-C(4)-C(5)	111.59(11)	N(1)-C(4)-H(4)	107.7
C(8)-C(4)-H(4)	107.7	C(5)-C(4)-H(4)	107.7
C(11)-C(5)-C(6)	110.01(10)	C(11)-C(5)-C(4)	113.10(10)
C(6)-C(5)-C(4)	107.28(10)	C(11)-C(5)-H(5)	108.8
C(6)-C(5)-H(5)	108.8	C(4)-C(5)-H(5)	108.8
O(3)-C(6)-O(4)	123.17(11)	O(3)-C(6)-C(5)	124.74(11)
O(4)-C(6)-C(5)	112.08(10)	O(4)-C(7)-H(7A)	109.5
O(4)-C(7)-H(7B)	109.5	H(7A)-C(7)-H(7B)	109.5
O(4)-C(7)-H(7C)	109.5	H(7A)-C(7)-H(7C)	109.5
H(7B)-C(7)-H(7C)	109.5	C(9)-C(8)-C(4)	123.32(14)
C(9)-C(8)-H(8)	118.3	C(4)-C(8)-H(8)	118.3
C(8)-C(9)-C(10)	125.61(17)	C(8)-C(9)-H(9)	117.2
C(10)-C(9)-H(9)	117.2	C(9)-C(10)-H(10A)	109.5
C(9)-C(10)-H(10B)	109.5	H(10A)-C(10)-H(10B)	109.5
C(9)-C(10)-H(10C)	109.5	H(10A)-C(10)-H(10C)	109.5
H(10B)-C(10)-H(10C)	109.5	C(16)-C(11)-C(12)	118.80(12)
C(16)-C(11)-C(5)	121.54(11)	C(12)-C(11)-C(5)	119.57(11)
C(11)-C(12)-C(13)	119.87(13)	C(11)-C(12)-H(12)	120.1
C(13)-C(12)-H(12)	120.1	C(14)-C(13)-C(12)	120.58(14)
C(14)-C(13)-H(13)	119.7	C(12)-C(13)-H(13)	119.7
C(13)-C(14)-C(15)	119.78(14)	C(13)-C(14)-H(14)	120.1
C(15)-C(14)-H(14)	120.1	C(14)-C(15)-C(16)	120.28(15)
C(14)-C(15)-H(15)	119.9	C(16)-C(15)-H(15)	119.9
C(15)-C(16)-C(11)	120.67(14)	C(15)-C(16)-H(16)	119.7
C(11)-C(16)-H(16)	119.7		

Table 27. Bond lengths [Å] and angles [°] for 1. Symmetry transformations used to generate equivalent atoms.

Atom	U11	U22	U33	U23	U13	U12
O(1)	80(1)	34(1)	57(1)	6(1)	41(1)	17(1)
O(2)	114(1)	24(1)	77(1)	8(1)	57(1)	7(1)
O(3)	34(1)	37(1)	59(1)	21(1)	13(1)	4(1)
O(4)	26(1)	42(1)	47(1)	18(1)	11(1)	6(1)
N(1)	34(1)	22(1)	30(1)	3(1)	11(1)	1(1)
C(1)	59(1)	26(1)	37(1)	2(1)	20(1)	7(1)
C(2)	59(1)	40(1)	58(1)	1(1)	34(1)	4(1)
C(3)	45(1)	31(1)	40(1)	8(1)	20(1)	3(1)
C(4)	28(1)	26(1)	30(1)	2(1)	9(1)	-1(1)
C(5)	25(1)	22(1)	30(1)	4(1)	7(1)	0(1)
C(6)	27(1)	25(1)	28(1)	1(1)	7(1)	1(1)
C(7)	26(1)	52(1)	54(1)	21(1)	11(1)	10(1)
C(8)	31(1)	37(1)	32(1)	4(1)	6(1)	2(1)
C(9)	31(1)	56(1)	37(1)	-7(1)	7(1)	0(1)
C(10)	31(1)	99(2)	44(1)	-11(1)	0(1)	13(1)
C(11)	24(1)	28(1)	29(1)	1(1)	5(1)	2(1)
C(12)	28(1)	30(1)	39(1)	-1(1)	3(1)	1(1)
C(13)	42(1)	38(1)	40(1)	-10(1)	5(1)	9(1)
C(14)	45(1)	57(1)	39(1)	-2(1)	19(1)	11(1)
C(15)	47(1)	48(1)	49(1)	2(1)	26(1)	-2(1)
C(16)	41(1)	32(1)	42(1)	-2(1)	18(1)	-4(1)

Table 28. Anisotropic displacement parameters ($Å^2$ x 10^3) for 1. The anisotropic displacement factor exponent takes the form: -2 gpi^2 [h^2 a^{*2} U11 + ... + 2 h k a b* U*

Atom	x	y	z	U(eq)
H(2A)	5230	2285	2960	59
H(2B)	5933	2545	3872	59
H(3A)	6980	536	3503	44
H(3B)	6207	-33	2651	44
H(4)	7866	3209	1855	33
H(5)	6869	-742	1455	31
H(7A)	4802	4002	800	66
H(7B)	4160	1958	764	66
H(7C)	4567	2512	-14	66
H(8)	8339	-840	2648	40
H(9)	9279	2984	2860	50
H(10A)	10137	837	4064	89
H(10B)	10569	641	3279	89
H(10C)	9904	-1185	3456	89
H(12)	7372	-3049	563	40
H(13)	8179	-3787	-441	49
H(14)	8998	-1121	-900	55
H(15)	9014	2311	-367	54
H(16)	8188	3102	606	44

Table 29. Hydrogen coordinates (x 10^4) and isotropic displacement parameters ($Å^2$ x 10^3).

C(3) – N(1) - C(1) - O(2)	176.38(17)
C(4) – N(1) - C(1) - O(2)	-3.6(3)
C(3) – N(1) - C(1) - O(1)	-3.66(18)
C(4) – N(1) - C(1) - O(1)	176.40(12)
C(2) – O(1) - C(1) - O(2)	177.21(17)
C(2) – O(1) - C(1) - N(1)	-2.75(19)
C(1) – O(1) - C(2) - C(3)	7.64(19)
C(1) – N(1) - C(3) - C(2)	7.94(16)
C(4) – N(1) - C(3) - C(2)	-172.12(12)
O(1) – C(2) - C(3) - N(1)	-9.00(17)
C(1) – N(1) - C(4) - C(8)	124.51(14)
C(3) – N(1) - C(4) - C(8)	-55.43(16)
C(1) – N(1) - C(4) - C(5)	-110.75(14)
C(3) – N(1) - C(4) - C(5)	69.32(15)
N(1) – C(4) - C(5) - C(11)	172.85(10)
C(8) – C(4) - C(5) - C(11)	-62.16(13)
N(1) – C(4) - C(5) - C(6)	51.36(13)
C(8) – C(4) - C(5) - C(6)	176.35(10)
C(7) – O(4) - C(6) - O(3)	-3.0(2)
C(7) – O(4) - C(6) - C(5)	175.93(12)
C(11) - C(5) - C(6) - O(3)	-46.73(17)
C(4) – C(5) - C(6) - O(3)	76.68(16)
C(11) - C(5) - C(6) - O(4)	134.35(11)
C(4) – C(5) - C(6) - O(4)	-102.24(12)
N(1) – C(4) - C(8) - C(9)	-95.81(16)
C(5) – C(4) - C(8) - C(9)	140.31(14)
C(4) – C(8) - C(9) - C(10)	179.00(14)
C(6) – C(5) - C(11) - C(16)	68.85(15)
C(4) – C(5) - C(11) - C(16)	-51.09(16)
C(6) – C(5) - C(11) - C(12)	-107.77(13)
C(4) – C(5) - C(11) - C(12)	132.29(12)
C(16) - C(11) - C(12) – C(13)	-1.51(19)
C(5) – C(11) - C(12) - C(13)	175.21(12)
C(11) - C(12) - C(13) – C(14)	1.2(2)
C(12) - C(13) - C(14) – C(15)	-0.1(2)
C(13) - C(14) - C(15) – C(16)	-0.8(2)
C(14) - C(15) - C(16) – C(11)	0.5(2)
C(12) - C(11) - C(16) – C(15)	0.7(2)
C(5) – C(11) - C(16) - C(15)	-175.96(13)

Table 30. Dihedral angles [°] for 1. Atom1 - Atom2 - Atom3 - Atom4, Dihedral Symmetry Transformations Used to Generate Equivalent Atoms.

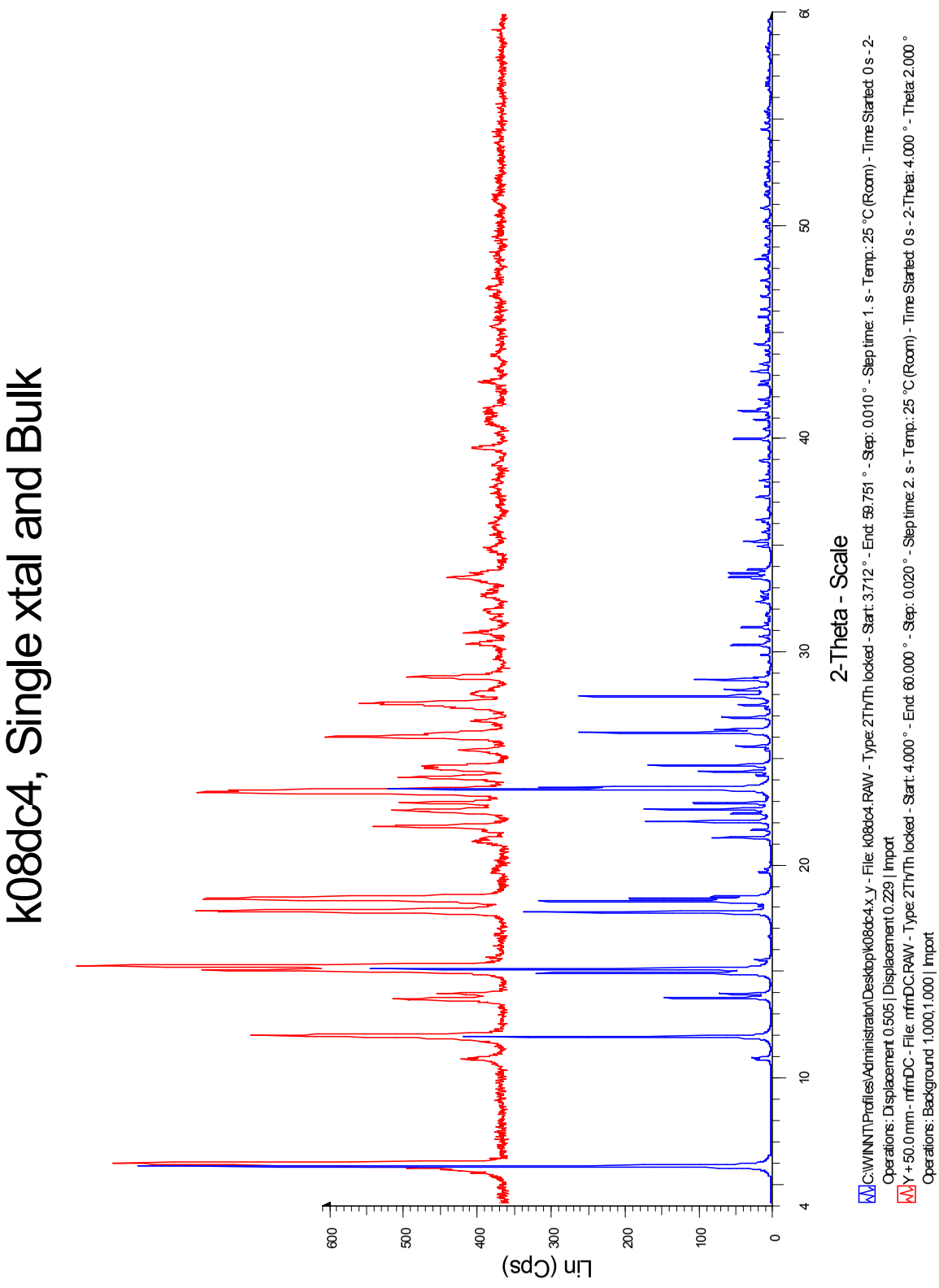

*Graph 26. Single Crystal & Bulk Powder Diffraction Patterns from **144**.*

7.2. Hammett Type Plots with Other σ-Values

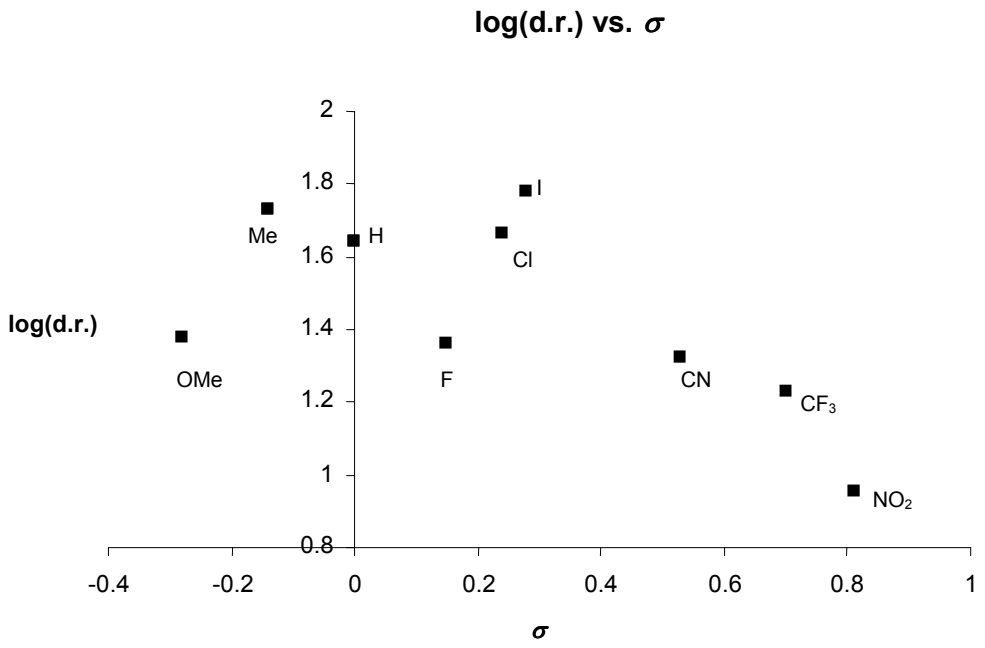

Graph 27. Log(d.r.) vs. σ.

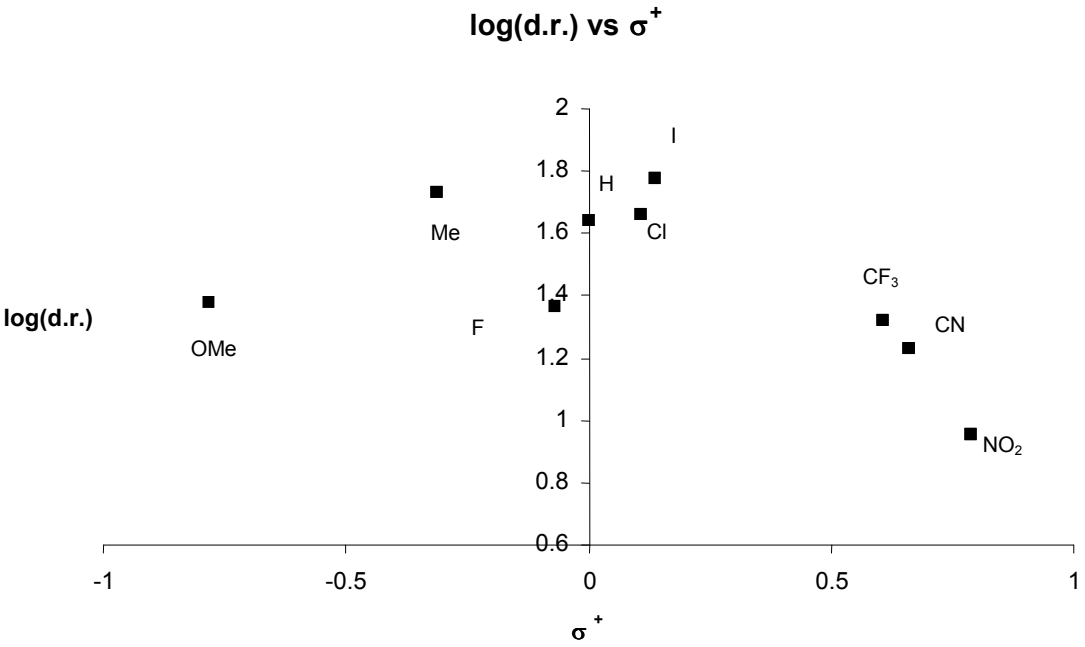

Graph 28. Log(d.r.) vs. σ^+.

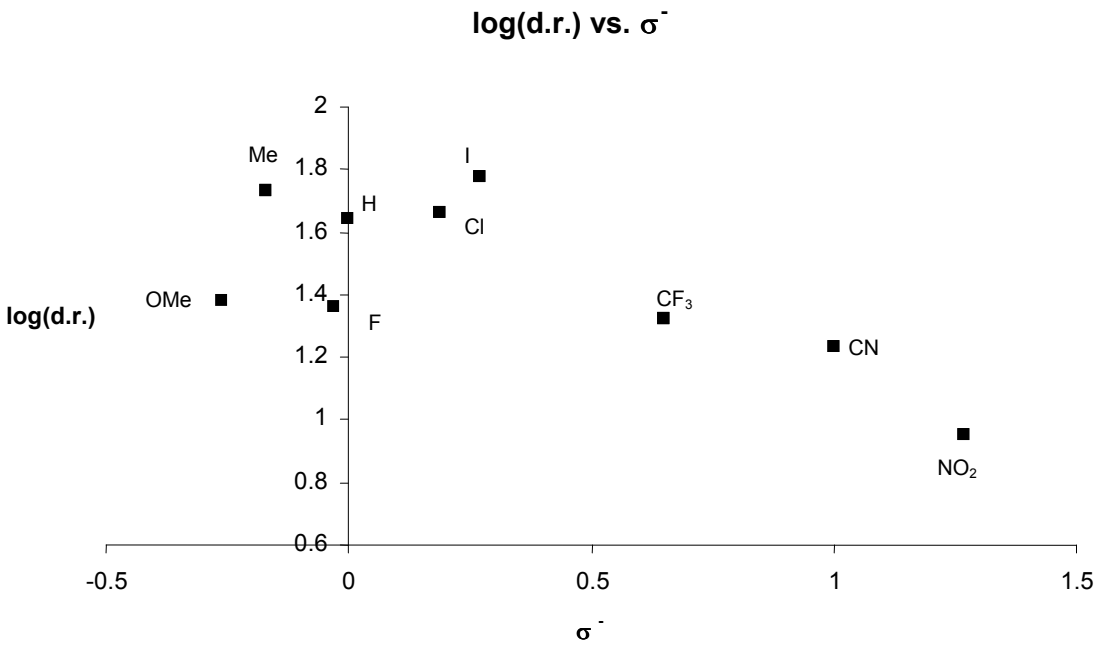

Graph 29. Log(d.r.) vs. σ^-.

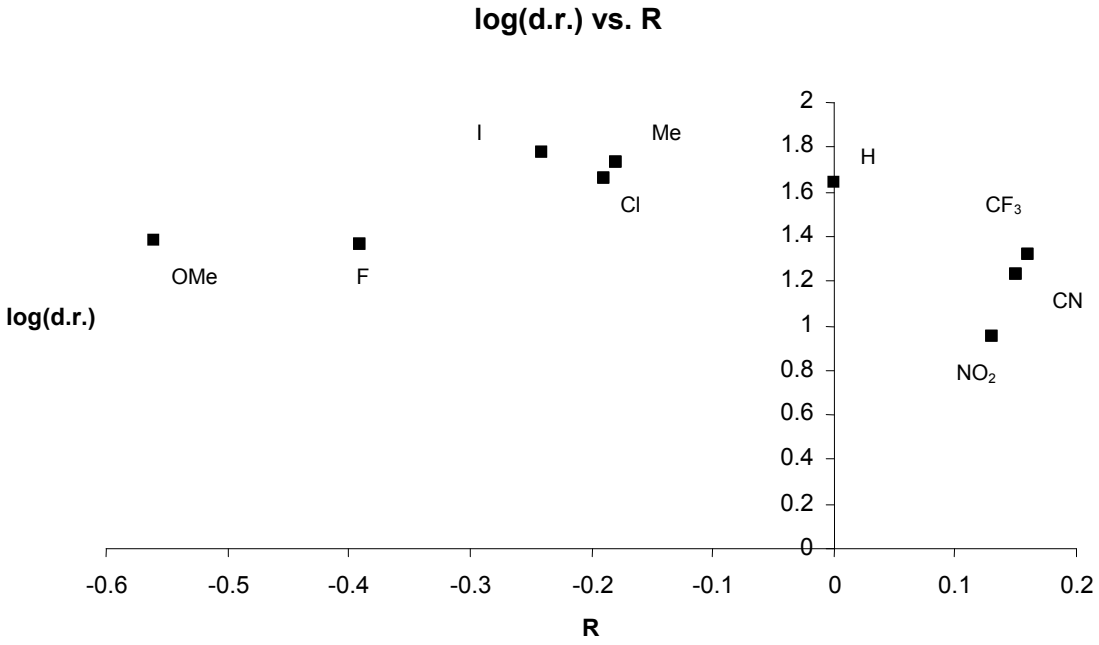

Graph 30. Log(d.r.) vs. Resonance Parameter R.

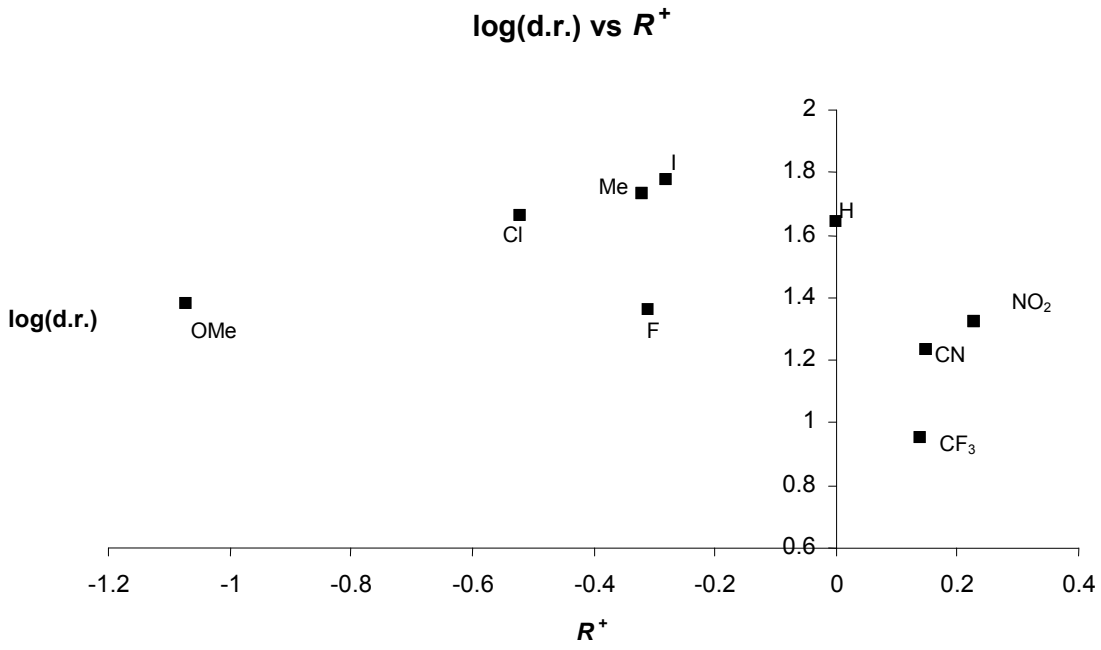

Graph 31. Log(d.r.) vs Resonance Parameter R^+.

7.3. 1D-NOE Data for Isolated Tolyl Derived SKAs

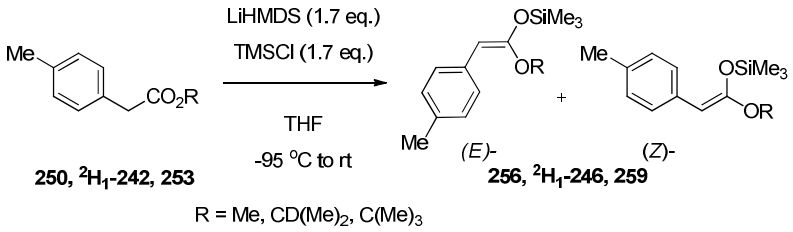

Entry	R	Product	$(E/Z)^a$	Yield (%)
1	Me	**256**	44:1	99
2	$CDMe_2$	**246**	68:1	99
3	CMe_3	**259**	68:1	99

Table 31. Yields & E/Z-Selectivity for 1°, 2° & 3° Derived Tolyl-SKAs.

(1-Methoxy-2-*p*-tolyl-vinyloxy)-trimethyl-silane 256

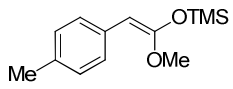

LHMDS (0.72 ml, 0.72 mmol, 1M in THF), TMSCl (0.10 ml, 0.72 mmol) and *p*-tolyl-acetic acid methyl ester **250** (0.10 g, 0.42 mmol) were combined according to general procedure 9a and purification was achieved by reported procedure to afford (1-methoxy-2-*p*-tolyl-vinyloxy)-trimethyl-silane **256** as a yellow oil (0.10 g, 99%, *E/Z* 44:1). ^{1}H NMR (400 MHz, $CDCl_3$) δ: 0.32 (s, 9H), 2.30 (s, 3H), 3.68 (s, 3H), 4.68 (s, 1H), 7.06 (app. d, 2H, J = 8.1 Hz), 7.31 (app. d, 2H, J = 8.1 Hz); ^{13}C NMR (100 MHz, $CDCl_3$) δ: 5.5, 21.0, 53.9, 86.0, 126.5, 128.8, 133.3, 133.7, 154.4. IR and HRMS not obtainable.

(1-Methoxy-2-*p*-tolyl-vinyloxy)-trimethyl-silane 256

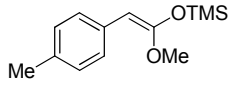


```
NAME      Primary tolyl SKA isolation
EXPNO                 1
PROCNO                1
Date_          20091217
Time              15.47
INSTRUM           spect
PROBHD   5 mm PABBO BB-
PULPROG            zg30
TD                65536
SOLVENT           CDCl3
NS                   13
DS                    0
SWH            8278.146 Hz
FIDRES        0.126314 Hz
AQ            3.9584243 sec
RG                  128
DW               60.400 usec
DE                6.00 usec
TE              298.0 K
D1           1.00000000 sec
TD0                   1

======== CHANNEL f1 ========
NUC1                 1H
P1                10.75 usec
PL1                0.00 dB
SFO1         400.1324710 MHz
SI                32768
SF           400.1300239 MHz
WDW                  no
SSB                   0
LB                 0.00 Hz
GB                    0
PC                 1.40
```

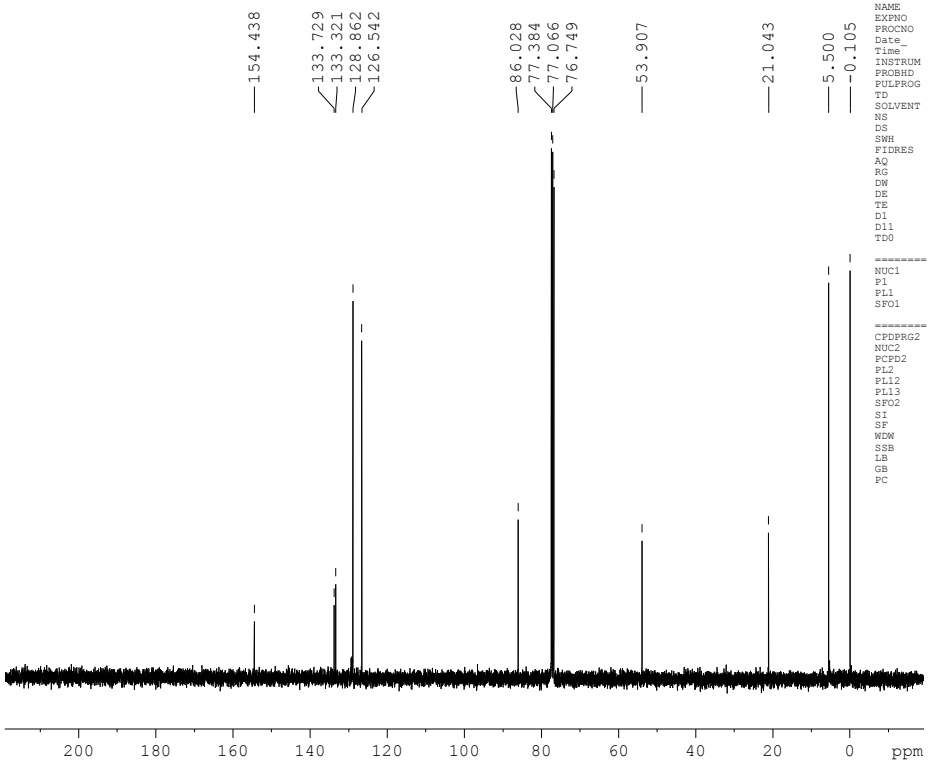


```
NAME      Primary tolyl SKA isolation
EXPNO                 2
PROCNO                1
Date_          20091217
Time              15.52
INSTRUM           spect
PROBHD   5 mm PABBO BB-
PULPROG          zgpg30
TD                65536
SOLVENT           CDCl3
NS                   49
DS                    4
SWH           23980.814 Hz
FIDRES        0.365918 Hz
AQ            1.3664756 sec
RG                13004
DW               20.850 usec
DE                6.00 usec
TE              298.0 K
D1           2.00000000 sec
D11          0.03000000 sec
TD0                   1

======== CHANNEL f1 ========
NUC1                13C
P1                 7.30 usec
PL1                0.00 dB
SFO1         100.6228298 MHz

======== CHANNEL f2 ========
CPDPRG2          waltz16
NUC2                 1H
PCPD2             80.00 usec
PL2                0.00 dB
PL12              17.23 dB
PL13              20.00 dB
SFO2         400.1316005 MHz
SI                32768
SF           100.6127690 MHz
WDW                  EM
SSB                   0
LB                 1.00 Hz
GB                    0
PC                 1.40
```

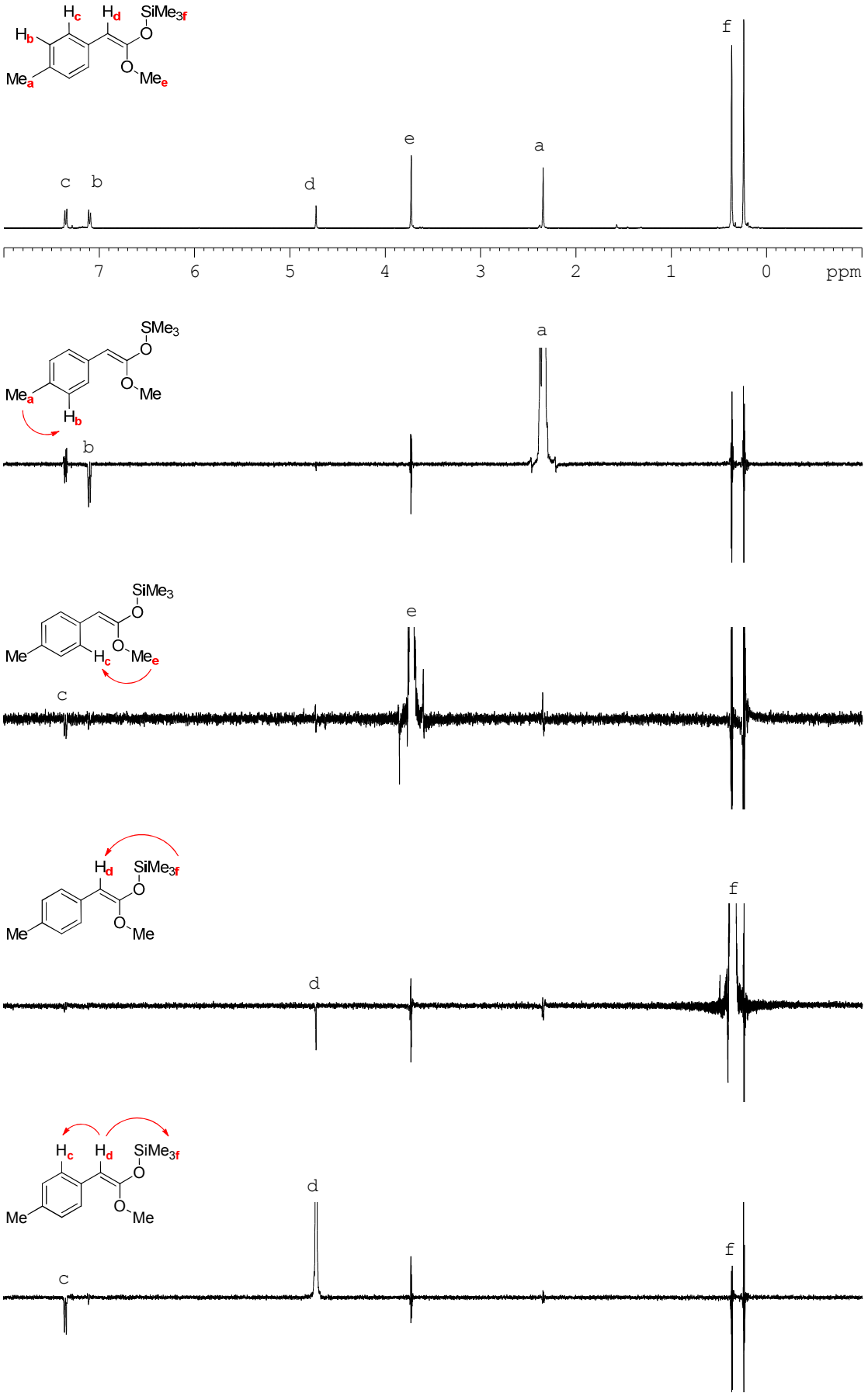
Hc
Hd
SiMe3f
Hb
O
Mea
Me
e
f
a
c
b
d
7
6
5
4
3
2
1
0
ppm
SMe3
Me
Hb
SiMe3
Hc
Hd

(1-d_1-Isopropoxy-2-*p*-tolyl-vinyloxy)-trimethyl-silane $^2H_1$-246

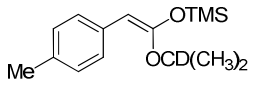

LHMDS (0.64 ml, 642 mmol, 1M in THF), TMSCl (0.09 ml, 642 mmol) and *p*-tolyl-acetic acid isopropyl-2-d_1 ester **239** (0.10 g, 0.38 mmol) were combined according to general procedure 9a and purification was achieved by reported procedure to afford (1-d_1-isopropoxy-2-*p*-tolyl-vinyloxy)-trimethyl-silane **240** as a yellow oil (0.10 g, 99%, *E/Z* 68:1). ^{1}H NMR (400 MHz, $CDCl_3$) δ: 0.31 (s, 9H), 1.29 (s, 6H), 2.29 (s, 3H), 4.72 (s, 1H), 7.04 (app. d, 2H, *J* = 7.8 Hz), 7.36 (app. d, 2H, *J* = 7.8 Hz); ^{13}C NMR (100 MHz, $CDCl_3$) δ: 5.5, 21.0, 22.2, 69.2 (t, *J* = 22.3 Hz), 88.1, 126.5, 128.7, 133.1, 134.0, 153.0. IR and HRMA not obtainable.

(1-d$_1$-Isopropoxy-2-*p*-tolyl-vinyloxy)-trimethyl-silane $^2H_1$-246

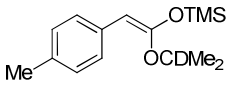

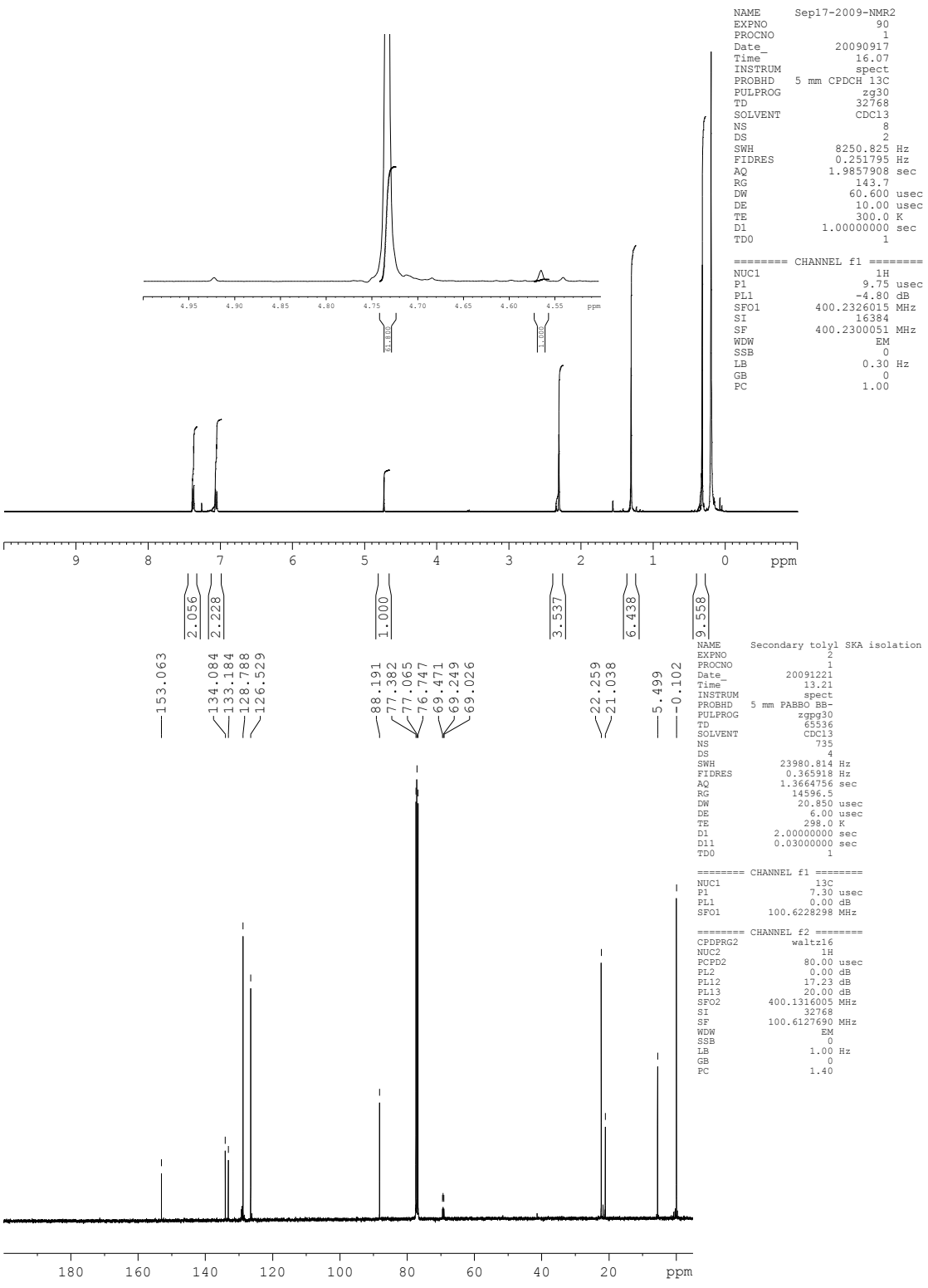

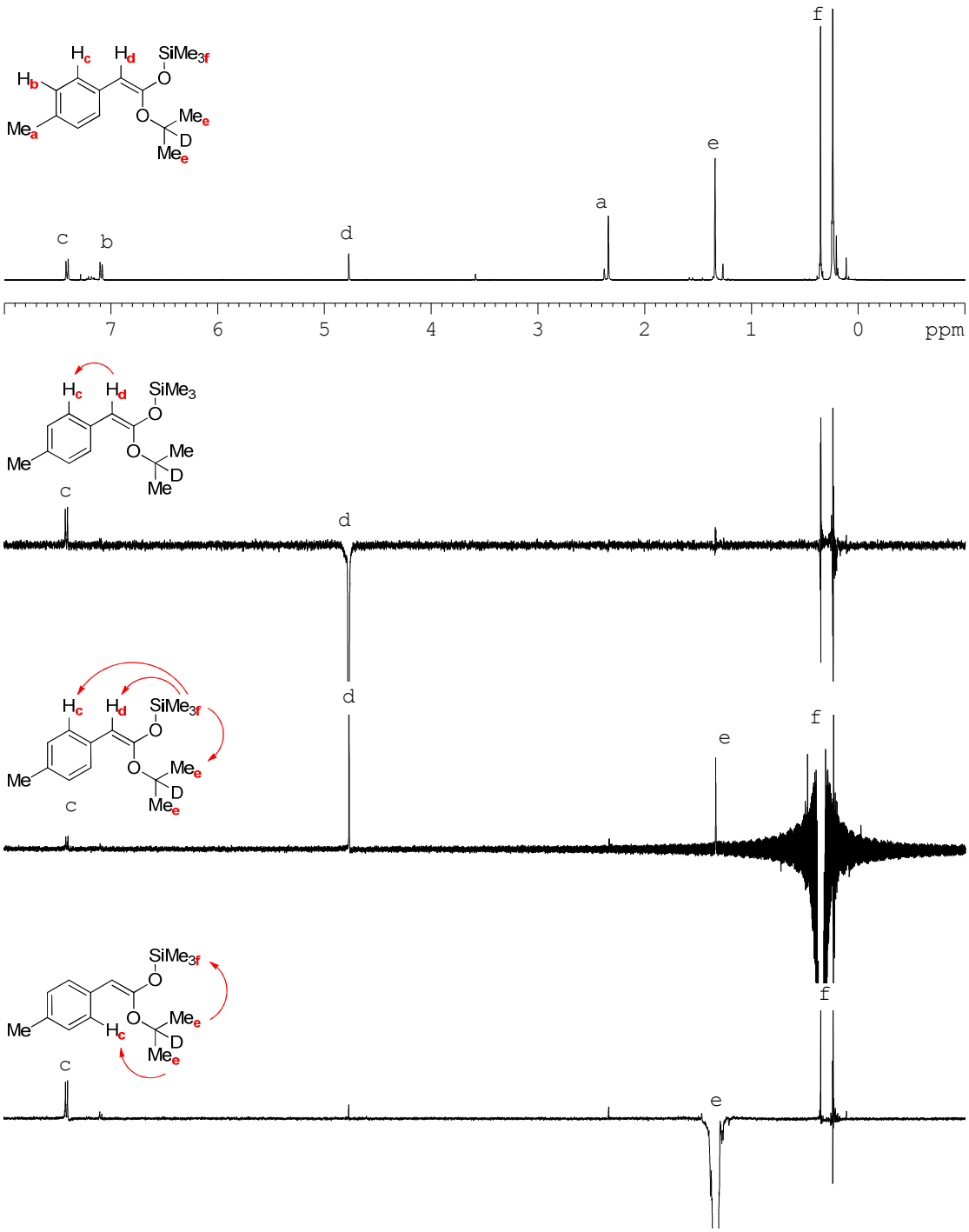

1D-NOE of Minor Z-SKA

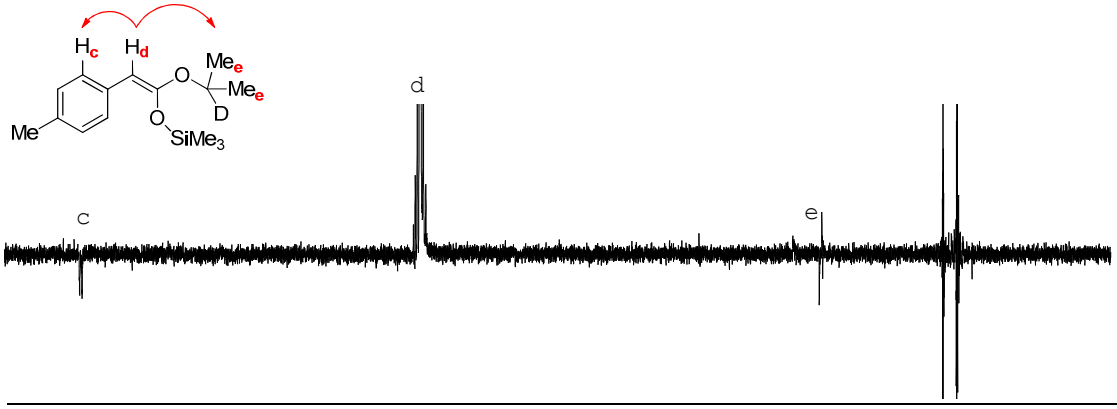

(1-*tert*-Butoxy-2-*p*-tolyl-vinyloxy)-trimethyl-silane 259

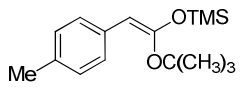

LHMDS (0.61 ml, 0.61 mmol, 1M in THF), TMSCl (0.08 ml, 0.61 mmol) and *tert*-butyl 2-*p*-tolylacetate **253** (0.10 g, 0.36 mmol) were combined according to general procedure 9a and purification was achieved by reported procedure to afford (1-*tert*-butoxy-2-*p*-tolyl-vinyloxy)-trimethyl-silane **259** as a yellow oil (0.10 g, 99%, *E/Z* 24:1). ^{1}H NMR (400 MHz, $CDCl_3$) δ: 0.34 (s, 9H), 1.49 (s, 9H), 2.33 (s, 3H), 4.86 (s, 1H), 7.08 (app. d, 2H, *J* = 8.0 Hz), 7.40 (app. d, 2H, *J* = 8.0 Hz); ^{13}C NMR (100 MHz, THF) δ: 2.9, 20.9, 29.3, 79.9, 92.9, 127.2, 128.8, 133.4, 134.6, 153.6. IR and HRMS not obtainable.

(1-*tert*-Butoxy-2-*p*-tolyl-vinyloxy)-trimethyl-silane 259

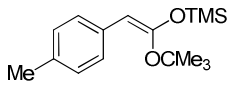

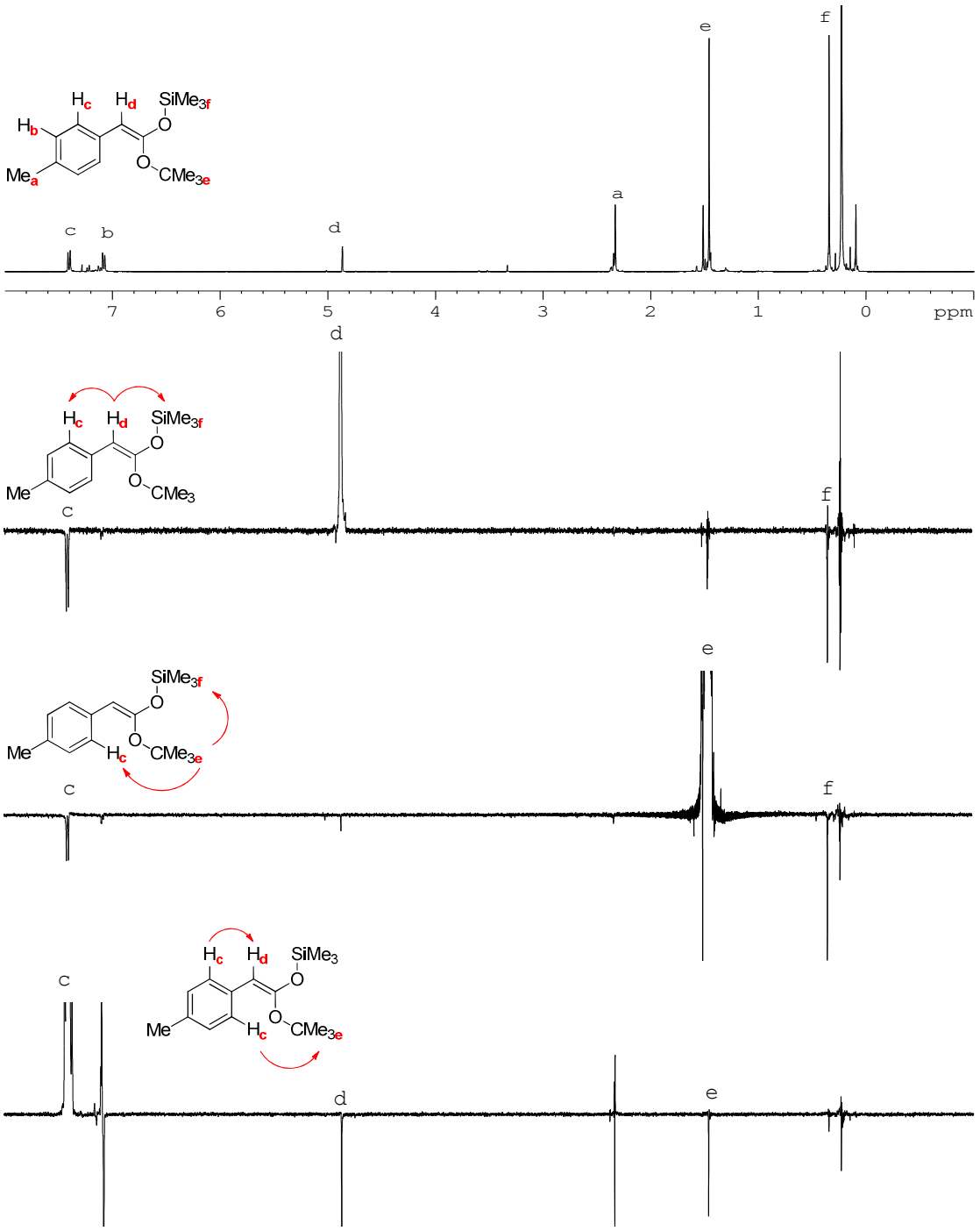

1D-NOE of Minor Z-SKA

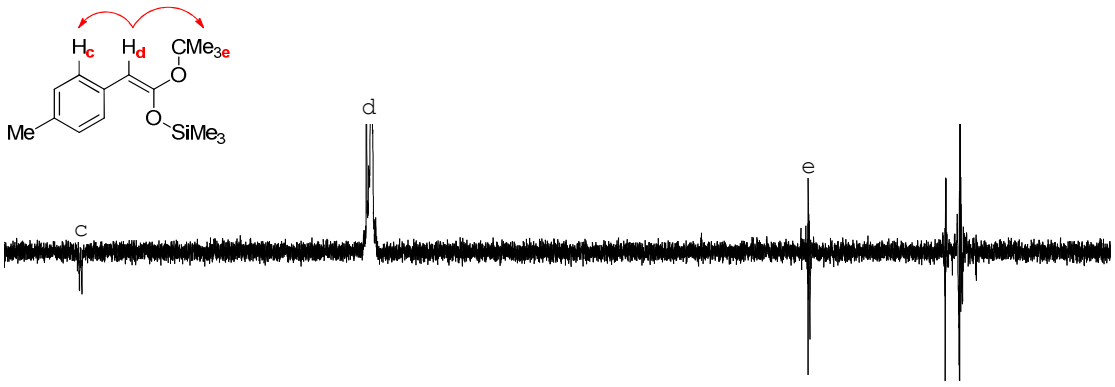

7.4. HPLC Data

(*anti-E*)-Methyl 3-(*N*-allyl-4-methylphenylsulfonamido)-2-phenylhex-4-enoate 333

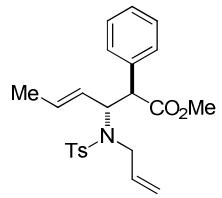

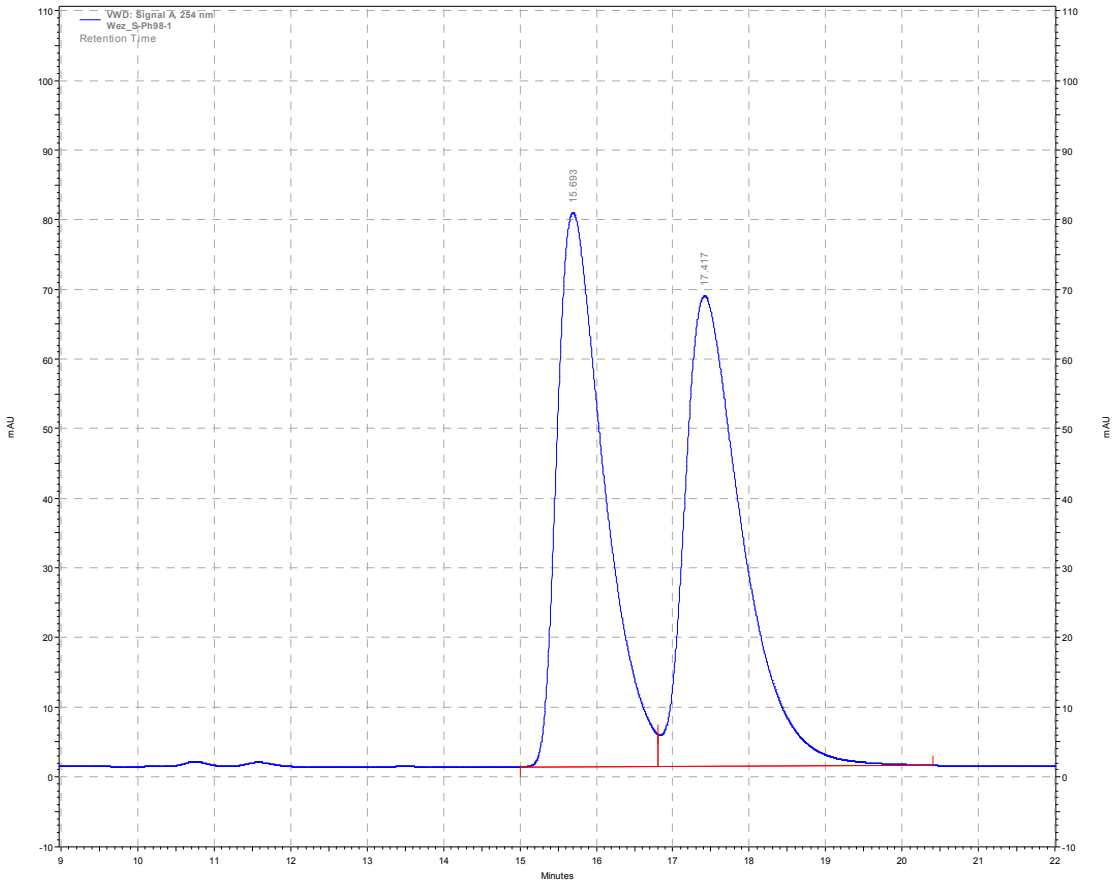

VWD: Signal A, 254 nm Results

Retention Time	Area	Area %	Height	Height %
15.693	57182044	49.13	1335586	54.09
17.417	59210450	50.87	1133646	45.91
Totals	116392494	100.00	2469232	100.00

(*2R,3R,E*)-methyl 3-(*N*-allyl-4-methylphenylsulfonamido)-2-phenylhex-4-enoate

(*S*)-333

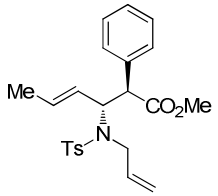

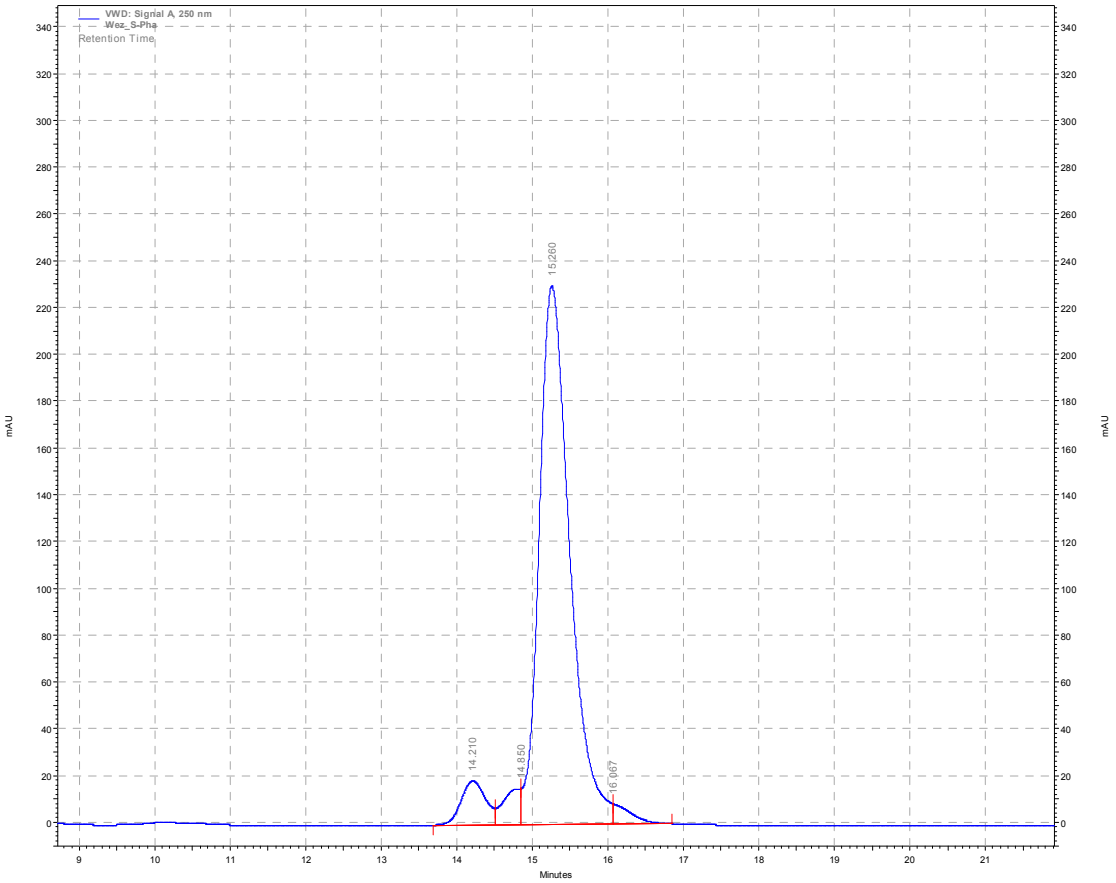

VWD: Signal A, 250 nm Results

Retention Time	Area	Area %	Height	Height %
14.210	7148487	5.83	316493	6.91
14.850	4240556	3.46	258057	5.63
15.260	108865486	88.76	3861193	84.27
16.067	2399737	1.96	146069	3.19
Totals	122654266	100.00	4581812	100.00

8. Bibliography

1. Seebach, D.; Gademann, K.; Schreiber, J. V.; Matthews, J. L.; Hintermann, T.; Jaun, B.; Oberer, L.; Hommel, U.; Widmer, H., *Helv. Chim. Acta* **1997,** *80* (7), 2033-2038.
2. Shideh, P.; Andrade, A. d.; Barbosa, J.; Cavalcanti, R. L.; Barreto, V. T. S.; Ward, C. J.; Preiser, W.; Grace, K. P.; Neild, G. H.; Codd, G. A., *The Lancet* **1998,** *352* (9121), 21-26.
3. Fischer, W. J.; Garthwaite, I.; Miles, C. O.; Ross, K. M.; Aggen, J. B.; Chamberlin, A. R.; Towers, N. R.; Dietrich, D. R., *Environmental Science & Technology* **2001,** *35* (24), 4849-4856.
4. Konishi, M.; Nishio, M.; Saitoh, K.; Miyaki, T.; Oki, T.; Kawaguchi, H., *Cispentacin, a new antifungal antibiotic. I. Production, isolation, physico-chemical properties and structure*. 1989; Vol. 42, p 1749-55.
5. Axten, J. M.; Krim, L.; Kung, H. F.; Winkler, J. D., *J. Org. Chem.* **1998,** *63* (26), 9628-9629.
6. Spiteller, P.; von Nussbaum, F., *β-Amino Acids in Natural Products*. John Wiley & Sons, Inc.: 2005; p 19-91.
7. Kimura, J.; Takada, Y.; Inayoshi, T.; Nakao, Y.; Goetz, G.; Yoshida, W. Y.; Scheuer, P. J., *J. Org. Chem.* **2002,** *67* (6), 1760-1767.
8. von Nussbaum, F.; Spiteller, P., *β-Amino Acids in Nature*. Wiley-VCH Verlag GmbH & Co. KGaA: 2005; p 63-89.
9. Buchwaldt, L.; Green, H., *Plant Pathology* **1992,** *41* (1), 55-63.
10. Engel, S.; Jensen, P. R.; Fenical, W., *J. Chem. Ecol.* **2002,** *28* (10), 1971-1985.
11. *Current Medicinal Chemistry* **2002,** *9*, 471-498.
12. Sridharan, V.; Menéndez, J. C., *Org. Lett.* **2008,** *10* (19), 4303-4306.
13. Hanbury, C. D.; White, C. L.; Mullan, B. P.; Siddique, K. H. M., *Animal Feed Science and Technology* **2000,** *87* (1-2), 1-27.
14. de Silva, E. D.; Williams, D. E.; Andersen, R. J.; Klix, H.; Holmes, C. F. B.; Allen, T. M., *Tetrahedron Lett.* **1992,** *33* (12), 1561-1564.
15. Eggen, M.; Georg, G. I., *Medicinal Research Reviews* **2002,** *22* (2), 85-101.
16. Kingston, D. G. I., *Chem. Commun.* **2001,** (10), 867-880.
17. Miller, M. L.; Ojima, I., *The Chemical Record* **2001,** *1* (3), 195-211.
18. Nicolaou, K. C.; Dai, W. M.; Guy, R. K., *Angewandte Chemie International Edition in English* **1994,** *33* (1), 15-44.
19. Shih, C.; Gossett, L. S.; Gruber, J. M.; Grossman, C. S.; Andis, S. L.; Schultz, R. M.; Worzalla, J. F.; Corbett, T. H.; Metz, J. T., *Bioorg. Med. Chem. Lett.* **1999,** *9* (1), 69-74.
20. Porter, E. A.; Wang, X.; Lee, H.-S.; Weisblum, B.; Gellman, S. H., *Nature* **2000,** *404* (6778), 565-565.
21. Woll, M. G.; Fisk, J. D.; LePlae, P. R.; Gellman, S. H., *J. Am. Chem. Soc.* **2002,** *124* (42), 12447-12452.
22. Duthaler, R. O., *Tetrahedron* **1994,** *50* (6), 1539-1650.
23. Ye, T.; McKervey, M. A., *Chem. Rev.* **1994,** *94* (4), 1091-1160.
24. Kirmse, W., *Eur. J. Org. Chem.* **2002**, 2193-2256.
25. Balenkovich, K., *Experientia.* **1947,** *3*, 369.

26. Baláspiri, L.; Penke, B.; Papp, G.; Dombi, G.; Kov´cs, K., *Helv. Chim. Acta* **1975,** *58* (4), 969-973.
27. Penke, B.; Czombos, J.; Baláspiri, L.; Petres, J.; Kovács, K., *Helv. Chim. Acta* **1970,** *53* (5), 1057-1061.
28. Jurczak, J.; Golebiowski, A., *Chem. Rev.* **1989,** *89* (1), 149-164.
29. Steurer, S.; Podlech, J., *Eur. J. Org. Chem.* **1999,** (7), 1551-1560.
30. Lubell, W. D.; Kitamura, M.; Noyori, R., *Tetrahedron: Asymmetry* **1991,** *2* (7), 543-554.
31. Hsiao, Y.; Rivera, N. R.; Rosner, T.; Krska, S. W.; Njolito, E.; Wang, F.; Sun, Y.; Armstrong, J. D.; Grabowski, E. J. J.; Tillyer, R. D.; Spindler, F.; Malan, C., *J. Am. Chem. Soc.* **2004,** *126* (32), 9918-9919.
32. Holz, J.; Monsees, A.; Jiao, H.; You, J.; Komarov, I. V.; Fischer, C.; Drauz, K.; Börner, A., *J. Org. Chem.* **2003,** *68* (5), 1701-1707.
33. Tang, W.; Wu, S.; Zhang, X., *J. Am. Chem. Soc.* **2003,** *125* (32), 9570-9571.
34. Weiner, B.; Szymanski, W.; Janssen, D. B.; Minnaard, A. J.; Feringa, B. L., *Chem. Soc. Rev.* **2010,** *39* (5), 1656-1691.
35. Eilitz, U.; Leßmann, F.; Seidelmann, O.; Wendisch, V., *Tetrahedron: Asymmetry* **2003,** *14* (2), 189-191.
36. Sammis, G. M.; Jacobsen, E. N., *J. Am. Chem. Soc.* **2003,** *125* (15), 4442-4443.
37. Wilsily, A.; Fillion, E., *Org. Lett.* **2008,** *10* (13), 2801-2804.
38. Myers, J. K.; Jacobsen, E. N., *J. Am. Chem. Soc.* **1999,** *121* (38), 8959-8960.
39. Saito, S.; Nakajima, H.; Inaba, M.; Moriwake, T., *Tetrahedron Lett.* **1989,** *30* (7), 837-838.
40. Kobayashi, S.; Ishitani, H.; Ueno, M., *J. Am. Chem. Soc.* **1998,** *120* (2), 431-432.
41. Kobayashi, S.; Kobayashi, J.; Ueno, M.; Ishiani, K., *Eur. J. Org. Chem.* **2002,** (8), 4185-4190.
42. Josephsohn, N. S.; Carswell, E. L.; Snapper, M. L.; Hoveyda, A. H., *Org. Lett.* **2005,** *7* (13), 2711-2713.
43. Brunel, J. M., *Chem. Rev.* **2005,** *105* (3), 857-898.
44. Taylor, M. S.; Jacobsen, E. N., *Angew. Chem. Int. Ed.* **2006,** *45* (10), 1520-1543.
45. Wenzel, A. G.; Jacobsen, E. N., *J. Am. Chem. Soc.* **2002,** *124* (44), 12964-12965.
46. Notz, W.; Tanaka, F.; Watanabe, S.-i.; Chowdari, N. S.; Turner, J. M.; Thayumanavan, R.; Barbas, C. F., *J. Org. Chem.* **2003,** *68* (25), 9624-9634.
47. Hayashi, Y.; Tsuboi, W.; Ashimine, I.; Urushima, T.; Shoji, M.; Sakai, K., *Angew. Chem. Int. Ed.* **2003,** *42* (31), 3677-3680.
48. Chowdari, N. S.; Suri, J. T.; Barbas, C. F., *Org. Lett.* **2004,** *6* (15), 2507-2510.
49. Bahmanyar, S.; Houk, K. N., *Org. Lett.* **2003,** *5* (8), 1249-1251.
50. Akiyama, T.; Saitoh, Y.; Morita, H.; Fuchibe, K., *Adv. Synth. Catal.* **2005,** *347* (11-13), 1523-1526.
51. Chen, Y. K.; Yoshida, M.; MacMillan, D. W. C., *J. Am. Chem. Soc.* **2006,** *128* (29), 9328-9329.
52. Vesely, J.; Ibrahem, I.; Rios, R.; Zhao, G.-L.; Xu, Y.; Córdova, A., *Tetrahedron Lett.* **2007,** *48* (12), 2193-2198.
53. Davis, F. A.; Reddy, R. E.; Szewczyk, J. M., *J. Org. Chem.* **1995,** *60* (21), 7037-7039.
54. Davis, F. A.; Reddy, R. T.; Reddy, R. E., *J. Org. Chem.* **1992,** *57* (24), 6387-6389.

55. Davis, F. A.; Szewczyk, J. M.; Reddy, R. E., *J. Org. Chem.* **1996,** *61* (6), 2222-2225.
56. Tang, T. P.; Ellman, J. A., *J. Org. Chem.* **1998,** *64* (1), 12-13.
57. Tang, T. P.; Ellman, J. A., *J. Org. Chem.* **2002,** *67* (22), 7819-7832.
58. Claisen, L., *Ber. Dtsch. Chem. Ges* **1912,** *45* (3), 3157-3166.
59. Claisen, L.; Eisleb, O., *Justus Liebigs Annalen der Chemie* **1913,** *401* (1), 21-119.
60. Ho, T.-L.; Chein, R.-J., *Chem. Commun.* **1996,** (10), 1147-1147.
61. Ireland, R. E.; Mueller, R. H., *J. Am. Chem. Soc.* **1972,** *94* (16), 5897-5898.
62. Wang, Y.-T.; Tseou, H.-F., *J. Chin. Chem. Soc.* **1937,** (5), 224-229.
63. Chai, Y.; Hong, S.-p.; Lindsay, H. A.; McFarland, C.; McIntosh, M. C., *Tetrahedron* **2002,** *58* (15), 2905-2928.
64. Angle, S. R.; Breitenbucher, J. G., *Tetrahedron Lett.* **1993,** *34* (25), 3985-3988.
65. Stivala, C. E.; Zakarian, A., *Org. Lett.* **2009,** *11* (4), 839-842.
66. Ireland, R. E.; Willard, A. K., *Tetrahedron Lett.* **1975,** *16* (46), 3975-3978.
67. Ireland, R. E.; Mueller, R. H.; Willard, A. K., *J. Am. Chem. Soc.* **1976,** *98* (10), 2868-2877.
68. Ireland, R. E.; Wipf, P.; Armstrong, J. D., *J. Org. Chem.* **1991,** *56* (2), 650-657.
69. Ireland, R. E.; Wipf, P.; Xiang, J. N., *J. Org. Chem.* **1991,** *56* (11), 3572-3582.
70. Khaledy, M. M.; Kalani, M. Y. S.; Khuong, K. S.; Houk, K. N.; Aviyente, V.; Neier, R.; Soldermann, N.; Velker, J., *J. Org. Chem.* **2002,** *68* (2), 572-577.
71. Ireland, R. E.; Daub, J. P., *J. Org. Chem.* **1981,** *46* (3), 479-485.
72. Ireland, R. E.; Thaisrivongs, S.; Vanier, N.; Wilcox, C. S., *J. Org. Chem.* **1980,** *45* (1), 48-61.
73. Bartlett, P. A.; Barstow, J. F., *J. Org. Chem.* **1982,** *47* (20), 3933-3941.
74. Bartlett, P. A.; Pizzo, C. F., *J. Org. Chem.* **1981,** *46* (19), 3896-3900.
75. Katzenellenbogen, J. A.; Christy, K. J., *J. Org. Chem.* **1974,** *39* (23), 3315-3318.
76. Ireland, R. E.; Varney, M. D., *J. Am. Chem. Soc.* **1984,** *106* (12), 3668-3670.
77. Fleischhacker, W.; Richter, B., *Monatshefte für Chemie / Chemical Monthly* **1992,** *123* (8), 837-848.
78. Kawasaki, T.; Ohtsuka, H.; Mihira, A.; Sakamoto, M., *ChemInform* **1998,** *29* (16), no-no.
79. Lee, T.-j., *Tetrahedron Lett.* **1979,** *20* (25), 2297-2300.
80. Egert, E.; Beck, H.; Schmidt, D.; Gonschorrek, C.; Hoppe, D., *Tetrahedron Lett.* **1987,** *28* (7), 789-792.
81. Johnson, W. S.; Werthemann, L.; Bartlett, W. R.; Brocksom, T. J.; Li, T.-T.; Faulkner, D. J.; Petersen, M. R., *J. Am. Chem. Soc.* **1970,** *92* (3), 741-743.
82. Mori, K.; Nukada, T.; Ebata, T., *Tetrahedron* **1981,** *37* (7), 1343-1347.
83. Overman, L. E., *J. Am. Chem. Soc.* **1974,** *96* (2), 597-599.
84. Anderson, C. E.; Overman, L. E., *J. Am. Chem. Soc.* **2003,** *125* (41), 12412-12413.
85. Burrows, C. J.; Carpenter, B. K., *J. Am. Chem. Soc.* **1981,** *103* (23), 6983-6984.
86. Bourgeois, D.; Craig, D.; King, N. P.; Mountford, D. M., *Angew. Chem. Int. Ed.* **2005,** *44* (4), 618-621.
87. Craig, D.; Grellepois, F., *Org. Lett.* **2005,** *7* (3), 463-465.
88. Inada, S.; Kurata, R., *Bull. Chem. Soc. Jpn* **1981,** *54*, 1581-1582.
89. Nubbemeyer, U., *J. Org. Chem.* **1995,** *60* (12), 3773-3780.
90. Yu, C.-M.; Choi, H.-S.; Lee, J.; Jung, W.-H.; Kim, H.-J., *J. Chem. Soc., Perkin Trans. 1* **1996,** (2), 115-116.
91. Kwart, H.; Evans, E. R., *J. Org. Chem.* **1966,** *31* (2), 413-419.

92. Aggarwal, V. K.; Lattanzi, A.; Fuentes, D., *Chem. Commun.* **2002,** (21), 2534-2535.
93. Nubbemeyer, U.; Öhrlein, R.; Gonda, J.; Ernst, B.; Belluš, D., *Angewandte Chemie International Edition in English* **1991,** *30* (11), 1465-1467.
94. Liu, D.; Acharya, H. P.; Yu, M.; Wang, J.; Yeh, V. S. C.; Kang, S.; Chiruta, C.; Jachak, S. M.; Clive, D. L. J., *J. Org. Chem.* **2009,** *74* (19), 7417-7428.
95. Carbery, D. R., *Organic & Biomolecular Chemistry* **2008,** *6* (19), 3455-3460.
96. Matsubara, R.; Kobayashi, S., *Accounts Chem. Res.* **2008,** *41* (2), 292-301.
97. Guo, Q.-X.; Peng, Y.-G.; Zhang, J.-W.; Song, L.; Feng, Z.; Gong, L.-Z., *Org. Lett.* **2009,** *11* (20), 4620-4623.
98. Terada, M.; Sorimachi, K., *J. Am. Chem. Soc.* **2006,** *129* (2), 292-293.
99. Jia, Y. X.; Zhong, J.; Zhu, S. F.; Zhang, C. M.; Zhou, Q. L., *Angew. Chem. Int. Ed.* **2007,** *46* (29), 5565-5567.
100. Baudequin, C.; Zamfir, A.; Tsogoeva, S. B., *Chem. Commun.* **2008,** (38), 4637-4639.
101. Carbery, D. R.; Marsh, B. J.; Heath, E. L., *Chem. Commun.* **2010,** *ASAP*, 10.1039/C0CC02272A.
102. Li, G.; Antilla, J. C., *Org. Lett.* **2009,** *11* (5), 1075-1078.
103. Bennasar, M. L.; Roca, T.; Monerris, M.; García-Díaz, D., *J. Org. Chem.* **2006,** *71* (18), 7028-7034.
104. Huang, Y.; Iwama, T.; Rawal, V. H., *J. Am. Chem. Soc.* **2000,** *122* (32), 7843-7844.
105. Huntley, R. J.; Funk, R. L., *Org. Lett.* **2006,** *8* (15), 3403-3406.
106. Barbazanges, M.; Meyer, C.; Cossy, J., *Org. Lett.* **2007,** *9* (17), 3245-3248.
107. Taniguchi, T.; Iwasaki, K.; Uchiyama, M.; Tamura, O.; Ishibashi, H., *Org. Lett.* **2005,** *7* (20), 4389-4390.
108. Movassaghi, M.; Hill, M. D.; Ahmad, O. K., *J. Am. Chem. Soc.* **2007,** *129* (33), 10096-10097.
109. Ylioja, P. M.; Mosley, A. D.; Charlot, C. E.; Carbery, D. R., *Tetrahedron Lett.* **2008,** *49* (7), 1111-1114.
110. Hong, S.-p.; Lindsay, H. A.; Yaramasu, T.; Zhang, X.; McIntosh, M. C., *J. Org. Chem.* **2002,** *67* (7), 2042-2055.
111. Zhang, X.; McIntosh, M. C., *Tetrahedron Lett.* **1998,** *39* (39), 7043-7046.
112. Ito, H.; Taguchi, T., *Chem. Soc. Rev.* **1999,** *28*, 43-50.
113. Janey, J. M.; Iwama, T.; Kozmin, S. A.; Rawal, V. H., *J. Org. Chem.* **2000,** *65* (26), 9059-9068.
114. Fan, M.-J.; Li, G.-Q.; Liang, Y.-M., *Tetrahedron* **2006,** *62* (29), 6782-6791.
115. McAlonan, H.; Murphy, J. P.; Nieuwenhuyzen, M.; Reynolds, K.; Sarma, P. K. S.; Stevenson, P. J.; Thompson, N., *J. Chem. Soc., Perkin Trans. 1* **2002,** (1), 69-79.
116. Kühnel, E.; Laffan, D. D. P.; Lloyd-Jones, G. C.; Martínez del Campo, T.; Shepperson, I. R.; Slaughter, J. L., *Ang. Chem. Int. Ed.* **2007,** *46*, 7075-7078.
117. Toyohiko, A.; Takayuki, S., *Chem. Pharm. Bull.* **1981,** *29* (11), 3249-3255.
118. Moreland, D. W.; Dauben, W. G., *J. Am. Chem. Soc.* **1985,** *107* (8), 2264-2273.
119. Corset, J.; Froment, F.; Lautie, M. F.; Ratovelomanana, N.; Seyden-Penne, J.; Strzalko, T.; Roux-Schmitt, M. C., *J. Am. Chem. Soc.* **1993,** *115* (5), 1684-1694.
120. Tanaka, F.; Fuji, K., *Tetrahedron Lett.* **1992,** *33* (51), 7885-7888.
121. Doering, W. v. E.; Wang, Y., *J. Am. Chem. Soc.* **1999,** *121* (43), 10112-10118.
122. Hrovat, D. A.; Beno, B. R.; Lange, H.; Yoo, H.-Y.; Houk, K. N.; Borden, W. T., *J. Am. Chem. Soc.* **1999,** *121* (45), 10529-10537.

123. Siebert, M. R.; Tantillo, D. J., *J. Am. Chem. Soc.* **2007,** *129* (28), 8686-8687.
124. Hansch, C.; Leo, A.; Taft, R. W., *Chem. Rev.* **1991,** *91* (2), 165-195.
125. Hammett, L. P., *Chem. Rev.* **1935,** *17* (1), 125-136.
126. Dippy, J. F. J.; Lewis, R. H., *Journal of the Chemical Society (Resumed)* **1936**, 644-649.
127. Dippy, J. F. J.; Williams, F. R., *Journal of the Chemical Society (Resumed)* **1934**, 1888-1892.
128. Dippy, J. F. J.; Williams, F. R.; Lewis, R. H., *Journal of the Chemical Society (Resumed)* **1935**, 343-346.
129. Hammett, L. P., *J. Am. Chem. Soc.* **1937,** *59* (1), 96-103.
130. Hammett, L. P., *Transactions of the Faraday Society* **1938,** *34*, 156-165.
131. Schreck, J., *J. Chem. Educ.* **1971,** *48* (2), 103-null.
132. Swain, C. G.; Langsdorf, W. P., *J. Am. Chem. Soc.* **1951,** *73* (6), 2813-2819.
133. Hart, H.; Sedor, E. A., *J. Am. Chem. Soc.* **1967,** *89* (10), 2342-2347.
134. Okamoto, Y.; Inukai, T.; Brown, H. C., *J. Am. Chem. Soc.* **1958,** *80* (18), 4969-4972.
135. Brown, H. C.; Okamoto, Y., *J. Am. Chem. Soc.* **1958,** *80* (18), 4979-4987.
136. Taft, R. W., *J. Am. Chem. Soc.* **1952,** *74* (12), 3120-3128.
137. Taft, R. W., *J. Am. Chem. Soc.* **1952,** *74* (11), 2729-2732.
138. Taft, R. W., *J. Am. Chem. Soc.* **1953,** *75* (18), 4538-4539.
139. Swain, C. G.; Lupton, E. C., *J. Am. Chem. Soc.* **1968,** *90* (16), 4328-4337.
140. Swain, C. G.; Unger, S. H.; Rosenquist, N. R.; Swain, M. S., *J. Am. Chem. Soc.* **1983,** *105* (3), 492-502.
141. Yukawe, Y.; Tsuno, Y., *Bull. Chem. Soc. Jpn* **1959,** *32* (9), 965-971.
142. Yajima, T.; Okada, K.; Nagano, H., *Tetrahedron* **2004,** *60* (27), 5683-5693.
143. Morgan, A. J.; Masse, C. E.; Panek, J. S., *Org. Lett.* **1999,** *1* (12), 1949-1952.
144. Gugelchuk, M. M.; Chan, P. C. M.; Sprules, T. J., *J. Org. Chem.* **1994,** *59* (25), 7723-7731.
145. Aviyente, V.; Houk, K. N., *J. Phys. Chem. A* **2001,** *105* (2), 383-391.
146. Burrows, C.; Carpenter, B. K., *J. Am. Chem. Soc.* **1981,** *103* (23), 6984-6986.
147. Curran, D. P.; Suh, Y. G., *J. Am. Chem. Soc.* **1984,** *106* (17), 5002-5004.
148. Gajewski, J. J.; Jurayj, J.; Kimbrough, D. R.; Gande, M. E.; Ganem, B.; Carpenter, B. K., *J. Am. Chem. Soc.* **1987,** *109* (4), 1170-1186.
149. Ollevier, T.; Nadeau, E., *Organic & Biomolecular Chemistry* **2007,** *5* (19), 3126-3134.
150. Denmark, S. E.; Chung, W.-j., *J. Org. Chem.* **2008,** *73* (12), 4582-4595.
151. Notte, G. T.; Baxter Vu, J. M.; Leighton, J. L., *Org. Lett.* **2011,** *13* (4), 816-818.
152. Solladie-Cavallo, A.; Csaky, A. G., *J. Org. Chem.* **1994,** *59* (9), 2585-2589.
153. Pinheiro, S.; Lima, M. B.; Gonçalves, C. B. S. S.; Pedraza, S. F.; de Farias, F. M. C., *Tetrahedron Lett.* **2000,** *41* (21), 4033-4034.
154. Heurtaux, B.; Lion, C.; Le Gall, T.; Mioskowski, C., *J. Org. Chem.* **2005,** *70* (4), 1474-1477.
155. Tanaka, M.; Kurosaki, Y.; Washio, T.; Anada, M.; Hashimoto, S., *Tetrahedron Lett.* **2007,** *48* (50), 8799-8802.
156. Akiyama, T.; Takaya, J.; Kagoshima, H., *Adv. Synth. Catal* **2002,** *344* (3-4), 338-347.
157. Itoh, J.; Fuchibe, K.; Akiyama, T., *Synthesis* **2006**, 4075-4080
158. Ollevier, T.; Nadeau, E., *Synlett* **2006**, 219-222.
159. Su, S.; Porco, J. A., *Org. Lett.* **2007,** *9* (24), 4983-4986.

160. Harker, W. R. R.; Carswell, E. L.; Carbery, D. R., *Org. Lett.* **2010,** *12* (16), 3712-3715.
161. Pfeffer, P. E.; Foglia, T. A.; Barr, P. A.; Obenauf, R. H., *J. Org. Chem.* **1978,** *43* (17), 3429-3431.
162. Seebach, D., *Ang. Chem. Int. Ed.* **1988,** *27*, 1624.
163. Laube, T.; Dunitz, J. D.; Seebach, D., *Helv. Chim. Acta* **1985,** *68*, 1373.
164. Lipshutz, B. H.; Wood, M. R.; Lindsley, C. W., *Tetrahedron Lett.* **1995,** *36* (25), 4385-4388.
165. Hall, P. L.; Gilchrist, J. H.; Collum, D. B., *J. Am. Chem. Soc.* **1991,** *113* (25), 9571-9574.
166. DePue, J. S.; Collum, D. B., *J. Am. Chem. Soc.* **1988,** *110* (16), 5518-5524.
167. DePue, J. S.; Collum, D. B., *J. Am. Chem. Soc.* **1988,** *110* (16), 5524-5533.
168. Hall, P. L.; Gilchrist, J. H.; Harrison, A. T.; Fuller, D. J.; Collum, D. B., *J. Am. Chem. Soc.* **1991,** *113* (25), 9575-9585.
169. Goo, *Chem. Commun.* **2001,** (7), 669-670.
170. Hama, T.; Liu, X.; Culkin, D. A.; Hartwig, J. F., *J. Am. Chem. Soc.* **2003,** *125* (37), 11176-11177.
171. Angle, S. R.; Breitenbucher, J. G.; Arnaiz, D. O., *J. Org. Chem.* **1992,** *57* (22), 5947-5955.
172. Funk, R. L.; Stallman, J. B.; Wos, J. A., *J. Am. Chem. Soc.* **1993,** *115* (19), 8847-8848.
173. Godenschwager, P. F.; Collum, D. B., *J. Am. Chem. Soc.* **2008,** *130* (27), 8726-8732.
174. Zhao, P.; Collum, D. B., *J. Am. Chem. Soc.* **2003,** *125* (14), 4008-4009.
175. Kim, Y.-J.; Streitwieser, A., *Org. Lett.* **2002,** *4* (4), 573-575.
176. Gallardo, G. L.; Butler, M.; Gallo, M. L.; Rodríguez, M. A.; Eberlin, M. N.; Cabrera, G. M., *Phytochemistry* **2006,** *67* (21), 2403-2410.
177. Roe, S. J.; Hughes, D. L.; Aggarwal, P.; Stockman, R. A., *Synthesis* **2009,** *22*, 3775-3784.
178. Smulders, M. M. J.; Stals, P. J. M.; Mes, T.; Paffen, T. F. E.; Schenning, A. P. H. J.; Palmans, A. R. A.; Meijer, E. W., *J. Am. Chem. Soc.* **2009,** *132* (2), 620-626.
179. Bucciarelli, M.; Forni, A.; Moretti, I.; Torre, G., *J. Org. Chem.* **1983,** *48* (16), 2640-2644.
180. Goldstein, S. W.; Overman, L. E.; Rabinowitz, M. H., *J. Org. Chem.* **1992,** *57* (4), 1179-1190.
181. Laguzza, B. C.; Ganem, B., *Tetrahedron Lett.* **1981,** *22* (16), 1483-1486.
182. Barbazanges, M.; Meyer, C.; Cossy, J., *Tetrahedron Lett.* **2008,** *49* (18), 2902-2906.
183. Gillard, J. W.; Belanger, P., *J. Med. Chem.* **1987,** *30* (11), 2051-2058.
184. Clayden, J., *Tetrahedron Organic Chemistry Series* **2002,** *23*.
185. Aviyente, V.; Houk, K. N., *The Journal of Physical Chemistry A* **2000,** *105* (2), 383-391.
186. Cerezo, S.; Cortés, J.; Moreno-Mañas, M.; Pleixats, R.; Roglans, A., *Tetrahedron* **1998,** *54* (49), 14869-14884.
187. Furstner, A.; Ackerstaff, J., *Chem. Commun.* **2008,** (25), 2870-2872.
188. Igawa, K.; Sakita, K.; Murakami, M.; Tomooka, K., *Synthesis* **2008,** *10*, 1641-1645.
189. Hofmann, P.; Shishkov, I. V.; Rominger, F., *Inorg. Chem.* **2008,** *47* (24), 11755-11762.

190. Hamper, B. C.; Kolodziej, S. A.; Scates, A. M.; Smith, R. G.; Cortez, E., *J. Org. Chem.* **1998,** *63* (3), 708-718.
191. Belanger, P. C.; Rooney, C. S.; Robinson, F. M.; Sarett, L. H., *J. Org. Chem.* **1978,** *43* (5), 906-909.
192. Lumma, W. C.; Berchtold, G. A., *J. Org. Chem.* **1969,** *34* (6), 1566-1572.
193. Krüger, T.; Vorndran, K.; Linker, T., *Chem. Eur. J.* **2009,** *44*, 12082-12091.
194. Kurimoto, A.; Hashimoto, K.; Nakamura, T.; Norimura, K.; Ogita, H.; Takaku, H.; Bonnert, R.; McInally, T.; Wada, H.; Isobe, Y., *J. Med. Chem.* **2010,** *53* (7), 2964-2972.
195. Motoyama, Y.; Kamo, K.; Nagashima, H., *Org. Lett.* **2009,** *11* (6), 1345-1348.
196. Moreau, E.; Fortin, S.; Lacroix, J.; Patenaude, A.; Rousseau, J. L. C.; C-Gaudreault, R., *Biorg. Med. Chem.* **2008,** *16* (3), 1206-1217.
197. Owston, N. A.; Nixon, T. D.; Parker, A. J.; Whittlesey, M. K.; Williams, J. M. J., *Synthesis* **2009,** *9*, 1578-1581.
198. Ni, A.; France, J. E.; Davies, H. M. L., *J. Org. Chem.* **2006,** *71* (15), 5594-5598.
199. Bodnar, B. S.; Vogt, P. F., *J. Org. Chem.* **2009,** *74* (6), 2598-2600.
200. Lambert, J. B.; Mark, H. W.; Magyar, E. S., *J. Am. Chem. Soc.* **1977,** *99* (9), 3059-3067.
201. Barua, A. K.; Chakrabarty, M.; Datta, P. K.; Ray, S., *Phytochemistry* **1988,** *27*, 3259-3261.
202. Eißler, S.; Bogner, T.; Nahrwold, M.; Sewald, N., *Chem. Eur. J.* **2009,** *15*, 11273-11287.
203. Roy, S.; Roy, S.; Gribble, G. W., *Org. Lett.* **2006,** *8* (21), 4975-4977.
204. Cabedo, N.; Andreu, I.; Ramírez de Arellano, M. C.; Chagraoui, A.; Serrano, A.; Bermejo, A.; Protais, P.; Cortes, D., *J. Med. Chem.* **2001,** *44* (11), 1794-1801.
205. Altermann, S. M.; Richardson, R. D.; Keri Page, T.; Schmidt, R. K.; Holland, E.; Mohammed, U.; Paradine, S. M.; French, A. N.; Richter, C.; Masih Bahar, A.; Witluski, B.; Wirt, T., *Eur. J. Org. Chem.* **2008**, 5315-5328.